

AD-A955 062

DTIC ACCESSION NUMBER

PHOTOGRAPH THIS SHEET



INVENTORY

LEVEL

DESIGN ANALYSIS OF A
PREPACKAGED NUCLEAR POWER
PLANT FOR AN ICE CAP
LOCATION

DOCUMENT IDENTIFICATION

DDI-44-669-226-3638

DISTRIBUTION STATEMENT A

Approved for public release;
Distribution Unlimited

DISTRIBUTION STATEMENT

ACCESSION FOR

NTIS GRA&I

DTIC TAB

UNANNOUNCED

JUSTIFICATION

BY

DISTRIBUTION /

AVAILABILITY CODES

DIST

AVAIL AND/OR SPECIAL

A-1

DISTRIBUTION STAMP

UNANNOUNCED

DTIC
ELECTE

JAN 29 1986

DATE ACCESSIONED

DATE RETURNED

86 1 28 065

DATE RECEIVED IN DTIC

REGISTERED OR CERTIFIED NO.

PHOTOGRAPH THIS SHEET AND RETURN TO DTIC-DDAC

APAE-39-56-553

APAE-39

REACTORS—POWER

AD-A955 062

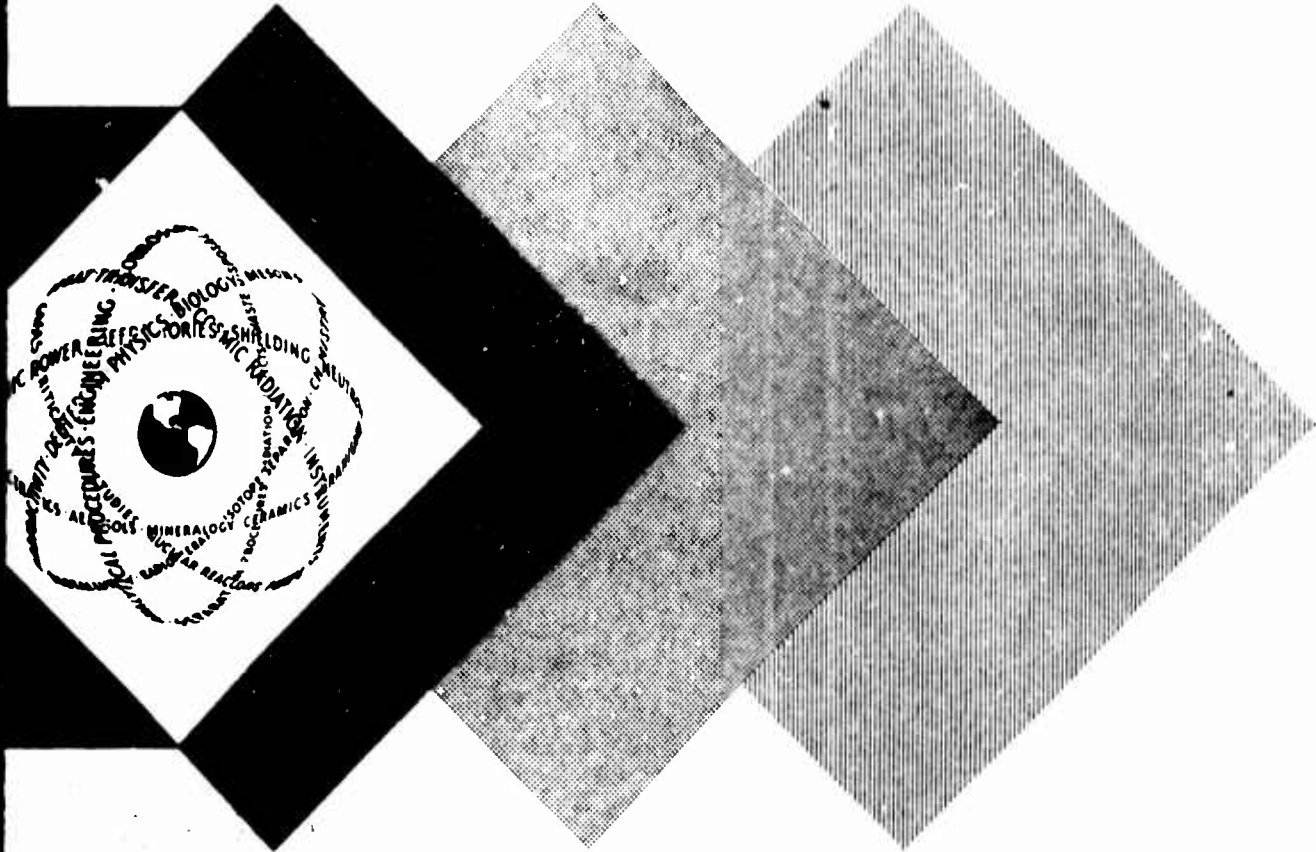
DESIGN ANALYSIS OF A PREPACKAGED NUCLEAR POWER PLANT FOR AN ICE CAP LOCATION

56-553

January 15, 1959

Alco Products, Inc.
Schenectady, New York

DISTRIBUTION STATEMENT A
Approved for public release
Distribution Unlimited



UNITED STATES ATOMIC ENERGY COMMISSION
Office of Technical Information

DC 43 564

LEGAL NOTICE

This report was prepared as an account of Government sponsored work. Neither the United States, nor the Commission, nor any person acting on behalf of the Commission:

A. Makes any warranty or representation, expressed or implied, with respect to the accuracy, completeness, or usefulness of the information contained in this report, or that the use of any information, apparatus, method, or process disclosed in this report may not infringe privately owned rights; or

B. Assumes any liabilities with respect to the use of, or for damages resulting from the use of any information, apparatus, method, or process disclosed in this report.

As used in the above, "person acting on behalf of the Commission" includes any employee or contractor of the Commission, or employee of such contractor, to the extent that such employee or contractor of the Commission, or employee of such contractor prepares, disseminates, or provides access to, any information pursuant to his employment or contract with the Commission, or his employment with such contractor.

This report has been reproduced directly from the best available copy.

Printed in USA. Price \$5.50. Available from the Office of Technical Services, Department of Commerce, Washington 25, D. C.



APAE-39
DESIGN ANALYSIS
OF A
PREPACKAGED NUCLEAR POWER PLANT
FOR AN
ICE CAP LOCATION

Issued January 15, 1959

Contract DA-44-009-eng-3638

Alco Products, Inc.
P.O. Box 414
Schenectady, N.Y.

SKID MOUNTED DESIGN ANALYSIS

MASTER INDEX

- Section P - Plant
Drawings for Plant
- Section A - Primary System
Drawings for Primary System
- Section B - Reactor Design
- Section C - Secondary System
Drawings for Secondary System

PLANT SECTION

INDEX

SECTION P

- 1.0 Plant design requirement
 - 1.1 Type of plant
 - 1.2 Generating requirements and heating load
 - 1.3 Site Conditions
 - 1.4 Air Transportability
 - 1.5 Standby Power Availability
 - 1.6 Building Structures and Foundations

- 2.0 Plant Design Philosophy
 - 2.1 Reliability
 - 2.1.1 Fuel Elements and Control Rods
 - 2.1.2 Primary System Components
 - 2.1.3 Closed Systems
 - 2.1.3.1 Vapor Containment
 - 2.1.3.2 Heating System
 - 2.1.3.3 Auxiliary Cooling System
 - 2.1.4 Condenser System
 - 2.1.5 Duplication of Rotating Equipment
 - 2.1.6 Instrumentation
 - 2.1.7 Testing
 - 2.1.8 Primary System Components
 - 2.1.9 Secondary System Components
 - 2.1.10 Packaging
 - 2.1.11 Steam Cycle
 - 2.1.12 Components
 - 2.1.13 Vapor Containment
 - 2.1.14 Spent Fuel Storage
 - 2.1.15 Hazards Requirement
 - 2.1.16 Consideration of Installation under Snow
 - 2.1.16.1 Layout Approach
 - 2.1.16.2 Enclosures
 - 2.1.17 Ventilation

- 3.0 Plant Arrangement
 - 3.1 Description
 - 3.2 Location of Packages

- 4.0 Operating Data, Weights and Dimensions
 - 4.1 Plant Performance
 - 4.2 Thermal Data of Reactor at Full Power
 - 4.3 Steam Generator
 - 4.4 Pressurizer
 - 4.5 Primary Coolant Pump
 - 4.6 Primary Coolant Piping
 - 4.7 Vapor Container
 - 4.8 Core Design

- 4.9 Shielding Design
- 4.10 Thermal Design
- 4.11 Weight and Dimensional Data of Major Items
- 5.0 Ethylene Glycol Diversion and Steam Extraction for Additional Heat
 - 5.1 Ethylene Glycol Diversion Provisions
 - 5.2 Steam Extraction from Main Steam Header for Additional Heat
- 6.0 Engineering, Procurement, Fabrication, Factory Testing, Site Installation, Site Testing
- 7.0 Plan for Installation of the Plant at a Site
- 8.0 Plan of operation of the Installed Plant Including Number and Qualifications of the Operating Personnel Required
- 9.0 Plant Relocation following extended power operation
- 10.0 Testing of Plant
 - 10.1 Individual Item Tests
 - 10.2 Plant Factory System Test
 - 10.3 Low and High Power Performance Test at the Site
 - 10.4 Plant Performance Test at the Site
- 11.0 Testing (In Service and Developmental)
 - 11.1 Fuel Elements
 - 11.2 Boron
 - 11.2.1 Boron
 - 11.2.2 Europium Oxide
 - 11.3 Control Rod Drives
 - 11.4 Reactor Vessel, Steam Generator and Pressurizer
 - 11.5 Primary Coolant Pump
 - 11.6 Primary Coolant Auxiliaries
 - 11.7 Secondary System and Equipment
 - 11.8 Instruments and Controls

INDEX

| SECTION P | DRAWINGS | PAGE NUMBER |
|-----------------------|--|-------------|
| <u>Drawing Number</u> | <u>Title</u> | |
| R9-47-1012 | Piping and Instrument Diagram (Primary) | P-55 |
| MO2M1 | Station Flow Diagram (Secondary) | P-57 |
| MO2M2 | Heat Balance Diagram | P-59 |
| MO2E2 | Single Line Wiring Diagram | P-61 |
| MO2E1 | Schematic and Connection Diagrams | P-63 |
| MO2M11 | General Arrangement (Plant) | P-65 |
| R9-43-1004 | Primary System (Installation) | P-67 |
| MO2M12 | Piping Plan | P-69 |
| MO2M13 | Piping Sections | P-71 |
| MO2E8 | Electrical Plan | P-73 |
| MO2S6 | Piling Diagram | P-75 |
| MO2S7 | Location of Centers of Gravity (Secondary) | P-77 |
| AES-268 | Primary Skid for Reactor and Steam Gen- erator Weight Distribution and Center of Gravity | P-79 |
| AES-270 | Vapor Container and Components Weight Distribution and Center of Gravity | P-81 |
| R9-43-1005 | Primary System (Installation) without Vapor Containment | P-83 |
| AES-269 | Primary Skid with Reactor and Steam Generator Generator Weight Distribution | P-85 |
| MO2S8 | Foundation Load Diagram (Secondary) | P-87 |
| MO2S9 | Turbine Generator Package - Typical Foundation Section | P-89 |
| MO2S10 | Typical Package Foundation - Cross Section | P-91 |

PLANT SECTION

1.0 Plant Design Requirement

1.1 Type of Plant

It is a Nuclear Power Steam-Electric generating plant. It is air transportable, skid mounted designed for an ice cap installation. The reactor is a pressurized water design.

1.2 Generating Requirements and Heating Load

The plant shall be capable of producing a minimum of 1500 Kw net 6 electrical energy at 4160/2400 volts, three phase, 60 cycles and 1.0×10^6 Btu/hr for space heating at 165 psia saturated steam at evaporator outlet.

1.3 Site Conditions

The plant is designed for the conditions imposed by a remote ice cap site, specifically the site conditions require the plant to be located on an ice cap at an elevation up to 5500 ft. above seal level with no cooling water for condensing steam available. Severe climatic conditions with surface temperatures ranging from -75° F to $+35^{\circ}$ F, and constant winds from 5 to 100 m.p.h. velocity, dictate the location of the entire power plant in tunnels below the snow surface. Average annual snow accumulation of approximately 2 ft. indicates the relocation of the entire power plant every six to seven years.

1.4 Air Transportability

In order to meet the limitations imposed by the site and air transportation, as well as to minimize field erection time, the plant components shall be pre-assembled and tested.

The weight and dimensional limitations are based on the use of the C-130 Air Craft and air shipment of all packages and components. All transportable packages do not exceed 30 ft. long x 9 ft. wide x 9 ft. high and/or 30,000# in weight.

All packages are designed to meet the permissible floor loading and the center of gravity location for C-130 Air Craft, and structurally able to provide proper tie-down connections to meet external forces experienced in flight.

1.5 Standby Power Availability

Standby power by diesel engine generator sets capable of producing 2000 Kw gross capacity will be furnished by others in a facility independent of the nuclear power plant. This standby power will represent 100% of nuclear power capacity.

The power generated by the diesel electric units is supplied at 4160/2400 volts, three phase, 60 cycles on a four-wire system. The nuclear plant switch gear and instrumentation are designed to receive and tie-in the standby power to the station bus.

1.6 Building Structures and Foundations

The design of the plant includes foundation requirement information as shown by the drawings included at the end of this section. The drawings also provide information to permit enclosure cost estimation. The buildings, structures, and foundations for support and enclosure will be supplied by others.

2.0 Design Philosophy

The plant design incorporates the maximum degree of reliability, simplicity, minimum maintenance and cost, within the scope of the design requirements stated heretofore.

2.1 Reliability

Due to the remote application and inaccessibility of the Site the proposed design incorporates the use of proven components wherever possible. In those areas where new components are required all of our past experience plus sound engineering judgment has been utilized to select or design the new components.

2.1.1 Fuel Elements and Control Rods

The successful operation of the APPR-1 fuel elements and control rods permit us to offer a proven core for the reactor. As such, development of such a core is not required. We are, therefore, offering a proven core which will permit us to meet the fabrication, erection and testing schedule as required and in addition the highest degree of operating reliability.

2.1.2 Primary System Components

The primary system design is an improved design based on the successful APPR-1 unit. As a result the systems and components utilize proven techniques and in addition will reflect the high degree of reliability of the APPR-1 both in engineering and the fabrication.

2.1.3 Closed Systems

Since minimum makeup water is available at the Site and no water is available for cooling the turbine exhaust steam the complete plant will be made up of closed water and coolant systems.

2.1.3.1 Vapor Containment

This system due to the potential hazards of radioactive corrosion products in the coolant, and the high quality of water required is a completely closed system. Primary system arrangement without vapor containment is shown on drawing R9-43-1005.

2.1.3.2 Heating System

Due to the high quality water desired in the secondary system the supplying of bleed steam for heating load directly from the cycle would require considerable water treatment of the heating system return drains. To eliminate the necessity of this water treatment and its high cost, the use of an evaporator reboiler was selected.

2.1.3.3 Auxiliary Cooling System

All auxiliary cooling systems throughout the plant will be closed systems.

As a result of this approach, the amount of make-up to this plant will be small.

2.1.4 Condenser System

Consideration was given to the use of a direct air cooled condenser to remove the latent heat from the turbine exhaust steam and as an alternative the use of an intermediate glycol loop between a surface condenser and an air blast cooler.

Investigation into the two types of cooling systems indicated that the direct air cooled surface condenser has three major problem areas.

- (1) Minimum experience to date.
- (2) Experience shows that tempering of air to prevent freezing of the condensate in the tubes is an unreliable method.
- (3) In the case of plant shutdown the unit should be immediately drained to prevent freezing.

On the basis of the Site conditions for this plant and anticipating a continual rotation of personnel on approximately a nine month basis, it was determined that the glycol intermediate loop arrangement would provide the highest degree of reliability, although it would result in a lower overall station thermal efficiency. With the continual changing of personnel it is rather obvious that the possibility of the direct air blast cooler being neglected during an emergency shutdown could freeze and damage the condenser. The result of this would prevent the startup of the plant until repairs could be made. Should such an emergency exist with the glycol intermediate loop arrangements no trouble would be anticipated since draining the system will not be necessary.

2.1.5 Duplication of Rotating Equipment

In order to maintain the continuity in operation all pumps in the secondary system whose failure would cause shutdown are duplicated. This in itself permits reliable performance of the plant while repairs are made.

2.1.6 Instrumentation

Due to the site conditions the use of air for any purpose where instruments are concerned is determined undesirable. Therefore, all instrumentation is either entirely mechanical or electrical.

To permit minimum operating personnel all plant parameters directly effecting plant operation are indicated on the console together with the controls for such items as pumps and rod drives while all variables which affect plant safety are annunciated.

All other instrumentation and controls are local in order to insure visual inspection of equipment when instrumentation information is required or control functions are to be performed.

2.1.7 Testing

To insure performance the testing of components by the manufacturer wherever practical will be done. In addition a complete plant will be assembled and a non-nuclear performance test will be run. Upon completion of this test connecting piping and wiring will be dis-assembled and units prepared for shipment.

2.1.8 Primary System Components

The steam generator design is of the horizontal evaporator type to comply with shipping dimensional limitations on the primary skid. The design takes into consideration maintenance features such that tubes can be plugged if necessary and is readily accessible to do this. This design will produce steam of 98% purity delivering dry and saturated steam to the turbine generator through a moisture separator just before the turbine generator.

This type of steam generator presents no difficult fabrication problems and can be manufactured in a minimum of time.

A natural convection cooling loop has been provided in the primary system for the removal of heat generated in the core after shutdown following complete loss of electrical power.

The primary coolant pump is of a canned rotor pump with flanged connections for ease of maintenance and shipping purposes. This type of pump has proved to be reliable and given satisfactory service in APFR-1.

The primary system is made up of two skids which are shipped as individual sections along with the primary shield rings. The skid bases are flanged and doweled for field assembly with minimum of time and labor. Refer to Drawing R9-43-1004.

Vapor containment is provided for this design and is a shop fabricated cylindrical vessel made up in sections to meet air transportability requirements.

2.1.3 Secondary System Components

The secondary system is provided in packaged and preassembled units and include the following packages:

- Turbine generator package
- Condenser Package
- Switchgear Packages
- Feedwater Package
- Heat Exchanger Package
- Air Blast Cooler Packages
- Interconnecting Piping
- Interconnecting Wiring

Refer to package drawings.

A single turbine generator set and secondary system is provided because a single turbine generator which meets the power requirements will result in a minimum plant cost, a minimum number of packages and interconnecting piping which must be shipped to a plant site and a minimum amount of erection time and labor for the plant. The overall plant efficiency will be improved and auxiliary power requirements are a minimum as a result of going to the single secondary system.

The turbine generator is rated at 2000 KW at .8 power factor and operation at 8 in. Hg exhaust pressure. A maximum of 2250 KW can be obtained with 3 inch exhaust pressure with 450 psig steam delivered to the turbine.

At the 3 inch turbine exhaust the condenser flow will be the same as at the 8 inch exhaust condition.

With the reduced back pressure of 3 inches the condenser cooling inlet and outlet temperatures will be approximately 100°F and 63°F respectively with the inlet air to the air blast coolers at -10°F.

The 2000 KW turbine generator requires shipment in two sections. One of which is the turbine and gear on its base and the other being the generator on its base.

Turbine generators as provided in this design with split bases which are flanged and doweled in the field are not out of the ordinary and no problem is anticipated during field erection.

Alignment is made in the manufacturer's plant before testing and shipment. This alignment requires approximately 4-6 hours.

In the field, the two sections would be installed on the foundation pad. The two base plates will be aligned and leveled and bolts and dowels inserted in the base plates. Alignment couplings would be checked and corrected if necessary. Following this, normal alignment procedures are followed which would require less time than that followed in the shop.

2.1.10 Packaging

Design of the complete plant and the organization of all components have been directed in such a manner that the minimum number of packages will be utilized and meet the air transportability requirements as well as reduction in erection time desired.

2.1.11 Steam Cycle

Careful consideration has been given to the primary and secondary conditions based on physical size, thermal efficiency, auxiliary load requirement, development, required costs and reliability.

2.1.12 Components

Due to the short delivery schedule and high reliability required, the use of standard equipment which has been manufactured and operated successfully is used.

2.1.13 Vapor containment

The arrangement of the primary system is such that a small high pressure vapor container can be utilized. In order to meet air transportability requirements, field erection is required for the vapor container.

2.1.14 Spent Fuel Storage

Since the spent fuel must cool for a period of time prior to shipment the storage pit will be a distance from the vapor container to permit access for shipment of fuel without shutting down the plant.

2.1.15 The plant is designed to meet what is understood by Alco to be the presently acceptable hazards requirements of pressurized water nuclear power plants so that no delay in approval of such requirements is expected. In addition, all necessary radiation monitoring devices for the safety of the performance is incorporated.

2.1.16 Consideration of Installation Under Snow

2.1.16.1 Layout Approach

The layout of the component packages will be such that the minimum piping and wiring runs are installed without sacrificing ease of operation and minimum operating crew.

2.1.16.2 Enclosures.

The enclosures for the component packages will be supplied by others, however, estimated heat losses are given herein.

2.1.17 Ventilation

The ventilation of the component packages and pipe enclosures to prevent heating of snow tunnels and freezing of lines during shutdown will be supplied by others.

3.0 Plant Arrangement

3.1 Description

The plant is designed for the placement of all component packages and interconnecting piping and wiring in snow tunnels below the surface of the snow. All packages will be placed in tunnels approximately 24 feet wide and 24 feet deep. The tunnels will be covered with arched plates and a minimum of snow backfill. Piping and wire-way tunnels between certain packages will be approximately 6 feet wide by 10 feet high and at suitable elevations above the main tunnel floor to give convenient access between main tunnels. Where freezing of interconnecting pipe runs could take place during shutdown others will provide heated enclosures. The foundations for the component packages will consist of hollow metal piles driven into the floor of the tunnels to a depth of approximately 30 feet. The number and location of the piles is dependent on the weight distribution of the package skids, and the arrangement of the piles is shown on drawing No. MQ2S6. The enclosures for the component packages will consist of insulated panels and roofs to protect and enclose the operating equipment. The enclosures and the space between the enclosures and the tunnel walls will require ventilation to remove the heat losses from the equipment and piping. The design of the enclosures and the ventilation requirements are not a part of this design analysis, but will be furnished by others. The anticipated differential settlement between packages is in the order of 0.1 to 0.2 inch per year.

The piping is designed to accept this differential settlement by the use of expansion joints and swivel type of fittings, as required by the particular service of the different pipe lines and by the change in direction and bends to provide sufficient flexibility as in the case of the high pressure and temperature in the steam and feed water piping. The settlement between packages, will be adjusted if required by jacking devices supplied by others placed between the pile caps and the underside of the skid supports, to maintain not more than 1

inch differential settlement between packages. Electrical wiring in cable trays is inherently flexible, and no special provision for differential settlement is required. Piping between packages which must pass through the cold branch tunnels will be grouped, generally, in two levels, to permit compactness in overall space requirements, they are to be insulated and enclosed in insulated panels forming a duct, through which heated air, can be delivered to prevent freezing during shutdown periods. During operation, heat from the hot lines will protect the adjacent unheated lines.

3.2 Location of Packages

The physical arrangement of the component packages was based on the following considerations: first; maximum safety to operators and equipment, second; greatest convenience to the plant operators, and third; the most direct routing of the principle piping and electrical systems. The principle equipment packages; namely, the primary containment vessel, the turbine generator, the condenser, the heat exchanger skid, and one unit of the air blast cooler, are arranged along the major axis of the plant. The primary system vapor container is in a tunnel at one end of the plant and separated from the secondary system by 25 ft. of undisturbed snow which acts as a radiation shield. Refer to Dwg. MO2M1.

The waste storage tank is located in a snow tunnel perpendicular to the vapor container with access provided from the vapor container tunnel and also from the tunnel containing the switchgear skid.

A spent fuel tank outside of the vapor container is provided to store spent fuel elements and is located in a separate tunnel perpendicular to the vapor container tunnel. Spent fuel elements will be moved by means of transfer casks from the reactor vessel to the spent fuel tank where they may be installed in a spent fuel shipping cask.

The spent fuel elements can be removed and transferred to the spent fuel tank during plant shutdown and refueling. After cool-down in the spent fuel tank they can be put in the spent fuel shipping cask without shutting the plant down.

The turbine, condenser, and heat exchanger skids are arranged with their long axis on a common centerline for the most direct connection of their interconnecting piping. The turbine is at the end nearest the primary package for the shortest routing of the main steam piping. The air blast cooler capacity requires that this equipment be divided into three units for shipping reasons. One section of the air blast cooler is located on the major axis beyond the heat exchanger package, and the other two sections of the air blast cooler are located in separate tunnels perpendicular to the main tunnel and located one on each side of the main tunnel near the heat exchanger package. This arrangement shortens the large size glycol solution piping since the main circulating pumps are on the heat exchanger skid and are connected to the main condenser on the adjacent condenser skid.

The arrangement of the air blast coolers in separate tunnels improves the dependability of the plant; that is, in the event of one snow tunnel around an air blast cooler collapsing, then operation can be continued on the other two sections at somewhat reduced capacity while repairs are being made. Thus, the collapse of a snow tunnel will not shut down the plant as might be the case if all coolers were placed in a single tunnel. The feed water package and the switchgear packages are placed in two separate snow tunnels perpendicular to and on opposite sides of the main tunnel. The feedwater package is placed conveniently for the branch piping from the turbine and condenser, and also arranged to permit direct connections by branch tunnels of the piping between the feed water package and the primary equipment in the vapor container. The switchgear packages are placed in line with the generator for the shortest and most direct connection of the generator leads to the enclosed switchgear, and to simplify the arrangement of the low voltage power and control wiring between the motor control center, the instrument panel, and the various packages.

4.0 Operating Data, Weight and Dimensional Data

4.1 Plant Performance

| | |
|---|---|
| Thermal power developed in reactor | 10 MW |
| Reactor Life | 8 MW years |
| Gross electrical power generated | 2000 KW |
| Electrical power required for auxiliaries | 315 KW |
| Net electrical power delivered with 8" Hg back pressure at turbine generator | 1685 KW |
| Net electrical power delivered with 3" Hg back pressure at turbine generator. | 1935 KW |
| Steam supplied for outside heating purposes | 1×10^6 BTU/hr (Net coincident with above values) |

4.2 Thermal Data of Reactor at Full Power

| | |
|----------------------------|-----------|
| Operating Pressure | 1750 psia |
| Design Pressure | 2000 psia |
| Coolant flow | 4219 gpm |
| Coolant inlet temperature | 500°F |
| Coolant outlet temperature | 518.6°F |

4.3 Steam Generator

| | |
|--------------------|-----------|
| <u>Tube Side</u> | |
| Operating Pressure | 1750 psia |
| Design Pressure | 2000 psia |
| Flow | 4219 gpm |
| Inlet Temperature | 518°F |
| Outlet Temperature | 500°F |

Shell Side

| | |
|--------------------|------------|
| Operating Pressure | 465 psia |
| Outlet Temperature | 463°F |
| Inlet Temperature | 306°F |
| Flow | 37055 #/hr |
| Blowdown | 400#/hr |

4.4 Pressurizer

| | |
|-----------------------|-----------|
| Operating Pressure | 1750 psia |
| Design Pressure | 2000 psia |
| Design Temperature | 650°F |
| Number of Heaters | 20 |
| Total heat output | 30 KW |
| Steam volume (cu.ft.) | 12.1 |
| Water volume (cu.ft.) | 5.9 |

4.5 Primary Coolant Pump

| | |
|---------------------|--------------|
| Type | Canned Rotor |
| Rated Flow | 4219 gpm |
| Operating Head | 42 ft. |
| Suction temperature | 500°F. |

4.6 Primary Coolant Piping

| | |
|------|-----------------------------------|
| Type | 304 Stainless steel, schedule 120 |
| Size | 10" Nom. |

4.7 Vapor Container

| | |
|-----------------------|----------------------------------|
| Design Pressure | 240 psi |
| Material | Carbon steel CR-212 to SA-300 |
| Operating Temperature | 120°F |

4.8 Core Design

| | |
|----------------------------|---|
| Configuration | 7 x 7 array - 3 elements in each corner missing |
| Equivalent diameter-in | 20.16 |
| Active Core height-in | 22 |
| Material content of core: | |
| U ²³⁵ - Kg | 18.49 |
| B ¹⁰ - gm | 16.66 |
| SS -kg | 172.10 |
| H ₂ O(68°F) -kg | 91.54 |

Stationary Fuel Element

| | |
|------------------------------------|-----------------|
| Type | APFR-1, Core II |
| Number of Elements | 32 |
| Plates/element | 18 |
| Active length-in | 22 |
| Clad thickness-in | 0.005 |
| Meat thickness | 0.020 |
| Meat Width | 2.500 |
| wt. U ²³⁵ /element - gm | 515.16 |
| wt. B ¹⁰ /element - gm | 0.464 |

Control Rod Fuel Elements

| | |
|--------------------|-----------------|
| Type | APFR-1, Core II |
| Number of Elements | 5 |
| Plates/element | 16 |
| Active length-in | 21-1/8 |

4.9 Shielding Design

Design Basis

| | |
|---|-----|
| Access after shutdown - hr | 8 |
| Dose in Control Console and Turbine Generator | 0.1 |
| Skid, 0.1 x tolerance - mr/hr | |

Primary Shield Type

Similar to APFR-1 (Concentric annuli of H₂O and steel. Steel ring clad on both sides with Boral. Inner surface of shield tank and outer surface of Pressure Vessel support ring clad with Boral)

| | |
|--------------------------------------|----------|
| Number of Steel Rings | 4 |
| Thickness -in | 3-1/4 |
| Boral clad; thickness-in | 1/8 |
| Water annuli; thickness-in | 1-1/4 |
| Dose rate 8 hr. after shutdown-mr/hr | 50 mr/hr |
| Dose rate during operation - R/hr | 247 |

Secondary Shield

| | |
|---|------|
| Type | Snow |
| Thickness -Ft. | 25 |
| Dose Rate on Surface; 0.1 x tolerance-mr/hr | 0.1 |

Core Shielding

| | |
|-----------------|-------|
| Type | Water |
| Shutdown - days | 1 |
| Thickness - Ft. | 11 |

| | |
|--|--------------------------|
| Dose Rate - mr/hr | 20 |
| Internal Flux Suppressor | |
| Material | Europium Oxide |
| Wt. of Eu/suppressor-gm | 1 |
| Length-in | 7/8 |
| thickness-in | 0.020 |
| width-in | 2.281 |
| Clad thickness -in | 0.005 |
| Meat thickness-- in | 0.020 |
| Meat width-in | 2.281 |
| wt. U^{235} /element .. gm | 401.12 |
| wt. B^{10} /element .. gm | 0.362 |
| Control Rod Absorbers | |
| Type | APFR-1, Core I: Low CoSS |
| B^{10} - gm | 56.4 |
| Absorber plates/Rod | 4 |
| Travel - in | 22 |
| Initial Reactivities - % | |
| Cold (68°F) - no xenon | 14.11 |
| Hot (512°F)-no xenon | 7.65 |
| Hot (512°F)-equilibrium xenon | 5.15 |
| Initial Bank Position - inches from bottom | |
| Cold (68°F) - no xenon | 5.0 |
| Hot (512°F) - no xenon | 9.7 |
| Hot (512°F) - equilibrium xenon | 11.6 |
| Power - Peak to Average | |
| Hot (512°F) - no xenon | |
| 0-MWYR | |
| Radial (center) | 1.46 |
| Axial (center) | 1.65 |
| 8-MWYR | |
| Radial (center) | 1.55 |
| Axial (center) | 1.47 |
| Average Thermal Flux-neutrons/cm ² -sec | |
| 0 MWYR | 1.67×10^{13} |
| 8 MWYR | 2.33×10^{13} |
| Expected Total Energy Release - MWYR | 10 |
| Burnup : 10 MWYR | |
| Average Fuel - % | 26 |
| Maximum Fuel - % | 49 |
| Maximum Control Rod-% | 27 |
| Temperature Coefficient | |
| Cold (68°F) - °F ⁻¹ | -0.22×10^{-4} |
| Hot (512°F) - °F ⁻¹ | -3.4×10^{-4} |

| | | |
|--|-----|---------------------------------------|
| Pressure Coefficient | | |
| Hot (512°F, 1750 psia) - psi ⁻¹ | | 43.1 x 10 ⁻⁶ |
| Control Rod Worth | | |
| Five Rod Bank | | |
| Cold (68°F) - % | | 19.9 |
| Hot (512 F) - % | | 19.5 |
| Center Rod | | |
| Cold (68 F) - % | | 4.5 |
| Hot (512°F) - % | | 4.0 |
| Spent Fuel Transfer Casks | | |
| Thickness -in | | |
| Single element cask | | 10.1 |
| Four element cask | | 10.5 |
| Dose Rate on Surface of Cask - mr/hr | | 200 |
| Spent Fuel Shipping Cask | | |
| Elements/cask | | 6 |
| Weight - Tons | | 10 |
| Thickness - in | | 10.5 |
| Dose Rate one meter from source -- mr/hr | | 10 |
| Demineralizer Shielding | | |
| Type | | APFR-1 |
| Shielding Material | | Lead |
| Thickness (Radial) -in | | 3-11/16 |
| Thickness (Axial) -in | | 3-3/16 |
| Dose Rate | | |
| Surface of Shield - mr/ hr | | 70 |
| One meter from source - mr/hr | | 10 |
| Waste Tank | | |
| Active Source | | Primary coolant Normal Plant Waste |
| Shield Thickness - in | | |
| Steel (= 7.9) | | 0.6 |
| Concrete (= 2.4) | | 1.32 |
| Water (= 1.0) | | 2.52 |
| Snow (= 0.495) | | 6.6 |
| Dose rate on surface of shield - mr/hr | | 500 |
| (Dose Rate on surface of APFR-1 | | |
| (waste tank with Normal Plant Waste only- mr/hr 20) | | |
| Gamma Heating in Snow | | |
| Surface of snow - Btu/Ft ³ - hr | | 0.14 |
| | R-3 | |

4.10 Thermal Design

| | |
|--|-------------------------|
| Type of flow | Uniform |
| Inlet Temperature - °F | 500°F |
| Outlet Temperature - °F | 517.6 |
| Maximum plate surface temperature - °F | 610. |
| Flow per fixed fuel element - gpm | 98.5 |
| Flow per control rod fuel element - gpm | 94.5 |
| Lattice flow - gpm | 595 |
| Total core flow - gpm | 4219 |
| Fixed Fuel Element - Btu/hr-Ft ² | |
| Maximum operating heat flux | 1.772 x 10 ⁵ |
| Burnout heat flux | 1.263 x 10 |
| Maximum ratio of operating to burnout heat flux | 0.1489 |
| Control rod Fuel Element-Btu/hr-Ft ² | |
| Maximum operating heat flux | 1.78 x 10 ⁵ |
| Burnout heat flux | 1.282 x 10 |
| Maximum ratio of operating to burnout heat flux | 0.1474 |
| Maximum internal plate temperature - °F | 632.3 |
| Ratio of peak to average power | 2.46 |
| Maximum stress in fuel elements - psi | 22,490 |
| Temperature difference across reactor vessel wall - °F | 46.9 |
| Thermal stress in reactor vessel - psi | 6800 |
| Thermal stress in thermal shield - psi | 62,000 |
| Thermal stress in vessel flange - psi | 7,470 |
| Thermal stress in outlet integral nozzle-psi | 5,390 |
| Allowable thermal stress in vessel, flange, and nozzle - psi | 8,750 |
| Total core pressure drops = control rod pressure drop - FT of H ₂ O | 5.07 |
| Pressure drop through fixed elements - FT of H ₂ O | 2.37 |
| Required fixed element orificing -FT of H ₂ O | 2.70 |
| Maximum pressure differential between fuel plates and lattice - psi | 0.03 |
| Maximum allowable pressure differential between fuel plates and lattice - psi | 3.0 |

4.11 Weight and Dimensional Data of Major Items

| | |
|------------------------|-----------------------------------|
| Turbine Generator | |
| Dimensions installed | 26'-3" x 9'-1" x 6'-4" High |
| Shipping Dimensions | |
| Turbine, gear and base | 15'-10" x 8'-10" x 5'-11" High |
| Generator and base | 13'-8" x 8'-10" x 6'-4" High |

| | |
|------------------------|--------------------------------|
| Total Weight Installed | 69000 lbs |
| Turbine, gear and base | 30000 lbs |
| Generator and base | 30000 lbs |
| Auxiliaries | 90000 lbs |
| Condenser Package | |
| Dimensions | 24'-3"x8'-4-1/2"x 9'-0"High |
| Weight | 28250 lbs |
| Feedwater Package | |
| Dimensions | 27'-9"x9'-0" x9'-0"High |
| Weight | 28900 lbs |
| Heat Exchanger Package | |
| Dimensions | 26'-9" x9'-0"x8'-10" High |
| Weight | 23250 lbs |
| Air Blast Coolers | |
| Number Required | |
| Dimensions ea. | 30'-0" x9'-0"x9'-0" High |
| Weight ea. | 25200 lbs. |
| Switchgear Packages | |
| Control Panel Section | |
| Dimensions | 29'-8"x9'-0"x9'-0"High |
| Weight | 25300 lbs |
| Switchgear Section | |
| Dimensions | 14'-7"x9'-0"x9'-0"High |
| Weight | 23000 lbs |
| Primary Package | |
| Reactor Skid Section | |
| Dimensions | 12'-2-1/2"x9'-0"x9'-0" High |
| Weight | 28388 lbs |

| | |
|---|----------------------------|
| Steam Generator Skid Section | |
| Dimension | 11'-8-1/2"x9'-0"x9'-0"High |
| Weight | 29343 lbs |
| Primary Shield Rings | 29000 lbs |
| Vapor Container | |
| Total weight, installed | 83400 lbs |
| Dimensions installed | 13' Dia. x 43'-5" lg. |
| As shipped condition | |
| Shell | 8 pcs |
| Heads | 4 pcs |
| Upper Shield Tank | 1 pc |
| Spent Fuel Tank | |
| Total weight, installed | 10000 lbs |
| Dimensions, installed | 12' Dia. x 20' High |
| Waste Storage Tank | |
| Weight | 7100 lbs |
| Dimensions | 7' Dia x 18' long |
| Fuel Transfer Conveyor | |
| Weight | 26,500 lbs |
| Spent Fuel Cask | |
| Shipping Casks 7 ea. | 17,800 lbs |
| Transfer Casks 2 ea. | 8,000 lbs |
| Interconnecting Piping | |
| Weight | 60,000 lbs |
| Shipping Packages | 3 |
| Interconnecting Wiring | |
| Weight | 12,000 lbs |
| Chemistry and Health | |
| Physics Packaged Lab. | 8,000 |
| Total Estimated Number of Packages (excluding Spent fuel Casks) | 23 |

Total Estimated Weight of
Equipment to be shipped

575,600 lbs.

5.0 Ethylene Glycol Diversion and Steam Extraction for Additional Heat

5.1 Ethylene Glycol Diversion Provisions

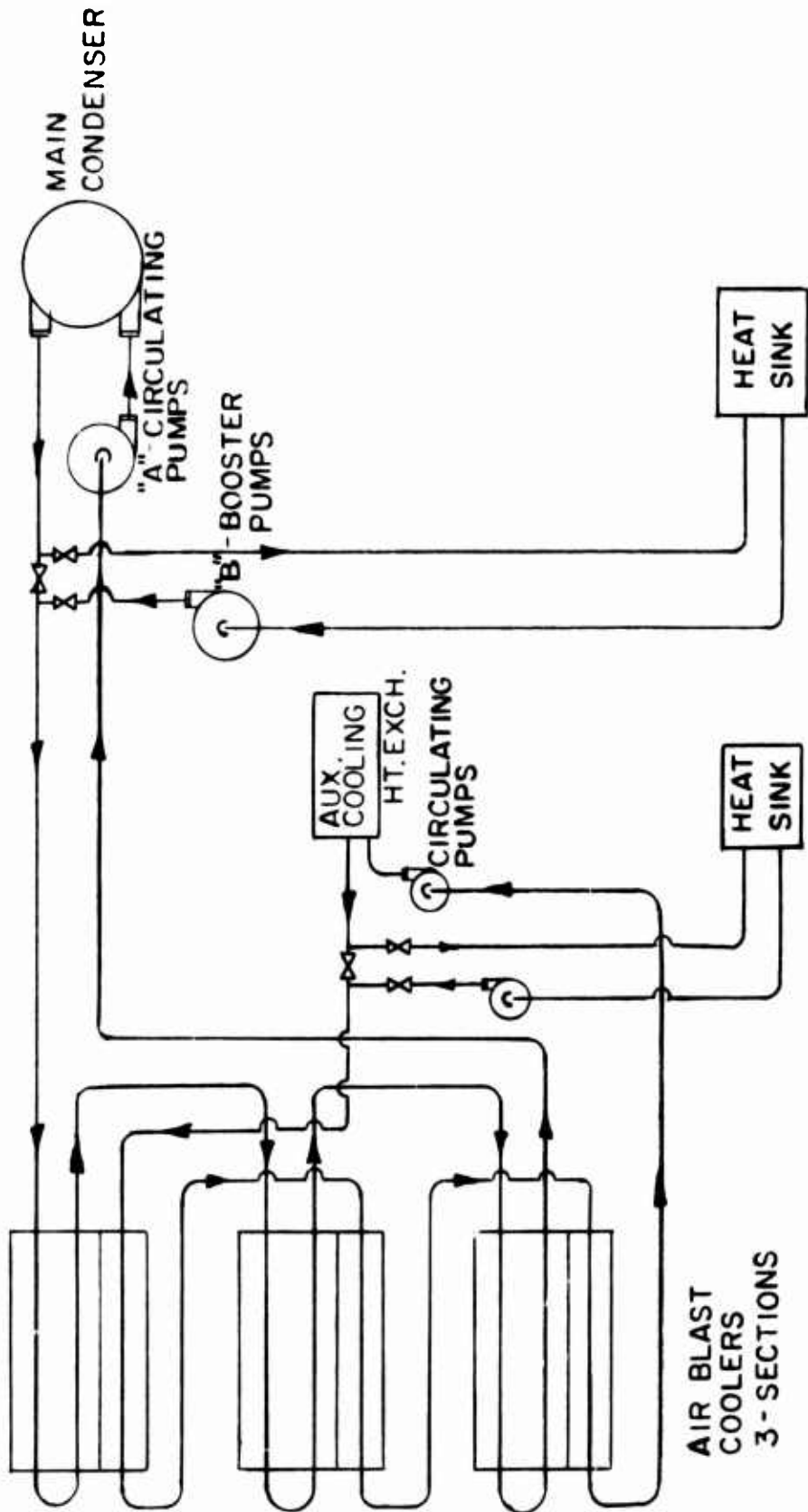
Insulated tees and valves are provided in the design of the ethylene glycol loop to permit diversion to another heat sink. However, the location of the tees and valves would have to be changed from those shown on drawing MO2M1 to permit return of the glycol from this heat sink to a point in the system that will allow additional cooling, if required, before entry into the condenser. This is shown schematically on the attached sketch AES-277. This arrangement, of course, presumes that the alternate heat sink is a closed circuit heat exchanger, the type of which is unknown at the present time. It must be pointed out that the circulating pumps and their motors marked "A", as presently designed, are sized to circulate the glycol solution through the main condenser, the air blast coolers, and their inter-connecting piping only. The diversion of the glycol solution to the alternate heat sink would in all probability increase the pumping head on the circulating pumps, because of the increased length of inter-connecting piping, and possibly a greater pressure drop through the heat sink, than through the air blast coolers. Therefore, either booster pumps at "B" would be required, or the present pumps and their motors at "A" would have to be reselected for the greater head required. With higher head pumps at "A", under normal operation with the air blast coolers, the excess head would require throttling to reduce the flow, with resultant operation at low pumping efficiency and excessive pumping horsepower.

The air blast coolers as designed, place a section of auxiliary cooling surface on each cooler package, requiring two one-pass series arrangements, as indicated on one for the main condenser circuit the other for the auxiliary cooling circuit.

5.2 Steam Extraction from Main Steam Header for Additional Heat

Included in this design are the necessary reducing valves, isolation and by-pass valves and fittings, not inter-connecting piping, for supplying the government furnished closed heat exchanger with steam from the main steam line after the dryer; the drain from the heat exchanger being returned directly to the main condenser.

Assuming a constant 10 megawatt reactor load and a constant condenser backpressure of 8 inches of mercury, the curve MO2G2 shows the predicted diversion for any given gross or net generation. With the turbine operating and holding its own auxiliaries, approximately 25,000 pounds of steam per hour could be diverted to the heat exchanger. There would, of course, be no electrical power for the base at that time.



ETHYLENE GLYCOL DIVERSION
R-21

ALCO
ALCO PRODUCTS, INC.
ATOMIC ENERGY DEPT.
SCHENECTADY, N. Y., U. S. A.

AES-277

As this system is envisioned, there are several limitations that should be considered:

1. It would not be advisable to divert more than 60 percent to 70 percent of the steam to the heat exchanger for any extended period of time without special design of the equipment, due to the poor deaeration that could be expected at loads below this point and consequent possibility of corrosion.

2. It is expected that the load to the heat exchanger would be relatively constant while operating, and the load on the generator could be manually adjusted to maintain the 10 megawatt reactor output. If this is not true, the turbine could be base loaded at some point where the total steam flow would not exceed the reactor capacity, or a pressure control added to the turbine to maintain a constant inlet steam pressure, which is a function of the reactor load.

While it is shown on the curve that the maximum steam that could be diverted would be 31,500 pounds per hour when the turbine is not operating, there is an even more serious deaeration problem should this be attempted, and it would be necessary to supply approximately 200 kilowatts auxiliary power to the plant at this time.

7.0 Plan for Installation of the Plant at a Site

The installation plan which is herein outlined assumes that all snow trenches will have been dug by the Government and supporting piers and foundations for modules are installed by the Government.

In order to expedite the installation of the turbine generator, condenser heat exchanger and air blast cooler modules (refer to Drawing MO2M11) it would be desirable to have the foundation pad for these modules in the main tunnel, installed as one continuous structure or with bridging between foundations such that the turbine generator can be skidded from the transporting sled on to the foundation and then skidded along the foundation pad to its installed position at the end of the tunnel. This same procedure would be used for the condenser, heat exchanger and air blast cooler modules.

This procedure will allow these modules to be installed in a minimum of time without having to wait for supporting piers and foundations to be installed before the individual modules can be installed in the main tunnel.

In order to utilize the installation crew to the maximum effort, it will be necessary to have sufficient hauling equipment and crews to install at least three modules simultaneously.

The sequence of module installation will be as follows so that alignment, pipe fitting, electrical and other personnel can proceed immediately after installation on their phase of the work.

1. Three hauling and rigging crews will install simultaneously the turbine generator module, feedwater and switch gear modules. Immediately after installation the turbine generator sections will be leveled, aligned and fastened together after which alignment of couplings and final alignment can be followed through.
2. The condenser, heat exchanger and air blast cooler modules in the main tunnel will be hauled into position immediately after the turbine generator sections have been set in position. The hauling and rigging crew which installed the turbine generator will be utilized for these modules.
3. The hauling and rigging crew which installed the feedwater package will then bring in the air blast cooler package in the side tunnel.
4. The third air blast cooler in the other side tunnel will be installed by the rigging crew which installed the switchgear packages.
5. After completing their work in (3) above this rigging crew will begin the assembly of the vapor container.
6. The installation of module inclosures can be initiated after the modules are installed in position. After final placing of secondary packages the exhaust stacks for the air blast coolers can be installed. It is assumed that the trenches for the air blast coolers will be left open; that is without roofs, until the exhaust stacks have been set in place.

This can be done with a mobile crane having at least a 40 ft. beam. If a mobile crane is not available, this can be performed with a gin-pole rig constructed of timbers. After the exhaust stacks are placed then the enclosing sheet metal housing can be placed with the same lifting rig and the roof construction can be completed.

7. The installation of prefabricated piping, wiring and necessary supports and enclosures for secondary system piping can be initiated after Step 1 and during Step 2 above.
8. The vapor container erection procedures are listed below. In order to handle, ship and erect the vapor container at a remote site, it will be necessary to fabricate the vessel so that shipping limitations are met for air transport regarding weight and size of packages. Total weight of the vapor container is 83,400#.

To meet the shipping requirements the vessel will be fabricated in 12 pieces and each piece clearly match-marked for each of erection and weights clearly shown on each piece. All pieces have weld bevels and bolted angle clips for fitup and erection before welding. The

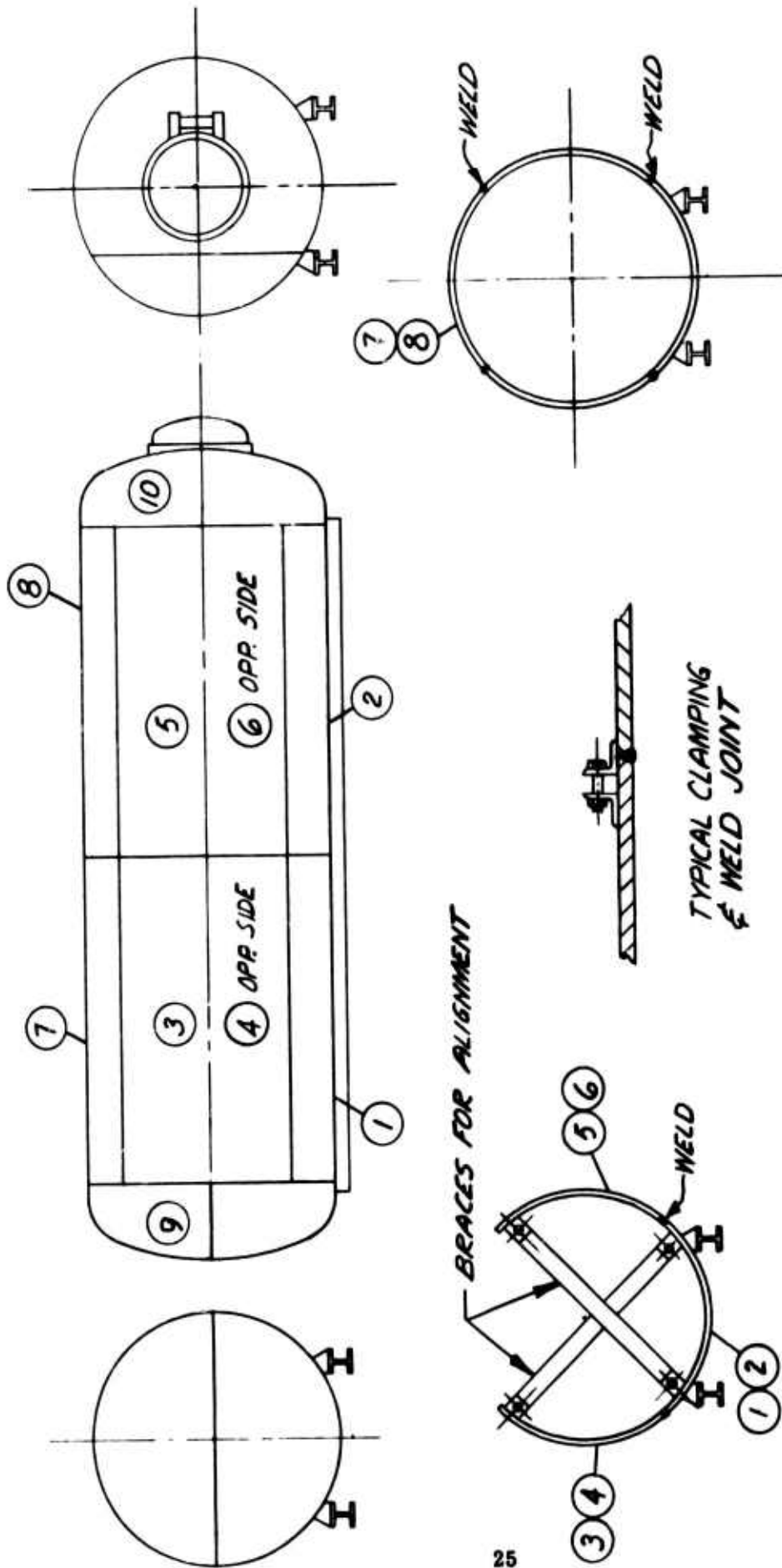
lower 100° segment pieces will be shipped with I-beam supports for ease of erection. The top segment will be a 90° piece and the two intermediate segments will be 85° pieces. The two elliptical heads will be shipped in two pieces each.

A cat crane of 15 ton capacity or some other lifting rig of equal capacity will be required to erect the vapor container pieces and can be utilized in handling other components of the plant during erection.

Vapor Container Erection Procedure (Refer to AES-267, Vapor Container Field Erection Procedure)

- a. Piece #1 will be rolled into place on base.
- b. Piece #2 will be rolled into place and butted to Piece #1.
- c. Align the above pieces, secure to base and bolt sections together.
- d. Pieces #3 and #4 opposite side will be installed using guide clips for fitting and aligning and angle supports must be used to retain pieces in place. Bolt sections together using angle clips as shown on Sketch #AES-267,
- e. Pieces #5 and #6 opposite side will be installed using same procedure as in Item #4 above.
- f. The two parts of the access head will be welded together before installing on V.C. and the same will be done with the rear elliptical head.
- g. The top 90° section of V.C. will be installed and secured for welding.
- h. Rear elliptical head will be installed, fitted and secured for welding.
- i. Access head will be installed, fitted and secured.
- j. Vessel shall be welded in accordance with ASME Code for Unfired Pressure vessels.
- k. All welds shall be 100% radiographed.
- l. A helium leak test will be placed on vessel in accordance with test procedures and will be done after primary module installation in the vapor container has been completed.

After the vapor container erection has been completed with the exception of the one elliptical head for module entry, the primary system package sections will be installed. The steam generator skid



VAPOR CONTAINER
 FIELD ERECTION PROCEDURE
 AES-267

section will be skidded into position into the vapor container first. The reactor skid section with the primary shield rings installed in the shield tank will then be pulled into the vapor container. The bases of each section will be fastened and piping assembled at the flanged joints.

The upper shield tank will be installed on the vapor container and elliptical entry head welded into position to complete the vapor container structure.

9. Piping and wiring between the primary and secondary systems can be installed after the vapor container is completed. At this time, all piping and wiring inside the vapor container leading to penetrations on the elliptical head can be completed.
10. After completing the rigging work on the vapor container, the installation of the waste storage tank, spent fuel tank and spent conveying system can be done.

Erection Man Hours, Time, Equipment and Materials Required

It is estimated that approximately 10486 man hours will be required for the installation of the plant. On the basis of using a total of 34 men as a minimum for the installation crew, 291 hours will be required for plant erection. Assuming a 10 hour day, 6 day work week for the installation of this plant the total installation time will be approximately 5 weeks which will meet the specified installation time of 6 weeks maximum.

A breakdown of equipment and material required for installation of the plant is as follows:

| | |
|--|-------------|
| Equipment required for erection of plant at the site | |
| Erection equipment required for primary and secondary system | |
| 4 - 300 amp. welding machines | Full period |
| 1 - Air compressor 315 CFM | " " |
| 1 - Air hoist | " " |
| 1 - 15 KW portable light plant | " " |
| 1 - 1/2" to 2" pipe machine | " " |
| 1 - D-4 Cat w/winch & dosn. | " " |
| 2 - 2-ton chain hoists | |
| 1 - 1-ton chain hoist | |
| Misc. tools, jacks | |
| Misc. Lumber (Cribbing) | |
| Cat. Crane 15-Ton capacity | 1 month |
| Misc. Angle 2", 3", 4" radom to 20'-0" | |
| Torches and burning equipment | |
| Trades and hours required for erection of plant at the site | |

ERECTION PLANT MODULES - BREAKDOWN

| | <u>Riggers</u> | <u>Pipe-fitters</u> | <u>Elect.</u> | <u>Insulators & Laborers</u> | <u>Hoisting Engr.</u> | <u>Millwright</u> | <u>Total M.H.</u> |
|---------------------------------|----------------|---------------------|---------------|----------------------------------|-----------------------|-------------------|-------------------|
| 3 - Air blast coolers | 450 | 432 | 96 | 240 | 128 | 112 | 1458 |
| Turbo-Generator module | 320 | 384 | 240 | 240 | 64 | 160 | 1408 |
| Condenser Module | 192 | 376 | 240 | 240 | 32 | 48 | 1128 |
| Heat exchanger module | 192 | 384 | 240 | 240 | 32 | 48 | 1136 |
| Feedwater Module | 192 | 504 | 256 | 240 | 32 | 48 | 1272 |
| Switchgear Module | 228 | | 384 | 240 | 64 | 72 | 988 |
| Primary System Module & V.C. | 750 | 520 | 408 | 240 | 128 | 112 | 2158 |
| Spent Fuel Pit & Hot Waste Tank | 128 | 144 | 64 | 240 | 64 | 48 | 688 |
| Miscellaneous | | | | | | | 250 |
| | <u>2452</u> | <u>2744</u> | <u>1928</u> | <u>1920</u> | <u>544</u> | <u>648</u> | <u>10,486</u> |

| | <u>M.H.</u> |
|--|-------------|
| 2 - Millrights | 648 |
| 8 - Riggers | 2452 |
| 10 - Pipefitters (4 welding pipefitters) | 2744 |
| 6 - Electricians | 1928 |
| 6 - Laborers | 1920 |
| 2 - Hoisting engineers | <u>544</u> |
| <u>34 Men Total</u> | 10,486 |

A breakdown by trades and hours which will be required for installation is tabulated on the following page.

8.0 Plan of operation of the installed plant including number and qualifications of the operating personnel required

The following personnel are estimated as being required for the operation of the installed plant.

| | |
|---|--------|
| 1. Plant Superintendent | 1 each |
| 2. Shift Engineers (Plant Superintendent will handle day shift) | 3 each |
| 3. Operator (Reactor Console) | 4 each |
| 4. Mechanic | 1 each |
| 5. Instrument Technician | 1 each |
| 6. Process Control (Health Physics and Chemistry) | 1 each |
| 7. Power Plant Electrician | 1 each |

The above will comprise the complete operating crew and should be set up by shifts as tabulated below:

| <u>Shift #1</u> | <u>Shift #2</u> | <u>Shift #3</u> | <u>#4 Relief</u> |
|--|------------------|------------------|------------------|
| Plant Supt.--Shift Engr. | Shift Engineer | Shift Engineer | Shift Engineer |
| Operator (Reactor) | Operator | Operator | Operator |
| Turbine Operator | Turbine Operator | Turbine Operator | Turbine Operator |
| Instrument Technician | -- | -- | -- |
| Process Control (Health Phy. & Chem.) | -- | -- | -- |
| Power Plant Electrician | -- | -- | -- |
| Mechanic | -- | -- | -- |

The duties of each of the members of the operating crew are tabulated below:

| <u>Personnel</u> | <u>Duties</u> |
|----------------------|---|
| Plant Superintendent | Overall plant responsibility |
| Shift Engineers | Supervision of Shift personnel and plant operation |
| Operators (Reactor) | Console Operator - under shift engineer |
| Turbine Operator | Responsible for turbine and misc. turbine equipment operation |

Personnel

Duties

| | |
|--|--|
| Instrument Technician | Responsible for Inst. Control and on call status |
| Process Control (Health Phy. & Chem.) | Responsible for Health Physics and Water Chem. and on-call status |
| Power Plant Electrician | Responsible for all power plant electrical equip- ment and on-call status |
| Mechanic | Responsible for maintenance of all mechanical equipment. |

While it is perfectly possible for two men to operate the plant under normal conditions which should prevail the bulk of the time, we would recommend that three men be on duty at all times; namely, shift engineer, console operator, and roving operator. The shift supervisor would be able to relieve either of the others and be available to act and assist during periods of emergency operation. During the day when trained maintenance people and the plant superintendent are around, this third man might not be necessary.

The shift supervisor should be more experienced than the control operator, but both should be well trained in the operation of the equipment involved. Both should be capable of rapid interpretation of data and capable of making decisions under emergency stress.

The roving operator need not be so highly skilled, but should understand the equipment and carry out such tasks as regeneration and checking of demineralizer, operate the oil purifier, and operate the valves and equipment. He should be capable of being trained for control operator.

The qualifications of the operating personnel are listed as follows:

| Personnel | Qualifications |
|----------------------------|--|
| Plant Superintendent | Mechanical and Nuclear Engineering |
| Shift Engineers (4) | Power Plant and Nuclear Plant Training |
| Electrical Supervisor | Electrical Engineering |
| Instrument Supervisor | Electrical, Electronic or Mechanical Engineering |
| Electrical Technicians (2) | Electronics and Electrical Training |
| Instrument Technicians (2) | Electronics and Electrical Training |
| Process Control | Health Physics and Chemical Engineering |

9.0 Plant Relocation Following Extended Power Operation

The relocation of the plant can be accomplished without severe difficulty as far as the secondary system is concerned. The primary system will require special equipment and handling procedures for the relocation.

In order to relocate the primary system as proposed; either of two types of sleds must be available:

- (1) One which is capable of carrying 120,000 lbs. or
- (2) Two sleds which are capable of carrying 60,000 lbs. with special rigging which will carry the primary system sections as proposed to be relocated. The purpose of the rigging being to distribute 120,000 lb. weight over the two sleds, so that a 30 ton sled must be available to do this.

Plans for relocation of the plant following extended power operation to a site approximately 250 yards from initial site will require about the same numbers in man-power, vehicles, equipment, etc. as were required for the initial installation.

The procedure for handling modules and relocating to the new site will be the installation procedure in reverse with the exception of the Primary System Module which will require special attention and will be clearly explained later as a separate item.

The new site trenches and module foundations shall be completed before disassembly of plant. Hauling vehicles, transport sleds, hoisting equipment, manpower, and other miscellaneous materials and equipment shall be at the disassembly site.

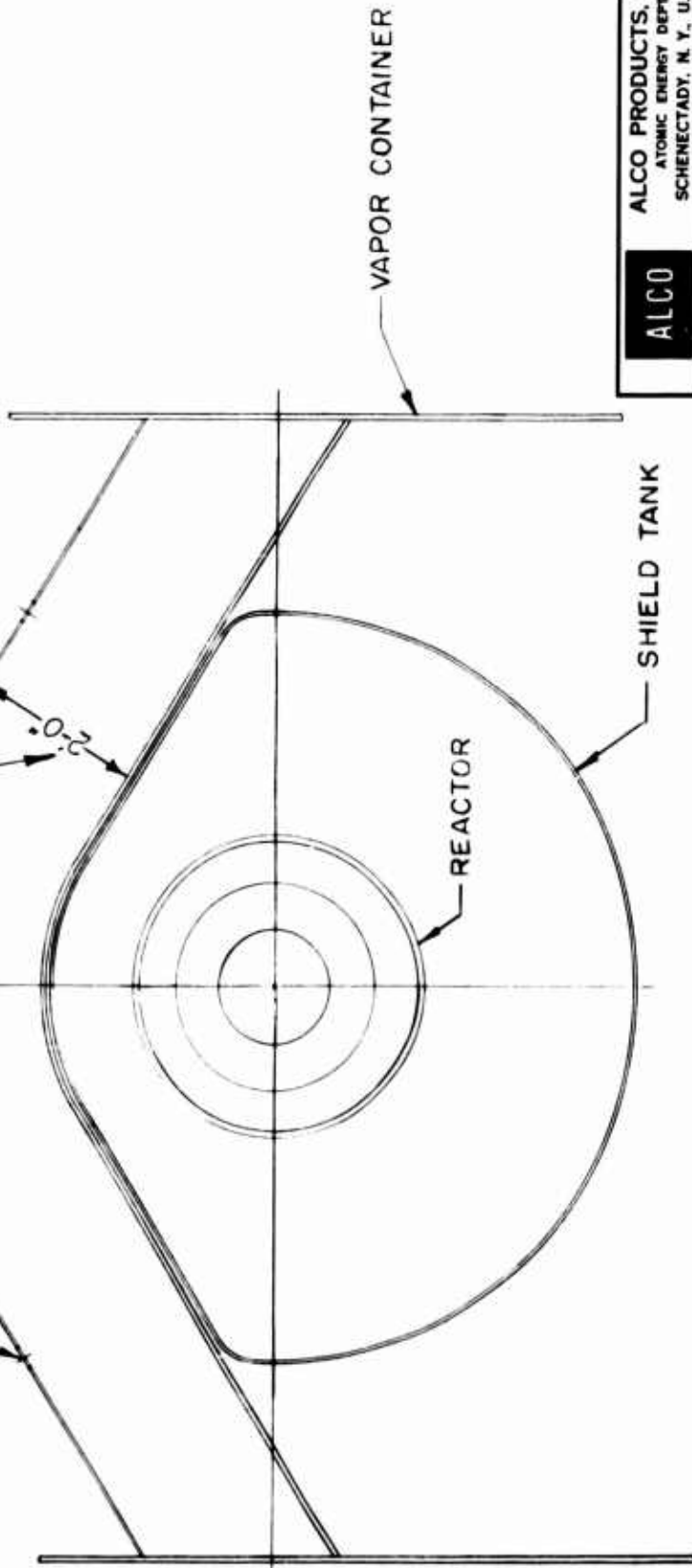
Disassembly and transporting packages to a new location will take place simultaneously. Four pipefitting crews of four men each will start disassembly of interconnecting piping and clearly indexing same for re-erection. Two rigging crews of six men each plus two vehicles and four sled crews will remove packages as they are disconnected. On the short distant change of location it may be possible to extend trench to new location without surfacing in the case of the main power plant trench which contains one air blast cooler, heat exchanger package, condenser package, turbine generator package could be handled below the surface to their new location and be in the proper sequence of erection.

The remaining packages, the two air blast coolers, the feedwater and switchgear and control packages would have to be surfaced and handled in the manner of original installation.

In order to relocate the primary system and stay within safe radiation limits a partition plate will be installed in the vapor container during the initial plant installation. This partition plate is shown on Sketch AES-274 and will contain a two foot thickness of water to reduce the radiation to safe levels during plant relocation. It is proposed to cut the vapor container around its circumference at the mid-point or parting point of the primary skid and also remove the elliptical head of the vapor container at the reactor vessel end. Before removing this head, the shielding water at this end of vapor container will be drained except for the 2 foot thickness of water required for shielding during relocation.

WATER SHIELD USED FOR RELOCATION TO NEW PLANT SITE, TO REDUCE DOSE RATE TO SAFE LEVELS.

3" DIA. HOLE FOR OVERFLOW 3 REQD



| | | | |
|--------------------------------------|-----|------------------------------|---------|
| ALCO | | ALCO PRODUCTS, INC. | |
| ATOMIC ENERGY DEPT. | | SCHENECTADY, N. Y., U. S. A. | |
| SCALE | REP | DIR | DATE |
| 3/4" = 1'-0" | | Revised | 12-4-58 |
| MATERIAL SPEC. | | TR | |
| | | CHK. | |
| | | APPR | |
| | | APPR | |
| | | MET. | |
| NAME: RELOCATING WATER SHIELD | | | |
| PART NO.: AES-274 | | | |

BREAK SHARP EDGES
REMOVE ALL BURRS

UNLESS OTHERWISE SPECIFIED
DIMENSIONS ARE IN INCHES
TOLERANCES ON FINISHED
FRACTIONAL DIMENSIONS
TO RL 2

√ FINISH AS INDICATED
IN MICRONS

(f1) MACHINE FINISH - ROUGH

(f10) FLAME CUT OR SAW

Fuel elements will be removed from the core and placed in the spent fuel tank.

The upper shield tank will be drained and removed from the vapor container.

The reactor skid section will be disconnected from the steam generator skid section. The shielding water in the shield tank will remain in place for shielding purposes.

After separating the primary reactor skid from the steam generator skid, the complete segment of the vapor container and reactor skid will be skidded on to the transporting sled or rig, whichever is available.

The breakdown of weights for this portion of the primary system will be as follows:

| | | |
|-------------------------|---|---------------|
| Vapor Container Segment | - | 42,000 lbs. |
| Shield Rings | | 30,000 |
| Reactor and Skid | | 30,000 |
| Shield Water | | <u>18,000</u> |
| Total | | 120,000 lbs. |

The same sled or rig will be used for the steam generator section of the primary skid and its portion of the vapor which has a total weight of approximately 70,000 lbs.

The two vapor container half sections including skids will be installed on the new bases aligned, bolted and rewelded. The upper shield tank will be rebolted to the vapor container. After the vapor container is welded, the skid sections will be aligned, bolted and leveled and the vapor container will be helium leak tested as in initial installation.

For relocating the plant in excess of 25 miles the same procedure will be required as used in the short haul with the following exceptions:

1. This plan will require sufficient sleds to handle all packages so that lags will be prevented in case of an exceptionally long haul.
2. Packages will be securely tied down on sleds and equipment, protected from the weather using

The breakdown of men, materials, vehicles, equipment, and time required in each case are as follows:

| <u>Personnel</u> | <u>No.</u> | <u>Time Required</u> |
|------------------|------------|----------------------|
| Riggers | 12 | 5 weeks |
| Pipe fitters | 16 | 6 weeks |
| Electricians | 6 | 6 weeks |
| Mechanics | 4 | 6 weeks |
| Welders | 2 | 4 weeks |
| Welders Helpers | 2 | 4 weeks |

| <u>Equipment</u> | <u>Time Required</u> |
|---|----------------------|
| 15-ton capacity cat.crane and crew | 6 weeks |
| 3 - 30,000 # capacity sleds | 5 weeks |
| 2 - 60,000 # capacity sleds | 1 week |
| 2 - Cat. tractors for hauling sleds | 5 weeks |
| 4 - 10-ton hydraulic jacks | 6 weeks |
| Misc. lumber (cribbing) | - |
| Misc. pipe for rollers | - |
| 2-300 Amp Welding machines, gasoline driven | 6 weeks |
| D-4 Cat. w/winch, doser and F.E.L. for utility | 6 weeks |
| 2 - Handi-crane 6000# cap. with 20' ext. boom | 6 weeks |
| Air compressor - gasoline driven, 300 CFM | 4 weeks |
| Tugger hoist - air driven | 6 weeks |
| Misc. shop equipment and small tools | - |
| Acetylene cutting equipment, torches, hose, etc. | 6 weeks |
| Acetylene gas supply | - |
| Oxygen supply | - |
| 1 - 15 KW Portable lighting plant | 3 months |
| 1 - Pipe cutting and threading machine 1/2" to 2" | - |
| Chain hoists 1 and 2 ton capacity | - |

10.0 Testing of Plant

The following tests are proposed to be performed by Alco Products Inc., and/or other manufacturer's supplying equipment to Alco for the Plant.

1. Individual item test.
2. Components and Assemblies Test
3. Plant Factory System Test
4. Low and High Power Performance Test
5. Plant Performance Test

Tests 1, 2 and 3 will be performed directly after manufacture and assembly and prior to shipment to a Site.

Tests 4 and 5 will be performed under Alco Products, Inc. supervision, after installation of the plant at a Site.

The following outline basically covers the testing to be made since the specific details covering the testing requirements and procedures to be followed, and how the testing is to be accomplished, will be developed by Alco Products, Inc. and submitted to the Government for review and approval prior to the execution of the proposed tests as outlined in this proposal. These test procedures will be submitted as specified not later than one month prior to factory testing and by April, 1960 for on-site testing.

10.1 Individual Item Tests

Alco Products, Inc. will be responsible and provide to the Government for Alco fabricated items and where required from other suppliers to Alco Products, as follows:

- ASME certificates for pressure vessels and code stamps.
- Calibration curves for instruments, gauges and meters.
- Performance curves and test results on pumps.
- Rating curves and test results on the turbine generator.
- Test results of cladding material.
- Core flow and orificing test results.
- Performance Test on Control Rod Drives.
- Fuel Element Tests.

The testing of components will be performed as required by Alco Products for Alco fabricated components and by other manufacturer's for components purchased by Alco, prior to assembly on modules to demonstrate their functional integrity.

Components and Assemblies Test

Following fabrication and individual item testing, these items will be assembled on the plant modules and subjected to subassembly tests outlined as follows:

1. Inspection of mountings and supports for equipment on the modules to preclude damage due to vibration and insure proper securement.
2. Valves and shutoff controls associated with pressure vessels and their piping will be tested for functional operation and leakage.
3. Primary system will be helium leak tested.
4. Hydrostatic test will be performed on the assembled primary system module in accordance with applicable codes to insure integrity of the primary system piping and connections.
5. Leakage of fluid from the primary system will be checked for excessive amounts beyond design conditions.
6. Rotating machinery, pumps, motors will be tested for proper rotation, operation and excessive vibration.

10.2 Plant Factory System Test

Prior to preparation for shipment, the secondary system modules will be tested in the assembled configuration. The primary system will be checked and tested separately.

The plant modules will be assembled in the overall configuration as shown on drawing M02M12 with the exception of the primary system and waste tank which are at elevations of 20 ft. and 24 ft. respectively below the secondary system as shown on drawing M02M12. The piping between the primary and secondary system will be assembled and checked for fit up and coding.

It is proposed to test the primary and secondary system separately. The secondary system will be supplied with steam from an external source and checked for integrity, operation and performance.

The secondary system modules including the air blast coolers and piping will be placed as shown in Dwg. M02M12 and all prefabricated interconnecting piping and wiring installed to check proper fitup, coding and integrity.

The primary steam generator skid and reactor skid sections will be assembled and bolted together and tested for integrity and operation using a dummy core.

An external steam source will be utilized to supply steam to the secondary system, at the design flow and pressure.

The physical integrity of the piping and vessels will be checked when simulating operating temperature pressure and flow conditions on the primary system and to check instruments, controls pumps and pressurizer heating elements, control rod drives and insure that all modules are stable and free from excessive vibration.

The capability of the system to deliver the required amount of electrical power within the required quality limits shall be checked.

Readings on all necessary flows, temperatures and other instruments will be made to record operating conditions such that a heat balance can be calculated.

An outline of the proposed plant factory test is given as follows:

Test Procedure

A helium leak test followed by a hydrostatic test will be performed on primary system in accordance to the specified requirements. Flanges and heads will be checked for leaks at this time. To attain operating temperature on the primary system, steam from an external steam generator will be introduced into the secondary side of the steam generator.

The main steam line, boiler feed and all other piping from steam generator will be blanked off or valved off during this heating-up period. Primary pump will be started, rotation checked and circulation established to pick up the heat being released in the secondary side (tubes) of steam generator.

Pressure will be brought up on primary loop by placing the heating elements into operation in the pressurizer and controlled at 1750 psi. Temperature of the primary circulating water will be raised at a rate of 50 F per hour maximum, until operating temperature of 520 F is attained and held at that point until a satisfactory inspection has been made of the entire primary system.

The control rod drives will be operated at operating temperature to check out rod drops, controls, wiring, clutch operation, etc. Primary system instrumentation will be checked during flushing and cleanup. Final check of the non-nuclear instrumentation will be made during operational test.

Secondary System Test

All the pressure piping of the secondary system will be hydrostatically tested upon completion of erection in conformance with A.S.A. code for pressure piping. This test shall be performed on each set of lines to a pressure conforming to A.S.A. code and of sufficient duration to make satisfactory inspection of all joints for leakage. A complete set of marked piping prints shall constitute record of the leak tightness of the secondary system.

Secondary system instrumentation will be checked and tested during erection, and during flush out and clean-up. Final checks and adjustments will be made during the initial phases of the operating test at Dunkirk.

Primary System

The items listed below will be checked during electrical check out. Operational checks i.e., rotation, vibration overheating and design conditions check will be made during operation test.

P.C. Pump

P.C. Makeup Pump

Seal Leakage Pump

Rod Drive Motors

Motor Operated Blowdown Valve

Spent Fuel Pit Recirculating Pump

Heating Procedure to Simulate Operating Press. & Temp.

1. At this time the primary system will be completely filled with clean demineralized water with reduced oxygen content. All pumps will be off and all valves on the primary system will be closed.
2. The external steam jenny will be put into operation and brought up to pressure.
3. Pressurize the primary system to a minimum of 50 psig by means of P.C. makeup pump. Regulate pressure by adjusting makeup and blowdown.
4. Start up P.C. pump.
5. Start pressurizer heaters as required to raise pressurizer temperature at a rate of 50 F/hr.
6. Introduce steam to the secondary side of the steam generator. Start at a very low rate and gradually increase flow until heating rate reached 50 F/hr. Keep the primary system temperature at least 20 F below the pressurizer temperature.
7. Throttle the valve in the blowdown jumper line to control condensate flow from the steam generator.
8. When the temperature of the water in the pressurizer reaches saturation temperature, steam will form and water will be displaced in the pressurizer. While this is taking place the blowdown rate will have to be increased and/or the makeup rate reduced to maintain a constant pressure in the system.
9. When the pressurizer water level reaches normal operating level, put the P.C. make-up pump on automatic control.
10. The primary system pressure will now start to rise and blowdown should be reduced to a minimum.
11. Continue heating until normal operating temperature and pressure is reached.

12. Manually control pressurizer heaters and raise primary system pressure to 2000 psig and check safety valve operation.
13. Reduce system pressure to normal operating pressure (1750#) and operate at design conditions for specified time.
14. Shutdown the pressurizer heaters and the external steam source.

Cool the Primary System

1. Start boiler feed pump.
2. Gradually admit water to steam generator until normal operating level is reached.
3. Put steam generator level control into operation.
4. Gradually open steam hand valve to the evaporator. Control the steam flow to lower the temperature of the primary system at a maximum rate of 50 F per hour.
5. When primary system pressure drops to 50 psig put the pressurizer level control on hand operation and maintain a minimum of 50 psig pressure on the system by means of the P.C. makeup pump.
6. As system temperature approaches 212 F the cooling rate will drop. Additional cooling may be attained by blowing down the primary and/or secondary system. When blowing down the primary system the blowdown cooler must be used.
7. When desired cooling has been attained shut down the various systems in reverse of startup. Drain and dry system. Prepare for loading and shipping.

10.3 Low and High Power Performance Test at the Site

Prior to pressurizing the primary system, the vapor container shall be tested for leakage rates with a helium mass spectrometer to insure that leakage rates are not exceeded.

Core loading and unloading procedures and transfer of fuel elements in transfer casks shall be test demonstrated.

The low and high power testing will include the following:

1. Each control rod shall be calibrated over its entire length with various settings of other control rods utilizing sufficient combinations of rod settings to determine all significant control rod effects.
2. Individual rod scram will be checked with coolant flow in the core at the design conditions.

3. Rod calibration shall be performed at temperatures from ambient to design level.
4. The temperature and pressure coefficients of reactivity will be measured at several points ranging from room temperature to design operating temperature while the primary coolant temperature is raised at approximately 30 F per hour.
5. Safe plant shutdown shall be tested according to the approved stuck rod criteria.
6. Tests and calibrations of process control instruments and radiation monitors will be made to insure proper operation and accuracy for safe plant operation.
7. Control mechanisms and circuits will be checked and tested for reliable operation.

All instrumentation will be inspected and tested for proper installation and connection. Check lists will be furnished to the government covering instrumentation calibration and performance check out indicating that each instrument and instrumentation system has met performance test recommended by the manufacturer.

Instrument calibration shall include the following:

- a) Continuity and signal test of all detecting components, recording circuits and control circuits will be made after installation.
- b) Signals simulating high flux levels and short periods will be applied to trip circuits to insure approved design response.
- c) Mouule radiation detectors will be tested and calibrated by means of standard radiation sources.
- d) All failures that relate to safety of the operating system will be induced and response checked against design requirements.
- e) All control rod elements shall be loaded into the reactor vessel and filled with water at design temperature and pressure and the action of all control rod elements shall be initiated singly and in bank to indicate freedom from binding.

10.4 Plant Performance Test at the Site

The plant performance test will include the following items:

1. The ability of the plant to deliver a minimum of 1500 KW electrical power (depending on existing camp loads at the time) at the design conditions.
 - a) The procedures for shifting and dividing of electrical and steam loads between the nuclear plant and the camp standby power shall be demonstrated.

2. Demonstration test of the radiation monitoring system will be made for proper operation during full load operation of the reactor. Three radiation surveys of the entire camp will be made.
3. Leakage rates of the primary and secondary systems shall be made to insure limitations within the design conditions.
4. Chemical analysis of the primary and secondary system water will be made to check impurity content within the design conditions.
5. Decay heat removal from the primary system following loss of power without bulk boiling of the primary system coolant will be checked.
6. Temperature of the tunnel walls shall be monitored to show that gamma heating does not exceed specified levels.
7. An endurance test shall be performed for 400 hours with less than 24 hours total planned and unplanned downtime and will include one 96 hour uninterrupted run with existing camp loads.

The construction progress schedule on the following page indicates manpower requirements and time requirements for erection and testing at the site.

11.0 Testing (In Service and Developmental)

11.1 Fuel Elements

The stationary fuel elements for this core will be identical to those in APPR-1 except for end boxes. These stainless steel plate type fuel elements have an excellent performance record both in in-pile and reactor operation.

Irradiation Tests - Irradiation tests performed in conjunction with APPR-1 Core I consisted of both small sized samples and full sized elements. Test variations in the small sized samples included matrix material, type of oxide, amount or reduction, oxide particle size, oxide and burnable poison contents, clad-core-clad proportions and amount of burnup. In brief, all samples showed no structural failures, even at burnups as high as 57% U²³⁵. Matrix hardening was evident, with the effect increasing as particle size decreased. In no case, however, was the hardening sufficient to cause structural failure. All small sized samples were exposed at MTR temperature.

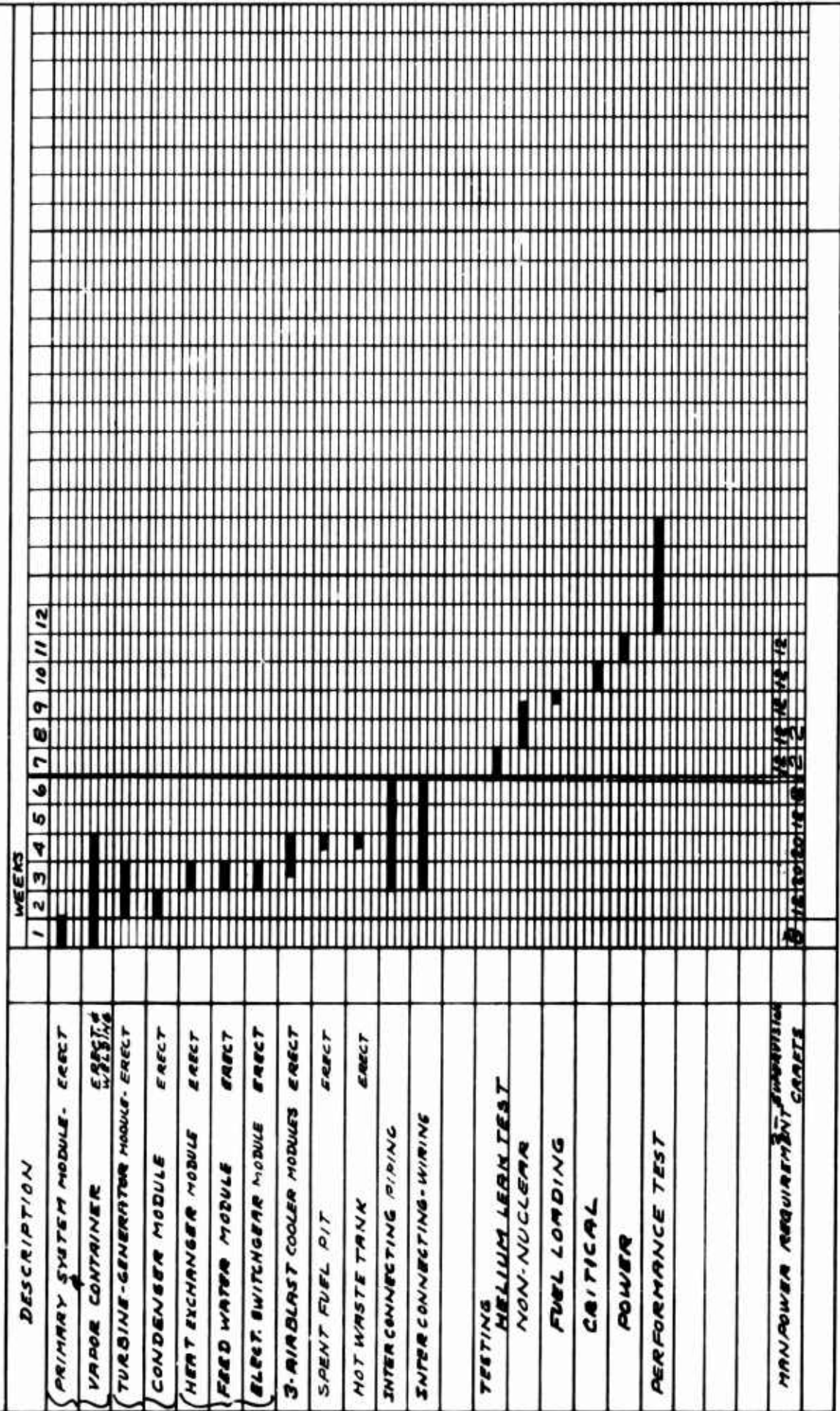
A full sized fuel element exposed to an estimated 25-40% U²³⁵ burnup at MTR temperature showed no evidence of structural failure.

Another full sized element was exposed in the STR core at Arco. However, this element received only about 3% U²³⁵ burnup before removal from the core. No metallurgical examination has been made, but visual inspection revealed no sign of any defect.

Reactor Operation - The APPR-1 has been in operation since April, 1957. The fuel plates in this core consist of about 26 weight % of fully enriched UO₂ and a small amount of B₄C as a burnable poison dispersed in a stainless steel

AE-33

ALCO PRODUCTS, INC.
CONSTRUCTION PROGRESS CHART
JCF CAP INSTALLATION



matrix and clad with stainless steel. The fuel plates are brazed into side plates and end boxes or handles attached to form the fuel elements. To date, average U^{235} burnup is about 22% and maximum U^{235} is in the vicinity of 35%. No evidence of malfunction has been found.

Other reactors have been operated with stainless steel plate type elements of about the same UO_2 content. These elements, however, are formed by welding the fuel plates to two side plates. The fuel plates were made by a commercial fuel element manufacturer. Operation of these fuel elements is reported as very satisfactory.

Further Development Work On Stainless Steel Plate Type Cores -
Development work on the APPR-1 Core II has recently been completed at ORNL. Core II elements will also be clad with stainless steel. Integral flux suppressors will be used in the control rod fuel elements to minimize flux peaking. APPR-1a Core I will also employ stainless steel fuel elements similar to the APPR-1 elements. It is evident that considerable confidence is placed in stainless steel plate type fuel elements of the APPR-1 type.

Status of Stainless Steel Plate Type Fuel Elements -
The extensive research, development and production experience gained from the APPR-1 Core I fuel element program is readily available. No further development work will be required for a similar core, except that normally expected due to changes in vendor, method of assembly, etc. The pre-packaged reactor core has been designed within the limits of APPR-1 experience. The extensive irradiation tests usually required for a new core design thus can be safely eliminated. The only significant difference in fuel plates is the incorporation of integral flux suppressors in the control rod fuel element plates.

A development program on integral flux suppressors and dispersions of Eu_2O_3 in stainless steels for APPR-1 Core II has been completed at ORNL. APPR-1 Core II fuel elements will be fabricated in approximately 3 months. It is evident that the necessary experience in manufacturing control rod fuel elements with integral Eu_2O_3 flux suppressors will be available for the pre-packaged core. A considerable amount of irradiation experience in the APPR-1 on these fuel elements will also be available before operation of the proposed plant.

Alco recommends a welded rather than a brazed fuel element for this core. The advantages of welded fuel element construction are significant. The elimination of braze metal removes the always present possibility of contamination with high neutron absorbing elements. The possibility of galvanic effects, peeling, etc. arising from the use of a different material is eliminated. The fuel plates can have considerably higher strength, since dead soft fuel plates are not required. Fuel element cost can be reduced. The possibility of rejection of fuel elements in assembly operations will be reduced. Other advantages include less dead material resulting from the use of thinner side plates and a faster production rate.

Alco Products, Inc. has conducted a development program on welded fuel elements. Several different welding designs have been investigated, and two very promising designs have resulted. In both cases, a reduced thickness side

plate is used. Welding is performed by a mechanized tungsten electrode inert gas shielded set-up. No filler metal is added, thus eliminating compatibility. Results of this program are most encouraging. Distortion has been held within established tolerances.

Further development work will be limited to that normally required by the introduction of a new fabrication method, and will require only relatively small expenditures in time and cost and will not delay the completion of the subject core.

11.2 Absorbers and Absorber Materials

11.2.1 Boron

The APPR-1 Core I utilizes B^{10} as the absorbing material in the form of a dispersion in iron clad with stainless steel. Content of B^{10} in the iron matrix is about $3\frac{1}{4}$ weight %.

Performance of these absorbers to date has been entirely satisfactory. However, the results of other irradiation programs indicate the possibility of future difficulty in operation. Irradiations of small sized samples and of one full sized sample have been at low ambient temperatures. Post-irradiation heat treatments have been applied to unblistered samples in order to obtain some simulation of reactor temperature conditions.

Samples with about 30-35% actual B^{10} burnup blistered and swelled severely in-pile. Samples with about 9 - 17% B^{10} burnup blistered to some extent after short heat treatments at 500° - 600° F. Samples with burnups of about 4% maximum showed no blistering after heat treatments as long as 312 hours. These tests indicate that blistering and swelling of such nature as to cause control rod malfunction might occur at some B^{10} burnup between 4 and 17%. Since B^{10} burnup in the pre-packaged reactor core is expected to be considerably in excess of 4%, the use of B^{10} as the absorbing material is not recommended.

11.2.2 Europium Oxide

APPR-1 Core II will use europium oxide as an absorber material dispersed in stainless steel (elemental powders) and clad with stainless steel. Content will be 33 weight %. Reactor performance is expected to be completely satisfactory on the basis of work to date.

Irradiation tests have been performed by KAPL on 25 and 30 weight % europium oxide extrusions. No difficulties were found in fabrication. Bend tests before and after irradiation indicated about a $\frac{2}{3}$ reduction in ductility.

In development work in connection with APPR-1 Core II absorbers, ORNL experienced reactions of Eu_2O_3 with the matrix during hot working operations. These reactions were traced to silicon present in the matrix material. It has been found that maintaining the silicon content of the matrix powers at a very low level will eliminate this reaction.

Metallographic studies of KAPL samples after irradiation and ORNL reacted samples after fabrication indicate similar effects. KAPL dispersions were subjected to a lower working temperature for much shorter periods of time than the ORNL samples. Since the reaction is undoubtedly time-temperature dependent, the difference in as-fabricated results is understandable.

The loss in ductility of the KAPL samples is thus indicated to be a delayed europium oxide-silicon reaction occurring in-pile rather than in fabrication. Consequently, it is believed that dispersions of europium oxide with matrix silicon content low enough to prevent reaction during absorber plate hot working operations will not suffer a significant loss in ductility during irradiation. Satisfactory operation is thus expected for absorbers consisting of europium oxide dispersions in stainless steel clad with stainless steel made with proper matrix material and low silicon content.

The absorbers proposed for this core will be identical to APPR-1 Core II absorbers containing 33 weight % europium oxide in low silicon elemental stainless steel powder dispersions clad with stainless steel. The absorber section will be composed of four hot rolled plates welded together at the corners to form a hollow rectangle. Although there is believed to be no question of europium oxide absorber integrity, actual operating experience in APPR-1 Core II will be available before operation of this reactor.

11.3 Control Rod Drives

A multiple rig with six complete drive mechanisms were placed in operation in February 1956 primarily for severe endurance testing. These drives operated approximately one year under these conditions with no serious malfunction of any component.

Some of the results of the testing are as follows:

| | Individual | Cumulative (all drives) |
|------------------------------------|------------------------|-------------------------|
| Scram cycles | 2 drives 15,000 ea. | 60,000 |
| Continuous Operation | 1 drive, 15,000 ft. | |
| Total travel in scram cycling | 2 drives 60,000 ft.ea. | 240,000 ft. |
| Operating hours at Temp. and press | 5 drives 2,250 ea. | 13,000 |

Tests were also made leaving rods in a stationary position at various points in the operating cycle for periods up to two months. Rods were then scrambled. No indication of any sticking or malfunction was observed.

It was found that one material used in certain specific locations in the prototypes showed rather severe corrosion upon metallurgical examination of the drive components after test. This material was changed in the final production design to one with essentially the same physical properties, but better corrosion resistance. The final design also provided for grouping the components in subassemblies to greatly facilitate maintenance.

The production drives were built and installed in the Alco Criticality Facility for the final critical checkout of the APPR-1 core. They were operated for a period of approximately four months under cold conditions. Each one was installed in the multiple test rig and operated for two weeks under APPR-1 conditions of temperature and pressure. No troubles were encountered during any of this operation.

The drives were shipped to Fort Belvoir for installation in APPR-1 in February 1957. After installation and debugging of the control equipment an intensive period of testing was done under actual operating conditions with a dummy core in place. Approximately 500 scram cycles were run on each rod with no indications of sticking or malfunction. A requirement of the APPR-1 contract specified a complete drive change demonstration would be made. This was to be done in a period of twenty-four hours by four men. The actual time recorded at the demonstration was five hours twenty-one minutes from the time the power was shut off until the mechanisms including seals had been removed and reinstalled and the rods were again being run from the Control Room. This demonstration was performed with the reactor at operating temperature and pressure.

The APPR-1 went critical on April 8, 1957 and, after the initial shake-down period and preliminary testing, completed a 700 hour acceptance test at full power. Subsequent to this test, a six month test at power conditions specified by the customer has been completed.

The APPR-1 is presently operated by Alco under contract with the Army Power Branch of ERDL. Operator training is a part of this contract. During this training program, the reactor has been made subcritical and returned to critical power operation approximately 1000 times. Approximately 400 of these cycles were accomplished by manually scrambling the reactor. The remaining cycles were accomplished by driving control rods into the core. To date, no false scrams or other operating difficulties have been experienced which are attributable to any rod drive component.

Alco designed and built for ANL a prototype drive for the ALFR. This prototype was extensively tested and approved by ANL. As a result of this program, Alco received a production contract for drives which are presently installed in the ALFR. Alco has been informed that the drives are operating quite satisfactorily.

The ALFR drive is basically similar to the APPR-1 drive, but is modified for top rather than bottom drive. A similar prototype, but for a bottom drive was designed and built for ANL as a back-up effort for the EBWR drives. The general arrangement of both of these drives is quite similar to that given in this proposal and helps to illustrate the adaptability of the basic drive to operating conditions different than APPR-1.

The success of this drive concept, which exceeded all expectations, is best exemplified by its acceptance by the reactor industry. Alco manufactured drives based on this concept are presently being fabricated for the APPR-1a and the Elk River power plants.

11.4 Reactor Vessel, Steam Generator and Pressurizer

These components are of the same type of design and materials which have been used in PWR programs with complete success. Each component will be tested in accordance with design requirements. Use of such proven conventional type components provides the maximum reliability and assurance of meeting operational requirements.

11.5 Primary Coolant Pump

The pump which will be used in the proposed Alco plant is a "canned rotor" type pump which has been successfully used and proven in numerous applications for several years. This type of pump is widely used in the PWR field and its reliable performance record is evident.

Alco is experienced in the packaged plant application of this type pump. It's reliability at APPR-1, as well as in the Navy and other PWR programs, has exceeded all expectations.

The pump to be furnished by Alco will be individually tested at the manufacturer's plant. It will be given a minimum performance test at operating temperature of 200 hours with one hundred (100) starts and stops. Required helium mass spectrometer leak and hydrostatic tests will be performed.

The pump will also be tested in the plant test prior to shipment.

11.6 Primary Coolant Auxiliaries

The auxiliary systems are similar to those utilized and proven in APPR-1 and designed for APPR-1a. All equipment will be of the "commercial" type which has been completely proven in service.

11.7 Secondary System and Equipment

The secondary system and equipment is of "commercial" design which has proven extremely reliable in service.

11.8 Instruments and Controls

Operations at APPR-1 indicate that tubes and relays contribute significantly to unreliability and maintenance problems of nuclear instruments. Therefore, a nuclear instrumentation system containing only transistors and magnetic amplifiers for sensing and control is being developed for APPR-1a in which some amplifiers are card mounted and interchangeable. Relays are utilized only to accomplish a function requiring a high current rating. Components of this transistorized system will be fully tested at APPR-1 prior to the fabrication of this plant.

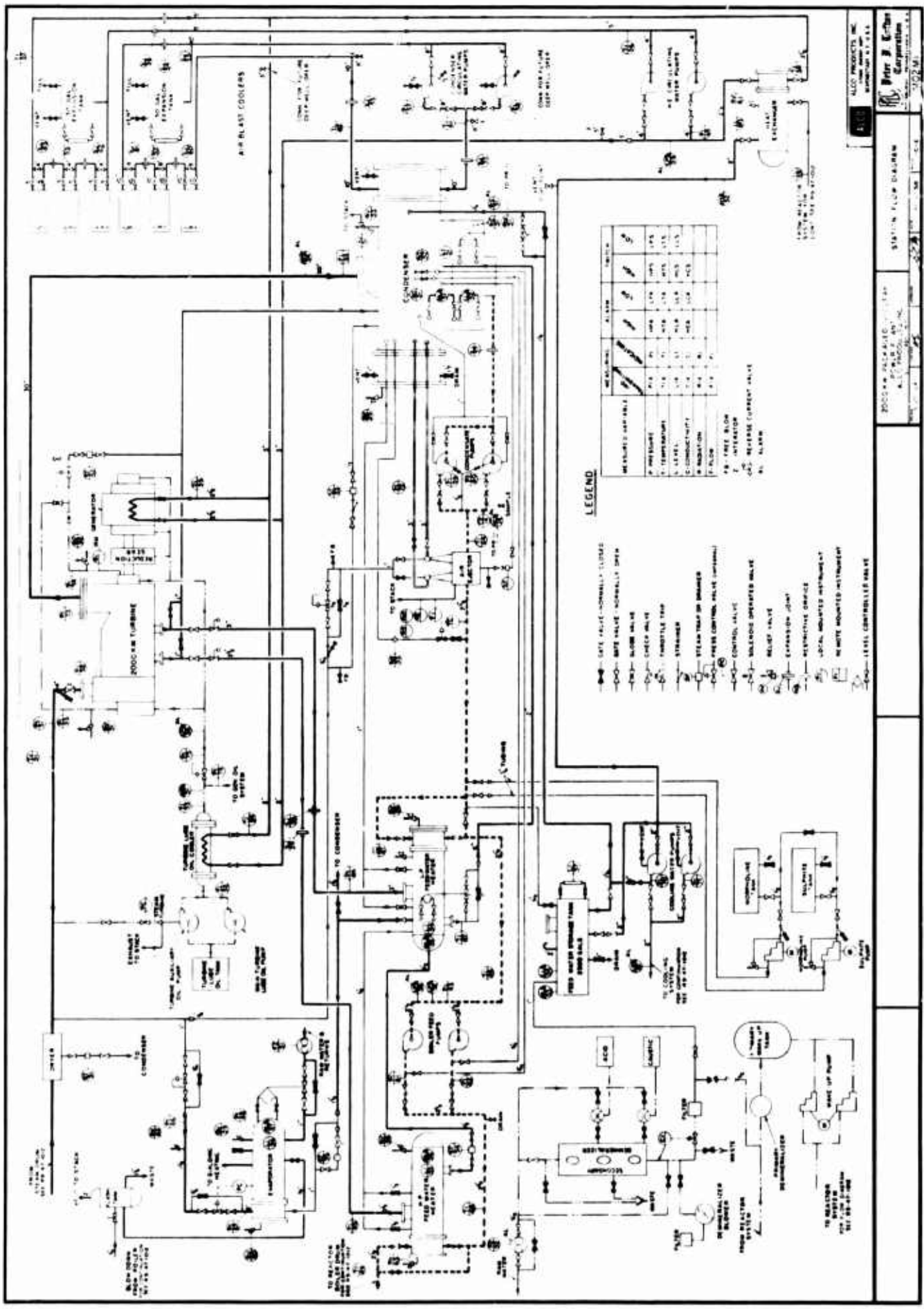
Recorders and controllers specified for this plant are of the latest commercial design and require no vacuum tubes. This equipment has been thoroughly field tested by the manufacturer at isolated stations. It will also be tested

under plant conditions at APPR-1 and APPR-1a before this proposed plant is fabricated.

Operations at APPR-1 have indicated the need for complete isolation of instrument power from any plant voltage transients. The use of solid state components has reduced the power required by the instrumentation and permitted the use of one isolated supply for all of the instrumentation.

The use of this type of design will provide maximum plant reliability, minimize maintenance and greatly improve overall plant performance.

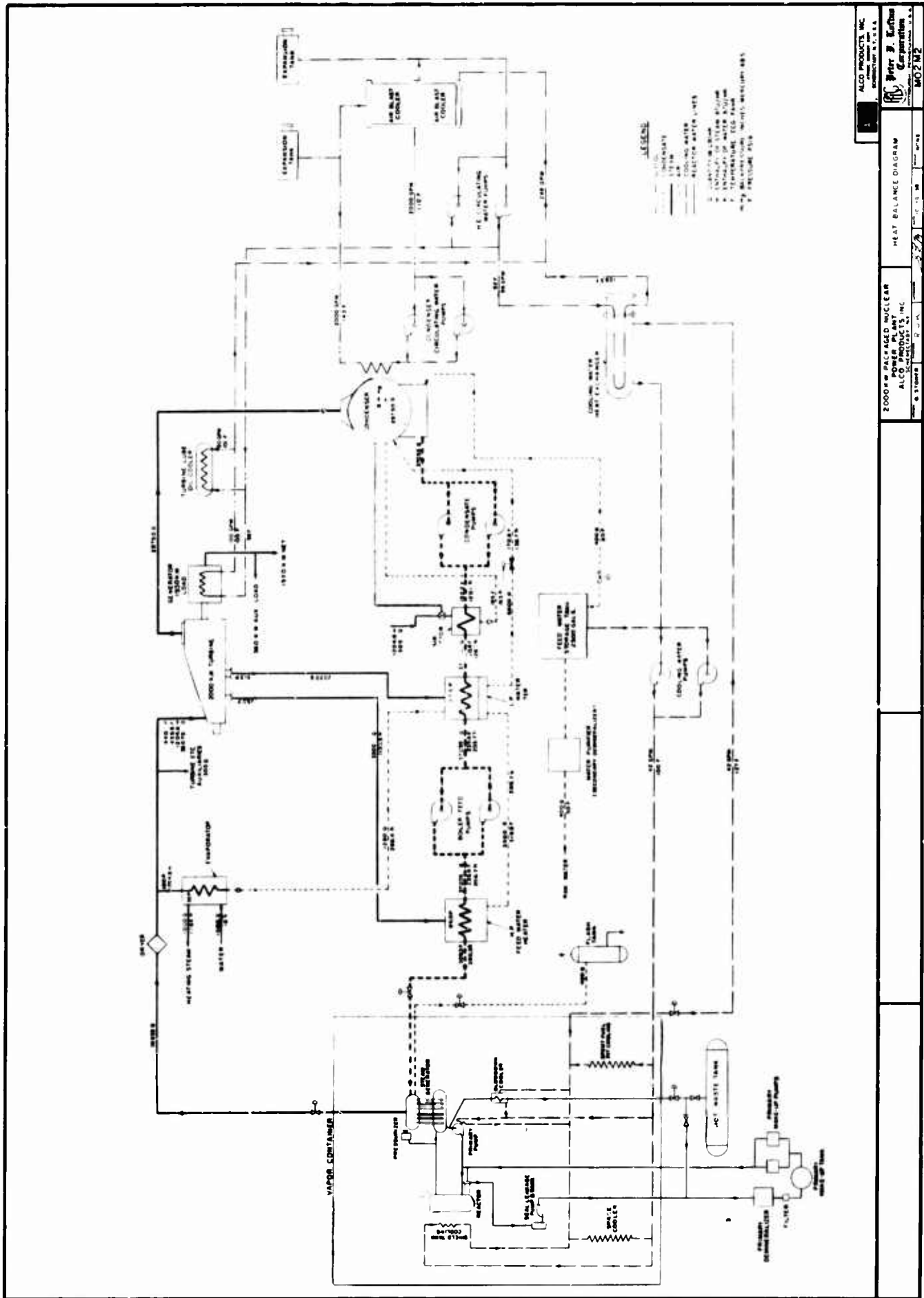
All equipment and systems will be checked at operating conditions (non-nuclear) prior to shipment to the site. Using proven equipment which has been thoroughly and satisfactorily checked at operating conditions will provide a plant having the maximum reliability.



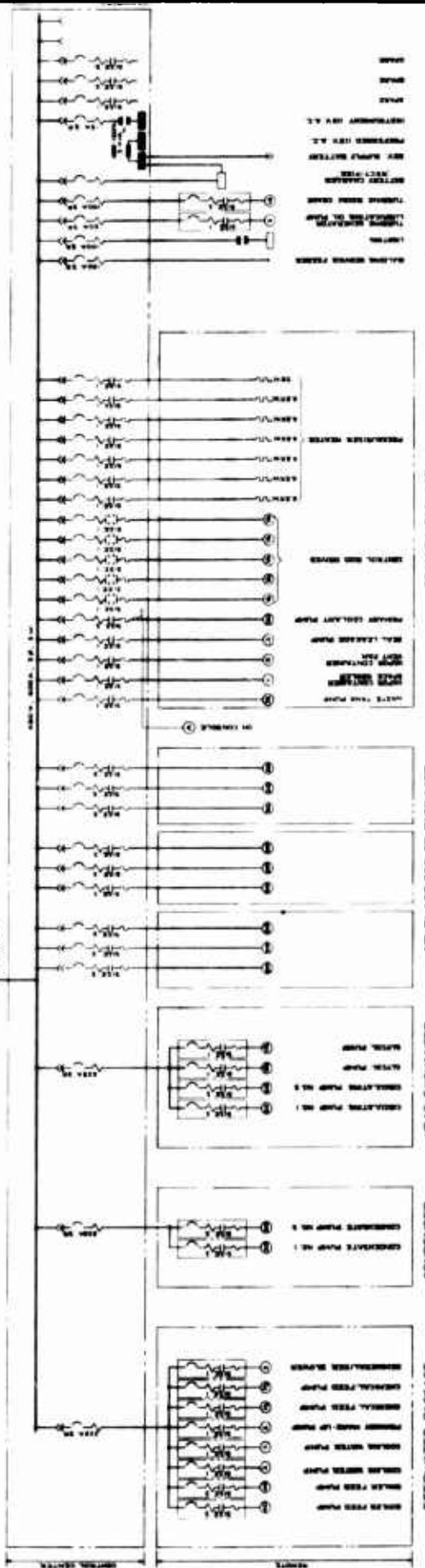
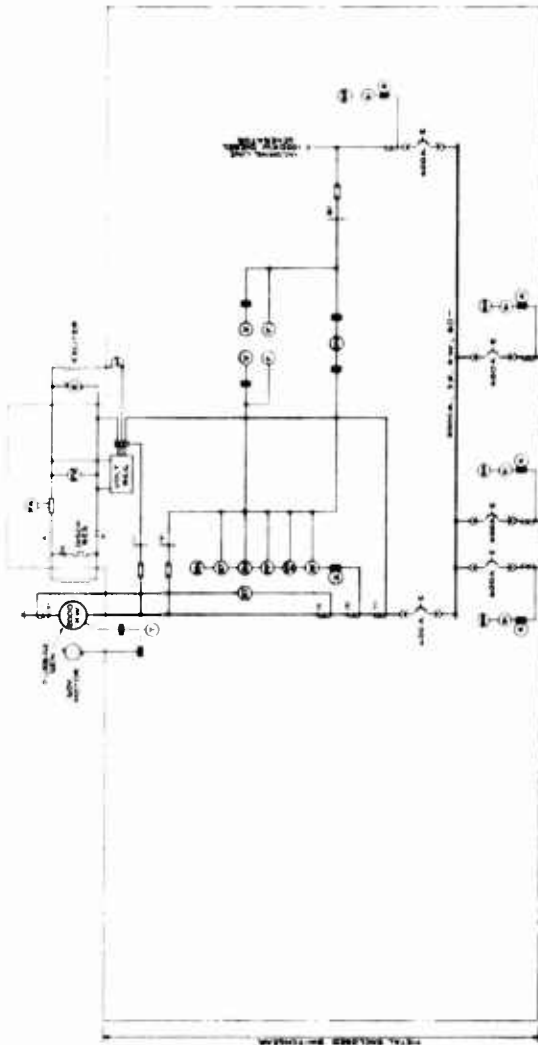
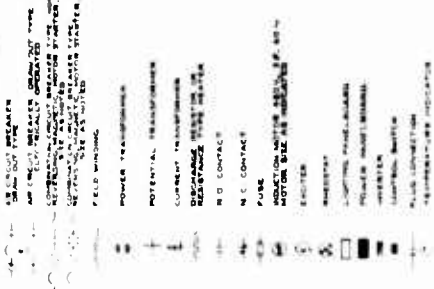
ALCO PRODUCTS, INC.
 1000 W. 10TH AVENUE
 DENVER, COLORADO 80202

Page 3 of 4
Station Flow Diagram

2000-1-15
 ALCO PRODUCTS, INC.



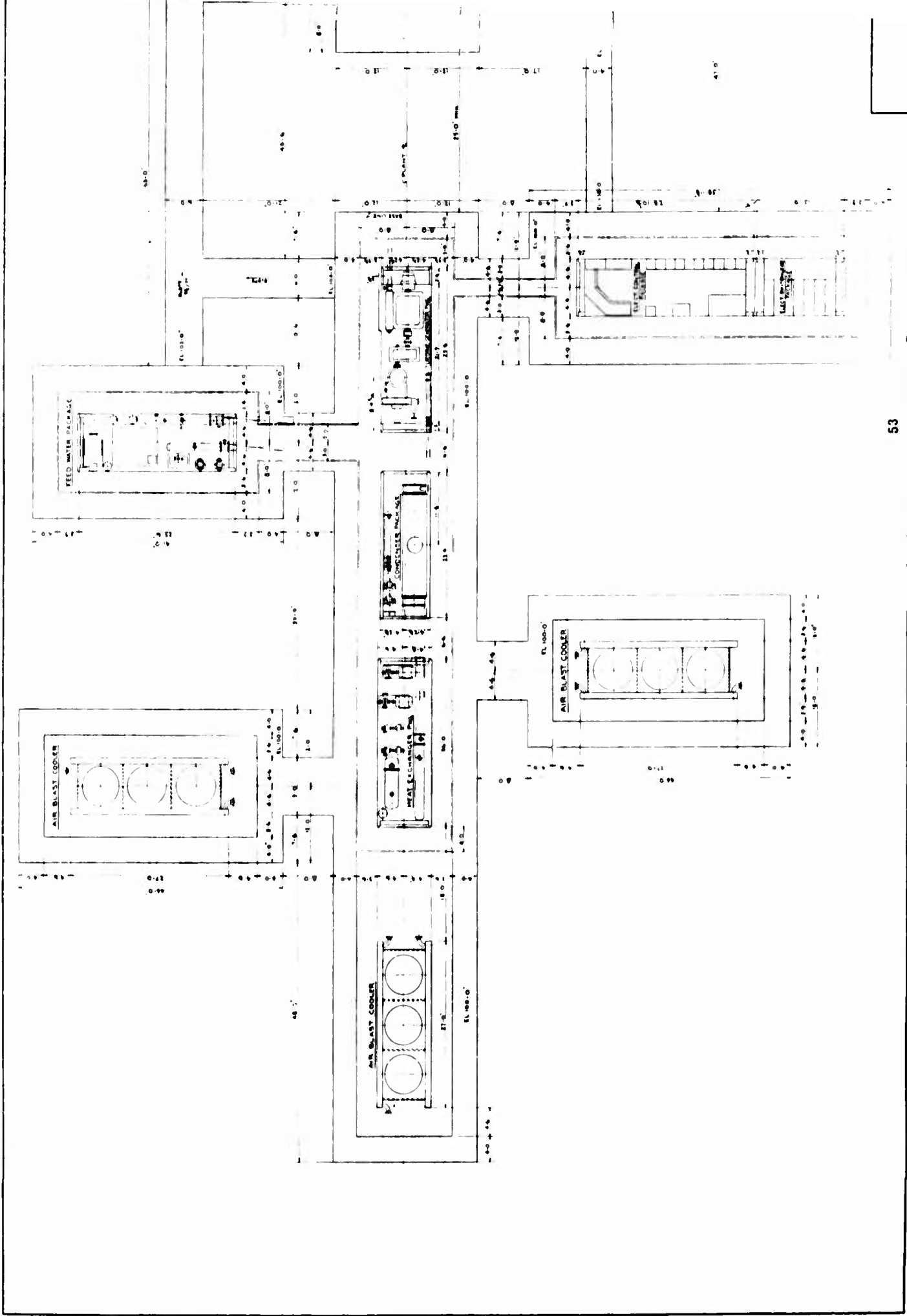
- 1 AMPHETER
- 2 VOLTMETER
- 3 WATTMETER
- 4 WATTMETER
- 5 POWER FACTOR METER
- 6 FREQUENCY METER
- 7 FIELD VOLTMETER
- 8 SYNCHROSCOPE
- 9 OVERCURRENT RELAY
- 10 OVERCURRENT GROUND RELAY
- 11 DIRECTIONAL OVERCURRENT RELAY
- 12 DIFFERENTIAL RELAY
- 13 OVERHEAT RELAY



NOTE: ALL VALUES SHALL BE KEPT IN RANGE AS SHOWN IN THIS WIRING DIAGRAM.

ALCO PRODUCTS, INC.
 2000KVA PACKAGE NUCLEAR POWER PLANT
 ALCO PRODUCTS, INC.

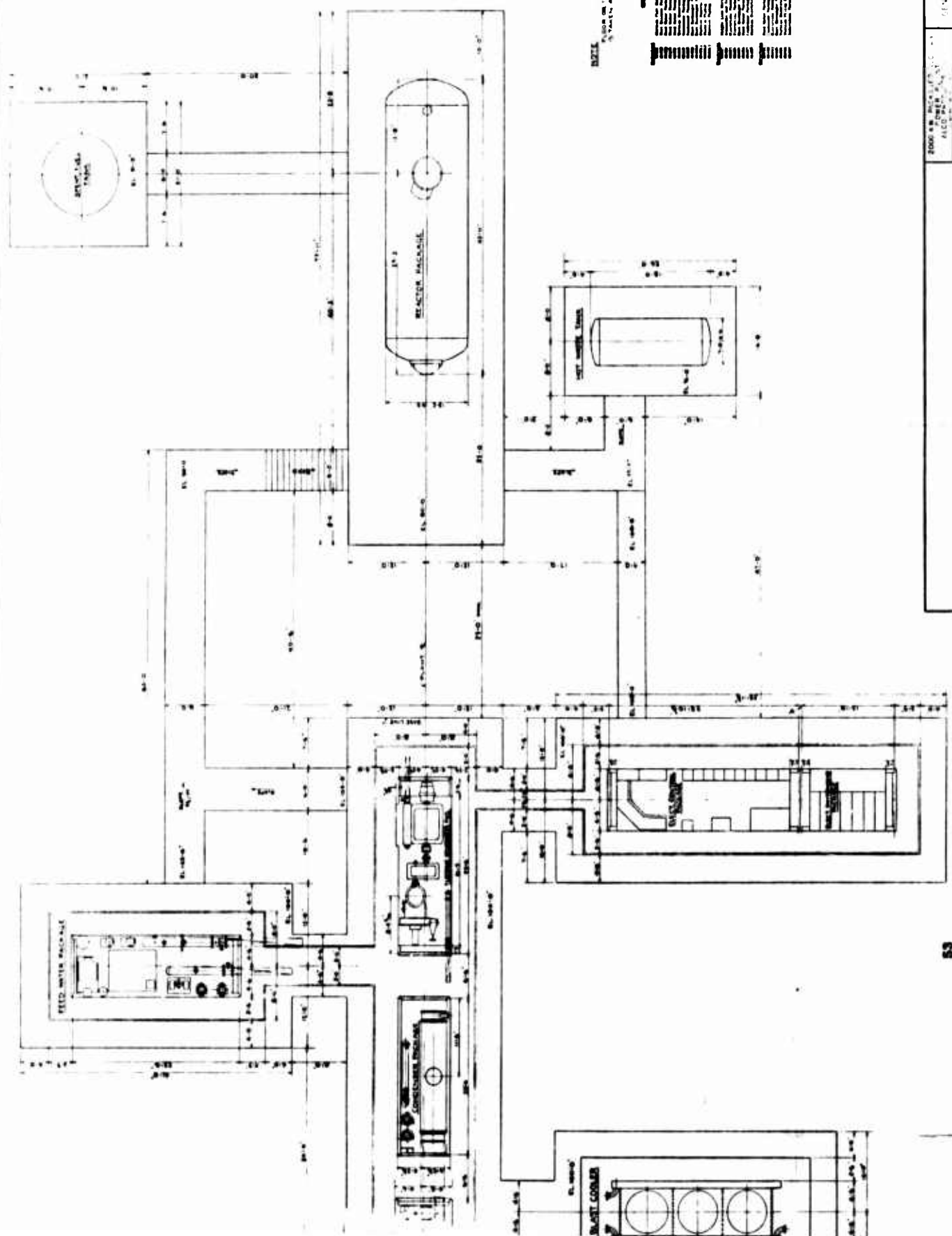
MOZEL

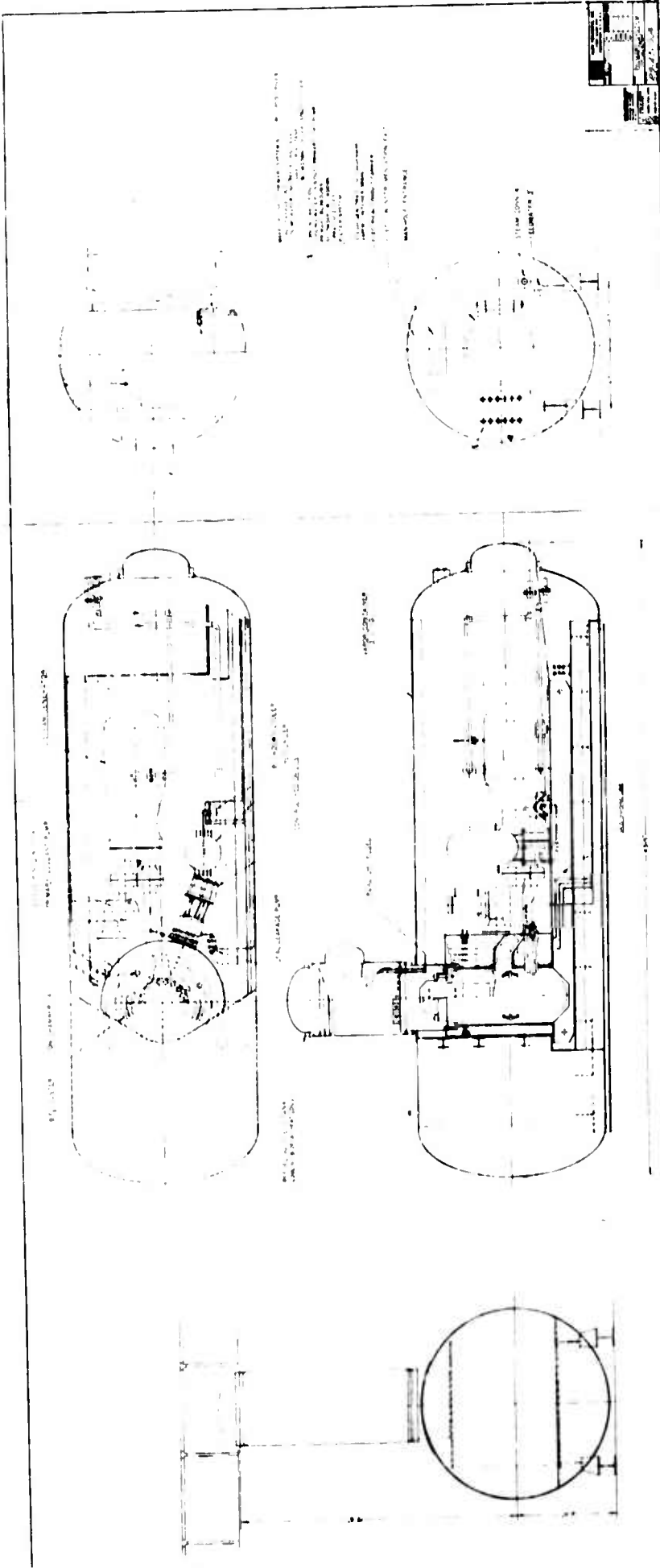


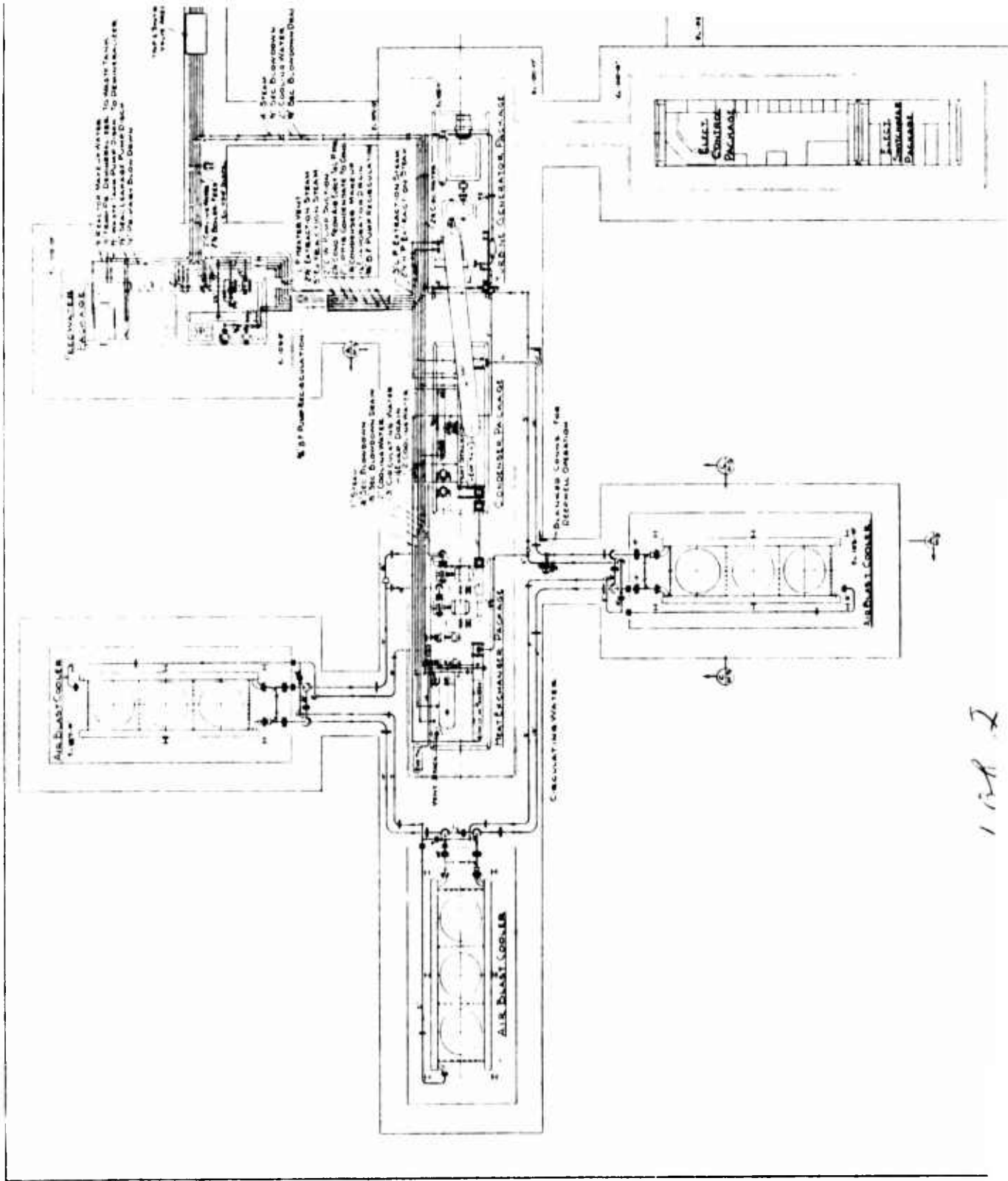
10

NOTE: SEE DRAWING L-1000 FOR LAYOUT OF
STATION 43 & 100 0

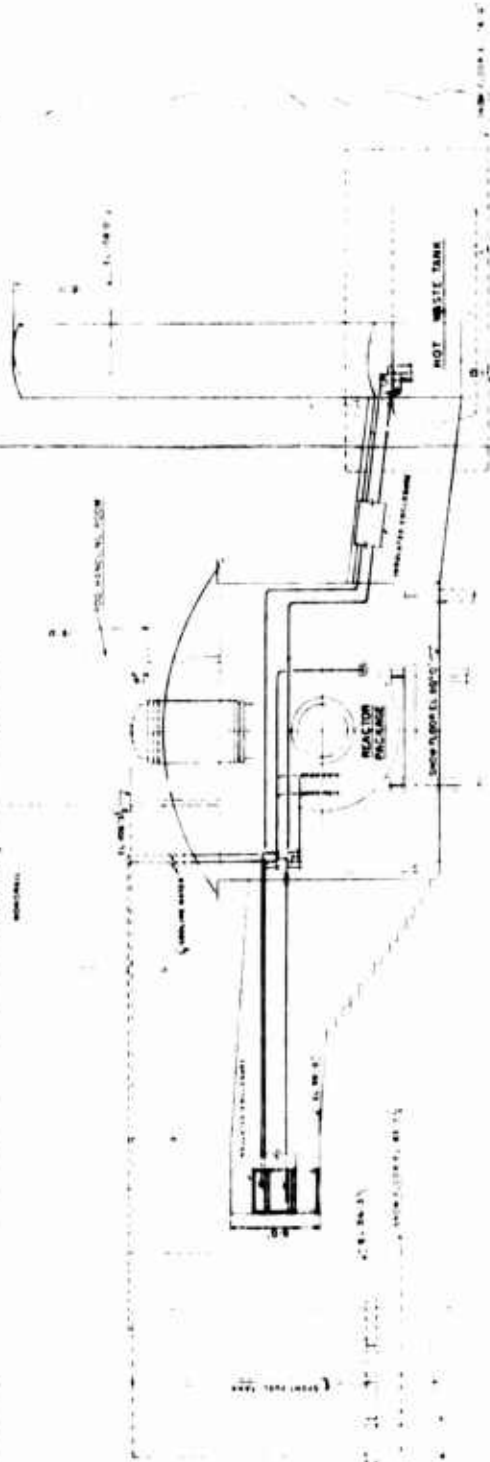
REVISIONS
NO. 1
DATE
BY
REASON



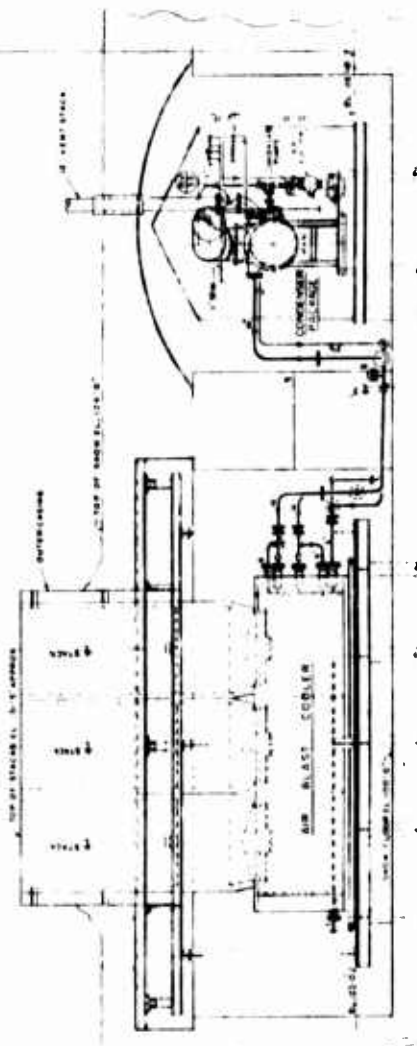




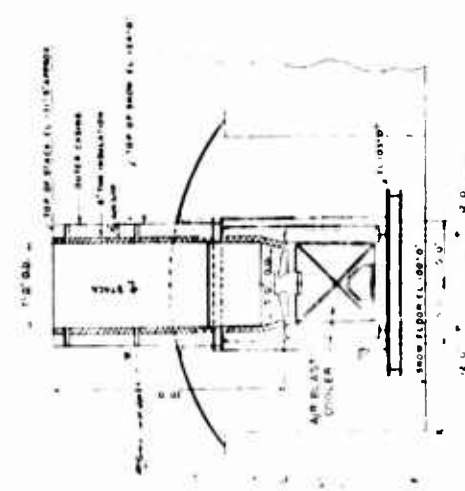
1002



SECTION-B-B
DWG NO. W212



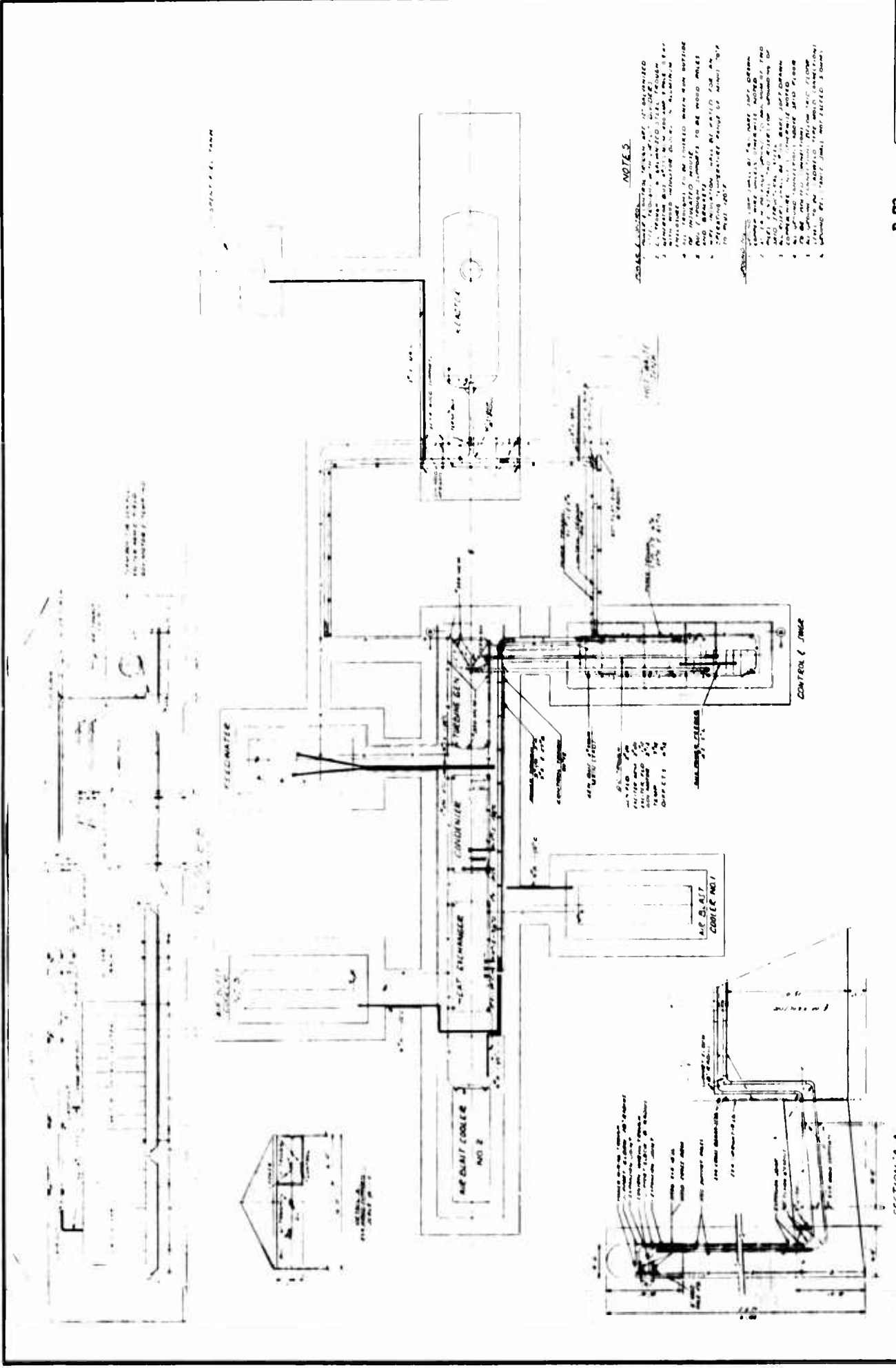
SECTION-A-A
DWG NO. W212



SECTION-C-C
DWG NO. W212


MCO PRODUCTS INC.
 A DIVISION OF
Pratt & Whitney Corporation
 10000 W. 10th Ave.
 MOBILE, ALA. 36688

20000 W. 10th Ave. MOBILE, ALA. 36688
 STATION
 PIPING SECTIONS
 MCO 212



NOTES

1. CONDENSER COILS TO BE 1 1/2" DIA. WITH 12" PITCH.
2. CONDENSER COILS TO BE 1 1/2" DIA. WITH 12" PITCH.
3. CONDENSER COILS TO BE 1 1/2" DIA. WITH 12" PITCH.
4. CONDENSER COILS TO BE 1 1/2" DIA. WITH 12" PITCH.
5. CONDENSER COILS TO BE 1 1/2" DIA. WITH 12" PITCH.
6. CONDENSER COILS TO BE 1 1/2" DIA. WITH 12" PITCH.
7. CONDENSER COILS TO BE 1 1/2" DIA. WITH 12" PITCH.
8. CONDENSER COILS TO BE 1 1/2" DIA. WITH 12" PITCH.
9. CONDENSER COILS TO BE 1 1/2" DIA. WITH 12" PITCH.
10. CONDENSER COILS TO BE 1 1/2" DIA. WITH 12" PITCH.

SECTION A-A
PAGE 57

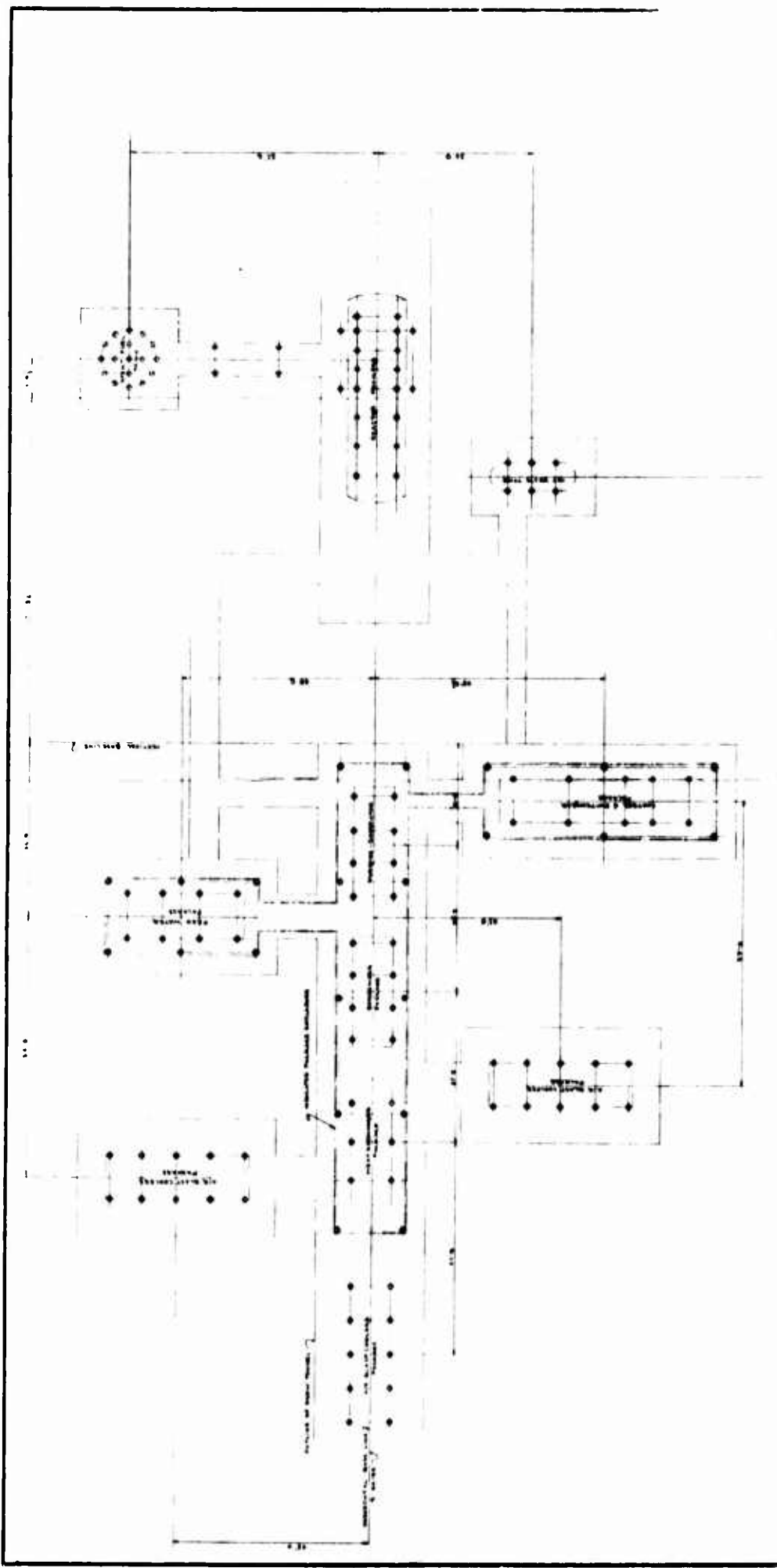
P-73

ALCO PRODUCTS, INC.
ALCO PRODUCTS, INC.
ALCO PRODUCTS, INC.

ALCO PRODUCTS, INC.
STATION
ELECTRICAL PLAN
ELECTRICAL PLAN

ALCO PRODUCTS, INC.
STATION
ELECTRICAL PLAN
ELECTRICAL PLAN

ALCO PRODUCTS, INC.
STATION
ELECTRICAL PLAN
ELECTRICAL PLAN



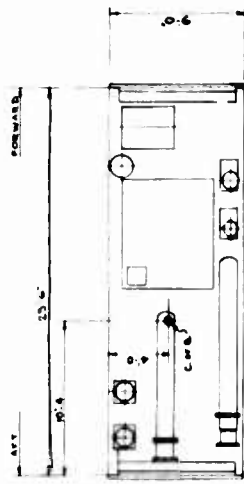
PLAN

ALL PILES SHOWN IN THIS DRAWING ARE OF THE TYPE SHOWN IN THE DRAWING

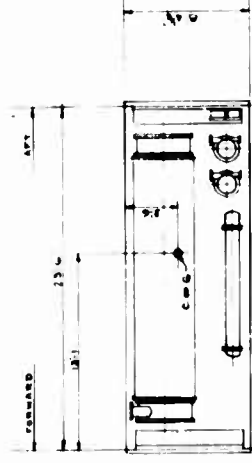
P-75

ALCO PRODUCTS, INC.
 1.00
 Peter B. Luthi
 Corporation
 MOORE

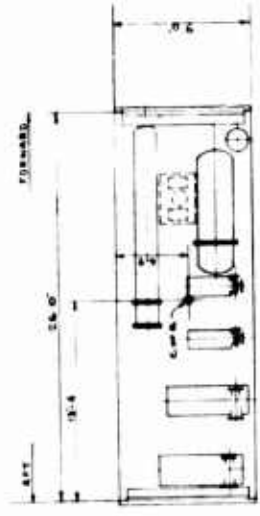
1000 W. PARKLAND AVENUE
 ALCO PRODUCTS, INC.
 SCHENECTADY, N.Y.
 O. WILSON
 1954



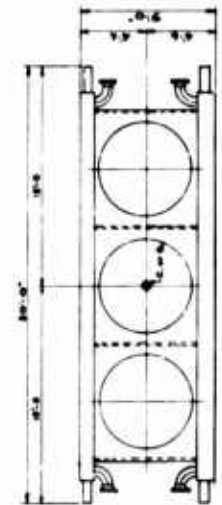
FEEDWATER SKID



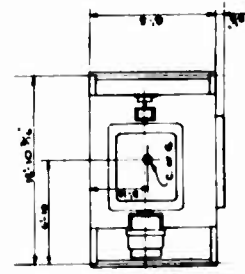
CONDENSER SKID



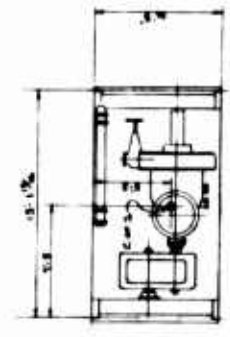
HEAT EXCHANGER SKID



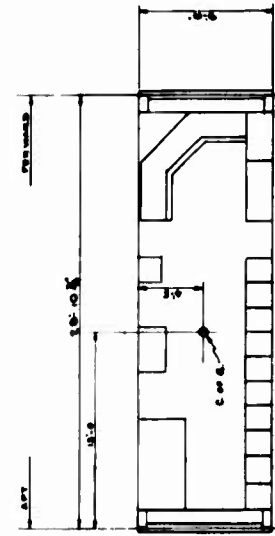
AIR BLAST COOLER SKID



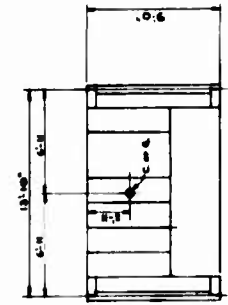
GENERATOR SKID



TURBINE SKID




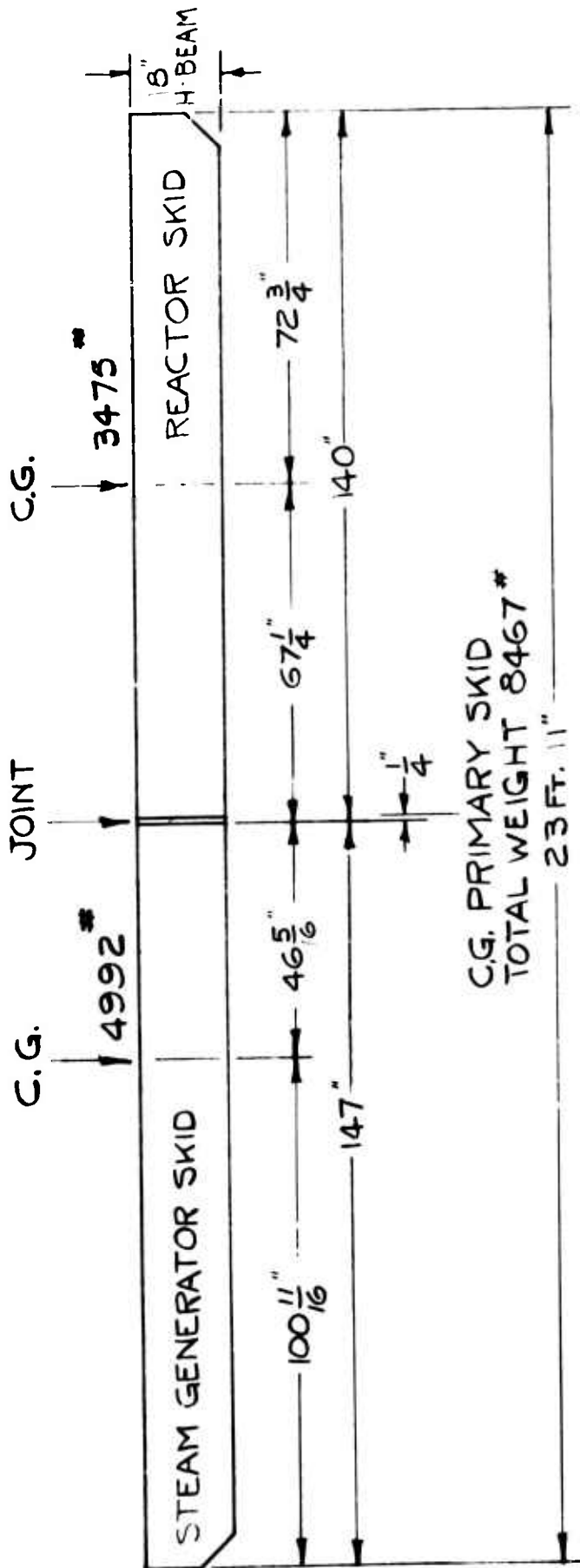
CONTROL SKID



SWITCH GEAR SKID

NOTE
CENTERS OF GRAVITY SHOWN ARE FOR
CARGO LOADING REQUIREMENTS ONLY.

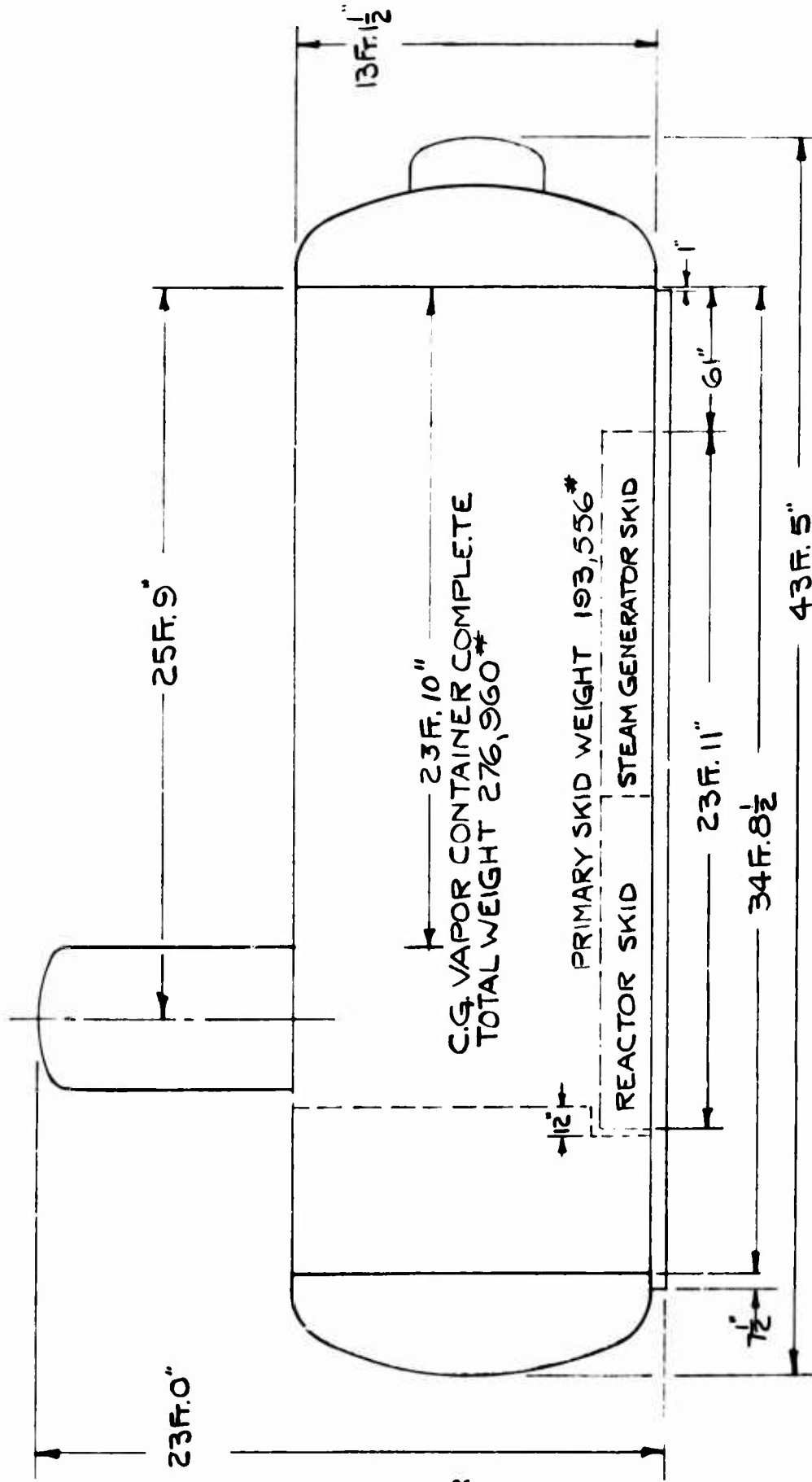
| | |
|--|---|
| ALCO PRODUCTS, INC. FRENCH CREEK, PA. CONTRACTORS, E. I. S. S. A. | |
|  Walter S. Gardner Corporation MANUFACTURERS OF SKIDS AND CONTAINERS 1000 W. 11th St., Erie, Pa. 16591, U.S.A. | |
| 2000 KW PACKAGED NUCLEAR POWER PLANT ALCO PRODUCTS, INC. ERIE, PA. | INDIVIDUAL PACKAGES CENTERS OF GRAVITY MOZ 57 11-10-58 11-10-58 |



PRIMARY SKID FOR
REACTOR & STEAM GENERATOR
WEIGHT DISTRIBUTION & CENTER OF GRAVITY

ALCO PRODUCTS INC.
SCHENECTADY, N.Y.
NOV. 21, 1958

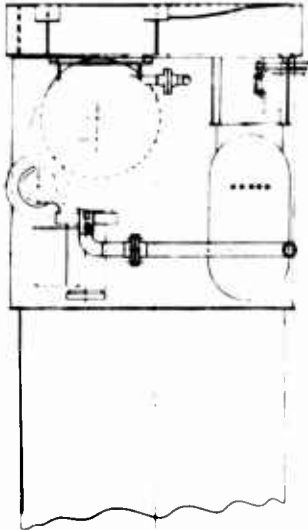
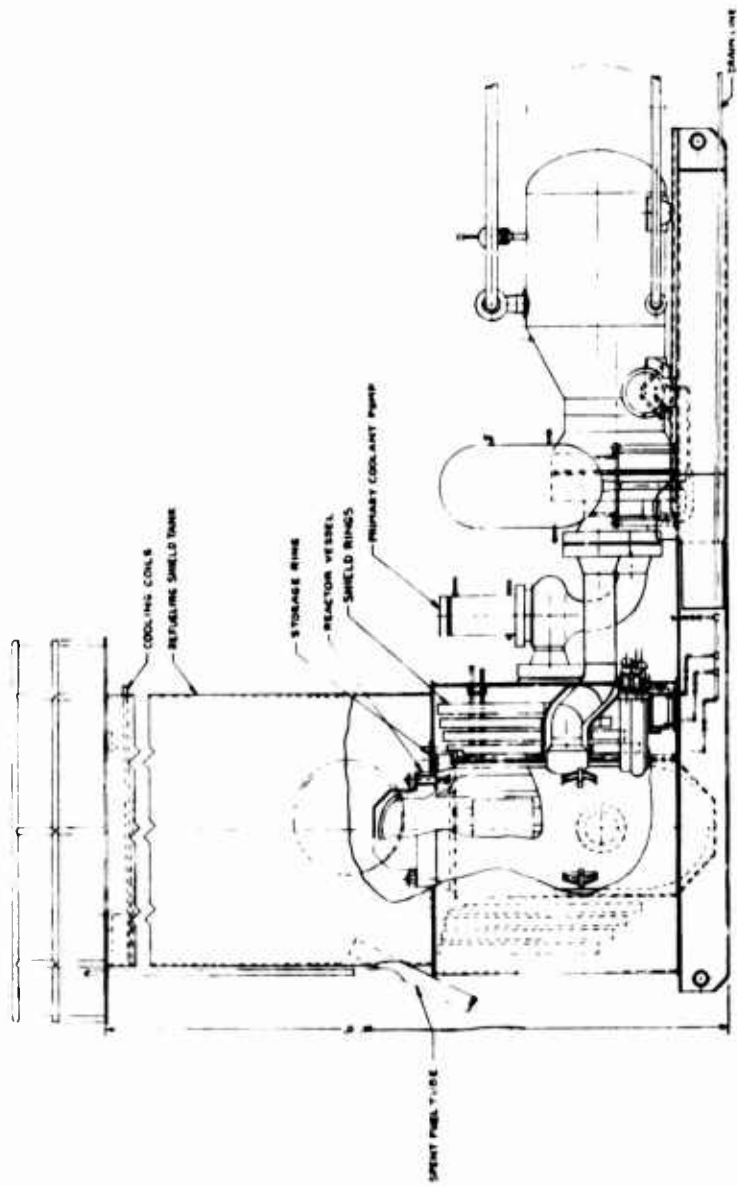
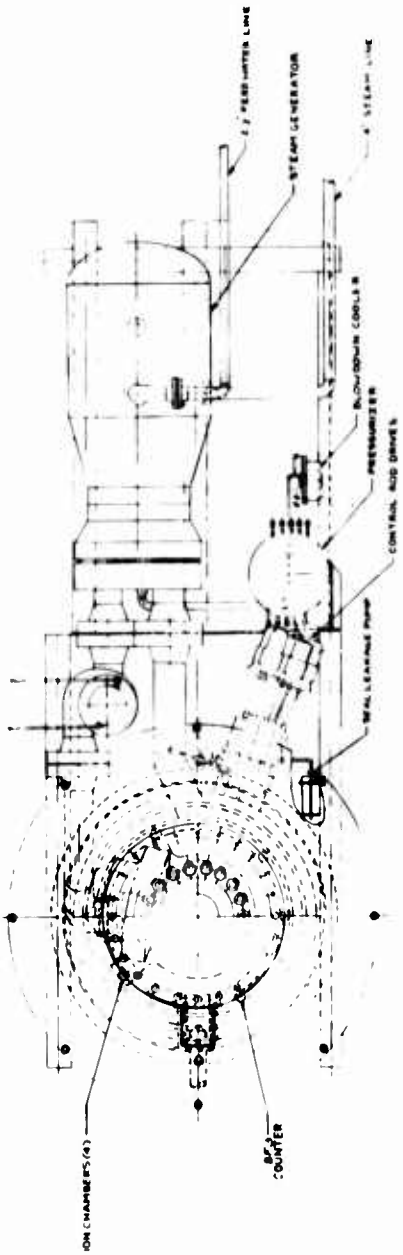
AES 268



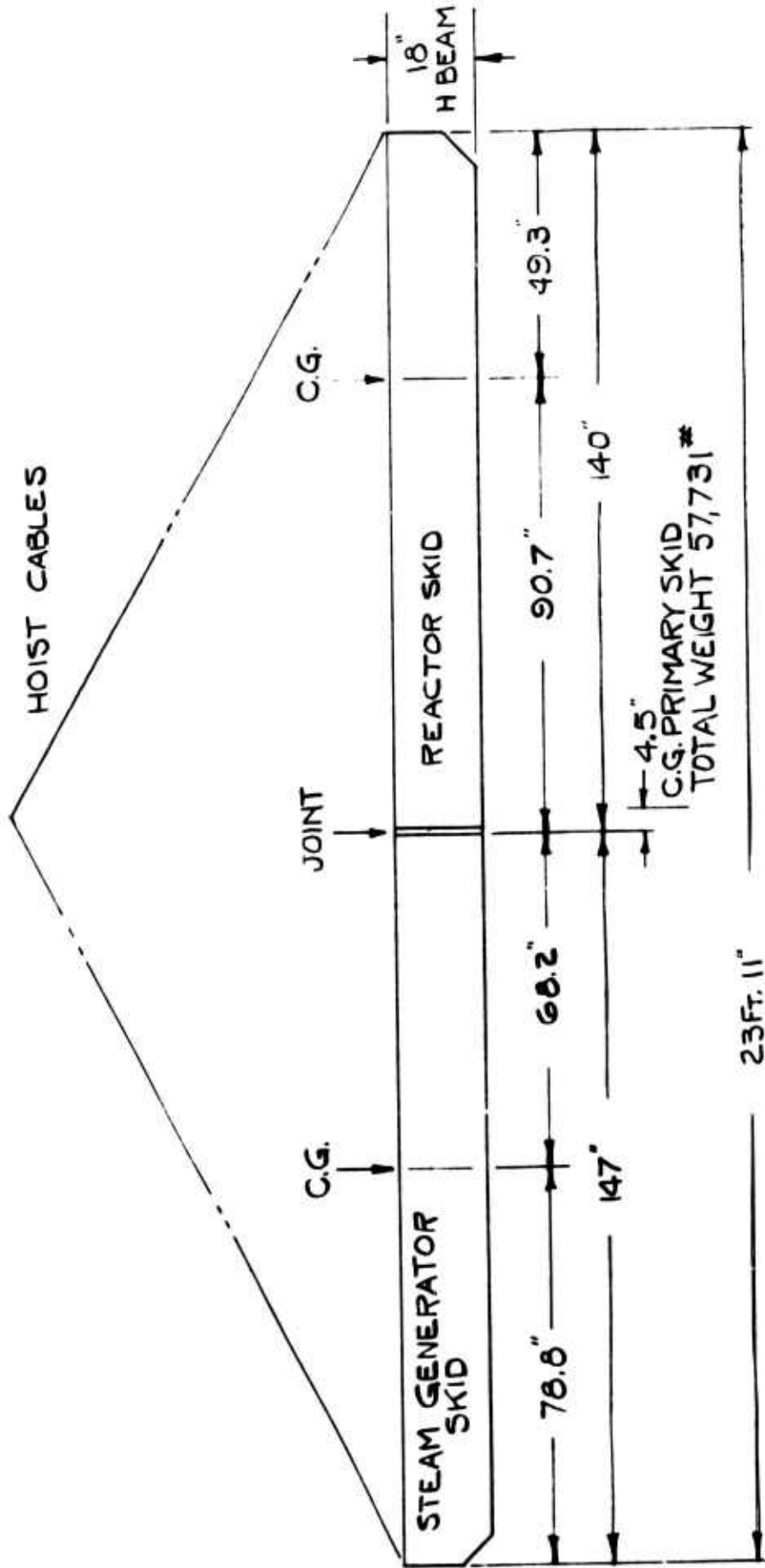
ALCO PRODUCTS INC.
 SCHENECTADY, N.Y.
 NOV. 21, 1958

AES 270

VAPOR CONTAINER COMPLETE
 WITH ALL COMPONENTS
 WEIGHT DISTRIBUTION & CENTER OF GRAVITY



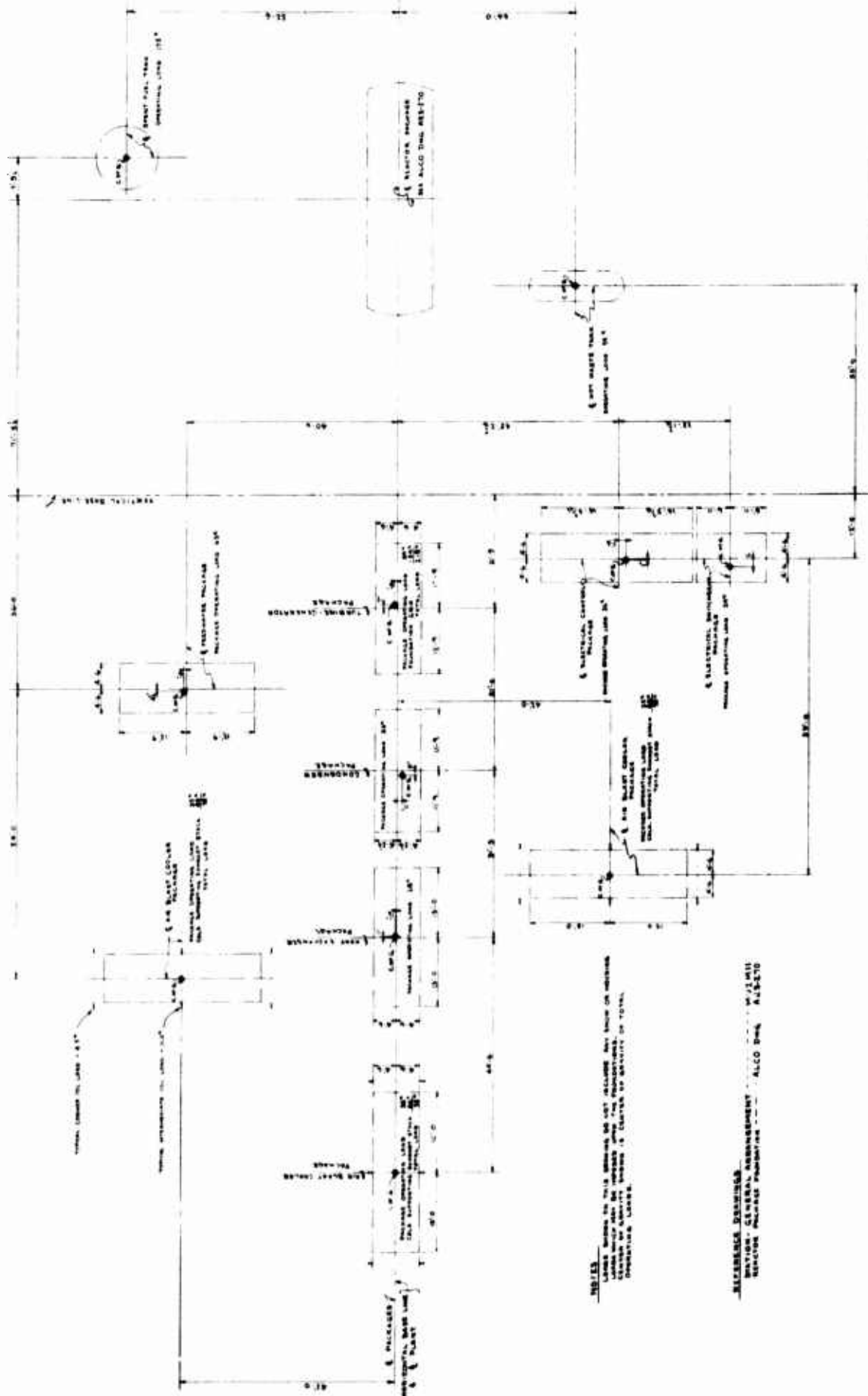
| | |
|-----------------------------|---------------------|
| ALCO PRODUCTS, INC. | |
| 1000 WEST 10TH AVENUE | |
| DENVER, COLORADO, U. S. A. | |
| DATE | 1/15/57 |
| BY | W. J. B. / J. W. B. |
| PRIMARY SYSTEM INSTALLATION | |
| R9-43-1005 | |



PRIMARY SKID WITH
 REACTOR & STEAM GENERATOR
 WEIGHT DISTRIBUTION & CENTER OF GRAVITY

ALCO PRODUCTS, INC.
 SCHEMECTADY, N.Y.
 NOV. 21, 1958

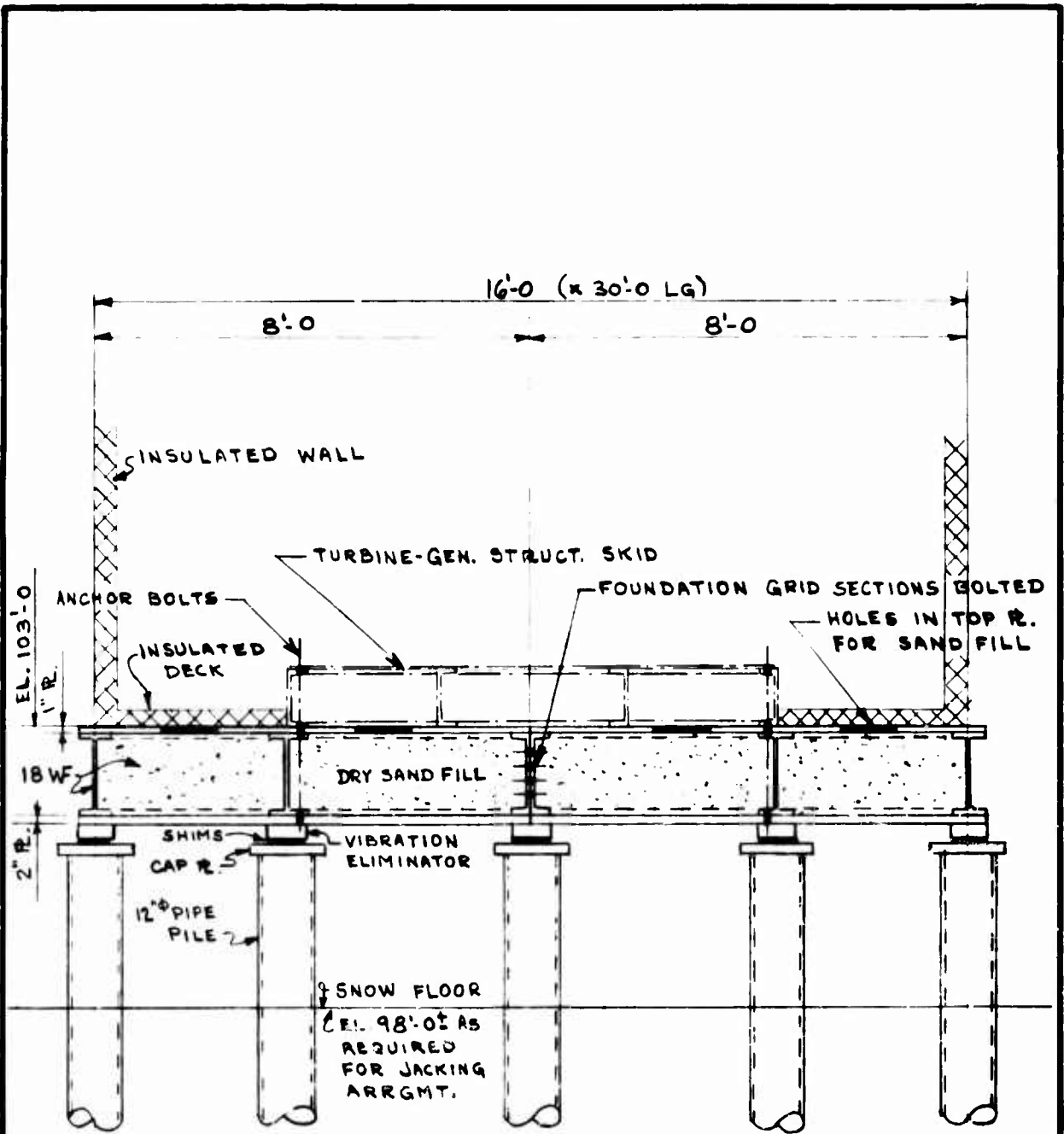
AES 269



NOTES
 1. LOADS SHOWN ON THIS DIAGRAM ARE THE ALLOWED AND NOT THE ACTUAL LOADS. THE ACTUAL LOADS SHOULD BE CHECKED BY A REGISTERED PROFESSIONAL ENGINEER.
 2. ALL DIMENSIONS ARE IN FEET AND INCHES UNLESS OTHERWISE SPECIFIED.

REFERENCE DRAWINGS
 FOUNDATIONS - ALCO DIST. A-15270
 STRUCTURAL - ALCO DIST. A-15270

| | | | |
|---|---------------|---|-------------|
| ALCO PRODUCTS, INC. ALCO DIST. A-15270 | | ALCO PRODUCTS, INC. ALCO DIST. A-15270 | |
| EDGEMAN NUCLEAR ALCO DIST. A-15270 | | FOUNDATIONS LOAD DIAGRAM | |
| ALCO PRODUCTS, INC. SHEPHERD, N. Y. | | Peter J. Korfus Corporation | |
| Scale: 1/4" = 1'-0" | Date: 12-1-58 | Sheet: 10258 | Proj: 10258 |



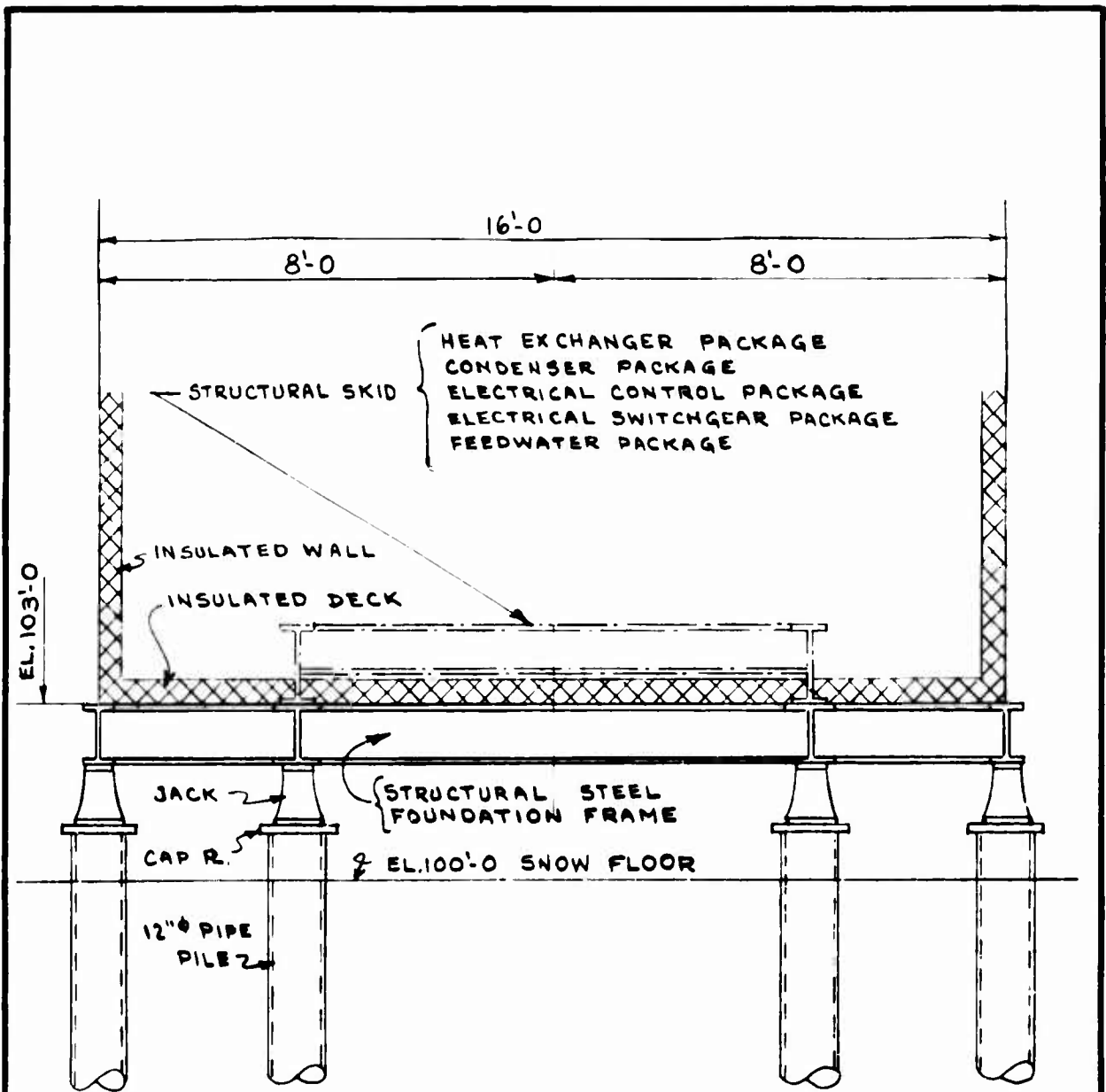
TYPICAL CROSS-SECTION THRU TURBINE-GENERATOR FOUNDATION

SAND FILL TO BE COMPACTED BY VIBRATION.

FOUNDATION GRID OF STEEL RS. & STRUCTURAL MEMBERS TO BE SHOP WELDED IN SECTIONS SUITABLE FOR AIR SHIPMENT—SECTIONS BOLTED TOGETHER IN FIELD.

ALCO PRODUCTS, INC.
ATOMIC ENERGY DEPT.

| | | |
|--|---|---|
| 2000 K.W. PACKAGED NUCLEAR POWER PLANT ALCO PRODUCTS INC. SCHENECTADY, N.Y. | TURBINE-GENERATOR PACKAGE TYPICAL FOUNDATION SECTION | Peter F. Loftus Corporation PITTSBURGH • PENNSYLVANIA • U.S.A. |
| DRAWN ROMRS | APPROVED <i>BEM</i> | DATE 12-4-58 |
| | | SCALE $\frac{3}{8}'' = 1'-0$ |
| | | M0259 |



FOUNDATION FRAME TO BE SHOP WELDED IN SECTIONS SUITABLE FOR AIR SHIPMENT - SECTIONS BOLTED TOGETHER IN FIELD.

ALCO PRODUCTS, INC.
ATOMIC ENERGY DEPT.

2000 K.W. PACKAGED NUCLEAR
POWER PLANT
ALCO PRODUCTS INC.
SCHENECTADY, N.Y.

TYPICAL PACKAGE FOUNDATION
CROSS-SECTION

Peter f. Loftus
Corporation
PITTSBURGH · PENNSYLVANIA · U.S.A.

DRAWN
ROHRS

APPROVED
[Signature]

DATE 12-4-58

SCALE 3/8" = 1'-0

M02510

SKID MOUNTED DESIGN ANALYSIS

INDEX

| | |
|-----------|--|
| SECTION A | General Description of Secondary Packages |
| 1.0 | Reactor Vessel |
| 1.1 | Description |
| 1.2 | Design Data |
| 1.3 | Thermal Shield Requirements |
| 1.4 | Closure Design |
| 1.5 | Control Rod Drive Penetration |
| 1.6 | Insulation and Jacket |
| 2.0 | Description of the Skid Mounted Core |
| 2.1 | Core Description |
| 2.1.1 | Fuel Element Description |
| 2.2 | Material and Nuclear Parameters |
| 2.3 | Startup Neutron Source |
| 2.4 | Spent Fuel Pit Criticality |
| 2.5 | Core Thermal and Hydraulic Design Analysis |
| 2.5.1 | Thermal Analysis |
| 2.5.2 | Ratio of Operating to Burnout Heat Flux |
| 2.5.3 | Thermal Stress in Fuel Elements |
| 2.5.4 | Thermal Stress in Pressure Vessel |
| 2.5.5 | Fuel Plate Deflection |
| 3.0 | Control Rod Drives |
| 4.0 | Steam Generator |
| 4.1 | Description |
| 4.2 | Selection of Horizontal |
| 4.3 | Operating and Design Conditions |
| 4.4 | Construction and Maintenance Features |
| 5.0 | Primary Loop Pressure Drop |
| 5.1 | Piping |
| 5.2 | Steam Generator |
| 5.3 | Reactor Vessel and Core Pressure Drop |
| 5.4 | Total Drop in Primary Loop |
| 6.0 | Primary Coolant Pump |
| 6.1 | Description |
| 6.2 | Design and Operating Data |
| 7.0 | Pressurizer |
| 7.1 | Description |
| 7.2 | Volume Requirements |

- 8.0 Primary Piping
 - 8.1 Description
 - 8.2 Operating Conditions and Design Data
 - 8.3 Flanging and Gasket Description

- 9.0 Shielding
 - 9.1 Primary Shielding
 - 9.1.1 Shutdown Dose Rate
 - 9.1.2 Operating Dose Rate
 - 9.2 Secondary Shielding
 - 9.3 Spent Fuel Shielding
 - 9.3.1 Water Tank Above Core
 - 9.3.2 Shielding Spent Fuel Pit
 - 9.3.3 Shipping Cask
 - 9.4 Demineralizer Shielding
 - 9.5 Waste Tank Shielding
 - 9.6 Cooling Provisions in Reactor Lower Shield Tank

- 10.0 Primary Skid Design
 - 10.1 Components on Primary Skid
 - 10.2 Design Features
 - 10.2.1 Provisions for Air Transportability
 - 10.2.2 Total Weights and Size of Complete Skid and Sections
 - 10.2.3 Description of Skid Bases

- 11.0 Vapor Container
 - 11.1 General Description
 - 11.2 Normal Operating Temperatures
 - 11.3 Vapor Container Design Conditions
 - 11.4 Fabrication Features and Materials
 - 11.5 Upper Shield Tank
 - 11.5.1 Description and Material
 - 11.5.2 Reactor Vessel Cover Storage Provisions
 - 11.5.3 Shielding Water Depth Requirements
 - 11.5.4 Provisions for Cooling
 - 11.6 Spent Fuel Tank
 - 11.6.1 Descriptions and Materials
 - 11.6.2 Cooling Provisions
 - 11.6.3 Transfer of Spent Fuel Elements
 - 11.7 Vapor Container Penetrations
 - 11.8 Space Cooler Requirements
 - 11.9 Insulation Requirements
 - 11.10 Decay Heat Removal Analysis

- 11.10.1 Decay Heat Removal Provisions
- 11.10.2 Sizing of Cooling Coil
- 11.10.3 Analysis of the Decay Heat Removal System
 - 11.10.3.1 Analysis of the Heat Removal System
 - 11.10.3.1.1 Analog Kinetic Model
 - 11.10.3.1.2 Plant Operating Constants
 - 11.10.3.1.3 Time and Amplitude Scaling Factors
 - 11.10.3.1.4 Potentiometer Settings
 - 11.10.3.1.5 Analog Circuit Diagram
 - 11.10.3.2 Results of the Analog Analysis
- 11.10.4 Reverse Flow Analysis
- 11.10.5 Results and Conclusions
- 11.10.6 References
- 11.11 Air Filtering
- 12.0 Fuel Handling Tools
 - 12.1 Description
 - 12.2 Fuel Element Handling System and Procedure
- 13.0 Primary System Instrumentation
 - 13.1 Design Considerations and Description of System
 - 13.2 Electro-Hydraulic Control Valves
 - 13.3 Radiation Monitoring
 - 13.4 Nuclear Instrumentation
 - 13.5 Startup Considerations
 - 13.6 Interlocks and Scram Actions
 - 13.7 Control Console
 - 13.7.1 General
 - 13.7.2 Primary System Instruments
 - 13.7.3 Nuclear Instruments
 - 13.7.4 Secondary Instruments
 - 13.7.5 Console Construction
 - 13.7.6 Annunciator
 - 13.7.7 Reactor Rod Control and Indication
 - 13.8 External Wiring
 - 13.8.1 Wireways
 - 13.8.2 Cables
- 14.0 Primary Purification and Make-up System
 - 14.1 Functional Requirements
 - 14.2 Summary Description of System
 - 14.3 Design Requirements
 - 14.4 System Design Data
 - 14.5 Detailed Description of Equipment and Components
 - 14.5.1 Purification Heat Exchanger (Blowdown Cooler)
 - 14.5.2 Pressure Reducing - Flow Control Station
 - 14.5.3 Demineralizer
 - 14.5.4 Purification Filter

- 14.5.5 Primary Make-up Tank
 - 14.5.6 Primary Make-up Pump
 - 14.5.7 Hydrogen Addition Flask
 - 14.6 Boron Injection
 - 14.6.1 Poison Tank
 - 14.7 Seal Leakage System
 - 14.7.1 Seal Leakage Tank
 - 14.7.2 Seal Leakage Pump
 - 14.8 Spent Fuel Tank Recirculating Equipment
 - 14.9 Initial Fill
 - 14.10 Activity Buildup Considerations
- 15.0 Waste Disposal System
- 15.1 Functional Requirements
 - 15.2 Summary Description of System
 - 15.3 Design Requirements

SKID MOUNTED DESIGN ANALYSIS

INDEX

SECTION A

DRAWINGS

| <u>Drawing Number</u> | <u>Title</u> | <u>Page Number</u> |
|-----------------------|-------------------------------------|--------------------|
| AEL 389 | Reactor Vessel | A-97 |
| R9-15-1002 | Core Support Structure | A-99 |
| R9-11-1018 | Control Rod Drives | A-101 |
| R9-45-1023) | Fuel Handling Tools | A-103 |
| D9-45-1025) | | A-105 |
| R9-46-1039 | Shield Rings and Shield Tank | A-107 |
| R9-47-1013 | Primary System Skid Arrangement | A-109 |
| R9-42-1001 | Skid Assembly | A-111 |
| R9-43-1002 | Vapor Container and Spent Fuel Tank | A-113 |
| R9-47-1011 | Control Console | A-115 |
| D47210-1 | Pressurizer | A-117 |
| H 47210-3-1 | Steam Generator | A-119 |
| D9-48-2035 | Basket-Fuel Element Shipping Cask | A-121 |
| R9-48-2036 | Spent Fuel Shipping Cask | A-123 |
| D9-13-2094 | Absorber | A-125 |
| R9-13-2075 | Fuel Element (Stationary) | A-127 |
| D9-13-2007 | Fuel Plates (Stationary) | A-129 |
| D9-13-2073 | Fuel Plates (Control Rod) | A-131 |
| D9-13-1011 | Fuel Element (Control Rod) | A-133 |
| D9-13-2092 | Absorber Plate (Drilled) | A-135 |

1.0 Reactor Vessel (Drawing No. AEL 389)

1.1 Description

The reactor vessel drawing AEL 389 has been designed in accordance with Case 1234 of the ASME Unfired Pressure Vessel Code which refers to vessels subject to gamma radiation. The cover flange, shell flange, shell and nozzles are low alloy steel forgings overlaid with stainless steel. Dished stainless clad heads provide the end closures. A removable cover at the top provides access to the vessel core. The lower portion of the vessel contains penetrations and mounting provisions for the five control rod drive mechanisms.

The coolant nozzles are located below the active core of the reactor. The mounting flange for the core structure is located between the nozzles and, with the core structure, becomes the flow divider between the inlet and outlet chambers of the vessel. The coolant enters the vessel through the lower nozzle, flows upward through the core, down between the thermal shield and the vessel wall and out of the vessel through the upper nozzle. A certain portion is bypassed between the core and the thermal shield to provide adequate cooling of the thermal shield. The core support plate is mounted on brackets attached to the vessel wall. Provision is made by dowels and bolting to properly secure the support plate, still leaving freedom for differential thermal expansion between the vessel and support plate.

Low alloy carbon steel, clad with type 304 stainless steel, has been selected for the vessel material.

1.2 Design Data

| | |
|---------------------------------------|--------------|
| Design Pressure | 2000 psi |
| Design Temperature | 600°F. |
| Design Stress | 17500 psi |
| Wall Thickness | 2-3/8 in. |
| Overall Length of vessel | 125-5/16 in. |
| Overall Length of vessel without head | 102-5/16 in. |
| Inside diameter of vessel | 37-3/4 in. |
| Insulation thickness | 2 in. |

1.3 Thermal Shield Requirements

A single two inch thick thermal shield has been added to keep the thermal stress at the vessel wall to a level consistent with Code Case 1234 which allows thermal stress to be up to 50% of the pressure stress.

1.4 Closure Design

The reactor cover is secured in place by 18 - 2-3/4 diameter studs and nuts. The pressure seal is made by use of an octagonal dead soft stainless steel ring. This type of closure has been used on APFR-1 and has given excellent service.

1.5 Control Rod Drive Penetration

To provide penetration of the control rod drive tubes through the shield tank a water jacket is provided. This jacket consists of 5 inch diameter tubes surrounding the drive tubes with flanges at each end. These flanges are welded to the shield tank inner and outer walls at assembly of the reactor vessel in the shield tank. This method of construction eliminates the need for a separate water box as used in APFR-1.

1.6 Insulation and Jacket

The entire vessel and cover are encased in a stainless steel jacket to minimize heat losses from the vessel. The two inch space between the vessel and jacket is filled with glass wool insulation.

2.0 Description of the Skid Mounted Core

2.1 Core Description

The skid mounted core is composed of 32 fixed fuel elements of APFR-1 Core II Specifications, 5 control rod fuel elements of APFR-1 Core II specifications, and 5 boron absorber sections of APFR-1 Core I specification. These elements are arranged in the basic 7 x 7 element array of APFR-1 with three elements missing in each corner. This results in a core which has an equivalent diameter of 20.16 inches and an active height of 22 inches. The arrangement of the 37 elements in the core support structure and control rod baskets is very similar to that of the APFR-1 which has proven itself from all viewpoints.

2.1.1 Fuel Element Description

Each stationary fuel element consists of 18 fuel plates 0.020" x 2.50" x 22" with 0.005" thick stainless steel cladding on each side of the plate. The water gap between plates is 0.133". The control rod fuel element plates are 0.020" x 2.281" x 21.125" with 0.005" steel cladding. There are only 16 plates to a control rod fuel element. The water gap is also 0.133". A flux suppressor 0.020" x 2.281" x 0.875" is above the control rod fuel element meat. It consists of 1 gm of europium in the form of Eu_2O_3 dispersed in a low cobalt stainless steel.

2.2 Material and Nuclear Parameters

The material composition of the core includes 18.5 kg of U-235, 16.7 gm of B^{10} , 172.1 kg of S.S., and 91.5 kg of H_2O . The core will provide 10th MW of power for one year at 0.8 load factor. There is a negative temperature coefficient of reactivity at all temperatures which keeps the core stable during changes in the power level ($-3.4 \times 10^{-4} \text{ } ^\circ\text{F}^{-1}$ at 512 $^\circ\text{F}$). The maximum reactivity occurs at the beginning of operation and decreases with core lifetime.

More extensive nuclear parameter data is given in a following section of this report. From the wealth of experimental data on the APPR-1, the characteristics and core performance of the skid mounted reactor can be accurately determined.

2.3 Startup Neutron Source

The startup neutron sources incorporated in the skid mounted core are:

1. a 15 curie Po-Be source
2. a 0.5" x 3" x 12" Beryllium block, a "photoneutron" source utilizing gamma radiation from fission products.

The combination of these neutron sources will insure a sufficiently large count rate at the neutron counters. In order to insure a safe startup, the sources are designed to achieve 10 counts per second at all times. The Po-Be source gives 32 counts per second at the start of core life. This falls off during core lifetime, and therefore a photoneutron source consisting of a beryllium block was added. The count rate at 1000 hours of operation and 10 days shutdown from the photoneutron source is 131 counts per second. At the end of core life, the photoneutron source gives a count rate of 43 counts per second.

A new Po-Be source must be used everytime a new core is inserted into the reactor.

2.4 Spent Fuel Pit Criticality

Calculations were performed to determine the criticality of a spent core in the spent fuel pit. The reactivity in the spent fuel pit criticality must at no time be greater than 0.70.

To insure sub-criticality of the spent fuel pit, the stored fuel element should be placed in individual cells of a lattice possessing the following characteristics.

1. Minimum height of lattice is equal to that of the active fuel element height with element in stored position.
2. Lattice material consists of 1% boron steel in 1/4" plates.
3. Center to center dimension of an individual cell is 3.5".
4. For shielding and cooling purposes the entire pit is filled with water.

The reactivity of such a spent fuel pit loaded to maximum capacity (52 elements) with fresh APPR-1 type elements will not exceed 0.70 and hence pose no criticality problem.

2.5 Core Thermal and Hydraulic Design Analysis

2.5.1 Thermal Analysis

The core thermal analysis is the determination of the core flow requirements. The skid mounted reactor has been designed thermally so that the maximum surface temperature in the hot channel does not exceed the saturation temperature at the system pressure. The coolant flow requirements calculations for each fuel element are minimized to the extent that the maximum surface temperature on the hottest plate is equal to the allowable surface temperature which in turn is less than the saturation temperature. The difference between maximum surface temperature and the saturation temperature is due to deviations in system pressure, core power, and inlet temperature. The thermal parameter for the cores of tailored and uniform flow is given in Table 2-1. As can be seen from Table 2-1, the tailoring of the flow through the skid mounted core would save only 102 gpm or about 2% of the total flow. Therefore, it was decided to use uniform flow.

2.5.2 Ratio of Operating to Burnout Heat Flux

In the case of pressurized water reactor, the specific power is proportional to the thermal neutron flux. As the power is increased, the increased heat flux will cause only a moderate rise in the surface temperature of the fuel element. However, if the heat flux increased to a certain value (burnout heat flux), the surface temperature of the fuel element will suddenly jump to about 1500° F. or greater. Since conventional structural materials cannot withstand such temperatures, there will be almost instantaneous failure or burnout of the fuel element. In order to determine if the reactor is safe, the ratio of the operating heat flux to burnout heat flux must be known. For the skid mounted core, the ratios are as follows:

Fixed Fuel Element:

$$\frac{\phi_{OP}}{\phi_{BO}} = 0.1489$$

TABLE 2 - 1

THERMAL PARAMETER

| | CASE | |
|--|---------------|--------------|
| | Tailored Flow | Uniform Flow |
| Inlet Temperature - °F | 500 | 500 |
| Outlet temperature - °F | 518.1 | 517.6 |
| Maximum plate surface temperature - °F | 610 | 610 |
| Flow of Coolant | | |
| Fixed fuel element gpm/element | - | 98.5 |
| Control rod fuel element gpm/element | 94.5 | 94.5 |

| | | |
|-------------------------------|-------|------|
| Element type 34 gpm/element | 98.5 | - |
| Element type 33 - gpm/element | 97.0 | - |
| Element type 23 - gpm/element | 87.5 | - |
| Element type 22 - gpm/element | 98.0 | - |
| Latticeflow gpm | 594.3 | 595 |
| Total flow gpm | 4117 | 4219 |

Control Rod Fuel Element:

$$\frac{\phi_{OP}}{\phi_{80}} = 0.1474$$

From this it can be concluded that the operating heat flux in all elements is low enough to provide a safe margin against abnormal power excursion.

2.5.3 Thermal Stress in Fuel Elements

The maximum internal plate temperature is calculated and is of interest for the determination of the thermal stress in the elements. The maximum temperature was found to be 632.3 F. From the temperature distribution in the hot element, the maximum thermal stress in the element is 22,490 psi. The calculated thermal stress for APFR-1 elements is 28,300 psi. Since the APFR-1 has operated satisfactorily, it can be concluded that the skid mounted reactor will also operate satisfactory.

2.5.4 Thermal Stress in Pressure Vessel

The pressure vessel is constructed of carbon steel with a stainless steel cladding of 1/8 inch on the inside surface. The outside diameter of the vessel is 42.75 inches and the thickness is 2-3/8 inches. In order to calculate the thermal stress in the vessel, the heat generation and the temperature difference across the vessel wall must be known. The heat generation in the vessel wall is described by the following equation:

$$H(\text{BTU}/\text{IN}^3\text{-SEC}) = 0.0185C^{-0.674X}$$

The temperature difference across the vessel wall is 46.9 F and the thermal stress in the vessel is 6800 psi. The allowable thermal stress for the carbon steel vessel is 8750 psi. Therefore, the vessel conforms to code regulations.

2.5.5 Fuel Plate Deflection

The maximum pressure differential is based on the allowable deflection in fuel plates that can be tolerated. If this deflection becomes greater than the allowable tolerance, burnout may result. For the skid mounted core, the maximum pressure differential is 3 psi. The calculated pressure differential is 0.12 and 0.03 psi for tailored and uniform flow respectively.

3.0 Control Rod Drives (Drawing No. R9-11-1018)

The control rod drive mechanisms are identical with minor modifications to those used so successfully in APFR-1 and being built for APFR-1a. They are of similar type to the Alco built drives now in operation in ALPR and the back up prototype for EBWR which has been thoroughly tested at ANL. Alco is now building similar drives for ACF for the Elk River Boiling Water Reactor.

Basically the drive consists of a rack and pinion with associated shafting inside the primary system, a mechanical seal to control leakage of primary water where the drive shaft penetrates the reactor vessel wall, and the external assembly comprising the position indication mechanism, emergency scram clutch, an accelerating spring and drive motor. The torque capacity of the clutch exceeds that necessary to raise the control rods by a factor of nearly 3. A shear element is provided at the motor to protect the mechanism from excessive torques resulting from possible malfunction of the limit switches, improper installations, etc. Torque capacity of nearly ten times that necessary to raise the rods is provided at this point and all other component stresses have safety factors well above this.

Driving speed of the rods, both up and down, is 3" per minute. Release time of the scram clutch is approximately 50 milliseconds and acceleration of the rods in the downward direction is ample to insert negative reactivity at a rate sufficient to shutdown the reactor on an emergency basis under both steady and transient power conditions.

An accelerating spring has been added to the basic APFR-1 drive to provide an additional downward force on the control rod during scram. While the overall control rod weight has been reduced from the 72 lbs of APFR-1 to 45.5 lbs. there has also been a considerable reduction in the pressure drop across the core which acts against the rod in scrambling. The net result shows a slight decrease in scram time (.4 g for APFR-1 vs. .37 g) for a free falling rod. It was therefore deemed prudent to incorporate the accelerating spring mechanism of APFR-1a but using a lighter spring of approximately 20 lbs to give a resultant rod acceleration of approximately .7g. This type spring mechanism has been installed with good results on the Alco built ALPR rod drives now in operation at Arco.

Rod position indication is by means of 2 synchros which are gear driven on the rod side of the scram clutch. Thus, position indication is positive for both normal operation and after a scram. Rod position can be read within less than 0.050". Limit switches are provided to prevent overtravel in both the full up and full down positions.

The seal is an all-metallic unit of the floating ring labyrinth type. Leakage under operating conditions is approximately 3 lbs. per hour per seal and has remained essentially constant over long operating periods in APFR-1 without maintenance. Makeup water is provided under pressure to the reactor side of the seals so that leakage from the seals is essentially pure makeup water which is returned to the demineralizers for reuse in the system.

All elements of the drive system external to the reactor vessel, including the seal, can be removed for maintenance or replacement without draining or depressurizing the primary system. All adjustment of the limit switches, synchros, etc., can be made on the bench prior to installation to minimize the time required for replacement of drive components in the pit. Drive motor is conventional, commercially available three phase unit with integral spur gear reduction.

Bearings, motor, tear box and other components external to the reactor vessel employ conventional lubricants and insulation. Structural parts external to the reactor vessel are made of stainless steel or other corrosion-resistant material to permit operation in high humidity atmospheres without experiencing damaging corrosion. All parts and components are interchangeable without shimming or fitting or installation.

4.0 Steam Generator

4.1 Description

As shown in the accompanying drawings, the steam generator is a kettle-type unit, a U-bend, double pass, tube-in-shell, heat exchanger, horizontally mounted. Overall dimensions are 11' - 7 $\frac{1}{2}$ " long and 4' - 2 - 5/8" wide (exclusive of side nozzles and support attachments). Dry weight is 17,600 lbs. and flooded weight is 22,850 lbs.

4.2 Selection of Horizontal

The kettle-type design has been selected because it employs fully understood technology and poses no difficult or unanticipated stress concentration problems, such as occur with risers when a separating drum is used. Also, fabrication is more economical and quicker. The only other type worth considering is the vertical type, and for this particular installation, the 9' dimension limitation does not make it practical. Similarly, final field welding under Arctic conditions did not seem practical.

4.3 Operating and Design Conditions

Steam purity from the steam generator is 98%. This is readily accomplished in the kettle-type and is allowable here because of the line dryer being installed immediately before the turbine throttle valve. The separator built into the generator is the simplest type of dry pipe.

Tube side operating conditions are 1750 p.s.i.g., 518^oF. in and 500^oF. out. Shell side operating conditions are 465 p.s.i.g., 306^oF. in and 463^oF. out. Vapor generation rate is 37,055 lbs. per hour with a continuous blow-down of about 400 lbs. per hour.

Tube side design conditions are 2000 p.s.i.g. and 600^oF. Shell side design conditions are 800 p.s.i.g. and 600^oF. Test pressures are at 50% above design ratings.

In general, for the steam generator the following additional operating requirements hold:

| | |
|---------------|--------------------|
| Heat Load | 35,000,000 Btu/hr. |
| Primary Flow | 4240 GPM |
| Pressure Drop | 13 ft. (tube side) |

4.4 Construction and Maintenance Features

Material specifications are shown on Drawing No. H 47210-3-2. A bolted cover is used on the channel end and the primary fluid is retained within a permanently welded gasket, assuring full integrity of the system. The advantage of this bolted head over a welded one is better access to tubes for inspection and repair, since working through the small openings is impractical both for fabrication and field servicing.

Finally, further economy is possible by fabricating the channels, tube sheet and primary fluid nozzles of carbon steel overlaid with Type 304 S.S. Welding the tube sheet to the shell, and the tubes to the overlay, is then possible without encountering any bi-metallic weld problem.

5.0 Primary Loop Pressure Drop

The following calculations have been made for the total pressure drop in the primary coolant loop. Pressure drops for the active core and steam generator tube section have been determined elsewhere and the results only are presented here.

Pressure drops through the various fittings and restrictions of the loop were determined by obtaining velocity head loss coefficients to apply to the local velocity head. Sources used for these coefficients were "The Reactor Handbook", Volume Two and J. K. Vennard "Elementary Fluid Mechanics".

The primary loop can be divided into three major sections: piping, reactor vessel, and steam generator. A summary of the loop pressure losses is presented in Table 5-1.

5.1 Piping

Flow of 4240 gpm in 10 inch schedule 120 pipe develops a velocity head of 6.90 feet of fluid. Piping losses were subdivided into the friction loss and fitting loss. Fittings included:

1 - 90 deg. L.R. ell, 1 - 90 deg. S.R. ell, 2 - 45 deg. L.R. ells
and 1 - 45 deg. S.R. ell.

5.2 Steam Generator

Pressure drop through this steam generator was divided into entrance

and exit losses and tube friction loss. The tube friction loss has been determined elsewhere. Entrance and exit losses were based on abrupt expansion and contraction losses respectively.

5.3 Reactor Vessel and Core Pressure Drop

Entrance: the entrance loss to the reactor vessel was examined in two parts; the conical diffuser section and the abrupt expansion into the lower plenum chamber. The abrupt expansion loss was assumed to be the total velocity head at that point.

Core: See Sec. B. IV 7.2

Annulus: The contraction outside the top of the thermal shield was treated as an abrupt entrance and a gradual enlargement with the pressure drop based on the local velocity head.

Exit: The reactor vessel exit loss was considered due to an abrupt contraction from an infinite area with a correction for the rounded edges.

5.4 Total Drop in Primary Loop

Table 5-1 indicates a total loop head loss of 39.3 feet. This result is slightly conservative since no correction was made for the close proximity of various fittings. Also the assumption of total velocity head loss at the reactor vessel entrance may be slightly conservative since some velocity will be maintained in the plenum chamber.

TABLE 5-1

Pressure Lossed in Primary Coolant Loop

| LOCATION | HEAD LOSS (ft.H ₂ O) |
|-----------------------------------|------------------------------------|
| Pipe Friction | 1.46 |
| Pipe Fittings | 5.25 |
| Reactor Entrance Nozzle Cone | 1.25 |
| Reactor Entrance Abrupt Expansion | 2.67 |
| Reactor Core | 5.07 |
| Thermal Shield Annulus | 2.56 |
| Reactor Vessel Exit | 2.62 |
| Steam Generator Entrance | 5.18 |
| Steam Generator Exit | 2.68 |
| Steam Generator Tubes | <u>13.5</u> |
| Loop Total | 42.3 |

6.0 Primary Coolant Pump

6.1 Description

Flow of the primary coolant is powered through an hermetically-sealed, integral liner - motor pump*, engineered and manufactured for zero leakage in nuclear power service. This unit is equipped with a double thrust bearing assembly in the top of the motor, the unit being vertically mounted. All parts in contact with the fluid are fabricated of Type 304 Stainless Steel. The canned motor is a 65 HP, 1800 RPM, 440 Volt, 3 phase, 60 cycle unit. Total weight of this equipment is 3700 lbs.

6.2 Design and Operating Data

Primary coolant pump operation is as follows:

Capacity 4240 GPM
Fluid Temperature 500°F
Pumping Head 43 ft. water
Normal System Pressure 1750 p.s.i.

The pump is to be capable of pumping the liquid at a temperature of 100°F. and the motor drive is sized accordingly.

7.0 Pressurizer - AEL - 348

The pressurizer is mounted in a vertical position in the primary loop and has the function of maintaining a constant system pressure, and to absorb the pressure variations caused by the changes in load on the system.

7.1 Description

The pressurizer is a cylindrical pressure vessel with hemispherical heads. It is designed in accordance with the ASME Unfired Pressure Vessel Code, using a material of stainless steel type 304. It has an inside diameter of 25-1/2 inches with a nominal wall thickness of 2-1/8 inches in the cylindrical portion and a nominal thickness of 1-1/4" in the hemispherical heads. The design pressure is 2000 psi at 650°F. The overall vessel length is 6'-0".

Steam saturation temperature and pressure is maintained by commercial type electric heaters mounted in individual heater wells located in the lower section of the pressurizer. The heater wells are sealed against system water making replacement of heaters possible without having to drain the primary systems. Twenty heaters, are arranged in two banks of 10 heaters each, having a total output of 30 KW, each heater producing 1.5 KW. Clearance between heater element and the wall of the heater well is held to a minimum to obtain a maximum heat transfer efficiency. The heaters are seated in the heater wells by weatherhead end connectors designed to withstand full system pressure should a leak occur in the heater well.

* Centrifugal Type

Normal operating pressure of the pressurizer is 1750 psi and operating temperature is approximately 620°F (saturation temperature).

7.2 Volume Requirements

The steam volume of the pressurizer is 12.1 cubic feet, and the liquid volume is 5.9 cubic feet under normal operating conditions, at full load. The normal liquid water level is approximately twelve (12) inches above the centerline of the lower row of heater well tubes. The variations in steam and liquid volumes, and transient conditions are covered in detail in Section B-III - 1.0

8.0 Primary Piping

8.1 Description

The components of the primary system are connected by 304 stainless steel pipe. Pipe runs and elbows are standard pipe with a nominal outside diameter of 10.75 inches and a nominal inside diameter of 9.064.

All pipe flanges are standard ASA weld neck type, made of 304 stainless steel. All welded connections are made in the shop using the consumable insert method. Ends of the pipe are machined and beveled on outside to permit full penetration welds. Reactor vessel nozzles are made of carbon steel with a type 304 stainless steel overlay. At the point of pipe and nozzle weld connection the nozzle has an extra heavy overlay so that all weld connections in the primary loop involve similar materials.

The pressurizer connection to the primary loop is made at the steam generator. This connection is a 2-1/2 inch schedule 80 304 stainless steel pipe.

The primary pump is connected into the primary loop using standard ASA weld neck type 304 stainless steel flanges. All breaks in the primary piping for skid shipment will take place only at the flanged connections at the steam generator. This involves two flange connections, one at the primary pump and one in the primary piping. Flange connections will eliminate all field welding of the relatively large primary piping.

8.2 Operating Conditions and Design Data

The primary piping design pressure is 2000 psi at 600°F and has been designed in accordance with the ASA code standards. The test pressure for the primary piping and flanging 2275 psi. The coolant flow rate through the primary loop is 4240 g.p.m. The actual operating pressure is 1750 psi and the core outlet temperature is 518°F.

8.3 Flanging and Gasket Description

The three weld neck flange bolted connections use 12 - 1-7/8 inch bolts. The gasket mean diameter is 12-3/4 inches and is of the octagonal type. It has a width of 5/8 inch and is made of dead soft type 304 stainless steel. This type gasket has been used with good success for the top vessel closure of APPR-1.

9.0 Shielding

The following sections contain a detailed description of shielding which has been designed for the skid mounted reactor.

9.1 Primary Shielding

The primary shielding of the skid mounted reactor is made up of concentric annuli of steel and water with the steel being covered with Boral. Boral is a dispersion of B_4C in aluminum; the boron absorbs thermal neutrons and therefore reduces activation and $n-\gamma$ reactions of the steel. In the shield tank there are four 3-1/4 inch steel rings sandwiched between 1/8 inch Boral sheets. The Boral-steel sandwiches are separated by 1-1/4 inches of water. The outer surface of the pressure vessel support ring and the inner surface of the shield tank wall are also covered with Boral. Drawing No. R9-46-1039 shows the primary shielding. Table 9-2 contains a complete description of the primary shielding.

9.1.1 Shutdown Dose Rate

All shutdown dose rates were calculated on the basis of infinite operation at 10 Mw. In addition to the dose rate from the core and shield tank activation, activated corrosion products distributed throughout the primary loop contribute to the dose rate in the vapor container after shutdown. Fig. 2-1 in the shielding design analysis of Section B shows shutdown dose rates at the primary shield tank as a function of shutdown time. The total dose rate curve includes an estimate of the dose rate from the distributed corrosion products.

Table 9-1 contains shutdown dose rates in and around the vapor container after shutdown.

Table 9-1

SHUTDOWN DOSE RATES

Dose rate on surface of primary shield tank (from core and shield tank)

| Time after shutdown, hrs. | Design Specification, Mr/hr | Calculated Mr/hr |
|---------------------------|-----------------------------|------------------|
| 2.5 | 50 | 50 |
| 8.0 | - | 28.0 |

| | | |
|------|---|------|
| 12.0 | - | 23.5 |
| 24.0 | - | 16 |

Dose rate between vapor container and tunnel wall (worst point)

| | | |
|-----|----|----|
| 2.5 | 80 | 75 |
| 8.0 | -- | 40 |

9.1.2 Operating Dose Rates

The operating dose rate from the core and primary shield on the surface of the shield tank during operation at 10 Mw is 247 R/hr.

9.2 Secondary Shielding

In the skid mounted ice cap installation the packed snow around the vapor container tunnel will act as secondary shielding to protect uncontrolled areas during reactor operation.

Table 9-2

Description of Primary Shield-Radial

| Description | Material | Outer Radius Inches | Thickness Inches |
|---------------------------------|-------------------|------------------------|---------------------|
| Core | - | 10.08* | - |
| Reflector | Primary Water | 11.76 | 1.68 |
| Thermal Shield | Stainless Steel | 13.76 | 2.00 |
| Cooling Passage | Primary Water | 18.88 | 5.12 |
| Pressure Vessel Cladding | Stainless Steel | 19.00 | 0.12 |
| Pressure Vessel | Carbon Steel | 21.38 | 2.38 |
| Insulation | (Considered Void) | 23.38 | 2.00 |
| Insulation Retainer | Steel | 23.50 | 0.12 |
| Clearance | Void | 24.05 | 0.55 |
| Pressure Vessel Support Ring | Steel | 25.05 | 1.00 |
| P.V. Support Ring Cladding | Boral | 25.175 | 0.125 |
| Cooling Passage | Shield Water | 26.425 | 1.25 |
| Shield Ring Cladding | Boral | 26.550 | 0.125 |
| 1st Shield Ring | Steel | 29.800 | 3.25 |
| Shield Ring Cladding | Boral | 29.925 | 0.125 |
| Cooling Passage | Shield Water | 31.175 | 1.25 |
| Shield Ring Cladding | Boral | 31.300 | 0.125 |
| 2nd Shield Ring | Steel | 34.550 | 3.25 |
| Shield Ring Cladding | Boral | 34.675 | 0.125 |
| Cooling Passage | Shield Water | 35.925 | 1.25 |

* Equivalent radius based on actual core cross-section

| | | | |
|----------------------|--------------|--------|-------|
| Shield Ring Cladding | Boral | 36.050 | 0.125 |
| 3rd. Shield Ring | Steel | 39.300 | 3.25 |
| Shield Ring Cladding | Boral | 39.425 | 0.125 |
| Cooling Passage | Shield Water | 40.675 | 1.25 |
| Shield Ring Cladding | Boral | 40.800 | 0.125 |
| 4th Shield Ring | Steel | 44.050 | 3.25 |
| Shield Ring Cladding | Boral | 44.175 | 0.125 |
| Neutron Shield | Shield Water | 51.000 | 6.825 |
| Tank Wall Cladding | Boral | 51.125 | 0.125 |
| Tank Wall | Steel | 51.500 | 0.375 |

During operation, the primary coolant loop becomes a source of gamma radiation. Dose rates from the primary coolant as well as the core and shield tank were calculated through the snow. The primary coolant dose rate was found to be insignificant compared to the core and shield tank dose rate.

Table 9-3 contains operating dose rates at various areas of the skid mounted ice cap installation. Distances used in the calculation of these dose rates were taken from drawing No. M02M11. The minimum thickness of snow used in the calculations was 25 feet.

Table 9-3

Operating Dose Rate - 10 MW

| | Design Specification, mr/hr | Calculated mr/hr |
|---------------------------|--------------------------------|---------------------|
| Turbine Generator Package | 0.1* | 0.086 |
| Elect. Control Package | 0.1* | 0.050 |
| Condenser Package | 0.1* | 0.086 |
| Feedwater Package | 1.5** | 1.5 |
| Heat Exchanger Package | 0.1 * | 0.086 |

* One-tenth tolerance dose rate

** Demineralizer located on this package. Dose rate is principally from demineralizer.

9.3 Spent Fuel Shielding

Provision must be made in the Skid Mounted Installation for removing the spent core and storing it until it is shipped off the ice cap. The spent fuel shielding must do the following:

- 1 - Protect personnel from the complete core whether in the pressure vessel or in the spent fuel pit.
- 2 -- Protect personnel from the single element being transferred from the pressure vessel to the spent fuel pit.

9.3.1 Water Tank Above Core

The water tank above the core performs the function of shielding personnel transferring spent fuel elements from the pressure vessel to the spent fuel pit and also provides a medium for removing decay heat from the spent core in the pressure vessel. The actual height of water above the core is determined from shielding considerations.

The water tank height above the core has been sized so that during element transfer a minimum of seven feet of water is always above the fuel element. Through seven feet of water the dose rate one foot above the surface of the water is 84 mr/hr. This calculation was made for an average fuel element removal 24 hours after shutdown after infinite operation at 10 MW.

9.3.2 Shielding Spent Fuel Pit

At end of life, the spent fuel elements are transferred to a storage area where the elements are cooled down before being shipped for reprocessing. While the elements are in the spent fuel pit, shielding must be provided so that personnel working above the pit do not receive excessive radiation. The shielding is in the form of water placed above the spent core.

The dose rate was calculated for 11, 12 and 13 feet of shield water. For 11 feet of shield water, the dose rate was 17.858 mr/hr on top of the spent fuel pit. With 12 and 13 feet of shield water, the dose rates are 3.985 and 0.903 mr/hr respectively. The results of the calculation are given in Fig. 4-2 of the shielding design analysis of Section B. For a dose rate no higher than 5 mr/hr on the top of the spent fuel pit 24 hrs. after shutdown, approximately 12 ft of shield water is required above the center of the core.

9.3.3 Shipping Cask

After the core burns out, the spent elements are shipped for reprocessing. The shipment of radioactive sources is controlled by I.C.C. regulation. The required shielding for the spent fuel cask is based on the regulation that the dose rate one meter from the radioactive source be no more than 10 mr/hr.

The shipping cask was designed to hold six (6) spent fuel elements 90 days after shutdown as shown in Dwg. nos. R9-48-2036 and D9-48-2035.

The required thickness of lead shielding to limit the dose rate one meter from the source to 10 mr/hr is 10.5 inches.

9.4 Demineralizer Shielding

Although the N^{16} activity in the primary system has a 7.4 sec half-life and therefore quickly dies after reactor shutdown, corrosion products are activated and distributed throughout the primary system constituting a source of radioactivity after shutdown. In order to remove the corrosion products, a resin-filled demineralizer is placed in the primary coolant blowdown line.

Since the demineralizer removes the activated corrosion products from the primary water and concentrates them, shielding must be provided around the demineralizer. Therefore, the skid mounted demineralizer will be operated in its own shipping cask which is shown in Fig.6-1 in the shielding design analysis in Section B.

The demineralizer shipping cask as shown has 3 - 11/16 inches of lead around the sides of the demineralizer and 3-3/16 inches of lead on the top and bottom. In addition the lead is contained between two 5/8 inch steel plates. This shielding will reduce the dose rate on the surface of the cask to 70 mr/hr during extended normal full power operation. Within one day after shutdown the dose rate one meter from the source will decrease to a value less than 10 mr/hr, thus meeting I.C.C. shipping regulations.

9.5 Waste Tank Shielding

The shielding of the waste tank is based on normal expected activity in the tank. This radioactive source consists of activity present in the normal waste of the plant. The dose rate on the surface of the waste tank shall be no greater than 500 mr/hr. The measured activity on the surface of the AFPR-1 waste tank containing normal plant waste is 20 mr/hr. From this, it can be concluded that there is no need of extra integral shielding on the waste tank.

9.6 Cooling Provisions in Reactor Lower Shield Tank

During normal operation gamma and thermal energy released from the reactor vessel to the lower shield tank must be dissipated by internal cooling coils.

The gamma heat loss has been evaluated elsewhere as 110,000 Btu per hour maximum. The thermal heat loss ordinarily is through the air space between the reactor and support ring to the vapor container space. Here, however, complete stagnation of that air space is assumed and maximum possible thermal flow to the shield tank by conduction is calculated to be 8750 Btu/hr. Thus the total design load for the cooling coil sizing is 118,750 Btu/hr. Other design criteria are coil water temperature rise, 100°F to 130°F.; shield tank water temperature, 150°F.; heat transfer coefficients, 133 Btu/hr. Ft.² °F. outside coil and 842 inside. Type 304 S.S. 1/2" pipe is used in three parallel loops to minimize pumping head pressure losses.

The calculated results are:

- 1) 7.98 GPM, total cooling water flow
- 2) 11 ft.² external area per each of 3 coils, or 50 lineal ft. per coil.
- 3) Head pressure loss of 1.6 psi per coil (at an average water temp. of 115°F.)

The three coils are installed in the upper shield tank off common inlet and outlet manifolds. Since the length of the outer periphery of the tank is approximately 22 ft., in order to obtain the total required length, all of the coils have a 2-1/2 loop configuration (around the reactor cavity).

10.0 Primary Skid Design

The primary skid carries the reactor vessel primary shielding, primary pump, pressurizer, steam generator, blowdown cooler and their necessary piping. In order to meet air shipment requirements the skid must be made on two halves.

10.1 Components on Primary Skid

The shield tank, shield rings, reactor vessel and primary pump are the main components on the reactor end of the skid. The seal leakage pump, and seal leakage tank are also located on this end of the skid. Because of shipping weight limitations the primary pump and the removable sections of the shielding will be shipped as a separate package. The reactor vessel cover will be removed for shipping to keep within the height limitations and a thin cover plate installed.

The steam generator, pressurizer, and blowdown cooler are the main components located on the steam generator end of the skid. The reactor vessel cover is carried on this skid during shipping.

10.2 Design Features

The main requirements of the design are to meet the size and weight requirements for air transportation, but yet be strong enough to withstand forces of 8 times gravity during shipment. Proper placing of the components on the skids to insure accessibility for erection and maintenance are also necessary.

10.2.1 Provisions for Air Transportability

In order to meet the size and weight requirements for air shipment the skid is made in two halves. The parting line is directly under the flanges of the pump and primary coolant line near the center of the skid. The two halves of the skid are bolted together. Provision for lifting each half of the skid separately or as an assembly has been made. By using six

points of suspension after bolting the deflection will be kept to an acceptable minimum.

10.2.2 Total Weights and Size of Complete Skid and Sections

The overall dimensions of the primary skid are, 23 ft. 11 in. long, 9 ft. 0 in. wide and 9 ft. 0 in. high. The total weight of the skid with the equipment in place is 91251 lbs. This does not include shielding water.

The reactor end of the skid with all its equipment in place weighs 64,619 lbs and is 11 ft. 8.5 in. long, 9 ft. 0 in. wide and 9 ft. 0 in. high. This weight does not include primary or shielding water. With the shielding, cover and pump removed the reactor end of the skid weighs 28,388 lbs. The steam generator end of the skid with all its equipment in place weighs 26,632 lbs. and is 13 ft. 10.5 in. long, 9 ft. 0 in. wide and 9 ft. 0 in. high. With the reactor vessel cover on this skid for shipping the total weight is 29,343.

10.2.3 Description of Skid Bases

The basic construction of the skid drawing R9-42-1001 includes two 18 x 8-3/4 x 64 lb "H" beams at the sides joined by cross ties and partial top deck. The weight requirement makes it necessary to build the skid in two halves. The parting plane is at the center of the skid and directly under the flanges at the steam generator. Fitted plates between the sections of the skids insure good field alignment. The halves of the skid are held together with bolting plates and ream bolts. Jacking screws are provided for leveling after installation of the skid in the vapor container.

11.0 Vapor Container (Dwg No. R9-43-1002)

11.1 General Description

The vapor container is a shop fabricated, cylindrical vessel made up of 3 segments and two heads which are welded together in the field. The size and weight requirements for air transportability make this construction necessary. Welding of the rear dished head of the vapor container is done after installation of the primary skid. Stress relieving of the field welds is not necessary to meet the code requirements for a welded vessel of this size and wall thickness. All welds are readily accessible for field X-ray.

A bulkhead separates the skid compartment from the front end of the skid. The front chamber is filled with water to provide shielding for this end of the reactor.

An access hatch is located in the head at the steam generator end of the skid which is large enough to remove the primary pump or the steam generator bundle, if necessary. Most of the penetrations to the vapor container are also made in this head.

The refueling shield tank is bolted and seal-welded to a flange on the vapor container.

11.2 Normal Operating Temperatures

The operating temperature inside the vapor container is expected to be 120°F and 95% relative humidity. The temperature of the water in both upper and lower shield tanks is expected to be 150°F.

11.3 Vapor Container Design Conditions

A vapor container 13 feet in diameter by 32 feet long is necessary to contain the primary package and provide proper access for servicing. Substitution of the primary component and shielding volumes leaves a net volume of approximately 4200 ft³ of air space available for expansion of released coolant in case of rupture.

The vessel has been designed according to the ASME Unfired Pressure Vessel Code for failure of either the primary or secondary system. It has also been so designed that in case of the remote possibility of both a primary and secondary system rupture that the stresses in the vessel are well below both the yield and ultimate strength of the materials. A design stress of 25,000 psi which is approximately one third the ultimate and two-thirds the yield for Grade 212-B material was selected. This results in a vessel wall thickness of 3/4 inch. Release of either the primary or secondary coolant results in a stress in the vessel of approximately 20% of the code allowable.

11.4 Fabrication Features and Materials

To meet the shipping requirements, the vapor container will have to be sectioned and assembled on the site. Each head will be in two pieces and the cylindrical portion in 8 pieces. Erecting lugs will be installed at the factory and the sections prefit to insure proper installation in the field. The materials of construction are carbon steel SA 212 for the main cylinder and heads. The shield tank will be carbon steel clad with 304 stainless steel on the inside.

The wiring for the motors and instrumentation will be carried in a trough along the top of the vapor container and dropped down at the appropriate locations for connection to the primary components.

11.5 Upper Shield Tank

The upper shield tank is a cylindrical pressure vessel having an inside diameter of 60 inches and an overall length of 146 inches. The primary function of this tank is to shield personnel while refueling the reactor core.

11.5.1 Description and Material (R9-46-1034)

The upper shield tank is designed in accordance with the ASME Unfired Pressure Vessel Code using a design pressure of 150 psi at 500^oF. The material for the tank walls and cover is SA-212 carbon steel with a 304 stainless clad. All flange connections are made of SA-212 carbon steel with a 1/8 inch thick 304 stainless steel overlay. All flange bolting material is SA-193-B7 carbon steel.

The shield tank has an overall length from flange to flange of 146 inches and a nominal inside diameter of 60 inches. The tank walls have a nominal overall clad plate thickness of 3/8 inches, and the 2:1 elliptical cover also has a nominal overall clad plate thickness of 3/8 inches.

The bottom flange connection to the lower shield tank is a gasketless joint using 40-1 inch studs and is field seal welded after bolting of the joint. The upper flange uses a rubber gasket and requires 68 3/4-inch studs to seal against design pressure.

The shield tank has provisions in the form of shelves to store reactor vessel stud nuts, and control rod caps. It also has support plates for the reactor vessel cover and a receptacle in the tank wall for vessel cover storage during refueling.

Cooling and decay heat removal coils are located in shield tank approximately 9-5/8 inches from top cover flange and extend downward into the tank approximately 45-5/8 inches.

11.5.2 Reactor Vessel Cover Storage Provisions

As mentioned above there are two reactor vessel cover support plates welded to the inside of the shield tank. These plates are notched as shown to take the edge of the pressure vessel flange. There is also a dome-shaped receptacle to allow the reactor vessel cover to be stored in shield tank and still permit access to the core. This receptacle has an inside diameter of 36 inches and an overall depth from shield tank centerline to inside of dome of 45 inches. The vessel cover is stored in a nearly vertical position with the flange resting in the support plates and the cover insulation protruding into the dome.

11.5.3 Shielding Water Depth Requirements

A minimum of 7 feet of water is required above the uppermost part of the fuel element during any fuel handling operation. The normal depth of the shielding water is 17 ft 3 in. above the core center line which will allow the necessary water above the fuel element while being transferred from the core to the transfer cask.

11.5.4 Provisions for Cooling

An upper shield tank cooling coil is required during normal operation to dissipate the heat losses from the reactor vessel head and flange.

The top head of the reactor is an elliptical, dished head which is covered with a fiberglass insulation inside a 4/16" stainless steel jacket. Average thickness of this covering is two inches.

Based on ambient temperatures of 500°F for the primary coolant inside the reactor head and 150°F for the water reservoir in the upper shield tank, and using the vessel dimensions shown in Dwg. No. 389, thermal conduction losses through the insulated section of the reactor head are found to be negligible (457 Btu/hr).

Consideration of the losses from the uninsulated flange, bolts, and nuts, reveals a much greater thermal flow through these portions of the vessel to the water reservoir. By graphic analysis the flange shape factor is found to be 2, and from the heat flow equation (p. 16, Heat Transmission by W. H. McAdams), the heat loss is found to be 128,000 Btu/hr. Allowing a 20% safety factor, so that the design criterion is 150,000 Btu/hr; the required cooling coil area is found to be 42 sq. ft. With a 1" Schedule 40, S. S. Pipe, and a coil centerline diameter of 56" a total of 8.5 turns are required in the upper shield tank.

Finally, evaluation of the thermal drop across the free convection film on the outside of the flange, by taking the total exposed metal area as 18 sq. ft. and balancing the conductive flow against the convective flow, yields a surface temperature of 219-220°F. With a 15 ft. hydraulic head, giving a 21.2 psia pressure at the cap, the boiling point is 230°F, considerably above the calculated metal temperature.

11.6 Spent Fuel Tank

11.6.1 Description and Materials

The spent fuel tank is located remotely from the vapor container in a tunnel which is at right angles to the main tunnel. The tank is approximately 20 ft. high, 12 feet in diameter and is made from 1/4 inch thick stainless steel. A storage rack of 1/4"-1% boron steel is provided to store a complete core. Space is provided for underwater loading of two shipping casks.

11.6.2 Cooling Provisions

Cooling in the spent fuel tank is required continuously during normal operation to remove the decay heat from stored elements. The maximum condition assumed here is an entire spent core in the tank 36-40 hours after shutdown. At this time, the heat release rate is 130,000 BTU/hr (Cf. Fig. 1, Section 11.6.2), and a design basis of 150,000 BTU/hr has been selected.

Final design calculations yield a coil of 1 inch Schedule 40, stainless steel pipe, 123 feet long in 3.6 turns with a centerline diameter of 11.0 feet. Circulation rate is 10 G.P.M. with a 2.2 ft. pressure drop.

11.6.3 Transfer of Spent Fuel Elements

Two lead transfer casks will be used to speed up the core unloading. The casks will be 26 inches in diameter and 3.5 feet long. A plug cover on each cask will insure operator protection when the cask is out of water.

An over-head monorail system with a switching arrangement will be used to transfer the fuel from the core to the spent fuel tank. The same type tool as used in unloading the core in the reactor is used to transfer the elements from the storage rack to the fuel shipping casks.

11.7 Vapor Container Penetrations

The penetrations to the vapor container are made through the head at the steam generator end. There are, in this head, 12 water lines, 4 drain lines, one 4-inch steam line, and 11 electrical penetrations. The drain water and steam lines will be of varying size but all require the same type of penetration. A nipple will be welded through the head and will be flanged on each end. The inside and outside prefabricated piping is attached to these flanged nipples with appropriate gaskets and bolts.

The electrical penetrations will also be a nipple welded through the head. A double ended cannon type plug will be used to make quick connections on both the inside and outside of the vapor container.

11.8 Space Cooler Requirements

Thermal heat losses from the reactor vessel, the pressurizer, the steam generator, the primary loop piping, and the lower shield tank necessitate the installation of a space cooler inside the vapor container. To the above losses must be added gamma heat generation during operation outside the lower shield tank.

For this evaluation of the heat accumulation in the vapor container, radiation losses have been taken into account, a temperature basis of 120°F in the space has been assumed, and no heat loss from the vapor container to the outside is considered, all heat removal to be through a finned, unit cooler circulating 100°F water.

Calculations show that the following heat buildup will exist in the vapor container:

| <u>Source</u> | <u>Flow</u> |
|------------------------------------|----------------|
| Gamma | 3000 BTU/hr |
| Steam Generator | 6700 |
| Pressurizer | 3020 |
| Reactor Vessel | 91.00 |
| Primary Piping | 5430 |
| Lower Shield Tank (Uninsulated) | <u>12560</u> |
| TOTAL | 39,810 BTU/hr. |

To handle this load a self-contained unit cooler with integral fan has been selected.

11.9 Insulation Requirements

The vapor container is insulated to prevent excessive heat losses to the snow (ambient temperature - 15°F) and to keep the metal walls at a temperature (100-120°F) which will definitely be above the transition point thus insuring maximum strength for a max crack condition.

11.10 Decay Heat Removal Analysis

11.10.1 Decay Heat Removal Provisions

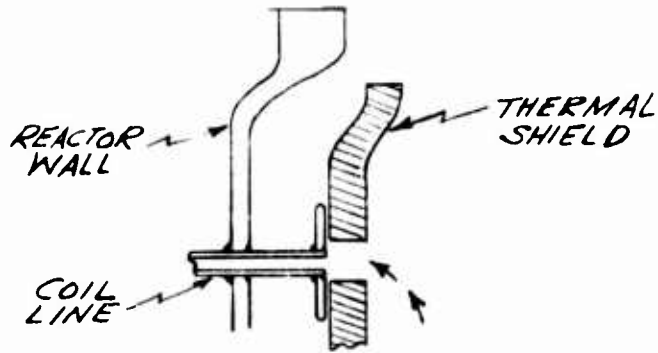
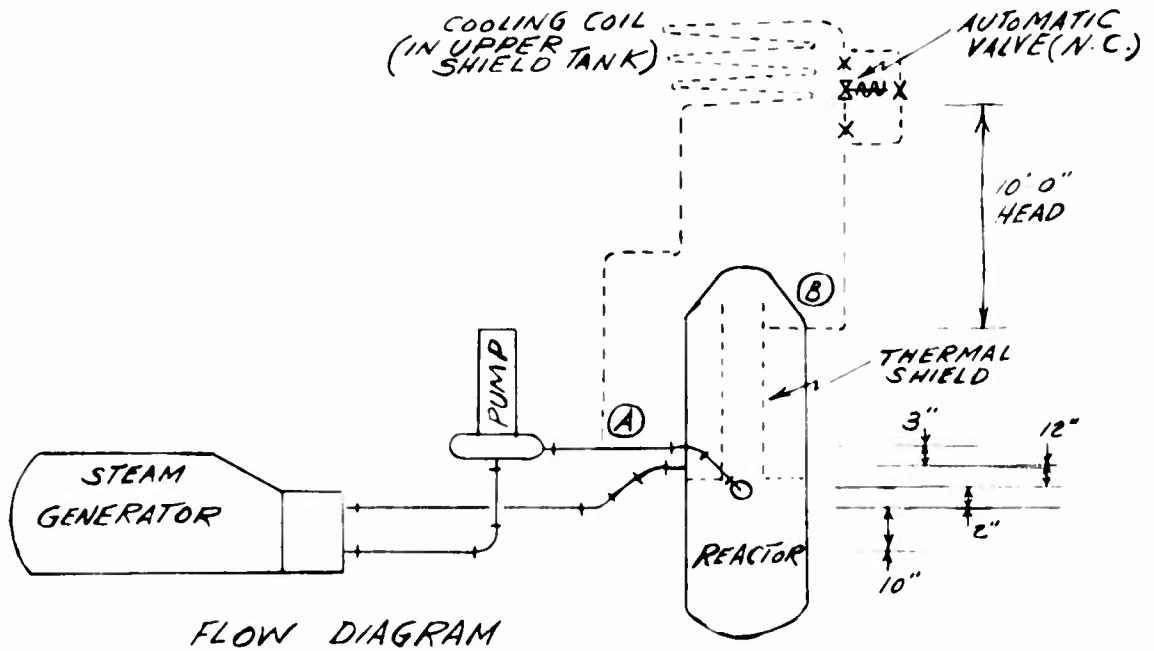
In the event of power failure or primary pump breakdown the reactor is scrammed automatically as soon as the primary coolant flow reaches 94% of full flow value. However heat generation due to fission product decay constitutes a significant source of heat that must be removed from the core to prevent overheating. This decay heat accumulation is to be dissipated in the water reservoir of the upper shield tank. Transfer of the heat is accomplished by a cooling coil circuit that utilizes natural convection induced by the thermal head resulting from the decay heat. This separate system is necessary since the location of the horizontal steam generator below the reactor core level prevents adequate natural convection in the primary loop alone. The system is shown in Figure 1.

The automatic valve as shown in Fig. 1 prevents primary coolant from heating the upper shield tank during normal operation. In the event of pump failure this valve is actuated at the time of reactor scramming; ie, when the primary coolant has dropped to 94% of full flow value. The cooling coil will then be in operation when the primary flow due to inertia has decayed to a negligible value.

11.10.2 Sizing of Cooling Coil

Preliminary design calculations yield a minimum coil length requirement of 52 ft. with 1 1/4", schedule 40, S.S. pipe. The thermal head attainable under the specified conditions is 0.58 p.s.i. at a flow of 7 g.p.m.

DECAY HEAT COOLING



REACTOR COIL TAP DETAIL

FIGURE 1
(SECTION 11.10)

allowing a total resistance of 240 ft. of equivalent pipe in the system.

CALCULATIONS

1. Cooling Coil Size

- Design Basis:
1. 500° F. temp. coolant to coil
 2. 300° F. temp. coolant leaving coil
 3. Minimum pipe leg of 10 ft.
 4. 212° F. temp. upper shield tank water
 5. Boiling condition at external pipe surface
 6. Coil operating pressure, 1750 psig

$$\text{Thermal head} = B = \frac{(d_1 - d_2) L}{144} \quad \text{lbs./in}^2$$

where d_1 and d_2 = wt. density at diff. temps., lbs/CF.
and L = length of pipe leg, ft.

$$\text{Then } d_{300} = 57.3 \text{ lbs/ft.}^3$$

$$d_{500} = 49.0 \text{ lbs/ft.}^3$$

$$L = 10 \text{ ft.}$$

$$\text{and } B = (57.3 - 49) 10/144 = 0.576 \text{ lbs/in.}^2 \text{ thermal head.}$$

$$\text{Heat Transfer: } Q = A \Delta T/R$$

$$\text{where } R = \frac{1}{h_o} + \frac{1}{h_i} + \frac{tw}{k} + \frac{1}{f} \quad \text{where } tw = \text{pipe wall thickness.}$$

$$Q = 540,000 \text{ Btu/hr. (cf. Ref.6)}$$

$$h_o = 273 \text{ Btu/hr. ft}^2\text{°F. (cf. Ref. 1) for boiling}$$

$$h_i = 700 \text{ Btu/hr. ft}^2\text{°F. (cf. Ref. 2) *}$$

$$k = 16.2 \text{ Btu/hr. ft.}^2\text{°F. ft. for type 304 S.S. (cf. Ref.4)}$$

$$1/f = \text{fouling resistance; assume } f = 1000.$$

* This heat transfer coefficient is based on the following assumptions and calculations of the inside fluid velocity:

$$\Delta t \text{ coolant water} = 500 - 300 = 200^\circ \text{F.}$$

$$w = \text{flow, lbs./hr.} = \frac{Q}{C_p \Delta t} = \frac{540000}{(1)(200)} = 2700 \text{ lbs/hr.}$$

At an average density (for 400° F.) of 53.6 lbs./C.F., the flow = 51 C.F./hr. If a 1-1/4" pipe is used with O.D. = 1.66", i.d. = 1.38" and transverse area = 0.010 ft.², velocity, $v = 5100 \text{ ft./hr.}$ or 1.42 ft./sec. Also, the mass velocity, $G = 75 \text{ lbs/sec. ft}^2$

$$\text{Then, } R = \frac{1}{273} + \frac{1}{700} + \frac{0.14 \times 0.083}{16.2} + \frac{1}{1000} \quad (\text{for fouling})$$

$$R = 0.00366 + 0.00143 + .0007 + .001 = 0.007$$

Now $\Delta T_{LM} = \text{Log Mean Temp. Diff.}$

$$\text{and with } \Delta T_1 = 500 - 212 = 288$$

$$\text{and } \Delta T_2 = 300 - 212 = 88$$

$$\Delta T_{LM} = 168.5$$

$$\text{So, } A = QR/\Delta T_{LM} = 540000 (0.007) / 168.5 = 22.4 \text{ ft.}^2$$

From Ref. (3), 1 1/4" Sch. 40 S.S. pipe is suitable for 650°F. and 1750 p.s.i. operation.

With an external area of 0.435 ft² / ft. of pipe, the required length, $L = \frac{22.4}{0.435} = 51.5$ ft.

From Ref. (4), using the Fanning equation or the empirical variation, $h = 0.5 v^{1.85}$, where $h =$ pressure drop in ft. of fluid per 100 ft. of pipe, $v =$ fluid velocity in ft. per sec. and $D =$ pipe i.d. in inches, the pressure drop,

$h = 0.5 (1.42)^{1.85} / (1.38)^{1.26} = 0.64$ ft/100 ft. which at an average temperature of 400°F. is equivalent to 0.24 p.s.i./100 ft.

With the thermal head of 0.576 p.s.i., the total allowable piping (with its equivalent for fittings and valves) is $(0.576/0.24) 100 = 240$ ft.

A similar calculation using 1" pipe shows a required coil length of 66 ft. and a pressure drop of 0.86 p.s.i./100 ft., which is too high for the thermal head available. Therefore, 1-1/4" pipe is the best selection.

2. Cooling Coil Configuration and Location

For the 60" shield tank, a coil diameter of 4-1/2' is used. Then, the minimum number of turns required is

$$n = \frac{L}{3.14D} = \frac{51.5}{3.14 (4.5)} = 3.64$$

3. Total Pressure Drop - Decay Heat Loop

Flow: 1.42 ft/sec. (0.75 lbs/sec.)

Average Water Density: 53.6 lbs per cu ft. (400°F.)
(7.17 lbs. per gal.)

At 4240 gpm in the primary loop the following head losses exist:

| | |
|---|-----------------|
| Piping and fittings pump discharge to reactor | 1.6 ft. |
| Reactor entrance | 3.9 |
| Reactor core | 5.1 |
| Total | <u>10.6 ft.</u> |

A. Pressure Drop of Primary Loop Section

If $v =$ g.p.m.
 $h_A =$ ft., loss
 $K^A =$ constant
 and $v = K \sqrt{h_A}$

$$\text{then } K = \frac{4240}{3.26} = 1300$$

$$\text{So, } h_A = \frac{V^2}{K} = \frac{10.6}{3.26}$$

$$\text{For, } V = (0.75/7.17)60 = 6.27 \text{ g.p.m.} \\ h_A = \frac{(6.27)^2}{1300} = \frac{1}{42,800} = 23.3 \times 10^{-6} \text{ ft.}$$

B. Pressure Drop of 1 1/4" Pipe and Coil

Given: 75 ft. total length

3.64 coil turns (ϕ dia. = 4 1/2 ft.)

From Reference (5), Equation 3-15,

$K = f L/D$, resistance of various fittings and valves.

Now $Re = DV\rho/u$ Reynolds number

where $D = 0.115 \text{ ft. (1.38")}$

$V = 1.42 \text{ ft./sec.}$

$\rho = 53.65 \frac{\text{lbs}}{\text{ft}^3}$ (400°F.)

$\mu = 0.13 (6.72) (10^{-4})$ pound mass /ft. sec.
 $(0.115 \text{ ft.}) (1.42 \frac{\text{ft.}}{\text{sec.}}) (53.65 \frac{\text{lbs}}{\text{ft}^3})$

and $Re =$

$$8.74 \times 10^{-5} \text{ lb. mass/ft. sec.}$$

$$Re = 100,000$$

Therefore $f = 0.0235$

Tabulation of Resistances:

- K (contraction) = 0.5
- or K (entrance) = 0.5
- K (exit) = 1.0
- or K (enlargement) = 1.0
- K (90° L.R. Ell) = 0.42
- L/D (open globe) = 340 ($K = 7.$)
- L/D (open gate) = 13 ($K = 0.27$)

Coil

$$\frac{R}{D} = \frac{27}{1.38} = 19.6$$

Total resistance of 90° bend = 49 (L/D)

Resistance due to length = 31 (L/D)

Bend Resistance = 18 (L/D)

$$\text{Then total Coil } \frac{L}{D} = [4(3.64) - 1] (31 + \frac{18}{2}) + 49$$

$$= 13.56 (40) + 49 = 591.4$$

Total K for entrance, exit, turns (6)

$$= 0.5 + 1.0 + 6 (.42) = 4.02$$

$$\text{Equiv. } \frac{L}{D} = 4.02 / 0.0235 = 171$$

Total $\frac{L}{D}$ for 1-1/4" loop, with 1 auto globe and 2 gate valves fully open,

$$= 171 \neq 591 \neq 340 \neq 13 \neq 13$$

$$= 1128$$

$$L = 1128 (0.115) = 130 \text{ ft.}$$

$$\text{Thus, } h_p = \frac{0.64 \text{ ft. of fluid} \times 130}{100 \text{ ft. of system}} = 0.832 \text{ ft.}$$

$$\text{and } h_A \neq h_B = 0.8320233$$

$$= 0.83 \neq \text{ft. at } V = 1.42 \text{ ft./sec.}$$

$$\text{and } p = \frac{0.83 \times 53.6}{144} = 0.31 \text{ p.s.i. loss}$$

Since, available thermal head is 0.576 p.s.i., flow can increase as follows:

$$V_1^2 = h_1$$

$$\frac{V_2^2}{h_2} = \frac{V_1^2}{h_1} \quad V_2 = 1.42 \text{ ft./sec.}$$

$$V_1 = V_2 \sqrt{\frac{h_1}{h_2}} \quad h_1 = 0.576 \text{ p.s.i.}$$

$$\quad \quad \quad \quad \quad \quad \quad h_2 = 0.31$$

$$V_1 = 1.42 \sqrt{\frac{0.576}{0.31}} = 1.42 (1.364)$$

$$= 1.94 \text{ ft./sec.}$$

Final balance between flow velocity and thermal head is determined by analysis with the analog number.

11.10.3 Analysis of the decay heat removal system

The sequence of events following failure of the primary coolant pump were investigated assuming the pump impeller becomes frozen. Initially the reactor power is constant while the coolant flow rate decreases. It was assumed that the coolant entering the reactor remained at its steady state value during this period and that the reactor power decreased only due to the effect of the negative temperature coefficient of reactivity. The reactor kinetic equations were solved for these circumstances yielding values of the average fuel surface temperature and the average coolant temperatures as a function of time. The design of this system provides for a low coolant flow scram initiated when coolant flow decreases to 94% of its steady state value. It was found that boiling did not take place before reactor scram.

By conservatively assuming a 1.55 second delay between pump failure and initiation of reactor scram, temperatures in the core were established.

FIG. 2 (SECTION II.10)

PRIMARY COOLANT FLOW
AFTER PUMP FAILURE

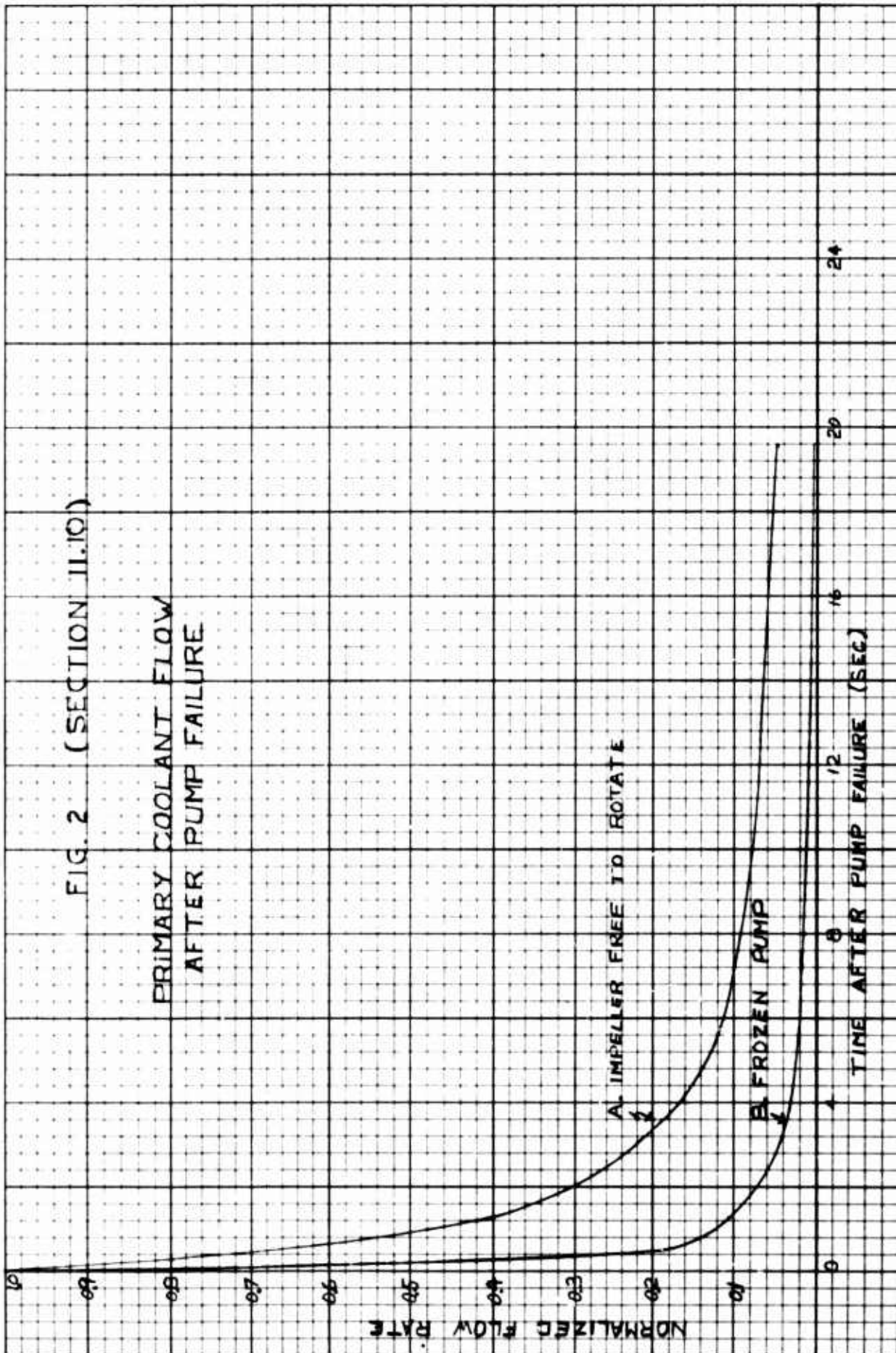


TABLE I - NOMENCLATURE

Symbols:

| | |
|--------|--|
| A | Heat Transfer Surface Area, ft ² |
| C | Specific Heat, Btu/lb ^o F. |
| g | Acceleration due to gravity, ft/sec. ² |
| L | Length of component, ft. |
| P | Power output of core, BTU/sec. |
| ρ | Density of liquid, lbs/ft ³ |
| R | Rate of primary coolant flow, lb/sec. |
| t | Time, sec. |
| T | Temperature, ^o F |
| U | Overall Heat transfer coefficient, BTU/ft ² - ^o F - Sec. |
| W | Weight, lb. |
| x | Distance along tube, ft. |
| z | Vertical distance, ft. |

Subscripts:

| | |
|---|-----------------------------------|
| c | Mean core coolant condition |
| D | Design condition, steady state |
| E | Mean exchanger coolant condition |
| f | Friction loss term |
| F | Mean fuel plate surface condition |
| i | The i th increment |
| s | Mean heat sink condition |

Power was assumed to decrease linearly during the next 1.45 seconds to that level predicted as a result of decay heat only. The following equations were numerically integrated from 1.55 seconds after the accident:

$$W_F C_F \frac{dT_F(t)}{dt} = P(t) - A_F U_F (T_F(t) - T_C(t)) \quad (1)$$

$$W_C C_C \frac{dT_C(t)}{dt} = A_F U_F (T_F(t) - T_C(t)) - 2RC_C (T_C(t) - T_{inlet}) \quad (2)$$

The rate of decay heat generation is given by: (8)

$$P(t) = P(o) (0.05225 t^{-0.2} - 0.05225 (t' / t)^{-0.2}) \quad (3)$$

where: P(o) = Normal power generation rate, Btu/sec.

$$= 9486 \text{ Btu/sec.}$$

t' = reactor operating time, sec.

At the end of 23 seconds after pump failure the average fuel surface temperature (T_p) was found to be 600°F. The average coolant temperature (T_c) was 570°F. These temperatures established the initial conditions for the analog study of the heat removal system.

11.10.3.1 Analysis of the Heat Removal System

The performance of the heat removal system was analyzed by analog computer methods. It was assumed that the system did not make appreciable contributions until 23 seconds after the pump accident. This assumption is very conservative in light of the analysis in section 11.10.4 in which the cooling loop is shown to operate almost immediately after pump failure.

11.10.3.1.1. Analog Kinetic Model

A lumped kinetic model was used in which time lags in piping were neglected. (9) This is possible because the intervals investigated were long compared to these delays. Equations representing the temperature distributions in the system as well as the coolant flow rate through the heat removal coils were solved subject to the initial conditions existing at 23 seconds after the pump accident.

The rate of change of momentum of the fluid circulating in the heat removal loop was equated to the sum of forces acting on it. This yields a differential equation representing the coolant mass flow rate in the cooling loop.

$$\sum_i \frac{\Delta x_i}{A_i g} \frac{dR}{dt} + \sum_i (\Delta p_f)_i - \sum_i \rho_i \Delta z_i = 0 \quad (4)$$

Evaluating the existing thermal head due to the position of the heat removal coils equation (4) becomes:

$$\frac{dR}{dt} = \frac{\sum_i \frac{D}{L_i}}{\sum_i \frac{L_i}{A_i g}} (T_c - T_o) - \frac{(\Delta p_f)_o}{\sum_i \frac{L_i}{A_i g}} \left(\frac{R}{R_o} \right)^{1.8} \quad (5)$$

The frictional pressure drop in equation (4) has been written as:

$$\sum_i (\Delta p_f)_i = (\Delta p_f)_o \left(\frac{R}{R_o} \right)^{1.8} \quad (6)$$

Here $(\Delta p_f)_o$ represents the calculated frictional pressure drop in the circuit at an assumed flow rate (R_o). The exponent 1.8 stems from a combination of basic turbulent flow relations. By choosing R_o larger than that expected to exist in the loop the exponent 1.8 can be conservatively replaced by 2. This function is simpler to generate on the analog computer.

Performing a heat balance on the fuel elements the lumped equation is:

$$W_F C_F \frac{dT_F}{dt} = P(t) - (U_F A_F)_O \left(\frac{R}{R_O} \right)^{0.8} (T_F - T_C) \quad (7)$$

The 0.8 power dependence of the heat transfer coefficient is in accord with the usual heat transfer equation of Nusselt:

$$N_N = \frac{h D}{K} = 0.023 (N_{Re})^{0.8} (N_{Pr})^{0.4} \quad (8)$$

By evaluating the heat transfer coefficient at an arbitrary flow rate (R_O) larger than that expected we may replace the exponent 0.8 by 1.

Similarly the equations for the other temperatures in the system become:

Average Coolant Temperature

$$W_C C_C \frac{dT_C}{dt} = (U_F A_F)_O \left(\frac{R}{R_O} \right) (T_F - T_C) - R C_C (T_C - T_E) \quad (9)$$

Average Temperature of Coolant in the Heat Removal Coils

$$W_E C_E \frac{dT_E}{dt} = R C_C (T_C - T_E) - (U_E A_E)_O \left(\frac{R}{R_O} \right) (T_E - T_S) \quad (10)$$

Average Temperature of Water in the Upper Shield Tank

$$W_S C_S \frac{dT_S}{dt} = (U_E A_E)_O \left(\frac{R}{R_O} \right) (T_E - T_S) - U_S A_S (T_S - 120) \quad (11)$$

11.10.3.1.2 Plant Operating Constants

$$C_C = 1.27$$

$$C_E = 1.084$$

$$C_S = 1.004$$

$$C_F = 0.121$$

$$D = 8.70$$

$$R_O = 1.2$$

$$R_D = 466.8 \text{ (at 4238 gpm)}$$

$$\begin{aligned}
(U_E) &= 0.0397 \\
A_E &= 22.6 \\
U_s &= 1.2916 \times 10^{-4} \\
A_s &= 2447 \\
\gamma &= 4.62 \times 10^{-2} \\
\sum_i \frac{L_i}{A_{ig}} &= 216 \\
W_F &= 429.7 \\
W_C &= 157.8 \\
W_E &= 28.7 \\
W_B &= 1.7689 \times 10^4 \\
(\Delta p_f)_0 &= 21.191 \text{ ft.}
\end{aligned}$$

11.10.3.1.3 Time and Amplitude Scaling Factors

In order to keep the length of computing time at a minimum a time scale was chosen such that one computer second would be equivalent to ten real seconds. Thus the problem was solved in a time scale ten times faster than it actually takes place.

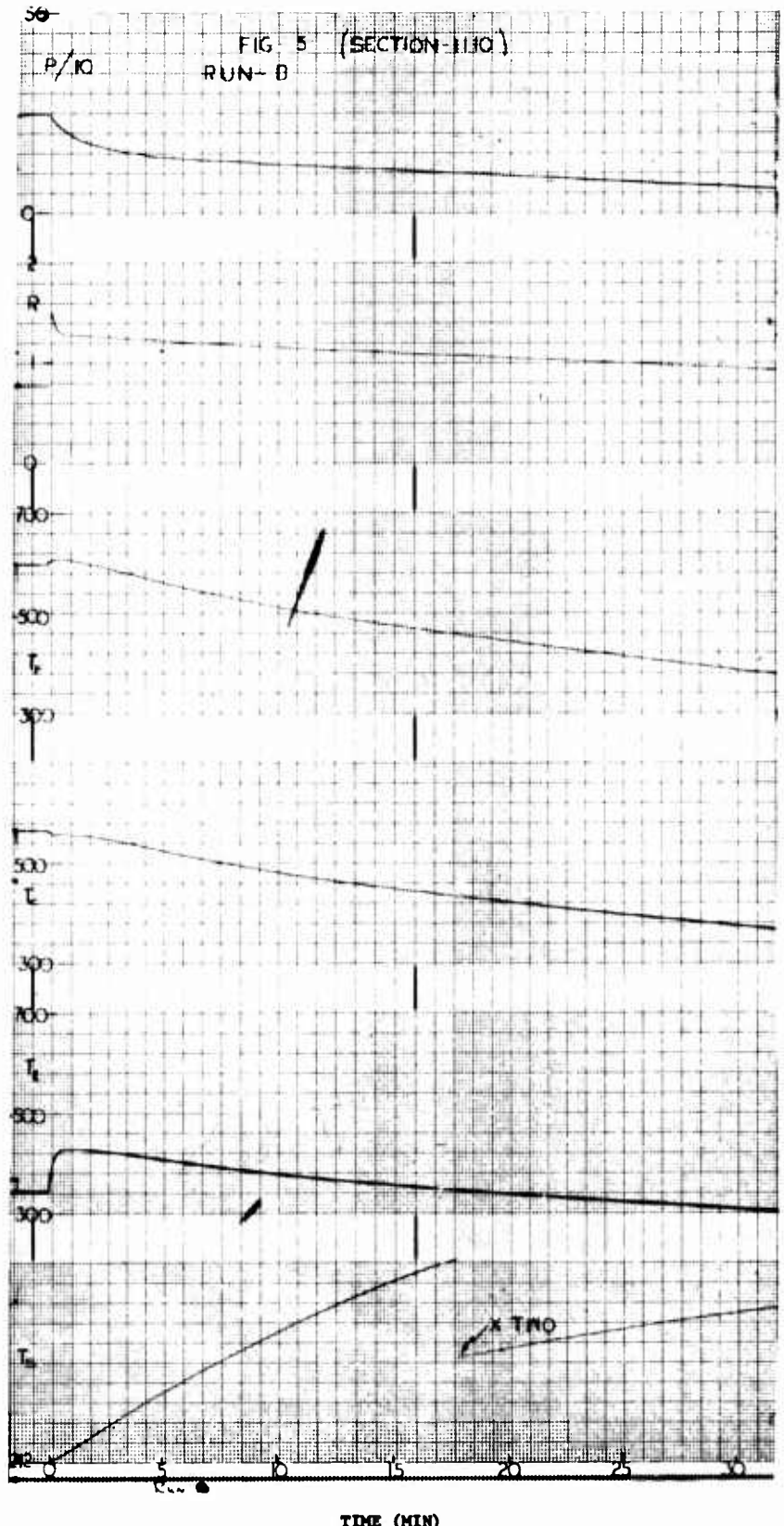
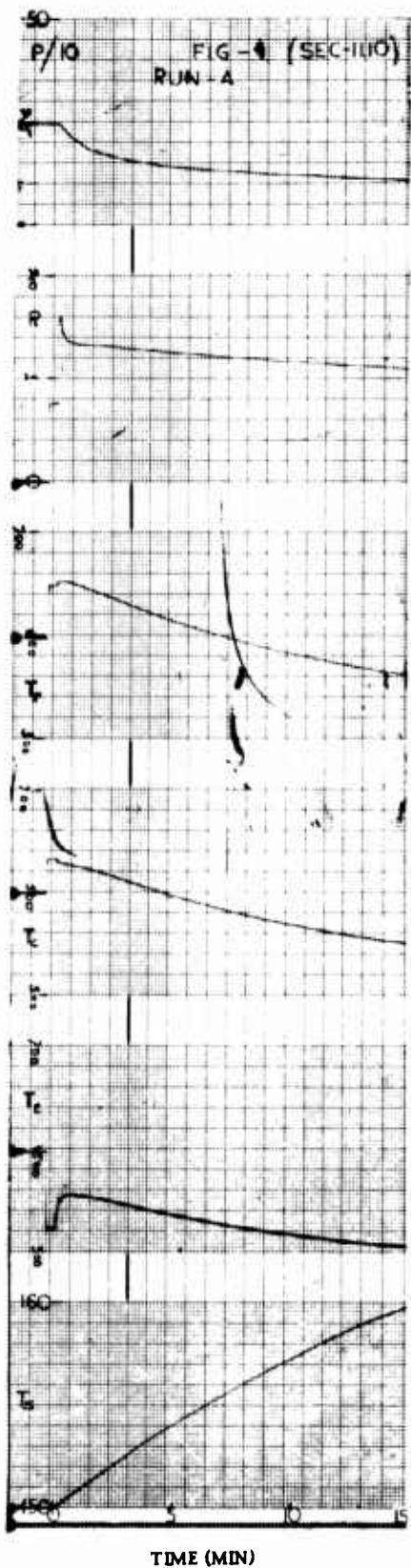
It was found that results could be more easily interpreted if a scaling factor of unity was chosen for problem amplitudes (one volt is equivalent to one physical unit). The resulting amplitudes were generated in sub-multiples to prevent them from exceeding ± 100 volts. A reference level for temperatures was established at 500°F. Temperatures were then generated above and below this reference level.

11.10.3.1.4 Potentiometer Settings

Servo set coefficient potentiometer values are listed in Table 2. Both the absolute magnitude of the setting and the physical symbols are listed.

TABLE 2 - POTENTIOMETER SETTINGS
(Section 11.10)

| <u>Number</u> | <u>Value</u> | <u>Physical Quantity</u> |
|---------------|--------------|--|
| 7 | 0.0970 | 100/100 |
| 12 | 0.2604 | $4U_E A_E 10^3 / W_S C_S R_O$ |
| 13 | 0.0200 | 1/50 |
| 19 | 0.7000 | 70/100 |
| 38 | 0.3500 | 35/100 |
| 40 | 0.6337 | 100/W _c |
| 41 | 0.5000 | 50/100 |
| 42 | 0.9617 | 50/W _F C _F |
| 43 | 0.1465 | $2U_F A_F / W_C C_C R_O$ |
| 45 | 0.4082 | $10 C_C / W_E C_E$ |
| 47 | 0.1857 | $100 \gamma D / \sum_I \frac{L_i}{A_i g}$ |
| 48 | 0.1857 | $100 \gamma D / \sum_I \frac{L_i}{A_i g}$ |
| 49 | 0.1626 | $(\Delta P_f)_O / R^2_O \frac{L_i}{A_i g}$ |
| 54 | 0.3880 | 38.8/100 |
| 56 | 0.3801 | $20 (U_F A_F)_O / W_C C_C R_O$ |
| 57 | 0.0100 | 1/100 |
| 60 | 0.0743 | $2(U_E A_E)_O / W_E C_E R_O$ |
| 64 | 0.2000 | 1/5 |
| 66 | 0.8100 | 81/100 |



11.10.3.1.5 Analog Circuit Diagram

The analog circuit used in this study is shown in Fig. 3. The notation is the same as used in APAE-38. Feed-back connections have been shown in order to indicate the coupled nature of the problem.

11.10.3.2 Results of the Analog Analysis

Figures 4 through 7 indicate analog solutions under different initial conditions and plant parameters.

Run A most closely approximates the design parameters envisioned. It is seen from Fig. 4 that the average fuel surface temperature increases by 10 F after the decay heat removal system takes over. After a period of 30 seconds this temperature begins to decrease reaching 420°F approximately 15 minutes after pump failure. Since the hot channel temperature is considerably higher than the average fuel surface temperature, local nucleate boiling will exist there. The average coolant temperature never exceeds saturation. General boiling will not take place after pump failure.

The analog results were checked for consistency by performing a heat balance on the entire system. This accounted for all heat generated within the limits of error of the problem.

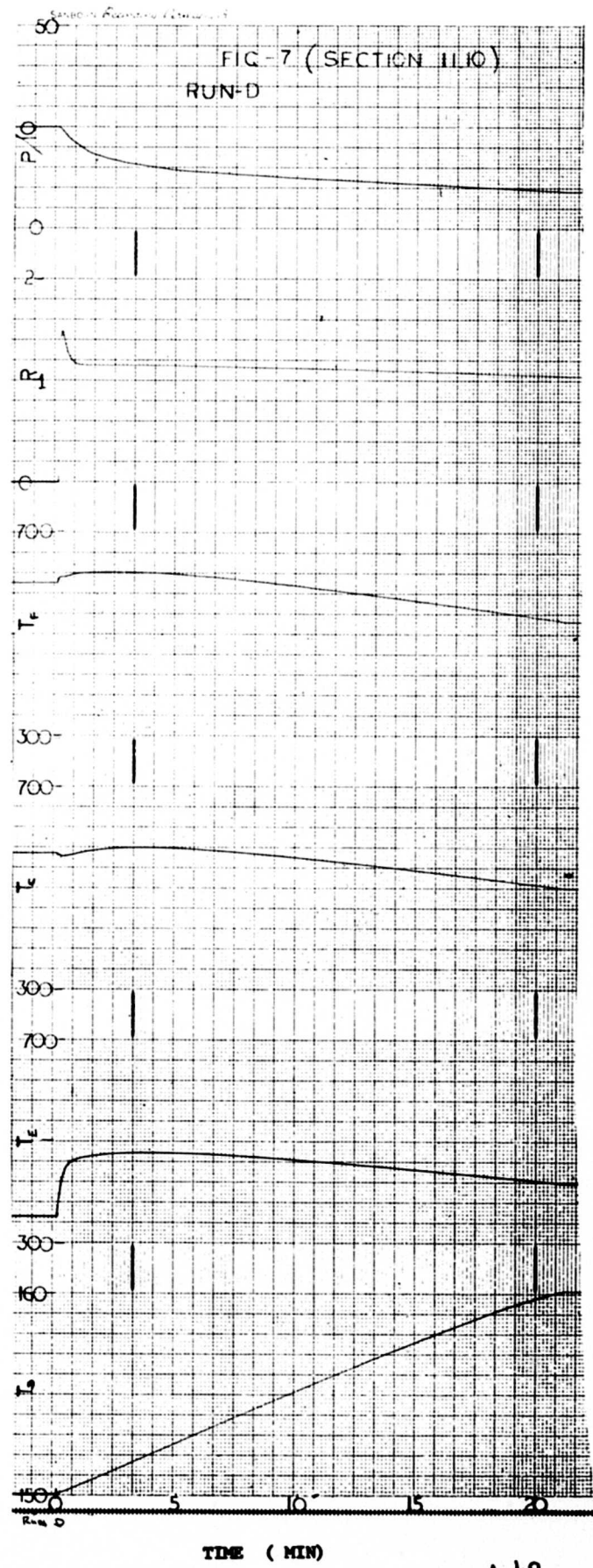
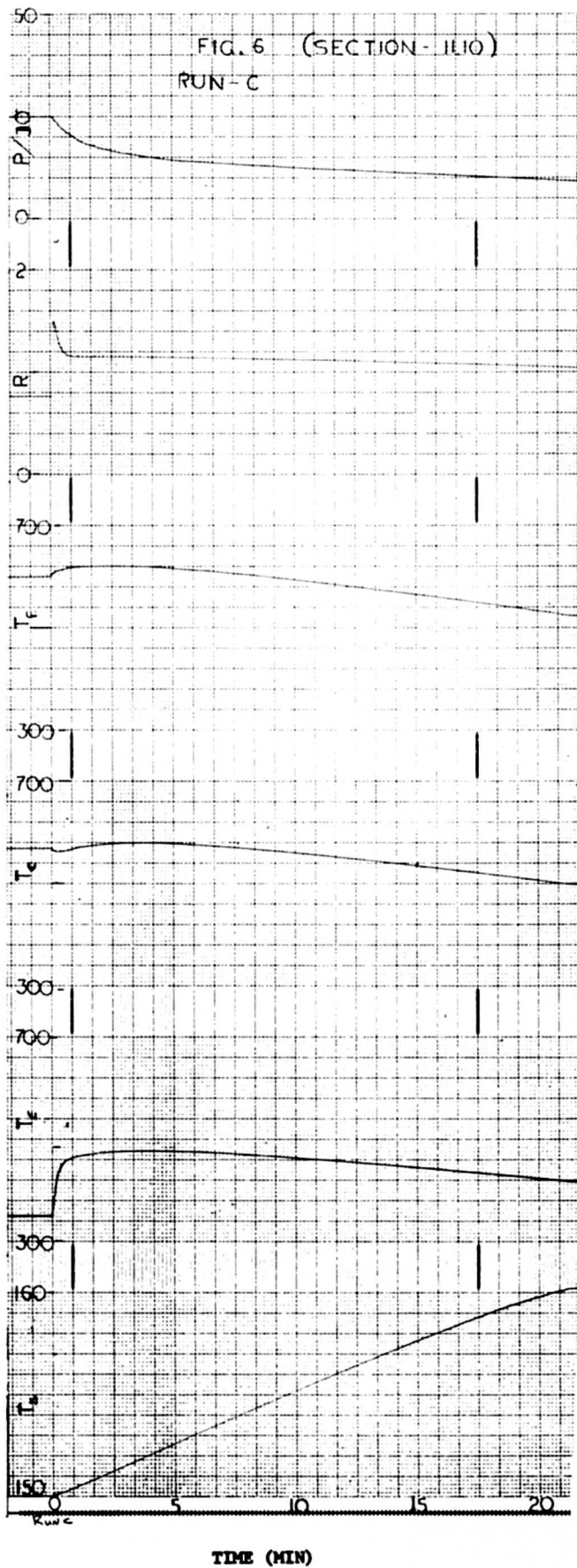
11.10.4 Reverse Flow Analysis

During normal operation the automatic valve in the cooling coil circuit is closed. In the event of pump failure the valve opens when the primary coolant flow has dropped to 94% of full flow value. Valve is actuated by same signal that scrams reactor. At this instant some water at steam generator exit temperatures (500°F) will be forced into the cooling coil. Such flow is in the opposite direction of that intended for the cooling coil circuit; also, the presence of 500°F. water in the cold leg of the cooling coil circuit will reduce the thermal head intended for the decay heat removal.

However, analysis will show that if the valve is opened as early as the instant of pump failure, the undesirable flow will quickly reverse its direction and the original thermal head will re-establish itself. These conditions will be reached while there is still considerable flow due to primary coolant inertia. Hence, opening of the automatic valve as designated above will not interfere with the proper operation of the cooling coil.

Analysis upon which this conclusion is based follows.

The automatic valve will be assumed to open at the instant of pump failure. The amount of 500°F water pushed into the cooling coil loop will depend on how fast the primary pump driving head decreases. To be conservative in this computation it will be assumed that the impeller



TIME (MIN)

TIME (MIN)

A-49

is free to rotate with coastdown following the curve A of Fig. 2.* Also, the force tending to drive the water into the cooling coil will be taken as that due to friction pressure drop of the primary coolant between points A and B of Fig. 1. This friction head at any given time will be based on the flow at the given time.

The force tending to prevent 500°F water from entering the cooling coil is due to the associated thermal head. At the instant of valve opening, this thermal head consists of a 13 foot cold leg (150°F) opposing a 13 foot hot leg 530°F. However, as soon as hot water (500°F.) from the steam generator begins to push its way into the cold leg (with an equal amount of 150°F. water forced into the hot leg) the thermal head is reduced correspondingly. A parameter of this effect is the distance beyond point A of Fig. 1 that 500°F. slug of water has been forced into the cooling coil. Fig. 8 gives thermal pressure as a function of this distance.

A force opposing flow in either direction is the friction of the coil circuit itself. This force is negligible in this analysis until flow velocity in the coil has reached approximately 1.6 ft/sec. At this point, it is taken into account.

Newton's second law is applied to the mass of water in the cooling coil between points A and B of Fig. 1. "Up" is taken as the positive direction. Pipe size is 1-1/4 inches.

$$F_T = ma \quad (1)$$

F_T is the sum of the three forces previously discussed.

$$F_T = F_f + F_{th} + F_L$$

F_f = driving force due to friction drop of primary coolant between points A and B of Fig. .

* This curve was based on methods given in reference (10). Coastdown parameters incorporated follows:

| | |
|--------------------------|---------------------------|
| Normal flow rate | = 466 lb/sec |
| Total loop pressure drop | = 39.31 ft. |
| Rated pump speed | = 91.8 rad/sec |
| Moment of inertia, pump | = 55 lb - ft ² |
| Rated efficiency | = 65% |

$$= 5.58 G^{1.8} \text{ lbs (always positive)}$$

Based on 106ft. head at full flow

F_{th} = driving force due to thermal head

= values given in Figure 8 (always negative)

F_f = friction force due to motion of cooling coil fluid

(assumed zero until $v = 1.6$ ft/sec)

$$= \frac{25}{1.42} \left(\frac{v}{1.42} \right)^{1.8}$$

G = normalized flow rate of primary coolant. Values as a function of time after pump failure are given by Curve A, Figure 2.

v = velocity of flow in cooling coil pipe (ft/sec)

m = mass of water in cooling coil from point A to point B of Fig. 1.

= 1.19 slugs (assumed constant for this analysis)

a = acceleration of mass m . (ft/sec²)

Once an average acceleration "a" has been established for a time interval, t , the corresponding velocity achieved (v) and distance traversed (s) during this interval may be determined from the following formulas.

$$v = v_0 + a \Delta t \quad (2)$$

$$s = v_0 \Delta t + 1/2 a (\Delta t)^2 \quad (3)$$

where v_0 = velocity at beginning of time interval.

By solving equations (1), (2), and (3) for such discrete time intervals*, the motion of water mass m was established. Results are given in the form of a graph (Fig. 9, Curve A) showing the distance that the slug of 500°F. feedwater has moved into the cooling coil as a function of time after the pump failure and simultaneous valve opening. It can be seen that this water enters, reaches zero velocity, and is driven back out by the

* Time interval was taken to be 0.5 seconds.

FIG - 8
(SECTION 11.10)

THERMAL PRESSURE
AS A FUNCTION OF LENGTH
OF 500°F FEEDWATER SLUG
FORCED INTO COOLING COIL

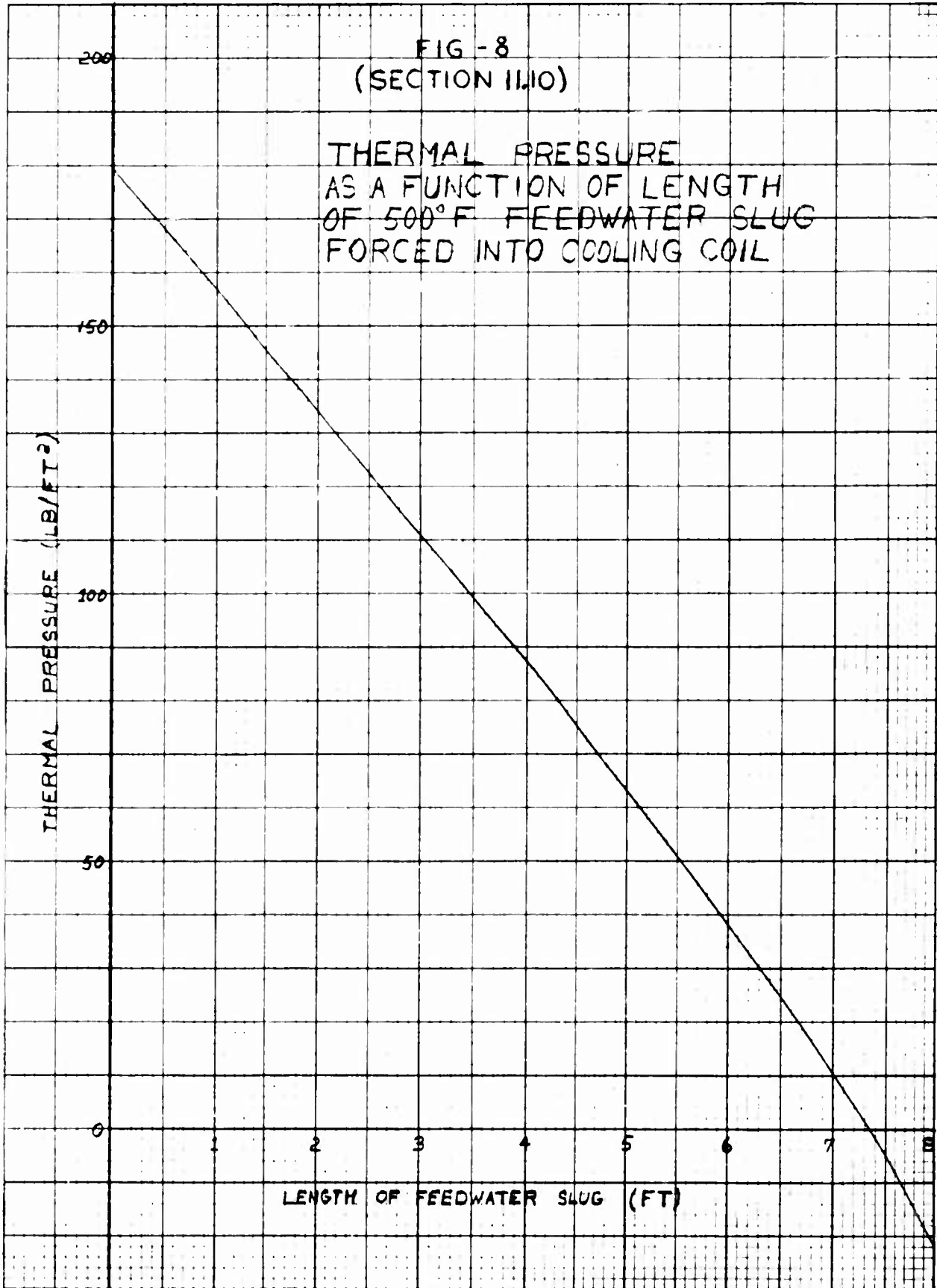
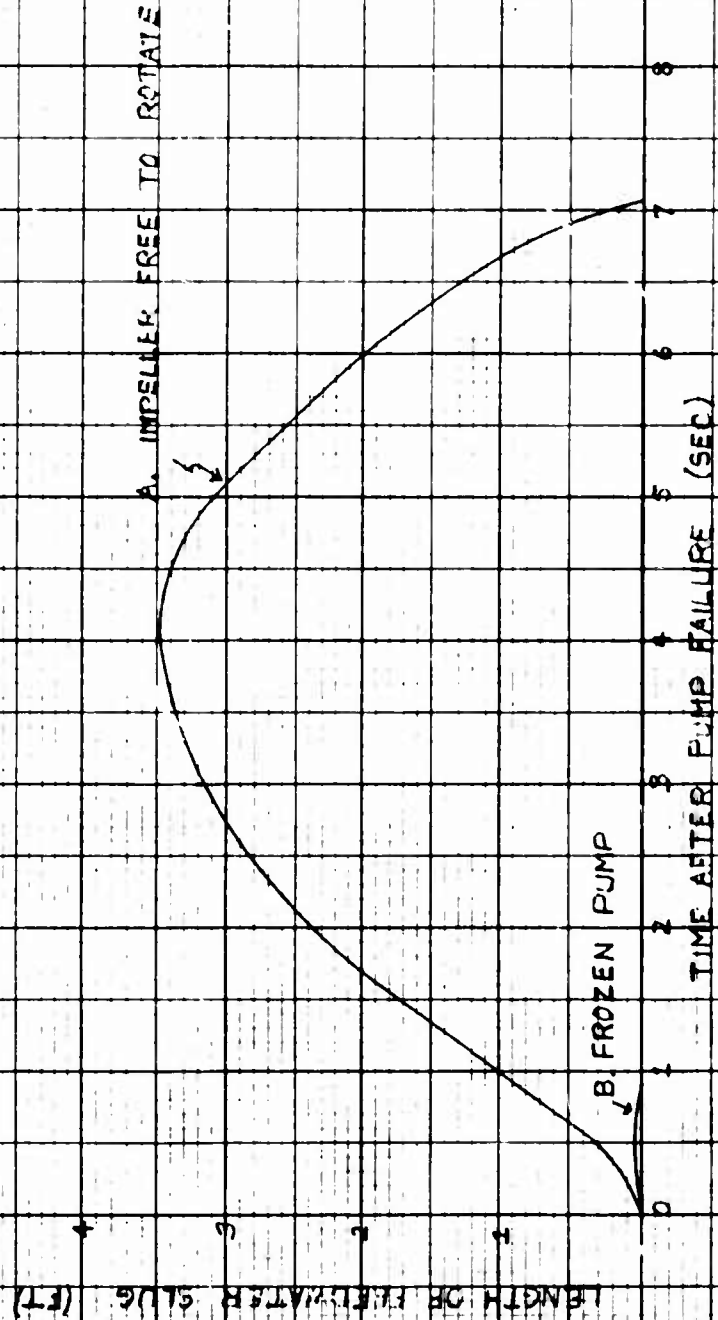


FIG. 9

(SECTION 11.10)

LENGTH OF 500 °F FEEDWATER SLUG
FORCED INTO COOLING COIL AFTER
PUMP FAILURE



thermal head in about 7 seconds. Comparison with curve A of Fig. 2, indicates that at this time there is still approximately 10% of full flow through the main primary coolant loop.

An identical type analysis performed for the case of a frozen pump (flow coast down given by Curve B of Fig. 2) shows that is a negligible amount of steam generator exit water entering the cooling coil pipe. See Curve B of Fig. 9.

11.10.5 Results and Conclusions

In the event of primary pump failure the decay heat removal system is sufficiently adequate to prevent generalized boiling of the coolant within the core. The analysis is conservative in that it neglects heat lost through the pressure vessel cap.

The investigation was conducted both for the case of a frozen pump impeller and for the instance where normal electrical power is not available for the pump.

11.10.6 References:

- (1) Table V, p. 315, Heat Transmission, 2nd Ed., by W.H. McAdams, McGraw - Hill, N.Y., 1942
- (2) p.86, Fan Engineering, Buffalo Forge Co. 1949
p.251, Proc. Eng'g. Calculations Manual, by L. Clarke, McGraw - Hill, N.Y., 1947
- (3) Catalogs TT 330, 640, & 724, by Tube Turns, Louisville, Ky.
- (4) p.93, Cameron Hydraulic Handbook, Ingersoll - Rand, 1951
p.1610, Mark's Handbook, Fifth Edition.
- (5) Crane Co. Flow of Fluids Handbook, 1957
- (6) AP Note 38 - "Reactor Power and Integrated Heat After Shutdown" by R.C. DeYoung
- (7) This Report - Part B - Kinetic Analysis Section 2.0 - "Reactor Behavior Following Pump Failure."
- (8) Second United Nations Conference on the Peaceful Uses of Atomic Energy - Paper 1070 - J.R. Stehn and E.F. Clancy - "Fission Product Radioactivity and Heat Generation".
- (9) APAE Memo 144 - Notes on Decay Heating After Power Failure by R.L. Murray
- (10) KAPL - M - TWT - 1 "Hydraulic Flow Transients" by T.W. Trout

11.11 Air Filtering

A ventilating system for the vapor container air space is shown schematically on Dwg. No. R9-47-1012 of the piping and instrument diagram for the primary section of the plant.

An external centrifugal fan and filter are installed with duct connections to and from the vapor container. A fresh air intake, a vent stack outlet and a filter by-pass are also provided with suitable manual valving for the various operations involved.

The "empty" volume of the vapor container is 5184 cu. ft. With a design air change of 100% every 15 mins., a fan capacity of 345 c.f.m. is required.

The filter housing, installed on the discharge side of the fan, holds two Cambridge 1D-1250 Absolute Filters in series. D type filters are selected because they are built to operate in 100% relative humidity air at temperatures up to 250°F. Their efficiency is 99.95% on 0.3 micron diameter particles. A specification set by the AEC for whom they are originally designed.

The filters are only used before the vapor container is to be entered, to bring the internal atmosphere down to a safe radiation level. Under this condition, the filters rarely become saturated according to APPR- 1 experience.

12.0 Fuel Handling Tools

12.1 Description

The handling equipment and tools for fuel handling are designed keeping in mind that a complete fuel change will be completed in 24 hours.

Operation 1 - Remove Shield Tank Cover - The shield tank cover is removed by first unbolting the covering and hoisting it to a storage space on the working level. No special tools are required for this operation since the workman has direct access to the cover.

Operation 2 - Loosen Vessel Cover Nuts - A torque multiplying wrench is lowered into the water tank directly over the pressure vessel cover. The design of this tool is such that the socket of the tool can be located and lined up with the nut. Physically, the tool is a simple gear torque multiplying device as used in APPR-1 with a 16-foot extension shaft attached. Final tightening of the extension shaft with a torque wrench insures all studs being stressed to the proper level. In this way evenly distributed gasket tightening and proper initial loosening of the nuts is assured. Approximately three full turns of the extension shaft are required to loosen or tighten the nuts.

Operation 3 - Remove Vessel Cover Nuts - After the cover nuts have been loosened an extension shaft with a hex socket is lowered into the shield tank. The hex socket has spring loaded balls on two of the flats that engage spot drill holes on the nut. The tool is engaged on the stud nuts and is then turned until the nuts have been unthreaded from the studs. The nuts are then picked up, the spring loaded balls carrying the nut weight, and stored on the 18 studs mounted on the storage shelves in the shield tank.

Operation 4 - Install Stud Caps - To prevent damage to studs during removal of cover, three stud caps are installed approximately 120° apart. The same tool extension is used as with the nut runner.

Operation 5 - Remove Vessel Cover - Once the cover nuts have been removed a three legged cable sling is lowered into the shield tank. Each cable leg has a specially designed safety hook. The hooks are engaged on the three lifting rings by means of an extension handle with square drive that engages the socket of the safety hook, providing a means for handling the hook. Once a hook is engaged on a lifting ring, the tool engaged in the square drive socket is turned seating the safety rod against the hook lip.

When all the hooks have been attached to the lifting rings, the cover is lifted by means of the overhead crane. When the cover has cleared the vessel and studs, it is tipped into a nearly vertical position by means of a small lever operated puller inserted in one leg of the sling.

The differential hoist leg will carry the entire load of the cover. The lifting ring on this leg is located so that when the entire load is being supported by that leg the cover will hang approximately 5° from the vertical. The cover is placed for storage on two brackets mounted on the shield tank wall.

Operation 6 - Removal of Top Grid and Orifice Plate - The fixture used to remove the top grid and orifice plate is supported on a four legged sling that is lowered into the shield tank. This tool has two basic parts, a lifting plate and a jacking plate. The lifting plate is lowered and engaged on the four grid retainers. Slight pressure applied from the working level through a tool extension and hex socket on the jacking screw positively engages the lifting plate. The above operation disengages the grid retainers from the rods and also locks grid to lifting plate. The grid can now be removed and stored on shield tank wall. The jacking portion of this fixture is used to disengage lifting plate from grid, by turning the compound jacking screw with the tool extension and the hex socket. The jacking plate holds grid in place while the lifting plate is disengaged.

Operation 7 - Place Fuel Transfer Cask in Shield Tank - The fuel transfer cask is moved from storage area by overhead crane to shield tank. The cask is lowered into shield tank and placed on a shelf mounted on the shield tank wall. The top cover plug is removed and placed on shelf inside the tank.

Operation 8 - Remove Stationary Elements - The stationary fuel elements can now be removed by inserting an expandable tool into the opening of the element. The tool is designed so that the expanding arms can never come in contact with the fuel plates. After the tool has been engaged in the fuel element it is raised to a position over the fuel transfer cask. The element and tool are then lowered into the cask. Once the element has reached the bottom the tool is disengaged from the element and removed. The fuel transfer cask top cover plug is now replaced and the loaded cask is now ready for removal from shield tank.

Operation 9 - Place Element in Shipping Cask - The fuel element transfer cask is picked up and removed from shield tank. It is then transferred to the shipping cask loading pit. Once the transfer cask has reached the loading pit, it is set down, the cover plug removed, and the element transferred from transfer cask to shipping cask, using an identical tool as used in operation 8. When the storage rack has been unloaded, it is returned to the shield tank for the next element.

Operation 10- Replaced Top Grid and Orifice Plates - The top grid is replaced as explained in operation 8. This step is required to add support to the control rod so that it is not damaged during rod cap or element removal.

Operation 11 - Remove Control Rod Cap - The control rod caps are removed by placing a square socket over the cap. By pushing down on cap with tool and turning 45° the cap can be removed. The square has spring loaded balls that engage the cap and carry its weight while it is being transferred from control rod to storage shelf on side of shield tank wall.

Operation 12 - Remove Control Rod and Absorber Elements - The tool used to remove control rod fuel and absorber elements has two jaws that close around 3/8" diameter pin on top of element. The tool can be engaged around pin in only one position and is designed such that the tool can never come in contact with fuel plates. When tool has been engaged in an element it is removed from core and placed in transfer cask. From this point on, the control rod absorber and fuel elements are handled in exactly the same manner as the stationary elements as explained in operations 8 and 9.

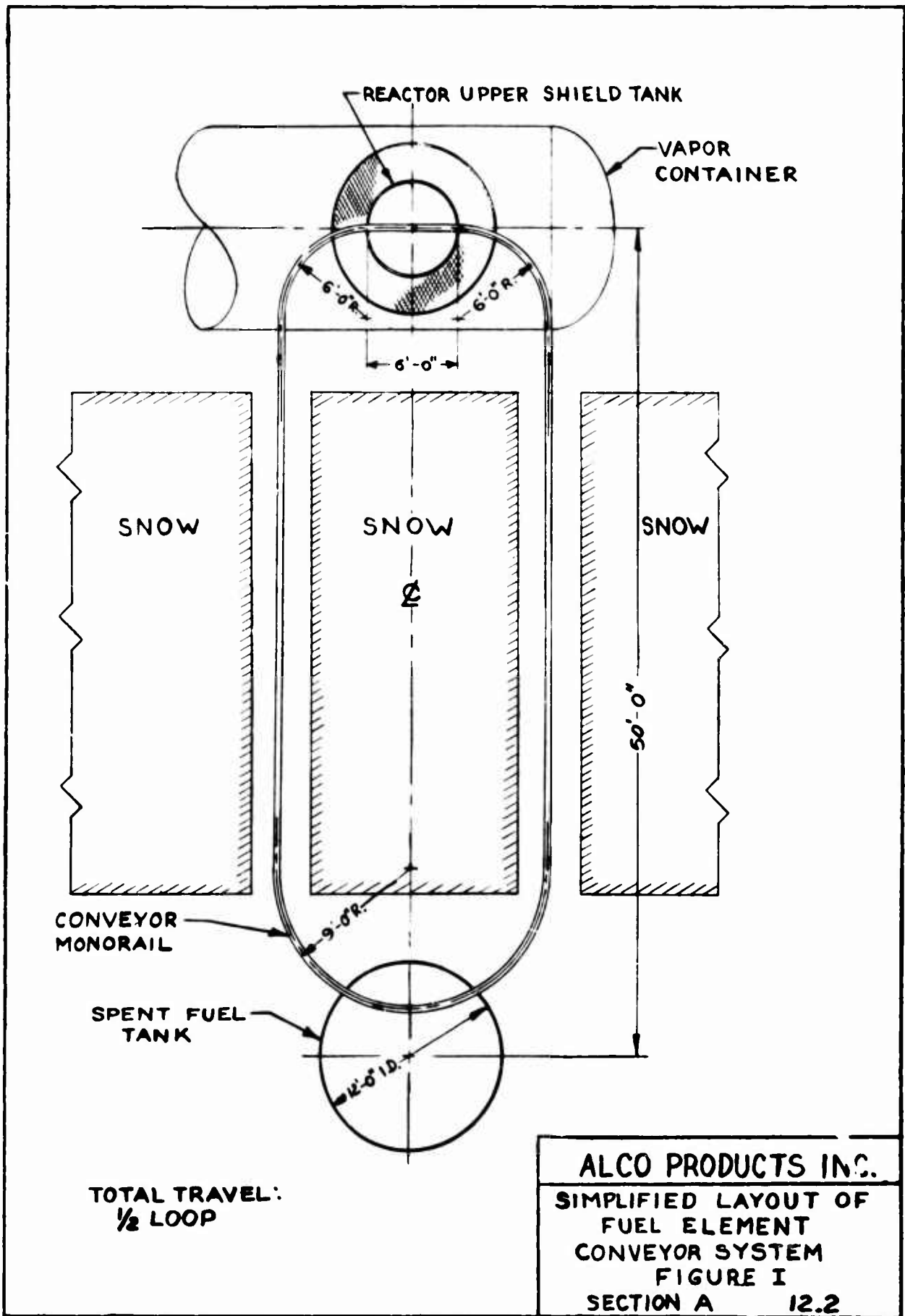
Operation 13 - Refueling - The core is ready for refueling. This is accomplished essentially in the reverse of the above procedure.

12.2 Fuel Element Handling System and Procedure

A general outline of the fuel element handling system is shown in Fig. 1 (Section A 12.2). The main conveyer consists of a suspended monorail loop carrying two electrically-propelled trolleys which, in turn, are each equipped with electrically driven five ton hoists. Each hoist can operate at a lift speed of 13 feet per min. and travel along the rail is rated at 60 feet per min. Power transmission to the hoists and trolley will be through a cable and shoe collection arrangement, with the power cables divided into four main segments, one at each end of the loop and one on each of the loop and one on each of the long runs. Power to the long runs is through interlocking switches at each of the loading points, to insure against collision of the two trolleys. The segments at the load points are energized through local switches only, to permit isolated maneuvering at the load points during cask handling in and out of the tanks.

Procedure during the 48 hour fuel element change period is in accordance with the following time cycle:

| | | |
|------------|-------------------------------------|---------|
| Step 1. | System cool-down and depressurizing | 12 hrs. |
| 2. | Upper Shield Tank opening | 2 hrs. |
| 3. | Reactor Cap removal | 4 hrs. |
| 4. | Spent Fuel Element removal | 7 hrs. |
| 5. | New Fuel Element placement | 4 hrs. |
| 6. | Reactor Cap replacing | 5 hrs. |
| 7. | Upper Shield Tank Closing | 2 hrs. |
| 8. | Reactor Startup and System Warmup | 12 hrs. |
| Total Time | | 48 hrs. |



It should be noted that the primary coolant loop and all the auxiliary cooling coils are circulated during the first two steps to effect the cool-down. At the start of Step 3, the primary coolant pump is shut down. At this point, the decay heat generation rate is down to about 160,000 Btu per hour, which can be handled adequately by the upper shield tank cooling coil and vapor container space coil.

During the unloading period, the spent fuel elements are placed individually in one of the two transfer casks used. They are unloaded in the spent fuel tank, from the transfer cask into a support lattice (Drg. R9-43-1002).

All handling of the elements is manual with special tools as described in the preceding section.

The support lattice is eventually emptied into the shipping casks at a later time, beyond the 48 hr. shutdown period. While one transfer cask is being loaded at the reactor, another is being unloaded at the spent fuel tank. Manipulation of the transfer casks is facilitated by a guide stanchion in each tank, which also holds a camming guide device for opening the cask lid by means of the the cask weight as it reaches the end of its travel near the tank bottom.

One main advantage of this method of operation is that during the removal of the spent fuel, two elements can be handled at the same time, allowing a major time saving in Step 4.

Since the spent fuel tank is located remote from the vapor container, radiation level during plant operation is low enough to permit loading of spent fuel into shipping casks at any time. This operation can thus be done at times independent of scheduled (plant shut-downs with attendant advantages from both the shipping schedule and plant shut-down time standpoints.)

13.0 Primary System Instrumentation

13.1 Design Considerations and Description of System

The controls and instrumentation for the plant is generally similar to APPR-1 and reflects Alco's operating experience on APPR-1 and design experience in APPR-1a.

Emphasis has been placed on simplifying the instrumentation and obtaining a compact, economical packaged system consistent with preserving plant safety, reliability and operability, and reducing downtime due to failures.

Instrumentation and controls are provided for the complete nuclear powered steam source. They include instruments, controls and safety devices for the reactor, the primary coolant system, the steam boiler feedwater system and the radiation monitoring system. Prefabricated units are used to lower the installed cost of the equipment, whenever possible. The physical size of the units is small to minimize initial costs, space requirements, weight and transportation costs to afford convenience of operation. The central location of equipment and the use of maintenance aids keep maintenance costs to a minimum.

Locally mounted controls and indicators are utilized only in cases where complete plant operation is not affected. These instruments are monitored and off-normal conditions alarmed. Remote mounting of control, recording and indication is employed as required where radiation hazards, inaccessibility or good operating practice dictate.

The control console carries the recorders and indicators necessary to keep the plant operator informed of pertinent plant parameters and the minimum controls necessary to operate the plant. The console is located on the skid with the instrument supply distribution panel, secondary switchgear and motor control centers so that all electrical controls are easily accessible to the operator. The nuclear channels, radiation monitoring, primary and secondary system recorders and indicators, rod-drive controls, primary system pump controls, pressurizer heater controls, scram and trip functions, trip valve controls and the annunciator are included on the control console.

Consistent with the use of all electric and solid state type instrumentation, the trip valves on outgoing lines from the vapor container are of electric solenoid or electro-hydraulic type which close on power failure in a fail-safe condition.

A radiation monitoring system is provided as a permanent integrated part of the plant to detect, record and alarm and presence and level of potential radiation hazards. It serves to alert the operating personnel to any abnormal situations which may become hazardous to personnel and plant operation both on and/or off the site.

After a 1957 survey of process instruments made of commercial manufacturers, Alco has selected the latest type miniature instruments incorporating transistors, magnetic amplifiers and solid state components using electrical circuitry throughout, and electro-hydraulic valves with self-contained hydraulic power source. This type of instrumentation reduces and simplifies maintenance by the use of modular construction, plug-in and "throw-away" components.

Pneumatics is eliminated for signal processing, transmission and for air loading of valves because of problems of low temperature and moisture and during shipment at any site.

Where components of questionable reliability cannot be eliminated military and industrial "ruggedized" long life types, hermetically sealed will be used. In the more critical applications, parallel and coincidence circuitry is used so that failure of a component cannot cause system failure.

All units are terminated in plug-in type electrical connectors and are factory pre-tested as complete channel systems.

They are disconnected and reconnected as a plug-in operation on the final destination where another check is made before operation.

13.2 Electro-Hydraulic Control Valves

Electro-hydraulic control valves are used in the all electrical instrumentation system in lieu of air operated valves. While an electric operated valve is about two to three times the cost of an air control valve, the overall plant cost is less because few valves are needed and the complete instrument air system with its associated piping is eliminated. Elimination of air type controls is also highly desirable for this plant to obviate the possibility of freezing of moisture in air supply and control lines.

Self-contained electrically powered hydraulic piston type control valves position with a high order of accuracy and have excellent frequency response. The stability of positioning in this type valve is superior to a pneumatic diaphragm operator that is a resilient assembly moving in response to dynamic forces transmitted from the valve or plug proper on the fluid stream. The hydraulic piston is positioned by a non-compressible fluid that dampens vibration and prevents jumping of the inner valve with resultant rough control and wear inherent in the pneumatic operator.

The electro-hydraulic valves are self-contained requiring no inputs other than the electrical control signal and a.c. power from the distribution line.

Electro-hydraulic trip valves will "fail-safe" on loss of power and close. Control valves will lock in position and annunciate the condition, or close on loss of power as specified.

13.3 Radiation Monitoring

A radiation monitoring system is provided for the protection of personnel and plant operation. Radiation levels of 5 mr/hr will be alarmed both locally and in the control room to warn personnel in a particular area and the control room operator of a hazardous condition. Also by positioning detectors in certain areas any malfunction which would result in the release of radioactive waste is detected and alarmed so that corrective action may be taken by the operator. For the protection of off-site personnel and to double check the in-plant monitoring systems, two analyzers monitoring plant water and all effluents are provided. These analyzers are also provided with suitable means of indication and alarm.

The in-plant monitoring systems is gamma sensitive only since both primary and secondary reactor shielding contains all neutrons and the pipe walls are of sufficient thickness to contain beta radiation.

Both the water and air effluent monitors are beta and gamma sensitive because the effluents are not contained.

13.4 Nuclear Instrumentation

Drawing heavily on APPR-1 operating experience and APPR-1a design experience, Alco has simplified the former nuclear instrumentation system. Neutron detecting chambers used in startup operations and their connectors have been a major problem. For protection of these chambers and their connectors our design calls for withdrawal of this chamber when not in use. At the same time, one startup channel is eliminated because this withdrawal will be made in calibrated steps providing the usual two decade overlap of the power channel. When the reactor is at power the chamber will be fully withdrawn to extend the life of the chamber and connector.

The safety level chambers are used in a two out of two coincidence circuit requiring both chambers to initiate a scram at 150 percent of design level power. Failure of one of the fail safe safety channels will be annunciated without scrambling the reactor and will allow time for a replacement of parts in the channel without a shutdown. But, if the other channel calls for a scram, (legitimate or not), before the defective channel is corrected, the reactor will be scrambled.

Five (5) nuclear channels will be provided using six recorders. High and low level periods are recorded on a dual channel instrument.

1. Startup - BF₃ counter with low level period
2. Log N and Period
3. Linear power
4. Safety #1
5. Safety #2

The BF_3 proportional counter channel with a minimum sensitivity of 4 counts/nv will cover the neutron flux range from source level to the range where the Log N channel gives accurate indication. This startup range corresponds to a power level of from about 0.01 watt to about 100 watts. The Log N channel will cover the power range from about 10 watts to over 10 megawatts. Associated with the Log N channel is a period amplifier, and a period of 3 seconds will cause a scram. At a period of 10 seconds rod withdrawal is stopped.

A linear power channel with range selector switch is provided with the same operating range as the Log N.

Use of only five nuclear channels, and reduction of the APPR-1 three safety channels with a two out of three coincidence scram circuit to the two safety channel system with two out of two coincidence circuit is based on the following:

1. Use of solid state systems and elimination of vacuum tubes, including solid state preamplifiers for the chambers which increases reliability and stability.
2. Use of regulated and isolated power supplies reduces the chance of false scrams due to outside interference.
3. Use of chamber wells extending to the outside of the vapor container with improved type connectors for the chamber leads.
4. Use of a BF_3 - chamber raising mechanism to remove the BF_3 counter tube from the region of high flux level during power operation. The mechanism will extend the useable life of the tube and reduce tube connector failure.

13.5 Startup Considerations

An adequate initial start-up count rate on the BF_3 counter channel is afforded by the use of a polonium-beryllium neutron source. After the initial startup the polonium-beryllium source is complemented by a photoneutron source that yields neutrons upon bombardment by gamma radiation from fission products. This source consists of a beryllium slab encased in stainless steel and welded to the core tank. After 1000 hours operation at 10 MW, the photoneutron source strength is considerably greater than the original source at initial startup and continues to increase in strength as fission products build up. Therefore, the count rate for startup procedure will be well within the range of the BF_3 counter channel for the life of the core.

After reloading the reactor with fresh fuel elements a new polonium-beryllium source equal in strength to the original source will be required.

13.6 Interlocks and Scram Actions

Rod Travel Limit Switches

The rod travel limit switches are the simplest interlocks preventing travel of rods beyond predetermined limits and protecting the rod drive starter and motor from overheating and possible burnout.

Rod Automatic Drive Down

There is a contact in parallel with the "in" contact of the "gang" switch which is closed during any "scram" condition, energizing rod drive motors "in". The main clutches are disengaged and the rod drive motors, when energized in this manner, operate through the overrunning clutches to break loose any rod that may hang up during the "scram". Once broken loose the rod will again fall freely to complete the scram action.

Nuclear Interlocks and Scrams

In either the low-power level or the intermediate power level regions, a reactor period shorter than some predetermined value prevents rod withdrawal. Both period channels function continuously in the low-power region with the low-level channel losing its value above 10 watts. This interlock accomplishes its function by making it impossible to apply power to the rod drive motor starters when any attempt is made to withdraw rods.

A rod minimum startup count rate interlock is used to guard against reactor runaway during startup because of lack of neutrons when achieving a critical mass.

A low-level protection by-pass in the log N channel by-passes both the short period and minimum count rate interlocks at some predetermined higher power level. This by-pass interlock protects against failure of either of the interlocks described above which prevent rod withdrawal at high power levels. Actuation of this interlock will be annunciated by a momentary audible alarm and switching on of a yellow warning light on the annunciator panel. This procedure is reversed during shutdown of the reactor.

The period scram is automatically by-passed when the following conditions have been satisfied.

1. Primary Coolant Average Temperature 480°F
2. Power Level 80%

If either or both of these parameters drop below 480°F and 80% power, respectively, the period scram is automatically activated. Deactivation of the by-pass is clearly annunciated to alert the operator.

Results of analog computer studies to date indicate that any rod withdrawal above the temperature and power conditions listed above will result in a power level scram before a period scram. These same studies also indicate that at other power levels of power and temperature it is possible to limit rod withdrawal in conjunction with a period scram by-pass. However, this has not been incorporated in our designs because normal operation of a plant is usually nearly design power. In a special case, however, circuitry to by-pass the period scram at lower levels may be incorporated in the design.

A primary coolant pump interlock prevents rod withdrawal when the pump is not operating. This prevents reactor startup and overheating of the primary system because of lack of primary coolant flow. The closure of this interlock on the pump motor starter allows withdrawal. Since there is a backup low flow scram action, starter actuation is considered satisfactory evidence that the pump is running.

Whenever conditions satisfy any or all of the rod withdrawal interlocks specified above, rod withdrawal is prohibited. It is then not possible to energize the rod withdrawal permissive relays. The operator is warned of this condition by the turning on of a rod (not permissive) light and the extinguishing of the green (permissive) light on the control console panel. The reverse is true when rod withdrawal is permitted.

The rod drive "In" contactor will always override the "out" contactor in the event that both of the contactors are energized simultaneously. This is a fail-safe interlock which would assist in shutting down the reactor.

The rod transfer lock switch requires initiation of reactor operations by a keyed switch. Also, if an attempt is made to start up in the "off" or "zero" positions, the reactor will scram.

During zero power operations very low limits must be maintained since the reactor pressure vessel cover may be off as in criticality tests. A scram contact is provided in the log N channel set at some predetermined level, such as 1 KW.

Routine power operation required by-passing the zero power scram through the transfer lock switch. However, the safety channels remain in the protective circuitry. A power level of 120% will initiate a scram action through the safety channels.

High rates of flux increase in the reactor coinciding with increased rate of heat production, are detrimental to the normal operation of the power plant and can cause serious damage. Therefore this rate of flux increase is monitored and the reactor is scrammed if too high a period is reached. Two period channels with overlapping ranges are used as monitors and scrams are affected by opening contacts in their signal circuits to the final output stage of the safety channel. The low level period scram utilizing the BF₃ channel is only in effect at low-period levels and is by-passed by the same log N contacts specified above.

The intermediate level scram channel remains in the circuit to scram the reactor on a prescribed period below those encountered during normal system load transients.

There are seven scrams which do not depend upon nuclear channels for their scram signals. The three scrams which depend upon a pressure signal are made up of three pressure switches for each scram. These three pressure switches are connected in coincidence so that if any two of the three switches are actuated a scram is initiated. Alarms are also provided through the same pressure switches. The alarms will also detect a defective pressure switch when an erroneous alarm is made.

1. Low primary coolant pressure will first alarm and then scram the reactor.
2. High primary coolant pressure will first alarm and then scram the reactor. Together with this scram the power to the pressurized heaters is cut off since the condition of high pressure may be caused by the heaters rather than the reactor.
3. High pressure secondary steam will alarm and scram the reactor. This control implies a primary coolant break through in the steam generator.
4. Low primary coolant flow is alarmed at approximately - 3% and a scram occurs at approximately -6%. This control guards against boiling in the reactor.

During zero power operation there is no necessity for primary coolant flow and low pressure controls because (a) the low power developed, (b) the pressure vessel cover may be off. Because of this the low flow and low pressure alarm and scram specified above are by-passed by the transfer lock-switch located in the control unit.

5. High reactor outlet temperature of primary coolant is alarmed and scrambled. A high reactor outlet temperature indicates higher rate of heat generation than the steam generator and primary coolant system are capable of handling.
6. High temperature steam is alarmed and scrambled. High steam temperature exists when the secondary system is incapable of removing heat from the primary system.
7. High primary coolant flow is also alarmed and scrambled.

13.7 Control Console

13.7.1 General

The control console is sized to provide uninterrupted one-man operation of the power plant. Recorders and controllers for the steam

and feed-water parameters are included in the console. As indicated on the layout of the switchgear control skid, associated controls for operation of the power plant such as switchgear, turbine-generator controls, etc., are adjacent to the operator. A graphic panel is not used since this is an operating plant.

The control console is functionally arranged for simplicity and ease of operation of the plant. The nuclear recorders and control rod drives necessary to control the primary system are on panels directly in front of the operator, with the controls mounted on an inclined panel at desk top levels. The annunciator unit and associated test panel is directly above this instrumentation within reach of the operator to acknowledge alarms. Additional nuclear instrumentation and radiation monitoring equipment is at the operator's left. The instruments and controls for the primary system are to the right of the operator. All recorders and indicators of variables are mounted on vertical panels in the console at operating eye level; controls are on inclined panels at desk top level. All of the sections mentioned above will be covered in more detail in the following paragraphs.

13.7.2 Primary System Instruments

The vertical eye-level panels of the console contain instruments which record and/or indicate all necessary system variables. These are:

1. Primary Coolant Mean Temperature
2. Primary Coolant Temperature
3. Primary Coolant Pressure
4. Primary Coolant Flow
5. Pressurizer Level and Temperature
6. Vapor Container Pressure
7. Primary System Temperature Monitor Indicator
8. Primary Coolant Pump Motor Ammeter
9. Waste Tank Level Indicator
10. Spare Position for Additional Recorder

The recorders are specified on the data sheets accompanying this report. Miniature electric type two-channel recorders with 4-inch strip charts are used to conserve space.

The right and left inclined control panels at desk top level contain switches and indicator lights used in the control of primary system pumps, pressurizer heaters, and trip valves.

13.7.3 Nuclear Instruments

The vertical panels contain all nuclear recorders which are specified in detail in attached data sheets. These recorders are -

1. Safety Channel No. 1
2. Safety Channel No. 2
3. Period, 2-channel, high and low level
4. Log N
5. Log Count Rate BF₃
6. Linear Power
7. Spare position for additional recorder

Amplifiers used in conjunction with these instruments are mounted in these recorders. Any controls requiring attention of the operator will be included on a panel on the front to the unit.

The center panel contains controls and indication for the reactor rod drives. The indicators are dual synchro receivers. The short needle is the "coarse" indicator of rod position making approximately one revolution for full rod travel. The longer needle is the "fine" indicator making one revolution for each 3 inches of rod travel. The combined indication of the two needles is the rod position within ± 0.020 of an inch.

Each of the five rods drive positions is indicated by a separate instrument. Upper and lower limits of travel are indicated by red and green lights, respectively. At these limits of travel the circuit to the rod drive motor starter is broken, preventing further motor rotation by either manual or automatic means. A double pole-double throw center off-switch, located near each indicator controls direction of individual rod travel. A ten-pole-double throw-center off switch is used for gang control of the regulating and shim rods so that the rods may be moved in unison.

13.7.4 Secondary Instruments

The right panel contains the instruments necessary to record and control steam output of the plant to the secondary system. These are:

1. Main Steam Pressure Recorder
2. Main Steam Temperature Recorder
3. Main Steam Flow Recorder
4. Steam Generator Level Recorder-Controller
5. Feedwater Flow Recorder
6. Feedwater Pressure Recorder
7. Turbine Exhaust Pressure Indicator

13.7.5 Console Construction

The control console structural members will be steel channeling, using U-shaped channels welded in a manner so as to serve as both structural support for the control unit equipment and wiring duct for electrical leads from the main internal wiring ducts. Using the channel as wiring duct reduces the amount of harnessing necessary, improves appearance and facilitates maintenance by allowing easy identification of cables, their routing and replacement.

The inclined panels containing equipment control will be mounted individually and hinged at the bottom so that they may be opened from the front for any maintenance or repair that is necessary. The upper or top sixteen inches of the three vertical panels of the control console containing the annunciator unit and test panel may be inclined forward to about 60° from the vertical to allow easier reach to the annunciator switches.

The instrument distribution panel will be built integral with the console and will also have structural channels to form wiring ducts similar to the construction described above for the console. The unit shall be completely enclosed and provided with access doors. Power and control cables will be connected to vertical termination boards in the lower section of the distribution panel.

The annunciator panels will be treated the same as the equipment control panels. They will be hinged at the bottom so that the panel may be rotated exposing the circuitry for repair.

All cables and wires entering the control console from the vapor container, nuclear rack and other locations will be plugged into connectors wired to the termination boards in the distribution panel section of the control console. These cables shall enter the distribution panel via overhead raceway except for power supplies from the control skid or nuclear panel. The leads from the distribution terminal boards will enter the control console through three wire-ways in the rear base of the console, accessible from the rear of the console. The three section wire-ways will segregate signal, high power and low power cables for ease of trouble shooting and to insure no signal distortion due to pickup caused by proximity to unshielded power leads. From this wireway, cables will be placed directly into the "channel" construction members. Wires and cables from the controls and equipment in the console will be permanently wired to connectors mounted on the terminal boards.

13.7.6 Annunciator

The annunciator will occupy the vertical panels of the console and will annunciate 96 variables. The relays, lamps and horn mounted in the same section of the control unit. All external connections will be of the plug-in type. Two relays and two lights will be used for each annunciating station. The annunciator panel shall be hinged at the bottom to allow the panel to be rotated around a horizontal axis for any maintenance to components located on the rear of the panel. The annunciator horn shall be provided with adjustable volume control and shall be audible a distance of 30 feet. Individual audible alarms are provided with radiation monitors in areas occupied by personnel. These audible alarms can be heard above the noise level of operating machinery.

The operator is required to acknowledge both the off-normal and the return to normal conditions of both the local and control room annunciation.

13.7.7 Reactor Rod Control and Indication

Each rod position is indicated on a single indicator unit utilizing two independently mounted and geared synchro transmitters electrically connected to their respective receivers. These receivers are directly mechanically to two concentrically driven pointers and contained in the indicator unit. The coarse indicator pointer travels approximately 360° for the full rod travel. The short pointer and smaller dial is used for this indication. The fine indicator pointer, which is the longer of the two, travels 360° for each three inches of rod travel. Rod position may be read to at least within ± 0.02 of an inch. The receiver dials are mounted on the control console directly in front of the operator together with associated rod drive control levers and indicator lights.

Rod position at either extreme of travel is indicated by lights mounted directly to the right of the synchro indicators. A green light for "down" or "in" position and a red light for "up" or "out" position. These lights are push-to-test lights allowing periodic testing of lights locally instead of from some remote control.

Each reactor rod is rack and pinion driven by a 3-phase, 440 volt, 60-cycle motor. This power is transmitted through a main clutch and a smaller over-running clutch when traveling in the "down" or "in" direction and through the main clutch only in the "out" or "up" direction. The over-running clutch drives any rod down which may not fall freely after a "scram" has been initiated. This clutch actuation will continue until the full "down" or "in" position is reached.

From the control unit all five rods may be controlled individually through their respective three-position lever switches. These three-position switches have spring return to the neutral-off position. When either "in" or "out" contactor is energized by correctly positioning the three position lever switch, 3-phase power is supplied through the starter to the motor. The motor then drives the rod "up" or "down" through a gear box and rack and pinion assembly.

To speed up additions of negative or positive reactivity during startups, etc., all five rods may also be controlled in a group or "gang". A switch for controlling the "gang" of five rods is located below the panel of the console containing the individual rod drive controls. Besides being at definitely offset location, the handle of this switch is of distinctive color and shape to further decrease the chance of operator error.

The limits of rod travel are controlled by "in" and "out" limit switches located on the actual rod drive. These switches prevent travel beyond the normal rod travel limits. Upon actuation of either limit switch, the respective limit light is energized and all power through the individual and gang control switches to the motor contactor is cut off, preventing further rod travel.

13.8 External Wiring

13.8.1 Wireways

All instrumentation cables, wires, power and control cables external to the panels and units will be carried in standard wireways with hinged and gasketed areas. These will be bolted or screwed together to form wireways interconnecting the panels and units. The wireways will be run in two sections so that low-level and signal cables can be isolated from power and control cables.

13.8.2 Cables

All instrumentation cables used to connect the panels and units are cut to length at the factory and wired into plug-in type connectors at each end and completely coded. The resulting leads are tested at the factory and prior to installation for continuity and insulation resistance. The cables will be laid in wireways in which provisions are made for segregating signal and power leads and plugged into the correct receptacles at the plant site. All cables have waterproof jacketing to suit the required temperature and humidity conditions and shall be terminated in water-resistant connectors.

14.0 Primary Purification and Make-up System

14.1 Functional Requirements

In conventional power and utility plants, the purity of the boiler water is controlled by a continuous schedule of blowdown and make-up. The same principle was followed in design of the purification system for the APPR-1, the APPR-1a, and this skid mounted nuclear power plant. The Fort Belvoir Plant was the first pressurized water reactor to utilize a low-pressure purification system; because of its many advantages and proven performance, this type of system has been used in most succeeding land-based plants, including Indian Point, Yankee, Savannah, etc. In the APPR-1 design, a small portion of water is continuously withdrawn from the main primary system, purified by mixed-bed demineralization, and reintroduced as make-up to the primary system and control rod seals. Advantages include simplicity of operation, minimum capital investment, and elimination of any waste disposal problems with normal operation.

The purification and make-up system is designed to perform the following functions:

- 1) Continuously remove dissolved and suspended impurities.
- 2) Control system pH.
- 3) Scavenge dissolved oxygen from the coolant by the addition of suitable chemicals (e. g. hydrogen during operation or hydrazine during start-up).
- 4) Prevent deposition on heat transfer surfaces.
- 5) Minimize possibility of fuel element failures.
- 6) Minimize corrosion.
- 7) Protect moving parts and small orifices from clogging or sticking.
- 8) Minimize radioactivity buildup on primary system components.
- 9) Attempt to eliminate radiological hazards to operating personnel and the environment.

14.2 Summary Description of System

The purification and make-up system contains five basic components; 1) a non-regenerative heat exchanger (blowdown cooler), 2) a pressure reducing-flow control station consisting of orifices, a self contained pressure reducing valve and an electro-hydraulic valve, 3) a non-regenerative disposable mixed-bed demineralizer, 4) a make-up tank, and 5) a positive displacement make-up pump.

In addition, the system contains valves, instruments, and auxiliary equipment required for operation and isolation. The blowdown cooler, as shown on R9-47-1013 - Primary System Skid Arrangement - is located on the steam generator skid. The other components are located on the feedwater skid as illustrated by drawing MO2M3 - Feedwater Package General Arrangement.

The basic flow diagram for the purification and make-up system of this skid mounted nuclear power plant is diagramed on drawing R9-47-1012 - Primary System P. & I.D. Primary water enters the purification system at approximately 510°F and 1750 psia. The temperature is reduced to about 110°F in the blowdown cooler to protect the demineralizer resins from thermal damage. A pressure reducing flow control station consisting of orifices, one self-contained pressure reducing valve and one electro-hydraulic valve reduces the pressure to less than 100 psia before the water is processed through a mixed-bed demineralizer. Flow through the purification system is regulated at about 1 gpm, although instantaneous flow is controlled by pressurizer level. Demineralizer influent also includes a small amount of control rod seal leakage water, and as required, make-up condensate to replace system or sampling losses.

A radiation monitor located on the demineralizer constantly monitors radioactivity buildup in this unit. Should radiation levels exceed preset values - as would probably occur during fuel element failure - an alarm in the control room signals the plant operator to discontinue purification flow. When the source of activity is analyzed, flow may either be diverted to the hot waste tank or processed through the demineralizer.

The demineralizer functions both as a filter and an exchanger. Actual operating experience with the APPR-1 has proven that this demineralizer design effectively maintains primary coolant purity and, by removing radioactive nuclides from the water, minimizes radiation and maintenance problems throughout the plant. Since regeneration of radioactive resins is not feasible, and since removal of the resins introduces major handling, storage, and disposal problems, the demineralizer is designed as an inexpensive, low-pressure unit that can be quickly and easily discarded and replaced. The unit is equipped with quick-disconnect seals that completely seal in all radioactive water and resins. The discarded unit can be disposed of either by burial or dumping at sea.

After passing through a filter designed to remove any resin fines that might have entered the water, the purified water is collected and stored in a 60 gallon stainless steel tank. A positive hydrogen pressure is maintained over the water in the tank to prevent air in-leakage and to introduce hydrogen into the make-up water. This hydrogen is automatically supplied from cylinders through regulating valves. Under a gamma flux, hydrogen not only suppresses dissociation of primary coolant, but scavengers any dissolved oxygen that might enter the system. By excluding air from the system, corrosion problems are minimized and air-borne radiation hazards, such as the formation of argon-41, are eliminated.

From the make-up tank, purified coolant is recirculated to the primary system and control rod seals by the primary make-up pump. Pump output can be manually adjusted from 0.17 to 1.7 gpm.

The make-up system provides means for adding a controlled, measured amount of hydrogen to the system during normal operation (through the hydrogen addition flask), hydrazine for oxygen scavenging prior to start-up, and, if necessary, a decontamination or soluble poison solution.

Since all primary water is collected and returned to the system, waste disposal problems are almost eliminated. No primary coolant is discharged to the environment. Thus, this design is suitable for even the most populated area and eliminates any possible public repercussions that might result from the discharge of radioactive water.

Design of this typical purification and make-up system is based on operating experience with the APPR-1. All components have been tested under conditions similar to those that will exist in this plant and have proven that the design is not only effective and reliable, but requires a minimum of operational manpower.

14.3 Design Requirements

The basic design requirements and conditions for the primary purification and make-up system are as follows:

a. The system shall maintain primary coolant purity to such a degree that radiation dose levels due to activated corrosion products, impurities, and deposited "crud" external to piping and components will not pose hazardous accessibility or maintenance problems. The effectiveness of the purification system in minimizing transport and deposition of activated corrosion products is as yet not fully known; however, this design utilizes the best information available from Task I - Activity Buildup Testing Program - of the research and development programs being performed by Alco under Contract AT(30-3)-326.

b. To minimize radiological hazards from gaseous impurities such as A^{41} and N^{16} , and to minimize corrosion due to oxygen or radiation synthesized products such as NH_3 and HNO_3 , the make-up system must be designed to prevent introduction of air with the make-up water.

c. To minimize corrosion by scavenging oxygen and effecting a recombination of the H_2 and O_2 produced by dissociation of the coolant under a neutron flux, the system shall be designed to maintain in the coolant 15-30 cc of hydrogen per kg of water.

d. The required operating life of the demineralizer shall be the maximum consistent with arrangement and component removal considerations, but not less than 90 days.

e. Means shall be provided to protect the demineralizer resin from water exceeding 140° Fahr. to avoid thermal decomposition of the resin and the resultant loss of capacity.

f. To facilitate field modifications or insertions, connections between the major components of the system shall use tubing and compression fittings unless welding is required by the type of service.

g. Primary coolant inlet temperature during operation will vary from 509°F to 500°F.

h. System operating pressure shall be 1750 psig upstream of the pressure reducing-flow control station and less than 2000 psi downstream of the make-up pump. The remaining parts of the system shall be designed for operation at 50 to 100 psig, depending on location.

i. The design corrosion rate of Type 304 or 316 stainless steel under the thermal and hydraulic conditions existing in the primary system is 5 mg/dm²/mo.

j. System equipment may be stored for an indeterminate time at -50°F, although minimum temperature during movement of packages will be -20°F. Since all nuclear grade resins (OH- and H⁺, NH₃⁺, or Li⁺ form) must be shipped as a water slurry, the possibility exists of cracking the resin beads by freezing. The need for protection during transit and/or storage is dependent on the outcome of a proposed research and development program on this subject.

k. Plant radiation levels under normal operating conditions shall be such that the dose received by plant personnel working 84 hours per week shall not exceed 300 mr.

l. The equipment shall be designed or braced to withstand 8 G's of shock during transit only.

m. Leakage from the five control rod seals will be less than 0.1 gpm.

n. Primary system volume control shall be based on adjustment of purification rate rather than make-up rate. Although no plant operating data is available on this control arrangement, discussions with manufacturers indicates that this will permit closer control of large transient variations than is possible with the APPR-1 setup.

o. Resin bed depth in the demineralizer shall be a minimum of 30 inches. In the absence of APPR-1 operating data on the effect of flow loadings on optimum demineralizer decontamination factors (gross D. F.'s as well as individual nuclides), flow loading specifications shall be based on conductivity data available from resin manufacturers. During normal operation, flow loadings shall be about 7.5 gpm per square foot of bed surface.

p. The primary coolant shall be maintained at essentially neutral pH. Although data from other installations indicates operation at high pH may be beneficial, the effect of high pH on APPR-1 operation (activity build-up, corrosion rates, corrosion product release rates, heat transfer, gas activity, fission product levels, etc.) has not been demonstrated.

q. Based on data obtained under Task I - Activity Buildup Studies under Contract AT(30-3)-326 and APPR-1 operating data, 25% of the total solids in the coolant are conservatively assumed to be soluble for design purposes. The average chemical combining weight of the corrosion products is assumed to be 50. Capacity of the resin is 10,000 grains/ft³ as CaCO₃.

r. Based on APPR-1 operating results, system design will not include an in-line gamma radiation monitor to measure primary purification radiation levels. Experience indicates that crud bursts, activity deposition on the chamber surface, and other factors nullify attempts to use this type of monitor to detect failed fuel elements. The need for a failed fuel element detection system is presently being evaluated under Task III - Fission Product Study of Contract AT(30-3)-326. Area monitors are included for personnel protection.

s. A connection shall be provided on the suction of the primary make-up pump to introduce hydrazine for oxygen scavenging during initial startup, a decontaminating solution, and a soluble poison solution. Although the latter two are not required by plant design criteria, their inclusion is considered desirable emergency features. The decontamination solution would be used in the event of fuel element failure, excessive buildup of long-lived deposited activity on primary system surfaces, or to facilitate relocation of the plant. The soluble poison solution would be used to control hot-to-cold reactivity changes in the event a control rod becomes stuck in the "full out" position or two rods become stuck in the operating position during the first part of core life.

t. Mixed-bed resin specifications are as follows:

Mixture: mixture of strongly acidic cation resin in the hydrogen form and strongly basic anion exchange resin in the hydroxyl form in proportions of 1.0 equivalent of hydroxyl ion to 1.0 equivalent of hydrogen ion.

Particle Size: both the cation and anion resins shall have a mean particle size of 16 to 50 mesh and a uniformity coefficient of less than two.

Capacity: the cation resin shall have a total finished capacity of not less than 47 milliequivalents per dry gram, of which not less than 95 equivalent percent shall be in the hydrogen form.

The anion resin shall have a total finished capacity of not less than 3.5 milliequivalents per dry gram, of which as great a proportion as is feasible, but not less than 80 equivalent percent shall be in the hydroxyl form.

Impurities: The resins shall be specially treated to remove any soluble organic contaminants which may be present. The resin shall not contain impurities of foreign cations greater than the following:

| | <u>Parts per million</u> <u>(of dry resin)</u> |
|------------------------|---|
| iron | 200 |
| copper | 100 |
| heavy metals (as lead) | 100 |

The resin shall not contain impurities of foreign anions greater than the following:

| | <u>Percent (equivalent)</u> |
|-----------|-----------------------------|
| chloride | 5 |
| carbonate | 15 |

14.4 System Design Data

Primary system piping and vessels will be fabricated of AISI type 304 stainless steel. All other system components exposed to the primary water will be of type 304 stainless steel with the following exceptions:

- (1) Rod drive mechanism

| | |
|-----------------------|-------------------------------|
| Valve seat and pinion | type 410 stainless steel |
| water seal shaft | Armco 17-4 PH stainless steel |

- (2) Instrumentation

| | |
|--|--|
| | type 441 stainless steel (where no flow exists) |
|--|--|

Purification system flow rates are based on the design requirements outlined in 14.3. The primary system surface area and volume used for corrosion and activity buildup considerations were $2.48 \times 10^6 \text{ cm}^2$ and 600 gallons, respectively. The calculated values for the individual components are as follows:

Primary System Surface Areas and Volumes

| | <u>Area, Ft²</u> | <u>Volume, Ft³</u> |
|--------------------------------------|-----------------------------|-------------------------------|
| Thermal Shield | 60.8 | |
| Core and Control Rod Drive Mechanism | 1580.0 | |
| Reactor Vessel (net water) | 91.2 | 42.8 |
| Primary Piping | 39.8 | 7.6 |
| Primary Coolant Pump | 2.5 | 3.0 |
| Steam Generator | 894.0 | 20.6 |
| Pressurizer | | <u>6.0</u> |
| Total | <u>2668.3</u> | <u>80.0</u> |

Based on the above, and assuming that at equilibrium the soluble and insoluble corrosion products entering the coolant are equal to the corrosion rate of the material under consideration, the impurities added to the coolant by corrosion were calculated to be $3.79 \times 10^{-4} \text{ lb/hr}$ or 124 grams per month. Using various assumptions for demineralizer efficiency, purification system effectiveness in competing with system surfaces for circulating "crud", deposition rates on heat transfer and nonheat transfer surfaces, demineralizer decontamination factors, etc., the required purification flow rate was calculated to be 1.1 to 1.5 gpm. Evaluation of standard pump capacities and designs offered by manufacturers indicated that a positive displacement pump with a 1.7 gpm maximum output would be sufficient

to meet system make-up and control rod drive seal requirements.

Assuming that all soluble corrosion products stay in solution and using 0.25 as the ratio of soluble to insoluble impurities (see 14.3, q), the volume of resin required per month can be calculated. The effect of filtered crud on the exchange capacity of the resin is unknown and is not factored into the calculations. For this prepackaged nuclear plant, a minimum of 0.12 Ft³ of resin will be exhausted per month or 0.36 Ft³ in 3 months of operation at system temperature. To account for unknown factors, the design value used was 1.5 times the minimum value or 0.54 Ft³ of resin for 3 months operation.

For comparison, with improvements in influent distribution to prevent the channeling found under Task VI - Shielding Studies of Contract AT(30-3)-326, an APPR-1 type demineralizer would last about 9 months. This coincides reasonably well with APPR-1 operating experience.

Pressure drop data used to determine design pressure requirements of individual components in the purification system were a combination of manufacturers' data and measured values during APPR-1 operation. The head loss due to friction/100 ft. of 1/2" 16 BWG stainless steel tubing was calculated using the Fanning equation:

$$h = \frac{fLv^2}{2gd} \quad \text{or} \quad \frac{0.03112 fLq^2}{d^5} \quad (1)$$

where:

- h = Head loss to friction, ft.
- f = Friction factor, dimensionless
- L = Length of pipe, ft. (100 ft.)
- v = Velocity of flow, ft. sec.
- g = Acceleration of gravity, ft/sec² (32.2)
- q = Flow of liquid, gal/min
- d = Internal Diameter of pipe, in (0.370 in.)

Substitution of known constants in equation

(1) yields:

$$h = 9.1 \times 10^7 f q^2$$

The friction factor is determined as a function of Reynolds number by the equation

$$N_{Re} = \frac{DV_p}{u}$$

where:

- D = Dia. of pipe, ft.
- V = Velocity of fluid, ft/sec.
- p = Density of fluid, lbs/ft³ (assumed temperature of 120°F Ave.)
- u = Viscosity, lbs-mass/ft-sec. or centipoises/1488

Assuming various flow rates in the purification system, the head loss per 100 ft. of 1/2" stainless steel tubing was calculated. The results are tabulated below:

Head Loss/100 ft. of 1/2" S. S. Tubing

| <u>gal/min</u> | <u>ft³/sec</u> | <u>ft⁶/sec²</u> | <u>D Ft.</u> | <u>V ft/sec</u> | <u>P # Mass/ft³</u> |
|----------------|---------------------------|---------------------------------------|--------------|-----------------|--------------------------------|
| 1 | .0022 | 485 x 10 ⁻⁸ | .0309 | 3 | 61.5 |
| 2 | .0044 | 1940 x 10 ⁻⁸ | .0309 | 6 | 61.5 |
| 5 | .0110 | 12,100 x 10 ⁻⁸ | .0309 | 15 | 61.5 |
| 10 | .0220 | 485 x 10 ⁻⁶ | .0309 | 30 | 61.5 |
| 20 | .0440 | 1940 x 10 ⁻⁶ | .0309 | 60 | 61.5 |

| <u>q gal/min</u> | <u>u Centipoises</u> | <u>DVp/u Dimensionless</u> | <u>f x 10³</u> | <u>Head Loss Ft.</u> | <u>Psig</u> |
|------------------|----------------------|----------------------------|---------------------------|----------------------|-------------|
| | <u>1488</u> | | | | |
| | x10 ⁻⁴ | | | | |
| 1 | 4.05 | 14,100 | 6.25 | 2.76 | 1.2 |
| 2 | 4.05 | 28,200 | 6.0 | 10.6 | 4.6 |
| 5 | 4.05 | 70,500 | 4.5 | 49.5 | 21.5 |
| 10 | 4.05 | 141,000 | 4.0 | 177 | 76.5 |
| 20 | 4.05 | 282,000 | 3.5 | 618 | 268 |

The values used for pressure drop through valves, fittings, and other system components was as follows:

Pressure Drop Through Purification System Components
Downstream of the Pressure Reducing - Flow Control Station

| | <u>Pressure Drop Psig</u> | <u>Equivalent ft. of 1/2" tubing</u> |
|-------------------------|---------------------------|--------------------------------------|
| Demineralizer ("dirty") | 10 | |
| Filter | 5 | |
| Valves | | 23.75 |
| Flow Indicator | 2 | |
| Tees, elbows, fittings | | 25.6 |
| | <u>17</u> | <u>49.35</u> |

For 50 equivalent feet of tubing in valves and fittings, the total pressure drop due to system components was calculated for various flow

rates. Results are listed below:

Head Loss Due to System Components

| <u>gal/min</u> | <u>pressure drop for 50 eq. ft.</u> | <u>Total pressure drop</u> |
|----------------|-------------------------------------|----------------------------|
| 1 | 0.6 | 17.6 |
| 2 | 2.3 | 19.3 |
| 3 | 4.2 | 21.2 |
| 4 | 7.0 | 24 |
| 5 | 11.0 | 28 |
| 6 | 16.0 | 33 |

From the above calculations, it is apparent that designing the demineralizer to withstand 100 psig will be more than adequate with expected flow rates.

14.5 Detailed Description of Equipment and Components

14.5.1 Purification Heat Exchanger (blowdown cooler)

The purification heat exchanger consists of a spiral shaped series of coils held between two flat surfaces - a base plate and casing. These parts when bolted together form closed spiral shaped fluid circuits outside of the coils and in between the two surfaces previously referred to, running counterflow to the companion circuits inside of the coils. Coils are stacked on top of one another and held together by the base plate and casing. Each coil is attached to a manifold located at either end of the coil. These manifolds are then bolted to the base plate matching up with the piping connections to an from the coil side of the unit. The connection that admits cooling water to the outside of the coils is located on the base plate.

The heat exchanger will have the following characteristics:

a. Type: spiral tube, counterflow

b. Materials of Construction:

Coil: 3/8 x 18 BWG stainless type 304
Manifold: bar stock stainless type 304
Base plate: steel plate
Casing: fabricated steel

c. Performance

| | <u>Conditions</u> | |
|-----------------------------------|--------------------|---------------------|
| | <u>Inside Coil</u> | <u>Outside Coil</u> |
| 1. Fluid Circulated | Primary Coolant | Cooling Water |
| 2. Rate of Flow | 104 g.p.h. | 600 g.p.h. |
| 3. Max. Entering Temp, °F. | 600 | 100 |
| 4. Max. Leaving Temp, °F | 120 | 183 |
| 5. Max. press.drop, psig | - | less than 1 |
| 6. Operating Press., psig | 1750 | |
| 7. Design Press., psig | 2000 | 100 |
| 8. Hydrostatic Test Press., psig | 2275 | 150 |
| 9. Total duty, BTU/hr | 416,000 | |
| 10. Total Surface ft ² | 11.6 | |

14.5.2 Pressure Reducing - Flow Control Station

Purification flow is controlled by use of 1) a pressure reducing orifice, 2) a pressure control valve, and 3) a flow control valve. The pressure control valve is a self-contained control valve that senses the pressure downstream of itself and adjusts accordingly. The flow control valve is an electro-hydraulically actuated valve. The electrically operated valve actuator produces high performance without the use of electronic amplification, utilizing only a simple force motor to control the hydraulic pilot. The pilot system incorporates no close fitting parts, such as sliding plate or spool valves, using instead simple nozzle-flapper combinations to control hydraulic pressure. Although no operating experience is available with this setup in an APPR-1 type system, it is believed to offer a marked improvement over the motor-operated throttling valve installed in the Fort Belvoir plant.

The pressure reducing orifice is sized to reduce the pressure in the purification system from 1750 psig to approximately 450 psig. The pressure regulating valve downstream of the orifice controls effluent pressure at 100 psig (or other preset value). Since the flow control valve is not involved in pressure regulation, it can accurately control purification flow as required.

14.5.3 Demineralizer

The demineralizer is a vertically mounted cylindrical vessel constructed of Type 304 stainless steel with a design pressure of 100 psig. It serves simply as a container for the resin used to purify the primary coolant. The resin purifies the water by removing radioactive and non-radioactive corrosion product, serving both as a filter for insoluble material and exchanger for soluble ionic impurities. Since regeneration of radioactive resins is not feasible, the demineralizer is designed as an

inexpensive unit that can be discarded and replaced. To facilitate replacement, minimize radiation exposures, and to prevent contamination of the shipping cask, inlet and outlet connections are provided with self-sealing quick disconnect couplings.

Influent water enters the top of the vessel through a distribution assembly which retains the resin in the unit and evenly distributes the water to minimize channeling. A similar assembly is also installed in the bottom of the demineralizer vessel to collect the purified water and prevent resin escaping into the outlet line. The distribution assembly chosen for the design consists of a number of slotted pipes radiating from the center inlet and outlet manifolds similar to spokes on a wheel.

To minimize radiation exposures to the operating crew, the demineralizer will be kept within the shipping cask which will be used to dispose of the unit when the resin is exhausted. Cask shielding design is covered in another section of the report.

14.5.4 Purification Filter

A cartridge type filter is included in the purification system to catch any resin fines leached from the demineralizer or, in the event of malfunction, any crud that might channel through the resin bed. Mean pore size of the filter is 5 microns, rated to remove any particles over 2 microns in diameter. Pressure drop across a clean unit is about 1 psi; however, entrapped material may increase this to over 5 psi. If pressure drops exceed the latter value, the housing is designed so that the cartridge can easily be replaced with a new unit.

14.5.5 Primary Make-up Tank

To provide a positive net suction head on the primary make-up pump and to provide an immediate supply of purified water for the primary system during possible emergencies, a 60 gallon make-up storage tank is included in the system. Assuming the maximum addition rate, the tank will hold a 30-minute supply of water. This time interval will permit the flow rate of make-up condensate from the secondary system to be increased to handle reasonable leakage rates.

A positive hydrogen blanket is maintained automatically over water in the tank to prevent in-leakage of air. The hydrogen is supplied from a cylinder with discharge pressure regulated by a pressure control valve. Since sufficient hydrogen may not be introduceable by this method to maintain 15-30 cc of hydrogen per kg. of coolant, particularly if appreciable air enters the primary system, a hydrogen addition system is included in the make-up system design.

14.5.6 Primary Make-up Pump

The primary make-up pump is a positive displacement, constant speed, controlled volume duplex pump rated at 1.7 gpm, maximum output under expected operating conditions. Discharge capacity can be ad-

justed from 0.17 gpm to 1.7 gpm by manually resetting the plunger stroke lengths while the pump is at rest. The pump motor is rated at 5 H.P., 440V, 3-phase, 60-cycles and is suitable for boiler-house installation.

14.5.7 Hydrogen Addition Flask

A hydrogen addition flask is provided in the purification and make-up system design to permit addition of a controlled known volume of hydrogen to the primary coolant in excess of that introduced in the make-up tank. The addition assembly is illustrated on R9-47-1012 - Piping and Instrument Diagram, Primary Coolant System. Hydrogen is supplied to the addition flask from a cylinder of the gas and is used both to purge and pressurize the flask. When required, the flask is valved into the make-up line, the by-pass valve closed, and the make-up water sweeps the hydrogen into the primary system.

14.6 Boron Injection

In the event the reactor could not be brought to zero power because of a stuck rod condition, a secondary means of accomplishing this would be boron poisoning. One side rod stuck in the full up position is the most critical case and would require 9 grams of boron-10 dispersed within the core to effect zero power under these conditions. This could be accomplished by injecting 14.9 lbs. of boric acid in solution into the primary system.

14.6.1 Poison Tank

To prepare a 50% solution of boric acid at room temperature, 72 gals. of water are required, therefore a 75 gal. tank could serve as a mixing and storage tank and with the necessary piping to the suction side of the primary make-up pump the required injection force could be provided by this pump. The injection could be completed in 42 minutes.

14.7 Seal Leakage System

14.7.1 Seal Leakage Tank

A closed 20-gallon type 304 stainless steel tank is provided in the plant design to collect control rod seal leakage water. The tank is equipped with level control switches to automatically actuate the seal leakage pump. Pump effluent is discharged into the purification system upstream of the demineralizer. The tank is also provided with a high-pressure alarm, and a vent and relief valve connected to the stack through a flame arrester.

14.7.2 Seal Leakage Pump

A canned rotor centrifugal pump is provided to empty the seal leakage collection tank as required. Pump output was sized so as to net

adversely affect demineralizer efficiency due to high flow loadings. The level control switches which actuate the pump are designed to permit frequent operation of the pump to minimize seizure due to exposure in a moist atmosphere.

14.8 Spent Fuel Tank Recirculating Equipment

On the bottom of the spent fuel tank, inlet and outlet gate valves with 1/2" flanged connections are provided. A portable centrifugal pump is used to recirculate the water through a cartridge type filter whenever such action is dictated by excessive turbidity of the water. The use of a portable centrifugal pump has proved its usefulness at the APPR-1 installation at Fort Belvoir for such uses as recirculating, filling, draining and other general utility purposes.

14.9 Initial Fill

The primary system may be initially filled at a rate of 25 gpm from the secondary feedwater storage tank by utilizing one of the cooling water circulating pumps and the necessary piping and valves. The water will be pumped directly into the primary system and avoid the 1/2" primary blowdown line.

14.10 Activity Buildup Considerations

Radioactivity isodose levels around the primary system eight hours after shutdown from prolonged full power operation cannot be accurately predicted with present technology. Development work on this technology is presently proceeding under Task I of Contract AT-(30-3)-326. The following information on radioactivity levels in the primary system of the Army Package Power Reactor at Ft. Belvoir, Virginia is indicative of what can be expected in this similar skid mounted nuclear reactor. The data are based on least mean square values of dosage eight hours after shutdown following one year of extrapolated full power operation. Radiation measurements in pipe lines were taken on contact with the four inches of insulation surrounding the 12-inch outside diameter pipe.

| <u>Location in System</u> | <u>Radiation Level Due to Deposition Activity on Primary System Surfaces (Mr/hr)</u> |
|---|--|
| Crud Piping Elbow below Steam Generator | 850 |
| Traps Piping Elbow below Pressurizer | 1900 |
| Reactor Inlet Pipe | 270 |
| Side of Steam Generator | 200 |

It should be noted that the piping elbows were crud traps and the activity could be reduced rapidly by flushing the crud from these points. The 200 mr/hr value in the steam generator appears to be the normal radiation level at points where crud does not concentrate.

The following table gives approximate radiation levels at given distances from the steam generator eight hours after shutdown.

| <u>Distance from Steam Generator</u> | <u>Radiation Level (mr/hr)</u> |
|--------------------------------------|--------------------------------|
| Contact with Steam Gen. Insulation | 200 |
| 1 foot | 112 |
| 2 feet | 76 |
| 3 feet | 40 |
| 4 feet | 36 |
| 5 feet | 24 |

15.0 Waste Disposal System

15.1 Functional Requirements

The waste disposal system is sufficient to collect and process the entire liquid contents of the primary and secondary systems plus normal waste accumulation over a 2-month period. This is a total of 4450 gallons. However, the design capacity is based more realistically on the total volume of water in the primary system, the shield tank above the pressure vessel, and two months accumulation of normal radioactive plant wastes (hot laboratory wastes, active wastes from equipment and floor drains, and active wastes from sampling). In addition, sufficient extra capacity is included to accommodate decontamination and rinsing of the primary system.

15.2 Summary Description of System

The hot waste storage tank shown on R9-47-1012 - Piping and Instrument Diagram - Primary Coolant System - is the major facility for containment of radioactive liquids. Radioactive water will be added to the tank from a number of sources and for various reasons. During normal operation of the purification system, settings on the relief valves may be momentarily exceeded, dumping a small amount of water into the tank. If primary coolant or demineralizer effluent exceeds preset limits due to crud bursts or fuel element failure, the demineralizer influent or effluent can be manually diverted to the tank. In the event of a steam generator tube failure which would contaminate the steam generator blowdown, the blow-off tank can be dumped into the hot waste tank. Hot waste tank influent can also include shield tank water if the latter is contaminated by intermixing with the primary coolant when the pressure vessel cover is removed. Other fluids that may be added to the tank are condensate from the vent stack if the latter becomes contaminated; hot laboratory wastes; equipment and floor drains from certain skids; sampling wastes; contaminated laundry wastes; and solutions used to decontaminate, rinse, or flush equipment and system components.

Whatever the source or activity in the solutions added to the hot waste tank, the contents must be stored and/or processed. If storage and decay sufficiently reduce the activity and the water is not required for plant

usage, the contents can be pumped into the ice cap for disposal. If purification is required, connections are provided on the discharge of the pump to process the tank contents through the purification system demineralizer. Demineralizer effluent from this operation can be returned to the plant via the make-up tank or can be returned to the hot waste tank for further processing or disposal.

15.3 Design Requirements

A 5000-gallon storage tank is used for the containment of radioactive liquid. This tank will provide for collection of the entire primary coolant, top shield water, one decontaminating flush, two rinses, and two months accumulation of normal plant wastes. The design capacity figures are listed below:

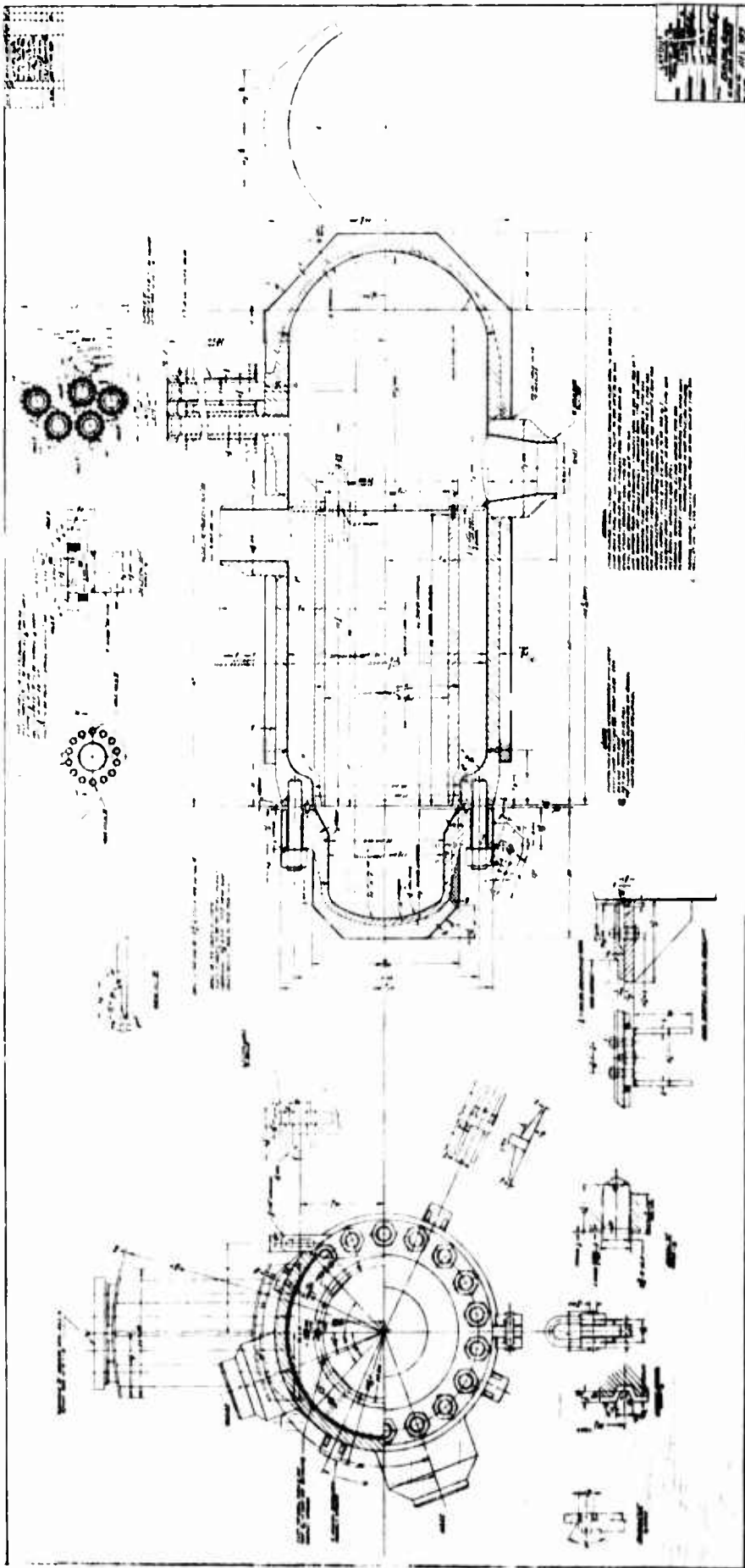
| | |
|------------------------------------|-----------------|
| Volume of primary coolant | 600 gal. |
| Volume of top shield tank | 2245 gal. |
| Volume of decontamination flush | 600 gal. |
| Volume of two rinses | 1200 gal. |
| Volume of two month's normal waste | <u>350 gal.</u> |
| | 4,995 gal. |

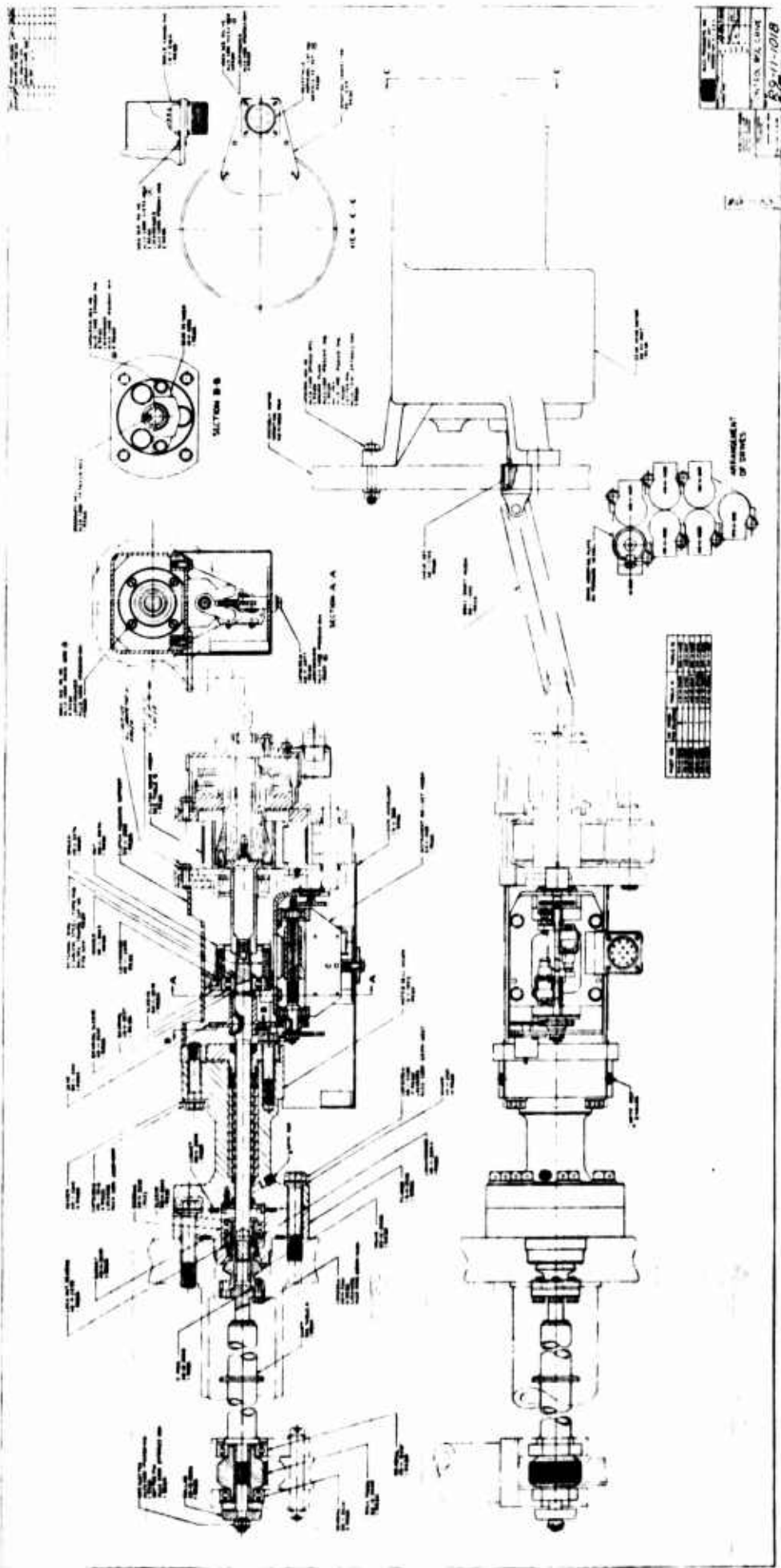
Alternately, the tank is capable of holding the entire primary and secondary system volume plus two months normal waste. The total capacity required in this case amounts to 4450 gallons, including 600 gal. for primary coolant, 350 gal. for normal wastes, and 3500 gal. for the secondary system. The latter comprises the following:

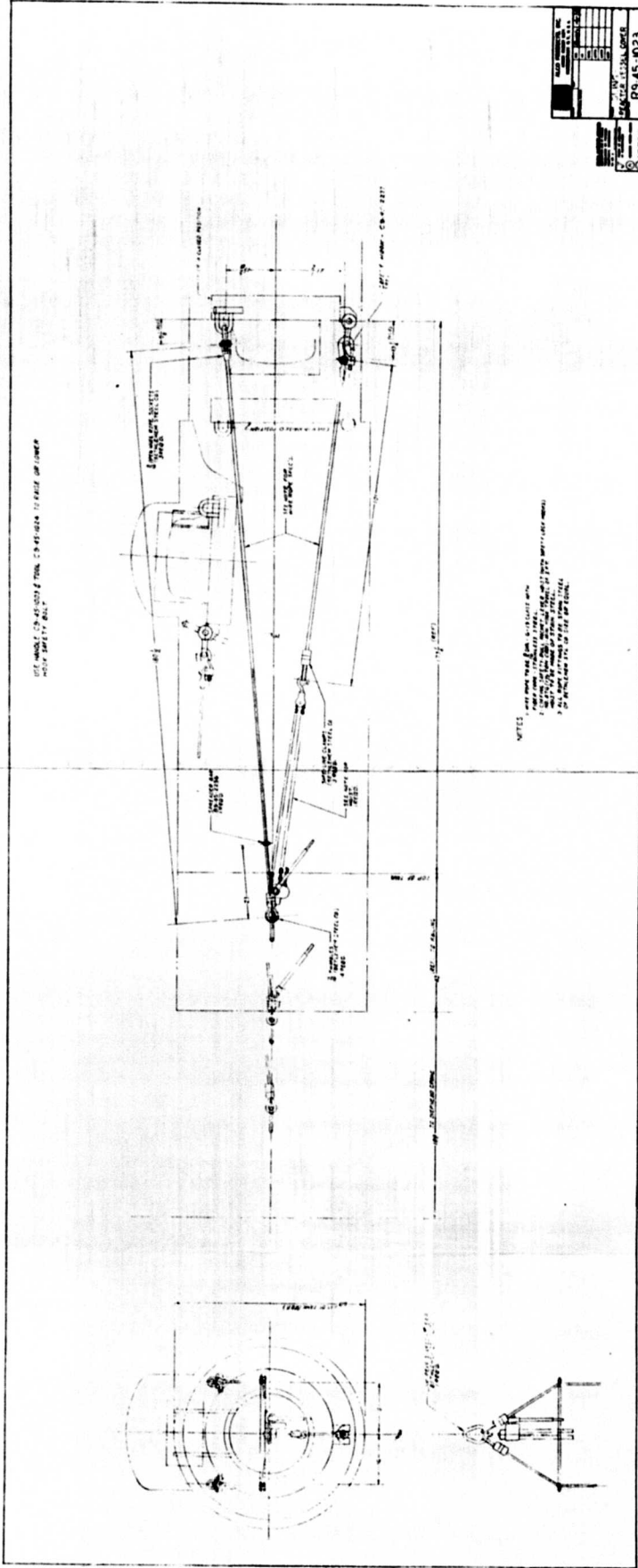
| | |
|-------------------------|------------------|
| Steam Generator | 690 gal. |
| Condenser Hotwell | 300 gal. |
| Pump and Piping | 10 gal. |
| Condensate storage Tank | <u>2500 gal.</u> |
| | 3500 gal. |

Since all of these solutions, including any reducing-complexing solution used as a decontaminating reagent, can be processed through the demineralizer, the storage volume required will be less than that listed above. It is anticipated that the hot waste tank will normally only have to provide temporary storage of solutions pending treatment and disposal. A decontamination flush into this tank with subsequent disposal of radioactive crud will be necessary prior to plant relocation. However, due to insufficient technology on control of activated corrosion products, it is not known if the decontamination flush will have the desired effectiveness in reducing the radiation level of primary system components.

An evaporator will be provided for concentration of radioactive waste and reclaiming of waste water if directed by the government. It is anticipated that an evaporative capacity of 30 to 50 gallons per hour will be sufficient for this purpose. This would allow processing of a full tank of waste water in less than one week of continuous operation.





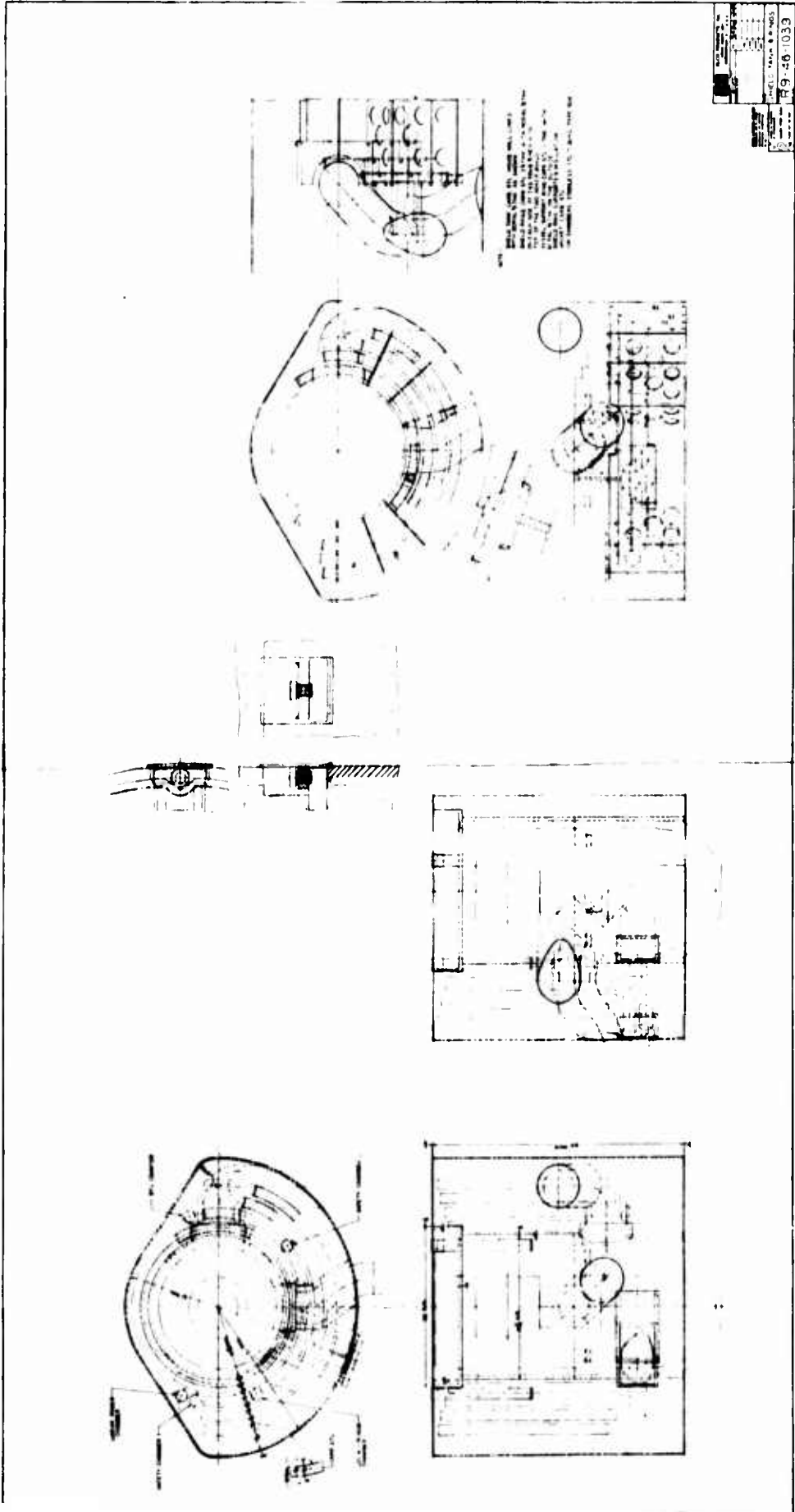


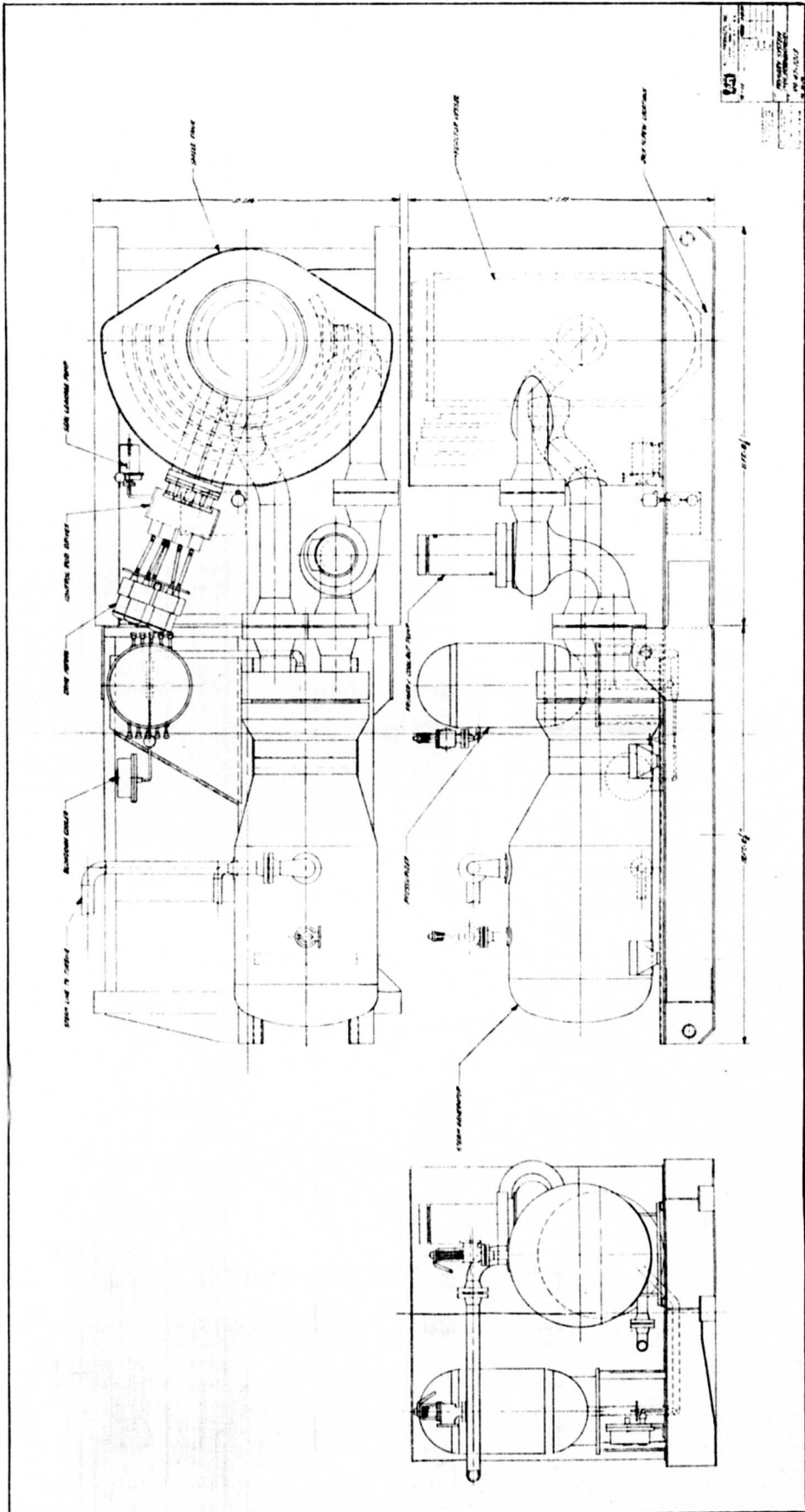
ALL DIMENSIONS ARE IN INCHES UNLESS OTHERWISE SPECIFIED.

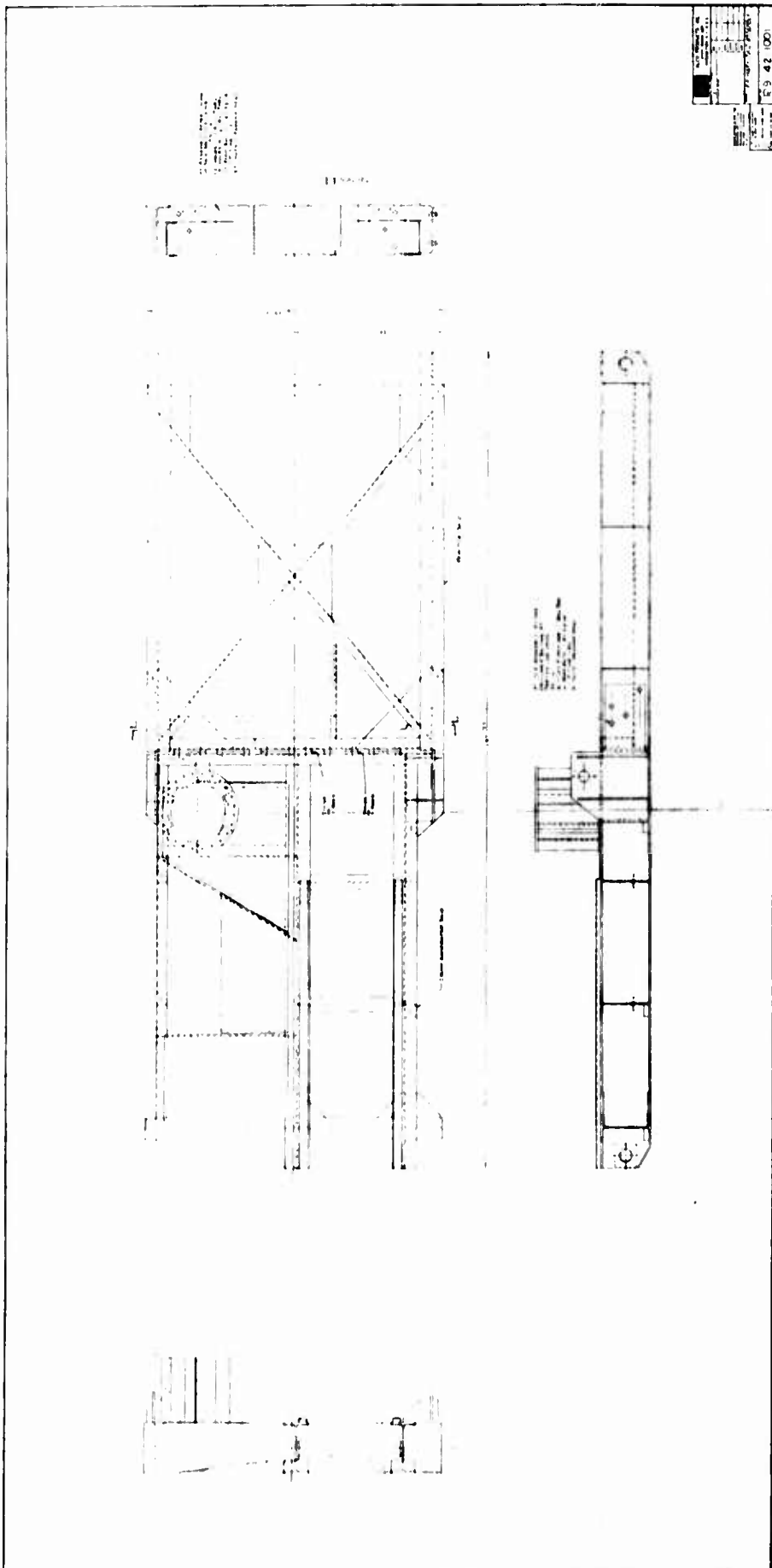
NOTES:

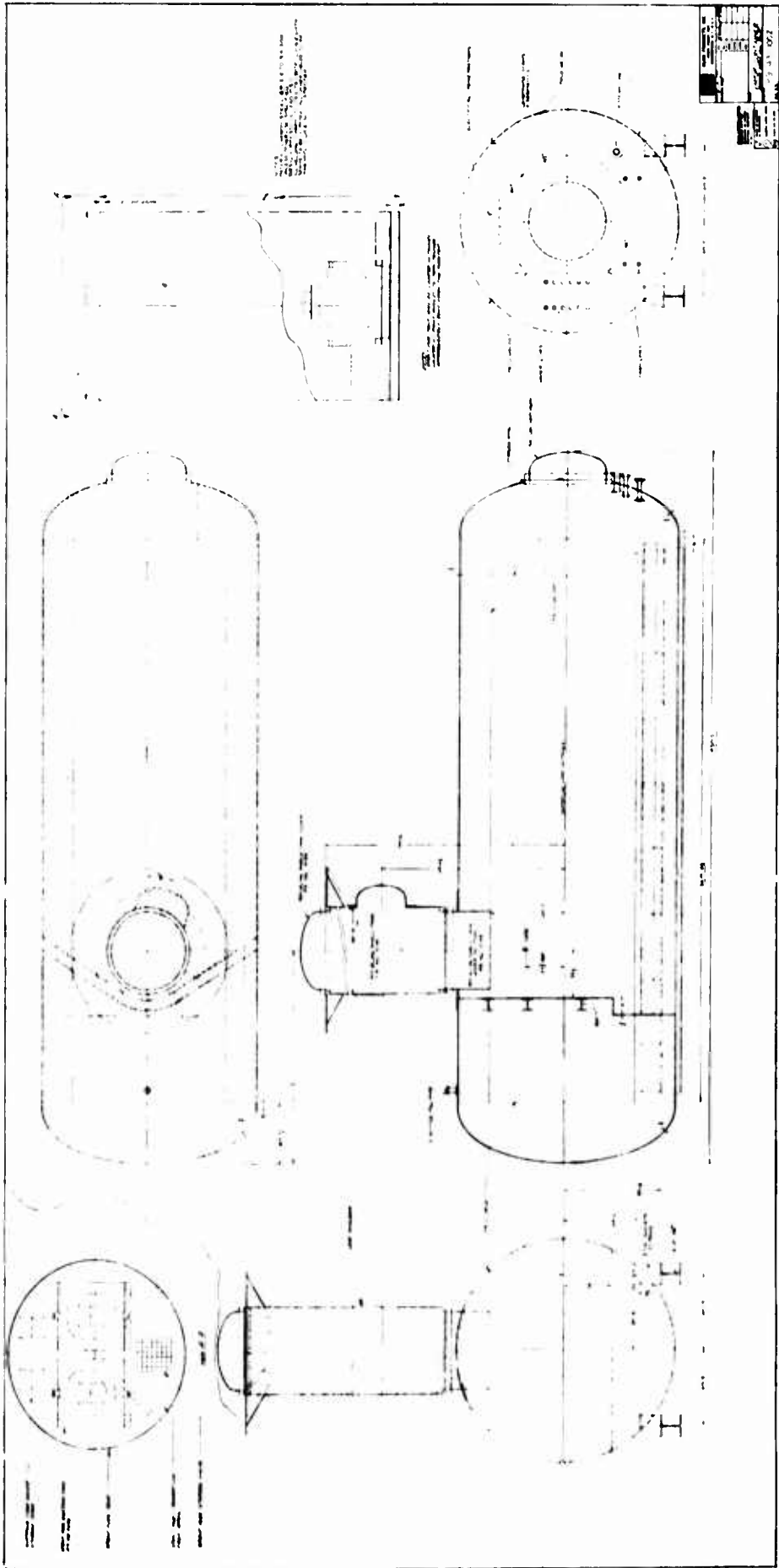
1. ALL DIMENSIONS ARE IN INCHES UNLESS OTHERWISE SPECIFIED.
2. ALL DIMENSIONS ARE TO BE TAKEN TO THE CENTER OF THE SHAFT UNLESS OTHERWISE SPECIFIED.
3. ALL DIMENSIONS ARE TO BE TAKEN TO THE CENTER OF THE HOLES UNLESS OTHERWISE SPECIFIED.

| | | | |
|---|-----|-------|--------|
| DATE | BY | CHKD. | APP'D. |
| 1954 | ... | ... | ... |
| DRAWING NO. 19-45-1023 PART NO. 19-45-1023 | | | |











| | | | |
|------|----|------|-------|
| DATE | BY | CHKD | APP'D |
| | | | |



GUIDES MADE FROM
2x1/2" D. x .049 WALL
TYPE 304 STAINLESS
STEEL TUBING

RAVET & W.C.'S
TYPE 304 STAINLESS STEEL
ALL WELDING IS TO BE
TYPE 304 STAINLESS STEEL
WELDING
NOTE: THIS FUEL ELEMENT
HAS WELDED JOINTS
BEFORE CONSTRUCTION TO
WELDED JOINTS
WELDED JOINTS

ESTIMATED WEIGHT = 26.6 LBS.

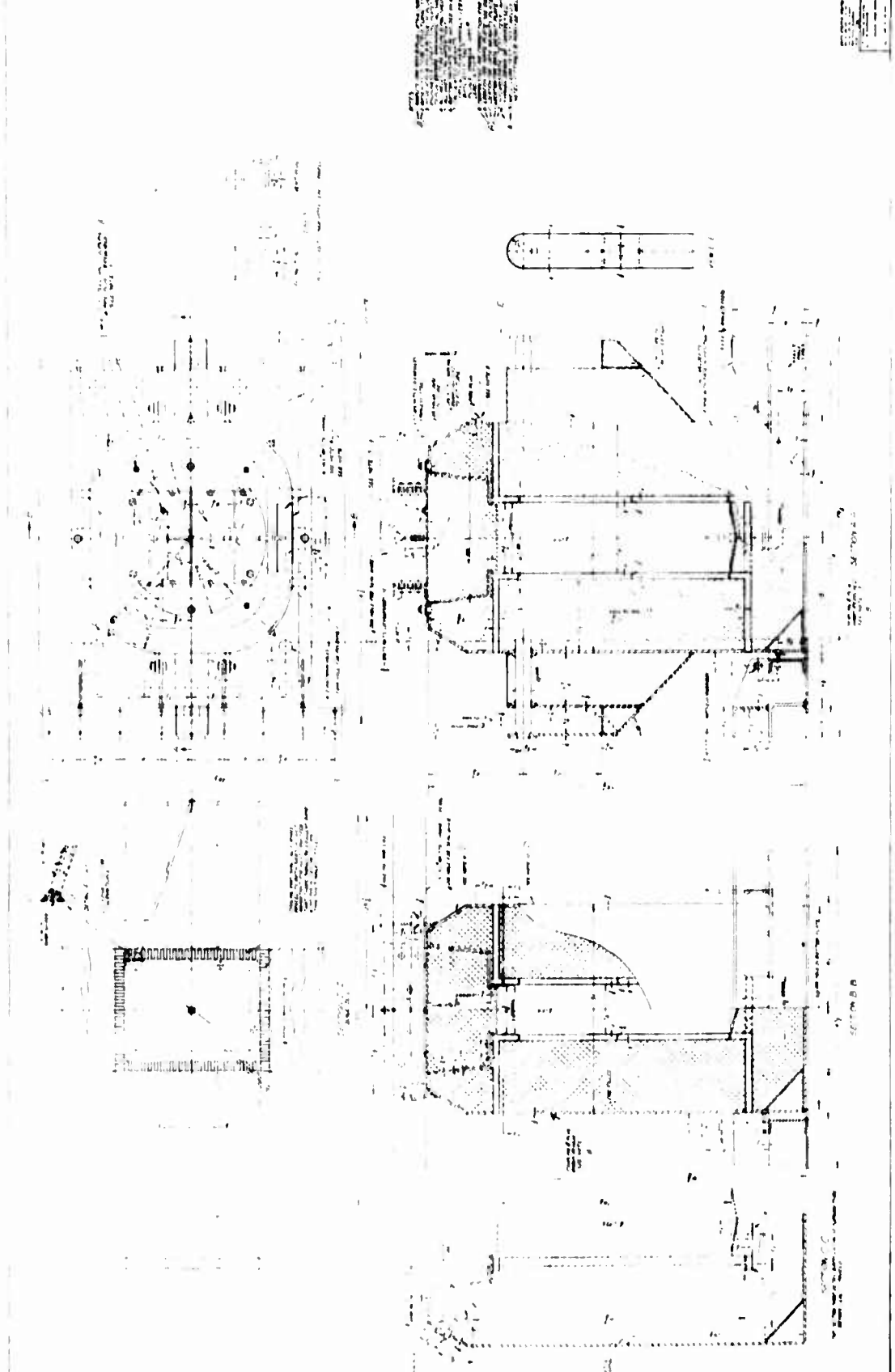
| | |
|--------------------------|--------------------------|
| ALCO PRODUCTS INC. | ALCO PRODUCTS INC. |
| MEMPHIS, TENNESSEE 38103 | MEMPHIS, TENNESSEE 38103 |
| SEE NOTES | SEE NOTES |
| DATE | DATE |
| BY | BY |
| CHKD | CHKD |
| APP'D | APP'D |

A-121

161

09-48-2035

Technical drawing header area containing a grid on the left and a title block on the right with fields for drawing title, scale, and date.

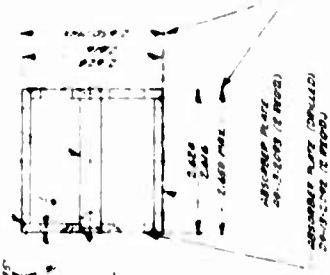


| | | | |
|--|--|--|--|
| | | | |
| | | | |
| | | | |
| | | | |



23 1/2"

2 1/2"



2 1/2"

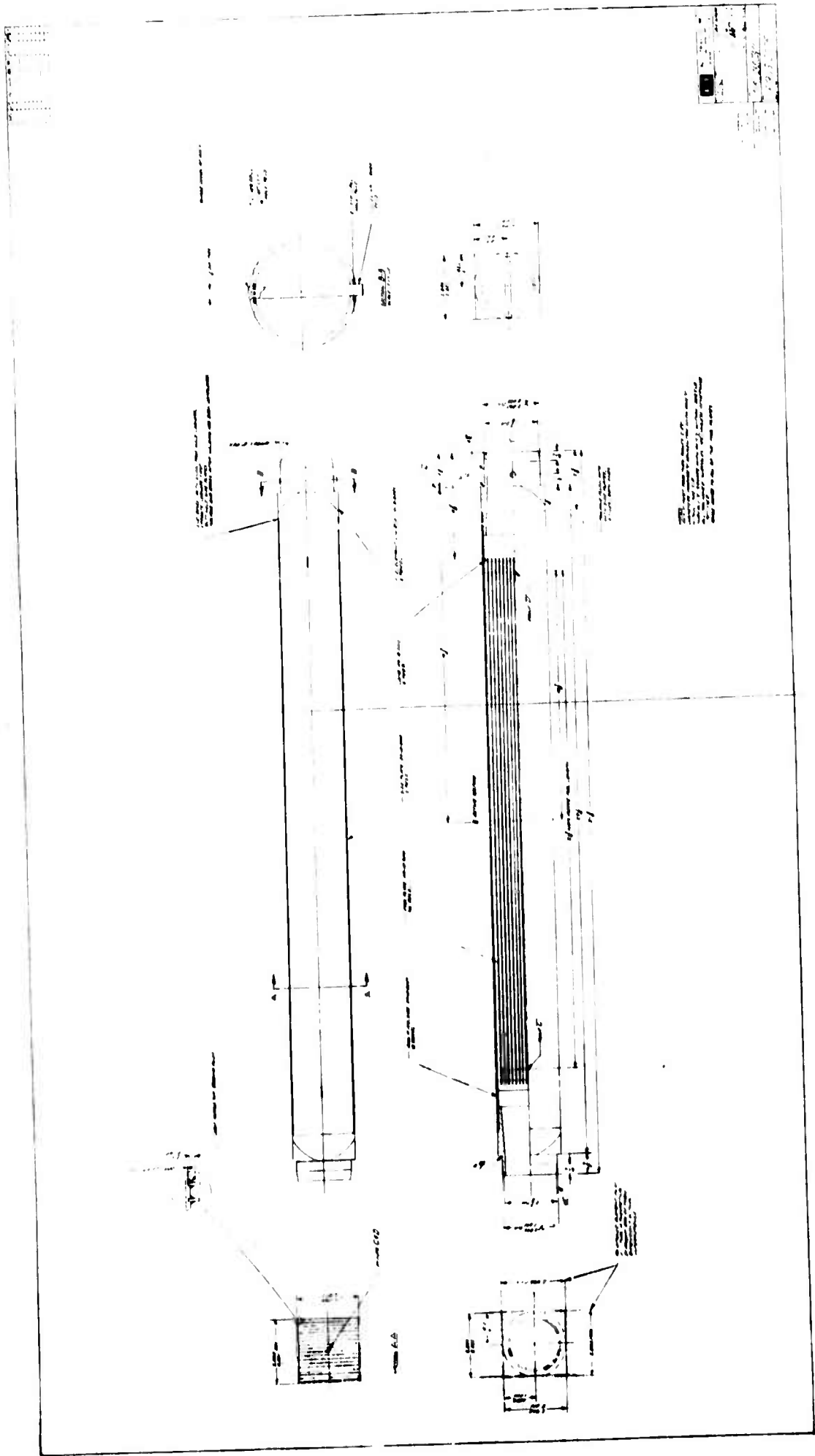
1.400"

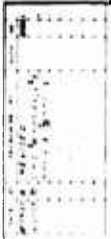
ALL DIMENSIONS MUST BE TAKEN AT
FACTORY TEMPERATURE AND AT THIS
DIMENSIONS TO 1/16" UNLESS OTHERWISE

ALCO PRODUCTS, INC.
ALCO
4530 BEECHER
D9-12-2024

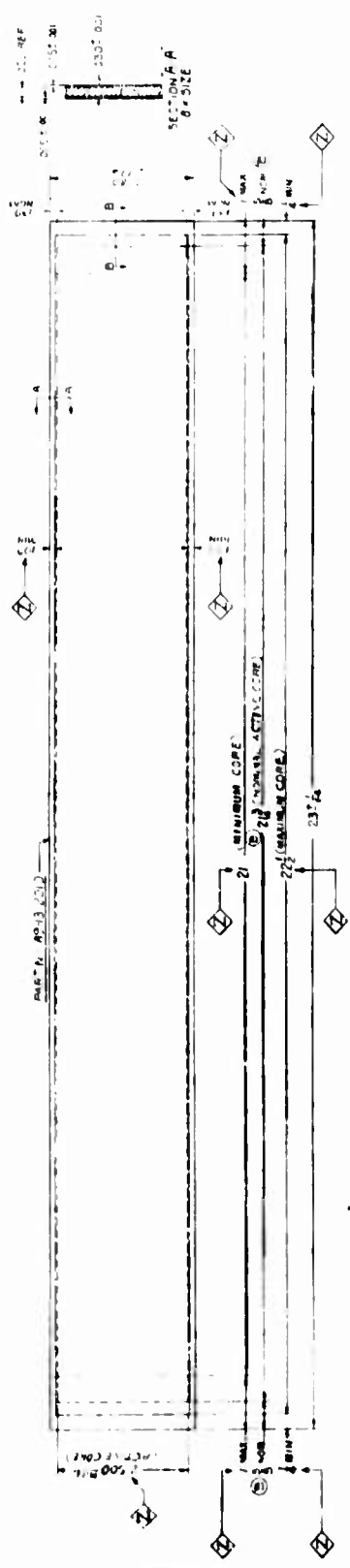
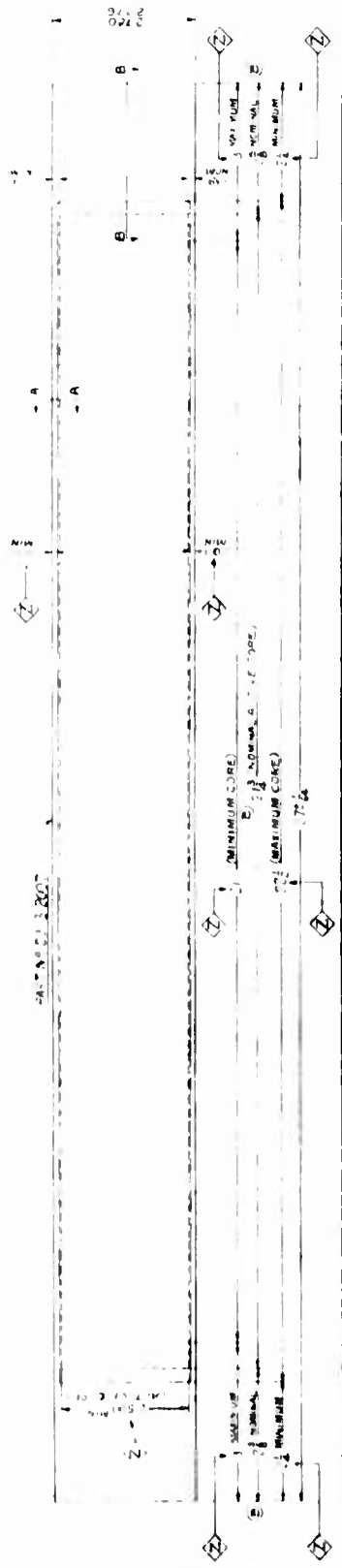
A-125

163





SECTION B-B
B-B SIZE



ALCOO PRODUCTS, INC.
 11000 W. 10TH AVE., DENVER, CO. 80202
 PHONE (303) 751-1000
 FAX (303) 751-1001
 WWW.ALCOO.COM

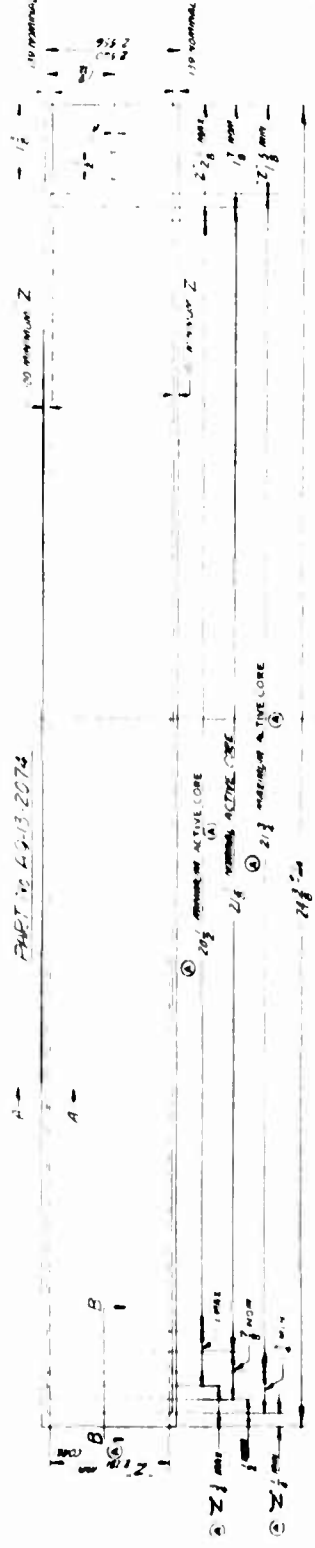
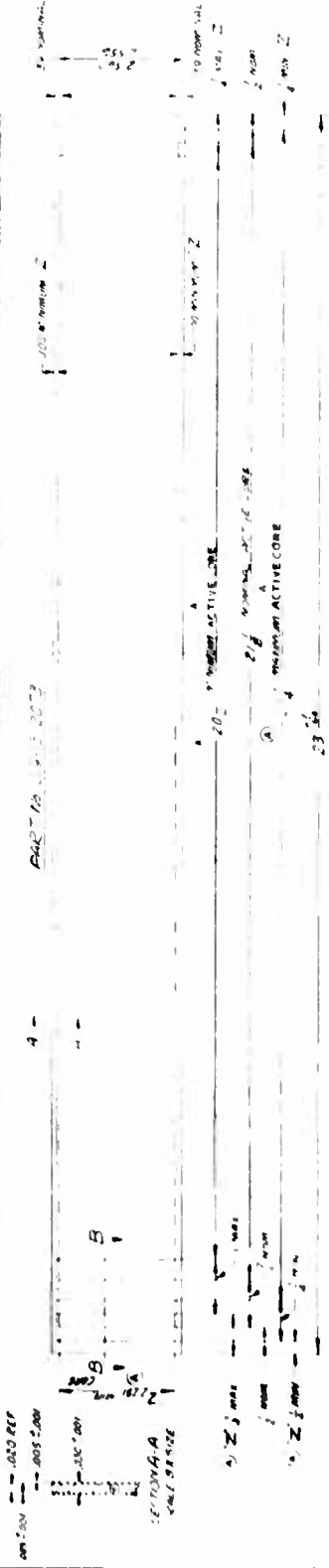
ALCOO
 PART NO. NAME
 09-13-2007 FUEL PLATE 21
 09-13-2007 FUEL PLATE

FUEL PLATES (DRAWING)
 09-13-2007

A-129

NOTE: ACTIVE CORE MUST FALL WITHIN DIMENSIONS MARKED.

| | |
|-----------|-----------|
| SECTION A | SECTION B |
| PLACES | PLACES |
| REVISIONS | REVISIONS |
| DATE | DATE |
| BY | BY |
| CHECKED | CHECKED |
| DATE | DATE |
| BY | BY |
| APPROVED | APPROVED |
| DATE | DATE |
| BY | BY |

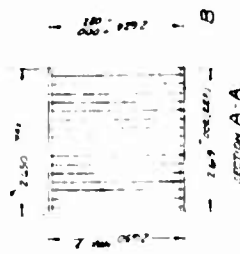


| | | |
|------------------------|----------|----------------|
| ALCO PRODUCTS, INC. | | |
| 11111 ALCO BLVD | | |
| ALCO, MO 65001 | | |
| TEL: (636) 335-1111 | | |
| FAX: (636) 335-1111 | | |
| WWW.ALCO.COM | | |
| E-MAIL: SALES@ALCO.COM | | |
| REVISIONS | | |
| NO. | DATE | DESCRIPTION |
| 1 | 10/13/13 | INITIAL REVISE |
| 2 | 10/13/13 | INITIAL REVISE |
| 3 | 10/13/13 | INITIAL REVISE |
| 4 | 10/13/13 | INITIAL REVISE |
| 5 | 10/13/13 | INITIAL REVISE |
| FILED DATE | | |
| CONTROL BOARD | | |
| D 9-13-2013 | | |

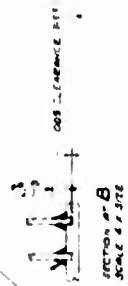
NOTE: SECTION A-A SCALE BY SIZE. DIMENSIONS SHOWN IN Z.

DATE 10-13-2013
INITIAL REVISE
INITIAL REVISE

ALCO PRODUCTS, INC.
 1000 WEST 10TH AVENUE
 DENVER, COLORADO 80202
 TEL. 333-2100

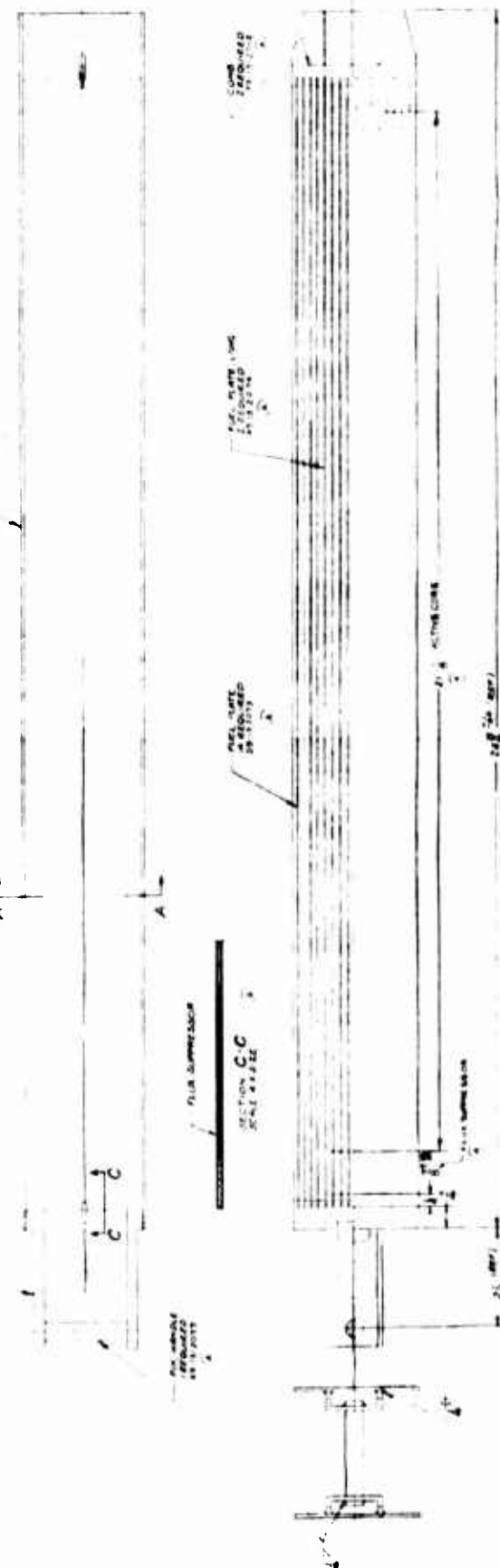


CONST. METALS UP BEARING ALLOY



EXHAUST
 09-13-1011

EXHAUST
 09-13-1011



- METHOD OF ASSEMBLY
1. PLACE CHANNELS TO FORM MATRIX AS SHOWN
 2. ASSEMBLE AND BAKE WITH CHANNELS AND COMES
 3. PLACE DOUBLE PER. LAYER TO FORM CORE
 4. ASSEMBLE TO FORM CORE
 5. BAKE TO FORM CORE AND REMOVE ALL GASES

A-133

ALCO PRODUCTS, INC.
 1000 WEST 10TH AVENUE
 DENVER, COLORADO 80202
 TEL. 333-2100

FUEL ELEMENT
 CONTROL ROD

D 9-13-1011

SKID MOUNTED

DESIGN ANALYSIS

INDEX

B. REACTOR ANALYSIS SECTION

- I CORE DESIGN ANALYSIS
- II SHIELDING DESIGN ANALYSIS
- III TRANSIENT ANALYSIS
- IV CORE THERMAL AND HYDRAULIC DESIGN ANALYSIS

SKID MOUNTED
DESIGN ANALYSIS

I. CORE DESIGN ANALYSIS

| INDEX | <u>PAGE NUMBER</u> |
|--|--------------------|
| 1.0 CONTROL DESIGN REQUIREMENTS | 13-19 |
| 1.1 Comparison with APPR-1 and 1a design requirements. | 13-19 |
| 2.0 CORE AND REFLECTOR CONFIGURATION | 13-19 |
| 2.1 APPR-1 Core I and Core II Characteristics | 13-20 |
| 2.2 Dimensional and Material tabulation | 13-20 |
| 3.0 APPR-1 MEASURED CORE CHARACTERISTICS | 13-23 |
| 3.1 Bank position under all conditions | 13-23 |
| 3.2 Control rod worth | 13-24 |
| 3.3 Stuck rod position | 13-24 |
| 3.4 Temperature coefficient | 13-24 |
| 3.5 Pressure coefficient | 13-24 |
| 3.6 Startup Count Rate | 13-24 |
| 3.7 Conclusions | 13-37 |
| 4.0 SKID MOUNTED CORE CHARACTERISTICS | 13-37 |
| 4.1 Method for establishing (calculation and measurements) | 13-37 |
| 4.1.1 Calculation model | 13-37 |
| 4.1.2 Thermal constants (68° and 500° F) | 13-37 |
| 4.1.3 Fast constants (68° and 500° F) | 13-40 |
| 4.1.4 Substitution effect | 13-40 |
| 4.1.5 Model correction | 13-40 |
| 4.2 Core reactivity at 68° F | 13-40 |
| 4.3 Control rod worth | 13-41 |
| 4.4 Core reactivity and bank position | 13-43 |

| | <u>PAGE NUMBER</u> |
|--|--------------------|
| 4.5 Stuck rod criticality | 13-44 |
| 4.6 Control rod burnup | 13-59 |
| 4.7 Temperature and pressure coefficient | 13-60 |
| 5.0 POWER AND FLUX DISTRIBUTIONS | 13-65 |
| 5.1 Power distribution calculation and experiments | 13-65 |
| 5.1.1 Axial distribution (most adverse) | 13-65 |
| 5.1.2 Radial distribution | 13-65 |
| 5.2 Flux distribution | 13-65 |
| 5.2.1 Axial | 13-65 |
| 5.2.2 Radial | 13-65 |
| 5.3 Flux at chamber position | 13-66 |
| 5.3.1 Startup level | 13-66 |
| 5.3.2 Operating level | 13-66 |
| 5.4 Fast flux on pressure vessel | 13-80 |
| 5.4.1 Method for calculation | 13-80 |
| 5.4.2 Comparison with APPR-1 and 1a | 13-81 |
| 5.5 Conclusions | 13-82 |
| 6.0 SOURCE STRENGTH DETERMINATION | 13-83 |
| 6.1 Correlation of APPR-1 Measurements with Theory | 13-83 |
| 6.1.1 APPR-1 Measurements | 13-83 |
| 6.1.2 Determination of Average Core Flux/Source Strength | 13-83 |
| 6.1.3 Correlation of Photo-neutron source | 13-84 |
| 6.2 Neutron Startup Source Strength | 13-91 |
| 6.2.1 Polonium-Beryllium Source | 13-91 |
| 6.2.2 Photo-neutron Source | 13-91 |
| 6.2.3 Conclusion | 13-95 |

| | <u>PAGE NUMBER</u> |
|--------------------------------|--------------------|
| 7.0 SPENT FUEL PIT CRITICALITY | 13-96 |
| 7.1 Computational Model | 13-97 |
| 7.2 Comparison with ZPE | 13-98 |
| 7.3 Conclusions | 13-99 |
| 7.4 Relocation effect | 13-100 |

SKID MOUNTED
DESIGN ANALYSIS
II SHIELDING DESIGN ANALYSIS

INDEX

| | <u>PAGE NUMBER</u> |
|--|--------------------|
| 1.0 CONTRACT DESIGN REQUIREMENTS | B-105 |
| 1.1 Design dose rates at various locations and operating Conditions | B-105 |
| 1.2 General design principles | B-106 |
| 2.0 PRIMARY SHIELD ANALYSIS | B-109 |
| 2.1 Configurations considered | B-109 |
| 2.2 Reference configuration | B-109 |
| 2.3 Shutdown dose calculation | B-109 |
| 2.3.1 Calculation model | B-110 |
| 2.3.1.1 Core source and attenuation | B-110 |
| 2.3.1.2 Activation sources and attenuation | B-110 |
| 2.3.1.3 Model comparison with APPR-1 measurements | B-113 |
| 2.3.2 Dose from core | B-113 |
| 2.3.2.1 Machine | B-114 |
| 2.3.2.2 Hand calculation | B-115 |
| 2.3.3 Dose from activated materials in the shield | B-118 |
| 2.3.4 Dose from sources outside shield tank | B-120 |
| 2.3.5 Total dose after shutdown | B-121 |
| 2.3.6 Conclusions | B-121 |
| 2.4 Operating dose calculation | B-122 |
| 2.4.1 Calculation model | B-122 |
| 2.4.1.1 Core source and attenuation | B-122 |
| 2.4.1.2 Capture sources and attenuation | B-125 |

| | |
|--|-------|
| 2.4.2 Model comparison with APPR-1 | B-125 |
| 2.4.3 Dose from core | B-125 |
| 2.4.4 Dose from capture sources | B-127 |
| 2.4.5 Total dose on surface of shield tank | B-127 |
| 2.5 Control rod drive shielding | B-127 |
| 2.6 Nozzle shielding | B-128 |
| 2.7 Radiation heating in the shield tank | F-129 |
| 2.7.1 Neutron heating | B-129 |
| 2.7.2 Heating from core and pressure vessel gammas | B-130 |
| 2.7.3 Heating from captures in the shield tank | B-131 |
| 2.7.4 Conclusions | B-132 |
| 2.8 Gamma flux on the instruments | B-133 |
| 3.0 SECONDARY SHIELDING ANALYSIS | B-134 |
| 3.1 N-16 Activity in primary water | B-134 |
| 3.1.1 Calculation of N-16 activity | B-134 |
| 3.1.2 Results | B-139 |
| 3.1.3 Comparison with APPR-1 | B-139 |
| 3.2 Attenuation of N-16 Gammas through secondary shielding | B-140 |
| 3.2.1 Calculation model | B-141 |
| 3.2.2 Calculated dose outside of secondary shield | B-141 |
| 3.3 Attenuation of radiation from shield tank | B-151 |
| 3.3.1 Calculation model | B-151 |
| 3.3.2 Conclusion | B-162 |
| 3.4 Secondary shield thickness required | B-162 |
| 3.5 Dose rate around vapor container after shutdown | B-167 |
| 3.6 Conclusions | B-168 |

| | <u>PAGE NUMBER</u> |
|--|--------------------|
| 4.0 SPENT FUEL SHIELDING | B-170 |
| 4.1 Water tank above core | B-170 |
| 4.1.1 Calculation model | B-170 |
| 4.1.2 Dose during element transfer in core | B-170 |
| 4.1.3 Dose after shutdown (full core) | B-178 |
| 4.1.4 Dose rate during transfer of element from shield tank to spent fuel pit | B-179 |
| 4.2 Water level in spent fuel pit | B-180 |
| 4.2.1 Calculation model | B-180 |
| 4.2.2 Dose rate on top of spent fuel pit | B-184 |
| 4.3 Shielding for shipping cask | B-184 |
| 4.4 Conclusions | B-187 |
| 5.0 HEAT RELEASE DISTRIBUTION | B-188 |
| 5.1 Reactor vessel wall at midplane | B-188 |
| 5.1.1 Calculation model | B-188 |
| 5.1.2 Application to APPR-1 | B-190 |
| 5.1.3 Calculated distribution (core gammas) | B-193 |
| 5.1.4 Calculated distribution (secondary gammas) | B-193 |
| 5.1.5 Calculated distribution (total gammas) | B-193 |
| 5.2 Axial heat distribution in reactor vessel wall | B-199 |
| 5.2.1 Outlet nozzle | B-199 |
| 5.2.2 Flange on top of reactor vessel | B-200 |
| 6.0 DEMINERALIZER SHIELDING | B-203 |
| 6.1 Corrosion product concentration in demineralizer | B-203 |
| 6.2 Volumetric source strength of demineralizer | B-206 |
| 6.3 Demineralizer shielding | B-208 |

| | |
|---|-------|
| 6.3.1 Radial shielding demineralizer | B-208 |
| 6.3.2 Vertical shielding of demineralizer | B-211 |
| 6.3.3 Dose rate after removal | B-212 |
| 6.3.4 Results | B-212 |
| 7.0 WASTE TANK SHIELDING | B-216 |
| 7.1 Primary coolant activation | B-216 |
| 7.2 Plant waste activity | B-218 |
| 7.3 Volumetric source strength in waste tank | B-218 |
| 7.4 Waste tank shielding | B-218 |
| 8.0 GAMMA AND NEUTRON HEATING THE SNOW-RADIAL DIRECTION | B-222 |
| 8.1 Calculation Model | B-222 |
| 8.1.1 Gamma Heating from Gammas from primary shield tank and primary coolant | B-222 |
| 8.1.2 Neutron heating from neutrons escaping primary shield | B-223 |
| 8.1.3 Gamma heating from hydrogen capture gammas in snow | B-224 |
| 8.2 Conclusions | B-226 |
| 9.0 GAMMA HEATING OF SNOW UNDER THE REACTOR | B-230 |
| 10.0 ACTIVATION OF COMPONENTS | B-234 |
| 10.1 Pressure vessel and primary shield components | B-234 |

SKID MOUNTED

DESIGN ANALYSIS

III. REACTOR AND PRIMARY SYSTEM KINETIC ANALYSIS

| | <u>Index</u> | <u>PAGE NUMBER</u> |
|-------|---|--------------------|
| 1.0 | Primary System Kinetics | B-241 |
| 1.1 | General Kinetic Model | B-241 |
| 1.1.1 | Description | B-241 |
| 1.1.2 | Nomenclature | B-241 |
| 1.1.3 | Differential Equations | B-242 |
| 1.2 | Scaled Kinetic Model | B-245 |
| 1.2.1 | Plant Constants | B-245 |
| 1.2.2 | Time and Amplitude Scaling Factors | B-246 |
| 1.2.3 | Potentiometer Settings | B-246 |
| 1.2.4 | Analog Circuit Diagram | B-246 |
| 1.3 | Analog Computer Model Response | B-246 |
| 1.4 | Selection of Pressurizer Size | B-246 |
| 2.0 | Reactor Behavior Following Pump Failure | B-257 |
| 2.1 | General Kinetic Model | B-257 |
| 2.1.1 | Description | B-257 |
| 2.1.2 | Pump Coastdown Characteristics | B-257 |
| 2.1.3 | Differential Equations | B-258 |
| 2.2 | Constants for Differential Equations | B-259 |
| 2.2.1 | Time and Amplitude Scaling Factors | B-259 |
| 2.2.2 | Potentiometer Settings | B-259 |
| 2.2.3 | Analog Circuit Diagram | B-260 |
| 2.3 | Results of Analog Pump Failure Simulation | B-260 |
| 2.4 | Conclusions | B-267 |

SKID MOUNTED

DESIGN ANALYSIS

IV CORE THERMAL AND HYDRAULIC DESIGN ANALYSIS

INDEX

| | <u>PAGE NUMBER</u> |
|---|--------------------|
| 1.0 THERMAL DESIGN CRITERIA | B-269 |
| 1.1 Heat transfer coefficient | B-269 |
| 1.2 Power distribution utilization | B-269 |
| 1.3 Hot channel factors | B-270 |
| 1.4 Lattice requirements | B-270 |
| 1.5 Instrumentation tolerance | B-271 |
| 1.6 Calculations | B-271 |
| 1.6.1 Hot channel factors | B-271 |
| 1.6.2 Lattice requirement determination | B-281 |
| 1.6.3 Heat release distribution | B-283 |
| 2.0 Thermal Analysis | B-284 |
| 2.1 General equations and results | B-284 |
| 2.2 Calculations | B-287 |
| 2.2.1 General constants and dimensions | B-287 |
| 2.2.2 Heat transfer area | B-288 |
| 2.2.3 Average heat flux | B-288 |
| 2.2.4 Bulk coolant temperature rise | B-288 |
| 2.2.5 Heat transfer coefficient | B-289 |
| 2.2.6 Water film temperature gradient | B-290 |
| 2.2.7 Maximum surface temperature | B-290 |
| 2.2.8 Flow requirements | B-293 |
| 2.3 Conclusions | B-294 |

| | <u>PAGE NUMBER</u> |
|--|--------------------|
| 3.0 RATIO OF OPERATING TO BURNOUT HEAT FLUX | B-297 |
| 3.1 Operating heat flux | B-297 |
| 3.2 Burnout heat flux | B-298 |
| 3.3 Flux ratios | B-299 |
| 3.4 Application of hot channel factors | B-299 |
| 4.0 INTERNAL PLATE TEMPERATURES | B-300 |
| 4.1 Method of calculation | B-300 |
| 4.2 Numerical calculation | B-300 |
| 4.3 Application of hot channel factors | B-300 |
| 4.4 Comparison with APPR-1 | B-302 |
| 5.0 THERMAL STRESS IN ELEMENTS | B-303 |
| 5.1 Use of experimental data | B-303 |
| 5.2 Experimental test conditions and results | B-303 |
| 5.3 Comparison with Skid-mounted core conditions | B-304 |
| 5.4 Conclusions | B-305 |
| 6.0 THERMAL STRESS IN REACTOR VESSEL | B-306 |
| 6.1 Method of calculations | B-306 |
| 6.2 Thermal stress in APPR-1 | B-309 |
| 6.2.1 Calculated and measured temperature difference | B-309 |
| 6.2.2 Thermal stress in APPR-1 | B-310 |
| 6.3 Calculated temperature difference and thermal stress at midplane | B-310 |
| 6.4 Calculated thermal stress in thermal shield | B-310 |
| 6.5 Calculated thermal stress in flange | B-313 |
| 6.6 Calculated thermal stress in integral nozzle | B-314 |
| 6.7 Conclusions | B-314 |

| | <u>PAGE NUMBER</u> |
|--|--------------------|
| 7.0 CORE PRESSURE DROP | B-315 |
| 7.1 Comparison of calculated and experimental data | B-315 |
| 7.2 Calculation of pressure drops | B-315 |
| 7.3 Results and conclusions | B-315 |
| 8.0 FUEL PLATE DEFLECTIONS | B-327 |
| 8.1 Calculation of pressure differential | B-327 |
| 8.2 Experimental data | B-328 |
| 8.3 Conclusions | B-328 |

CHAPTER I

| <u>FIGURE NUMBER</u> | <u>LIST OF FIGURES</u> | <u>PAGE NUMBER</u> |
|----------------------|--|--------------------|
| | <u>TITLE</u> | |
| 3-1 | Five Rod Shim Bank Vs Energy Release -APPR-1 | B-25 |
| 3-2 | Calibration of 5 Rod Bank - APPR-1 | B-27 |
| 3-3 | Stuck Rod Condition - APPR-1 | B-29 |
| 3-4 | Excess Reactivity Vs Energy Release - APPR-1 | B-31 |
| 3-5 | Temperature Coefficient Vs. Temperature-APPR-1 | B-33 |
| 3-6 | Pressure Coefficient Vs. Pressure - APPR-1 | B-35 |
| 4-1 a,b,c | Core Parameters Vs. Burnup | B-45,47, 49 |
| 4-2 | Reactivity Vs. Energy Release | B-51 |
| 4-3 | Five Rod Bank Position Vs. Energy Release | B-53 |
| 4-4 | Excess Reactivity with One Stuck Rod | B-55 |
| 4-5 | Critical Stuck Rod Position Vs. Core Lifetime | B-57 |
| 4-6 | Temperature Coefficient Vs. Temperature | B-61 |
| 4-7 | Pressure Coefficient Vs. Temperature | B-63 |
| 5-1 | Radial Power Distribution | B-67 |
| 5-2 | Axial Power Distribution | B-69 |
| 5-3 | Radial Thermal Flux Distribution, Beginning and End of Life | B-71 |
| 5-4 | Axial Flux Distribution, Beginning and End of Life | B-73 |
| 5-5 | Radial Flux Distribution for Infinite Water and Water-Steel Reflectors | B-75 |
| 5-6 | Radial Thermal and Fast Flux Distributions Through Primary Shield | B-77 |
| 6-1 | Average Core Flux Due to Neutron Source as Function of K_{eff} | B-85 |
| 6-2 | Beryllium (n, γ) Cross Section | B-89 |
| 6-3 | Startup Radial Flux Distribution to BF_3 Counter Tube (Thermal) | B-93 |

CHAPTER II

| <u>FIGURE NUMBER</u> | <u>TITLE</u> | <u>LIST OF FIGURES</u> | <u>PAGE NUMBER</u> |
|----------------------|---|------------------------|--------------------|
| 2-1 | Dose Rate on Surface of Shield Tank as a Function of Shutdown Time | | B-123 |
| 3-1a to 3-1e | Dose Point Location | | B-145,7 |
| 3-2 | Snow Density | | B-149 |
| 3-3a to 3-3c | N-16 Isodose Lines | | B-153,5,7 |
| 3-4 | Operating Dose Rate from Core and Shield Tank as a Function of Snow Penetration | | B-159 |
| 3-5 | Core and Shield Tank Isodose Lines around Vapor Container | | B-163 |
| 3-6 | Core and Shield Tank Isodose Lines on Surface of Icecap | | B-165 |
| 3-7 | Shutdown Dose Rate Outside Vapor Container in Snow | | B-169 |
| 3-8 | Isodose Lines Around Vapor Container - 8 hours after shutdown | | B-171 |
| 4-1 | Determination of Transfer Cask Shielding | | B-181 |
| 4-2 | Determination of Height of Water above Fuel Elements in Spent Fuel Pit | | B-185 |
| 5-1 | Volumetric Heat Release in APFR-1 Pressure Vessel | | B-191 |
| 5-2 | Volumetric Heat Release in Skid Mounted Pressure Vessel | | B-197 |
| 5-3 | Heat Release Distribution in Reactor Vessel Flange | | B-201 |
| 6-1 | Demineralizer Shipping Cask | | B-209 |
| 6-2 | Determination of Demineralizer Shielding | | B-213 |
| 7-1 | Determination of Waste Tank Shielding | | B-219 |
| 8-1 | Neutron and Gamma Heating in the Snow | | B-227 |
| 9-1 | Neutron Fluxes below Core | | B-231 |
| 9-2 | Gamma Heating in Snow under Reactor | | B-235 |

CHAPTER III

| <u>FIGURE NUMBER</u> | <u>TITLE</u> | <u>PAGE NUMBER</u> |
|----------------------|---|--------------------|
| 1-1 | Electronic Analog Computer Circuit Diagram of Plant Kinetic Model | B-251 |
| 1-2 | Plant Response to Instantaneous Load Reductions | B-253 |
| 1-3 | Plant Response to Instantaneous Load Increases | B-255 |
| 2-1 | Pump Failure Analog Circuit Diagram | B-261 |
| 2-2 | Pump Failure Analog Results, $\mathcal{J} = 3.4 \times 10^{-4} \quad \Delta k/^\circ F$ | B-263 |
| 2-3 | Pump Failure Analog Results, $\mathcal{J} = 2.55 \times 10^{-4} \quad \Delta k/^\circ F$ | B-265 |

CHAPTER IV

| | | |
|-----|---|-------|
| 2-1 | Core Fuel Element Arrangement and Numbering System | B-291 |
| 2-2 | Maximum Wall Temperature Versus Element Flow | B-295 |
| 6-1 | Thermal Stress in a Stainless Steel Pressure Vessel Versus Thermal Shield Thickness | B-311 |
| 7-1 | Comparison of Experimental And Calculated Pressure Drop Data | B-317 |
| 7-2 | Fuel Element Pressure Drop Versus Reynolds Number--Air Flow | B-319 |
| 7-3 | Fuel Element Pressure Drop Versus Reynolds Number--Water Flow | B-321 |
| 7-4 | Control Rod Pressure Drop Versus Flow Per Element | B-323 |
| 7-5 | Stationary Fuel Element Pressure Drop Versus Flow Per Element | B-325 |
| 8-1 | Location of Head Losses Through Core | B-329 |
| 8-2 | Head Loss Across Core -Stationary Element and Lattice | B-331 |

CHAPTER I

| <u>TABLE NUMBER</u> | <u>TITLE</u> | <u>PAGE NUMBER</u> |
|---------------------|--|--------------------|
| 2-1 | Comparison of Skid Mounted Core and APPR-1. | B-20 |
| 4-1 | Constants - Skid Mounted and APPR-1 | B-38 |
| 5-1 | Integrated Fast Flux Incident on the Pressure Vessel | B-81 |

CHAPTER II

| | | |
|-----|---|-------|
| 1-0 | Radiation Dose Rates from Skid Mounted Reactor (Ice Cap Installation) | B-106 |
| 1-1 | Description of Primary Shield | B-108 |
| 2-1 | Fission Product Source Strength after Shutdown | B-111 |
| 2-2 | Hand Calculation of Dose Rate from Core after Shutdown | B-117 |
| 2-3 | Fluxes Used in the Machine Calculation of the Dose Rate from Activated Materials | B-119 |
| 2-4 | Results of Machine Calculation of Operating Dose Rate from Core | B-126 |
| 2-5 | Results of Machine Calculation Operating Dose Rates from Capture and Activation Sources in the Shield | B-127 |
| 2-6 | Calculation of Heat Produced by Captures in Shield Tank | B-132 |
| 2-7 | Gamma Dose Rates on Instruments APPR-1 and Skid Mounted Reactors | B-133 |
| 3-1 | Calculation of Uncollided Flux | B-137 |
| 3-2 | Calculation of Collided Flux | B-138 |
| 3-3 | Total Energy Dependent Flux | B-138 |
| 3-4 | Shadow Shield Description | B-142 |
| 3-5 | Source Point Description | B-143 |
| 3-6 | Dose Point Description | B-144 |
| 3-7 | Dose Rates from RAS-I Program (Secondary Shield) | B-151 |

CHAPTER II

| <u>TABLE NUMBER</u> | <u>TITLE</u> | <u>LIST OF TABLES</u> | <u>PAGE NUMBER</u> |
|---------------------|---|-----------------------|--------------------|
| 3-8 | Dose Rates Through Snow from the Shield Tank | | B-161 |
| 4-1 | Calculation of Dose Rate from Single Fuel Element | | B-175 |
| 4-2 | Dose Rate Above Complete Core | | B-179 |
| 4-3 | Calculation of Spent Fuel Pit Shielding | | B-183 |
| 4-4 | Radial Dose Rates - Spent Fuel Casks | | B-187 |
| 5-1 | Reactor Vessel Configurations | | B-188 |
| 5-2 | Volumetric Heat Release in APFR-1 Thermal Shield and Reactor Vessel | | B-190 |
| 5-3 | Energy Group of Gammas | | B-193 |
| 5-4 | Volumetric Heat Release in Skid Mounted Pressure Vessel Due to Core Gammas | | B-194 |
| 5-5 | Volumetric Heat Release in Skid Mounted Pressure Vessel due to Secondary Gammas | | B-195 |
| 5-6 | Total Volumetric Heat Release in Skid Mounted Pressure Vessel | | B-196 |
| 5-7 | Volumetric Heat Release Distributions for all Pressure Vessel Configurations | | B-199 |
| 6-1 | Properties of Nuclides | | B-205 |
| 6-2 | Concentration of Active Nuclides in Demineralizer | | B-206 |
| 6-3 | Calculation of Volumetric Source Strength | | B-207 |
| 6-4 | Energy Grouping and Source Strength | | B-208 |
| 6-5 | Dose Rates on Surface of Loaded Demineralizer Shipping Cask | | B-211 |
| 7-1 | Corrosion Product Concentration in Primary Water | | B-217 |
| 7-2 | Total Source Strength due to Primary Coolant | | B-217 |

CHAPTER II

| <u>TABLE NUMBER</u> | <u>TITLE</u> | <u>LIST OF TABLES</u> | <u>PAGE NUMBER</u> |
|---------------------|--|-----------------------|--------------------|
| 7-3 | Volumetric Source Strength in Waste Tank | | B-278 |
| 7-4 | Shield Thickness for Waste Tank | | B-221 |
| 8-1 | Gamma Heating in Snow Due to Gammas from Shield Tank and Primary Coolant | | B-225 |
| 8-2 | Neutron Heating in Snow from Neutrons Escaping Primary Shield | | B-225 |
| 8-3 | Gamma Heating from Capture Gammas Produced in Snow | | B-229 |
| 9-1 | Gamma Heating in the Snow under the Reactor | | B-230 |
| 10-1 | Dose Rates from Activated Components | | B-237 |
| 10-2 | Feasibility of Relocation of Components | | B-238 |

CHAPTER III

| | | | |
|-----|---|--|-------|
| 1-1 | Servo-set Potentiometer Settings, Plant Kinetic Model | | B-248 |
| 1-2 | Analog Computer Model Runs | | B-250 |
| 2-1 | Pump Failure Potentiometer Settings | | B-260 |

CHAPTER IV

| | | | |
|-----|--|--|-------|
| 1-1 | Hot Channel Factors | | B-270 |
| 1-2 | Mechanical Specification Tolerances and Maximum Deviations Considered in Calculating Hot Channel Factors | | B-271 |
| 2-1 | Velocity Schedule | | B-287 |
| 2-2 | Total Required Flow | | B-293 |
| 5-1 | Comparison of Irradiation Conditions in the MTR and APPR-1 | | B-303 |
| 6-1 | Reactor Vessel Thermal Stresses | | B-310 |
| 8-1 | Head Loss through Stationary Elements | | B-327 |
| 8-2 | Head Loss through Lattice | | B-328 |

I. Core Design Analysis

1.0 Contract Design Requirements

The core design requirements are set forth in the general objective and project guide lines. The general objective for this project requires that the core be of the APFR type and be adaptable to skid mounting of the primary system. The project guide lines call for following items that affect core designs:

- a. System reliability with minimum down time for refueling.
- b. Minimum installed capital cost at a remote site.
- c. Utilization of proven technology.
- d. Availability for procurement by January 1, 1959.
- e. Minimum personnel requirements for operation and maintenance.
- f. Minimum of one year between refueling when operating at full power.

1.1 Comparison with APFR-1 and 1a design requirements

The contract requirements for this design are not inconsistent in any way with those for the APFR-1⁽¹⁾ and 1-a⁽²⁾ reactor cores. By relaxing design requirements the contractor is able to make improvements in core design and operating philosophy that are of benefit to the military.

2.0 Core and Reflector Configurations.

The core array selected for the skid mounted APFR is the basic 7 x 7 array of the APFR-1 with 3 elements missing in each corner which results in a core of 37 fuel elements. In this manner a reduction in effective core diameter is obtained of approximately 2 inches. The arrangement of the 32 fixed elements, 5 control rod fuel element, and 5 absorber sections in the core support structure and control rod baskets is very similar to that of the APFR-1 which has proven itself from all standpoints.

The reflector configuration originally envisioned for the skid mounted APFR (See APAE 33, Drawing AEL-335) employed a minimum water reflector followed by the reactor vessel. No thermal shielding was to be employed. It was intended to employ a solid stainless steel reactor vessel because of the high fast neutron flux on the reactor vessel. As will be discussed in II Shielding Design Analysis, Section 5.0, the heating in this vessel resulted in too high thermal stresses. It then became necessary to investigate the addition of thermal shielding which resulted in an increased diameter of the stainless steel vessel. A configuration employing a large thickness of thermal shielding (practically a stainless steel reflector) resulted in a stainless steel

(1) APAE-10 Vol.1, Phase 3 Design Analysis for the Army Package Power Reactor.

(2) APAE-17, Vol.1, Phase 3 of the report Army Package Power Reactor Field Unit #1, APFR-1a

vessel whose inside diameter was not significantly smaller than that of the carbon steel vessel. The inside diameter of the shield was such as to permit adequate water to be placed between it and the reactor vessel to reduce the fast neutron flux to a level such that the total integrated nvt over a 20-year life was not a problem. The basic characteristics of the reactor core together with a comparison with APFR-1, Core I are given in Section 2.2.

2.1 APFR-1 Core I and Core II Characteristics.

The project guide lines are consistent with the core design developed in "APAE-33, 2000 KW skid mounted APFR power plant". The core design proposed in AE-33 employed 32 fixed fuel elements of APFR-1 Core I or Core II specifications and 5 control rod fuel elements of APFR-1 Core II specifications and 5 boron absorber sections of APFR-1 Core I specifications. It is felt that this core configuration, as will be proven in the design analysis, meets all the project guide lines, such as utilization of proven technology, minimum of one year core life and minimum installed cost. By employing APFR-1 fuel elements in this core the installation becomes capable of receiving fuel elements of improved technology as they are developed for the APFR family.

2.2 Dimensional and Material Tabulation

All core dimensions and material for the Skid Mounted Reactor are listed in Table 2-1. Data for the APFR-1 core is also listed to supply the reader with a comparison between the two cores. All experimental information is marked with an asterisk (*).

TABLE 2-1

Comparison of Skid Mounted Core and APFR-1.

("Hot" means 512°F in Skid Core, 440°F in APFR-1 Core)

| Configuration | Skid Mounted | APFR-1 |
|-------------------------------|---|---|
| | 7 x 7 - 3 elements in each corner missing -37 elements | 7 x 7 - corners missing-45 elements |
| Equivalent diameter - in. | 20.16 | 22.20 |
| Active core height - in. | 22.0 | 22.0 |
| No. of fixed elements | 32 | 38 |
| No. of control rod elements | 5 | 7 |
| Material content of core | | |
| U ²³⁵ -kg. | 18.49 | 22.50 |
| B10 -gm. | 16.66 | 19.52 |
| ss - kg. | 172.10 | 208.92 |
| H ₂ O (68°F) - kg. | 91.54 | 111.08 |

Table 2-1 (Cont'd)

| Configuration | Skid Mounted | APPR-1 |
|--|--|---|
| | 7x7 - 3 elements in each corner missing-37 elements | 7x7 - corners missing-45 elements |
| Fixed element | | |
| U ²³⁵ - gm. | 515.16 | 515.16 |
| B ¹⁰ - gm. | 0.464 | 0.446 |
| Control Rod element | | |
| U ²³⁵ - gm. | 401.12 | 417.76 |
| B ¹⁰ - gm. | 0.362 | 0.363 |
| Control Rod Absorber Section | | |
| B ¹⁰ - gm. | 56.4 | 56.4 |
| Volume in core - cc | | |
| ss. UO ₂ , B ₄ C | 23,907 | 29,095 |
| H ₂ O | 91,195 | 110,894 |
| Total | 115,102 | 139,989 |
| Fuel elements | | |
| Fuel plate meat - rectangular flat UO ₂ - SS - B ₄ C | | |
| Fuel plate clad - type 304L stainless steel | | |
| Meat thickness - in. | | |
| Fixed element | 0.020 | 0.020 |
| Control Rod element | 0.020 | 0.020 |
| Meat width - in. | | |
| Fixed element | 2.500 | 2.500 |
| Control Rod element | 2.281 | 2.281 |
| Active length - in. | | |
| Fixed element | 22.0 | 22.0 |
| Control Rod element | 21.125 | 22.0 |
| Cladding - in. | | |
| Fixed element | 0.005 | 0.005 |
| Control Rod element | 0.005 | 0.005 |
| Fuel Plates per element | | |
| Fixed element | 18 | 18 |
| Control Rod element | 16 | 16 |
| Water gap between plates - in. | | |
| Fixed element | 0.133 | 0.133 |
| Control Rod element | 0.133 | 0.133 |
| Fuel plate meat composition - wt. % | | |
| UO ₂ | 25.032 | 25.98 |
| B ₄ C | 0.134 | 0.14 |
| SS | 78.834 | 73.88 |

Control Rods

Type - square stainless steel basket containing absorber section and control rod fuel element (7/8" Europium flux suppressor at top of meat - 1gm Eu)

Absorber section - four plates welded into a square tube

Composition - boron enriched in B¹⁰ isotope dispersed in iron and clad with type 304L stainless steel.

Travel-22 in.

Weight of one rod-55 lb.

Table 2-1 (Cont'd)

| Configuration | Skid Mounted 7x7 - 3 elements in each corner missing-37 elements | APFR-1 7x7 - corners missing-45 elements |
|--|--|---|
| <div style="border: 1px solid black; padding: 5px; display: inline-block;"> "Hot" means 512°F in Skid core, 440°F in APFR-1 core. * means experimental data. </div> | | |
| Initial reactivities - β | | |
| Cold - 68°F - no xenon | 14.11 | 15.35* |
| Hot - no xenon | 7.65 | 10.37* |
| Hot - eq. xenon | 5.15 | 8.15* |
| Initial bank positions - inches from bottom | | |
| Cold - 68°F - no xenon | 5.0 | 3.7* |
| Hot - no xenon | 9.7 | 6.8* |
| Hot eq. xenon | 11.6 | 8.3* |
| Power - peak to average, hot, clean | | |
| 0 MWYR | | |
| Radial | 1.46 | 1.49 |
| Axial | 1.65 | 1.71 |
| Average Thermal neutron flux (neutrons) (cm ² - sec.) | | |
| 0 MWYR | | |
| Expected total energy release - MWYR | 1.67x10 ¹³ | 1.36x10 ¹³ |
| Average fuel burnup | 10 | 15* |
| | (10 MWYR) | (15 MWYR) |
| Maximum fuel burnup | 26% | 32% |
| | 49% | 75% |
| Composition of core at end of life | | |
| U-235 left - Kg. | 13.7 | 15.3 |
| Original B-10 left -gms. | 3.0 | 2.3 |
| Maximum burnup of control rod material | 27% | 43% |
| Temperature coefficient | | |
| Cold - 68°F | - 0.22x10 ⁻⁴ | - 0.22x10 ⁻⁴ * |
| Hot | - 3.4 x10 ⁻⁴ | - 2.2 x10 ⁻⁴ * |
| Pressure Coefficient | | |
| | / 3.1 x10 ⁻⁶ (1750psia) | / 2.1 x10 ⁻⁶ (1200psia) |
| Five rod bank worth - β | | |
| Cold - 68°F | 19.9 | 19.0 |
| Hot | 19.5 | 19.2 |
| Center rod worth - β | | |
| Cold - 68°F | 4.5 | 4.1 |
| Hot | 4.0 | 4.1 |

Table 2-1 (Cont'd)

| Configuration | Skid Mounted | APFR-1 |
|--|--|---|
| | 7x7 - 3 elements in each corner missing-37 elements | 7x7 - corners missing-45 elements |
| Radial Reflector savings - S_r - cm. | | |
| Cold - 68°F | 6.117207 | 6.180821 |
| Hot | 8.248812 | 7.797679 |
| Axial reflector savings - S_z - cm. | | |
| Cold - 68°F | 6.030801 | 5.109191 |
| Hot | 7.978338 | 6.103367 |
| Radial buckling - B_r^2 - cm ⁻² | | |
| Cold - 68°F | 0.005747 | 0.004895 |
| Hot | 0.005046 | 0.004465 |
| Axial buckling - B_z^2 - cm ⁻² | | |
| Cold - 68°F | 0.002138 | 0.002259 |
| Hot | 0.001913 | 0.002129 |
| Total Buckling - B_T^2 - cm ⁻² | | |
| Cold - 68°F | 0.007885 | 0.007154 |
| Hot | 0.006959 | 0.006594 |

3.0 APFR-1 Measured Core Characteristics

Because of the fact that the skid mounted APFR employs 37 APFR-1 fuel elements the measurements made on the APFR-1 core employing 45 fuel elements are of particular significance. It is expected that the principal effect of employing 37 rather than 45 fuel elements is to reduce the reactivity of the core throughout lifetime. In addition, there will be some increase in temperature coefficient due to the reduced core size.

3.1 Bank Position

The 5 rod bank position in the APFR-1 has been measured under a wide range of conditions. These are -

| | |
|-------|-------------------|
| 70°F | No Xenon |
| 440°F | No Xenon |
| 442°F | Equilibrium Xenon |
| 442°F | Peak Xenon |

The results of these measurements through 7 MWR of core life are shown in Fig. 3-1 (Fig. 2A Progress Report #5, Task VII). It would be expected that the 5 rod bank position for the skid mounted reactor would be further withdrawn at room temperature because of the lower core reactivity

and higher rod worth and would be further withdrawn at operating temperature due to the same reasons together with the higher operating temperature (512°F vs 440°F).

3.2 Control Rod Worth

The 5 rod bank worth has been measured under a variety of conditions in the ZPE and at Ft. Belvoir. The measurements at Ft. Belvoir provide a comparison between the room temperature calibrations made in the ZPE and calibrations made at operating temperature. A summary of all the measurements is contained in Fig. 3-2. (Fig. 3D Progress Report #6)⁽¹¹⁾. It would be expected that the 5 rod bank calibration for the skid mounted APPR would not differ significantly from that in Fig. 3-2.

3.3 Stuck Rod Positions

With rods A&B fully withdrawn and considered stationary, the most reactive condition with a single stuck rod is that of an excentric rod stuck in its fully withdrawn position. The case of having the centerline rod stuck in its fully withdrawn position is less reactive.

Fig. 3-3 (Fig. 5: Progress Report #5) shows the critical position of the partially withdrawn rod as a function of lifetime. From calibrations of the critical rods and their position, the reactivity in the core can be determined if the partially withdrawn rod is completely withdrawn. This result is shown in Fig. 3-4 (Fig. 5D). It would be expected that the critical position of the partially withdrawn rod in the skid mounted APPR would be further out than that of the APPR-1. It should be noted that if APPR-1 Core II boron loading as specified in APAE 32 (7) can be employed, then the skid mounted APPR could be made sub-critical with one rod stuck full out.

3.4 The temperature coefficient has been measured in the APPR-1 during the course of core burnout. This data is shown plotted in Fig. 3-5 (Fig. 1A Progress Report #6). Two effects would be present in the skid mounted APPR that would tend to increase the temperature coefficient. These are reduced core size and higher operating temperature. The effect of core size has been investigated in ZPE II and can be used in interpreting this change.

3.5 Pressure Coefficient

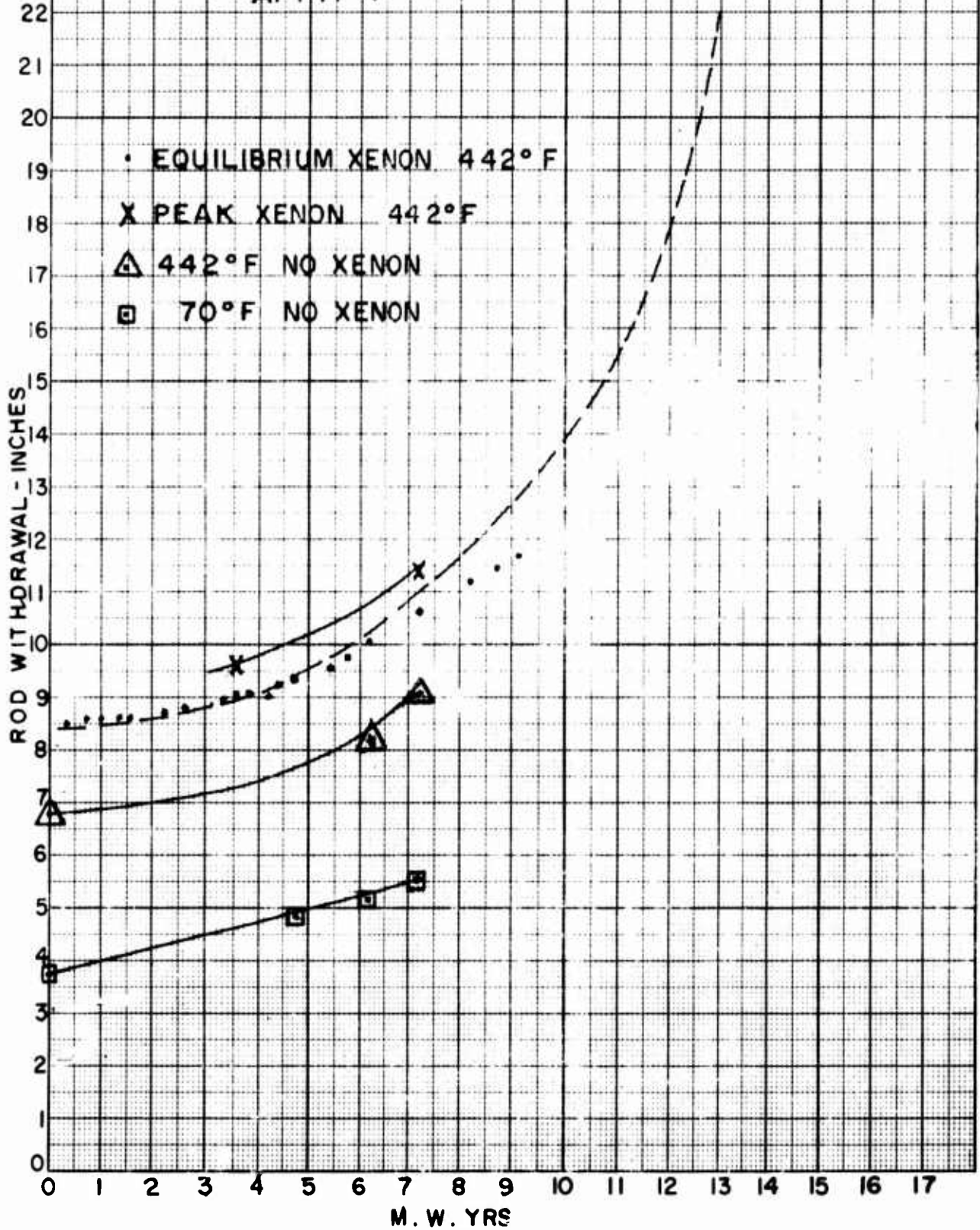
Pressure coefficient as measured in the APPR-1 is shown in Fig. 3-6 (Fig. 1A Progress Report #1).

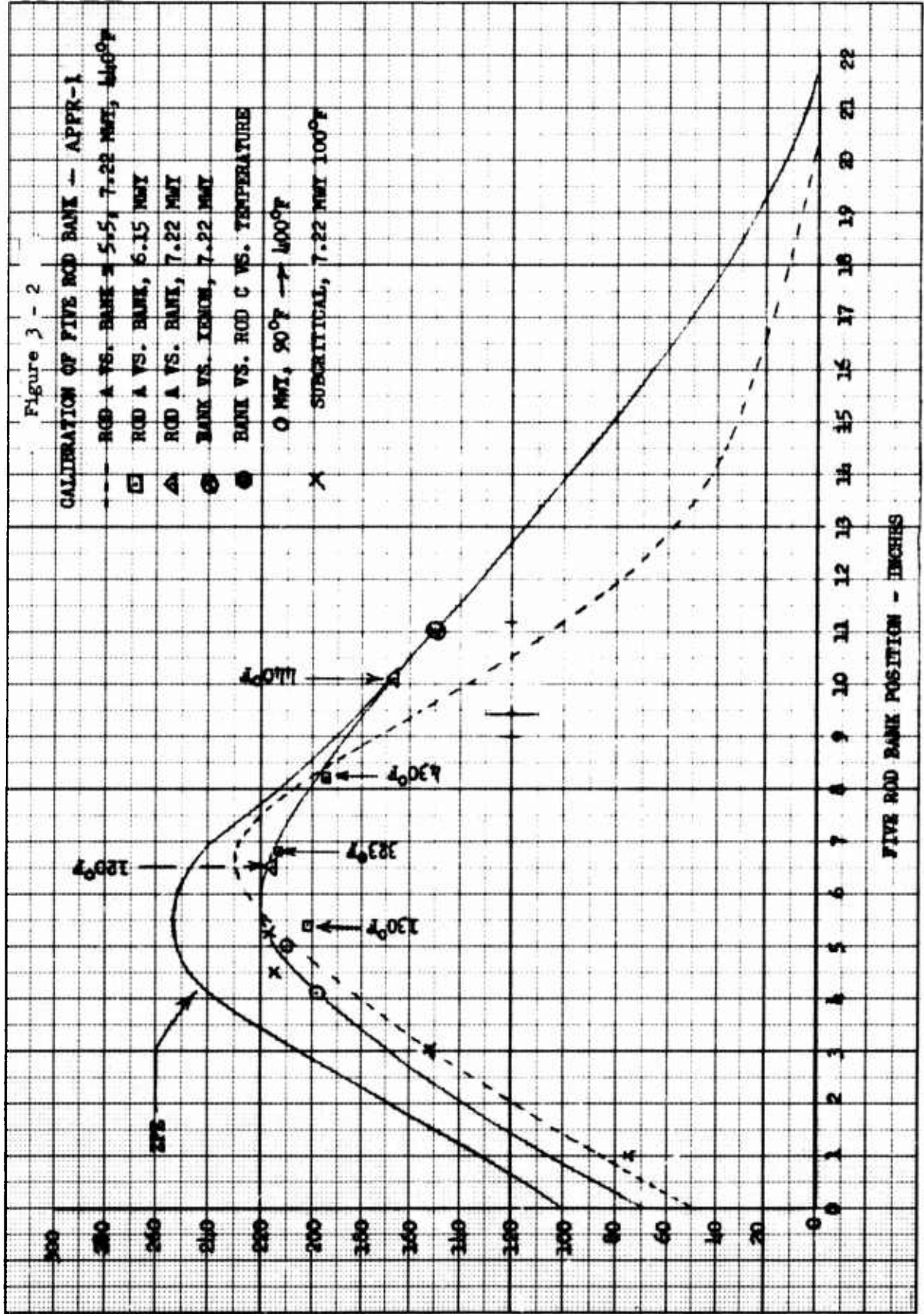
3.6 Startup Count Rate

The startup count rate is being measured in the APPR-1 during the course of core burnout. The count rate ranges from 3 to 5 counts per second with the beryllium photoneutron block installed in the APPR-1.

Fig. 3-1

FIVE ROD SHIM BANK VS. ENERGY RELEASE APPR - I



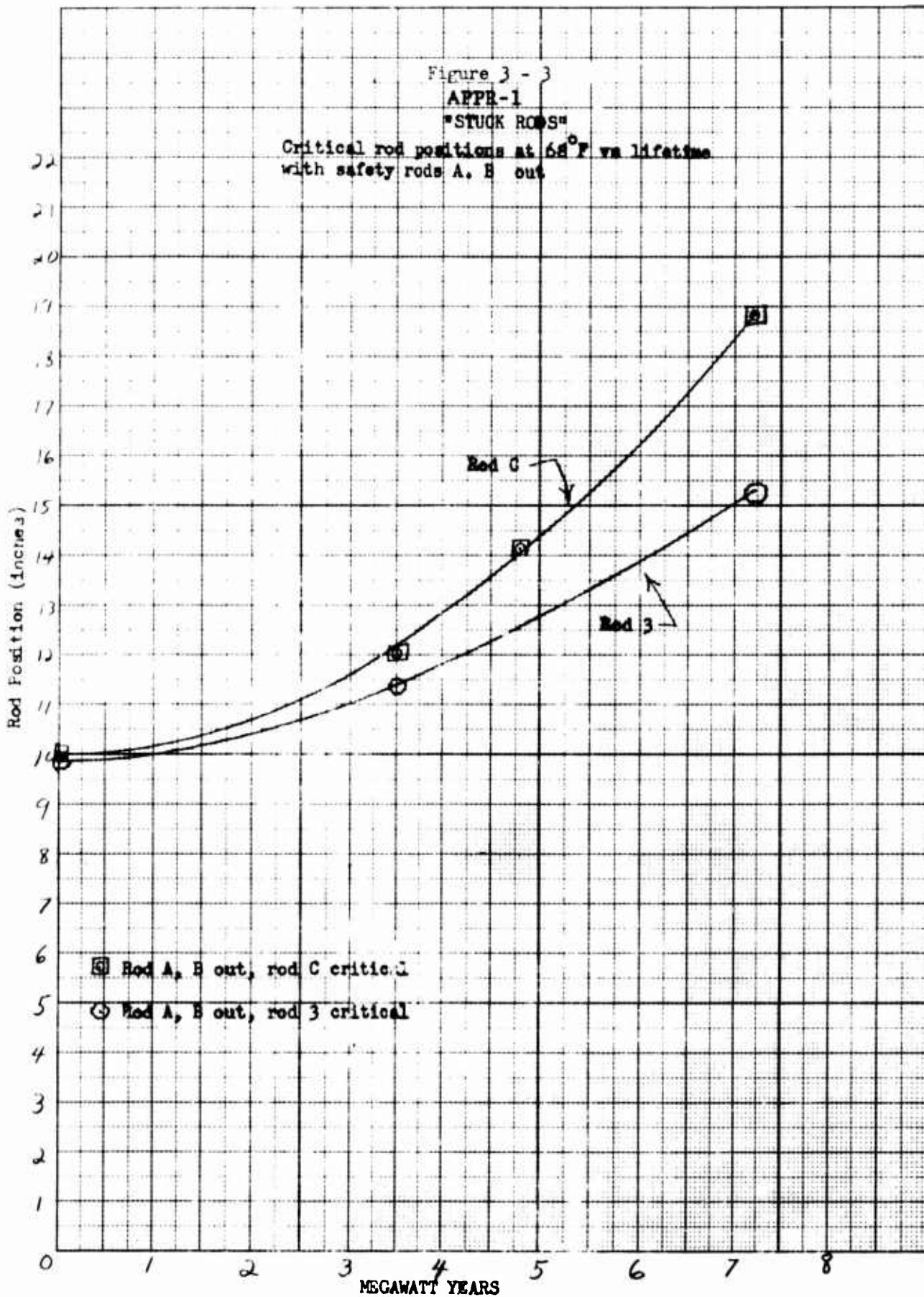


REACTIVITY - CENTS PER INCH

Figure 3 - 3
APPR-1

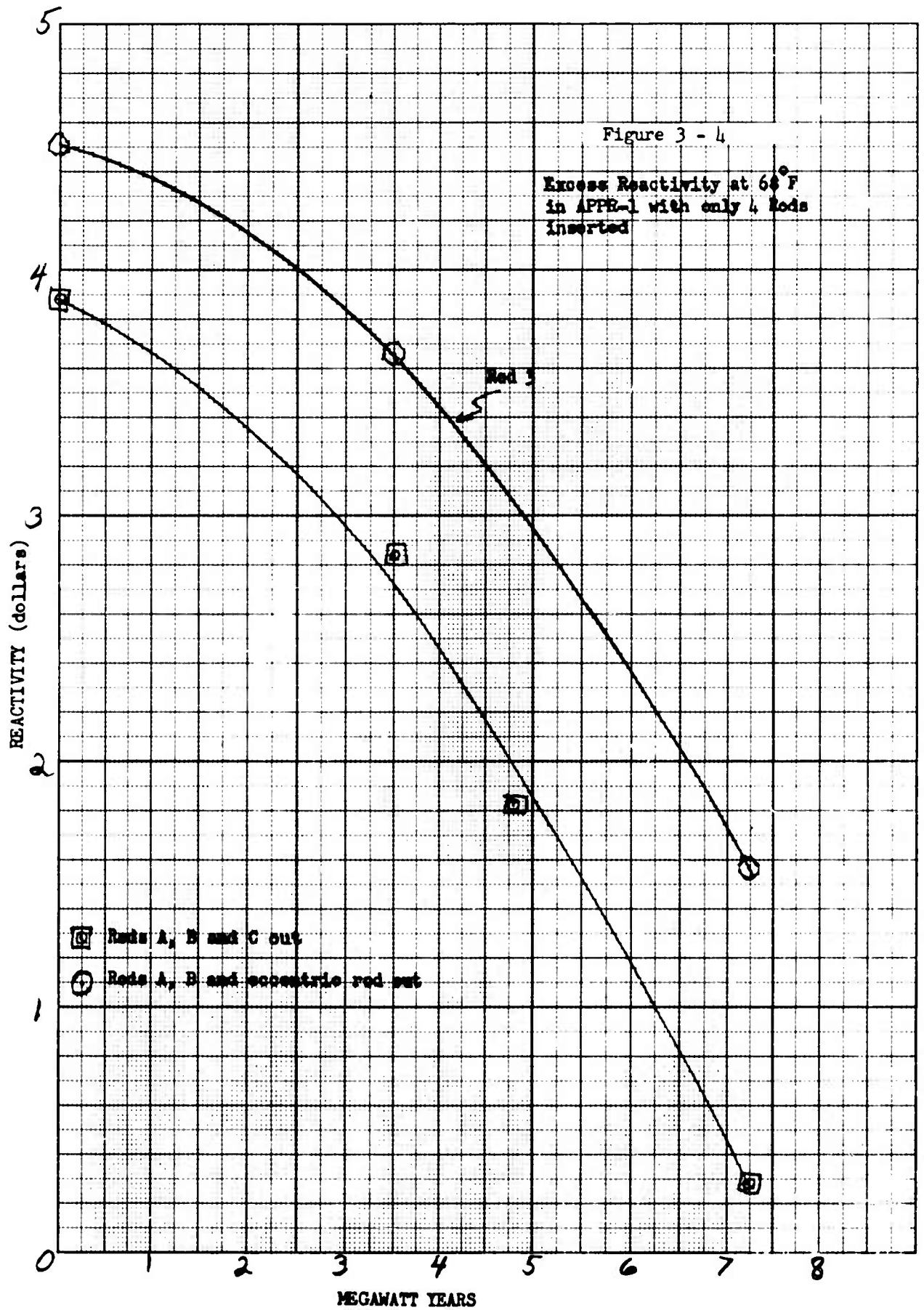
"STUCK RODS"

Critical rod positions at 68°F vs lifetime
with safety rods A, B out



□ Rod A, B out, rod C critical

○ Rod A, B out, rod 3 critical



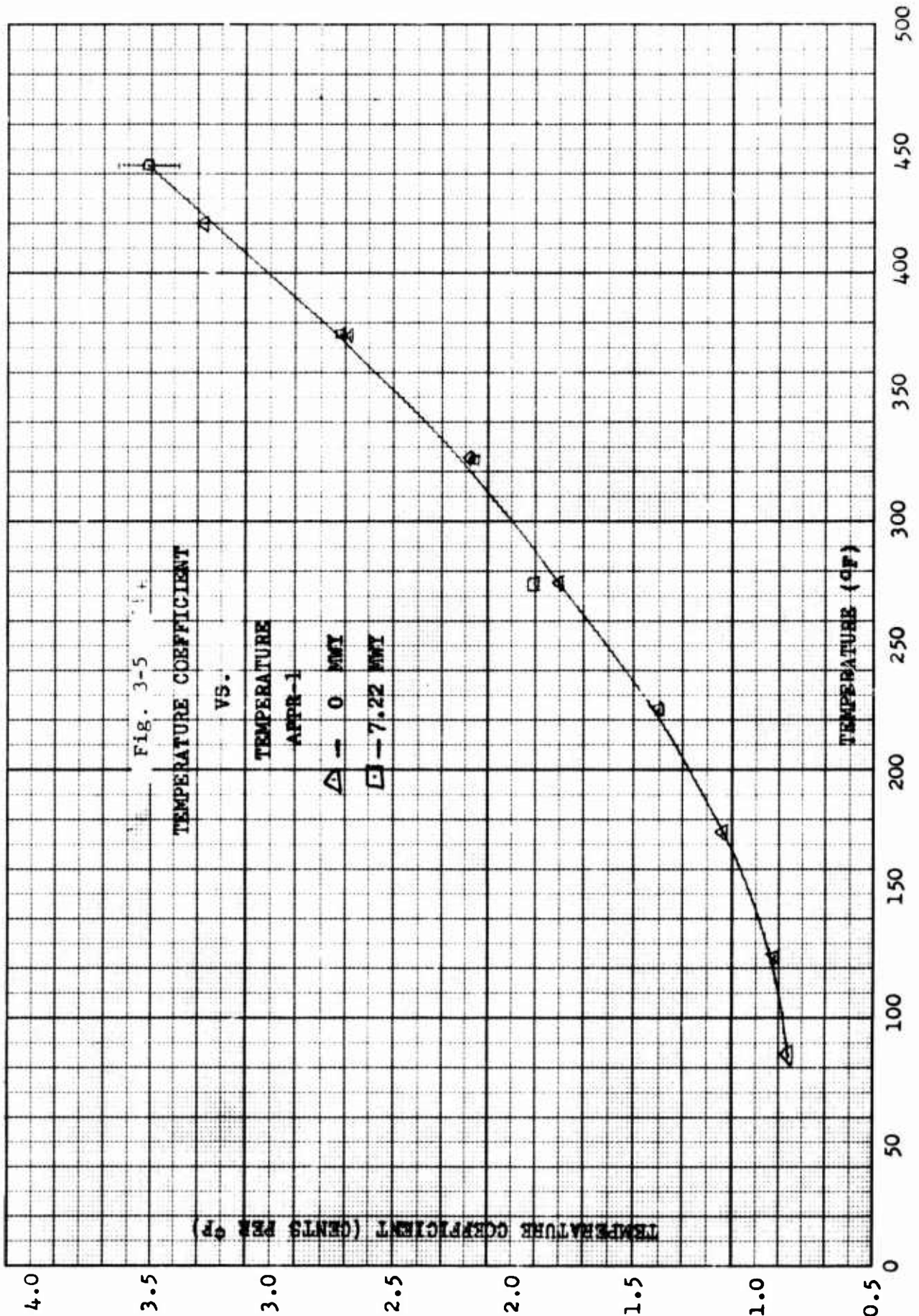
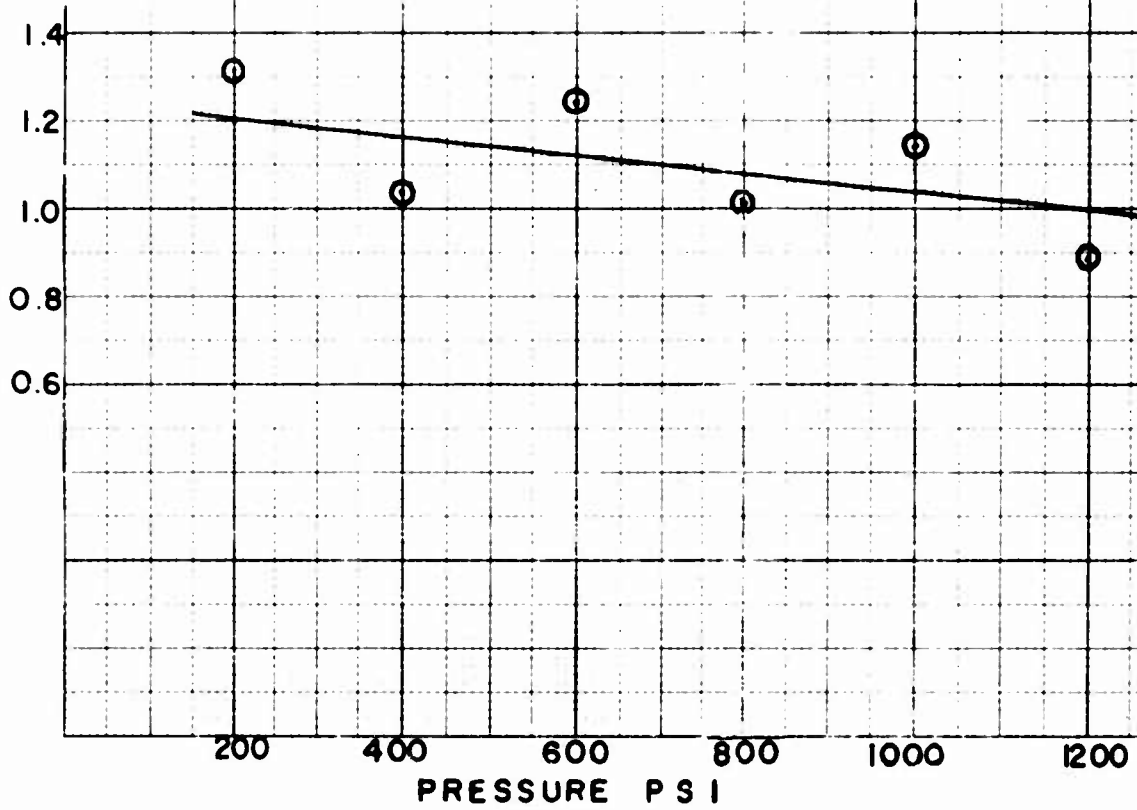


Fig. 3-6

PRESSURE COEFFICIENT
APPR-1

ZERO XENON
115° F
4.79 MWY

PRESSURE COEFFICIENT
CENTS / 100 PSI



3.7 Conclusions

It is apparent from the wealth of experimental data available on the **APPR-1** core that the characteristics of the skid mounted core can be predicted with high precision. This fact should place the core performance on a firm basis.

4.0 Skid Mounted Core Characteristics

The basis for determining the **Skid Mounted Core Characteristics** is through calculation and comparison with the **APPR-1** and zero power measurements.

The analytical model used in the **Skid-Mounted Core** calculation is one which was used in the analysis of the **Zero Power Experiments** (6) and the **APPR-1** (7).

4.1 Method for Establishing - Calculation and Experiment

4.1.1 **Calculational Model** - The basic model uses two neutron-energy group diffusion theory as defined by the equations:

$$\begin{aligned} -D_f \nabla^2 \phi_f(r, z) + \Sigma_{r,f}(r, z) \phi_f(r, z) &= k_{th} \Sigma_{th}^a \psi_{th}(r, z) + (1-p) k_f \Sigma_{r,f}(r, z) \phi_f(r, z) \\ -D_{th} \nabla^2 \psi_{th}(r, z) + \Sigma_{th}^a \psi_{th}(r, z) &= p \Sigma_{r,f}(r, z) \phi_f(r, z) \end{aligned}$$

The definitions of the symbols are given at the end of the report. Assuming separability of the radial (r) and axial (z) dimensions, the solution to these equations can be obtained from various codes for digital computers. (1) The **Valprod** (2) and **Windowshade** (3) codes, written for the **IBM-650** digital computer, were used to solve the multiregion diffusion equations in the radial and axial directions. The output of the codes include reactivity (K_{eff}), normalized power, and normalized thermal and fast flux distributions. In the **Windowshade** code, a uniform absorption cross-section simulating a bank of control rods can be specified. The code then adjusts the rod bank to the critical position.

4.1.2 Thermal Constants -68°F and 512°F

Since the **Skid-Mounted** core contains **APPR-1** type elements, the thermal group constants for the cold (68°F) core were abstracted from **APAE 27** (6). Constants for the homogenized hot (512°F) core were prepared by the **P-3** code (5). Neutron cross sections for each material were evaluated at a hardened energy of 0.0597 eV and the thermal cutoff was taken at 0.248 eV. The **P-3** code solves the one velocity transport equation to the third spherical harmonic approximation for plate type elements. Table 4-1 shows hot and cold **Skid Mounted** constants compared to **APPR-1** constants.

Table 4-1

Constants-Skid Mounted and APPR-1

Fixed Elements

| | Skid | APPR-1 | Skid | APPR-1 |
|---------------------|-------------|-------------|-------------|-------------|
| | Cold (68°F) | Cold (68°F) | Hot (512°F) | Hot (440°F) |
| τ | 32.403796 | 32.3788 | 48.438042 | 42.9631 |
| D_f | 1.321181 | 1.321185 | 1.565798 | 1.491955 |
| Σ_f^a | 0.010286 | 0.01102 | 0.009287 | 0.010867 |
| g' | 0.898091 | 0.898091 | 0.938302 | 0.933348 |
| $\nu \Sigma_f^f$ | 0.013235 | 0.014181 | 0.011910 | 0.013921 |
| p | 0.747733 | 0.747790 | 0.712723 | 0.729024 |
| k_f | 1.286758 | 1.286817 | 1.282469 | 1.280967 |
| Σ_{th}^a | 0.266734 | 0.266863 | 0.200244 | 0.207138 |
| $\nu \Sigma_{th}^f$ | 0.405789 | 0.405789 | 0.309479 | 0.317149 |
| k_{th} | 1.521326 | 1.520589 | 1.545509 | 1.53110 |
| D_{th} | 0.170539 | 0.170538 | 0.267920 | 0.245022 |
| Σ_{xe}^a | --- | --- | 0.006776 | 0.006272 |
| Σ_{SUB}^a | 0.005289 | 0.007846 | 0.003785 | 0.006131 |
| Σ_p | 0.095242 | 0.088263 | 0.073065 | 0.07756 |

CONTROL ROD FUEL ELEMENTS

| | Skid | Skid |
|---------------------|--------------------|--------------------|
| | <u>Cold (68°F)</u> | <u>Hot (512°F)</u> |
| τ | 32.763697 | 48 46 2583 |
| D_f | 1.288348 | 1.510167 |
| Σ_f^f | 0.039322 | 0.031162 |
| Σ_f^a | 0.009254 | 0.008411 |
| $\nu \Sigma_f^f$ | 0.010876 | 0.009798 |
| p | 0.764649 | 0.730070 |
| k_f | 1.175275 | 1.164865 |
| Σ_{th}^+ | 0.223360 | 0.169193 |
| $\nu \Sigma_{th}^f$ | 0.310757 | 0.241486 |
| k_{th} | 1.391283 | 1.427281 |
| D_{th} | 0.180707 | 0.275669 |
| L^2 | 0.809039 | 1.629316 |
| Σ^a | 2.003930 | 1.387063 |
| Σ^{tr} | 1.844579 | 1.209179 |

REFLECTOR PROPERTIES (PURE WATER)

| | Skid | APPR-1 | Skid | APPR-1 |
|-----------------|--------------------|--------------------|--------------------|--------------------|
| | <u>Cold (68°F)</u> | <u>Cold (68°F)</u> | <u>Hot (512°F)</u> | <u>Hot (440°F)</u> |
| D_{th} | 0.14340 | 0.172304 | 0.297171 | 0.264866 |
| D_f | 1.671769 | 1.596015 | 2.154495 | 1.893739 |
| Σ_{th}^a | 0.019470 | 0.016960 | 0.009849 | 0.011052 |
| τ | 34.9638 | 33.6945 | 57.373705 | 47.5034 |
| p | 0.985556 | 0.987116 | 0.986647 | 0.988482 |

4.1.3 Fast Constants - 68°F and 512°F

Constants for the fast group were also obtained from machine calculations. The Muft -III code ⁽⁴⁾ prepares the fast group constants using the P-1 Selengut-Goertzel approximation for slowing down of neutrons in hydrogenous mixtures.

4.1.4 Substitution Effect

Of the 37 APPR-1 type fuel elements, 5 are movable control rod fuel elements. These elements contain less uranium and more stainless steel cladding than the fixed elements. The effect of substituting control rod elements for fixed elements can be approximated by weighting the effect at the center of the core by a $J_0^2(\mu r)$ Bessel function where μ is the radial buckling. The effect of the center control rod fuel element on reactivity is found by running two Valprod calculations, one of which contains a control rod fuel element region at the centerline. The multiplication constant, K_{eff} , for the Skid-Mounted core can then be found from the equalities:

$$K_{eff} = K_{eff}^{F.E.} - \Delta K_{eff} - N (\Delta K_{eff}) \times J_0^2(\mu r)$$

$$\text{where } \Delta K_{eff} = K_{eff}^{F.E.} - K_{eff} \text{ (F.E. with central control rod fuel element)}$$

N = no. of rods excluding central rod.

F.E. = fixed fuel elements

It is assumed that the effect of substituting a control rod fuel element for a fixed element changes only the thermal absorption cross-section,

$$\Sigma_{th}^a = \Sigma_{th}^a \text{ (F.E.)} / \Sigma_{SUB}^a$$

4.1.5 Model Correction

Reactivity calculations using this analytical approach are different from measured values in the APPR-1 reactor. To compensate for this expected difference between calculation and measurement, a "model" correction is applied to the calculated reactivity of the Skid-Mounted Reactor.

4.2 Core Reactivity at 68°F

Using the model described in section 4.1, the effective multiplication of the Skid Mounted Core at 68°F was calculated to be 1.1693. This result was obtained from a Valprod calculation of a core composed of fixed fuel elements at a temperature of 68°F. The constants for this calculation are listed in Table 4-1.

The substitution effect for a central control rod fuel element was found by running a Valpro calculation with a cylindrical control rod fuel element at the center of the core. For this case, k_{eff} decreased to 1.1594. The substitution effect for all five elements is then:

$$\begin{aligned} \Delta k_{eff} &= 0.0059 \\ k_{eff} \text{ (actual core)} &= 1.1594 - 4 J_0^2 (\mu r) \Delta k_{eff} \\ &= 1.1594 - 4 (0.49673) (0.0059) = 1.1594 - 0.0117 \\ &= 1.147 \end{aligned}$$

This correction has reduced the reactivity to 1.1477 or 12.87 % ρ .

The measured cold reactivity for APPR-1 is 1.81% higher than the calculated value. (See APAE-27, (6) Pg. 48 and 49, APAE-32, (7) Pg. 49, 50, 56, 73) This difference is almost constant for a variety of core configurations ranging from 1.6 to 2.6% ρ . In all cases the measured reactivity was greater than the calculated reactivity. Thus, the Skid Mounted core should have an excess reactivity of about 14.98% at 68°F.

The measured reactivity of the APPR-1 is 15.35% ρ . This implies that the difference in reactivity between the Skid Mounted and APPR-1 is only 0.67%.

Measurements were made on the zero power experimental core (10) of the position of the five rod bank vs. number of elements in the core. The bank moved 1.7" further in, going from 37 to 45 elements, which corresponds to a reactivity change of 2.57% using the best available rod worth data. (1) However, these cores had two additional control rod elements present. In the Skid Mounted core, they are replaced by fixed elements. This difference amounts to 0.75% ρ . Therefore, we can infer from this experimental data that the Skid Mounted Reactor has a reactivity of 13.53% ρ or 1.82% ρ less than the APPR-1. In the interpretation of this experiment, the assumption was made that the rod worth does not change from 45 to 37 elements. There is probably a slight increase in rod worth in the 37 element core (about 0.9% for the 5 rod bank).

A difference of 1.15% exists between the two predicted reactivities. We will say, therefore, that the reactivity of the Skid Mounted core at 68°F is 14.11% ρ \pm 0.58% ρ .

4.3 Control Rod Worth

The worth of the central control rod and the bank of five rods were calculated using the Scram Code (8) for the IBM 650. This code solves a one velocity diffusion equation for a bare reactor with a ring of black absorbing shells including a shell placed at the center of the core. At 68°F, the calculated worth of the bank is 19.9% ρ ; at 512°F, it is 19.5% ρ . A homogeneous thermal poison cross section for the rod bank can then be defined as:

$$\Sigma_p = \Sigma_a \text{ rods in } \Sigma_a \text{ mixed element core}$$

This poison cross section is used to predict the critical rod bank position. The calculated worth of the center rod alone is 4.5% ρ at 68°F and 4.0% ρ at 512°F.

Experimental measurements on the APPR-1 Zero Power Reactor (9), Pg. 44 and 45, show a center rod worth of 4.0% ρ for a boron-steel poisoned core, and 4.8% ρ for a stainless steel poisoned core at 68°F. The integrated worth of the entire bank is 18.2% ρ (11). This is fairly good agreement as it is expected that the rod worth will be larger in the Skid Mounted Core. These experimental measurements (11) indicate no change in rod worth with changes in temperature.

4.4 Core Reactivity and Bank Position

The hot (512° F), clean reactivity for the skid mounted core with fixed elements was calculated using the "Valprod" code⁽²⁾. The constants used are listed in Table 4-1. The substitution effect reduced the reactivity from 8.4% ρ with all fixed fuel elements to 7.12% ρ with five control rod fuel elements. In APPR-1, this calculational model was 0.53% ρ too low. Therefore, the hot clean reactivity of the skid core is about 7.65% ρ .

In the hot (512°F) equilibrium xenon condition, the reactivity decreased to 4.9% ρ at 0 MWYR.

A "model" correction of 0.30% ρ brings the reactivity up 5.2% ρ for this case. This will be the maximum reactivity for the equilibrium xenon condition since the core will lose reactivity with burnup.

The uniform and one shot burnout models were the same as those used in the APPR-1 burnout calculations. (12) All equations can be found in this reference. Calculated core parameters as functions of uranium burnup are plotted in Fig. 4-1 a,b,c. The reactivity for uniform burnup can then be calculated from the two group bare equivalent core equation,

$$K_{\text{eff}} = \frac{K_{\text{thp}}}{(1 + \frac{B_T^2}{\beta}) (1 + L^2 B_T^2)} + \frac{K_f (1-p)}{(1 + B_T^2 \tau)}$$

The results are plotted in Fig. 4-2.

For the non-uniform burnup, the core was divided into seven radial regions and burned out in five time steps with an average flux for each region. The "Nub I" code⁽¹²⁾ was used to burn up these regions. However, no change in reactivity was found up to about 8.5 MWYRS. The initial case was at hot, equilibrium xenon, 0 MWYR. The flux distribution was kept constant but the magnitude of the fluxes varied with burnup.

In the axial direction, the core was divided into five regions and burned out in five time steps using the same assumptions applied to the radial burnout. The initial case was at hot, equilibrium xenon, 0 MWYR, with the rods at the critical position (11.6" out). At each time step, the "Windowshade" code⁽³⁾ was utilized in finding the critical rod bank position. A comparison between this calculation and APPR-1 results is found in Figure 4-3.

The excess reactivity can then be determined from rod worth measurements on the APPR-1. The rod worth per inch of the five rod bank is plotted in reference (11), and reproduced in Figure 3-2. It is assumed that the rod worth curve for the skid mounted APPR would not be significantly larger than for the APPR-1. The excess reactivity curve for the axial non-uniform burnout is plotted in Fig. 4-2 as is the curve for uniform burnout. If the APPR-1 non-uniform correction were applied to the uniform burnout curve the predicted lifetime would be less. This can be expected since the non-uniformity is greater in the APPR-1. The initial rod bank

position in the APPR-1 is 8.3" out of the core. This distorts the axial flux distribution much more than in the skid mounted core.

The lifetime of the skid mounted APPR should be about 10 ± 1 MWYR and will exceed the requirement to run for one year at 10 MW (0.8 load factor). The maximum fuel burnup for a region of the core is 49% for the center region. The maximum reactivity will occur at the beginning of life before Xenon builds up to equilibrium conditions.

4.5 Stuck Rod Criticality

In the skid-mounted core, the maximum reactivity will occur at the beginning of core life in the cold (68°F), clean condition. If the core can be shut down by any four rods of the five rod bank at this time, then those four rods should be able to shut down the core at any time. The stuck rod condition will not be as severe as in APPR-1 because of the smaller core size and increased rod worth.

Due to the flux perturbations that occur when a rod is stuck out, analytical techniques are not successful in predicting the core criticality. For instance, when one side rod is stuck out, that side of the core becomes essentially a slab reactor, and the flux shift to that side of the core increases the worth of the rod considerably. Fortunately, there is good experimental data from the APPR-1 core (13) showing the reactivity of the core with a side rod or center rod stuck out. Fig. 4-4 shows the excess reactivity of the APPR-1 and skid mounted cores for these cases. The rod worths for the skid mounted core are assumed to be the same as the APPR-1, but the initial reactivity is smaller by about $1.25\% \rho$. Since the initial skid reactivity is close to that of the APPR-1, the core will not shut down with a rod stuck all the way out. However, additional experimental data from the APPR-1 (10) shows the core to be critical with the center rod stuck out 9.98". The worth of this rod in this range is 50.6¢ per inch. Therefore, the critical position of the center rod in the skid core would be 14.5" out. The APPR-1 core is critical with a side rod out 9.84" where the rod is worth 65¢ per inch. In the skid core, the rod should make the core critical about 13 inches out. This is verified in Figure 4-5, reproduced from reference (13). These positions are above the equilibrium xenon operating condition where the rod bank is initially withdrawn 11.6". However, if a rod were stuck while overriding xenon, the core might not shut down.

Boron Injection System for Stuck Rods

The injection of boric acid into the skid mounted core will be necessary to insure complete shutdown in the event of some stuck control rod conditions.

The skid core will shut down with one rod stuck in the equilibrium xenon operating bank position. In the unlikely event of one rod stuck all the way out of the core, the core will not shut down at 68°F with the remaining four rods. The worst case is with one side rod stuck out. In this case, the side of the core becomes a slab reactor, and the flux shift to that side increases the worth of the side rod considerably. About 15 out of the 37 elements form this slab. The excess reactivity can be found from the

FIG 4-1a
 NUCLEAR PARAMETERS
 vs.
 U-235 BURNUP

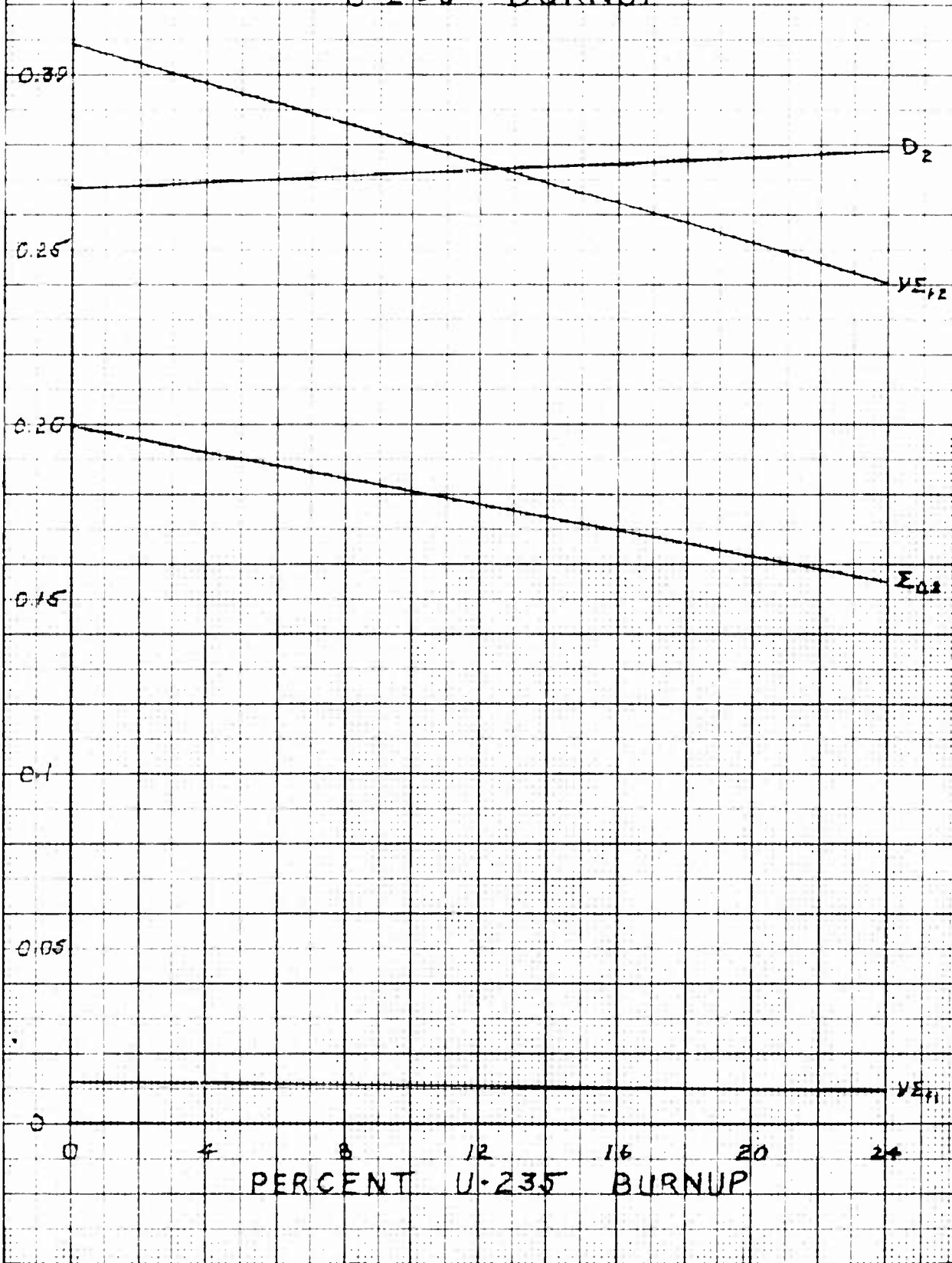
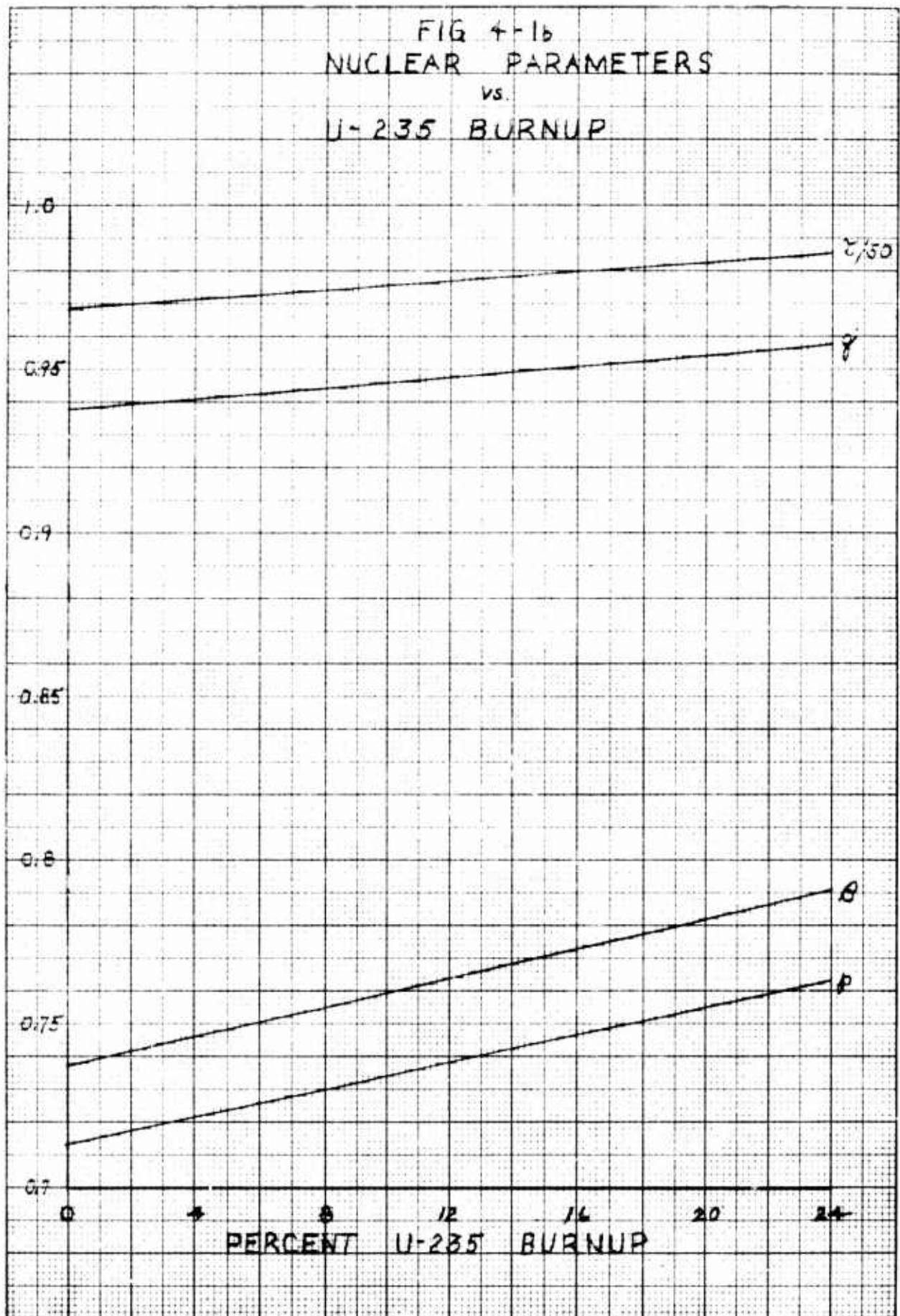


FIG 4-1b
 NUCLEAR PARAMETERS
 vs.
 U-235 BURNUP



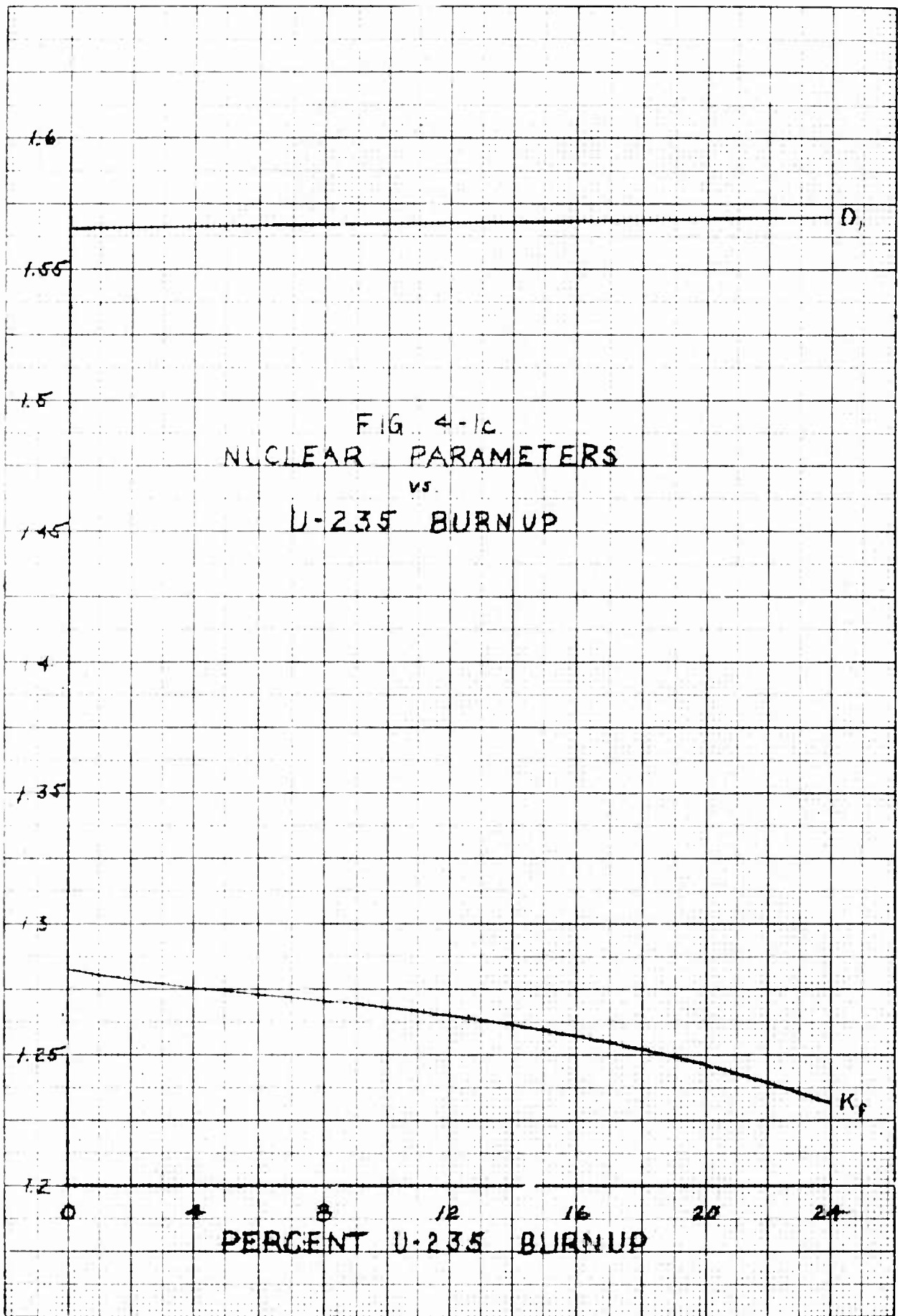


FIG. 4-2

SKID MOUNTED REACTIVITY

NOTE: SIZE PF & EQUILIBRIUM XENON

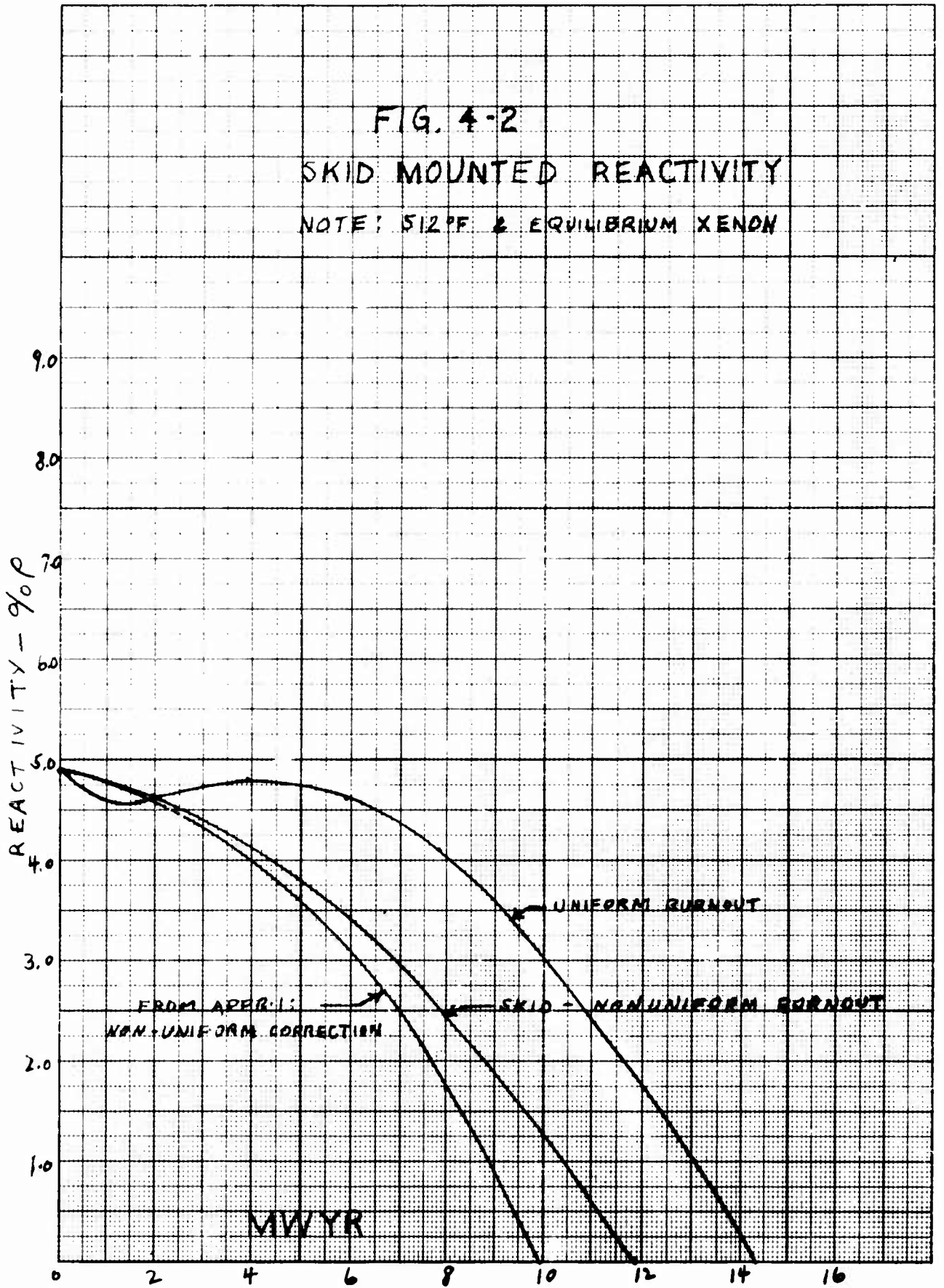


FIG. 4-3

FIVE ROD BANK POSITION vs LIFETIME

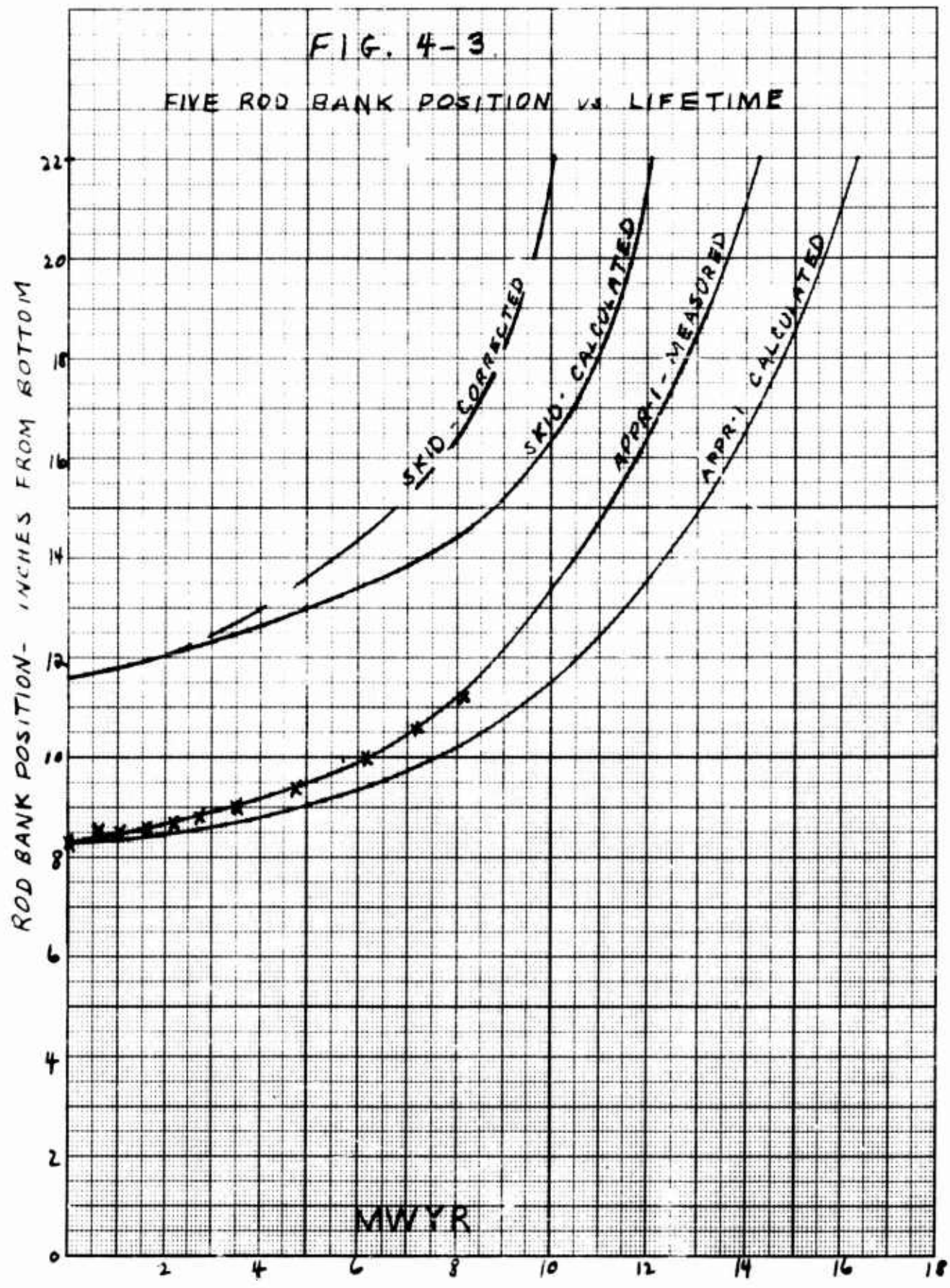


FIG 4-4

EXCESS REACTIVITY AT 68°F
WITH 4 RODS INSERTED

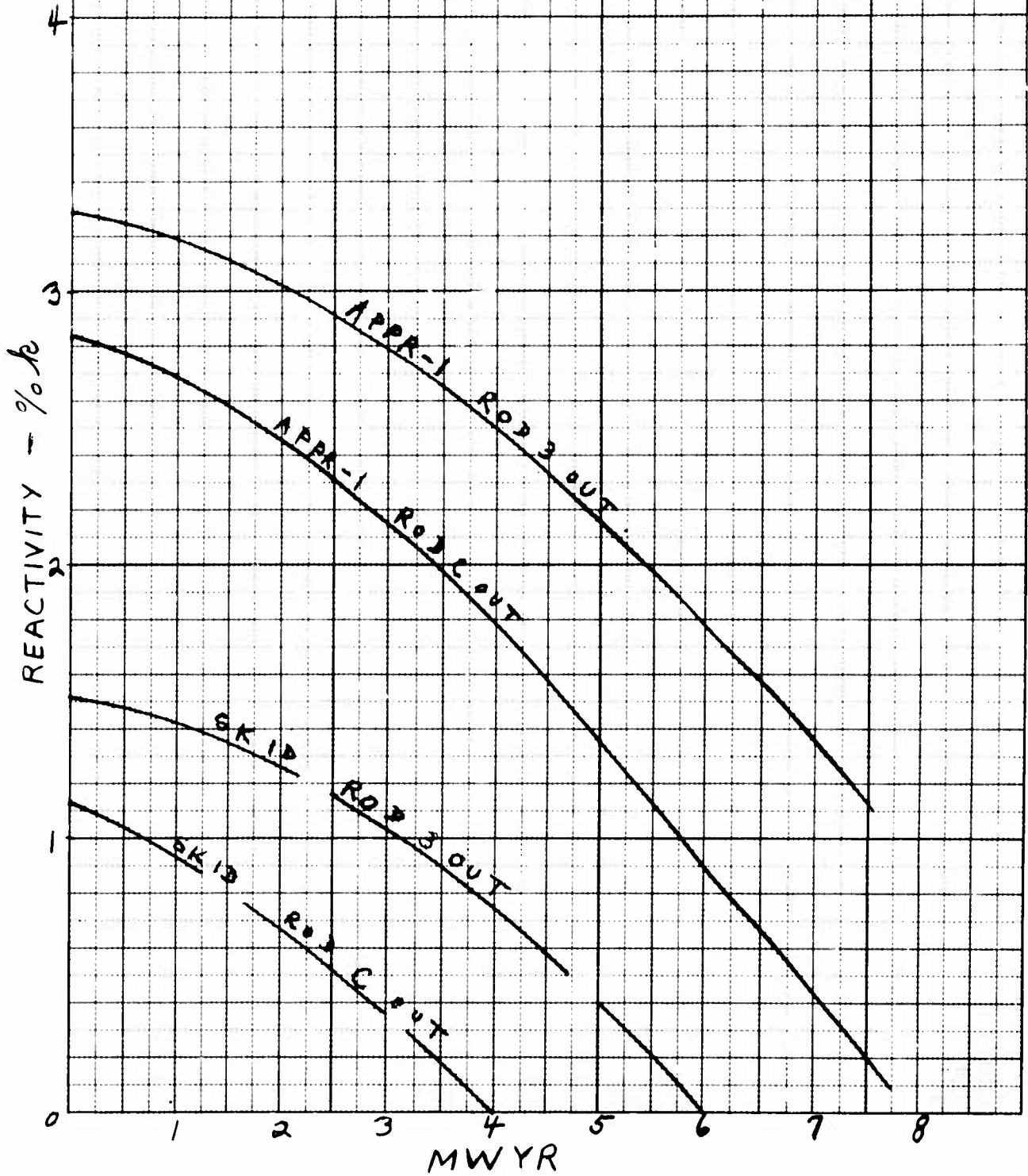
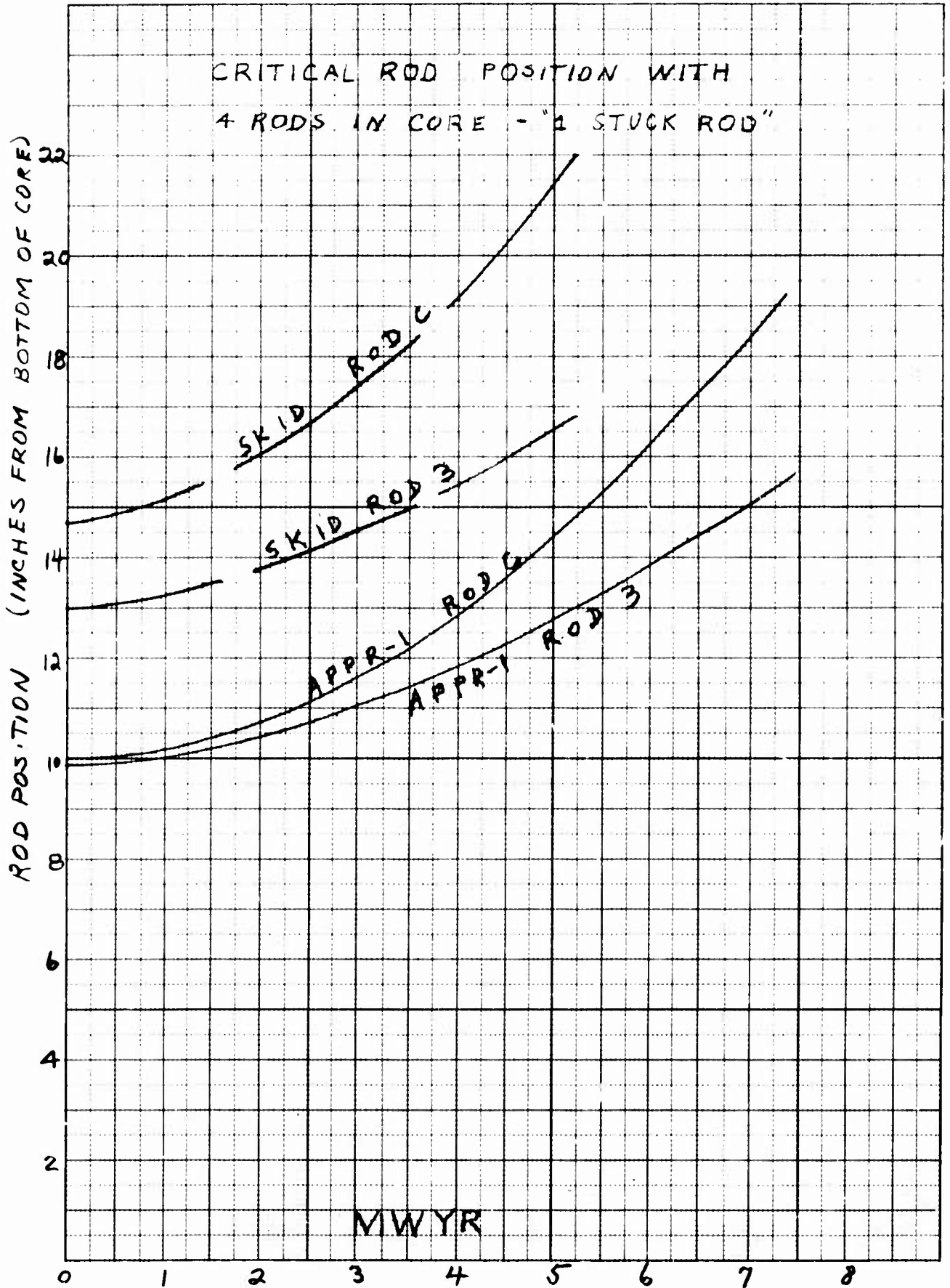


FIG. 4-5



experimental worth of this rod. (See Fig. 3-4 or Fig. 4-4) Subtracting the difference between the skid and APPR-1 cores, about 1.75% k, the excess reactivity is 1.55% k or \$2.12. Since the worth of B-10 to be injected is 70¢ per gm, about 3 grams of boron -10 would be needed in that side of the core. Assuming homogeneous injection of the boron,

$$\frac{37}{15} \times 3 = 7.4 \text{ grams B}^{10}$$

needed in entire core. A total of 9 gms of B¹⁰ was specified for the core to account for any experimental inaccuracies.

4.6 Control Rod Burnup

The fraction burnup in the control rod bank is defined as the total number of absorptions in the rods per original atom density of absorber, i.e.,

$$B = \frac{A_{\text{total}}}{N_0}$$

where N_0 is the atom density of absorber times the volume of absorber in the core at the average bank position. The assumption is made that all the excess neutrons ($k_{\text{ex}} = k_{\text{eff}} - 1$) were absorbed in the control rod absorber material.

$$A_{\text{total}} = P \delta \nu k_{\text{ex}} t$$

where

$$P = \text{power} = 10^7 \text{ watts}$$

$$\delta = \text{fissions/watt-sec.} = 3.24 \times 10^{10}$$

$$\nu = \frac{\text{neutrons}}{\text{fission}} = 2.46$$

$$k_{\text{ex}} = \text{average excess multiplication} = 0.05$$

$$t = \text{lifetime of core} = 3.1536 \times 10^7 \text{ sec.}$$

If the average bank position is 6" into the core, $N_0 = N_{B10}$ total rod atoms $\times 6/22 = 4.63 \times 10^{24}$ atoms in core.

$$N_{B10} \text{ total rod atoms} = 16.985 \times 10^{24}$$

$$\Delta \text{ total} = 1.257 \times 10^{24}$$

The maximum fractional burnup is then 0.27. Thus, the amount of original B_{10} absorber left after 10 MWYR is 3.37×10^{24} atoms for an average rod insertion of 6". The average burnup for the entire length of the rods would be 7.4%.

This amount of burnup is a less serious problem than in APPR-1 since the maximum fractional burnup in the APPR-1 is estimated to be 0.37. However, irradiation of APPR-1 rods will be examined and the results will be applicable to the control rods in the Skid Mounted Reactor. After 9 MWYR of operation in the APPR-1, there has been no malfunctioning of the rods due to control rod burnup. This is almost equal to the core lifetime of the skid. However, removal of the control rods from the reactor may present a problem.

4.7 Temperature and Pressure Coefficients

The temperature coefficient of the Skid Mounted core was primarily based upon extrapolation of existing experimental data. The Zero Power Experiment (9) predicts a temperature coefficient, at the operating temperature of 512°F, of $-3.1 \times 10^{-4} \frac{\Delta k}{\Delta T}$. Measurements on the APPR-1 (11) reactor predict the same values at 512°F although the curve is of a slightly different shape. Fig. 4-6 is a reproduction of the experimental curves which also show a rise in the temperature coefficient for a 32 element core. The skid mounted core will therefore have a temperature coefficient of about -3.4×10^{-4} at the operating temperature of 512°F.

The integral of this curve is -7.3% k for the 37 element core from 68°F to 512°F. This number can be checked from available rod bank data (11). In APPR-1 the rod bank is 3.7" out; at 440°F it is at 6.6". Extrapolating this curve to 512°F, the rods would be 8.2" out. This corresponds to 7.0% k and would be slightly higher in the Skid core due to increased rod worth. This is excellent agreement, and, together with the knowledge of the cold (68°F) reactivity of the Skid, should determine the hot (512°F), clean reactivity.

As expected, measurements of the pressure coefficient (24,25) show this to be smaller than the temperature coefficient by at least a factor of 100. In the Skid Mounted reactor, it is estimated to be $3.1 \times 10^{-6} \frac{\Delta k}{\Delta P}$ at 512°F and 1750 psi operating pressure. (See Fig. 4-7)

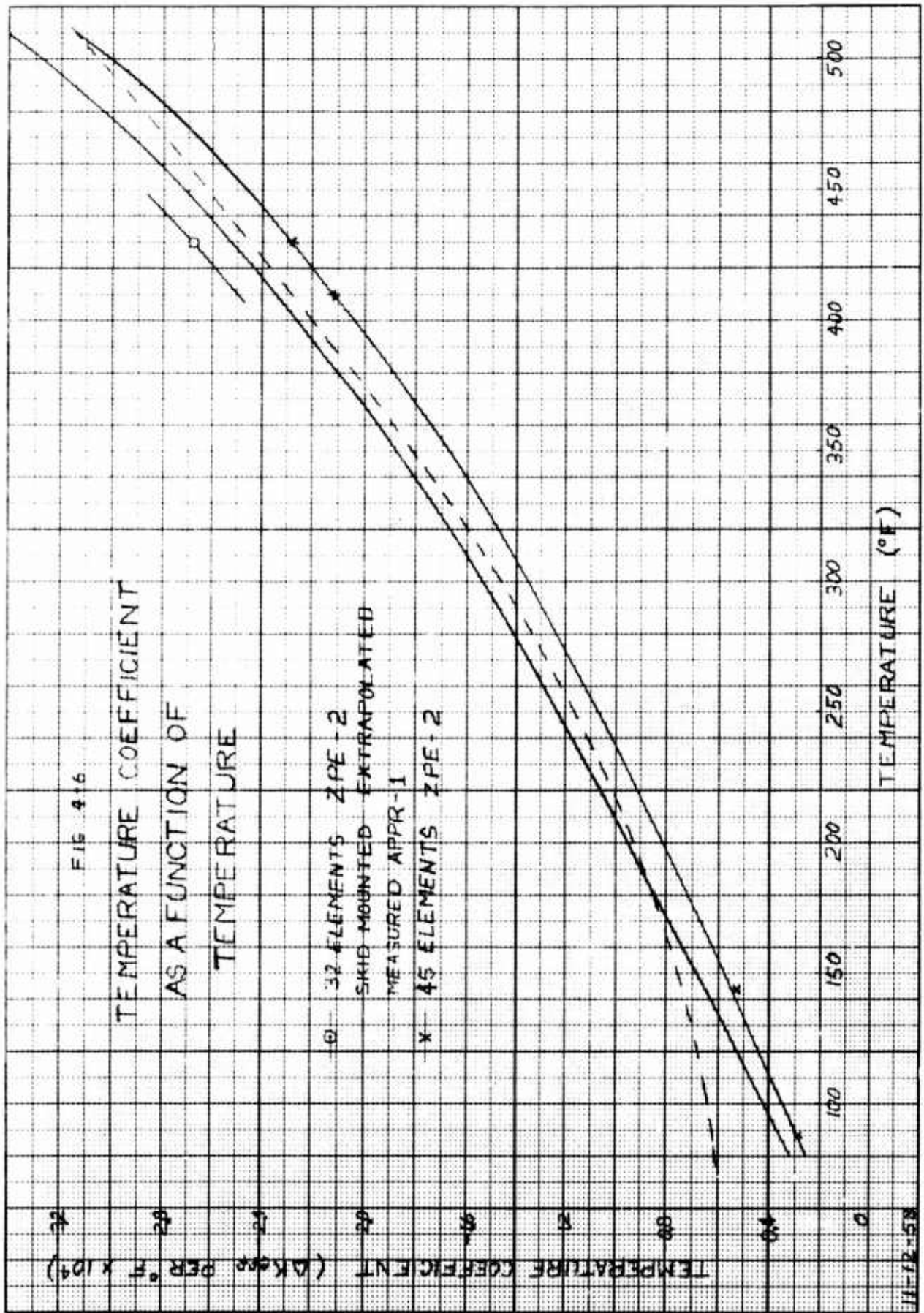


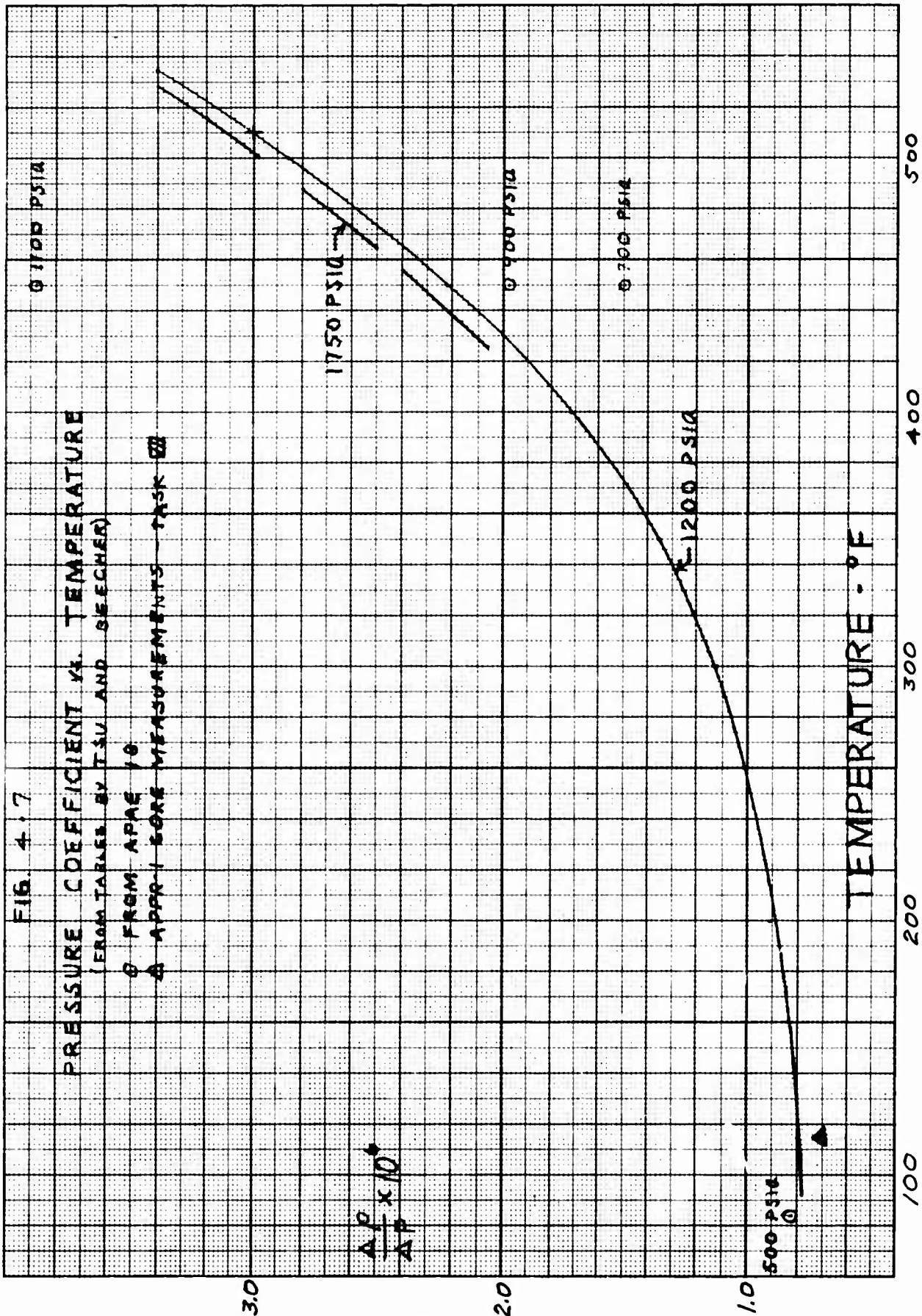
FIG. 4.7

PRESSURE COEFFICIENT VS. TEMPERATURE

(FROM TABLES BY TSU AND SEECHER)

○ FROM APAC 10

△ APPR. SCORE MEASUREMENTS TASK III



5.0 Flux and Power Distribution

Power distributions on the Skid-Mounted reactor were obtained for the Thermal Analysis section for determination of the coolant flow rate in each element. Power peaking at the edge of the core was not expected to be a problem because of the placement of the 2" thick stainless steel thermal shield only an average of 1.23" from the edge of the core. However, different reflector configurations were examined for effects on the power distribution, flux distributions, and reactivity of the Skid Mounted Core.

Fast and thermal flux distributions through the primary shield were graphed to show the flux level at various positions in the shield and in the pressure vessel. These calculations helped to set the inner diameter of the pressure vessel and location of the various neutron reading instruments in the primary shield.

5.1 Power Distribution calculations and experiments

The Valprod code, written for the IBM 650 digital computer, was utilized in determining thermal and fast flux distributions through the primary shield. The code also finds the power distribution and reactivity of the core by solving the two group, multiregion diffusion equations in one dimension. Material constants were calculated by the MUFT III and P-3 codes.

Experimental flux data is not available on a 37 element core. However, there is radial flux data for 32 and 45 element cores with water reflectors. As seen on Pgs. 78, 79 and 80 of APAE-27 (6), agreement between calculated thermal fluxes and experimental data is excellent. Since the power generation is almost directly proportional to the thermal flux in the core, we can expect the Valprod code to also predict the radial power distribution accurately.

In the axial direction, power distributions with a bank of control rods inserted into the core were obtained by assuming the bank could be replaced by a homogeneous thermal absorption cross-section (Σ_p). A one dimensional, two group code, the Windowshade code, iterates for the position at which the insertion of this Σ_p will result in a critical core. The most adverse power distributions occur at the beginning of full power operation because the rod bank is at its deepest penetration and the lower part of the core provides most of the power generation as shown in Fig. 5-1 and 5-2. The radial peak to average is 1.46. The axial center peak to average is 1.65; however, this improves as the rods are withdrawn.

5.2 Flux Distribution

As the uranium in the core burns up, the rod bank must be moved out to compensate for the reactivity decrease. This helps flatten the axial thermal flux distributions; however, the magnitude of the flux increases. The power level is a function of the flux times the fission cross-section. In order to maintain a constant power level, the flux increases as the fission cross-section decreases due to uranium burnup. Therefore the magnitude of the fluxes will be largest at the end of core life (10 MWYR). Fig. 5-3 and 5-4 show the radial and axial thermal flux distributions at 0 MWYR and at 8 MWYR at operating temperature (512°F).

Fig. 5-5 shows the radial thermal flux distribution for an infinite water reflector and for a 1 2/3" water gap followed by a 2" thick stainless steel thermal shield. The thermal shield depresses the thermal flux peak at the edge of the core considerably since steel does not scatter thermal neutrons back into the core as effectively as water and is a greater thermal neutron absorber. Reflector properties of stainless steel can be found in APAE-27.(6)

5.3 Flux at Chamber position

In order to determine the flux level in the primary shield rings for instrumentation and dosage purposes, radial flux distributions were calculated. The average thermal flux in the core is about 1.67×10^{13} at the beginning of core life for 10 MW operation. This increases to a maximum of 2.3×10^{13} after 10 MWYR. Fig. 5-6 shows the thermal flux, normalized to an average of 1 in the core, through the primary shield which consists of concentric rings of boral, water, and carbon steel. The absolute value of the thermal and fast fluxes at the end of life at full power can be found by multiplying the scale by 2.3×10^{13} .

After shutdown the average value of the thermal flux in the core is initially about 1.3×10^4 . This is a function of the polonium-beryllium and photoneutron sources in the core and the shutdown multiplication constant of the core. Section 6.0 will provide complete data on shutdown conditions.

Instrument chamber tubes are to be located at essentially two type positions within the shield.

Position 1:

Two tubes are located within a cut in the second shield ring on a center 33 inches from the core centerline.

Position 2:

Three tubes (including the BF_3 tube) are to be located within shield tank water on a center 33 inches from the core centerline. The second shield ring does not extend to these counter positions.

Estimates of the average thermal neutron flux at these positions follow, based on knowledge of the average core fluxes and flux distribution through the shield.

Position 1:

$$\phi_{\text{th}} = 1.19 \times 10^9 \text{ neutron/cm}^2\text{-sec} \quad \text{beginning of life}$$

$$\phi = 1.63 \times 10^9 \quad \text{end of life}$$

Position 2:

$$\phi = 0.89 \times 10^{10} \quad \text{beginning of life}$$

$$\phi = 1.22 \times 10^{10} \quad \text{end of life}$$

These values may be reduced considerably by proper positioning of the tubes in the vertical dimension.

FIG 5-1
RADIAL POWER
DISTRIBUTION

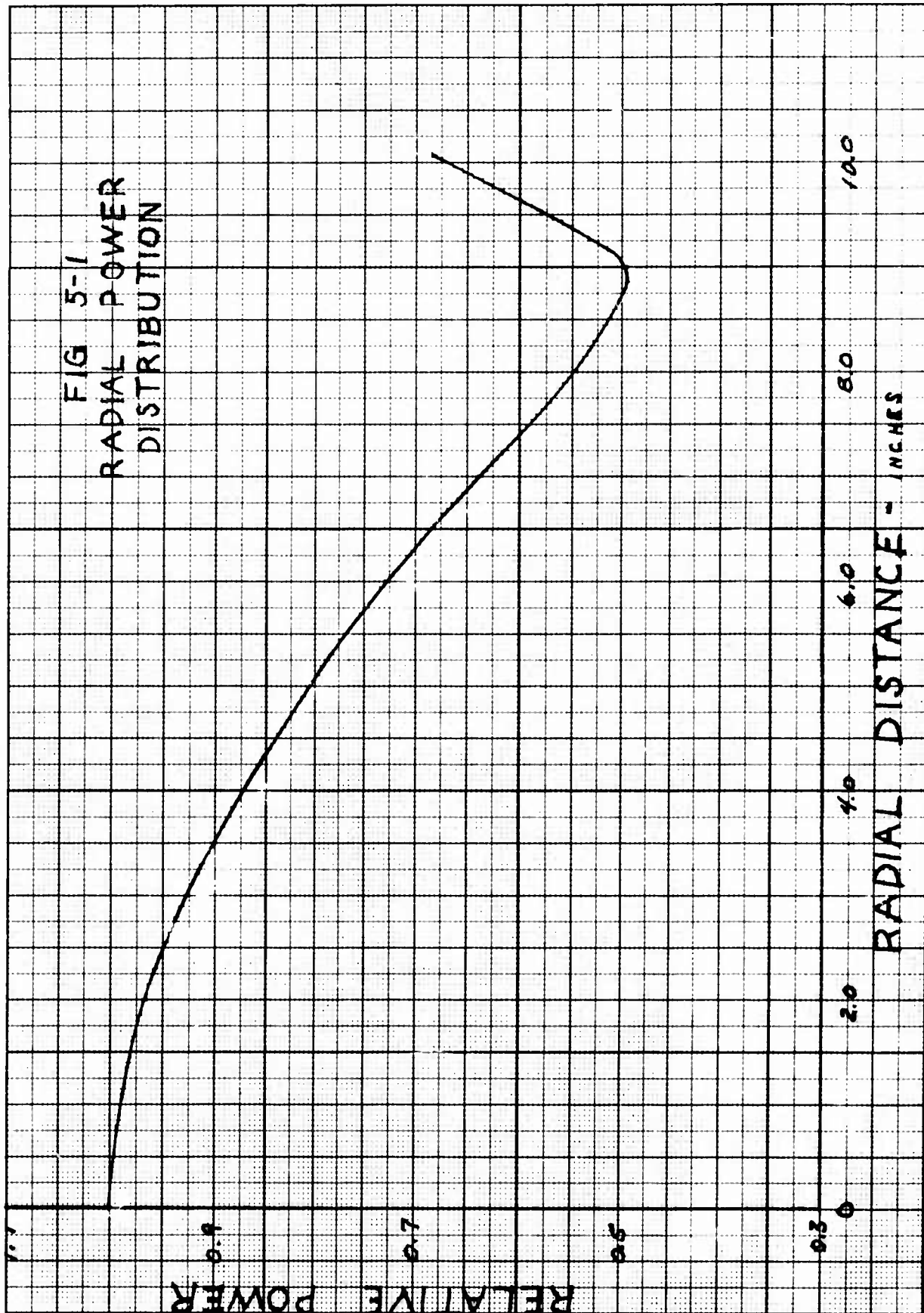


FIG. 5-2

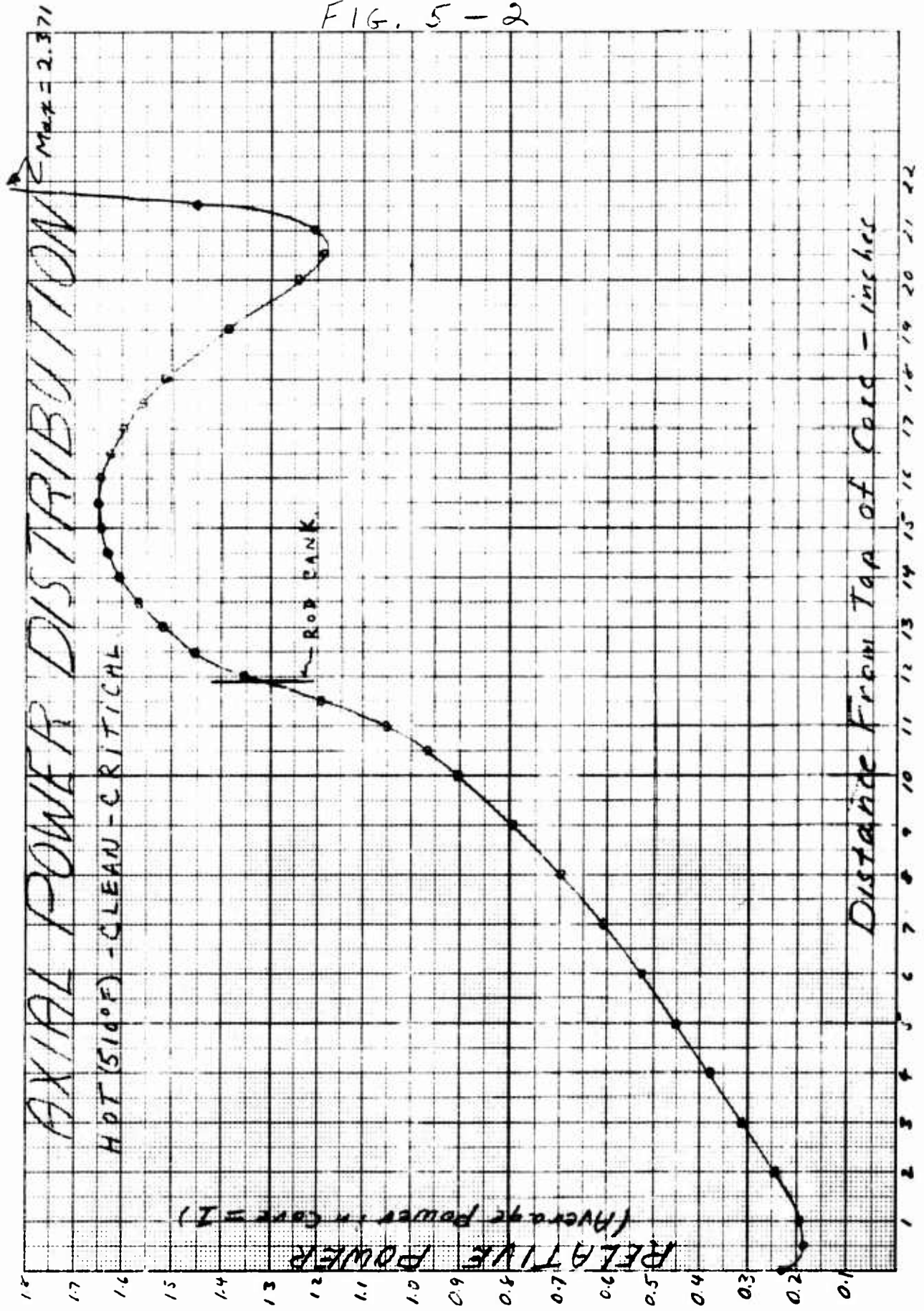
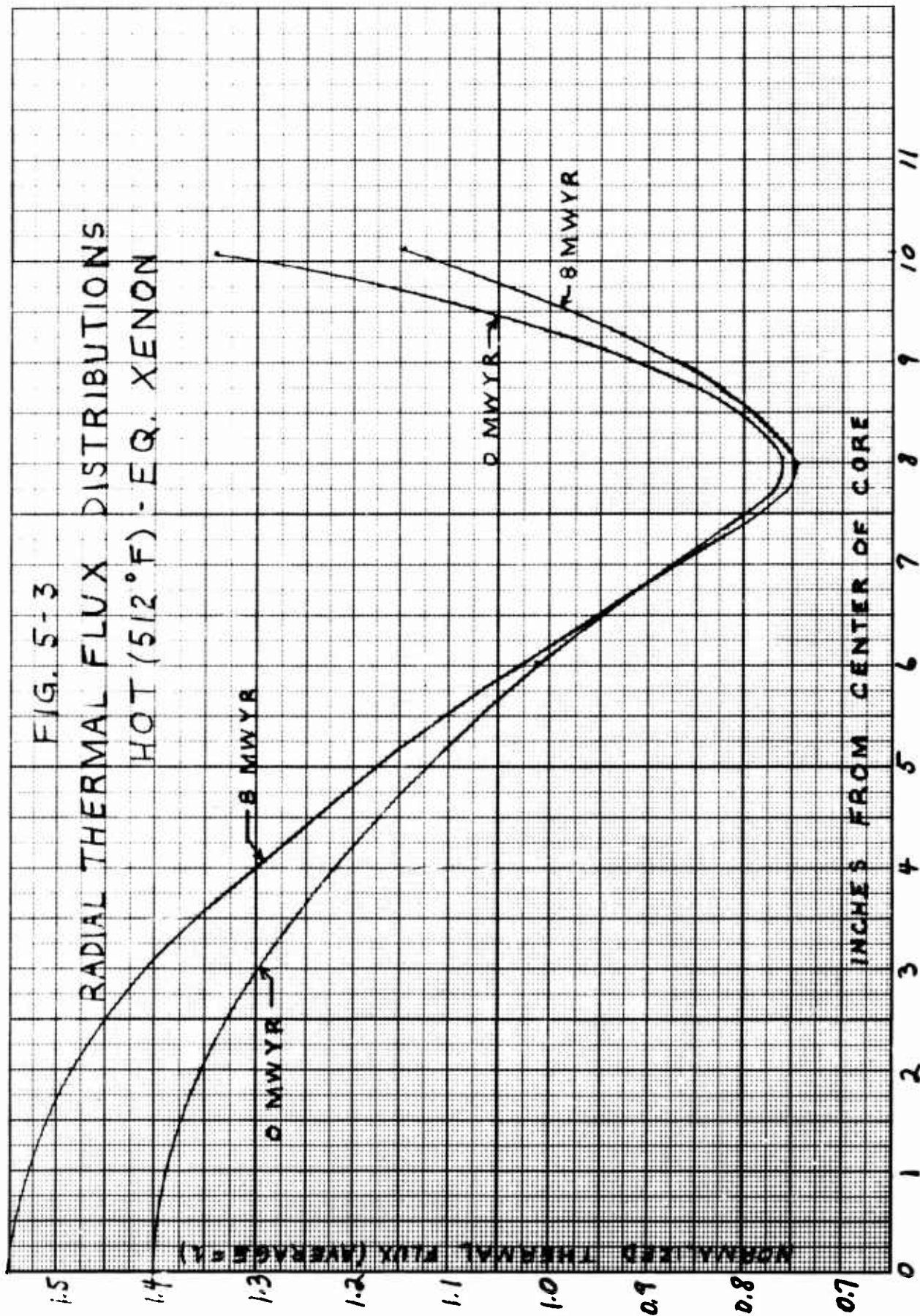


FIG. 5-3

RADIAL THERMAL FLUX DISTRIBUTIONS
HOT (512°F) - EQ. XENON



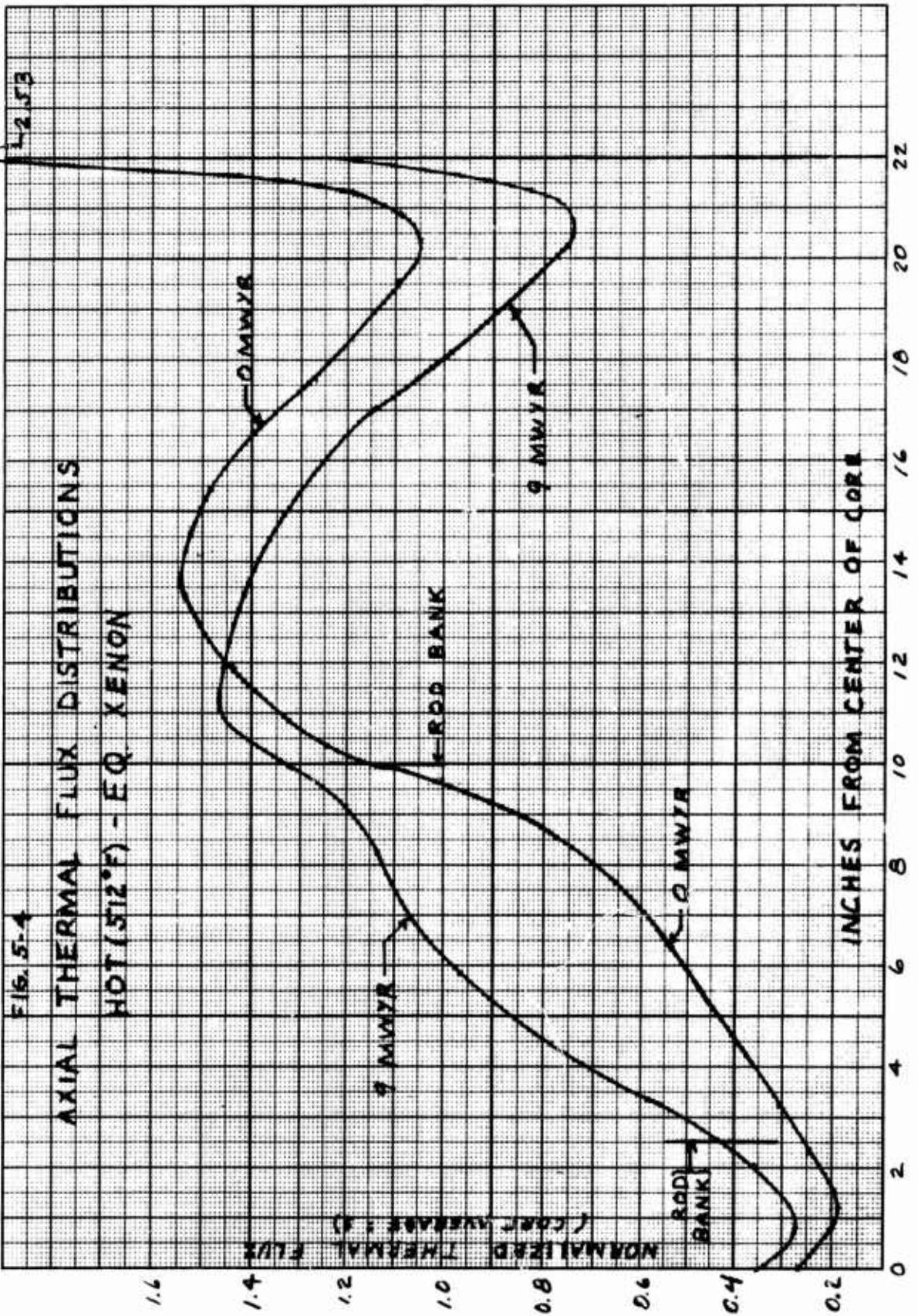
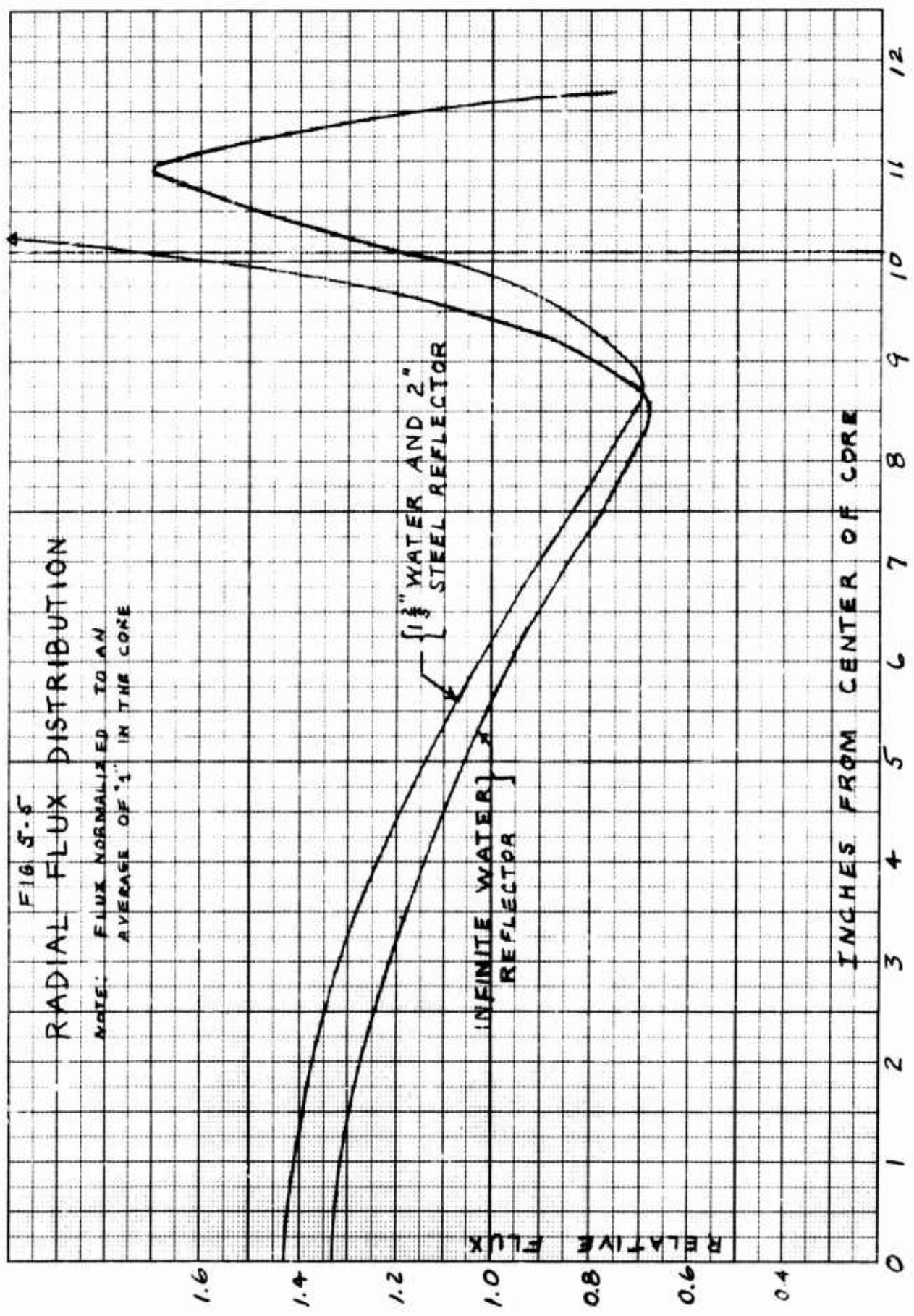
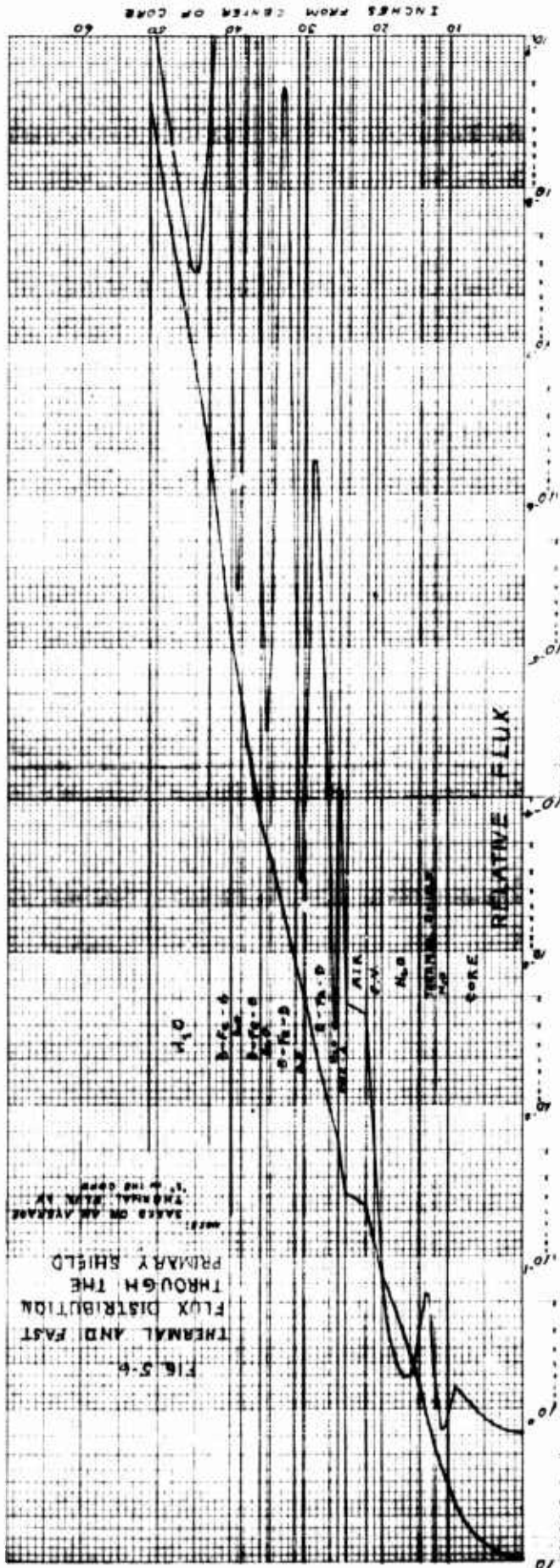


FIG. 5-5
 RADIAL FLUX DISTRIBUTION
 NOTE: FLUX NORMALIZED TO AN
 AVERAGE OF '1' IN THE CORE





Estimates of the average thermal neutron flux at these positions follow, based on knowledge of the average core fluxes and flux distributions through the shield.

Flux at 10 Megawatts

Position 1:

| | |
|---|-------------------|
| $\phi = 1.19 \times 10^9$ neutrons/cm ² -sec | beginning of life |
| $\phi = 1.63 \times 10^9$ | end of life |

Position 2:

| | |
|------------------------------|-------------------|
| $\phi = 0.89 \times 10^{10}$ | beginning of life |
| $\phi = 1.22 \times 10^{10}$ | end of life |

Shutdown Flux

Position 1:

| | |
|---------------|-------------------|
| $\phi = 0.96$ | beginning of life |
|---------------|-------------------|

Position 2:

| | |
|--------------|-------------------|
| $\phi = 7.2$ | beginning of life |
|--------------|-------------------|

Gamma flux at both positions for 10 megawatt operation is approximately 4×10^5 r/hr.

These values may be reduced considerably by proper positioning of the tubes in the vertical dimension.

5.4 Fast Flux on Pressure Vessel

In an attempt to reduce weight, the inside diameter of the pressure vessel of the Skid Mounted Reactor was reduced to 25" in the early stages of the design. Bringing the pressure vessel in so near the core increased the incident fast flux to such an extent that it became mandatory to change the pressure vessel material from carbon to stainless steel. The properties of stainless steel, however, increased the thermal stresses from gamma heating to such an extent that several inches of thermal shielding would have been necessary to reduce thermal stress to the desired value. Addition of thermal shields increased the diameter and weight of the pressure vessel - thermal shield combination. Therefore it proved advantageous to increase the diameter of the pressure vessel to 38" where the incident fast flux is tolerable on carbon steel, thus resulting in the reference design.

5.4.1 Method of Calculation

Two-group radial flux calculations gave the flux distributions shown in Fig. 5-6; the fast flux shown is distributed in energy between 0.4 ev and 10 Mev. The flux of interest, however, is that above 1 Mev since radiation damage to carbon steel is dependent upon the integrated flux above 1 Mev.

The method used to calculate the above -1- Mev flux is detailed in WAPD-45 (25). The basic equation is:

$$\phi_H(E) = \frac{\eta R_f}{N_H} \left[\frac{f(E)}{\sigma_H(E)} + \frac{1}{E\sigma_H(E)} \int_E^{\infty} f(E') dE' \right]$$

$\eta = 2.46$ neutrons per fission

R_f = fission rate, fissions/cm³-sec.

N_H = nuclear density of hydrogen, nuclei/cm³

$\sigma_H(E)$ = hydrogen scattering cross section, cm²/nucleus

$f(E)$ = fraction of fission neutrons born with energy E per unit energy interval

$\int_E^{\infty} f(E') dE'$ = fraction of fission neutrons born above energy E

The calculation above will overestimate the fraction of the total fast flux which is above 1 Mev since inelastic scattering with the heavy elements in the core is ignored.

After the above -1- Mev flux has been calculated in the core, it is still necessary to arrive at a corresponding flux on the pressure vessel. The Valpred code used to calculate the distribution of the fluxes is inadequate to investigate rigorously the effect of the thermal shield-water combination because of the two-group limitation. To assume that the spectrum

of the fast flux is the same on the pressure vessel as in the core would give an overestimate of the above -1- Mev flux because of the inelastic scattering in the steel thermal shields. Therefore an attempt has been made to estimate the effect of thermal shields and the inelastic scattering in the core on the above -1- Mev flux. It appears that a conservative estimate of these two effects would be:

- 1) Fast flux through a water reflector only has same spectrum as calculated core fast flux.
- 2) Through four inches of thermal shielding, the flux above 1 Mev is attenuated until it constitutes a fraction of the total fast flux equal to one-half its calculated fraction in the core.
- 3) Through two inches of thermal shielding, the flux above 1 Mev is attenuated until it constitutes a fraction of the total fast flux equal to three-fourths its calculated fraction in the core.

These estimates have been applied to the above -1- Mev fluxes of Table 5-1.

5.4.2 Comparison with APPR-1 and 1a

Table 5-1 contains calculated values of fast and above -1- Mev fluxes and "n v t" above 1 Mev for APPR-1, APPR-1a, and the Skid Mounted Reactor assuming a load factor of 100%.

Table 5-1

Flux and "n v t" above 1 Mev Incident on Pressure Vessel

| | $\phi_f (> 0.4 \text{ ev})$ | $\phi'_f (> 1 \text{ Mev})$ | $n \ v \ t$ |
|---|-----------------------------|-----------------------------|-----------------------|
| APPR-1 (20-yr. lifetime) | 3.8×10^{11} | 9.8×10^{10} | 6.2×10^{19} |
| APPR-1a (20-yr. lifetime) | 2.3×10^{12} | 4.1×10^{11} | 2.6×10^{20} |
| Skid Mounted (20-yr. lifetime) 25" Vessel | 3.54×10^{13} | 1.09×10^{13} | 6.86×10^{21} |
| 38" Vessel | 3.18×10^{12} | 7.4×10^{11} | 4.8×10^{20} |

5.5 Conclusions:

Power peaking will not be a problem in the Skid Mounted reactor. Radially, the presence of the thermal shield only an average of 1 2/3 inches from the core edge reduces the power peak at the edge of the core considerably from $1.47 \frac{P_{max.}}{P_{av.}}$ with an all water reflector to $0.95 \frac{P_{max.}}{P_{av.}}$.

In the axial direction the peaking will be lower than in the APPR-1 core because the rod bank controls less reactivity and is not inserted as deep. In the most adverse case (hot, clean, 0 MWYR), the APPR-1 five rod bank is inserted 15 inches while the Skid bank is inserted only 12 inches.

Thermal stress on the pressure vessel has been reduced to tolerable values by the addition of a thermal shield and increased diameter of the carbon steel pressure vessel.

6.0 SOURCE STRENGTH DETERMINATION

To insure a sufficient count rate on the BF_3 chamber during reactor start-up, a neutron source must be incorporated within the core area. Determination of the strength of such a source follows.

6.1 Correlation of APPR-1 Measurements With Theory

6.1.1 APPR-1 Measurements

Since the complete computation of required source strengths involves some rather complex theory, results of experimental measurements made on the APPR-1 will be incorporated wherever feasible. Source strength specification for the APPR-1 and experimental data are given below.

SOURCES

15 curie polonium - beryllium source (3.8×10^7 neutrons/sec. initial)

3" x 3" x 0.5" beryllium block as a photo-neutron source utilizing gamma rays from fission products

Measured Shutdown Count Rates, BF_3 Chamber

| Date Measured | Temp. | Megawatt Years Operation | Time After Shutdown | Count Rate |
|---------------|-------|--------------------------|---------------------|-----------------------|
| April 11, '57 | 68°F | 0 | 0 days | 7 counts per sec (17) |
| May 26, '58 | 112° | 6.15 | 5.08 | 4 counts per sec (22) |

6.1.2 Determination of Average Core Flux/Source Strength

One of the most difficult quantities to compute in predicting count rate due to a given source is average core flux/source strength. This quantity will be established for the APPR-1 by using the count rate measured during the early days of reactor operation. See page 130 of AP Note 59. (17)

Measured count rate = 7 cps
 Counter sensitivity = 4.5 cps/nv nv = thermal flux

$$\phi_{\text{eff}} / \phi_{\text{peak}} = 0.30 \quad \text{Figure I-21, APAE 17 (14)}$$

$$\phi_{\text{peak}} / \bar{\phi} = 3.6 \times 10^{-4} \quad \text{Figure I-21 APAE 17 (14)}$$

$$S = 3.8 \times 10^7 \text{ neutrons/sec.}$$

$$\text{Shutdown } k_{\text{eff}} = 0.93 \quad \text{initial excess reactivity - total rod worth}$$

where

S = neutron source strength

ϕ = average core flux due to source

ϕ_{peak} = value of flux peak in water gap preceding second shield ring.
BF₃ chamber is located in 2nd shield ring.

ϕ_{eff} = effective counter flux (an average around the counter tube
with attenuation due to steel tube taken into account)

$$\bar{\phi}/S = \frac{7}{(4.5) (.30) (3.6 \times 10^{-4}) (3.8 \times 10^7)}$$
$$= 3.79 \times 10^{-4} \text{ cm}^{-2}$$

This value will be used for APPR-1 type cores for a sub-initial k_{eff} of .93 and with the same ratio of thermal to fast core flux. For different values of k_{eff} the curve of Figure 6-1 will be utilized. The curve is based on a classified Westinghouse Reactor reactor but normalized to the preceding value of $\bar{\phi}/S$. The assumption is made that $\bar{\phi}/S$ is directly proportional to the ratio of thermal to fast core flux since $\bar{\phi}$ is taken as thermal flux. Hence, a corresponding correction should be employed for cores with a different thermal to fast flux ratio. For the skid mounted reactor this corrective ratio is 0.9. Figure 6-1 assumes this correction.

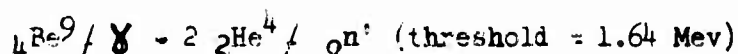
6.1.3 Correlation of photo-neutron source

The strength of the Po-Be source had fallen off more than a factor of ten when the count rate measurement of 4 cps was made on May 26, 1958. (See Figure J-25 APAE 17).⁽¹⁴⁾ Therefore, this measurement provided a good point of correlation for the beryllium block photo-neutron source. A prediction of this source strength and the resulting count rate was made. The factor necessary to force the predicted values of count rate into agreement with the measured 4 cps was retained as a correction factor to be used for count rate prediction on the Skid Mounted reactor.

The calculational procedure was based upon that used for the APPR-1a as given in APAE 17,⁽¹⁴⁾ page 47. More recent data was used where appropriate and simplifications made where possible.

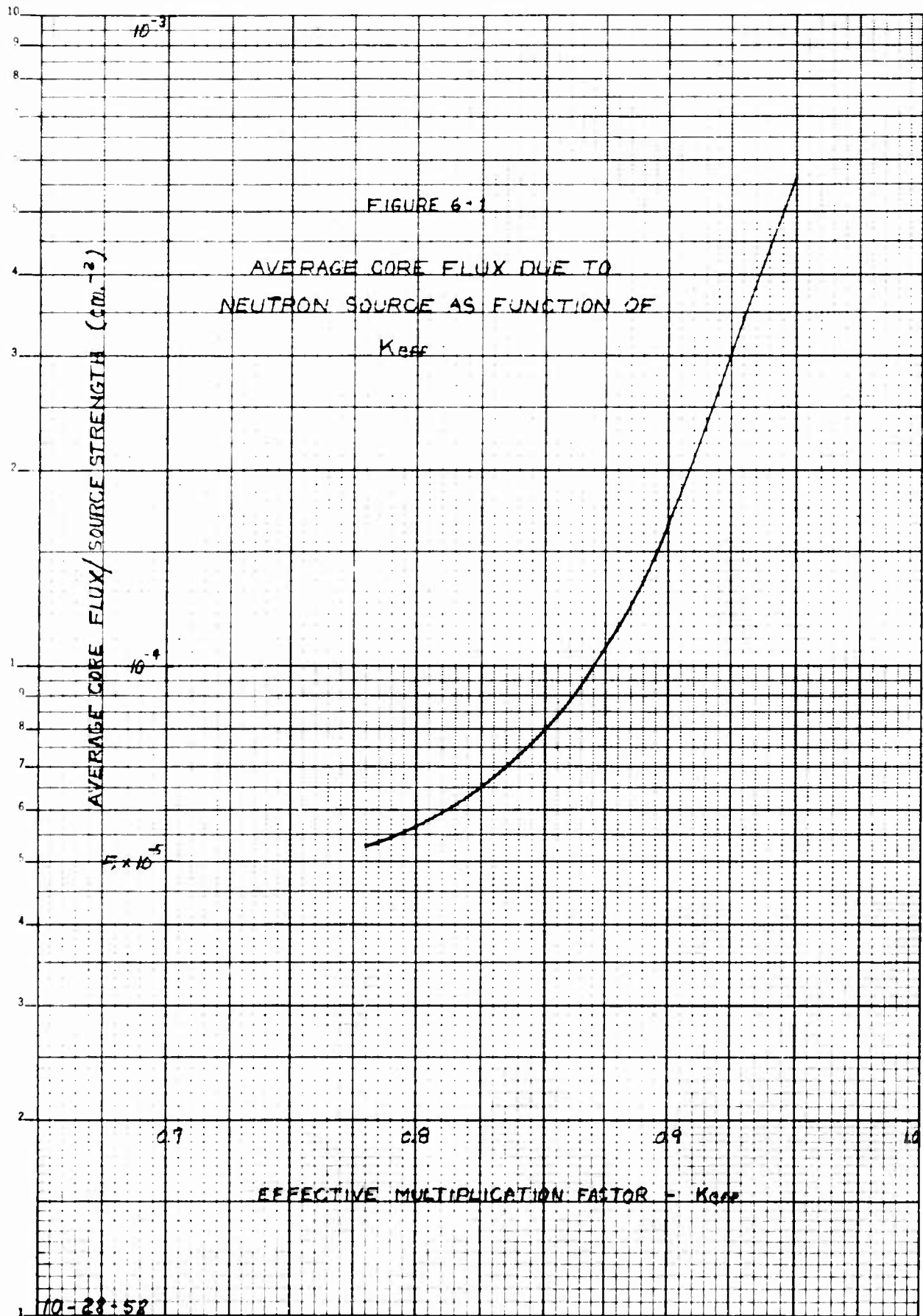
Photo-neutron source strength computation corresponding to the measured point follow.

The neutron source arises from the following reaction.



Source of the gamma ray are fission products. Hence, a gamma source strength of energy greater than 1.64 Mev must be established. Then the resulting gamma flux on the beryllium block attached to the side of the core determined. The resulting (γ, n) reaction rate immediately establishes the strength of the neutron source.

Gamma source strengths were based on gamma spectrum data from NDA-27-39.⁽¹⁹⁾ Establishment of the resulting gamma flux at the beryllium block was based on shielding methods given in TID 7004⁽²⁰⁾ for a cylindrical



source. Total gamma attenuation coefficients were also obtained from this reference. The microscopic beryllium (γ, n) cross section as a function of energy is given in Figure 6-2*.

Reference to the above sources of information reveals the following facts. Approximately 95 percent of the (γ, n) reaction is due to the 2.5 Mev gamma of La^{140} . For the other gammas of interest the attenuation coefficient differs little from that appropriate for the 2.5 Mev gamma. Therefore, gammas other than those of energy 2.5 Mev were weighted only with the Be cross section. Hence, only one shielding calculation is necessary. Further, gammas other than the 2.5 Mev of La^{140} can be considered as one gamma of energy 2 Mev with a yield equal to that of the total given in NDA-27-39 for Group V (1.8-2.3 Mev). Computations were based on yields given for 1000 hours and infinite operation at 10 megawatts (MW) and after one and ten days shut-down periods. The yield from La^{140} was taken as the total of Group VI (2.2-2.6 Mev).

| | Gamma Yield (S_γ) | | | |
|--------------------|----------------------------|----------------------|---|--|
| | Energy Group Mev | Energy Per Gamma Mev | 1 day shutdown photons-cm ² /sec | 10 day shutdown photons-cm ² /sec |
| 1000 hr operation | 2.2-2.6 | 2.5 | 2.64×10^{-13} | 1.80×10^{-13} |
| | 1.8-2.2 | 2 | 5.94×10^{-14} | 8.3×10^{-15} |
| | Total | | 3.23×10^{-13} | 1.88×10^{-13} |
| | Error due to grouping | | -11% | -1.1% |
| infinite operation | 2.2-2.6 | 2.5 | 3.24×10^{-13} | 2.04×10^{-13} |
| | 1.8-2.2 | 2 | 7.30×10^{-14} | 2.07×10^{-14} |
| | Total | | 3.97×10^{-13} | 2.25×10^{-13} |
| | Error due to grouping | | 0.65% | 3.7% |

Gamma Flux

The beryllium block was considered a field point located midway on the side of a finite cylinder equivalent to the core. The quantity ϕ_γ/S_γ at the beryllium block was computed from the shielding formula found in TID 7004 (20)

ϕ_γ = gamma flux

S_γ = gamma source strength per unit volume (gamma yield ÷ core volume; core volume = 1.395×10^5 cm.³)

* It will be noted that the gamma spectrum data and beryllium cross section used here are from different sources than that used in APAE 17. Those used here are felt to be more accurate.

One attenuation coefficient was used for a core consisting of 80% water, 19.6% iron, and 0.4% uranium. The total attenuation coefficient for an energy of 2.5 Mev was chosen. No build-up factor was used since scattering below the threshold energy of 1.64 Mev is effectively a removal.* (average attenuation coefficient = 0.0945 cm^{-1})

$$\bar{\phi}_v/S_v = 4.14 \quad \text{core radius} = 28.19 \text{ cm.}$$

The expression for the resulting neutron source strength follows.

$$S = \bar{\phi}_v \Sigma_{\text{BeN}} \text{Be} \nu_{\text{Be}} \quad \begin{array}{l} N_{\text{Be}} = \text{number density} \\ = .1236 \times 10^{24} \text{ nuclei/cm.}^3 \\ \nu_{\text{Be}} = \text{volume beryllium} \\ = 73.6 \text{ cm.}^3 \end{array}$$

Source strengths for 1000 hour and infinite operation times after one and ten day shutdown periods were readily obtainable with the use of the corresponding gamma yields. To obtain the source strength for operating times corresponding to 6.15 megawatt years and 5.08 day shutdown (needed to correlate measured count rate), linear interpolation between the above points was employed.** The result follows:

$$S = 7.4 \times 10^7 \text{ neutron/sec.}$$

Computation of the resulting count rate utilizes much of the same data used with the Po-Be source. However, the value $\bar{\phi}/S$ must be corrected for core burnout for 6.15 megawatt years of operation.

$$\Delta k_{\text{eff}} = -0.023 \text{ estimated from rod bank measurements}$$

Reference to Figure 6-1 gives the following corresponding correction factor.

$$\text{burnup correction} = .557$$

Therefore,
$$\bar{\phi}/S = (.557) (3.79 \times 10^{-4})$$

$$= 2.11 \times 10^{-4} \text{ cm}^{-2}$$

$$\text{count rate} = S \times \frac{\bar{\phi}}{S} \times \frac{\phi_{\text{peak}}}{\bar{\phi}} \times \frac{\phi_{\text{eff}}}{\phi_{\text{peak}}} \times \text{counter sensitivity}^{***}$$

* Difference in results obtained with this one cylinder method is only 10% from that obtained by use of the three cylinder method suggested in APAE 17.

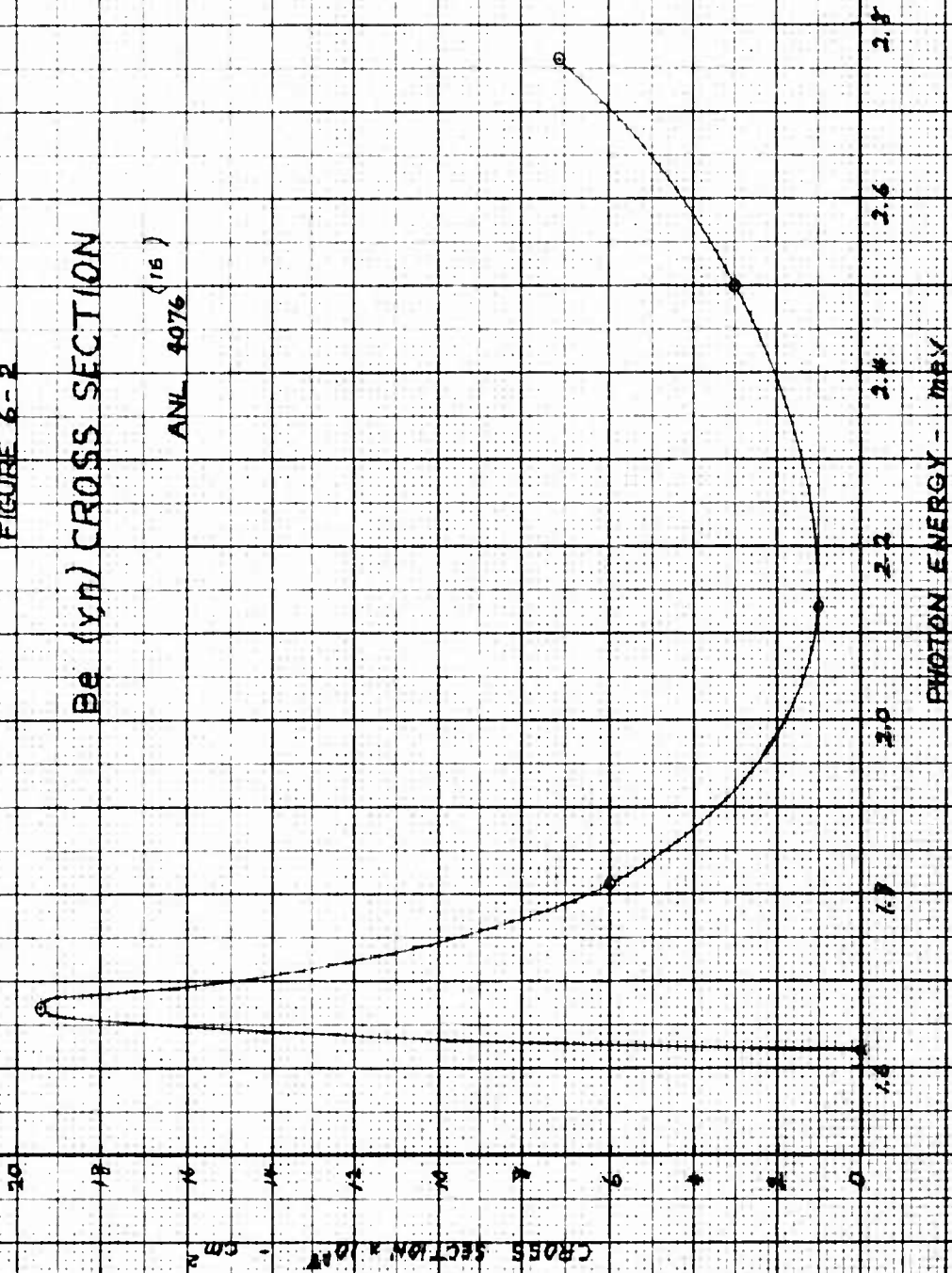
** Infinite operation was considered to be 10,000 hrs. Operation was assumed to be continuous at 10 Mw.

*** The values $\phi_{\text{peak}}/\bar{\phi}$ and $\phi_{\text{eff}}/\phi_{\text{peak}}$ used here differ from those employed in connection with the Po-Be source. The reason is due to the fact that boron was added to the shield water before the second count rate was measured. Flux distribution from which these values were obtained can be found in Figures 1.2 and 1.3 of APAE 35. (15)

FIGURE 6-2

Be (γn) CROSS SECTION

ANL 4976 (15)



9-38-57

$$= (7.4 \times 10^7) (2.11 \times 10^{-4}) (2.09 \times 10^{-4}) (.32) \\ \times (4.5)$$

$$\text{Count Rate} = 4.69 \text{ cps}$$

Measured value is 4 cps. Therefore, correction factor is

$$C = \frac{4}{4.69}$$

$$C = .85$$

6.2 Neutron start-up source strength - Skid Mounted Reactor

Count rates were computed for given neutron sources and were found to be sufficient. Hence, these sources are specified for the 10 Mw Skid Mounted Reactor. Initial source estimates were based on those used in the APPR-1 and the resulting count rates.

6.2.1 Polonium-beryllium source

Prediction of count rate due to a given polonium-beryllium source follows. The method employed follows directly from Section 6.1.

1. A 15 curie polonium-beryllium source was chosen. Corresponding neutron strength is

$$S = 3.8 \times 10^7 \text{ neutrons/sec. p. 41, APAE 17} \quad (14)$$

2. Shutdown initial k_{eff} was estimated to be 0.93 from rod worth and excess reactivity values.

$$\bar{\phi}/S = 3.41 \times 10^{-4} \text{ cm.}^{-2} \quad \text{Figure 6-1}$$

3. $\bar{\phi} = \bar{\phi}/S \times S$
 $\bar{\phi} = (3.41 \times 10^{-4}) (3.8 \times 10^7)$
 $\bar{\phi} = 1.295 \times 10^4 \text{ n/cm}^2\text{-sec}$
4. $\phi_{\text{eff}}/\bar{\phi} = 5.55 \times 10^{-4}$ (Includes transmission factor of) Fig.6-3
 (.88 through steel tube enclosing counter)
5. $\phi_{\text{eff}} = \phi_{\text{eff}}/\bar{\phi} \times \bar{\phi}$
 $= (5.55 \times 10^{-4}) (1.295 \times 10^4)$
 $= 7.2 \text{ neutrons/cm}^2\text{-sec}$ effective shutdown BF_3
 counter flux
6. counter sensitivity = 4.5 cps/nv typical value
7. count rate = $\phi_{\text{eff}} \times$ (counter sensitivity)
 $= (7.2) (4.5)$
 count rate = 32 cps

6.2.2 Photo-neutron source

Prediction of count rate due to a beryllium - fission product gamma photo-neutron source follows. The method employed follows directly from Section 6.1.

1. The source consists of a 0.5" x 3" x 12" beryllium block bombarded by fission product gammas.
2. Source strength calculations were based on 1000 hours of operation at 10 megawatts ten days after shut-down.
3. $S_{\gamma}^{Be} = 1.88 \times 10^{-13}$ photons-cm²/sec Section 6.1
4. $\phi_{\gamma}/S_{\gamma} = 4.17$ method of TID 7004(20)
 $S_{\gamma} = S_{\gamma}/\text{core volume}$ core volume = 1.15×10^5 cm.³
core radius = 25.6 cm.
assumed core composition = 80% H₂O;
19.6% Fe;
0.4% U
average attenuation
coefficient = 0.0945 cm.⁻¹
5. $S = \phi_{\gamma} S_{\gamma}^{Be} N^{Be} v^{Be} \times \text{correction factor}$ correction factor = .85
 $= 1.58 \times 10^8$ neutrons/sec $N^{Be} = 0.1236 \times 10^{24}$
 $v^{Be} = 220$ cm.³
This value
assumes effective volume
to be 0.75 actual volume.
6. $\bar{\phi}/S = 3.32 \times 10^{-4}$ cm.⁻² Figure 6-1
Assumes $\Delta k_{eff} = 0.02$ based on 1.14 mega-
watt year operation for APPR-1, See Fig-
ure 3E Progress Report No. 6.(18)
7. $\phi_{eff}/\bar{\phi} = 5.55 \times 10^{-4}$ Figure 6-3
Value includes transmission factor of 0.88
through steel tube enclosing counter.
8. Counter sensitivity = 4.5 cps/nv
9. Count rate = $S \times \frac{\bar{\phi}}{S} \times \frac{\phi_{eff}}{\bar{\phi}}$ x counter sensitivity
 $= (1.58 \times 10^8) (3.32 \times 10^{-4}) (5.55 \times 10^{-4}) (4.5)$
 $= 131$ counts per second

10. If the reactor remains shut-down for 92 days, the count will drop to approximately 2 cps. This value is based on the decay of the 2.2-2.6 Mev gamma group as given in NDA-27-39. (19)

11. Count rate at the end of core life was estimated as follows.

Infinite operation at 10 megawatts and ten day shut-down is assumed. The value of step 9 was corrected for this longer operation time and for the change in shut-down k_{eff} .

operation time correction = 1.13 reference (19)

correction due to k_{eff} = 0.29 Based on Figure 6-1

assuming k_{eff} = 0.062.
See reference (18).

count rate = (131) (1.13) (.29)

= 43 cps

6.2.3 Conclusion

The following start-up neutron sources should be incorporated in the 10 Mw Skid-Mounted Core.

15 curie Po-Be source

0.5" x 3" x 12" beryllium block

The resulting count rate at shut-down will be quite adequate for start-up for any reasonable operational program during the lifetime of the core. Sufficient margin is allowed in the event there is considerable delay in transporting the Po-Be source due to the unique geographical location of the reactor.

7.0 Analysis of Spent Fuel Pit Criticality

Calculations were performed to show that the reactivity of the spent fuel pit will at no time exceed 0.70

The calculated method chosen was that of modified two group theory. The expression for reactivity follows:

$$K = \frac{\eta f p}{(1 / B^2)(1 / L^2 L^2)} + \frac{\eta_r f_r (1 - p)}{(1 / B^2 \tau)}$$

- K = total reactivity
- η = neutrons per fuel absorption (thermal)
- f = thermal utilization
- η_r = neutrons per fuel absorption (resonance)
- f_r = resonance utilization
- B^2 = buckling
- τ = age to thermal
- L = thermal diffusion length
- p = resonance escape probability

The fuel elements are to be stored within a 1% boron steel lattice 1/4" thick immersed in water * To insure a conservative result the following assumptions were made:

1. Only fresh fuel elements are stored (no control rod elements).
2. Lattice is filled to capacity, including the space taken up by the hopper.
3. Self-shielding factor of one is used for the fuel element.
4. There is no thermal leakage. $(\frac{1}{10B^2L^2} = 1)$

Thermal constants were computed for a homogenized core but utilized a self-shielding factor for the boron steel absorption. This self-shielding factor was computed by the P₃ Code for slab geometry. Fast constants were computed by the Muft III Code, utilizing homogenized number densities. The final results follow:

- * Boron steel containing one percent boron possesses good mechanical properties and is readily available. Hence, this boron concentration was chosen, and the necessary total boron content of the pit adjusted by controlling the lattice thickness. The resulting 1/4" value is quite compatible with mechanical considerations.

Thermal contribution = .500
 Fast contribution = .144
 K = .644

7.1 Computational Model

Detailed steps of the computation are given below:

Diameter of spent fuel pit: $2R = 32$ in.
 $R = 40.6$ cm

Volume fractions:

fuel element $f^f = .526$
 1% boron steel lattice $f^b = .117$
 water gaps (exterior to fuel element) $f^w = .357$
 $\underline{1.000}$

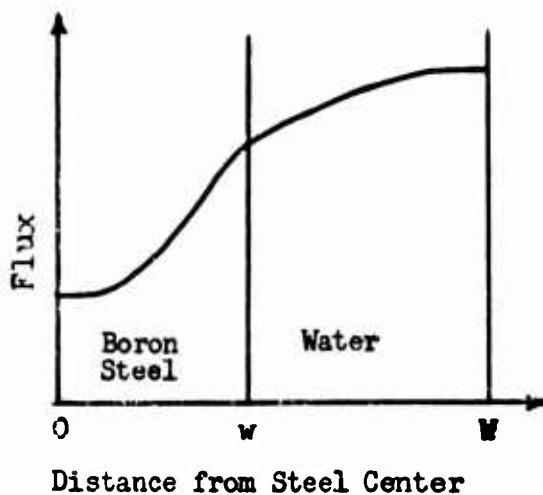
Thermal Contribution

Absorption cross sections:

fuel element $\Sigma^f = .3914$ cm⁻¹
 U^{235} $\Sigma^{25} = .302$
 1% boron steel $\Sigma^b = 3.58$
 water $\Sigma^w = .0221$

Self-shielding factor boron steel:

The P_3 approximation was used for slab geometry to determine a self-shielding factor for the boron steel absorption. The geometry incorporated is pictured below:



$$w = .318 \text{ cm (1/8")}$$

$$W-w = .320 \text{ cm}$$

W was taken where flux peak was thought to occur.

$$\Sigma^b = 3.58 \text{ cm}^{-1}$$

$$\Sigma_s^b = 0.918 \text{ cm}^{-1} \text{ boron steel scattering cross section}$$

$$1-\mu_0 = 0.988 \quad 1 - \text{average cosine of scattering angle, boron steel}$$

$$\Sigma^w = 0.0221 \text{ cm}^{-1}$$

$$\Sigma_s^w = 3.0 \text{ cm}^{-1} \quad \text{H}_2\text{O scattering cross section (based on measured diffusion length)}$$

$$1-\mu_c^w = .676 \quad 1 - \text{average cosine of scattering angle, H}_2\text{O}$$

Self-shielding factor was taken to be the value at the water-steel interface divided by the average flux in the steel. This self-shielding factor was found to be:

$$S = .40$$

Thermal utilization follows:

$$f = \frac{f^f \Sigma^{25}}{f^f \Sigma^f / S + f^b \Sigma^b / f^w \Sigma^w}$$

$$= \frac{(.526) (.302)}{(.526) (.391) + (.40) (.117) (3.58) + (.357) (.0221)}$$

$$= .418$$

$$\eta = 2.077$$

$$f = .870$$

Fast Contribution

Homogenized number densities corresponding to the core and volume fractions listed earlier were used as input for the Muft III Code. The resulting fast group constants appear below:

$$\gamma = 31.1 \quad \eta_a f_r = \frac{\nu \Sigma_f}{\Sigma_a} \quad p = .67$$

$$= 0.51$$

Axial buckling was taken to be that of the core. (Table 2-1)

$$B_z^2 = .00191$$

Geometric buckling is used in the radial direction.

$$\begin{aligned}
 B_r^2 &= \left(\frac{j_0}{R}\right)^2 \\
 &= \left(\frac{2.405}{40.6}\right)^2 \\
 &= .00352
 \end{aligned}$$

Total buckling

$$\begin{aligned}
 B^2 &= B_z^2 + B_r^2 \\
 &= .00543
 \end{aligned}$$

Fast leakage

$$\begin{aligned}
 L_f &= \frac{1}{1 + B^2 \tau} \\
 &= \frac{1}{1 + (.00543)(31.1)} = .856 \\
 &\quad \text{Total Reactivity}
 \end{aligned}$$

The expression for total reactivity follows. Recall that the thermal non-leakage factor is taken as unity.

$$\begin{aligned}
 K &= \frac{\eta f p}{1 + B^2 \tau} + \frac{\eta_n f_n (1-p)}{1 + B^2 \tau} \\
 &= (.870)(.67)(.856) + (.51)(.33)(.856) \\
 &= .500 + .144 \\
 &= .644
 \end{aligned}$$

7.2 Comparison with ZPE

This low value of reactivity is compatible with ZPE experiments. It will be noted on p. 50 of APAE-21 (21) that the value of B-10 mass per fuel element required for criticality is .775 gm per fuel element. The 1% boron steel lattice used in the Skid Mounted spent fuel pit results in a value of 9 gm per fuel element for lattice height equal to that of the active element.

7.3 Conclusion

To insure sub-criticality of the spent fuel pit, the stored fuel elements should be placed in individual cells of a lattice possessing the following characteristics:

1. Minimum height of lattice is equal that of the active fuel element height with element in stored position.
2. Lattice material consists of 1% boron steel in 1/4" plates.
3. Center-to-center dimension of an individual cell is 3.5".
4. For shielding and cooling purposes the entire pit is filled with water.

The reactivity of such a spent fuel pit loaded to maximum capacity (52 elements)* with fresh APPR-1 type elements will not exceed 0.70 and hence pose no criticality problem.

7.4 Relocation Effect

To facilitate a more feasible operating program and to reduce shielding requirements, the spent fuel pit has been relocated outside the vapor container. Though the design capacity has been increased to 49 fuel elements (7 x 7 array), the radius of the equivalent cylinder is smaller than that designated in the foregoing criticality calculation. Therefore, the corresponding value of effective multiplication will be lower, and the conclusions concerning criticality given in Section 7.3 remain valid.

* Design capacity is 46 elements. Conceivably, however, six additional elements could inadvertently be fitted into the space allowed for the loading hopper.

NOMENCLATURE

| | |
|-------------------------------|---|
| B | Fraction burnout |
| $B^2 \text{ Cm}^{-2}$ | Buckling |
| $D_f \text{ Cm}$ | Fast diffusion coefficient |
| $D_{th} \text{ Cm}$ | Thermal diffusion coefficient |
| g' | Thermal shielding factor |
| K_f | Fast multiplication factor |
| K_{th} | Thermal multiplication factor |
| K_{eff} | Effective multiplication factor of core |
| $L \text{ Cm}$ | Diffusion length |
| $N^{25} \text{ atoms/cm}^3$ | U-235 atom concentration |
| $N^{B-10} \text{ atoms/cm}^3$ | Boron 10 atom concentration |
| P | Resonance escape probability |
| P MW | Reactor power |
| S_r | Radial reflector savings |
| S_z | Axial reflector savings |
| t Sec | Time |
| V Cm^3 | Core volume |
| α | Xenon non-uniform factor |
| α_f | Fast U-235 capture to fission ratio |
| α_{th} | Thermal U-235 capture to fission ratio |
| β | Fraction thermal fissions |
| γ_1 | Iodine fraction fission yield |
| ∇^2 | La placian Operator |
| γ_2 | Xenon fraction fission yield |
| $\lambda_1 \text{ sec}^{-1}$ | Iodine decay constant |
| $\lambda_2 \text{ sec}^{-1}$ | Xenon decay constant |

| | | |
|--------------------------|----------------------------|---|
| $\nu \Sigma_{th}^f$ | neuts/cm | Neutrons per fission times thermal macroscopic fission cross section |
| ρ | | Percent reactivity $\frac{K_{eff}-1}{K_{eff}}$ |
| σ_{th}^{a-B} | cm ² | Boron-10 thermal absorption cross section |
| σ_f^{a-B} | cm ² | Boron-10 fast absorption cross section |
| σ_{th}^a | cm ² | U-235 thermal absorption cross section |
| σ_f^a | cm ² | U-235 fast absorption cross section |
| σ_{th}^f | cm ² | U-235 thermal fission cross section |
| σ_{fa}^f | cm ² | U-235 fast fission cross section |
| σ_{xe} | cm ² | Xenon thermal absorption cross section |
| Σ_{th}^a | cm ⁻¹ | Macroscopic thermal absorption cross section |
| Σ_{xe}^a | cm ⁻¹ | Macroscopic xenon absorption cross section |
| Σ^p | cm ⁻¹ | Rod bank equivalent poison cross section |
| Σ_a^{sub} | cm ⁻¹ | Cross section representing effect of substituting 5 control rod elements for 5 fixed elements |
| Σ^s | | Macroscopic scattering cross section |
| Σ^{tr} | | Macroscopic transport cross section |
| Σ^r | | Macroscopic removal (slowing down) cross section |
| τ | cm ² | Fermi age |
| ϕ_{th} | neuts/cm ² -sec | Thermal flux |
| ϕ_f | neuts/cm ² -sec | Fast flux |
| $\bar{\phi}_{real}^{th}$ | neuts/cm ² -sec | Real average thermal flux in core |
| $\bar{\phi}_{region}$ | | Average region flux from Valprod or Windowshade |
| $\bar{\phi}_{core}$ | | Average core flux from Valprod or Windowshade |

REFERENCES

- (1) G.J. Habetler "One Space Dimensional Multigroup for the IBM-650, Part I, Equations", KAPL -1415, December, 1955
- (2) P.V. Oby, "Modified Two-Group Multiregion Calculation using the Valprod Code for the IBM-650", APAE Note 24 (Revised) Aug. 14, 1957.
- (3) F.B. Fairbanks, "Two Group Multiregion Axial Windowshade Calculations on the IBM-650", APAE Memo 88, March 29, 1957.
- (4) S.S. Rosen, "Supplement to MUFT III Code Multiregion Fourier Transform Calculation," AP Note 90, Dec. 6, 1957.
- (5) B.J. Byrne, R.L. Caton, "Two Dimensional P_3 Calculation for APPR Type Fixed Fuel Elements", AP Note 96, February 14, 1958.
- (6) B.J. Byrne, P.V. Oby, "Analysis of Extended Zero Power Experiments on the Army Package Power Reactor ZPE-2," APAE 27, May 7, 1958.
- (7) T.G. Williamson, M.J. Leibson, B.J. Byrne, "Reactor Analysis APPR-1 Core II," APAE-32, July 15, 1958.
- (8) P.V. Oby, "Scram I: Control Rod Worth Calculation on the IBM 650," APAE Memo 89, April 16, 1957.
- (9) S.D. MacKay, H.W. Geisler, J.W. Noaks, "Extended Zero Power Experiments on the Army Package Power Reactor ZPE-2," APAE-21, Nov. 15, 1957.
- (10) J.W. Noaks, W.R. Johnson, "Army Package Power Reactor Zero Power Experiments ZPE-1," APAE 8, Feb. 8, 1957.
- (11) S.D. MacKay, "Progress report No. 6, Task Number VII Contract No. AT (30-3)-326", Aug. 21 to Sept. 20, 1958.
- (12) T.G. Williamson, "APPR-1 Burnout Calculations", APAE Memo 126, April 10, 1958.
- (13) S.D. MacKay, "Progress Report No. 5, Task Number VII, Contract No. AT (30-3)-326 July 21 to Aug. 20, 1958.
- (14) "Phase III Report Army Package Power Reactor Field Unit No. 1 APPR-1a Design Analysis, Volume 1" APAE 17, May 15, 1957
- (15) S.S. Rosen, et al, "APPR-1 Research and Development Program Shielding Experiments and Analysis Task No. VI", APAE 35, Oct. 15, 1958
- (16) "Experimental Nuclear Physics Div. and Theoretical Nuclear Physics Div. Report for July, Aug. and Sept. 1947" Argonne National Lab. 47, ANL-4076.
- (17) J. Meem, et al, APPR-1 "Operating Log, Feb. 28 to Apr. 23, 1957" AP Note 59

- (18) S.D. MacKay and D.C. Tubbs, Task No. VII, Program Report No. 6, Aug. 21, to Sept. 20, 1958.
- (19) F.J. Clark "Decay of Fission Product Gammas", NDA-27-39, Dec. 30, 1954.
- (20) Theodore Rockwell III, "Reactor Shielding Design Manual", TID-7004, March, 1956.
- (21) J.W. Noaks, et al, Extended Zero Power Experiments on the Army Package Power Reactor ZPE-2, APAE 21, Nov. 15, 1957.
- (22) S.D. Mackay, Task No. VII, Progress Report No. 4, June 21 to July 20.
- (23) Tau and Beecher "Thermodynamic Properties of Compressed Water"
- (24) S.D. MacKay, "Progress report No. 1, Task Number VII".
- (25) F.C. Brooks and H.L. Glick, "The Fast Neutron Flux Spectrum of a Proton Moderated Thermal Reactor", WAPD-45, November, 1951.

II SHIELDING DESIGN ANALYSIS

1.0 Contract Design Requirements

Shielding design requirements for the Skid Mounted Reactor ice cap installation are:

1. Shielding must be adequate to permit access to the primary skid 8.0 hours after shutdown.

2. Shielding must be adequate to permit operating personnel working an 84-hour week to conform to government established radiation tolerance standards which allow an average integrated total body dose of 300 millirem per week (mr/wk). A maximum permissible integrated total body exposure of 3 rem may be received in a period of any short duration within a thirteen consecutive week period and annual exposure may not exceed 5 Rem/year.

3. Shielding must be adequate to permit personnel to perform routine maintenance such as leveling, snow removal, etc., around the vapor container after shutdown.

1.1 Design Dose Rates at Various Locations and Operating Conditions

Table 1.0 indicates the maximum permissible design dose rates at selected important locations for both shutdown and operating conditions and includes calculated dose rates at these locations. The site layout is shown in Dwg. M02M11. Conservative calculational procedures would make the actual operating dose rates appreciably less than design values.

During normal operation, personnel at the control console and turbine-generator skids should not receive more than 0.1 times tolerance. (Dose rates at other skids will be smaller since they are farther from the vapor container.) As used here, tolerance refers to a dose rate of 1 mr/hr, which gives a dose of 84 mr in an 84-hour week. This low value of 0.1 tolerance allows a margin for performing short time maintenance operations in high level radiation areas. In addition, this procedure is consistent with that outlined in APAE 78, Revision II (1) for uncontrolled areas.

Since operating personnel will approach the feed water and heat exchanger skid only intermittently, design dose rate has been set at 1.5 mr/hr. The demineralizer is the chief source of radiation at this skid.

The primary shield has been designed to give the maximum permissible design rate of 50 mr/hr at the primary skid (see Table 1.0) at 8.0 hours after shutdown for infinite operation at 10 Mw. Again, conservative calculational procedures would make the actual dose rates somewhat less than calculated values.

Primary shielding has been designed to give the maximum permissible design rate of 80 mr/hr at the worst point outside the vapor container on the side of the reactor away from the steam generator. This is comparable to the dose rate experienced in the vapor container 2.5 hours after shutdown.

Design dose rates have not been established for the area on the surface of the ice cap. Dose rates have been calculated in this area and access must be restricted, possibly by fences.

Table 1-0

Radiation Dose Rate from Skid Mounted Reactor

(Ice Cap Installation)

| | Design Specification mr/hr | Calculated mr/hr |
|---|-------------------------------|---------------------|
| 1. Normal Operation | | |
| 1.1 Control Console Skid | 0.1 | 0.050 |
| 1.2 Turbine Generator Skid | 0.1 | 0.086 |
| 1.3 Feed Water and Heat Exchanger Skid | 1.5 | 1.5 |
| 2. Equipment Maintenance after Reactor Shutdown | | |
| 2.1 Dose rate on surface of primary shield tank | | |
| Time after Shutdown - Hours | | |
| 2.5 | 50 | 50 |
| 12 | --- | 23.5 |
| 24 | --- | 16 |
| 2.2 Dose rate between vapor container and snow wall (worst point) | | |
| Time after Shutdown - Hours | | |
| 2.5 (core in pressure vessel) | 80 | 80 |

1.2 General Design Principles

During the reactor operation, activation of the primary coolant results in all parts of the primary system becoming severe gamma sources. This radiation has a 7.4 sec half life. After shutdown this source decays rapidly and the activity drops to a level at which no shielding is required for this

radiation, even to work near the primary system. Consequently, considerable shielding of the primary system is necessary only during reactor operation. This shielding is accomplished by the packed snow which separates the vapor container from the manned stations of the ice cap installation.

The reactor requires a considerably greater amount of radiation attenuation during operation than the primary coolant. With the reactor shut down, the radiation level is greatly reduced, but considerable shielding is still needed to protect personnel working in the vapor container from accumulated fission product activity in the core. These two functions are accomplished by the primary shield surrounding the reactor vessel.

The shielding available in the primary shield is described in Table 1-1.

Since the Skid Mounted Reactor must be air transportable the primary shielding design principle is that the shielding weight on the primary skid must be kept to an absolute minimum. This principle dictates that the pressure vessel be of the minimum possible diameter which will survive radiation damage and thermal stresses. All shield rings must also be of a minimum diameter to give a shield tank of minimum weight.

Since snow will replace secondary shielding in the ice cap installation it is not necessary to attempt optimization of primary and secondary shielding. Therefore the primary shield has been designed simply to meet the requirement of access to the primary skid and sides of the vapor container after shutdown.

Table 1-1

Description of Primary Shield - Radial

| Description | Material | Outer Radius Inches | Thickness Inches |
|---------------------------|-------------------|------------------------|---------------------|
| Core | - | 10.08* | - |
| Reflector | Primary Water | 11.76 | 1.68 |
| Thermal Shield | Stainless Steel | 13.76 | 2.00 |
| Cooling Passage | Primary Water | 18.88 | 5.12 |
| Pressure Vessel Cladding | Stainless Steel | 19.00 | 0.12 |
| Pressure Vessel | Carbon Steel | 21.38 | 2.38 |
| Insulation | (Considered Void) | 23.38 | 2.00 |
| Insulation Retainer | Steel | 23.50 | 0.12 |
| Clearance | Void | 24.05 | 0.55 |
| Pressure Vessel | | | |
| Support Ring | Steel | 25.05 | 1.00 |
| P.V Support Ring Cladding | Boral | 25.175 | 0.125 |
| Cooling Passage | Shield Water | 26.425 | 1.25 |
| Shield Ring Cladding | Boral | 26.550 | 0.125 |
| 1st Shield Ring | Steel | 29.800 | 3.25 |
| Shield Ring Cladding | Boral | 29.925 | 0.125 |
| Cooling Passage | Shield Water | 31.175 | 1.25 |
| Shield Ring Cladding | Boral | 31.300 | 0.125 |
| 2nd Shield Ring | Steel | 34.550 | 3.25 |
| Shield Ring Cladding | Boral | 34.675 | 0.125 |
| Cooling Passage | Shield Water | 35.925 | 1.25 |
| Shield Ring Cladding | Boral | 36.050 | 0.125 |
| 3rd Shield Ring | Steel | 39.300 | 3.25 |
| Shield Ring Cladding | Boral | 39.425 | 0.125 |
| Cooling Passage | Shield Water | 40.675 | 1.25 |
| Shield Ring Cladding | Boral | 40.800 | 0.125 |
| 4th Shield Ring | Steel | 44.050 | 3.25 |
| Shield Ring Cladding | Boral | 44.175 | 0.125 |
| Neutron Shield | Shield Water | 51.000 | 6.825 |
| Tank Wall Cladding | Boral | 51.125 | 0.125 |
| Tank Wall | Steel | 51.500 | 0.375 |

* Equivalent radius based on actual core cross-section.

2.0 PRIMARY SHIELD ANALYSIS

The basic purpose of the primary shield is to attenuate neutron and gamma radiation escaping from the core to acceptable dose rate levels. However, the primary shield itself becomes activated due to capture of neutrons escaping from the core and therefore becomes a source of gamma radiation. The problem then becomes that of achieving the required attenuation of core radiation with the minimum amount of shielding activation. Shield activation may be minimized by judicious choice and spatial arrangement of shielding materials.

The primary shield analysis was completed using the shielding codes developed at Alco. Dose rates from these shielding codes have been checked against experimental measurements in the APPR-1 and calculated dose rates have been found to be consistently higher than those measured (see Ref. 2). In addition a hand calculation of the dose rate from the core after shutdown on the surface of the shield tank for the skid mounted configuration was made to check the machine output.

2.1 Configurations Considered

The basic configuration considered for the primary shielding is similar to that of APPR-1 in that it is made up of concentric annuli of water and steel. However, in the Skid Mounted shield the steel rings are clad on both sides with Boral to reduce activation by thermal neutron capture.

Since most of the dose after shutdown comes from the core, thermal shield and pressure vessel the dose is quite insensitive to the arrangement of the steel rings in the shield tank, that is, the calculated dose rate is a function only of the total steel thickness in the shield tank. Therefore, the arrangement of the shield rings in the tank was dictated by weight and mechanical rather than shielding considerations.

2.2 Reference Configuration

The reference configuration is shown in Dwg. No. R9-46-1039 of Section A and described in Table 1-1. There are four 3-1/4-inch steel rings sandwiched between 1/8-inch Boral sheets in the shield. The Boral-steel sandwiches are separated by 1-1/4 inches of water. The inner surface of the outer tank wall and the outer surface of the pressure vessel support ring are also clad with Boral. During the plant lifetime of 20 years, the maximum burnup in the Boral sheets will be about 0.5% based on the total number of original atoms.

2.3 Shutdown Dose Calculation

After shutdown significant contributions to the dose rate in the vapor container are made by:

1. Fission products and activated steel in core.
2. Activated steel in the primary shield.
3. Activated components around the primary shield.
4. Activated corrosion products in primary coolant.

Of the above four sources, only the first two lend themselves to fairly rigorous theoretical analysis. For the last two sources use must be made of data accumulated during APPR-1 operation.

2.3.1 Computational Model

2.3.1.1 Core Source and Attenuation

The core was considered a volumetric source uniformly distributed in the form of a cylinder. The well known equation for calculation of the dose rate from such a source was taken from the "Reactor Shielding Design Manual" (3) and for a point opposite the core midpoint is:

$$\text{Eq. 2.2} \quad D = \frac{BS_v R_o^2}{2(a \sqrt{s})} F(\theta, b_2) \times \frac{1}{K_D}$$

K_D = factor for converting from flux to dose

Other symbols defined in TID 7004 (3)

Fission product decay gammas are usually divided into seven energy groups. Data on the seven groups are available in "Decay of Fission Product Gammas" (4) and "Fission Product Decay Gamma Energy Spectrum" (5). Volumetric source strengths for the seven groups taken from Ref. 4 are listed in Table 2-1.

Activation gammas from stainless steel in the core were also considered. Activation gamma production calculations are outlined in Sections 2.3.1.2 and 2.3.3.

2.3.1.2 Activation Sources and Attenuation

The activated steel rings in the primary shield were treated as infinite slabs and a correction applied to account for the actual cylindrical geometry. The basic equation from TID 7004 (3) with the cylindrical correction is:

$$\text{Eq. 2.1} \quad D = \sqrt{\frac{r_s}{r_D}} \times \frac{BS_v}{2\mu_3} \left[E_2(b_1) - E_2(b_3) \right] \times \frac{1}{K_D}$$

r_s = radius of cylindrical source

r_D = radius of cylindrical surface through dose point

K_D = factor for converting from flux to dose

Other symbols as defined in TID 7004 (3).

Each steel slab is divided into thinner slabs and each thin slab is attenuated through all material between the slab and the dose point.

Since Boral is applied to steel surfaces exposed to water in the shield tank, thermal flux and hence thermal activation of the steel is reduced to a minimum. However, the Boral has a much smaller effect on the fast flux and fast activation. Resonance integrals of Pomerance and Macklin (6) were used to calculate activation of the shielding materials by the fast flux.

TABLE 2-1

Fission Product Source Strengths After Shutdown

| Group | Energy Range (Mev) | Effective Energy | 2.5 hrs. after shutdown | | | 1 day after shutdown | | |
|-------|--------------------|------------------|-------------------------|-----------------------|-----------------------|-----------------------|-------------------|-------------|
| | | | ∞ Operation | 1000-hr Operation | ∞ Operation | ∞ Operation | 1000-hr Operation | ∞ Operation |
| 1 | 0.1 - 0.4 | 0.35 | 1.37×10^{11} | 1.29×10^{11} | 1.11×10^{11} | 1.01×10^{11} | | |
| 2 | 0.4 - 0.9 | 0.75 | 8.87×10^{11} | 6.7×10^{11} | 6.35×10^{11} | 4.21×10^{11} | | |
| 3 | 0.9 - 1.35 | 1.35 | 9.31×10^{10} | 9.31×10^{10} | 1.05×10^{10} | 1.04×10^{10} | | |
| 4 | 1.35 - 1.8 | 1.6 | 3.70×10^{11} | 2.83×10^{11} | 2.70×10^{11} | 2.44×10^{11} | | |
| 5 | 1.8 - 2.2 | 2.10 | 1.04×10^{11} | 1.02×10^{11} | 7.05×10^9 | 5.75×10^9 | | |
| 6 | 2.2 - 2.6 | 2.5 | 2.91×10^{10} | 2.66×10^{10} | 2.34×10^{10} | 1.91×10^{10} | | |
| 7 | 2.80 | 2.80 | 1.39×10^9 | 1.39×10^9 | 6.7×10^6 | 6.7×10^6 | | |

$$\left(Sv \frac{\text{Mev}}{\text{sec} \cdot \text{cm}^3} \right)$$

Core Volume = $1.15 \times 10^5 \text{ cm}^3$

$P_0 = 10 \text{ Mw}$

Data on gamma yields from activated elements were taken from the Activation Handbook (7). The compositions of carbon and stainless steel used in the calculation follow.

Composition of 304 Stainless Steel
($\rho = 7.9 \text{ gm/cm}^3$)

| | |
|----------------------|-----------------|
| Carbon | 0.08% by weight |
| Manganese | 2.00 |
| Silicon | 1.00 |
| Chromium | 19.00 |
| Nickel | 9.50 |
| Cobalt | 0.05 |
| Iron (by difference) | 68.37 |

Carbon Steel - C-1015
($\rho = 7.84 \text{ gm/cm}^3$)

| | |
|----------------------|-----------------|
| Carbon | 0.15% by weight |
| Manganese | 0.53 |
| Phosphorus | 0.018 |
| Sulphur | 0.031 |
| Silicon | 0.17 |
| Cobalt | 0.01 |
| Iron (by difference) | 99.091 |

Stainless steel composition, except for cobalt content, was taken from Allegheny Ludlum Blue Sheet for Allegheny Metal 18-8 (8). Carbon steel composition, except for cobalt, was taken from Modern Steels and Their Properties (9). Cobalt content of both stainless and carbon steel was taken from Bopp and Sisman (10).

In the machine calculation, at 2.5 hrs after shutdown, the decay gammas from stainless and carbon steel are lumped into one energy group having an average energy of 1.65 Mev. Materials are assumed to have been exposed long enough so that all activities are saturated.

For short times after shutdown ($< 10 \text{ hrs}$) Mn^{56} is the chief source of radiation in carbon and stainless steels. For longer times after shutdown Fe^{59} and Co^{60} become the chief sources.

Activation analysis of the skid-mounted shielding is complicated by the fact that the steel surfaces exposed to water in the shield tank are covered with Boral to reduce activation due to thermal neutron capture. However, the Boral has a smaller effect on the fast flux and fast activation, which is ordinarily negligible when compared to thermal activation.

Little work has been done on fast flux activation of shielding materials in configurations such as the skid-mounted and APPR-1 shields. The approach used in the machine calculation is to use the resonance integrals of Pomerance and Macklin (6), and assume the fast flux to be proportional to $1/E$. The use of the resonance integrals of Ref. 6 will give an overestimate of fast

activation because they are based upon foil activation (no self-shielding) whereas the shield is made up of massive slabs of steel.

No experimental data are available on fast activation of large slabs of steel. Data are available on thermal activation (see Ref. 11); thermal activation sources from the machine were found to check closely with the data of Ref. 11.

2.3.1.3 Model Comparison with APPR-1 measurements

Since the skid mounted shielding is similar to that of APPR-1, it appears worthwhile to make use of APPR-1 experimental data to approximate the skid mounted dose rate. With this purpose in mind all the materials in the skid mounted shielding were combined and the calculated skid mounted dose rate compared to the measured dose rate at a corresponding point in the APPR-1 shield. Since the exposed steel in the skid mounted shield tank is Boral clad, the data from APPR-1 represents an upper limit for the skid mounted dose rate.

Total shielding between the skid mounted core and the outside of the shield tank is as follows:

6.79 inches water @ $\rho = 0.8 \text{ gm/cm}^3$
12.44 inches water @ $\rho = 0.98 \text{ gm/cm}^3$
18.775 inches steel

The closest corresponding point in the APPR-1 shield is between the seventh and eighth shield rings. This region has the following materials between the dose point and the core:

10.7 inches water @ $\rho = 0.8 \text{ gm/cm}^3$
6.25 inches water @ $\rho = 0.98 \text{ gm/cm}^3$
18.75 inches steel

The dose rate in this region of the APPR-1 at 2.5 hrs after shutdown from Fig. 2.3 of APAE 35(2) is about 130 mr/hr.

Comparison of the Skid Mounted dose rate to APPR-1 experimental measurements is valid at 2.5 hours after shutdown because the Mn^{56} activity is the chief source of radiation at this time and was saturated in APPR-1 before doses were measured.

2.3.2 Dose from Core

The dose rate from the core was calculated both by hand and with the IBM 650 machine code developed by Alco. The two calculations employ the basic equation of Section 2.3.1.1 with minor differences which will be detailed in the following sections.

2.3.2.1 Machine Calculation

Complete Details of the Machine Calculation are contained in APAE 35(2) and APAE Memo 142 (12)

In the machine calculation, at 2.5 hours after shutdown, the fission product decay gammas of Groups 3, 4, 5, 6, 7 of Table 2-1 are lumped into one group which is assumed to have an effective energy of 1.65 Mev and the 650 machine calculates attenuation through the shield and buildup for gammas of this energy. Groups 1 and 2 of Table 2-1 are also lumped into one group, but the dose rate from this group is negligible in comparison to Groups 3, 4, 5, 6 and 7 of Table 2-1.

The first part of the machine program calculates S_V (gammas/sec-cm³) and μ_c (cm⁻¹) the linear absorption coefficient in the core. S_V is calculated from the following equation (see Ref.2).

$$S_V = \sum_i v_i \left[\bar{\phi}_{th} F_i + \bar{\phi}_f G_i \right] \quad (2-3)$$

- S_V = source strength, gammas/sec-cm³ (assumed to be at 1.65 Mev)
- v_i = volume fraction of material i in the core
- $\bar{\phi}_{th}$ = average full power thermal neutron flux in the core, neutrons/cm²-sec
- $\bar{\phi}_f$ = average full power fast neutron flux in the core, neutrons/cm²-sec
- F_i = gammas/cm³-sec arising in material i per unit thermal neutron flux
- G_i = gammas/cm³-sec arising in material i per unit fast neutron flux

(See APAE 35 (2) for complete details.)

Files of F and G factors for core materials (U²³⁵ and stainless steel) are available for the machine calculation for various times after shutdown. Therefore, only the average fast and thermal neutron fluxes in the core and the material volume fractions are necessary as input to the machine calculations to calculate S_V .

The actual average thermal flux is 2.3×10^{13} . However, material in file on U²³⁵ is based upon the fission cross section of U²³⁵ at 0.025ev corrected for a Maxwellian distribution as follows:

$$\begin{aligned} \sigma_{0.025\text{ev}}^f &= 580 \text{ barns} \\ \sigma_{\text{thermal}}^f &= 0.886 \times 580 = 514 \text{ barns} \end{aligned}$$

However, according to Appendix III, APAE Memo 126 (13), temperature and heterogeneous effects in APPR-1 reduce this cross section to 327 barns or about 0.65 times the value used in the machine files. In order to keep the files general, the cross section was left as it was and the average thermal flux was multiplied by 0.65 giving the average thermal flux listed in the input which follows:

| Material | Volume Fraction* |
|---------------------------------|------------------|
| H ₂ O | 0.795207 |
| Stainless Steel | 0.173590 |
| U ²³⁵ O ₂ | 0.017259 |

$$\bar{\phi}_{th} = 1.5 \times 10^{13} \text{ neutrons/cm}^2\text{-sec}$$

$$\bar{\phi}_{fast} = 1.4 \times 10^{14} \text{ neutrons/cm}^2\text{-sec}$$

* Sum is not 100% because some materials such as U²³⁸O₂, B¹⁰, C which do not effect S_v have been omitted.

The core absorption coefficient, μ_c is calculated by the machine as follows:

$$\mu_c = \sum_i v_i \mu_i$$

v_i = volume fraction of material i in the core.

μ_i = absorption coefficient of material i in the core.

Files of absorption coefficients for materials of interest are available. After calculating S_v and μ_c the machine calculates dose rate by Eq. 2.2. Repeating Eq. 2.2

$$D = \frac{BS_v R_0^2}{2(a/s)} F(\Theta, b_2) \times \frac{1}{K_D}$$

Input to this part of the machine program is merely the dimensions of the core and shielding materials from Table 1-1.

The machine calculates geometric and material attenuation to get the unscattered dose and then calculates and applies the dose buildup factor B to get the total dose.

Buildups are calculated and used in the following manner:

- 1) All thicknesses of the same material are summed up and a buildup factor for each material is calculated by the equation (3)

$$B = A_1 e^{-\alpha_1 b} / (1 - A_1) e^{-\alpha_2 b}$$

Files of buildup parameters A, α_1 , α_2 from Ref 3 are available for materials of interest.

- 2) The buildup factors are then multiplied together and the the product applied to the unscattered gamma dose.

3) Buildup due to self-absorption in the core is not used.

Results of the machine calculation of the dose rate from the core at a point on the core midplane on the surface of the shield are:

$$\begin{aligned} \mu_c &= 0.1154 \text{ cm}^{-1} & \mu_0 Z &= 1.66 \\ S_v &= 4.76 \times 10^{11} \frac{\text{gammas}}{\text{sec-cm}^3} @ 1.65 \text{ Mev} & B &= 161 \\ \phi &= 1.59 \times 10^4 \frac{\text{gammas}}{\text{sec-cm}^2} @ 1.65 \text{ Mev} \\ D &= 44 \text{ mr/hr} \end{aligned}$$

2.3.2.2 Hand Calculation

In the hand calculation each group of gammas of Table 2-1 is treated separately using the appropriate gamma absorption coefficients and buildup factors. Groups 1, 2 and 3 give a dose rate insignificant compared to that of Groups 4, 5, 6 and 7; therefore only the dose rates of the last four groups were calculated. Eq. 2.2 is the basic equation used.

In the hand calculation the buildup factor is treated differently from the way it is treated in the machine calculation. In the hand calculation the total number of relaxation lengths in the shield plus the " μ_c^s " (a measure of self-absorption in the core) is used for attenuation. A dose buildup factor corresponding to the total number of shield relaxation lengths plus " μ_c^s " is applied. Iron buildup was used since steel is by far the most important shielding constituent of the shield. (Except for Group 4, water buildup is nearly the same as iron buildup.)

Complete details of the hand calculation are contained in Table 2-2. In addition to the calculation of Table 2-2 which is for 2.5 hours after shutdown, dose rates were also calculated at 12 and 24 hours after shutdown at a point on the shield surface opposite the core center. A summary of results follows:

| Time After Shutdown, Hr. | Dose Rate from Core, mr/hr |
|--------------------------|----------------------------|
| 2.5 | 24.3 |
| 12 | 11.5 |
| 24 | 9.9 |

TABLE 2-2

Hand Calculation of Dose Rate From Core

$R_0 = 25.6$ cm. $t_{Fe} = 48.2$ cm (Assumes contribution of 0.92 cm due to Boral.)
 $h = 55.9$ cm $t_{H_2O} = 44.4$ cm (Assumes density of 0.8 gm/cm³ for reflector H₂O)

Infinite operation at 10⁷ watts $a = 96.09$ cm
 2 1/2 hours after shutdown core composition: 79.5% H₂O; 20.5% Fe

| Gamma Group | Group Energy Yield (Mev/sec-watt) | Energy Per Photon (Mev) | Volumetric Source (Sv) (photons/cm ³ -sec.) | Linear Absorption Coefficient Fe (cm ⁻¹) | Linear Absorption Coefficient H ₂ O (cm ⁻¹) |
|-------------|-----------------------------------|-------------------------|--|--|--|
| IV | 4.25 x 10 ⁹ | 1.6 | 2.31 x 10 ¹¹ | 0.356 | 0.055 |
| V | 1.2 x 10 ⁹ | 2.1 | 4.97 x 10 ¹⁰ | 0.310 | 0.048 |
| VI | 3.4 x 10 ⁸ | 2.5 | 1.181 x 10 ¹⁰ | 0.293 | 0.0438 |
| VII | 1.6 x 10 ⁷ | 2.8 | 4.97 x 10 ⁸ | 0.284 | 0.041 |

| Gamma Group | μ_c (cm ⁻¹) | m | $(\frac{1}{m}) \mu_{c,z}$ | b_2 | $B_{Fe} (b_2)$ | Θ | $F (b_2, \Theta)$ |
|-------------|-----------------------------|------|---------------------------|-------|----------------|----------|-------------------------|
| IV | 19.6 | 1.68 | 1.31 | 21.8 | 40 | 13.5° | 6.0 x 10 ⁻¹¹ |
| V | 17.07 | 1.58 | 1.26 | 19.06 | 24 | 13.4° | 1.05 x 10 ⁻⁹ |
| VI | 16.07 | 1.53 | 1.24 | 17.97 | 20 | 13.4° | 3.1 x 10 ⁻⁹ |
| VII | 15.51 | 1.49 | 1.23 | 17.34 | 17.5 | 13.3° | 5.8 x 10 ⁻⁹ |

| Gamma Group | ϕ (photons/cm ² -sec) | K_D (photon hours/ roentgen-cm ² -sec) | Dose Rate = ϕ/K_D r/hr. |
|-------------|---------------------------------------|---|------------------------------|
| IV | 1.559 x 10 ³ | 3.7 x 10 ⁵ | 4.21 x 10 ⁻³ |
| V | 3.50 x 10 ³ | 3.0 x 10 ⁵ | 11.65 x 10 ⁻³ |
| VI | 2.04 x 10 ³ | 2.6 x 10 ⁵ | 7.85 x 10 ⁻³ |
| VII | 1.402 x 10 ² | 2.4 x 10 ⁵ | 0.59 x 10 ⁻³ |

Total = 24.3 milliroentgen/hour

2.3.3 Dose from Activated Materials in the Shield

The dose rate from the activated materials in the shield was calculated with the IBM 650 code developed by Alco. Complete details of the machine calculation are contained in APAE 35 (2) and APAE Memo 142 (12). Equation 2.1 is the basic equation employed.

Repeating Eq. 2.1:

$$D = \sqrt{\frac{r_B}{r_D}} \times \frac{BS_V}{2\mu_B} \left[E_2(b_1) - E_2(b_3) \right] \times \frac{1}{K_D}$$

(See Section 2.3.1.2 and TID 7004 (3) for definition of symbols.)

Briefly, S_V and B are calculated as in the core calculation described in Section 2.3.2.1. Files are available which contain data on neutron cross sections, gamma yields, gamma absorption coefficients and buildup parameters for different shielding materials including carbon and stainless steel. Files are also made up so that S_V may be calculated for various times after shutdown.

At times shorter than 12 hours after shutdown, gammas from activated shield materials are put into two energy groups. All gammas below 1 Mev are considered to have an average energy of 0.75 Mev; all gammas above 1 Mev are considered to have an average energy of 1.65 Mev.

At 12 hours and longer after shutdown, gammas above 1 Mev are considered to have an average energy of 1.25 Mev. This change is made because after 12 hours shutdown Co^{60} and Fe^{59} become more important than Mn^{56} as gamma sources since saturation of all activities is assumed.

Input to the machine calculation is merely the fast and thermal fluxes throughout the shield and the thicknesses of materials in the shield.

Table 2-3 contains fluxes used in the machine calculation. Fluxes in Table 2-3 were taken from Valprod Calculation No. 2624 results of which are plotted in Fig. 5-6 of Section 5 of Core Design Analysis. Thermal fluxes for points inside the pressure vessel have been multiplied by 0.8 to correct for temperature effects on thermal cross sections of water and stainless steel. (See Section 2.3.2.1.)

Boral in the shield has been treated as water as a source and shield after shutdown. Neither water nor Boral would contribute appreciably to dose rate after shutdown.

TABLE 2-3

Fluxes Used in the Machine Calculation of Dose Rate from Activated Materials.

| <u>Point</u> | <u>Location</u> | <u>ϕ_{th}</u> | <u>ϕ_r</u> |
|--------------|---------------------------------|-------------------------------|----------------------------|
| 1 | Core-Reflector I.F. (Interface) | 1.89×10^{13} | 7.44×10^{13} |
| 2 | Reflector Midpoint | 2.45×10^{13} | 5.75×10^{13} |
| 3 | Reflector-Thermal Shield I.F. | 1.07×10^{13} | 4.67×10^{13} |
| 4 | Thermal Shield Midpoint | 3.16×10^{12} | 3.07×10^{13} |
| 5 | Thermal Shield-Coolant I.F. | 5.21×10^{12} | 1.76×10^{13} |
| 6 | Coolant Passage -1 | 1.52×10^{13} | 9.2×10^{12} |
| 7 | Coolant Passage -2 | 1.17×10^{13} | 5.1×10^{12} |
| 8 | Coolant-Pressure Vessel I.F. | 2.94×10^{12} | 3.33×10^{12} |
| 9 | Pressure Vessel -1 | 6.35×10^{11} | 2.5×10^{12} |
| 10 | Pressure Vessel -2 | 1.86×10^{11} | 1.78×10^{12} |
| 11 | Pressure Vessel-Void I.F. | 4.68×10^{10} | 1.15×10^{12} |
| 12 | Void-Support Ring I.F. | 5.18×10^{10} | 9.56×10^{11} |
| 13 | Support Ring Midpoint | 1.7×10^{10} | 7.21×10^{11} |
| 14 | Support Ring-Boral I.F. | 2.28×10^9 | 5.05×10^{11} |
| 15 | Water Annulus Midpoint | 7.92×10^{10} | 3.35×10^{11} |
| 16 | Boral-1st. Shield Ring I.F. | 3.81×10^8 | 2.62×10^{11} |
| 17 | 1st. Shield Ring Midpoint | 2.42×10^7 | 1.37×10^{11} |
| 18 | 1st. Shield Ring-Boral I.F. | 4.36×10^7 | 5.88×10^{10} |
| 19 | Water Annulus Midpoint | 8.4×10^9 | 3.95×10^{10} |
| 20 | Boral-2nd Shield Ring I.F. | 3.12×10^7 | 3.07×10^{10} |
| 21 | 2nd. Shield Ring Midpoint | 1.45×10^6 | 1.61×10^{10} |
| 22 | 2nd. Shield Ring-Boral I.F. | 6.92×10^6 | 6.92×10^9 |
| 23 | Water Annulus Midpoint | 8.49×10^8 | 4.6×10^9 |
| 24 | Boral-3rd. Shield Ring I.F. | 2.77×10^6 | 3.6×10^9 |
| 25 | 3rd. Shield Ring Midpoint | 1.17×10^5 | 1.83×10^9 |
| 26 | 3rd. Shield Ring-Boral I.F. | 3.94×10^5 | 7.01×10^8 |
| 27 | Water Annulus Midpoint | 1.25×10^8 | 5.48×10^8 |
| 28 | Boral-4th. Shield Ring I.F. | 2.35×10^5 | 4.21×10^8 |
| 29 | 4th. Shield Ring Midpoint | 8.3×10^3 | 2.08×10^8 |
| 30 | 4th. Shield Ring-Boral I.F. | 3.67×10^4 | 7.11×10^7 |
| 31 | Water Annulus Midpoint | 3.8×10^6 | 1.68×10^7 |
| 32 | Boral - Tank Wall I.F. | 8.45×10^4 | 3.96×10^6 |
| 33 | Tank Wall Midpoint | 1.93×10^4 | 3.66×10^6 |
| 34 | Outside of Tank Wall | 1.62×10^4 | 3.38×10^6 |

Results of the machine calculation of dose rate due to shield activation after shutdown are as follows:

| <u>Group</u> | <u>Average Energy</u> | <u>Dose Rate</u> | |
|--------------|-----------------------|-------------------------------|------------------------------|
| | | <u>2.5 hrs after shutdown</u> | <u>24 hrs after shutdown</u> |
| 1 | 1.65 Mev | 48.2 mr/hr | 15.9 mr/hr |
| 2 | 0.75 Mev | <u>18.1 mr/hr</u> | <u>Negligible</u> |
| | Total | 66.3 mr/hr | 15.9 mr/hr |

2.3.4 Dose Rate from Sources outside Shield Tank

In addition to the radiation from the shield tank there are two other sources of radiation in the vapor container after shutdown. These are:

- 1) Activated corrosion products distributed throughout the primary system
- 2) Activated components in the vapor container

These two sources do not lend themselves to rigorous theoretical analysis, but health physics surveys made in APPR-1 give an indication of the relative importance of the two sources and the general dose rate level to be expected in the vapor container from the two sources.

Experimental data from APPR-1 are applicable to the Skid Mounted Reactor because:

- 1) Activation of corrosion products in the two plants is comparable.
- 2) Neutron fluxes escaping from the shield tanks of the two plants are comparable.

Surveys made in APPR-1 lead to the following conclusions which have been applied to the Skid Mounted Reactor:

- 1) Dose rate from vapor container component activation is small compared to dose rate from distributed activated corrosion products.
- 2) A general radiation field exists in the vapor container from these two sources which gives a dose rate of about 30 mr/hr at 2.5 hours after shutdown and about 6 mr/hr at 24 hours after shutdown.

2.3.5 Total Dose Rate after Shutdown

Results from the machine calculation indicate a dose rate on the shield surface of 110 mr/hr (66 mr/hr from shield activation and 44 mr/hr from fission product gammas) for infinite operation at 10 MW and 2.5 hours shutdown time. However, APAE 35 (2) shows that the machine calculation gives dose rates consistently higher than those measured in APPR-1. For instance, from Table 2.13 and Fig. 2.3 of APAE 35 (2) between the seventh and eighth shield rings of APPR-1 where total shielding is approximately equal to that in the Skid Mounted Reactor the machine calculated dose rate is about six times the measured dose rate. Therefore, it seems to be a conservative estimate to say that personnel standing at the primary skid 2.5 hours after shutdown would be subjected to 50 mr/hr from the primary shield rather than the 110 mr/hr calculated by the machine program.

Adding to the dose rate from the shield tank that from activated corrosion products and vapor container components gives a total dose rate of 80 mr/hr at 2.5 hrs. after shutdown for infinite operation at 10 Mw.

2.3.6 Conclusions

The important measure of the effectiveness of a shield is the dose accumulated by personnel outside the shield.

Fig. 2.1 is a plot of dose rate outside the shield tank, vs time after shutdown for infinite operation at 10 Mw and is based on the following data:

| Source | Time After Shutdown | | |
|------------------------------|---------------------|-----------|----------------|
| | 2.5 hrs. | 12 hrs. | 24 hrs. |
| Core | 24 mr/hr | 11.5 | 9.9 mr/hr |
| Shield | 26 | 12 | 6 |
| Activated Corrosion Products | <u>30</u> | <u>15</u> | <u>6 mr/hr</u> |
| Total | 80 mr/hr | 38.5 | 21.9 |

Core dose rates were calculated by hand (see Table 2-2 of Section 2.3.2.2). Shield dose rates were calculated by the machine; the dose rate at 2.5 hours after shutdown was reduced to give a total dose rate of 50 mr/hr at shield tank surface (see Section 2.3.5) including the 24 mr/hr from the core hand calculation. Shield dose rates at 12 and 24 hours after shutdown were reduced by the same factor. Dose rates from activated corrosion products were estimated from health physics surveys in APPR-1.

From Fig 2-1 it can be seen that the dose accumulated by personnel working at the shield tank for 4 hours from 8 to 12 hours after shutdown would be about 170 mr.

2.4 Operating Dose Calculation

Ordinarily operating dose rates from the reactor and shield tank must be calculated in order to determine thickness of secondary shielding necessary to reduce the operating dose rate to allowable levels. In the skid mounted ice cap installation it is necessary to calculate the operating dose rate in order to determine the distance between the vapor container tunnel and the manned stations of the installation since the snow between the tunnels acts as secondary shielding.

During operation significant sources of gamma radiation which escapes from the shield tank are:

1. Prompt fission gammas.
2. Fission product decay gammas.
3. Radiative capture gammas in U^{235} and in the shield.
4. Decay gammas from activated materials in the shield tank.

2.4.1 Calculation Model

2.4.1.1 Core Source and Attenuation

The calculation model used in the operating dose rate calculation was, in general, the same as that used in the shutdown dose rate calculation. Magnitude of the source strengths and energy spectrum, of course, are much different.

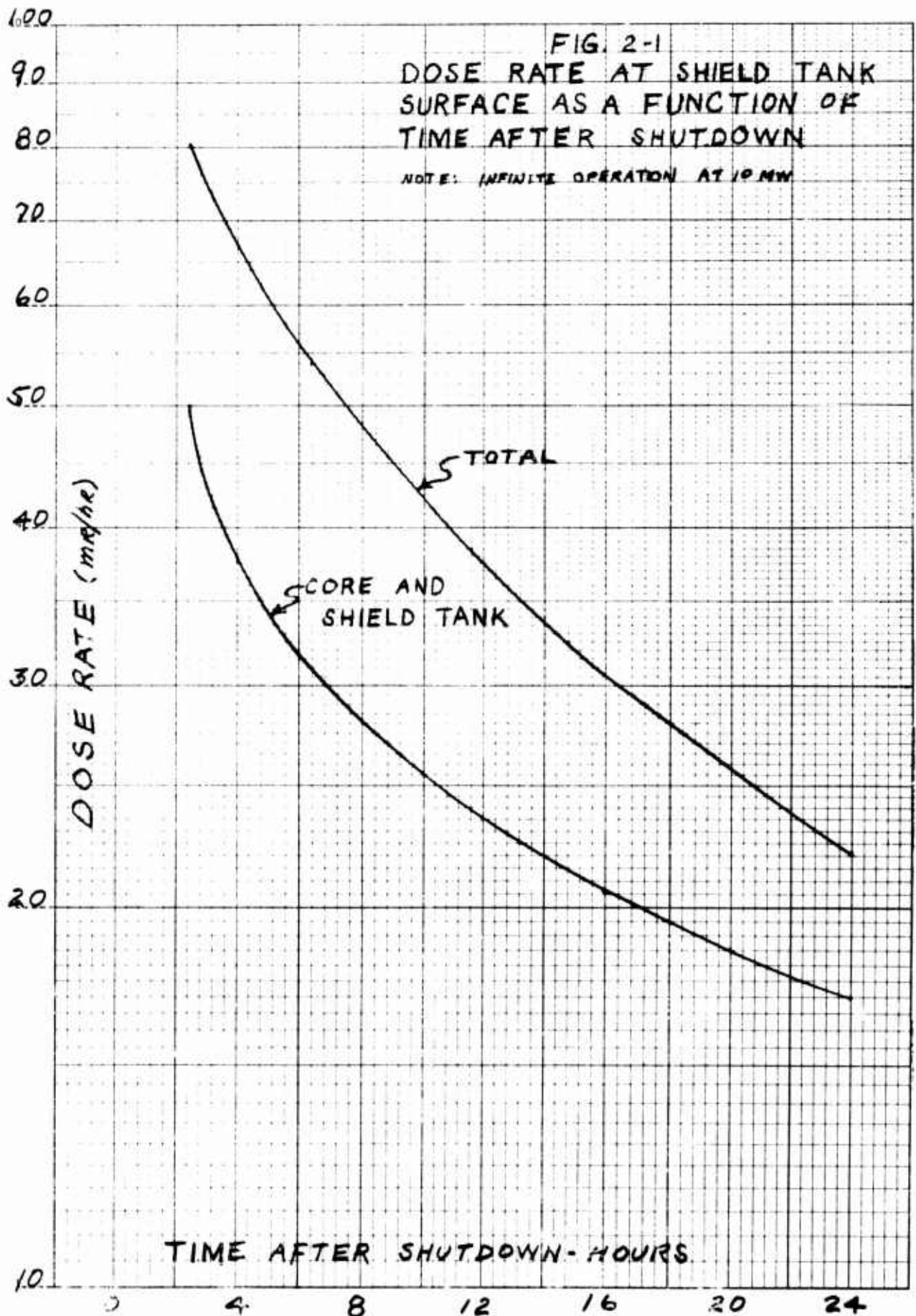
The machine program was used in the operating dose rate calculation. Files for the fission gamma yield are based upon the Motz spectrum for fission gammas as follows (see p. 47, Ref. 15):

$$N(E) dE = 18.5 e^{-1.24E} dE \quad \text{gammas/fission-Mev} \\ (E \text{ in Mev})$$

The above expression assumes a total of 12 Mev of gamma energy per fission event. Total gamma energy released from the fission event and its decay products is 11 Mev. One Mev is assumed to be released in radiative capture in U^{235} per fission and the radiative capture gammas are assumed to have the same spectrum as the fission gammas.

In addition to gammas from U^{235} , capture and activation gammas from stainless steel and capture gammas from water were considered. Data for the files for capture gamma production and energy spectra were taken from Table 3.6 of TID 7004 (3). Data for the files for activation gamma production were taken from Ref. 7.

In preparing the files, data on resonance capture integrals from Ref. 6 were used where available. For materials whose resonance capture integrals were not available a $1/v$ variation of absorption cross section was assumed. Thermal absorption cross sections for all the machine calculations were taken from BNL 325 (16). Thermal activation cross sections were taken from Ref. 7.



Capture and activation gamma sources in the core during operation were calculated basically in the same manner as outlined in the shutdown calculation (see Sections 2.3.1.2 and 2.3.3).

During operation gammas produced range in energy up to 7 Mev. All gammas are put into five energy groups as follows:

| Group | Energy Range, Mev | Average Energy, Mev |
|-------|-------------------|---------------------|
| 1 | > 7 | 7.0 |
| 2 | 5-7 | 6.0 |
| 3 | 3-5 | 4.0 |
| 4 | 1-3 | 2.0 |
| 5 | 0-1 | 0.75 |

2.4.1.2 Capture Sources in Shield and Attenuation

During operation, capture sources in the shield and their attenuation are calculated in much the same manner as activation sources after shutdown (see Sections 2.3.1.2 and 2.3.3). All activities are assumed to be saturated and operating at equilibrium values. Sources of data for capture and activation gammas are listed in Section 2.4.1.1. Activation and capture gammas produced during operation are put into the five energy groups listed in Section 2.4.1.1.

2.4.2 Model Comparison with APPR-1

As has been shown in Section 2.3.1.3, the primary shielding in APPR-1 out to the water annulus between the last two shield rings is approximately equal to the total primary shielding of the Skid Mounted Reactor. At this point in the APPR-1 shield the total measured dose rate during full power operation is 86.4 R/hr and the machine calculation gave 315 R/hr at the same point (see Table 2.12 of Ref.2).

Again the measured dose rate of 86.4 R/hr in APPR-1 would be expected to be an upper limit for the Skid Mounted Reactor. However, the machine calculated operating dose rate of 247 R/hr has been used in this report.

2.4.3 Dose from Core

Input to the core dose rate calculation during operation is the same as that for the shutdown calculation; the machine merely uses an operating file rather than a shutdown file. The input consists of core dimensions (height and radius), volume fractions in the core, kinds of materials and their thickness in the shield, and fast and thermal average fluxes in the core. Material types and thickness were taken from Table 1-1; volume fractions and fluxes are listed in Section 2.3.2.1.

Table 2-4 contains the output of the core operating dose rate calculation. Total calculated dose rate from the core is 73.8 R/hr.

Table 2-4
Results of Machine Calculation of Operating Dose Rate from Core

| Group | Energy Range, Mev | Average Energy Mev | Sv Gammas per sec per cm ³ | μ_c | $\mu_{c\gamma}$ | B(b) | ϕ Gammas per cm ² per sec | Dose Rate, R/hr |
|-------|-------------------|--------------------|---------------------------------------|---------|-----------------|-------|---|-------------------|
| 1 | >7 | 7.0 | 5.41 x 10 ¹¹ | 0.0661 | 1.46 | 11.5 | 2.59 x 10 ⁶ | 21.6 |
| 2 | 5-7 | 6.0 | 6.07 x 10 ¹¹ | 0.0675 | 1.47 | 14.2 | 2.76 x 10 ⁶ | 20.6 |
| 3 | 3-5 | 4.0 | 1.31 x 10 ¹² | 0.0749 | 1.52 | 26.2 | 3.20 x 10 ⁶ | 17.6 |
| 4 | 1-3 | 2.0 | 1.70 x 10 ¹³ | 0.0994 | 1.61 | 118 | 4.39 x 10 ⁶ | 14.0 |
| 5 | 0-1 | 0.75 | 4.44 x 10 ¹³ | 0.1712 | ----- | ----- | ----- | <u>Negligible</u> |
| Total | | | | | | | | 73.8 R/hr |

2.4.4 Dose from Capture and Activation Sources in the Shield

Input to the operating dose rate calculation for capture sources in the shield is the same as that for the shutdown activation calculation and consists of thicknesses and types of materials in the shield and fluxes throughout the shield. Fluxes used are listed in Table 2-3; types and dimensions of materials were taken from Table 1-1.

Table 2-5 contains the output of the operating dose rate calculation. Total calculated dose rate from the shield is 173.3 R/hr.

Table 2-5

Results of Machine Calculation of Operating Dose Rate from Capture and Activation Sources in the Shield.

| Group | Energy Range, Mev | Average Energy, Mev | Gammas/cm ² -sec | Dose Rate, R/hr |
|-------|-------------------|---------------------|-----------------------------|-------------------|
| 1 | > 7 | 7.0 | 1.32×10^7 | 110.4 |
| 2 | 5-7 | 6.0 | 5.59×10^6 | 41.7 |
| 3 | 3-5 | 4.0 | 3.36×10^6 | 18.4 |
| 4 | 1-3 | 2.0 | 8.88×10^5 | 2.8 |
| 5 | 0-1 | 0.75 | 2.72×10^4 | <u>Negligible</u> |
| | | | Total | 173.3 R/hr |

2.4.5 Total Dose on Surface of Shield Tank

The total dose rate on the surface of the shield tank is the sum of the core dose rate from Section 2.4.3 and the shield dose rate from Section 2.4.4. This total is 247 R/hr.

It has been shown in APAE 35 (2) that the machine calculation gives dose rates consistently higher than those measured. It has also been shown in Section 2.4.2 that the dose rate measured in APPR-1 outside a shield thickness corresponding approximately to total thickness of the skid mounted reactor is 86.4 R/hr and the machine calculated dose rate at the same point is 315 R/hr. Nevertheless, the 247 R/hr calculated outside the skid mounted shield has been used in following sections of this report.

2.5 Control Rod Drive Shielding

Control rod drive shielding after shutdown has been a difficult problem in both APPR-1 and APPR-1a. In these designs, to replace rod drives, personnel must approach quite close to the core.

Dose rates in APPR-1 control rod drive pit range from 940 mr/hr at 20 minutes after shutdown to 480 mr/hr at 2 1/2 hours after shutdown. (See Table 7, Ref. 14.) The geometry of the shield tank and control rod drive pit make it difficult to apply shielding effectively although this has been done in both designs.

The control rod drives of the skid mounted reactor and their relation to the core, pressure vessel, and shield tank may be seen in Dwg. Nos. R9-46-1039 and R9-47-1013. In the skid mounted configuration personnel do not have to approach any closer to the core than the outside of the shield tank. Therefore, shielding may be provided in the shield tank to protect personnel changing rod drives.

In addition to the fixed elements in the core there are five control rod fuel elements which are below the core after shutdown. To determine how far down the shield rings must extend to protect the control rod drive it was stipulated that the amount of shielding intersecting a ray from the bottom of any control rod fuel element to the control rod drives must be the same as is intersected by a ray from the core surface out horizontally to the shield tank surface.

In order to calculate the amount of shielding material intersected by a ray from the bottom of the fuel elements to the control rod drives it was necessary to determine equivalences of steel and water. (Boral was neglected.)

The equivalence of shield water and steel taken from Table 6.11 of Ref. 3 for 2 Mev gammas is: 1.7" steel = 11.6" water.

Water in the pressure vessel was assumed to have a density of 0.8 gm/cm³ and therefore its equivalence with steel is:

$$1" \text{ steel} = 8.53" \text{ Primary water}$$

The problem then becomes that of scaling off a drawing the thickness of materials intersecting a ray from the bottom of the control rod fuel elements to the area occupied by personnel changing control rod drives and extending the shield rings down until enough shielding material is intersected.

Dose rate from core and shield tank expected in this area would be less than the 50 mr/hr expected at the surface of the shield tank opposite the core.

2.6 Nozzle Shielding

Drawing No. R9-46-1039 shows the relation of the reactor outlet nozzle to the core and the shield rings. It can be seen that insulation around the nozzle and pipe in the shield tank affords a streaming path through the primary shield for radiation from the core and from the control rod elements below the core.

The approach to this problem was essentially the same as that used for the control rod drive shielding. That is, the nozzle and shield rings were drawn full size and rays drawn from the core and control rod fuel elements through the insulation to the outside of the primary shield tank.

The following equivalences of materials were used (see Table 6.11, Ref. 3):

$$1" \text{ Lead} = 11.6" \text{ water} = 1.7" \text{ Iron}$$

Where less than the full amount of shielding material was intersected, insulation will be taken off and replaced with lead until the desired amount of shielding is intersected.

2.7 Radiation Heating in the Shield Tank

During operation a significant amount of heat is deposited in the shield tank by radiation escaping from the core, pressure vessel and thermal shield. In order to size the cooling coil needed to remove the heat, the rate of heat deposition is calculated in the following section. A basic assumption is that all radiation incident on the pressure vessel support ring is absorbed in the shield tank.

2.7.1 Neutron Heating

All neutron heating is due to the absorption of the kinetic energy of fast neutrons.

From Table 2-3, the fast neutron flux incident on the pressure vessel support ring is 1.15×10^{12} n/cm²-sec. This is the fast flux averaged over the 22" height of the core. The corresponding area on the support ring is:

$$\begin{aligned}\pi \times 48'' \times 22'' &= 3.32 \times 10^3 \text{ in}^2 \\ &= 2.14 \times 10^4 \text{ cm}^2\end{aligned}$$

Assuming an average of 1 Mev per fast neutron the total amount of neutron energy incident on the support ring over the 22" height of the core is:

$$2.14 \times 10^4 \text{ cm}^2 \times 1.15 \times 10^{12} \text{ n/cm}^2\text{-sec} \times 1 \text{ Mev/n} = 2.46 \times 10^{16} \text{ Mev/sec}$$

Fluxes above and below the core are smaller than core fluxes and fall off rapidly (see Fig. 9.1). However, neutron energy incident on a 10" high section of the support ring below the level of the core was calculated as follows:

$$\begin{aligned}\bar{\phi}_F &= \text{average core fast flux} \\ \bar{\phi}_F &= 1.44 \times 10^{14}\end{aligned}$$

From Fig. 9.1 the ratio of the fast flux at the bottom of the core to the core fast flux is:

$$\frac{\phi_F}{\bar{\phi}_F} = \frac{0.95 \times 10^{14}}{1.44 \times 10^{14}} = 0.66$$

The ratio of the fast flux 10" below the core to the core fast flux is:

$$\frac{\phi}{\bar{\phi}_F} = \frac{5.9 \times 10^{12}}{1.44 \times 10^{14}} = 0.041$$

Taking a linear average from the bottom of the core to 10" below the core:

$$\begin{aligned}\frac{\phi}{\bar{\phi}_F} &= \frac{0.66 + 0.041}{2} = 0.35 \\ \phi &= 0.35 \times \bar{\phi}_F\end{aligned}$$

Or an average fast flux over the 10" section of the support ring would be:

$$\phi = 0.35 \times 1.15 \times 10^{12} \text{ n/cm}^2\text{-sec} = 4.02 \times 10^{11} \text{ n/cm}^2\text{-sec}$$

The area upon which this flux is incident is:

$$\begin{aligned} \pi \times 48'' \times 10'' &= 1.51 \times 10^3 \text{ cm}^2 \\ &= 9.74 \times 10^3 \text{ cm}^2 \end{aligned}$$

Total neutron energy incident on a 10" section of the support ring below the level of the core is:

$$\begin{aligned} 9.74 \times 10^3 \text{ cm}^2 \times 4.02 \times 10^{11} \text{ n/cm}^2 \text{ sec} \times 1 \text{ Mev/n} \\ = 3.92 \times 10^{15} \text{ Mev/sec} \end{aligned}$$

The fast flux below this 10" band below the core may be neglected. Since the flux above the core is much smaller than the flux below the core, the heat deposition above the core may also be neglected (see Fig. 7, Ref. 13)

Total heating due to neutrons is then:

$$2.46 \times 10^{16} \text{ Mev/sec} + 3.92 \times 10^{15} \text{ Mev/sec} = 2.85 \times 10^{16} \text{ Mev/sec}$$

2.7.2 Heating from Core and Pressure Vessel Gammas

A machine calculation was made to determine the gamma flux incident on a section of the support ring corresponding to the core height. The results, which include core gammas and capture gammas, follow:

| E(Mev) | ϕ , γ /sec-cm ² | ϕ_g , Mev/sec-cm ² |
|--------|--|--|
| 7 | 3.24×10^{11} | 2.27×10^{12} |
| 6 | 1.80×10^{11} | 1.08×10^{12} |
| 4 | 2.34×10^{11} | 9.36×10^{11} |
| 2 | 1.24×10^{12} | 2.48×10^{12} |
| 0.75 | 5.87×10^{11} | 4.4×10^{11} |
| | Total | $7.21 \times 10^{12} \text{ Mev/sec-cm}^2$ |

$$7.21 \times 10^{12} \text{ Mev/sec-cm}^2 \times 2.14 \times 10^4 \text{ cm}^2 = 1.54 \times 10^{17} \text{ Mev/sec}$$

From Fig. 80, Ref. 29, the total gamma flux below the core falls off similarly to the fast neutron flux. Therefore, the heating rate due to core gammas in the 10" section below the core is:

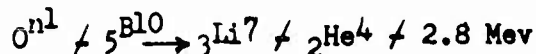
$$\frac{3.92 \times 10^{15}}{2.46 \times 10^{16}} \times 1.54 \times 10^{17} \text{ Mev/sec} = 2.46 \times 10^{16} \text{ Mev/sec}$$

Total gamma heating is:

$$2.46 \times 10^{16} \text{ Mev/sec} \neq 1.54 \times 10^{17} \text{ Mev/sec} = 1.79 \times 10^{17} \text{ Mev/sec}$$

2.7.3 Heating from Captures in the Shield Tank

Neutrons incident on the inner surface of the pressure vessel support ring are captured in the steel, boron and water in the shield tank resulting in the production of capture gammas except in the case of boron. The reaction in boron is as follows:



Thus, while boron serves as a gamma suppressor, appreciable amounts of heat are released in the shield tank in the form of kinetic energy of the boron reaction products. The heat release will in fact be greater than had the neutrons been absorbed in water.

The total amount of gamma radiation released per neutron capture is equal to the binding energy of the additional neutron. In the case of carbon steel, this has been taken to be 8 Mev; for water (hydrogen) it has been taken to be 2.2 Mev. It has been assumed that all capture gammas are absorbed in the tank.

The equation used to calculate heat production in the different materials in the shield tank is:

$$H = \sum_i \left[\sum_{th}^a \bar{\phi}_{th} + \sum_F^a \bar{\phi}_F \right] V_i E_i$$

$$\sum_{th}^a \bar{\phi}_{th} + \sum_F^a \bar{\phi}_F = \text{absorptions per cm}^3 \text{ of } i\text{th material}$$

V_i = volume of ith material

E_i = energy released per capture in ith material

Table 2-6 contains details of the calculation. To account for gamma production above and below the core, the radial fluxes which are averaged over the height of the active core were used over an area extending over the height of the core plus 10 inches below the core. Heat production rates were calculated for the first five regions of the shield. Since the

fluxes fall off exponentially, it is not necessary to calculate captures further out in the shield. Fast and thermal cross sections are the same as those used in the Valprod calculation, results of which are plotted in Fig. 5-6 of Core Design Analysis.

Table 2-6: Calculation of Heat Produced by Captures in the Shield Tank

| Region* | $\sum_{th}^a \text{cm}^{-1}$ | $\sum_F^a \text{cm}^{-1}$ | $\bar{\phi}_{th}$ n/cm ² -sec | $\bar{\phi}_F$ n/cm ² -sec | $\left[\frac{\sum_{th}^a \bar{\phi}_{th} + \sum_F^a \bar{\phi}_F}{\text{Captures}} \right]$ cm ³ -sec |
|---------|------------------------------|---------------------------|---|--|--|
| 1 | 0.16864 | 0.008 | 2.6×10^{10} | 7.21×10^{11} | 1.015×10^{10} |
| 2 | 16.715 | 0.59 | 8×10^9 | 4×10^{11} | 3.70×10^{11} |
| 3 | 0.115 | 0.001 | 4×10^{10} | 3.35×10^{11} | 4.94×10^9 |
| 4 | 16.715 | 0.59 | 8.5×10^9 | 8×10^{10} | 1.89×10^{11} |
| 5 | 0.16864 | 0.008 | 2×10^8 | 1.37×10^{11} | 1.1×10^9 |

| Region* | V, cm ³ | E, $\frac{\text{Mev}}{\text{Capture}}$ | $V \times E \times \left[\sum_{th}^a \bar{\phi}_{th} + \sum_F^a \bar{\phi}_F \right]$ | $\frac{\text{Mev}}{\text{sec}}$ |
|---|---------------------|--|--|---------------------------------|
| 1 | 5.6×10^4 | 8 | 3.98×10^{15} | |
| 2 | 1.033×10^4 | 2.8 | 1.07×10^{16} | |
| 3 | 1.26×10^5 | 2.2 | 1.38×10^{15} | |
| 4 | 1.28×10^4 | 2.8 | 6.8×10^{15} | |
| 5 | 3.52×10^5 | 8 | 1.17×10^{15} | |
| <u>H = 2.40 x 10¹⁶ Mev/sec</u> | | | | |

- *Region - 1 - Pressure Vessel Support Ring
 2 - Pressure Vessel Support Ring Boral Clodding
 3 - 1st. Water Annules
 4 - Boral Clodding on 1st. Shield Ring
 5 - 1st. Shield Ring

2.7.4 Conclusions

Total radiation heating rates in the shield tank as calculated in the preceding sections are:

| | |
|--|-------------------------------|
| Neutrons | 0.29×10^{17} Mev/sec |
| Gammas from Core, Thermal Shield and pressure vessel | 1.79×10^{17} Mev/sec |
| Captures in the shield tank | 0.24×10^{17} Mev/sec |
| Total | 2.32×10^{17} Mev/sec |

$$2.32 \times 10^{17} \text{ Mev/sec} \times 5.472 \times 10^{-13} \frac{\text{Btu-sec}}{\text{Mev-hr}} = 1.27 \times 10^5 \text{ Btu/hr}$$

Over 75% of the total heating rate is based upon the machine shielding calculation. Because the machine calculation has been shown to yield higher dose rates and heating rates than those measured, the heating coil for the shield tank has been sized to remove 110,000 Btu/hr of gamma and neutron heat.

2.8 GAMMA FLUX ON THE INSTRUMENTS

A machine calculation was performed to determine the operating dose rate on the nuclear instruments in the shield tank. Neutron fluxes used in this calculation were the same as those listed in Table 2-3 of Section 2.3.3. These are end of life neutron fluxes and therefore give the highest gamma dose rate to be expected on the instruments. Thermal neutron fluxes are markedly different for the two instrument positions shown in Drawing No. R9-46-1039 as a result of the different amounts of water behind the instruments. This difference will have little effect upon the gamma flux and the gamma dose rate has been assumed to be the same for all instruments.

Shutdown gamma dose rates on the instruments in the skid mounted shield tank have been estimated from experimental data taken in APPR-1. Table 2-7 contains a comparison of gamma dose rates measured in APPR-1 and calculated for the skid mounted reactor.

Table 2-7: Gamma Dose Rates on the Instruments in APPR-1 and the Skid Mounted Reactor

| | <u>Operating</u> | |
|-------------------------------|------------------------------|--------------------------------|
| | Calculated | Measured |
| APPR-1 | $5 \times 10^5 \text{ R/hr}$ | $2.5 \times 10^5 \text{ R/hr}$ |
| Skid Mounted | $4 \times 10^5 \text{ R/hr}$ | ————— |
| <u>24 Hrs. After Shutdown</u> | | |
| | Estimated* | Measured |
| APPR-1 | ————— | 10^3 R/hr |
| Skid Mounted | $7 \times 10^2 \text{ R/hr}$ | ————— |

*Estimated from APPR-1 measurements.

3.0 Secondary Shielding Analysis

The primary shield was designed on the basis of minimum weight and access to the primary skid 8.0 hours after shut-down. Therefore, a high level of radiation would be expected around the primary skid during operation.

The allowable continuous radiation received by any personnel is based on the amount that may be received in one year. This allowable radiation is 5 R/YR. In any one week, this is equivalent to a radiation level of 96.2 mr/week. Since base personnel are scheduled to be on duty 84 hours a week, the hourly permissible dose rate in operating areas can be approximately 1 mr/hr.

At the site, the radiation emanates from the core itself, the primary shield (shield tank) and N-16 activity in the primary water. In order to decrease the level of the operating radiation to base personnel, the primary system is located within the secondary shield, in this case, snow.

This section will deal with the thickness of secondary shielding required to decrease the operating radiation to 1 mr/hr. The operating radiation consists of the contribution from the N-16 activity of the primary water and from the activation of the primary shield.

3.1 N-16 Activity in Primary Water

In all reactors where water is used as a primary coolant, there is activation of the water. This is due to the capture of a neutron by O-16 as shown in the following reaction which has a threshold of approximately 10 Mev.



The extent of the activation is a sensitive function of the influx time and the total cycle time.

A simplified method was employed to calculate the N-16 activity. This method was used since it was shown to give comparable results to a more precise and lengthy method (2).

3.1.1 Calculation of N-16 Activity

In this reactor, the water will be activated in both the core and the reflector. The activity was calculated using the following equations:

core

$$A_c(0) = \sum_a \bar{\phi}_c \left(\frac{1 - e^{-\lambda t_c}}{1 - e^{-\lambda t_T}} \right) \quad (3-1)$$

reflector

$$A_R(0) = \sum_a \bar{\phi}_R \left(\frac{1 - e^{-\lambda t_R}}{1 - e^{-\lambda t_T}} \right) \quad (3-2)$$

Total

$$A_T(0) = A_c(0) + A_R(0) \quad (3-3)$$

where

$A_c(0)$ = activity due to activation in core, dis/sec-cm³

$A_R(0)$ = activity due to activation in reflector, dis/sec-cm³

$\bar{\phi}_c$ = average activation flux in core, neutrons/cm²-sec

$\bar{\phi}_R$ = average activation flux in reflector, neutrons/cm²-sec

\sum_a = activation cross section of O-16, cm⁻¹ = 4.274 x 10⁻⁴

λ = disintegration constant of N-16, sec⁻¹ = 0.0943

t_T = time for one complete cycle, sec = 8.024

t_c = time water spends in core, sec = 0.384

t_R = time water spends in reflector, sec = 2.449

The activation flux is that part of the fast flux above 10 Mev which consists of the uncollided and collided flux. The uncollided flux is described by equation 3-4 (17)

$$\phi_u(E) = \frac{\nu_{R_F} f(E)}{\sum_o(E) + \sum_H(E) + \sum_{Fe}(E)} \quad (3-4)$$

where

$\phi_u(E)$ = uncollided activation flux, neutrons/cm²-sec-Mev

ν = neutrons/fission = 2.46

R_f = (P) (CF)/V, Fissions/cm³-sec = 2.815 x 10¹²

P = Power output, watts = 10⁷

(CF) = Conversion factor, Fission/Watt-sec = 3.24 x 10¹⁰

V = Volume of core, cm³ = 1.151 x 10⁵

f(E) = Watt's fission spectrum, neutrons/fission neutron

$\Sigma_o(E)$ = macroscopic cross section of oxygen, cm⁻¹

$\Sigma_H(E)$ = macroscopic cross section of hydrogen, cm⁻¹

$\Sigma_{Fe}(E)$ = macroscopic cross section of iron, cm⁻¹

Watt's fission spectrum is defined by equation 3-5.

$$f(E) = 0.484 e^{-E} \text{ Sinh } \sqrt{2E} \quad (3-5)$$

where

E = neutron energy, Mev

Table 3-1 gives the calculation and numbers that were used to obtain the uncollided flux.

The collided flux above 10 Mev is defined by equation 3-6 (17).

$$\phi_c(E) = \frac{\nu R_f}{E \Sigma_H(E)} \left[(1-p) \int_E^\infty f(E') dE' / p e^{-E/T} \left\{ \left(\frac{E}{T}\right)^2 / \left(\frac{E}{T}\right) / 1 \right\} \right] \quad (3-6)$$

In this case the second term is negligible.

where

$$p = \frac{\int_E^{\infty} \frac{\sum_{\text{O}}(\text{E}') \sum_{\text{Fe}}(\text{E}')}{\sum_{\text{H}}(\text{E}') / \sum_{\text{O}}(\text{E}') / \sum_{\text{Fe}}(\text{E}')} f(\text{E}') d\text{E}'}{\int_E^{\infty} f(\text{E}') d\text{E}'}$$

E = energy, Mev

T = nuclear temperature of the residual nucleus, Mev

Table 3-1

Calculation of Uncollided Flux

| E(Mev) | f(E) | $\sigma_{\text{H}}(\text{E})$ (barns) | $\sigma_{\text{O}}(\text{E})$ (barns) | $\sigma_{\text{Fe}}(\text{E})$ (barns) | \sum_t^* (cm ⁻¹) | $\phi_u(\text{E})$ n/cm ² -sec-Mev |
|--------|--------------------------|--|--|---|-----------------------------------|--|
| 10 | 9.616 x 10 ⁻⁴ | 0.94 | 1.25 | 2.95 | 0.1092 | 6.096 x 10 ¹⁰ |
| 11 | 4.401 x 10 ⁻⁴ | 0.87 | 1.33 | 2.82 | 0.1061 | 2.871 x 10 ¹⁰ |
| 12 | 1.994 x 10 ⁻⁴ | 0.79 | 1.41 | 2.68 | 0.1025 | 1.347 x 10 ¹⁰ |
| 13 | 8.962 x 10 ⁻⁵ | 0.74 | 1.50 | 2.58 | 0.1009 | 6.149 x 10 ⁹ |
| 14 | 3.997 x 10 ⁻⁵ | 0.69 | 1.54 | 2.52 | 0.0988 | 2.801 x 10 ⁹ |
| 15 | 1.771 x 10 ⁻⁵ | 0.65 | 1.57 | 2.45 | 0.0968 | 1.268 x 10 ⁹ |
| 16 | 7.795 x 10 ⁻⁶ | 0.61 | 1.59 | 2.39 | 0.0947 | 5.701 x 10 ⁸ |
| 17 | 3.413 x 10 ⁻⁶ | 0.57 | 1.61 | 2.34 | 0.0927 | 2.548 x 10 ⁸ |

$$\sum_t^* = N_{\text{H}} \sigma_{\text{H}}(\text{E}) / N_{\text{O}} \sigma_{\text{O}}(\text{E}) / N_{\text{Fe}} \sigma_{\text{Fe}}(\text{E})$$

$$N_{\text{H}} = 4.1381 \times 10^{22} \text{ atoms/cm}^3$$

$$N_{\text{O}} = 2.1635 \times 10^{22} \text{ atoms/cm}^3$$

$$N_{\text{Fe}} = 1.4653 \times 10^{22} \text{ atoms/cm}^3$$

Table 3-2 outlines the calculation of the collided flux above 10 Mev. The total energy dependent flux is the sum of the uncollided and collided flux and is given in Table 3-3.

Table 3-2
Calculation of Collided Flux

| E(Mev) | $\Sigma_H(E)$ | $\Sigma_O(E)/\Sigma_{Fe}(E)$ | $\Sigma_t(E)$ | $\int_E f(E') dE'$ | p | ϕ_c n/cm ² -sec-Mev |
|--------|---------------|------------------------------|---------------|------------------------|-------|--|
| 10 | 0.03893 | 0.07027 | 0.1092 | 1.305×10^{-3} | 0.767 | 5.578×10^9 |
| 11 | 0.0360 | 0.07010 | 0.1061 | 5.477×10^{-4} | 0.891 | 1.04×10^9 |
| 12 | 0.03272 | 0.06978 | 0.1025 | 2.464×10^{-4} | 0.843 | 6.829×10^8 |
| 13 | 0.03064 | 0.07026 | 0.1009 | 1.077×10^{-4} | 0.811 | 3.55×10^8 |
| 14 | 0.02856 | 0.07024 | 0.0988 | 4.72×10^{-5} | 0.763 | 1.939×10^8 |
| 15 | 0.02692 | 0.06987 | 0.09679 | 1.84×10^{-5} | 0.649 | 1.11×10^8 |
| 16 | 0.02524 | 0.06942 | 0.09466 | 5.28×10^{-6} | 0.584 | 3.77×10^7 |
| 17 | 0.02359 | 0.06912 | 0.09271 | 2.3×10^{-6} | 0.513 | 1.939×10^7 |

Table 3-3
Total Energy Dependent Flux

| E(Mev) | $\phi(E)$ n/cm ² -sec-Mev |
|--------|--------------------------------------|
| 10 | 6.655×10^{10} |
| 11 | 2.976×10^{10} |
| 12 | 1.416×10^{10} |
| 13 | 6.504×10^9 |
| 14 | 2.994×10^9 |
| 15 | 1.378×10^9 |
| 16 | 6.078×10^8 |
| 17 | 2.742×10^8 |

The total flux above 10 Mev is defined by equation 3-7.

$$\phi_{\text{act}} \text{ (n/cm}^2\text{-sec)} = \int_{10}^{\infty} \phi \text{ (E) dE} \quad (3-7)$$

where

$$\phi \text{ (E)} = 1.707 \times 10^{14} e^{-0.7833E}$$

Therefore

$$\phi_{\text{act}} = 8.559 \times 10^{10} \text{ neutrons/cm}^2\text{-sec}$$

In order to obtain the average flux over 10 Mev in the core and reflector, the following assumption is made: the neutron flux above 10 Mev has the same radial distribution as the fast group flux. Therefore, the average fluxes above 10 Mev in the core and reflectors are 5.397×10^{10} and 1.538×10^{10} neutrons/cm²-sec respectively.

3.1.2 Results

From equations 3-1, 3-2, and 3-3 the activation of the primary water by the $^{16}\text{O} \text{ (n,p) } ^{16}\text{N}$ reaction is as follows:

Activation in disintegrations/sec-cm³

Core

$$A_{\text{C}}(0) = 1.545 \times 10^6$$

Reflector

$$A_{\text{R}}(0) = 2.553 \times 10^6$$

Total

$$A_{\text{T}}(0) = 4.098 \times 10^6$$

3.1.3 Comparison with APPR-1

A rough comparison can be obtained from the measured N-16 activity and known cycle times in the APPR-1. The experimentally obtained activity is 1.63×10^6 dis/sec-cm³. Therefore,

$$A_{\text{APPR-1}}(0) = 1.63 \times 10^6 = \sum_{a1} \phi_1 \left(\frac{1 - e^{-\lambda t_{c1}}}{1 - e^{-\lambda t_{t1}}} \right) = 0.0614$$

$$A_{\text{SKID}}(0) = A_2 = \sum_{a2} \phi_2 \left(\frac{1 - e^{-\lambda t_{c2}}}{1 - e^{-\lambda t_{t2}}} \right) = 0.06698$$

but

$$\frac{\sum_{a2} \rho_2}{\sum_{a1} \rho_1} = \frac{48.9 \text{ \#/ft}^3}{51.77 \text{ \#/ft}^3} = 0.9426$$

and assuming

$$\frac{(\phi_{\text{fast}})_{\text{APPR-1}}}{\phi_1} = \frac{(\phi_{\text{fast}})_{\text{SKID}}}{\phi_2},$$

$$\frac{\phi_2}{\phi_1} = \frac{1.5055 \times 10^{14}}{1.0095 \times 10^{14}} = 1.491,$$

and

$$\frac{\sum_{a2} \phi_2}{\sum_{a1} \phi_1} = 1.408$$

$$\therefore \frac{A_2}{1.63 \times 10^6} = \frac{0.06698 \sum_{a2} \phi_2}{0.0614 \sum_{a1} \phi_1} = 2.504 \times 10^6$$

From the scaling of the measured activity in the APPR-1, the activity in the skid mount would be 2.504×10^6 dis/sec-cm³ or approximately 39% lower than the previously calculated value of 4.098×10^6 dis/sec-cm³ which is the number that will be used on the secondary shielding calculations.

3.2 Attenuation of N-16 Gammas Through Secondary Shielding

In section 3.1, the N-16 activity in the primary coolant was calculated at the reactor outlet. This section describes the calculation of the attenuation of the N-16 gammas through the secondary shield.

3.2.1 Calculation Model

The method used to calculate the gamma dose rate from the primary coolant is described fully in RAS-I (18) and AP NOTE 63 (19) as developed by the Electric Boat Division of General Dynamics Corp.

RAS-I takes the source due to the N-16 activity and attenuates it through shields within the vapor container and the secondary shield. To obtain the source geometry, the primary coolant piping and steam generator is divided into sections about one foot in length. The foot long sources are then approximated by a point source at the center of the actual source having a strength of S_0 (gamma/sec). The point sources are then located in a three dimensional co-ordinate system. Essentially, the same setup is used to determine the shadow shields within the vapor container (including piping and steam generator). The input to the computer consists of the properties of the sources, piping, steam generator and other components in the vapor container. The points at which the dose rates are to be calculated are also included in the input. The shadow shield, source point and dose point descriptions are given in Tables 3-4, 3-5 and 3-6 respectively. The location of all dose points is given in Figs. 3-1a to 3-1e.

The computer calculates the inverse square attenuation and the self-absorption of the source to the selected dose point. After this, the machine checks to see if the gamma ray passes through a shadow shield. If it does, the computer attenuates the source through the shadow shield. For secondary shielding the machine uses two shields of specified thickness. Then it uses Peebles data (20) to compute slant attenuation and buildup in the shield. The dose rate at the selected dose point from all sources is summed up by the machine which then prints the dose rate as the output.

A unique property of the ice cap skid-mounted reactor is that the density of the secondary shielding (snow) varies in the vertical direction. This variation is shown in Fig. 3-2. In the calculation where the gamma rays from source to dose point were slanted in a vertical plane, an average snow density and linear absorption coefficient were used.

3.2.2 Calculated Dose Outside of Secondary Shield

During the shielding task conducted on the APPR-1 (2), measurements were performed determining the dose rate of various positions on the outside of the secondary shield. In all cases, the dose rate calculated by RAS-I was between a factor of $1\frac{1}{2}$ and 3 greater than the measured rate. According to Ref. (18) (pg. 93 and 94) the machine calculation has been checked against the STR Mark I shield test and the calculated dose rates were consistently higher than the measured doses. Therefore, the RAS-I calculation can be used to determine the dose rates on the outside surface of the secondary shielding.

The dose rates were calculated at 33 positions in the secondary shielding around the vapor container. The results from the RAS-I calculation are given in Table 3-7. The dose points were selected so that isodose lines could be determined as a function of depth and distance from

TABLE 3-4

| Type | Shadow Shield Description | IDA | R (ft) | X ₁ (ft) | Y ₁ (ft) | Z ₁ (ft) | \sqrt{OA} | X ₂ (ft) | Y ₂ (ft) | Z ₂ (ft) |
|----------------------------|---------------------------|-----|--------|---------------------|---------------------|---------------------|-------------|---------------------|---------------------|---------------------|
| Reactor | | 01 | 3.67 | 20.0 | 35.0 | 29.2 | .00 | 20.0 | 35.0 | 35.1 |
| Pump | | 02 | 0.58 | 26.3 | 32.4 | 32.0 | .00 | 26.3 | 32.4 | 34.8 |
| Reactor Tank (Top) | | 03 | 2.38 | 20.0 | 35.0 | 35.1 | .03 | 20.0 | 35.0 | 51.0 |
| Reactor Tank (side) | | 04 | 4.29 | 20.0 | 35.0 | 27.6 | .04 | 20.0 | 35.0 | 35.1 |
| Large upper boiler section | | 05 | 2.29 | 34.6 | 33.3 | 30.3 | .09 | 41.2 | 33.3 | 30.3 |
| Boiler end | | 06 | 1.58 | 29.3 | 33.3 | 29.5 | .10 | 30.6 | 33.3 | 29.5 |
| Small upper boiler section | | 07 | 1.88 | 31.6 | 33.3 | 29.9 | .13 | 34.6 | 33.3 | 29.9 |
| Lower pressurizer | | 08 | 1.25 | 30.2 | 37.9 | 30.0 | .13 | 30.2 | 37.9 | 32.2 |
| Boiler tube | | 09 | 1.33 | 31.1 | 33.3 | 29.5 | .24 | 41.1 | 33.3 | 39.5 |
| Upper pressurizer | | 10 | 1.25 | 30.2 | 37.9 | 32.2 | .29 | 30.2 | 37.9 | 34.4 |
| Schedule O Pipe | | 11 | 0.43 | 24.3 | 34.2 | 29.9 | .45 | 28.9 | 34.2 | 29.9 |
| | | 12 | 0.43 | 28.9 | 32.4 | 29.0 | .45 | 27.1 | 32.4 | 29.0 |
| | | 13 | 0.43 | 27.0 | 32.4 | 29.1 | .45 | 26.3 | 32.4 | 29.8 |
| | | 14 | 0.43 | 26.3 | 32.4 | 29.9 | .45 | 26.3 | 32.4 | 31.0 |
| | | 15 | 0.43 | 26.3 | 31.5 | 11.5 | .45 | 22.5 | 31.5 | 11.5 |

TABLE 3-5

Source Point Description


| Type | 1D _A | 1D _B | X _B (ft) | Y _B (ft) | Z _B (ft) | C |
|-----------------|-----------------|-----------------|---------------------|---------------------|---------------------|--|
| Boiler End | 06 | 001 | 29.3 | 33.3 | 29.5 | 293.05 |
| Boiler Tube | 09 | 001 | 31.6 | 33.3 | 29.5 | 90.20 |
| | 09 | 002 | 32.6 | 33.3 | 29.5 |  |
| | 09 | 003 | 33.6 | 33.3 | 29.5 | |
| | 09 | 004 | 34.6 | 33.3 | 29.5 | |
| | 09 | 005 | 35.6 | 33.3 | 29.5 | |
| | 09 | 006 | 36.6 | 33.3 | 29.5 | |
| | 09 | 007 | 37.6 | 33.3 | 29.5 | |
| | 09 | 008 | 38.6 | 33.3 | 29.5 | |
| | 09 | 009 | 39.6 | 33.3 | 29.5 | |
| | 09 | 010 | 40.6 | 33.3 | 29.5 | |
| Schedule 0 Pipe | 11 | 001 | 24.8 | 34.2 | 29.9 | |
| | 11 | 002 | 25.8 | 34.2 | 29.9 | 22.38 |
| | 11 | 003 | 26.6 | 34.2 | 29.9 | 22.29 |
| | 11 | 004 | 27.5 | 34.2 | 29.9 | 22.20 |
| | 11 | 005 | 28.4 | 34.2 | 29.9 | 25.26 |
| | 12 | 001 | 28.5 | 32.4 | 29.0 | 16.34 |
| | 12 | 002 | 27.6 | 32.4 | 29.0 | 19.51 |
| | 13 | 001 | 26.7 | 32.4 | 29.4 | 21.11 |
| | 14 | 001 | 26.3 | 32.4 | 30.4 | 22.15 |
| | 15 | 001 | 25.8 | 31.5 | 31.5 | 18.74 |
| | 15 | 002 | 24.8 | 31.5 | 31.5 | 17.11 |
| | 15 | 003 | 23.9 | 31.5 | 31.5 | 17.04 |
| | 15 | 004 | 23.0 | 31.5 | 31.5 | 18.50 |

TABLE 3-6

DOSE POINT DESCRIPTION

| Plane | Dose Pt. Identification | b ₁ | X _D | X _D | Z _D | C _{b1} | C _{b2} |
|-------|----------------------------|----------------|----------------|----------------|----------------|-----------------|-----------------|
| 1 | 001 | 0 | 20.0 | 35.0 | 66.9 | 10.000* | 02.318* |
| 1 | 002 | 0 | 30.0 | 35.0 | 66.9 | 10.000* | 02.318* |
| 1 | 003 | 0 | 47.7 | 35.0 | 66.9 | 10.000* | 02.318* |
| 2 | 004 | 5 | 82.2 | 35.0 | 66.9 | 20.500 | 01.600 |
| 2 | 005 | 5 | 99.9 | 35.0 | 66.9 | 20.500 | 01.600 |
| 3 | 006 | 5 | 20.0 | 65.5 | 66.9 | 20.500 | 01.600 |
| 2 | 007 | 5 | 82.2 | 80.0 | 66.9 | 20.500 | 01.600 |
| 2 | 008 | 5 | 82.2 | 65.5 | 54.9 | 20.500 | 01.600 |
| 2 | 009 | 5 | 82.2 | 47.0 | 54.9 | 20.500 | 01.600 |
| 2 | 010 | 5 | 82.2 | 35.0 | 54.9 | 20.500 | 01.600 |
| 2 | 011 | 5 | 82.2 | 23.0 | 54.9 | 20.500 | 01.600 |
| 2 | 012 | 5 | 82.2 | 04.5 | 54.9 | 20.500 | 01.600 |
| 2 | 013 | 5 | 82.2 | 65.5 | 42.9 | 20.500 | 01.600 |
| 2 | 014 | 5 | 82.2 | 35.0 | 42.9 | 20.500 | 01.600 |
| 2 | 015 | 5 | 82.2 | 04.5 | 42.9 | 20.500 | 01.600 |
| 2 | 016 | 5 | 82.2 | 65.5 | 30.7 | 20.500 | 01.600 |
| 2 | 017 | 5 | 82.2 | 47.0 | 30.7 | 20.500 | 01.600 |
| 2 | 018 | 5 | 82.2 | 35.0 | 30.7 | 20.500 | 01.600 |
| 2 | 019 | 5 | 82.2 | 23.0 | 30.7 | 20.500 | 01.600 |
| 2 | 020 | 5 | 82.2 | 04.5 | 30.7 | 20.500 | 01.600 |
| 3 | 021 | 5 | 00.0 | 80.0 | 66.9 | 20.500 | 01.600 |
| 3 | 022 | 5 | 30.0 | 80.0 | 66.9 | 20.500 | 01.600 |
| 3 | 023 | 5 | 20.0 | 95.0 | 66.9 | 20.500 | 01.600 |
| 3 | 024 | 5 | 00.0 | 65.5 | 54.9 | 20.500 | 01.600 |
| 3 | 025 | 5 | 20.0 | 65.5 | 54.9 | 20.500 | 01.600 |
| 3 | 026 | 5 | 40.0 | 65.5 | 54.9 | 20.500 | 01.600 |
| 3 | 027 | 5 | 60.0 | 65.5 | 54.9 | 20.500 | 01.600 |
| 3 | 028 | 5 | 00.0 | 65.5 | 42.9 | 20.500 | 01.600 |
| 3 | 029 | 5 | 20.0 | 65.5 | 42.9 | 20.500 | 01.600 |
| 3 | 020 | 5 | 00.0 | 65.5 | 30.7 | 20.500 | 01.600 |
| 3 | 031 | 5 | 20.0 | 65.5 | 30.7 | 20.500 | 01.600 |
| 3 | 032 | 5 | 40.0 | 65.5 | 30.7 | 20.500 | 01.600 |
| 3 | 033 | 5 | 60.0 | 65.5 | 30.7 | 20.500 | 01.600 |

* C_{b1} and C_{b2} have been multiplied by 10⁻² to fit input. Therefore calculated dose rates must be multiplied by 10².

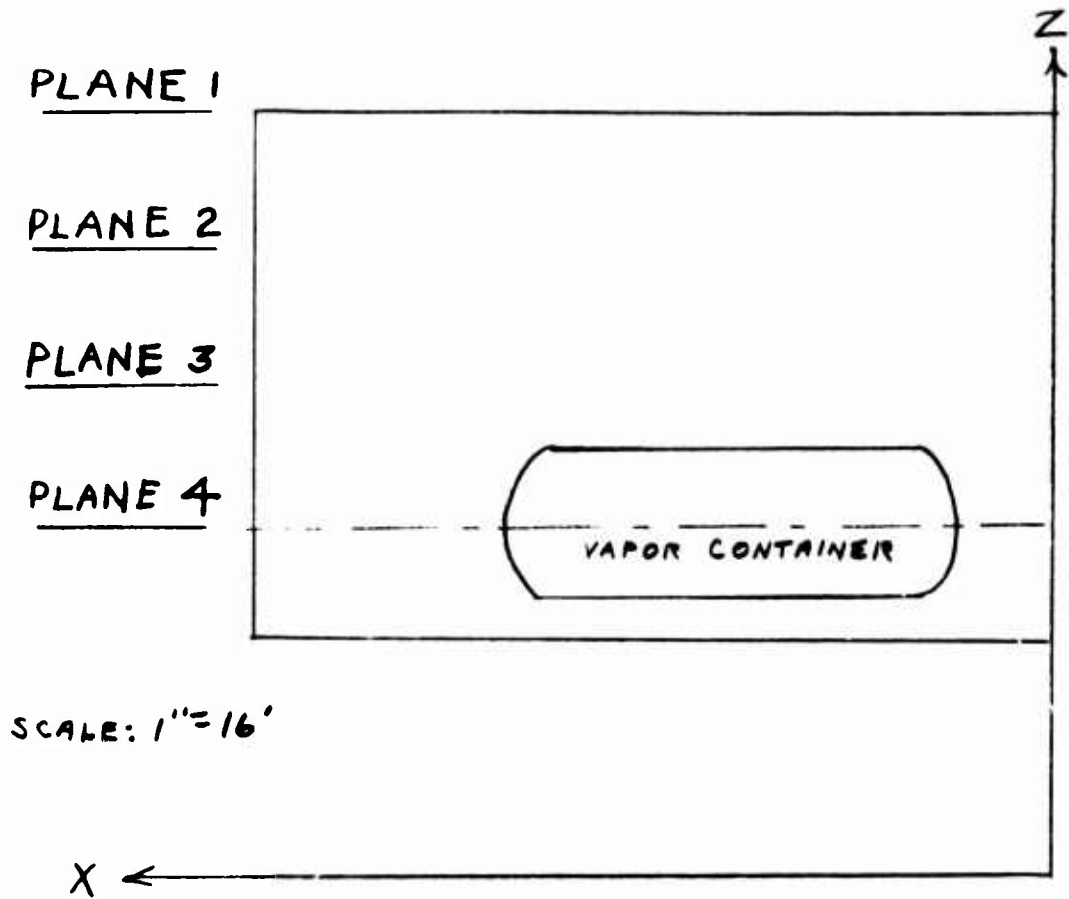


FIG. 3-1a. ELEVATION VIEW - DOSE POINT LOCATION

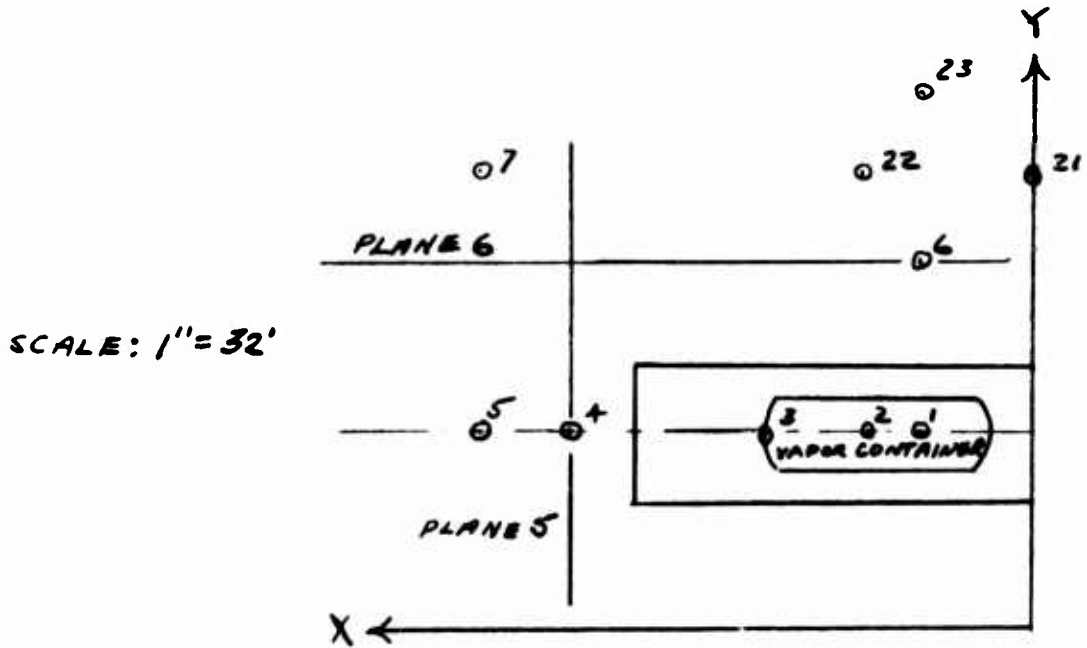


FIG. 3-1b. PLAN VIEW - DOSE POINT LOCATION ON PLANE 1

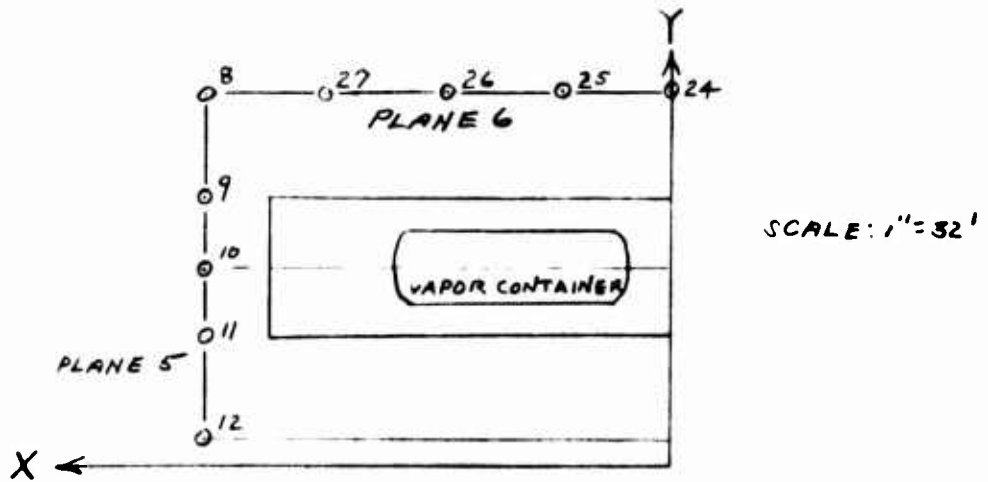


FIG. 3-1c. PLAN VIEW-DOSE POINT LOCATION ON PLANE 2

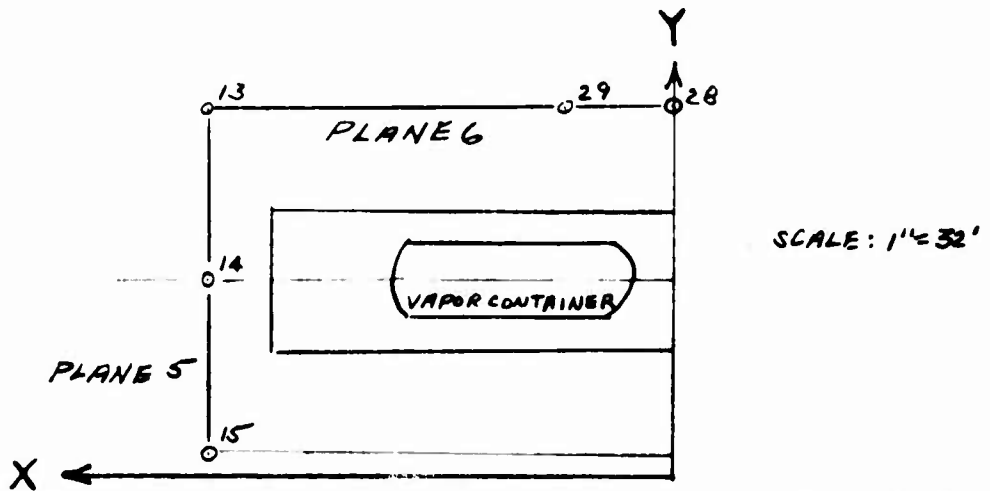


FIG 3-1d. PLAN VIEW-DOSE POINT LOCATION ON PLANE 3

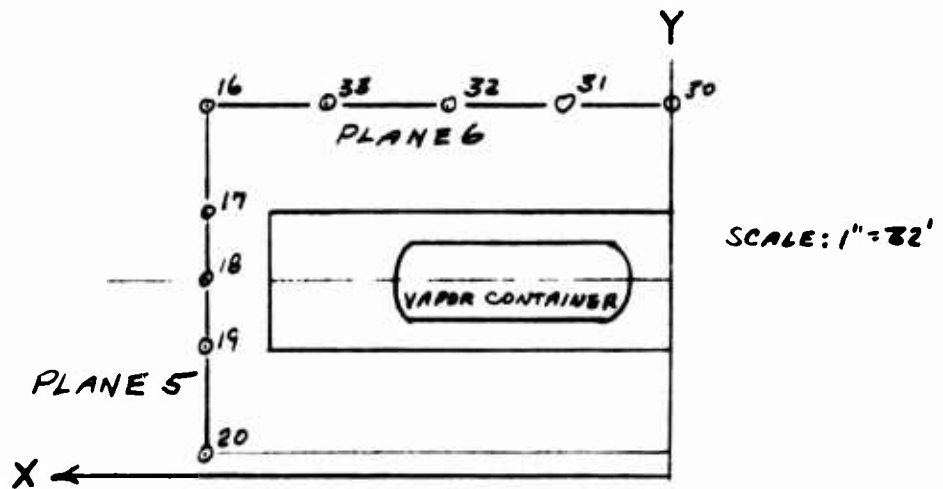
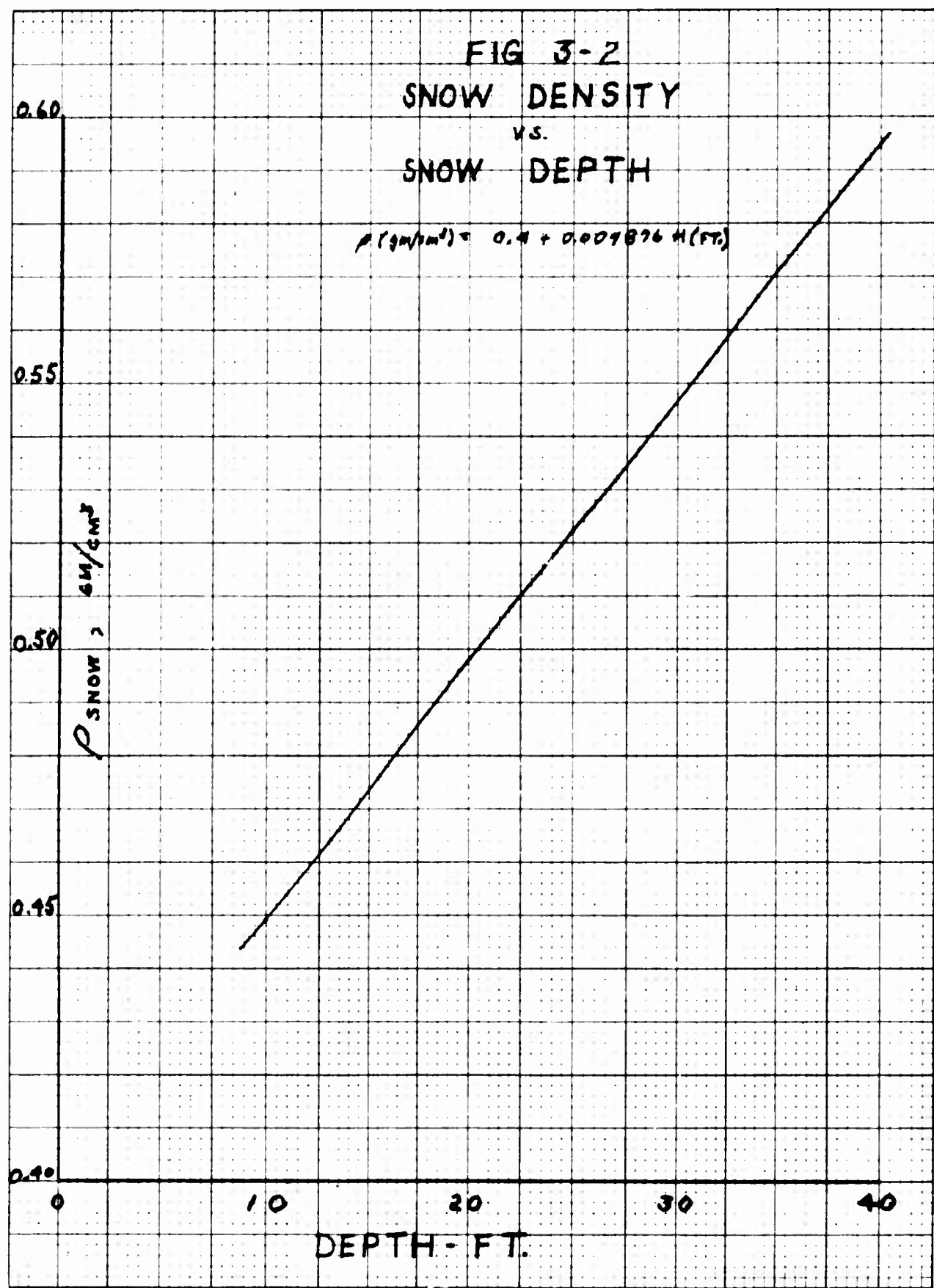


FIG. 3-1e. PLAN VIEW-DOSE POINT LOCATION ON PLANE 4

FIG 3-2
SNOW DENSITY
VS.
SNOW DEPTH

$$\rho \text{ (gm/cm}^3\text{)} = 0.4 + 0.009876 H \text{ (FT.)}$$



the vapor container. From the results given in Table 3-7, the various isodose lines in the different planes are given in Fig. 3-3a to Fig. 3-3c.

Table 3-7

Dose Rates from RAS-I Program (Secondary Shield)

| <u>Dose Point</u> | <u>Dose (mr/hr)</u> | <u>Dose Point</u> | <u>Dose (mr/hr)</u> |
|-------------------|---------------------|-------------------|---------------------|
| 1 | 92.5 | 18 | 0.0094 |
| 2 | 131.76 | 19 | 0.0761 |
| 3 | 62.98 | 20 | 0.0219 |
| 4 | 0.0087 | 21 | 0.0031 |
| 5 | 0.007 | 22 | 0.0084 |
| 6 | 0.0068 | 23 | 0.0128 |
| 7 | 0.0015 | 24 | 0.0023 |
| 8 | 0.0048 | 25 | 0.0220 |
| 9 | 0.0088 | 26 | 0.0096 |
| 10 | 0.0104 | 27 | 0.0019 |
| 11 | 0.0134 | 28 | 0.0050 |
| 12 | 0.0091 | 29 | 0.0666 |
| 13 | 0.0068 | 30 | 0.0136 |
| 14 | 0.0654 | 31 | 0.2329 |
| 15 | 0.0092 | 32 | 0.3603 |
| 16 | 0.0175 | 33 | 0.0357 |
| 17 | 0.0359 | | |

3.3 Attenuation of Radiation from Shield Tank

3.3.1 Calculation Model

With the primary shielding designed for access after shut-down, the dose rate from the reactor and the shield tank through the snow will be much greater than the dose rate from the primary coolant.

The following equation was used to calculate the reactor and shield tank dose rate through the snow:

$$D_2 = \left(\frac{r_1}{r_2} \right)^2 D_1 e^{-b} B(b) \quad (3-8)$$

where

D_2 = dose rate at a distance r_2 from the core center

D_1 = dose rate on the surface of the shield tank opposite the core midplane

D_1 = 247 R/hr (from Section 2.4)

r_1 = radius of shield tank

r_1 = 4.25 ft

r_2 = distance from core center to point at which dose rate is to be calculated

t = snow thickness

$b = \mu t$

μ = linear absorption coefficient of snow for 6 Mev gammas, cm^{-1}

$B(b)$ = dose buildup factor (for water)

Table 3-8 contains details of the operating dose rate calculation from the shield tank at various locations in the secondary system. At all these locations dose rate from primary coolant activation is negligible compared to the reactor dose.

In the calculations of Table 3-8, gamma radiation from the shield tank was assumed to be at 6 Mev. Snow density was assumed to be 0.517 gm/cm^3 which corresponds to a depth of 24 feet (see Fig. 3-2). The 24-ft. depth is minimal for the ice cap installation.

Fig. 3-4 shows the approximate dose rate as a function of penetration through snow. Points for the curve were calculated from Eq. 3.8. For the sake of generality and simplicity of calculation it was assumed that:

$$r_2 = r_1 + t$$

That is, geometrical attenuation between the shield tank surface and the snow wall was neglected.

SCALE: 1" = 16'

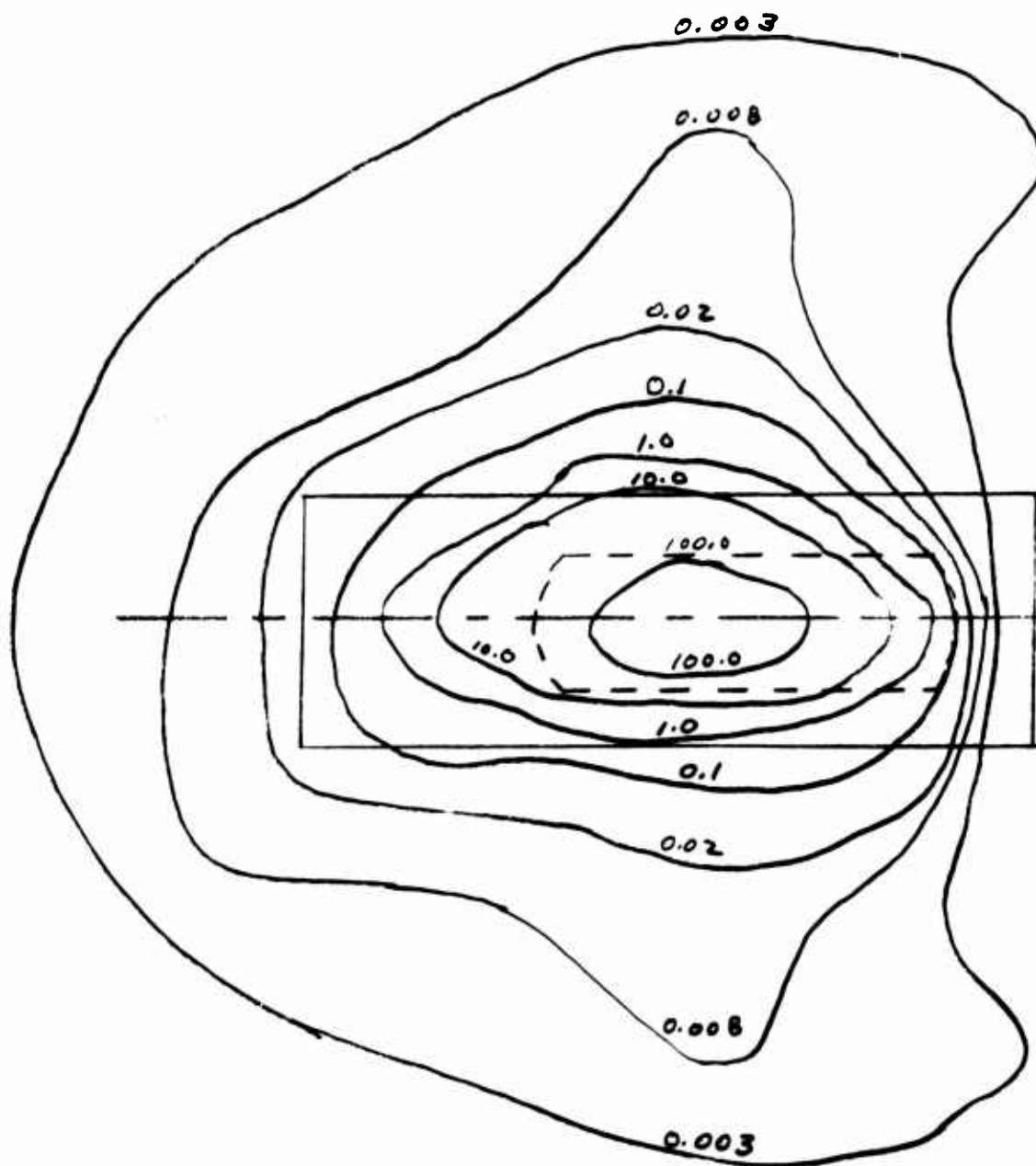


FIG. 3-3a. N-16 ISODOSE LINES ON PLANE 1
(MR/HR)

SCALE: 1" = 16'

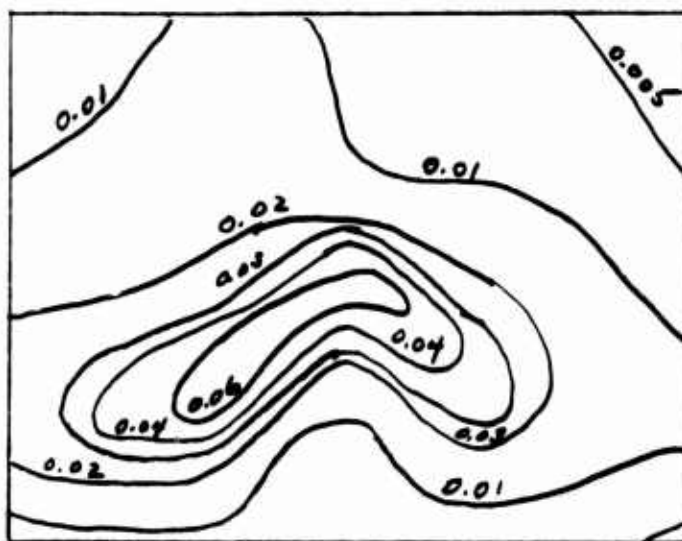


FIG. 3-36. N-16 ISODOSE LINES ON VERTICAL PLANES (MR/HR)

SCALE: 1" = 16'

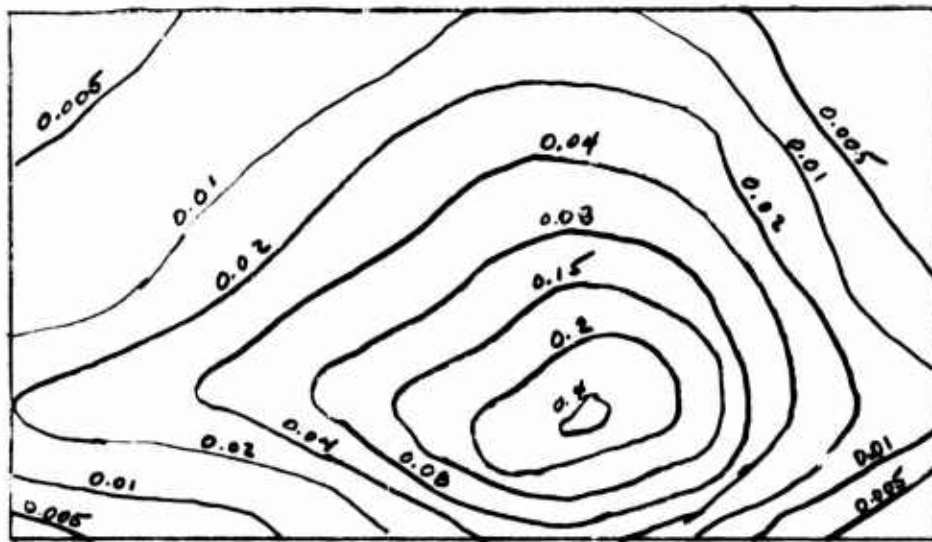


FIG. 3-3c. N-16 ISODOSE LINES ON
VERTICAL PLANE 6 (mr/hr)

1
9
8
7
6
5
4
3
2
1
9
8
7
6
5
4
3
2
1
9
8
7
6
5
4
3
2
1

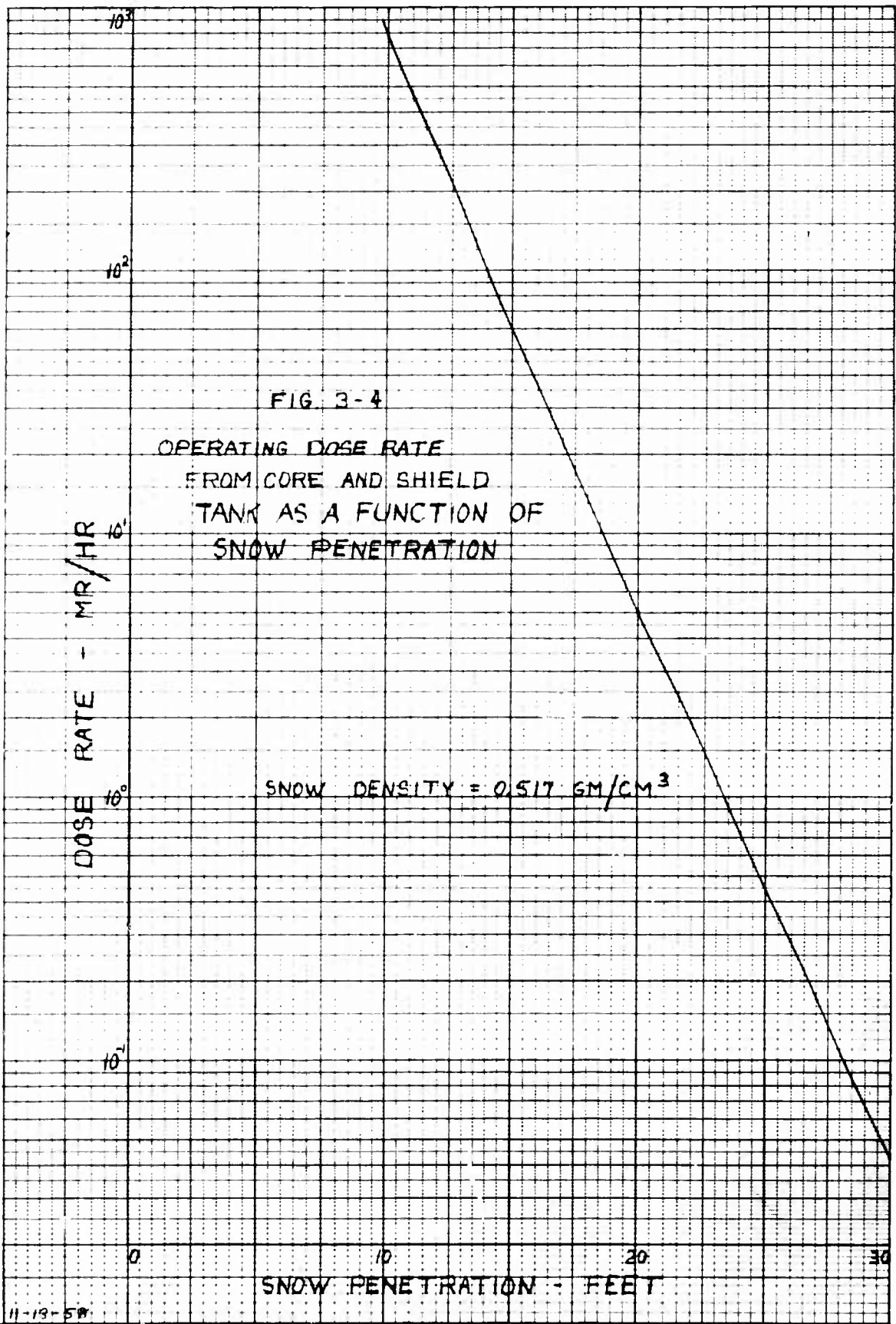


Table 3-8

Dose Rates through the Snow from the Shield Tank

| Area | r_2 (ft) | r_1/r_2 | $\left(\frac{r_1}{r_2}\right)^2$ | t (cm) | b | H_2O (b) | e^{-b} | Dose Rate (mr/hr) |
|-----------------------|------------|-----------------------|----------------------------------|--------------------|-------|------------|----------------------|-------------------|
| Turbine Gen. Pkg. | 68 | 6.25×10^{-2} | 3.91×10^{-3} | 7.62×10^2 | 11.05 | 5.6 | 1.6×10^{-5} | 0.086 |
| Elect. Control Pkg. | 72 | 5.9×10^{-2} | 3.48×10^{-3} | 7.92×10^2 | 11.5 | 5.8 | 1×10^{-5} | 0.050 |
| Condenser Package | 98 | 4.34×10^{-2} | 1.88×10^{-3} | 7.62×10^2 | 11.05 | 5.6 | 1.6×10^{-5} | 0.086 |
| Feedwater Package | 98 | 4.34×10^{-2} | 1.88×10^{-3} | 1.01×10^3 | 14.6 | 9.0 | 4.6×10^{-7} | 0.002 |
| Heat Exchange Package | 126 | 3.37×10^{-2} | 1.14×10^{-3} | 7.62×10^2 | 11.05 | 5.6 | 1.6×10^{-5} | 0.086 |

$$\mu_{H_2O} = 0.028 \text{ cm}^2/\text{gm for 6 Mev. gammas}$$

$$\mu_{\text{snow}} = 0.0145 \text{ cm}^{-1} \rho = 0.517 \text{ gm/cm}^3 \bullet 24 \text{ ft. depth}$$

Distances and snow thicknesses are approximate and were scaled from Dwg. No. M02M11 of Section A, Secondary System Mechanical and Electrical Design.

Knowing the thickness of snow between an area of interest and the vapor container, Fig. 3.4 may be used to find the approximate dose rate to be expected. However, dose rates taken from Fig. 3.4 for the specific areas listed in Table 3-8 will be higher than those calculated in the table. This is caused by neglecting the geometrical attenuation between shield tank and snow wall in the general calculations for Fig. 3.4 and taking the attenuation into account for the more specific calculations of Table 3-8.

Fig. 3-5 shows isodose regions in the snow around the vapor container; data for the isodose lines were taken from Fig. 3.4.

Fig. 3-6 shows isodose lines on the surface of the ice cap. Dose rates on the ice cap surface were calculated by Eq. 3.8 on the basis of the following assumptions:

1. $r = r_1 / t$ (geometrical attenuation between shield surface and snow is neglected)
2. t = slant thickness through snow
3. Average snow density between core and surface of ice cap is 0.48 gm/cm^3 (see Fig. 3.2).

3.3.2 Conclusions

From Table 3-8 it may be concluded that dose rates from the shield tank of manned stations of the skid mounted ice cap installation as shown in Dwg. No. M02M11 of Section C are well below the design dose rates of Section 1.1.

3.4 Secondary Shield Thickness Required

Comparing the dose rates calculated from the shield tank in Section 3.3.1 to those calculated from primary coolant activation in Section 3.2 it can be seen that the primary coolant dose rate is about a factor of ten smaller. Therefore, the necessary thickness of snow between the vapor container and the uncontrolled stations of the site may be determined from shield tank dose rate only.

Drawing No. M02M11 of Section A shows a site layout with 25 feet of snow between the vapor container and the nearest skid which must be accessible during operation (the turbine generator skid). From Table 3-8 which contains the dose rate at the turbine generator through twenty-five feet of snow, it can be seen that the dose rate calculated is 0.086 mr/hr. The design dose rate in this area from Table 1-0 of Section 1.1 is 0.1 mr/hr.

Therefore, it may be concluded that 25 feet of snow is adequate and desirable as a secondary shield.

SNOW DENSITY = 0.517 gm/cm³
OPERATING AT 10 Mw

- PT 1 - 12 FT. FROM TUNNEL FACE
- PT 2 - 24 FT. FROM TUNNEL FACE
- PT 3 - 36 FT. FROM TUNNEL FACE

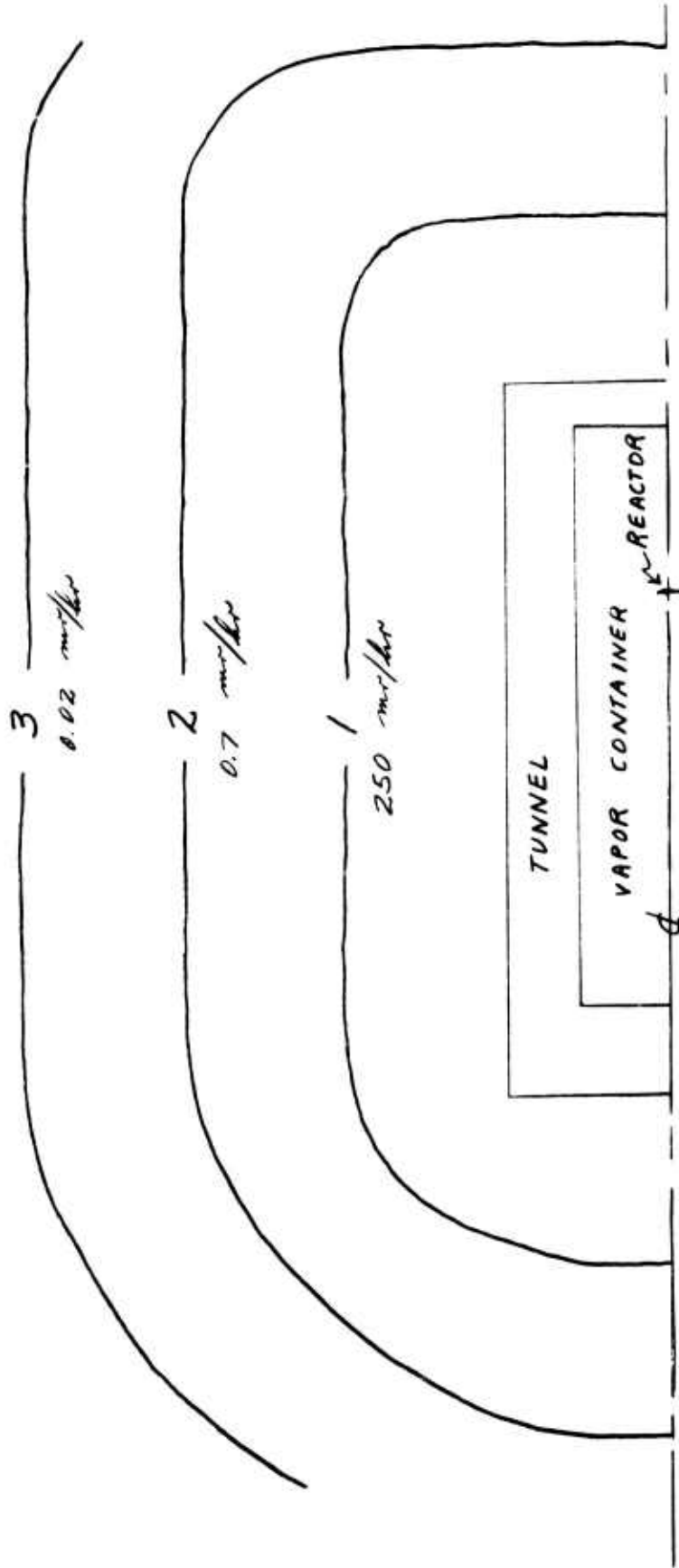
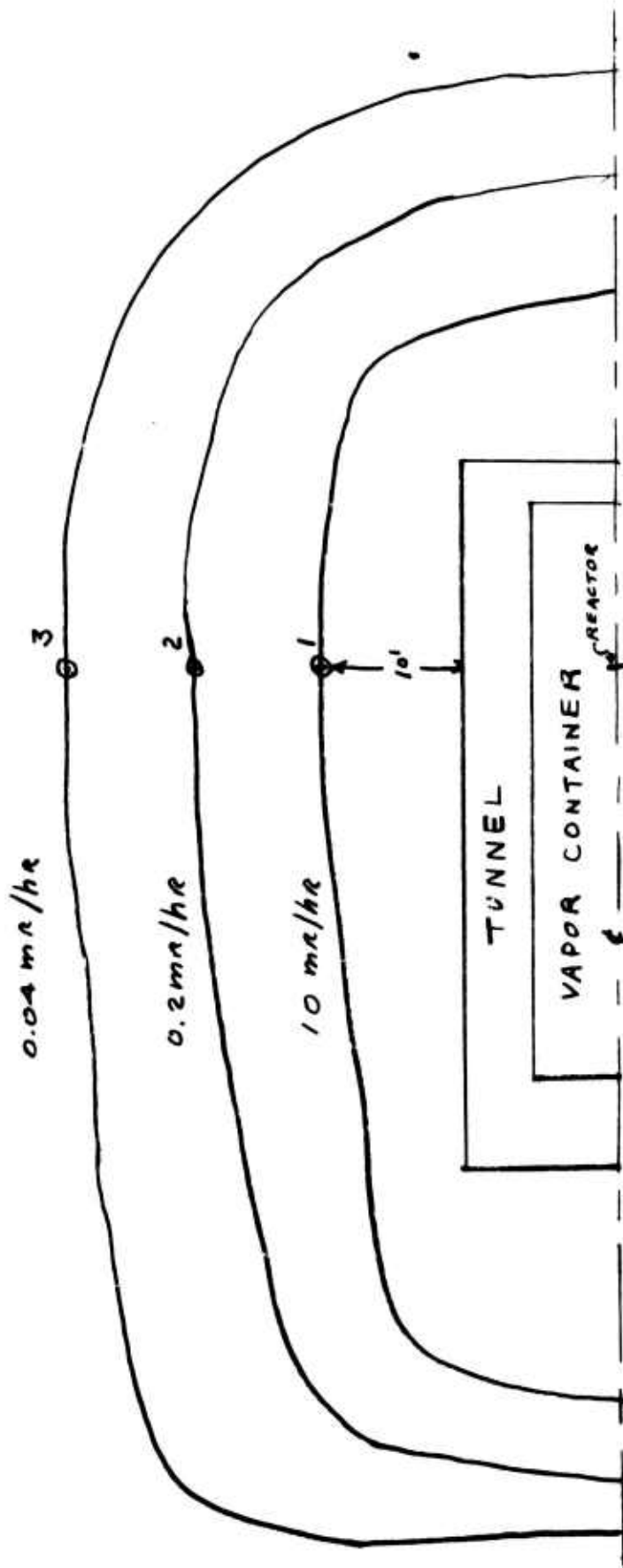


FIG. 3-5

CORE & SHIELD TANK ISODOSES AROUND VAPOR CONTAINER

FIG. 3-6
 CORE AND SHIELD TANK ISODOSE LINES
 ON SURFACE OF ICECAP (PLANE 1)

OPERATING AT 10 Mw



POINT 1 IS 10 FEET FROM TUNNEL FACE
 POINT 2 IS 20 FEET FROM TUNNEL FACE
 POINT 3 IS 30 FEET FROM TUNNEL FACE
 DIMENSIONS TAKEN FROM
 DWG. MD2M11, SECTION A

3.5 Dose Rates Around the Vapor Container after Shutdown

The basic equation used to calculate dose rates around the vapor container after shutdown is Eq. 3.8 of Section 3.3.1.

From Fig. 2.1 of Section 2.3.5 the dose rate just outside the shield tank is 50 mr/hr. at 8 hrs. after shutdown. An average gamma energy of 2 Mev was assumed. The 50 mr/hr. dose rate was attenuated through the vapor container with no distance attenuation as follows:

$$(B)(e^{-b})(50 \text{ mr/hr.}) = \text{dose rate outside vapor container}$$

$$\mu_{\text{Fe}} = 0.336 \text{ cm}^{-1} \text{ for 2-Mev gammas}$$

$$b = 0.75 \text{ inch} \times 2.54 \text{ cm/inch} \times 0.336 \text{ cm}^{-1} = 0.64$$

$$B = 1.5$$

$$D_1 = 1.5 \times e^{-0.64} \times 50 \text{ mr/hr} = 40 \text{ mr/hr}$$

This is the total dose rate on the surface of the vapor container between steam generator and shield tank 8 hours after shutdown. Going away from the steam generator the shield tank shadows out the sources outside the shield tank. Therefore, the shield rings have been wrapped around the core only for enough to give a dose rate of 40 mr/hr in this area.

Dose rates far from the reactor were calculated according to the following equation:

$$D_2 = B e^{-b} \left(\frac{r_1}{r_2} \right)^2 \times 40 \text{ mr/hr} \quad (3-9)$$

r_1 = distance at which 40 mr/hr dose rate was calculated
taken to be 10 ft.

r_2 = distance to point at which dose rate is to be calculated

t = snow thickness, cm

$b = \mu t$

$\mu = 0.0254 \text{ cm}^{-1}$ for 2-Mev gammas and snow $\rho = 0.517 \text{ gm/cm}^3$

Fig. 3-7 shows dose rates 8 hrs. after shutdown as a function of distance through the snow. Fig. 3-8 shows isodoses around the vapor container after shutdown.

The dose rates shown in Fig. 3-8 apply only radially around the vapor container. There is an area under the shield tank which will have a much larger dose rate and which will be inaccessible after shutdown.

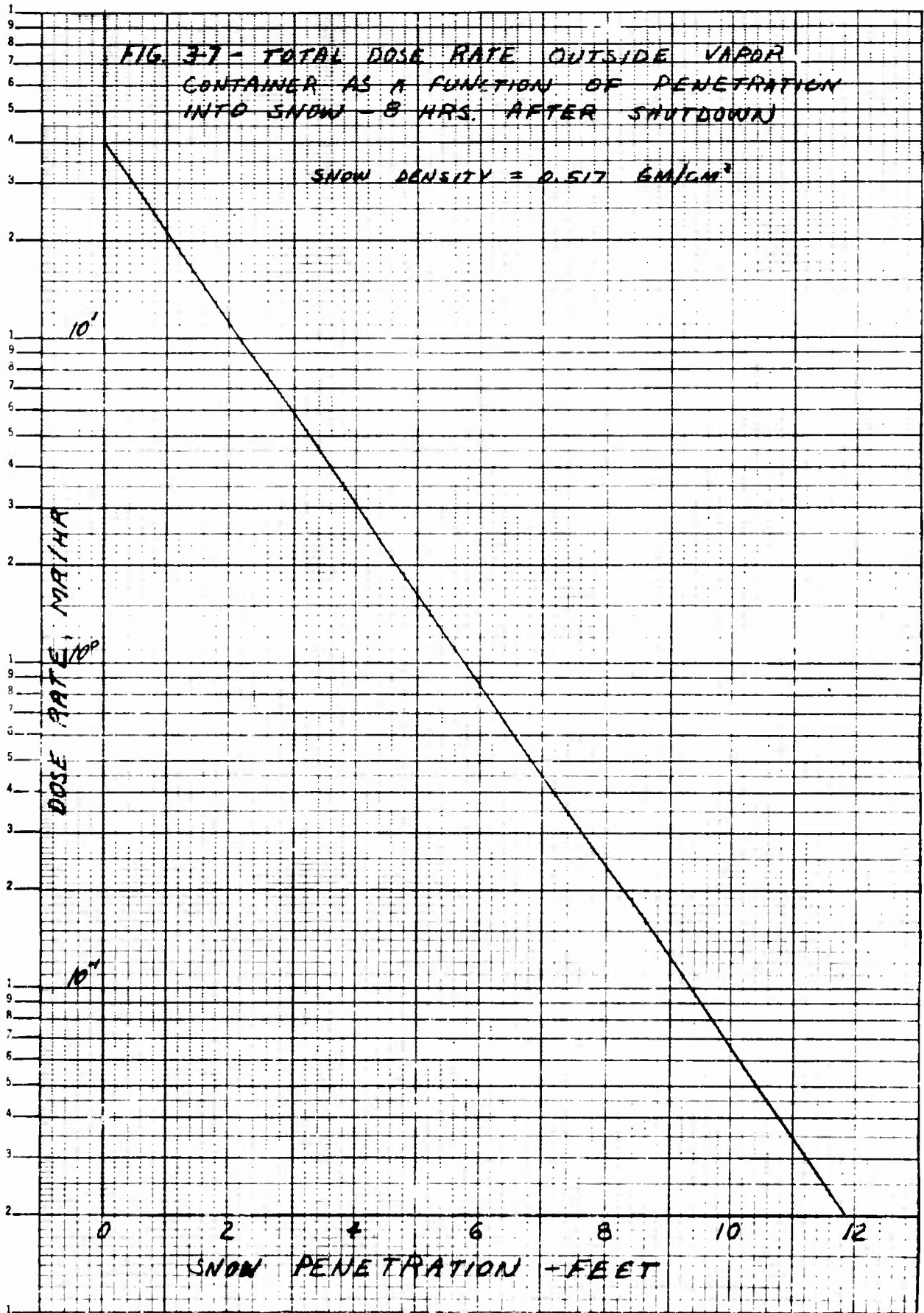
3.6 Conclusions

From the foregoing sections the necessary thickness of snow between vapor container and uncontrolled areas has been determined to be 25 feet for a vapor container located in a tunnel 44 feet deep.

From Fig. 3-6 and Fig. 3-3a it can be seen that dose rates on the surface of the ice cap fall off rapidly with distance back from the tunnel edge, being 0.04 mr/hr 30 feet back from the full diameter (24 feet) of the tunnel. Actual exclusion area on the surface of the ice cap would be determined by radiation surveys during operation. However, it may be concluded that an exclusion area extending no less than 50 feet back from all tunnel faces would be adequate and desirable. For the site layout shown in Dwg. No. M02M11 of Section A, this would give an exclusion area of about 150 x 125 feet.

FIG. 3-7 - TOTAL DOSE RATE OUTSIDE VAPOR CONTAINER AS A FUNCTION OF PENETRATION INTO SNOW - 8 HRS. AFTER SHUTDOWN

SNOW DENSITY = 0.517 GM/CM³



SCALE
8 FT.

SNOW DENSITY = 0.517 GM/CM³

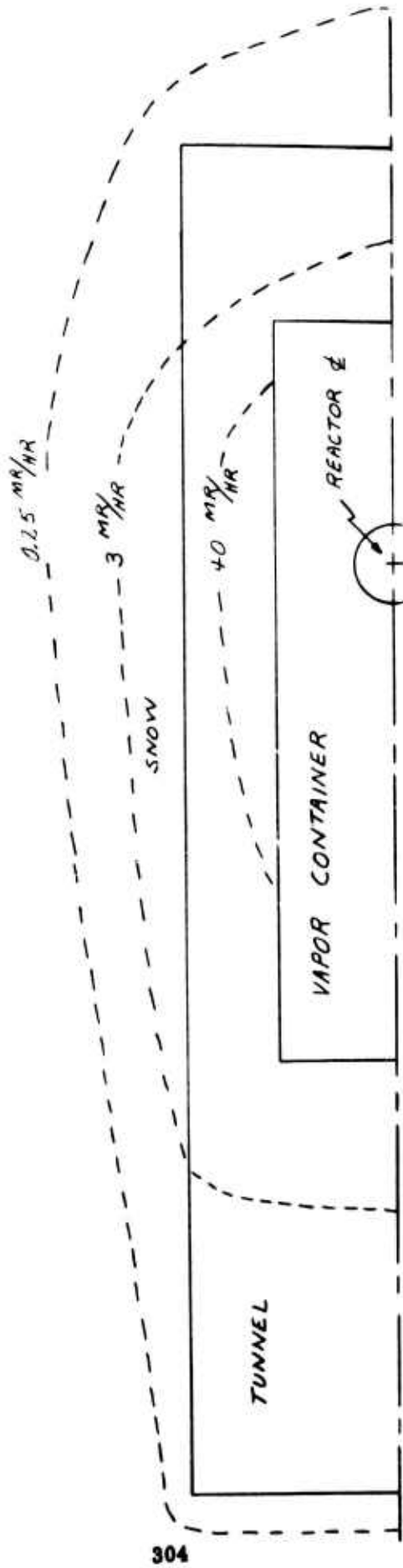


FIG. 3-8

HORIZONTAL SECTION THROUGH VAPOR CONTAINER CENTERLINE
SHOWING ISODOSE LINES AROUND CONTAINER - 8 HOURS
AFTER SHUT DOWN

4.0 Spent Fuel Shielding

Provision must be made in the Skid Mounted installation for removing the spent core and storing it until it is shipped off the ice cap. The spent fuel shielding must do the following:

- 1) Protect personnel from the complete core whether in the pressure vessel or in the spent fuel pit.
- 2) Protect personnel from the single element being transferred from the pressure vessel to the spent fuel pit.

4.1 Water Tank Above Core

The water tank above the core performs the function of shielding personnel transferring spent fuel elements from the pressure vessel to the spent fuel pit and also provides a medium for removing decay heat from the spent core in the pressure vessel. The actual height of water above the core is determined from shielding considerations.

To arrive at a necessary water depth above the core, it was first assumed that the allowable dose rate at the surface of the water would be received during the transfer of individual fuel elements since the fuel elements must be raised about seven feet above the core during transfer. Then the dose rate from the complete core was checked through the column of water.

4.1.1 Calculation Model

Because of the fairly large distance between the surface of the water tank above the core and the top of the core itself, the conventional methods for calculating dose rates above cylinder ends fail to give accurate answers. Therefore, the core was treated as a point source.

In calculating the dose rate from the individual fuel elements the same difficulty was encountered. However, since the fuel element height is much greater than its width, the fuel element was divided into eight smaller sections (approximately cubes) and dose rates calculated for each section. A correction factor was then applied to account for self-absorption in the small sections.

Calculations were made on the basis of 10 MW operation for infinite time; time after shutdown was 1 day.

4.1.2 Dose Rate During Element Transfer

The individual fuel element was divided into eight sections, each section having the dimensions 2.750 x 2.863 inches. The total dose rate from the eight sections one foot above the surface of

the water directly above the element was calculated using the following equation:

$$D = \sum_{j=0}^7 \sum_{i=1}^7 \frac{S_{v_i} V e^{-b_{ij}} B_i}{4\pi r^2 K_{D_i}}$$

S_{v_i} = specific activity of i th energy group Mev/sec-cm³

V = Volume of a section, 3.66×10^2 cm³

r = 244 cm (7 ft of water plus 1 ft)

K_{D_i} = factor for converting energy flux of i th energy group to dose rate

$$b_{ij} = \mu_{H_2O} \times t_{H_2O} + \mu_{\text{fuel element}} \times j \times 2.75 \text{ inches} \times 2.54 \frac{\text{cm}}{\text{inch}}$$

From the definition of b_j it can be seen that the dose rate from each section is attenuated through all the sections above it. Geometric attenuation, however, was kept constant (for ease of calculation) by using the minimum r for the eight sections.

Table 4-1 contains details of the calculation of the single element calculation.

Dose rates for the eight sections and total dose rate follow:

| Section | | Dose Rate (mr/hr) |
|---------|--------------------------------------|---|
| 1 | (top 2.75 inches of fuel element) | 46.25 |
| 2 | | 26.10 |
| 3 | | 14.24 |
| 4 | | 7.23 |
| 5 | | 3.70 |
| 6 | | 2.00 |
| 7 | | 1.05 |
| 8 | (bottom 2.75 inches of fuel element) | 0.57 |
| | | <hr style="width: 10%; margin-left: auto; margin-right: 0;"/> |
| | | 101.14 |

Table 4-1

Calculation of Dose Rate from Single Fuel Element

$$t_{H_2O} = 7 \text{ ft.} = 214 \text{ cm}$$

$$V_{\text{Section}} = 3.66 \times 10^2 \text{ cm}^3$$

$$R = 8 \text{ ft.} = 244 \text{ cm}$$

$$\mu_{\text{fuel element}} = \mu_{\text{core}} = \mu_c$$

Section 1

| Group | $S_v, \frac{\text{Mev}}{\text{sec-cm}^3}$ | μ_{H_2O} | b_{H_2O} | e^{-b} | $B_{H_2O} (b)$ |
|-------|---|--------------|------------|-----------------------|----------------|
| 4 | 2.7×10^{11} | 0.055 | 11.78 | 7.7×10^{-6} | 19 |
| 5 | 7.05×10^9 | 0.049 | 10.48 | 2.8×10^{-5} | 11.8 |
| 6 | 2.35×10^{10} | 0.044 | 9.41 | 8.05×10^{-5} | 9.2 |

| Group | K_D | $\frac{VS_v}{4\pi R^2 K_D}$ | D, mr/hr |
|-------|--------------------|-----------------------------|-------------|
| 4 | 6.05×10^5 | 2.18×10^2 | 32 |
| 5 | 6.5×10^5 | 5.31×10^0 | 1.75 |
| 6 | 6.8×10^5 | 1.69×10^1 | <u>12.5</u> |
| | | | 46.25 |

Section 2

| Group | μ_c | b_2 | $b_3 = \frac{b_2}{b_{H_2O}}$ | $B_{H_2O} (b_3)$ | e^{-b_3} | D, $\frac{\text{mr}}{\text{hr}}$ |
|-------|---------|-------|------------------------------|------------------|-----------------------|----------------------------------|
| 4 | 0.108 | 0.754 | 12.534 | 22 | 3.6×10^{-6} | 17.3 |
| 5 | 0.0941 | 0.658 | 11.138 | 13 | 1.45×10^{-5} | 1.0 |
| 6 | 0.0879 | 0.620 | 10.03 | 10.5 | 4.4×10^{-5} | <u>7.8</u> |
| | | | | | | 26.1 |

$$b_2 = \mu_c \times 2.75'' \times 2.54 \frac{\text{cm}}{\text{in}}$$

Table 4-1 (continued)

Section 3

| Group | b_2 | $b_3 = b_2 / b_{H_2O}$ | $B_{H_2O}(b_3)$ | e^{-b_3} | D, mr/hr |
|-------|-------|------------------------|-----------------|----------------------|-------------|
| 4 | 1.508 | 13.288 | 23 | 1.8×10^{-6} | 9.02 |
| 5 | 1.316 | 11.80 | 14 | 7.5×10^{-6} | 0.56 |
| 6 | 1.240 | 10.65 | 11.5 | 2.4×10^{-5} | <u>4.66</u> |
| | | | | | 14.25 |

$b_2 = 2 \times b_2$ of Section 2

Section 4

| Group | b_2 | b_3 | $B_{H_2O}(b_3)$ | e^{-b_3} | D, mr/hr |
|-------|-------|-------|-----------------|----------------------|-------------|
| 4 | 2.262 | 14.04 | 24.6 | 8×10^{-7} | 4.29 |
| 5 | 1.974 | 12.45 | 14.5 | 3.9×10^{-6} | 0.30 |
| 6 | 1.860 | 11.27 | 12.0 | 1.3×10^{-5} | <u>2.64</u> |
| | | | | | 7.23 |

Section 5

| Group | b_2 | b_3 | $B_{H_2O}(b_3)$ | e^{-b_3} | D, mr/hr |
|-------|-------|-------|-----------------|----------------------|-------------|
| 4 | 3.016 | 14.8 | 26.5 | 3.8×10^{-7} | 2.2 |
| 5 | 2.632 | 13.11 | 16 | 2×10^{-6} | 0.17 |
| 6 | 2.480 | 11.89 | 12.4 | 6.8×10^{-6} | <u>1.43</u> |
| | | | | | 3.70 |

Section 6

| Group | b_2 | b_3 | $B_{H_2O}(b_3)$ | e^{-b_3} | D, mr/hr |
|-------|-------|-------|-----------------|-----------------------|-------------|
| 4 | 3.770 | 15.55 | 28.5 | 1.75×10^{-7} | 1.09 |
| 5 | 3.290 | 13.77 | 16.7 | 1.01×10^{-6} | 0.09 |
| 6 | 3.100 | 12.51 | 13 | 3.75×10^{-6} | <u>0.82</u> |
| | | | | | 2.00 |

Table 4-1 (continued)

Section 7

| Group | b_2 | b_3 | $B_{H_2O}(b_3)$ | e^{-b_3} | D, mr/hr |
|-------|-------|-------|-----------------|----------------------|-------------|
| 4 | 4.524 | 16.30 | 30.5 | 8.2×10^{-8} | 0.54 |
| 5 | 3.948 | 14.43 | 17.5 | 5.3×10^{-7} | 0.05 |
| 6 | 3.720 | 13.13 | 13.7 | 2×10^{-6} | <u>0.46</u> |
| | | | | | 1.05 |

Section 8

Group

| | | | | | |
|---|-------|-------|------|-----------------------|-------------|
| 4 | 5.278 | 17.06 | 33 | 4×10^{-8} | 0.29 |
| 5 | 4.606 | 15.09 | 18.4 | 2.8×10^{-7} | 0.03 |
| 6 | 4.340 | 13.75 | 14.5 | 1.02×10^{-6} | <u>0.25</u> |
| | | | | | 0.57 |

The preceding calculation does not take into account the effect of self-absorption in the sections of the fuel elements. Equation 4-1 was taken from Ref. 21 to account for self absorption:

$$\text{S.A.} = \frac{3}{4(\mu_c a)^2} \left[\mu_c a / e^{-2\mu_c a} - \frac{1}{2\mu_c a} (1 - e^{-2\mu_c a}) \right] \quad (4-1)$$

a = half height of section, 1.375 inches

μ_c = total linear absorption coefficient of core, cm^{-1}

The minimum self-absorption factor will be calculated when μ is a minimum; that is, for Group 6 which has the highest energy gamma. The self-absorption factor calculated for this group was 0.83. If this factor is applied to the dose rate calculated without self-absorption, the result is 84 mr/hr one foot above the surface of the water in the tank above the core when the top of a single fuel element is 7 feet below the surface.

4.1.3 Dose After Shutdown. (Full Core)

The dose rate from the complete core on the surface of the water above the core was calculated using the following equation:

$$D = \sum_{i=1}^7 \frac{S_{v_i} V e^{-b_i} B_i}{4\pi r^2 K_{D_i}}$$

V = core volume, $1.15 \times 10^5 \text{ cm}^3$

b_i = $\mu_i \times 519 \text{ cm}$ (17 ft of water above core)

r = 519 cm

(See Section 4.1.2 for definition of symbols)

No self-absorption correction was made. The calculated dose rate was $2.7 \times 10^{-3} \text{ mr/hr}$.

Table 4-2 contains details of the calculation for the whole core.

Table 4-2

Dose Rate above Complete Core

$$t_{H_2O} = 17 \text{ ft} = 519 \text{ cm} \approx r$$

$$r^2 = 2.69 \times 10^5$$

| Group | $S_v, \frac{\text{Mev}}{\text{sec-cm}^3}$ | H_2O | b_{H_2O} | e^{-b} | B_{H_2O} | $D, \text{mr/hr}$ |
|-------|---|--------|------------|-----------------------|------------|---|
| 4 | 2.7×10^{11} | 0.055 | 28.5 | 4.2×10^{-13} | 60 | 2.38×10^{-4} |
| 5 | 7.05×10^9 | 0.048 | 25.4 | 9.1×10^{-12} | 33 | 7.15×10^{-5} |
| 6 | 2.35×10^{10} | 0.044 | 22.8 | 1.3×10^{-10} | 24 | $\frac{2.36 \times 10^{-3}}{2.67 \times 10^{-3}}$ |

The dose rate on the walkway above the vapor container from the complete core was calculated in a manner similar to that above. It was found that the equivalent of 11 feet of water was needed between the core and the walkway to reduce the dose rate on the walkway floor to 20 mr/hr. It was also found that rays from the core could go through the tank on a slant and intercept less than this minimum of eleven feet. Where this was possible lead was placed in the tank to attenuate core gammas to the allowable level. Lead, water and steel equivalences were taken from Table 6.11 of Ref. 3.

4.1.4 Dose Rate During Transfer of Element from Shield Tank to Spent Fuel Pit

In the process of moving the spent fuel elements from the core to the spent fuel pit, a transfer cask is used to protect personnel who are handling the spent elements. The size of the single element transfer cask is based on shielding requirements. The following assumptions were used in the calculation of the required shielding.

1. Dose rate on surface of cask to be no more than 200 mr/hr.
2. Infinite operation of reactor
3. 24 hours shutdown time
4. Transfer cask to be cylindrical
5. Dose rate due to three energy groups
6. Cask to contain either one or four elements

The dose rates were calculated for a cylindrical spent fuel element transfer cask of thicknesses of 8, 10 and 12 inches. The results are given in Fig. 4-1. To limit the dose rate to 200 mr/hr on the surface of the transfer cask, 10.1 inches of lead is required for the single element cask and 10.5 inches is required for the four element cask.

4.2 Water Level in Spent Fuel Pit

At end of life, the spent fuel elements are transferred to a storage area where the elements are cooled down before being shipped for reprocessing. While the elements are in the spent fuel pit, shielding must be provided so that personnel working above the pit do not receive excessive radiation. The shielding is in the form of water placed above the spent core.

4.2.1 Calculation Model

In order to determine the shielding required for the spent fuel pit, the following assumptions were made:

1. Infinite operation at 10 MW
2. 24 hours of shutdown
3. Equivalent sphere to determine self-absorption in core
4. Point source for attenuation of gamma-rays
5. Personnel are always directly above spent core
6. Radioactive sources can be divided into four energy groups.

The self-absorption in the core was calculated using a spherical source. On the basis of equivalent volumes ($1.15 \times 10^5 \text{ cm}^3$), the radius of the equivalent sphere is 30.17 cm. From Eq. 4-1, the self-absorption factor of the core was calculated for all four energy groups (21).

The numbers used in the calculations and results are given on Table 4-3.

The fission product gammas sources are also given in Table 4-3 for the four energy groups. The sources were obtained from NDA-27-39 (4) for infinite operation and 24 hours of shutdown.

The required amount of shield water above the spent core was based on the attenuation of gamma rays from a point source using equation 4-2 for all four energy groups.

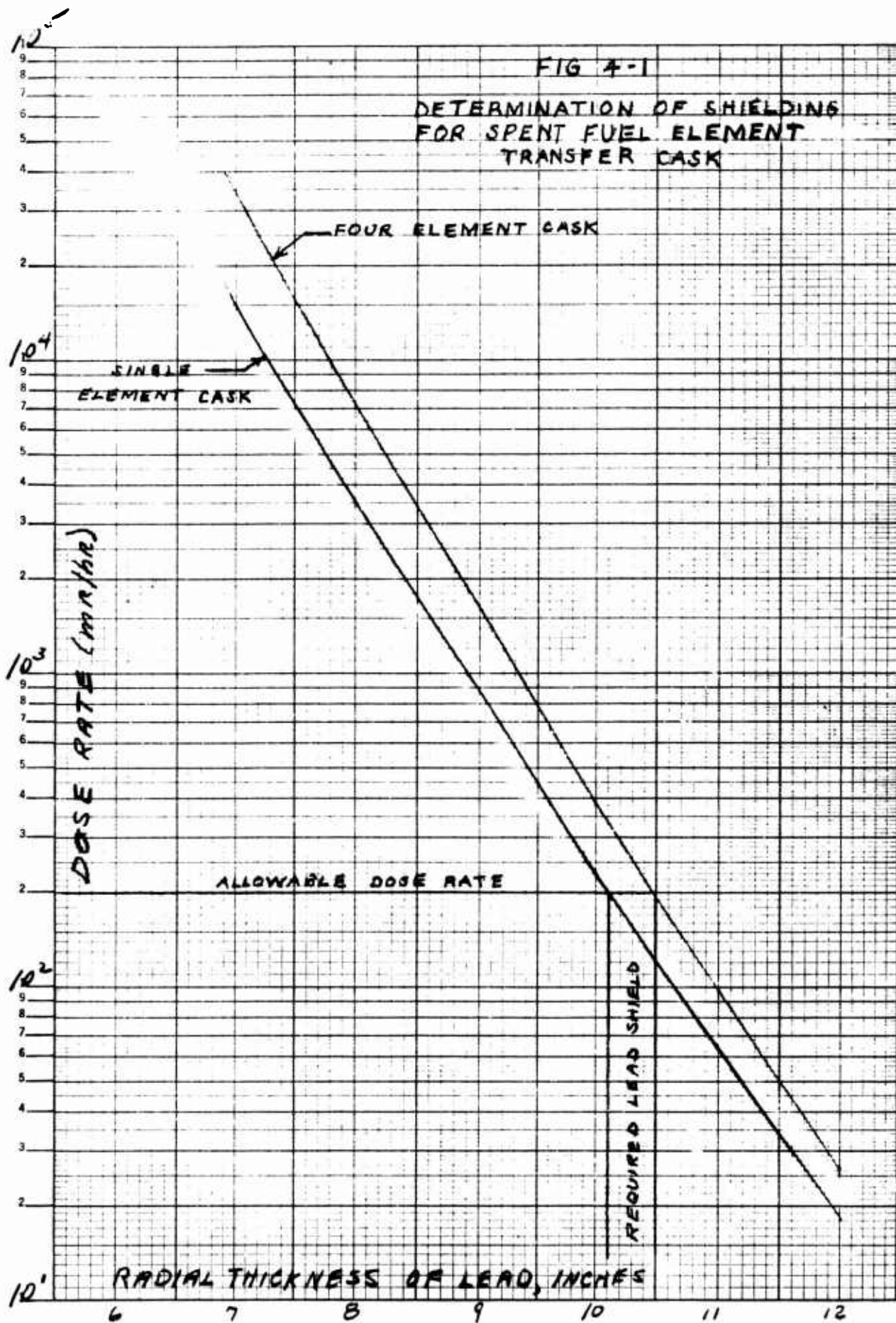


Table 4-3

Calculation of Spent Fuel Pit Shielding

| | Energy Group | | |
|--|-------------------------|------------------------|------------------------|
| | IV | V | VI |
| E(Mev) | 1.6 | 2.1 | 2.5 |
| $\mu_{\text{core}} (\text{cm}^{-1})$ | 0.108 | 0.0941 | 0.0879 |
| $(\mu r)_{\text{core}}$ | 3.258 | 2.839 | 2.652 |
| $SA(\mu r)_{\text{core}}$ | 0.219 | 0.247 | 0.263 |
| $\mu_{\text{H}_2\text{O}} (\text{cm}^{-1})$ | 0.055 | 0.048 | 0.0438 |
| S(Mev/sec-watt) | 3.1×10^9 | 8.1×10^7 | 2.7×10^8 |
| S_0 (Mev/sec) | 3.1×10^{16} | 8.1×10^{14} | 2.7×10^{15} |
| $C_e (\frac{\gamma/\text{cm}^2\text{-sec}}{\text{mr/hr}})$ | 365 | 315 | 255 |
| $(b_1)_1$ | 18.44 | 16.43 | 14.75 |
| $(b_1)_2$ | 21.79 | 19.42 | 17.43 |
| $(b_1)_3$ | 20.12 | 17.92 | 16.09 |
| B_1 | 41.0 | 21.8 | 15.9 |
| B_2 | 53.0 | 26.8 | 19.1 |
| B_3 | 47.0 | 24.2 | 17.6 |
| $e^{-(b_1)_1}$ | 9.808×10^{-9} | 7.318×10^{-8} | 3.927×10^{-7} |
| $e^{-(b_1)_2}$ | 3.441×10^{-10} | 3.68×10^{-9} | 2.693×10^{-8} |
| $e^{-(b_1)_3}$ | 1.828×10^{-9} | 1.65×10^{-8} | 1.028×10^{-7} |
| D_1 (mr/hr) | 5.294 | 0.717 | 11.847 |
| D_2 (mr/hr) | 0.172 | 0.032 | 0.699 |
| D_3 (mr/hr) | 0.950 | 0.151 | 2.884 |

$a_1 = 11 \text{ feet}$

$a_2 = 13 \text{ feet}$

$a_3 = 12 \text{ feet}$

$(D_1)_T = 17.858 \text{ mr/hr}$

$(D_2)_T = 0.903 \text{ mr/hr}$

$(D_3)_T = 3.985 \text{ mr/hr}$

$$D(E) = \frac{B(E) SA(E) S_o(E) e^{-b_1(E)}}{4\pi a^2} \quad (4-2)$$

where

$D(E)$ = dose at desired point, mr/hr

$SA(E)$ = self-absorption factor

$B(E)$ = dose buildup factor

$S_o(E)$ = source strength of point source, gammas/sec

a = distance from point source to dose point

$b_1(E) = \mu_{H_2O}(E) t_{H_2O}$

$\mu_{H_2O}(E)$ = linear absorption coefficient of water, cm^{-1}

t_{H_2O} = thickness of water shield

The calculation of the dose rate at the top of the spent fuel pit for 11, 12, and 13 feet of shield water for all energy groups is given in Table 4-3.

4.2.2 Dose Rate on Top of Spent Fuel Pit

The dose rate was calculated for 11, 12, and 13 feet of shield water. For 11 feet of shield water, the dose rate was 17.858 mr/hr on top the spent fuel pit. With 12 and 13 feet of shield water, the dose rates are 3.985 and 0.903 mr/hr respectively. The results of the calculation are given in Fig. 4-2. For a dose rate no higher than 5 mr/hr on the top of the spent fuel pit 24 hours after shutdown, approximately 12 feet of shield water is required above the center of the core.

4.3 Shielding for Shipping Cask

It was decided to use the spent fuel shipping cask that was designed for the APPR-1. The design analysis was presented in AP Memo 63 (22). The following assumptions were used in the calculation:

1. Fuel element activity 1.5 times the average activity
2. Six spent fuel elements per shipping cask

10²

FIG 4-2
DETERMINATION OF HEIGHT
OF WATER ABOVE FUEL
ELEMENTS IN SPENT FUEL PIT

NOTE:

- 1. INFINITE OPERATION
- 2. 24 HRS AFTER SHUTDOWN

DOSE RATE, mR/hr

10¹

HEIGHT OF WATER ABOVE CORE, FEET

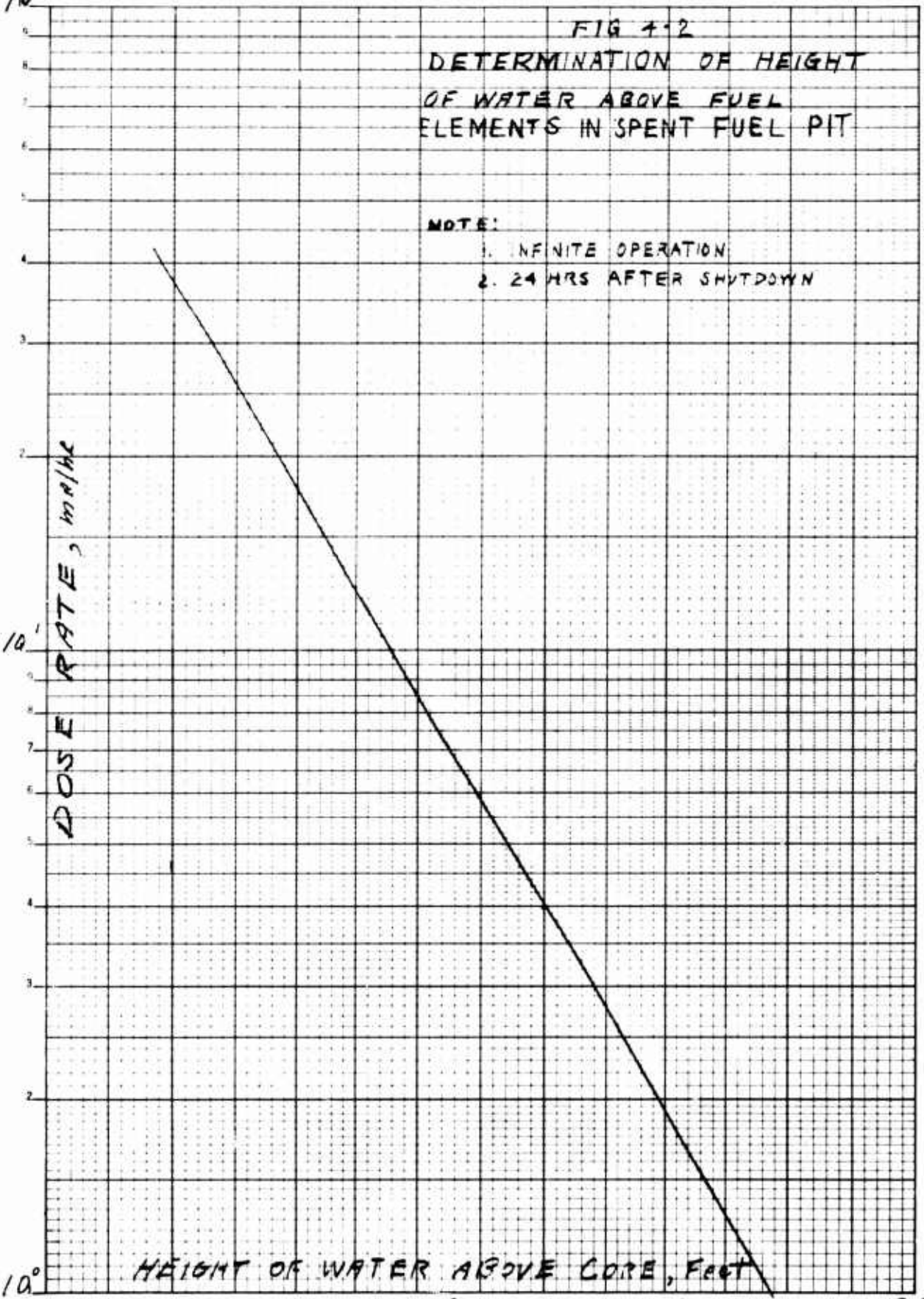
10⁰

10.5

11.5

12.5

13.5



3. Reactor operation time was taken as infinite

4. Four shutdown times: 10, 20, 30, and 90 days

The dose rates on the surface of the shipping cask and one meter from surface is given in Table 4-4 for different lead thicknesses and the four cooling times.

From the calculated results, 9.8 inches of lead is needed so that the dose rate one meter from the surface is less than 10 mr/hr with a cooling time of 90 days. The dose rate on the surface of the spent fuel shipping cask will be under 40 mr/hr for the conditions stated in the previous section.

TABLE 4-4

Radial Dose Rates - Spent Fuel Cask

| Lead Thickness Inches | Dose Rate in mr/hr at Surface after Shutdown | | | | Dose Rate in mr/hr one meter from Surface after Shutdown | | | |
|--------------------------|---|--------------------------|--------------------------|--------------------------|---|--------------------------|--------------------------|--------------------------|
| | <u>10</u> <u>days</u> | <u>20</u> <u>days</u> | <u>30</u> <u>days</u> | <u>90</u> <u>days</u> | <u>10</u> <u>days</u> | <u>20</u> <u>days</u> | <u>30</u> <u>days</u> | <u>90</u> <u>days</u> |
| 9.5 | - | - | - | 91.2 | - | - | - | 14.55 |
| 10.0 | 660 | 497 | 348 | 40.9 | 138 | 103 | 71 | 7.92 |
| 10.5 | 318 | 240 | 168 | 18.6 | 74 | 56 | 39 | 4.33 |
| 11.0 | 161 | 123 | 86 | - | 41 | 31 | 22 | - |
| 11.5 | 83 | 64 | 45 | - | 23 | 17 | 12 | - |
| 12.0 | 45.7 | 35.6 | 25.2 | - | 12.7 | 9.7 | 6.8 | - |

4.4 Conclusions

From the foregoing sections it may be concluded that adequate shielding has been designed for the spent core and that core removal operations may be carried out within the allowable dose rate limits of Section 1.0.

5.0 Heat Release Distribution

The reactor vessel as originally designed in APAE-33 (23) was based on a two inch thick vessel wall located 6.15 cm. from the edge of the core. In this design, there was to be no thermal shields between the core and the reactor vessel as can be seen in Drawing AEL-335 of APAE-33 (23). This was proposed because of the necessity of compactness. However, detailed calculations on this proposed design showed that the vessel was overstressed due to gamma heating. In order to decrease the stress to within the allowable stress, work was performed on various configurations. Table 5.1 gives the list of configurations that were investigated.

The gamma heating was calculated for all seven cases at a power output of 10 MW. Case 7 is the configuration that was finally selected.

5.1 Reactor Vessel Wall at Midplane

5.1.1. Calculation Model

The calculation of the gamma heating in the reactor vessel was based on a cylindrical core with the thermal shields and the reactor vessel as cylindrical shells. The calculation was performed at the mid-plane of the core and is divided into core and secondary gammas. The complete calculation was performed by an IBM 650 program (12). The code is divided into 4 parts. The first routine calculates the source strength, S_c , and the macroscopic cross section of source material, μ_c . The attenuation of core gammas is then computed by a second routine utilizing μ_c and S_c and material and geometrical specification set up by a third routine. The results of these operations is the volumetric heat release, H (BTU/in³ - sec), in the reactor vessel. The calculation of the gamma attenuation is based on equation 5-1.

TABLE 5-1

Reactor Vessel Configurations

| Case # | Reactor Vessel | | | Thermal Shield | | |
|--------|----------------|--------------------------------|-----------------|----------------|-----------|-------------------|
| | Inside Dia. | Thickness | Material | Inside Dia. | Thickness | Material |
| 1 | 25" | 2" | 304SS | | | None |
| 2 | 25" | 1-3/4" | 304SS | | | None |
| 3 | 28.5" | 2" | 304SS | 23.5" | 2" | 304-SS |
| 4 | 30.5" | 2" | 304SS | 23.5" | 3" | 304-SS |
| 5 | 30.5" | 2" | 304SS | 23.5" | 3" | Borated 304-SS |
| 6 | 37.75" | 1/8" Clad/ 2-3/8" Vessel | 304SS SA-212 | 33" | 1" | 304-SS |

TABLE 5-1 (Cont'd)

Reactor Vessel Configurations

| Case # | Reactor Vessel | | | Thermal Shield | | |
|--------|----------------|-----------------------------|------------------|----------------|-----------|----------|
| | Inside Dia. | Thickness | Material | Inside Dia. | Thickness | Material |
| 7 | 37.75" | 1/8" Clad/ 2 3/8" Vessel | 304-SS SA-212 | 23.5" | 2" | 304-SS |

$$H(E) = \frac{C_e B_a S_c R_o^2}{2(a/z)} F[\theta, b_2] \quad (5-1)$$

where B_a = Energy absorption build-up factor

S_c = Source strength of core, (cm⁻³ - sec⁻¹)

R_o = Radius of volume source, cm

a = distance from source to heat release point, cm

z = effective self-attenuation distance, cm

$$F[\theta, b_2] = \int_0^{\theta} e^{-t_2} \sec \theta' \, d\theta'$$

$$\theta = \tan^{-1} \left(\frac{h/2}{a/z} \right), \text{ degrees}$$

h = height of volume source, cm

$$b_2 = b_1 / \mu_c z$$

$$b_1 = \sum_i \mu_1 t_1$$

μ_c = Macroscopic cross section of core, cm⁻¹

μ_1 = Macroscopic cross section of i th shield, cm⁻¹

t_1 = Thickness of i th shield

$$C_e = H(E) / \phi_\gamma(E) = (2.488 \times 10^{-15} \frac{\text{BTU-cm}^3}{\text{Mev-in}^3}) \mu_a(E) E$$

$\phi_\gamma(E)$ = Gamma flux, photons/cm²-sec

$\mu_a(E)$ = energy absorption cross section for vessel, cm⁻¹

E = Energy of gamma, Mev

The second contribution to the volumetric heat release in the reactor vessel is due to capture and decay gammas emanating from various components of the shield. This calculation is also computed by the IBM 650 (12) and is based on equation 5-2.

$$H(E) = \frac{C_e B_a S_v}{2 \mu_s} [E_2(b_1) - E_2(b_3)] \quad (5-2)$$

where S_v = source strength of volume source, (cm⁻³-sec⁻¹)

μ_s = macroscopic cross section of source material, cm⁻¹

$$E_2(b) = b \int_b^{\infty} \frac{e^{-t}}{t^2} dt$$

$$b_3 = b_1 / \mu_s h$$

h = thickness of source slab, cm

5.1.2 Application to APFR-1

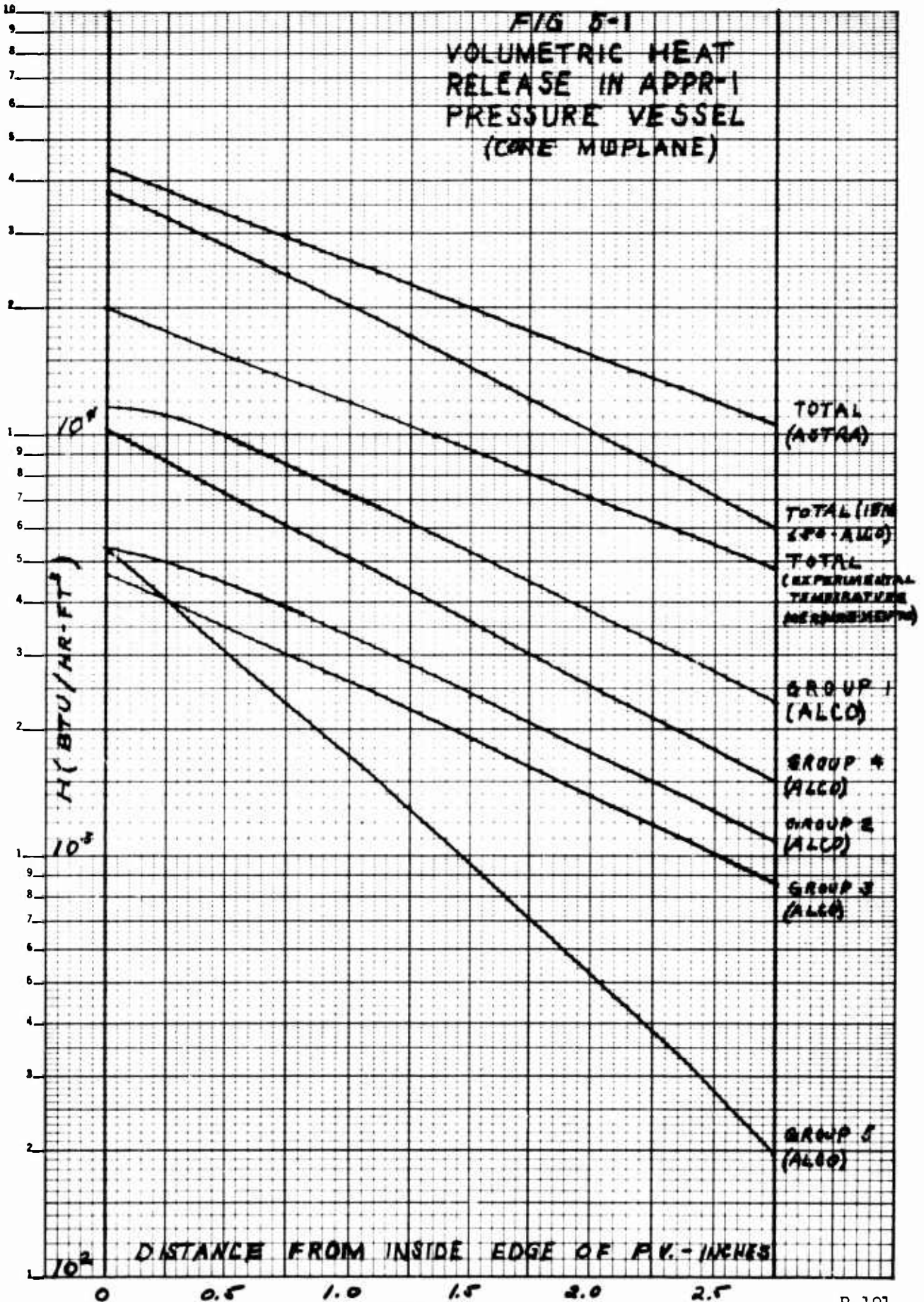
The volumetric heat release was calculated for the thermal shield and the reactor vessel of the APFR-1 by ASTRA (24). From experimental temperature measurements on the APFR-1 reactor vessel, a volumetric heat release was calculated. To compare with the above quantities, the heat release rate was calculated using the IBM 650 codes. The values of the volumetric heat releases on the inside surface of the reactor vessel and thermal shield is given in Table 5-2.

Table 5-2

| Volumetric Heat Release in APFR-1 Thermal Shield and Reactor Vessel | | |
|---|--------------------------------|---------------------------------|
| | Reactor Vessel | Thermal Shield |
| ASTRA | 43,300 BTU/Ft ³ -Hr | 249,000 BTU/Ft ³ -Hr |
| Alco (IBM 650) | 37,000 BTU/Ft ³ -Hr | 162,000 BTU/Ft ³ -Hr |
| Experimental Temperature measurements | 20,000 BTU/Ft ³ -Hr | None |

From the above table, the IBM 650 calculation gives results closer to the experimentally inferred number than does the ASTRA computation. The results from the machine calculation are within a factor of two to the volumetric heat release based on experimental temperature measurements. The heat release distribution through the reactor vessel is given in Fig. 5-1, for all calculation models. This figure shows that the machine calculation gives a reliable answer.

FIG 5-1
 VOLUMETRIC HEAT
 RELEASE IN APPR-1
 PRESSURE VESSEL
 (CORE MIDPLANE)



5.1.3 Calculated Distribution (Core gamma)

The gammas emanating from the core is divided into 5 energy groups as given in Table 5-3.

Table 5-3

Energy Groups of Gammas

| Group | Energy (Mev) |
|-------|----------------|
| 1 | Greater than 7 |
| 2 | 5-7 |
| 3 | 3-5 |
| 4 | 1-3 |
| 5 | less than 1 |

The gamma heating in the reactor vessel was calculated for all cases. The contribution from each energy group from the core is given in Table 5-4, for the final configuration, case 7.

5.1.4 Calculated Distribution (secondary gammas)

For each calculation of the distribution due to core gammas, the distribution due to secondary gammas was computed. The results that were obtained for case 7 is given in Table 5-5 based on the same energy grouping.

5.1.5 Calculated Distribution (Total Gammas)

The total volumetric heat release is the summation of the heat release due to core and secondary gammas. The results for the final configuration, case 7, are given in Fig. 5-2 and in Table 5-6.

At the interface between the clad and the reactor vessel, the total volumetric heat release, H , is $0.01781 \text{ BTU/in}^3\text{-sec}$ or $1.108 \times 10^5 \text{ BTU/FT}^3\text{-hr}$. The distribution can be described by the following equation:

$$H = 0.0185e^{-0.67395} \times \text{BTU/in}^3\text{-sec} \quad (5-3)$$

The volumetric heat release distribution for the other cases are given in Table 5-7.

Table 5-4

Volumetric Heat Release in Pressure Vessel at Core Midplane Due to Core
H (BTU/IN³-sec)

| Energy (Mev) | Inside Surface of Clad | Interface Between Clad & Vessel | 7/16" from Interface | 14/16" from Interface | 1-5/16" from Interface | 1-12/16" from Interface | Outside Surface of Vessel |
|--------------|------------------------|---------------------------------|------------------------|------------------------|------------------------|-------------------------|---------------------------|
| > 7 | 6.46 x10 ⁻⁴ | 5.88 x10 ⁻⁴ | 4.63 x10 ⁻⁴ | 3.51 x10 ⁻⁴ | 2.78 x10 ⁻⁴ | 2.18 x10 ⁻⁴ | 1.68 x10 ⁻⁴ |
| 5-7 | 6.28 x10 ⁻⁴ | 5.84 x10 ⁻⁴ | 4.57 x10 ⁻⁴ | 3.58 x10 ⁻⁴ | 2.80 x10 ⁻⁴ | 2.21 x10 ⁻⁴ | 1.72 x10 ⁻⁴ |
| 3-5 | 7.8 x10 ⁻⁴ | 7.25 x10 ⁻⁴ | 5.83 x10 ⁻⁴ | 4.65 x10 ⁻⁴ | 3.74 x10 ⁻⁴ | 2.91 x10 ⁻⁴ | 2.26 x10 ⁻⁴ |
| 1-3 | 3.534x10 ⁻³ | 3.263x10 ⁻³ | 2.844x10 ⁻³ | 2.358x10 ⁻³ | 1.920x10 ⁻³ | 1.493x10 ⁻³ | 1.142x10 ⁻³ |
| < 1 | 1.922x10 ⁻³ | 1.675x10 ⁻³ | 1.781x10 ⁻³ | 1.424x10 ⁻³ | 9.97 x10 ⁻⁴ | 6.48 x10 ⁻⁴ | 4.07 x10 ⁻⁴ |
| Total | 7.51 x10 ⁻³ | 6.835x10 ⁻³ | 6.128x10 ⁻³ | 4.956x10 ⁻³ | 3.849x10 ⁻³ | 2.871x10 ⁻³ | 2.115x10 ⁻³ |

Table 5-5

Volumetric Heat Release in Pressure Vessel at Core Midplane Due to Secondary Gammas
H (BTU/IN³-sec)

| Energy (MeV) | Inside Surface of Clad | Interface Between Clad & Vessel | 7/16" from Interface | 14/16" from Interface | 1-5/16" from Interface | 1-12/16" from Interface | Outside Surface of Vessel |
|--------------|--------------------------|---------------------------------|--------------------------|--------------------------|--------------------------|--------------------------|---------------------------|
| >7 | 4.140 x 10 ⁻³ | 6.441 x 10 ⁻³ | 4.589 x 10 ⁻³ | 3.182 x 10 ⁻³ | 2.202 x 10 ⁻³ | 1.521 x 10 ⁻³ | 1.034 x 10 ⁻³ |
| 5-7 | 1.602 x 10 ⁻³ | 2.346 x 10 ⁻³ | 1.713 x 10 ⁻³ | 1.200 x 10 ⁻³ | 8.37 x 10 ⁻⁴ | 5.83 x 10 ⁻⁴ | 3.99 x 10 ⁻⁴ |
| 3-5 | 8.65 x 10 ⁻⁴ | 1.279 x 10 ⁻³ | 1.015 x 10 ⁻³ | 7.26 x 10 ⁻⁴ | 5.12 x 10 ⁻⁴ | 3.58 x 10 ⁻⁴ | 2.46 x 10 ⁻⁴ |
| 1-3 | 8.21 x 10 ⁻⁴ | 7.66 x 10 ⁻⁴ | 5.12 x 10 ⁻⁴ | 3.57 x 10 ⁻⁴ | 2.50 x 10 ⁻⁴ | 1.75 x 10 ⁻⁴ | 1.21 x 10 ⁻⁴ |
| <1 | 8.9 x 10 ⁻⁵ | 1.44 x 10 ⁻⁴ | 8.6 x 10 ⁻⁵ | 5.5 x 10 ⁻⁵ | 3.3 x 10 ⁻⁵ | 1.9 x 10 ⁻⁵ | 1.1 x 10 ⁻⁵ |
| Total | 7.517 x 10 ⁻³ | 1.098 x 10 ⁻² | 7.915 x 10 ⁻³ | 5.52 x 10 ⁻³ | 3.834 x 10 ⁻³ | 2.656 x 10 ⁻³ | 1.811 x 10 ⁻³ |

Table 5-6

Volumetric Heat Release in Pressure Vessel at Core Midplane Due to Total Gammas
H (BTU/IN³-sec)

| Energy (Mev) | Inside Surface of Clad | Interface Between Clad & Vessel | 7/16" from Interface | 14/16" from Interface | 1-5/16" from Interface | 1-12/16" from Interface | Outside Surface of Vessel |
|--------------|------------------------|---------------------------------|------------------------|-------------------------|------------------------|-------------------------|---------------------------|
| > 7 | 4.786x10 ⁻³ | 7.029x10 ⁻³ | 5.052x10 ⁻³ | 3.533x10 ⁻³ | 2.48 x10 ⁻³ | 1.739x10 ⁻³ | 1.202x10 ⁻³ |
| 5-7 | 2.230x10 ⁻³ | 2.930x10 ⁻³ | 2.170x10 ⁻³ | 1.558x10 ⁻³ | 1.117x10 ⁻³ | 8.04 x10 ⁻⁴ | 5.71 x10 ⁻⁴ |
| 3-5 | 1.645x10 ⁻³ | 2.004x10 ⁻³ | 1.598x10 ⁻³ | 1.191x10 ⁻³ | 3.86 x10 ⁻⁴ | 6.49 x10 ⁻⁴ | 4.72 x10 ⁻⁴ |
| 1-3 | 4.355x10 ⁻³ | 4.029x10 ⁻³ | 3.356x10 ⁻³ | 2.715 x10 ⁻³ | 2.17 x10 ⁻³ | 1.668x10 ⁻³ | 1.263x10 ⁻³ |
| < 1 | 2.011x10 ⁻³ | 1.819x10 ⁻³ | 1.867x10 ⁻³ | 1.479x10 ⁻³ | 1.03 x10 ⁻³ | 6.67 x10 ⁻⁴ | 4.18 x10 ⁻⁴ |
| Total | 1.503x10 ⁻² | 1.781x10 ⁻² | 1.404x10 ⁻² | 1.048x10 ⁻² | 7.683x10 ⁻³ | 5.527x10 ⁻³ | 3.926x10 ⁻³ |

FIG 5-2
VOLUMETRIC HEAT RELEASE
IN PRESSURE VESSEL-CASE 7
(CORE MIDPLANE)

| | | |
|---------|-----|-----|
| GROUP 1 | 2.7 | MEV |
| GROUP 2 | 5.2 | MEV |
| GROUP 3 | 3.5 | MEV |
| GROUP 4 | 1.8 | MEV |
| GROUP 5 | 4.1 | MEV |

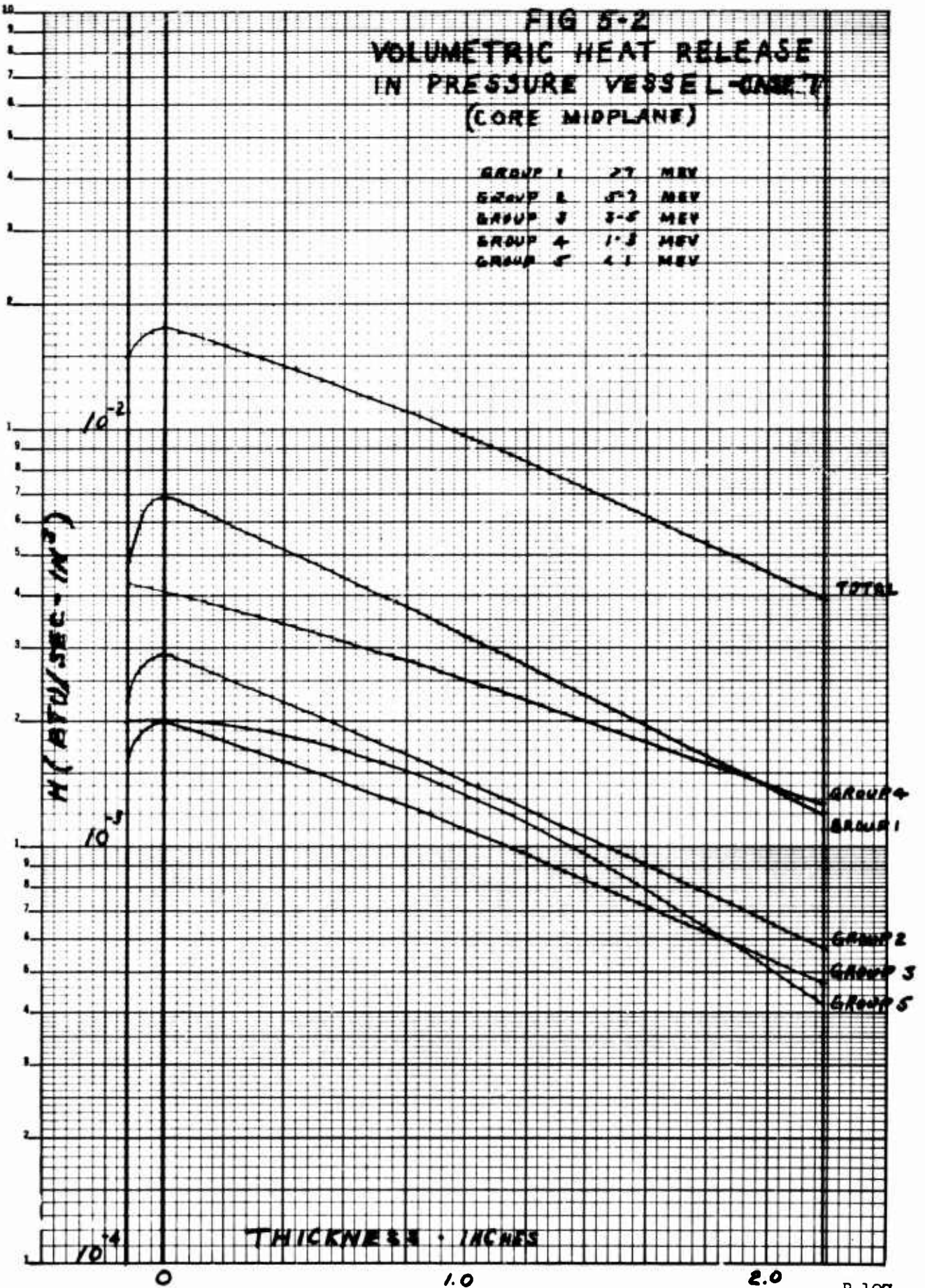


Table 5-7

Volumetric Heat Release Distributions for All Configurations

| <u>Case #</u> | <u>Equation</u> | <u>Average Heat Release</u> |
|---------------|--|--|
| 1 | $H = 0.1338e^{-0.762x} \text{ BTU/in}^3\text{-sec}$ | $\bar{H} = 0.0688 \text{ BTU/in}^3\text{-sec}$ |
| 2 | $H = 0.1338e^{-0.762x} \text{ BTU/in}^3\text{-sec}$ | $\bar{H} = 0.0741 \text{ BTU/in}^3\text{-sec}$ |
| 3 | $H = 0.0308e^{-0.6611x} \text{ BTU/in}^3\text{-sec}$ | $\bar{H} = 0.0171 \text{ BTU/in}^3\text{-sec}$ |
| 4 | $H = 0.0185e^{-0.6453x} \text{ BTU/in}^3\text{-sec}$ | $\bar{H} = 0.0104 \text{ BTU/in}^3\text{-sec}$ |
| 5 | $H = 0.015e^{-0.5736x} \text{ BTU/in}^3\text{-sec}$ | $\bar{H} = 0.0089 \text{ BTU/in}^3\text{-sec}$ |
| 6 | $H = 0.0341e^{-0.6868x} \text{ BTU/in}^3\text{-sec}$ | $\bar{H} = 0.0176 \text{ BTU/in}^3\text{-sec}$ |
| 7 | $H = 0.0185e^{-0.674x} \text{ BTU/in}^3\text{-sec}$ | $\bar{H} = 0.0097 \text{ BTU/in}^3\text{-sec}$ |

The thermal stress in the reactor vessel due to gamma heating was calculated on the basis of the above operations.

5.2 Axial Heat Distribution in Reactor Vessel Wall

A calculation was made to establish the heat release distribution at various axially positions in the vessel. The heat release distribution was calculated in the outlet nozzle and the flange above the core to facilitate the thermal stress calculations in these members.

5.2.1 Outlet Nozzle

The outlet nozzle is located about 6 inches below the bottom of the core. The average thickness of the nozzle is 10 inches.

The machine calculations of core gamma attenuation is set up to determine the heat distribution at the midplane of the core and therefore can not be used axially (12). A simplified model was used to calculate the volumetric heat release as a function of axial position as given in equation 5-4.

$$H_a = H_m e^{-\sum_i \mu_1 t_1 (1 - \sec \psi)} \quad (5-4)$$

where H_a = Volumetric heat release at any axial position, BTU/in³-sec

H_m = Volumetric heat release Core midplane, BTU/in³-sec

μ_1 = macroscopic cross-section of i^{th} shield, cm⁻¹

t_1 = thickness of i^{th} shield, cm

$\psi = \tan^{-1} \left(\frac{h}{a/R_o} \right)$, degrees

R_0 = Radius of cylinder source, cm

a = Distance from source to heat release point, cm

h' = Axial distance above midplane of core, cm

The heating at the inside surface of the nozzle calculated from equation 5-4 is 18,000 BTU/hr-ft³. At the midplane of the core, the heat release at the inside surface of the vessel due to secondary gamma is equal to that due to core gammas. As a conservative approach, it can be assumed that the secondary contribution is equal to the contribution from the core on the inside surface of the nozzle. Therefore, the volumetric heat release distribution at the nozzle is 36,000 BTU/hr-ft³.

5.2.2 Flange on Top of Reactor Vessel

The heat release distribution was calculated on the inside surface of the flange and at various interior points. The contribution of core gamma was based on the attenuation of the core gamma flux on the inside surface of the thermal shield through the shield, reflector and reactor vessel flange. Equations 5-5a and 5-5b were used to calculate the attenuation of the flux

$$\text{(Thru steel)} \quad \phi_2 = \phi_1 B_a e^{-\mu t} \quad (5-5a)$$

$$\text{(Thru water)} \quad \phi_2 = \phi_1 \quad (5-5b)$$

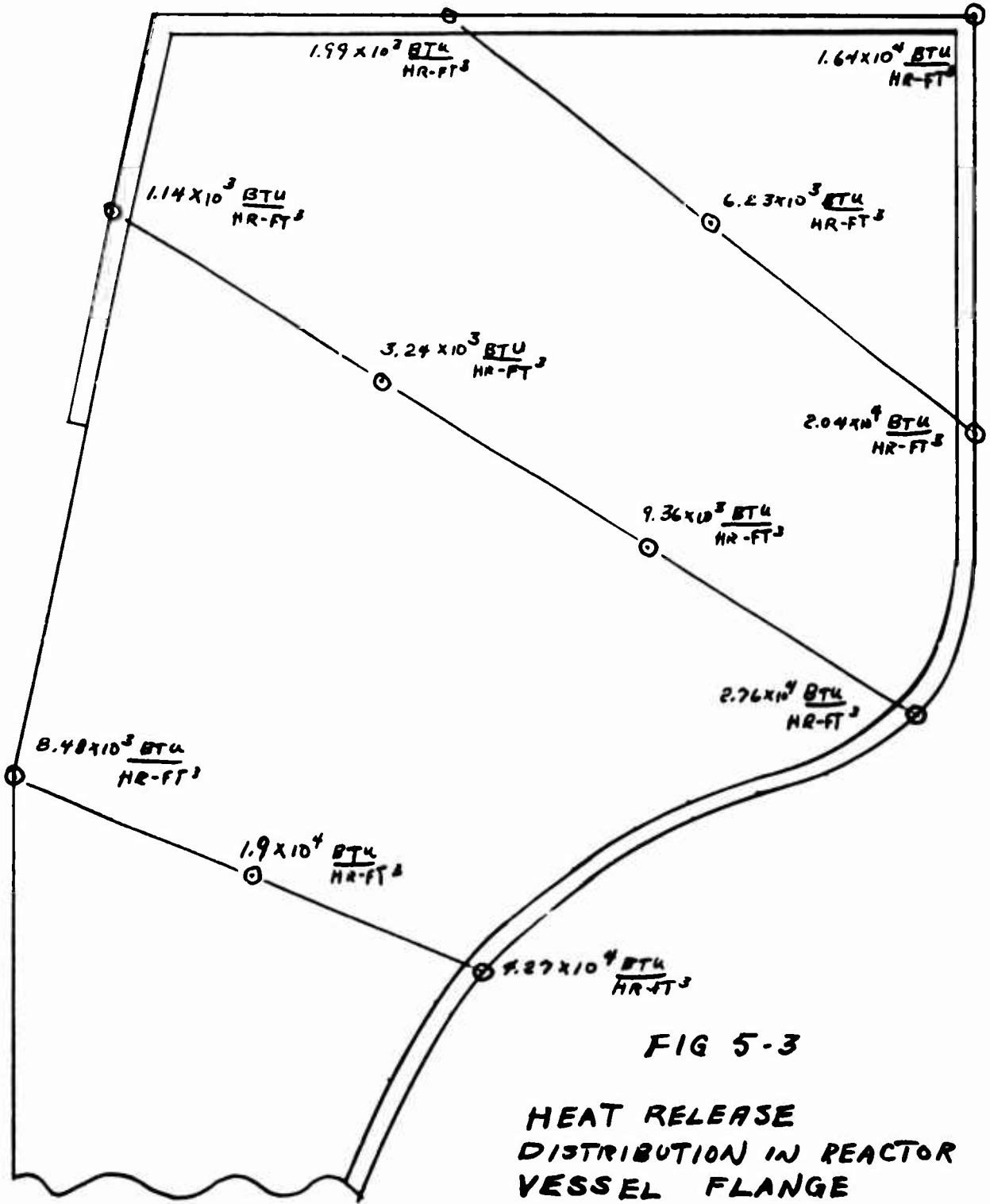
where

B_a = Energy absorption build-up factor

μ = macroscopic cross section of steel, cm⁻¹

t = thickness of steel, cm

These equations assume that the only attenuation is due to steel. Water was considered transparent to gamma rays. As another conservative assumption, the contribution due to secondary gammas was set equal to heat release distribution due to core gammas. The total heat release distribution is shown in Fig. 5-3.



6.0 Demineralizer Shielding

Due to corrosion and activation of the structural material in the primary system, the primary coolant becomes activated. This activity is due to both soluble and insoluble nuclides in the coolant. In order to remove these nuclides, a resin filled demineralizer is placed in the primary coolant blowdown line. Therefore, the demineralizer acts as a filter for insoluble nuclides and as a chemical exchange medium for soluble nuclides. In this manner, the activated nuclide concentration in the primary coolant is kept down.

The activation of the primary coolant is due to several nuclear reactions. With stainless steel as the structural material, the following reactions will take place in the material.

1. $\text{Cr}^{50} (n, \gamma) \text{Cr}^{51}$
2. $\text{Ni}^{64} (n, \gamma) \text{Ni}^{65}$
3. $\text{Fe}^{54} (n, p) \text{Mn}^{54}$
4. $\text{Mn}^{55} (n, \gamma) \text{Mn}^{56}$
5. $\text{Fe}^{56} (n, p) \text{Mn}^{56}$
6. $\text{Ni}^{58} (n, p) \text{Co}^{58}$
7. $\text{Co}^{59} (n, \gamma) \text{Co}^{60}$
8. $\text{Fe}^{58} (n, \gamma) \text{Fe}^{59}$

Since the demineralizer removes all the activated nuclides from the blow-down line, the demineralizer in turn becomes a radioactive source. This necessitates the shielding of the demineralizer by a lead cask.

6.1 Corrosion Product Concentration in Demineralizer

The concentration of active nuclides in the demineralizer was calculated from equations 6-1, 6-2, 6-3, and 6-4.

$$n_D = X + Y + Z \quad (6-1)$$

$$X = \frac{C_0 S_2 N_a F_n F_s \sigma \phi_e}{V_z A} \left[\frac{1 - e^{-\lambda t}}{\lambda(\lambda + Q/W_w)} + \frac{e^{-\lambda t} - e^{-(Q/W_w)t}}{\lambda(\lambda - Q/W_w)} + \frac{e^{-(\lambda + Q/W_w)t} - e^{-\lambda t}}{(\lambda + Q/W_w)(Q/W_w)} + \frac{e^{-\lambda t} - e^{-(\lambda + Q/W_w)t}}{\lambda(Q/W_w)} \right] \quad (6-2)$$

$$Y = \frac{QC_0 S_a N_a f_n f_s \sigma \phi_a}{V_s A \lambda V_w} \left[\frac{1 - e^{-\lambda t}}{\lambda(\lambda + Q/V_w)} + \frac{e^{-\lambda t} - e^{-(\lambda + Q/V_w)t}}{(Q/V_w)^2} \right] + \frac{t e^{-\lambda t}}{(Q/V_w)} + \frac{e^{-(\lambda + Q/V_w)t} - e^{-\lambda t}}{(\lambda + Q/V_w)(Q/V_w)} \quad (6-3)$$

$$Z = \frac{Q f_n f_s \rho N_a \sigma S_a \phi_a l}{4 A V_s (\lambda + Q/V_w)} \left[\frac{1 - e^{-\lambda t}}{\lambda V_w} + \frac{e^{-(\lambda + Q/V_w)t} - e^{-\lambda t}}{Q} \right] \quad (6-4)$$

- where n_D = concentration of active nuclides in demineralizer, atom/cm³
 C_0 = release rate, gm/cm²-sec = 0.965×10^{-11}
 S_0 = total primary system corrosion area, cm² = 2.763×10^6
 $(S_0)_N$ = for normal Co stainless steel, cm² = 1.296×10^6
 $(S_0)_L$ = for low Co stainless steel, cm² = 1.468×10^6
 S_a = primary system corrosion area exposed to flux, cm² = 1.524×10^6
 $(S_a)_N$ = for normal Co stainless steel, cm² = 5.65×10^4
 $(S_a)_L$ = for low Co stainless steel, cm² = 1.468×10^6
 N_a = Avogadro's number, atoms/mole = 6.02×10^{23}
 σ_1 = thermal activation cross section of target nuclide, cm²/atom
 A_1 = Atomic weight of target nuclide, gm/mole
 Q = flow rate through demineralizer, cm³/sec = 63.6
 λ_1 = disintegration constant of active nuclide, sec⁻¹
 V_w = volume of primary water, cm³ = 2.1×10^6
 ρ_1 = density of target nuclide, gm/cm³
 l = recoil distance, cm = 10^{-5}
 t = time of operation, sec = 3.156×10^7

TABLE 6-1

Properties of the Nuclides

| Reaction | f_g | f_n | σ (barn) | λ (sec ⁻¹) | ρ (gm/cm ³) | A (gram/mole) |
|--|--------|-------|-----------------|--------------------------------|------------------------------|---------------|
| Cr ⁵⁰ -Cr ⁵¹ | 0.19 | 0.043 | 7.4 | 3.03x10 ⁻⁷ | 7.1 | 52.01 |
| Ni ⁶⁴ -Ni ⁶⁵ | 0.095 | 0.012 | 1.066 | 7.433x10 ⁻⁵ | 8.9 | 58.71 |
| Fe ⁵⁴ -Mn ⁵⁴ | 0.6847 | 0.058 | 0.011 | 2.57x10 ⁻⁸ | 7.6 | 55.85 |
| Mn ⁵⁵ -Mn ⁵⁶ | 0.015 | 1.00 | 9.1 | 7.433x10 ⁻⁵ | 7.2 | 54.94 |
| Fe ⁵⁶ -Mn ⁵⁶ | 0.6847 | 0.917 | 0.0166 | 7.433x10 ⁻⁵ | 7.8 | 55.85 |
| Ni ⁵⁸ -Co ⁵⁸ | 0.095 | 0.678 | 0.0664 | 1.117x10 ⁻⁷ | 8.9 | 58.71 |
| Co ⁵⁹ -Co ⁶⁰ (normal) | 0.004 | 1.0 | 24.3 | 4.17x10 ⁻⁹ | 8.9 | 58.94 |
| (Low Co steel) | 0.0004 | 1.0 | 24.3 | 4.17x10 ⁻⁹ | 8.9 | 58.94 |
| Fe ⁵⁸ -Fe ⁵⁹ | 0.6847 | 0.003 | 0.6 | 1.74x10 ⁻⁷ | 7.8 | 55.85 |

- ϕ_e = thermal neutron flux; effective; weighted by core geometry and fraction of cycle time spent in each region-core, and reflectors, neutron/cm²-sec = 9.35×10^{12}
 ϕ_a = thermal neutron flux; averaged over core geometry - not dependent upon primary cycle time, neutrons/cm²-sec = 2.65×10^{13}
 f_s = fractional abundance of chemical element in system-material weight fraction.
 f_n = fraction abundance of target nuclide in chemical element - weight fraction.
 V_I = effective volume of resin bed in demineralizer, cm³ = 5.66×10^4

The derivation of the above equations is given in APAE-17 (25). Comparison of the analytic calculation with experimental measurements is given in ref. (2). The release rate, Co, was obtained from fitting APPR-1 data. The differences and the difficulties in performing these analytical calculations are also given in ref.

The properties of the various nuclides are given in Table 6-1.

The concentration of active nuclides in the demineralizer after one (1) year of full power operation at 10 MW is given in Table 6-2.

TABLE 6-2

Concentration of Active Nuclides in Demineralizer

| Nuclide | Concentration, n_D (atom/cm ³) |
|------------------|--|
| Cr ⁵¹ | 8.149×10^{14} |
| Ni ⁶⁵ | 7.533×10^8 |
| Mn ⁵⁴ | 1.108×10^{13} |
| Mn ⁵⁶ | 8.243×10^{10} |
| Fe ⁵⁹ | 4.133×10^{12} |
| Co ⁶⁰ | 3.598×10^{14} |
| Co ⁵⁸ | 2.695×10^{13} |

6.2 Volumetric Source Strength of Demineralizer

The next step in determining the shielding required for the demineralizer is the calculation of the volumetric source strength. The source strength is based on the buildup of active nuclides in the demineralizer.

Equation 6-5 was used to calculate the source strengths.

$$S_V = \lambda n_D \left(\frac{\gamma}{d} \right) E \quad (6-5)$$

where S_V = source strength of volume source, Mev/cm³-sec

n_D = concentration of active nuclides in demineralizer, atom/cm³

λ = disintegration constant, sec⁻¹

E = gamma energy, Mev

$\left(\frac{\gamma}{d} \right)$ = number of gammas of energy, E , released per disintegration

The constants to equation 6-5 and the source strength of the volume source, S_V , due to each of the activated nuclides are given in Table 6-3.

TABLE 6-3

Calculation of Volumetric Source Strength

| Nuclide | λ (sec ⁻¹) | $\left(\frac{\gamma}{d} \right)$ | E (mev) | S_V (mev/cm ³ -sec) |
|------------------|--------------------------------|-----------------------------------|-----------|----------------------------------|
| Cr ⁵¹ | 3.03x10 ⁻⁷ | 0.1 | 0.32 | 7.901x10 ⁶ |
| Ni ⁶⁵ | 7.433x10 ⁻⁵ | 0.4 | 0.37 | 8.287x10 ² |
| | | 0.25 | 1.49 | 2.086x10 ⁴ |
| | | 0.18 | 1.12 | 1.129x10 ⁴ |
| Mn ⁵⁴ | 2.57x10 ⁻⁸ | 1.0 | 0.84 | 2.392x10 ⁵ |
| Mn ⁵⁶ | 7.433x10 ⁻⁵ | 1.0 | 0.84 | 5.147x10 ⁶ |
| | | 0.3 | 1.81 | 3.327x10 ⁶ |
| | | 0.2 | 2.13 | 2.61x10 ⁶ |
| Co ⁵⁸ | 1.117x10 ⁻⁷ | 1.0 | 0.81 | 2.438x10 ⁶ |
| Fe ⁵⁹ | 1.74x10 ⁻⁷ | 0.5 | 1.3 | 4.674x10 ⁵ |
| | | 0.5 | 1.1 | 3.955x10 ⁵ |
| Co ⁶⁰ | 4.17x10 ⁻⁹ | 1.0 | 1.33 | 1.995x10 ⁶ |
| | | 1.0 | 1.17 | 1.755x10 ⁶ |

The different gammas emitted from the active nuclide were consolidated into five groups to facilitate the calculation of the dose rate due to the active nuclides in the demineralizer. The energy groups that were used and the volumetric source strength for each group is given in Table 6-4.

TABLE 6-4
Energy Grouping and Source Strength

| Group Number | Group Energy (mev) | S_v (mev/cm ³ -sec) |
|--------------|--------------------|----------------------------------|
| 1 | 2.13 | 2.61×10^6 |
| 2 | 1.81 | 3.327×10^6 |
| 3 | 1.2-1.5 | 2.483×10^6 |
| 4 | 1.0-1.2 | 2.162×10^6 |
| 5 | <1.0 | 1.573×10^7 |

3 Demineralizer Shielding

Since the Activity in the demineralizer builds up during reactor operation, it is desirable to operate it in a lead shield cask so that the dose rate on the surface of the lead cask be no more than 70 mr/hr. The following sections will discuss the selection of the size of the lead cask.

6.3.1 Radial Shielding Demineralizer

The IBM 650 shielding program (12) was modified in order to calculate the dose on the outside surface of the lead shield cask. This program calculates the dose rate at any desired point due to a cylindrical source with intervening shield materials. Fig. 6-1 shows the geometry of the demineralizer and lead cask. The equation that the machine solves is given on page 360 of Rockwell (3) where $\phi_1 = \phi_2 = \phi$.

The calculation was performed using the energy groups and volumetric source strengths given in Table 6-4. In order to determine the effect of lead thickness on dose rate, four different cases were calculated. They were two, three, four, and five inches of lead. The dose rates on the outside surface of the cask due to the different energy groups are given in Table 6-5 for each size of the lead cask.

FIG 6-1
DEMINERALIZER SHIPPING CASK
SCALE = $\frac{1}{8}$ SIZE

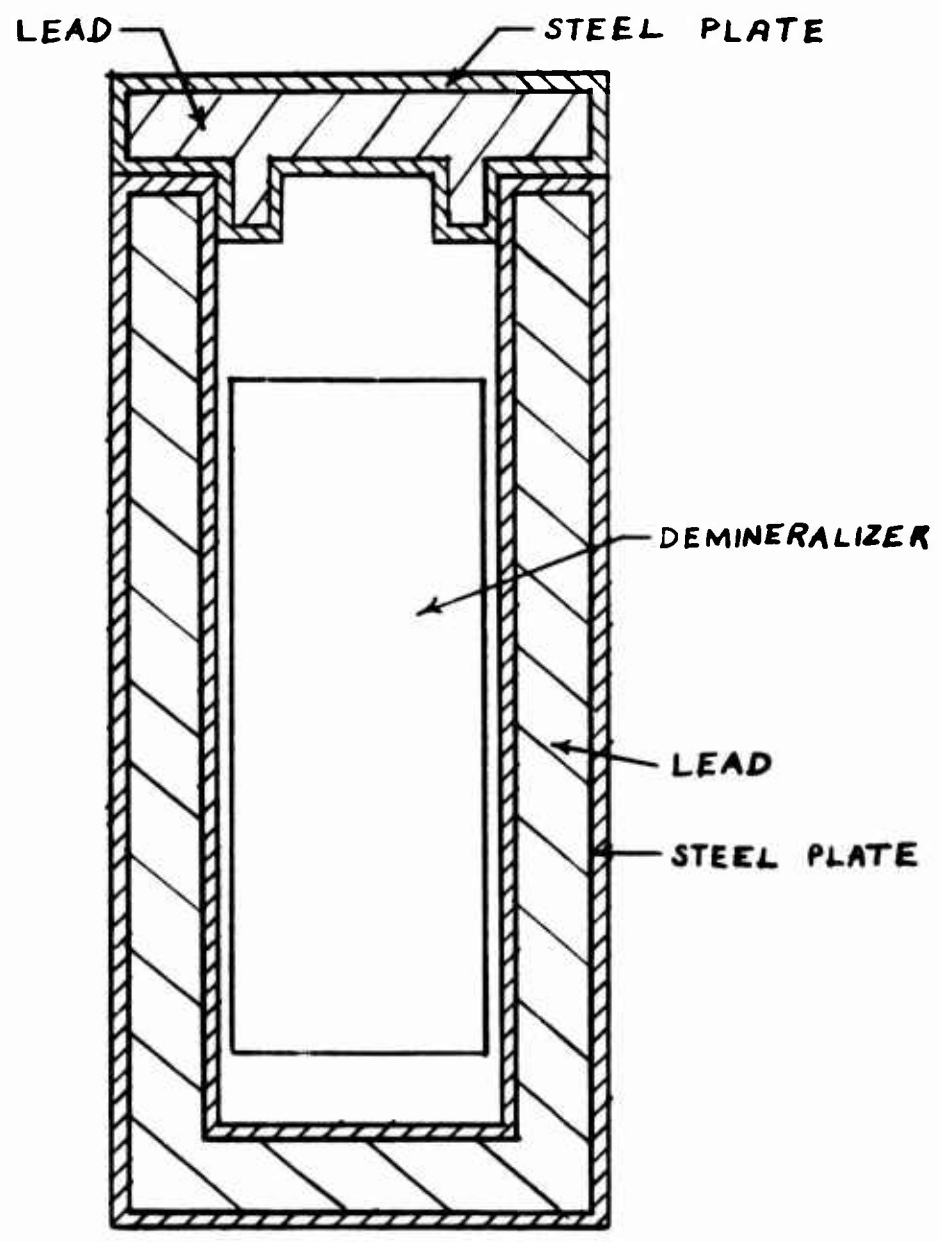


TABLE 6-5

Dose Rate on Surface of Loaded Demineralizer Shipping Cask

| Energy Group | Thickness of Lead in Cask | | | |
|--------------|---------------------------|-------------|-------------|-------------|
| | 2" of Lead | 3" of Lead | 4" of Lead | 5" of Lead |
| 1 | 353.7 mr/hr | 103.9 mr/hr | 29.92 mr/hr | 8.57 mr/hr |
| 2 | 380.0 " | 102.9 " | 27.11 " | 7.14 " |
| 3 | 157.7 " | 32.7 " | 6.53 " | 1.29 " |
| 4 | 88.6 " | 15.3 " | 2.51 " | 0.41 " |
| 5 | 153.9 " | 13.5 " | 1.39 " | 0.10 " |
| Total | 1133.9 mr/hr | 268.3 mr/hr | 67.46 mr/hr | 17.51 mr/hr |

The results are also shown on Fig. 6-2. For a maximum dose rate of 70 mr/hr on the surface of the lead cask, 4 inches of lead is required for the cask. This value is very conservative as the buildup factor is defined as follows:

$$B_T = \prod_1 B_1 \quad (6-6)$$

where B_1 = Buildup factor of i^{th} material

The buildup factor can be calculated in a different manner as follows:

$$B_T = A_1 e^{-\alpha_1 b_1} / (1 - A_1) e^{-\alpha_2 b_1} \quad (6-7)$$

where $b_1 = \sum_1 \mu_1 t_1$ for all shield materials. The buildup factors are smaller and therefore do not give as conservative an answer as the machine calculation. The results from the hand calculations are given in Fig. 6-2. From this curve a lead thickness of 3 9/16 inches will limit the dose rate on the outside surface of the lead cask to 70 mr/hr. It is recommended that the results from the hand calculation be used as the radial thickness of the lead cask.

6.3.2 Vertical Shielding of Demineralizer

From studies performed during the shielding program of Task VI (2), it is known that less lead shielding is needed for the top and bottom of the lead cask. The following equations were used to determine the maximum and minimum dose rates with a three inch lead cask.

Upper Limit

$$D = \frac{ES_V}{2M_B C_e} \left[E_2(b_1) - \frac{E_2(b_1 \text{ Sec } \Theta_1)}{\text{Sec } \Theta_1} \right] \quad (6-8)$$

Lower Limit

$$D = \frac{ES_V}{2M_B C_e} \left[E_2(b_1) - \frac{E_2(b_1 \text{ Sec } \Theta_3)}{\text{Sec } \Theta_3} \right] \quad (6-9)$$

where

$$E_2(b) = b \int_0^{\infty} \frac{e^{-t}}{t^2} dt$$

$$\Theta_1 = \text{Tan}^{-1} \left(\frac{R_o}{a'} \right), \text{ degrees}$$

$$\Theta_3 = \text{Tan}^{-1} \left(\frac{R_o}{a' - h'} \right), \text{ degrees}$$

$$h' = 3/M_B \text{ cm.}$$

a' = distance from top or bottom of cylindrical source to dose point, cm

For 3 inches of lead, the upper and lower limits on the top or bottom surfaces of the cask are such that the average value is a little greater than 70 mr/hr. Therefore about 3 1/16 inches of lead would be required for the top and bottom parts of the lead cask. This is shown in Fig. 6-1.

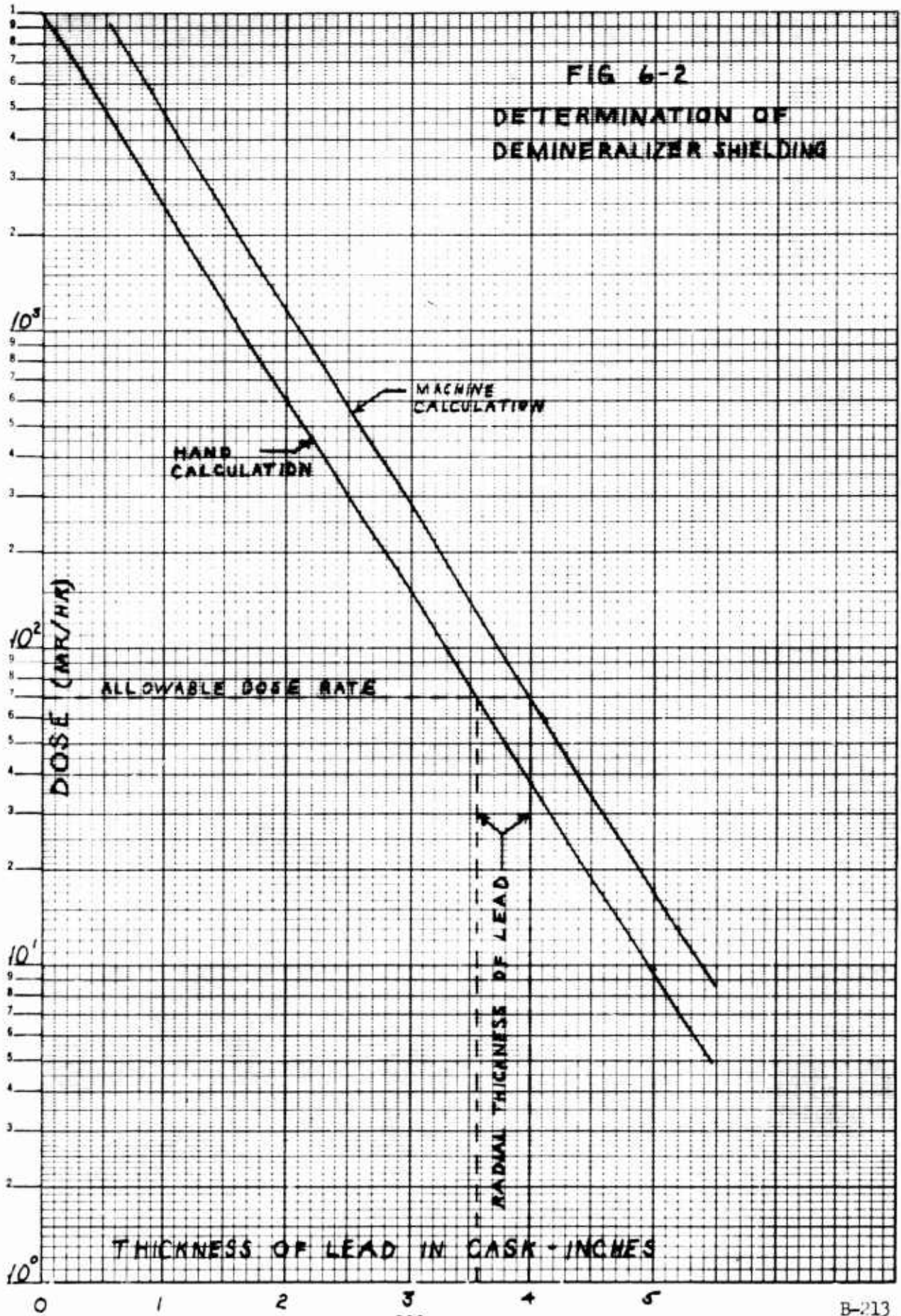
6.3.3 Dose Rate After Removal

After removal of the demineralizer from the system, the dose rate on the surface of the cask will decrease rapidly for the first forty hours. The decay of the dose rate will then decrease very slowly compared to the initial decrease. Within the first forty hours, all of the short lived activity will decay away giving an initial fast decrease in the dose. Thereafter, the dose rate decreased slowly due to the decay of the long-lived nuclides. Experimental and analytical work on this subject is given in APAE-35 (2). The dose rate after a cooling period of about two days would be within 40 mr/hr on the surface of the lead cask shielding.

6.3.4 Results

The shipping cask consists of two 3/4" thick concentric steel cylinders with 3 9/16" of lead between them. In the APPR-1 design, the cask consisted of two 5/8" thick steel rings with

FIG 6-2
DETERMINATION OF
DEMINERALIZER SHIELDING



3 1/2" of lead between them. For equivalent casks with 5/8" steel rings, 3 11/16" of lead will be needed radially in the skid mount demineralizer. Axially, 3 3/16" of lead will be needed with the 5/8" thick steel retaining walls.

For the above cask, the dose rate one meter from the source is 15% of the dose rate on the surface of the shipping cask. With a dose rate of 70 mr/hr on the cask surface, the dose rate one meter from the source would be 10.5 mr/hr. Within a day, the dose rate one meter from the source will decrease to a value less than 10 mr/hr. This radioactive source would then meet I.C.C. shipping regulations.

7.0 WASTE TANK SHIELDING

The waste tank will be used to store radioactive waste. This waste may include the primary coolant and two months plant waste. The shielding of the waste tank is based on normal usage and not on abnormal nuclear incidents. This means that the radioactive source in the waste tank will be due to activated corrosion products in the primary coolant and active material in the plant waste. The high energy gamma rays (energy groups 1 and 2) are from the disintegration of the short-lived nuclides present in the primary water. These nuclides have half-lives of approximately 2.6 hours (26). Therefore, the activity due to these nuclides will diminish rapidly and disappear within a day or two after the primary water is drained into the waste tank. The shielding required will be such that the allowable dose on the shield surface shall not exceed 500 mr/hr.

7.1 Primary Coolant Activation

The activity of the primary coolant is due to the activation and corrosion of structural materials in the primary system. The nuclear reactions giving rise to this activation are the same as described in Section 6.0.

The concentration of the various activated corrosion products in the primary coolant was calculated by equation 7-1, 7-2, 7-3, and 7-4. The derivation of the following equations is presented in APAE-17(25).

$$n_w = U / V / W \quad (7-1)$$

$$U = \frac{C_o S_o N_a \sigma_f s f_n \phi_e}{A Q} \left[\frac{1 - e^{-(\lambda + Q/V_w)t}}{(\lambda + Q/V_w)} + \frac{e^{-(\lambda + Q/V_w)t} - e^{-(Q/V_w)t}}{\lambda} \right] \quad (7-2)$$

$$V = \frac{C_o S_a N_a f_n f_a \sigma \phi_a}{A \lambda V_w} \left[\frac{1 - e^{-(\lambda + Q/V_w)t}}{(\lambda + Q/V_w)} + \frac{e^{-(\lambda + Q/V_w)t} - e^{-\lambda t}}{Q/V_w} \right] \quad (7-3)$$

$$w = \frac{f_n f_{s1} f_{s2} N_a \sigma_{sa} \phi_a}{4AV_w (\lambda + Q/V_w)} \left[1 - e^{- (\lambda + Q/V_w)t} \right] \quad (7-4)$$

where n_w = concentration of active nuclides in primary coolant, atom/cm³
and the other symbols are defined in section 6.1.

The preceding equations were solved for a power output of 10MW for one year at full power operation. The results of this calculation is given in Table 7-1.

TABLE 7-1

Corrosion Product Concentrations in Primary Coolant

| <u>Nuclide</u> | <u>Concentration (atom/cm³)</u> | <u>Total Atoms</u> |
|------------------|--|------------------------|
| Cr ⁵¹ | 2.194x10 ¹¹ | 4.607x10 ¹⁷ |
| Ni ⁶⁵ | 4.983x10 ⁷ | 1.046x10 ¹⁴ |
| Mn ⁵⁴ | 6.877x10 ⁸ | 1.444x10 ¹⁵ |
| Mn ⁵⁶ | 5.452x10 ⁹ | 1.145x10 ¹⁶ |
| Co ⁵⁸ | 1.248x10 ⁹ | 2.621x10 ¹⁵ |
| Fe ⁵⁹ | 6.515x10 ⁸ | 1.368x10 ¹⁵ |
| Co ⁶⁰ | 2.485x10 ¹⁰ | 5.219x10 ¹⁶ |

The gamma rays from all the nuclides were divided into five energy groups. The total source strength of the volume source due to the primary coolant is given in Table 7-2.

TABLE 7-2

Total Source Strength Due To The Primary Coolant

| <u>Group Number</u> | <u>Total Source Strength (mev/sec)</u> |
|---------------------|--|
| 1 | 3.625x10 ¹¹ |
| 2 | 4.62x10 ¹¹ |
| 3 | 3.341x10 ⁹ |
| 4 | 1.953x10 ⁹ |
| 5 | 7.197x10 ¹¹ |

7.2 Plant Waste Activity (28)

In two months of operation, the accumulation of normal waste would amount to about 300 gallons or 1.136×10^6 cm³. The average activity of the waste would be approximately 0.2 μ c/cm³ or 2.275×10^5 μ c. The total source strength due to this activity is 9.245×10^9 Mev/sec. The following was assumed in order to calculate the total source of the normal plant waste.

1. Average energy of radioactive nuclides = 1.1 Mev
2. One photon per disintegration of radioactive nuclide.

This radioactive source, since the average energy is 1.1 Mev, was included in Energy Group 4 along with the contribution from the primary coolant.

7.3 Volumetric Source Strength in Waste Tank

The source strength of the volume source in the waste tank is equal to the total source strength calculated in sections 7-1 and 7-2 divided by the volume of the waste tank. The volume of the waste tank assuming that it is filled to capacity is 1.939×10^7 cm³. A list of the volumetric source strength for each energy group is given in Table 7-3.

TABLE 7-3

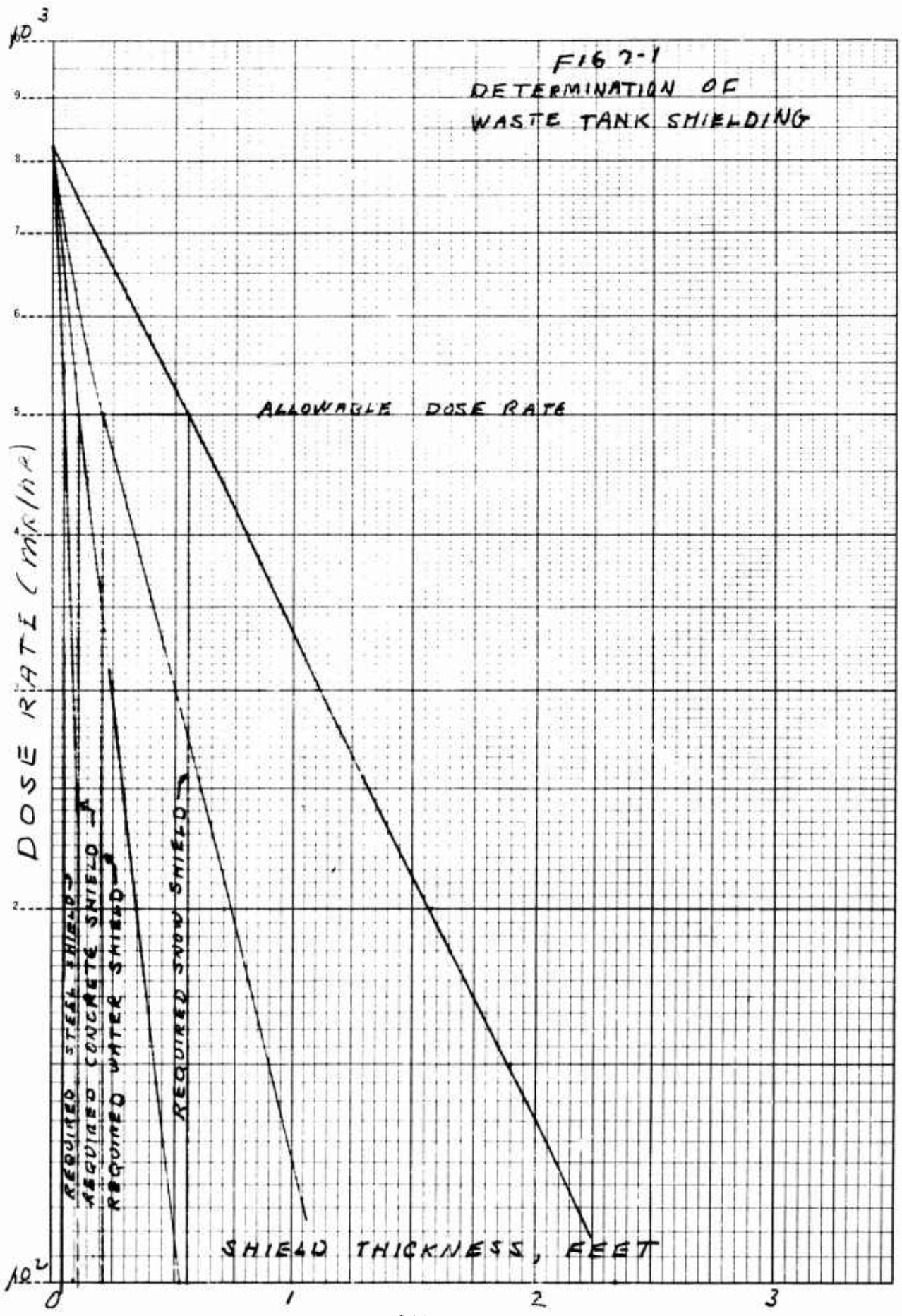
Volumetric Source Strength in Waste Tank

| Group Number | Total Source (Mev/sec) | Volumetric Source (Mev/cm ³ -sec) |
|--------------|---------------------------|---|
| 1 | 3.625×10^{11} | 1.87×10^4 |
| 2 | 4.62×10^{11} | 2.383×10^4 |
| 3 | 3.341×10^9 | 1.723×10^2 |
| 4 | 1.12×10^{10} | 5.776×10^2 |
| 5 | 7.197×10^{11} | 3.712×10^4 |

7.4 Waste Tank Shielding

The shielding of the waste tank was based on the use of any of the following material:

1. Concrete, $\rho = 2.4$ gm/cc.
2. Water, $\rho = 1.0$ gm/cc.
3. Snow, $\rho = 0.595$ gm/cc (Snow depth = 4.0')
4. Steel, $\rho = 7.9$ gm/cc.



The method used to calculate the dose rate on the surface of the different shields is identical to the method used in Section 6. The IBM Shielding code (12) was used to perform all the numerical calculations. The dose rates on the shield surface as a function of shield material and thickness is given in Fig. 7-1. The required shield thickness for each shield material is given in Table 7-4 for an allowable dose rate of 500 mr/hr on the shield surface.

TABLE 7-4

Shield Thickness for Waste Tank

| <u>Material</u> | <u>Thickness</u> |
|--------------------------------|------------------|
| Concrete ($\rho = 2.4$ gm/cc) | 1.32 inches |
| Water ($\rho = 1.0$ gm/cc) | 2.52 inches |
| Snow ($\rho = 0.595$ gm/cc) | 6.60 inches |
| Steel ($\rho = 7.9$ gm/cc) | 0.6 inches |

The shield thickness using snow is based on the tank being an average of 40 feet below the snow surface. This depth is considered to be the most adverse case as the snow becomes denser as it piles up on the top surface. Therefore, less snow is needed to adequately shield the waste tank with the passage of time.

8.0 GAMMA AND NEUTRON HEATING IN THE SNOW - RADIAL DIRECTION

Since the snow around the vapor container acts as secondary shielding and is subject to heating by radiation escaping from the vapor container, it is necessary to evaluate this heating to determine if it is necessary to remove the heat from the snow.

8.1 Calculation Model

The approach used in calculating the gamma and neutron heating in the snow was to use a conservative model which would overestimate the heating. Then if heating rates calculated are not prohibitive, a more detailed analysis is not necessary. The heating calculation was divided into three parts:

1. Gamma heating from primary shield and primary coolant gammas.
2. Neutron heating from neutron flux leakage from primary shield.
3. Gamma heating from capture gammas produced in snow.

8.1.1 Gamma Heating from Primary Shield and Primary Coolant

The dose rate on the surface of the primary shield during operation is 247 r/hr (see section 2.4.5). Dose rate from the primary coolant at the worst point is about one r/hr. A total of 300 r/hr is assumed for the sum of these two sources.

The equation used in gamma heating calculations is:

$$H_{\gamma} = C_e B_a \mu_a \phi_E \frac{\text{Btu}}{\text{in}^3 \text{- sec}} \quad (8.1)$$

where

$$\phi_E = \text{energy flux, Mev/cm}^2\text{-sec}$$

$$\mu_a = \text{energy absorption coefficient, cm}^{-1}$$

$$B_a = \text{buildup factor for energy absorption}$$

$$C_e = 2.488 \times 10^{-15} \frac{\text{BTU-cm}^3}{\text{Mev-in}^3}$$

In order to calculate the energy flux, ϕ_E on the face of the tunnel it was assumed that the gamma dose rate of 300 R/hr is at 2 Mev and that there is no geometrical attenuation between vapor container and snow. Therefore:

$$\phi_E(0) = 300 \text{ R/hr} \times 6.4 \times 10^5 \text{ Mev-hr/cm}^2\text{-sec-R}$$

$$\phi_E(0) = 1.92 \times 10^8 \text{ Mev/cm}^2\text{-sec}$$

Energy flux as a function of penetration into the snow is calculated as follows:

$$\phi_E(x) = \phi_E(0) e^{-\mu x}$$

where x = penetration into snow, cm

μ = total linear absorption coefficient, cm^{-1}

Table 8-1 contains details of the calculation of gamma heating in the snow from gammas born inside the vapor container.

8.1.2 Neutron Heating in the Snow

Neutron heating in the snow is calculated from the following equation:

$$H_N = C_e \sum_{\text{Rem}} \phi_N(0) e^{-\sum_{\text{Rem}} x} E \quad (8.2)$$

where

$\phi_N(0)$ = neutron flux on tunnel face, neutrons/ $\text{cm}^2\text{-sec}$

$\phi_N(0)$ is assumed to be the fast flux on the surface of the shield tank.

$\phi_N(0)$ was assumed to be 1×10^7 (fast flux is actually somewhat lower)

E = average energy of fast neutron

E was assumed to be 10 Mev

\sum_{Rem} = removal cross section of snow for fast neutrons, cm^{-1}
(other symbols defined in section 8.1.1.)

To arrive at \sum_{Rem} for snow a density of 0.6 gm/cm^3 was assumed for snow. From AECD 3978 (28), a representative relaxation length for fast neutrons in water is 10^7 cm or

$$\sum_{\text{Rem}}^{\text{H}_2\text{O}} = 0.1 \text{ cm}^{-1}$$

For snow at a density of 0.6 gm/cm^3 ,

$$\Sigma_{\text{Rem}} = 0.1 \times 0.6 = 0.06 \text{ cm}^{-1}$$

Results and details of the neutron heating calculation are contained in Table 8-2.

8.1.3 Gamma Heating from Capture Gammas in the Snow

Gamma heating from hydrogen capture gammas in the snow was calculated from Eq. 8.1 as follows:

$$H_{\gamma}^i = C_e B_a \mu_a \phi_E^i(x)$$

The infinite slab equation of Section 1-4, Chapter 9, Ref. 3, was used to calculate $\phi_E^i(x)$ as follows:

$$\phi_E^i(x) = \frac{S_v}{2\mu_B} \left[E_2(b_1) - E_2(b_3) \right] \quad (8.3)$$

The snow was divided into 3-ft. thick slabs and S_v was considered constant throughout the 3-ft. slab. S_v was calculated as follows:

$$S_v(x) = \frac{\rho_{\text{snow}}}{1 \text{ gm/cm}^3} \times \sum_a^{\text{H}_2\text{O}} \phi_N^{\text{th}}(x) \times 2 \text{ Mev/gamma}$$

$$S_v(x) = \text{Capture gamma production, Mev/sec-cm}^3$$

(one 2-Mev gamma/capture)

$$\rho_{\text{snow}} = 0.6 \text{ gm/cm}^3$$

$$\sum_a^{\text{H}_2\text{O}} = 0.0195 \text{ cm}^{-1} \bullet \rho = 1 \text{ gm/cm}^3$$

$$\phi_N^{\text{th}}(x) = \text{thermal flux at } x$$

$\phi_N^{\text{th}}(x)$ has been assumed equal to $\phi_N(x)$ of Section 8.1.2. In reality $\phi_N^{\text{th}}(x)$ is proportional to and less than $\phi_N(x)$, but the assumption of equality is conservative.

Table 8-1

Gamma Heating in Snow due to Gammas from Shield Tank and Primary Coolant

| x, cm | $\phi_E, \frac{\text{Mev}}{\text{sec-cm}^2}$ | B_a | μx | $e^{-\mu x}$ | $H_\gamma, \text{Btu/in.}^3\text{-sec}$ |
|--------|--|-------|---------|----------------------|---|
| 0 | 1.92×10^8 | 1.0 | 0 | 1.0 | 7.54×10^{-9} |
| 91.44 | 4.7×10^7 | 3.6 | 2.69 | 0.068 | 1.84×10^{-9} |
| 182.88 | 5.91×10^6 | 6.7 | 5.38 | 4.6×10^{-3} | 2.32×10^{-10} |

$$\mu_a = 0.6 \times 0.0263 \text{ cm}^{-1} = 0.01578 \text{ cm}^{-1}$$

$$\mu = 0.6 \times 0.049 \text{ cm}^{-1} = 0.0294 \text{ cm}^{-1}$$

$$\rho_{\text{snow}} = 0.6 \text{ gm/cm}^3$$

Table 8-2

Neutron Heating in Snow from Neutrons Escaping Primary Shield

| x, cm | $\phi_N(x) \text{ n/cm}^2\text{-sec}$ | \sum_{Rem^x} | $e^{-\sum_{\text{Rem}^x}}$ | $H_N, \text{Btu/in.}^3\text{-sec}$ |
|--------|---------------------------------------|-----------------------|----------------------------|------------------------------------|
| 0 | 1×10^7 | 0 | 1 | 1.492×10^{-8} |
| 91.44 | 4.1×10^4 | 5.49 | 4.1×10^{-3} | 6.11×10^{-11} |
| 182.88 | 1.68×10^2 | 10.98 | 1.68×10^{-5} | 2.51×10^{-13} |

S_v has been held constant in each 3-ft. slab of snow to permit use of Eq. 8.3. The constant value assumed for S_v is the maximum in each slab.

For the first 3-ft. slab of snow between $x = 0$ and $x = 91.44$ cm:

$$S_v = 0.6 \times (0.0195 \text{ cm}^{-1}) \times \phi_N(0) \times 2 \text{ Mev/gamma}$$

$$S_v = 2.34 \times 10^{-2} \times 1 \times 10^7 \text{ Mev/sec-cm}^3$$

$$S_v = 2.34 \times 10^5 \text{ Mev/sec-cm}^3$$

For the second 3-ft slab of snow between $x = 91.44$ cm and $x = 182.88$ cm:

$$S_v = 2.34 \times 10^{-2} \phi_N(91.44)$$

$$S_v = 2.34 \times 10^{-2} \times 4.1 \times 10^4 \text{ Mev/sec-cm}^3$$

$$S_v = 9.6 \times 10^2 \text{ Mev/sec-cm}^3$$

Calculation of the snow capture gamma heating rate is detailed in Table 8-3.

8.2 Conclusions

The total radiation heating rate in the snow is the sum of the different rates in Tables 8-1, 8-2 and 8-3.

Totals are:

| x , cm | H_T , Btu/in. ³ -sec |
|----------|-----------------------------------|
| 0 | 2.25×10^{-8} |
| 91.44 | 2.46×10^{-9} |
| 182.88 | 2.51×10^{-10} |

Results are plotted in Fig. 8-1. It has been concluded that heating rates such as these are not prohibitive and do not require a means of heat removal.

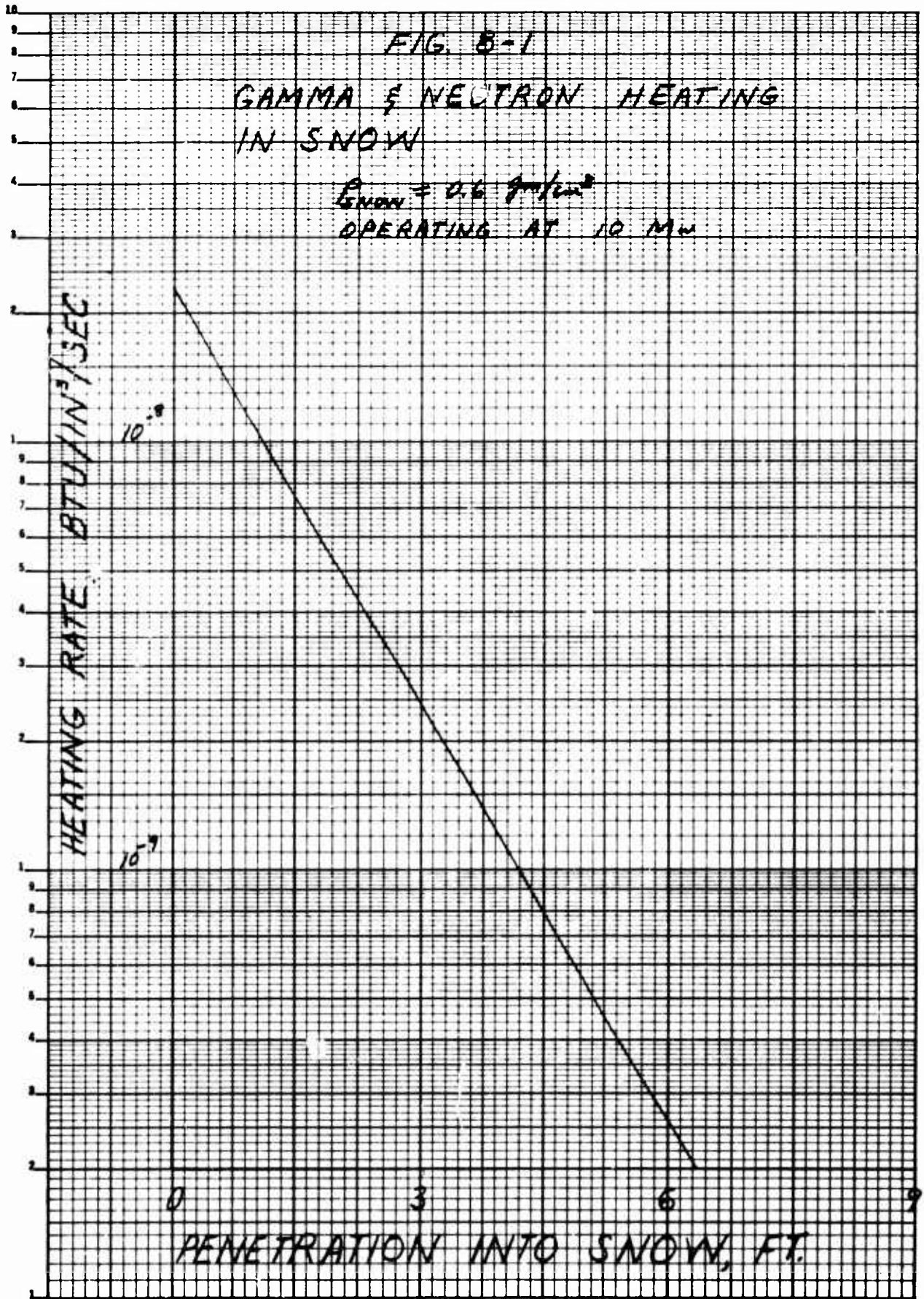


Table 8-3

Gamma Heating from Capture Gammas Produced in Snow

From 1st 3-ft thickness $S_v = 2.34 \times 10^5$ Mev/sec-cm³

| x, cm | b ₁ | E ₂ (b ₁) | M _g h | E ₂ (b ₃) | E ₂ (b ₁)-E ₂ (b ₃) |
|--------|----------------|----------------------------------|------------------|----------------------------------|---|
| 91.44 | 0 | 1 | 2.69 | 1.5 x 10 ⁻² | 1.0 |
| 182.88 | 2.69 | 1.5 x 10 ⁻² | 2.69 | 6.2 x 10 ⁻⁴ | 1.4 x 10 ⁻² |

| $\phi'_E(x)$ | x, cm | B _a (b ₃) | H' _g , Btu/in. ³ -sec |
|------------------------|--------|----------------------------------|---|
| 3.98 x 10 ⁶ | 91.44 | 3.6 | 5.63 x 10 ⁻¹⁰ |
| 5.57 x 10 ⁴ | 182.88 | 6.7 | 1.47 x 10 ⁻¹¹ |

From 2nd 3-ft. thickness $S_v = 9.6 \times 10^2$ Mev/sec-cm³

| x, cm | b ₁ | E ₂ (b ₁) | M _g h | E ₂ (b ₃) | E ₂ (b ₁)-E ₂ (b ₃) |
|--------|----------------|----------------------------------|------------------|----------------------------------|---|
| 182.88 | 0 | 1.0 | 2.69 | 1.5 x 10 ⁻² | 1.0 |

| $\phi'_E(x)$ | x, cm | B _a (b ₃) | H' _g , Btu/in. ³ -sec |
|------------------------|--------|----------------------------------|---|
| 3.04 x 10 ⁴ | 182.88 | 3.6 | 4.3 x 10 ⁻¹² |

$$\mu_a = 0.6 \times 0.0263 \text{ cm}^{-1} = 0.01578 \text{ cm}^{-1}$$

$$\mu = 0.6 \times 0.049 \text{ cm}^{-1} = 0.0294 \text{ cm}^{-1}$$

$$\rho_{\text{snow}} = 0.6 \text{ gm/cm}^3$$

9.0 Gamma Heating of Snow Under the Reactor

There is much less steel and much more water under the core than in the radial direction. Therefore, the gamma flux emerging from the vapor container under the reactor is much greater and the neutron flux is much smaller than in the radial direction. Since in the radial calculation neutron heating is smaller than gamma heating, only gamma heating will be calculated under the core.

A machine calculation was performed to find the gamma flux incident on the snow under the vapor container. Fluxes used in the calculation are shown in Fig. 9-1. These fluxes are from a Valprod calculation with water only below the core and will give an overestimate of the capture gamma flux since the steel members below the core would depress the thermal neutron flux.

Results of the shielding calculation follow.

| Group | \bar{E}_γ , Mev | ϕ_γ , $\delta/\text{sec-cm}^2$ | Mev/sec-cm ² |
|-------|------------------------|--|-------------------------|
| 1 | 7 | 3.284×10^9 | 2.3×10^{10} |
| 2 | 6 | 1.909×10^9 | 1.14×10^{10} |
| 3 | 4 | 1.999×10^9 | 8×10^9 |
| 4 | 2 | 8.195×10^9 | 1.74×10^{10} |

Gamma heating in the snow was then calculated in the same manner as in Section 8.1.1 except that each group above was calculated separately with appropriate absorption coefficients, etc. Table 9-1 contains details of the calculation. Fig. 9-2 is a plot of gamma heating rates in the snow under the reactor.

TABLE 9-1

Gamma Heating in the Snow under the Reactor

| E, Mev | μ_a , cm ² /gm | μ_a , cm ⁻¹ | μ , cm ² /gm | μ , cm ⁻¹ |
|--------|-------------------------------|----------------------------|-----------------------------|--------------------------|
| 7 | 0.018 | 0.0108 | 0.026 | 0.0156 |
| 6 | 0.019 | 0.0114 | 0.028 | 0.0168 |
| 4 | 0.0213 | 0.0128 | 0.034 | 0.0204 |
| 2 | 0.0263 | 0.0158 | 0.049 | 0.0294 |

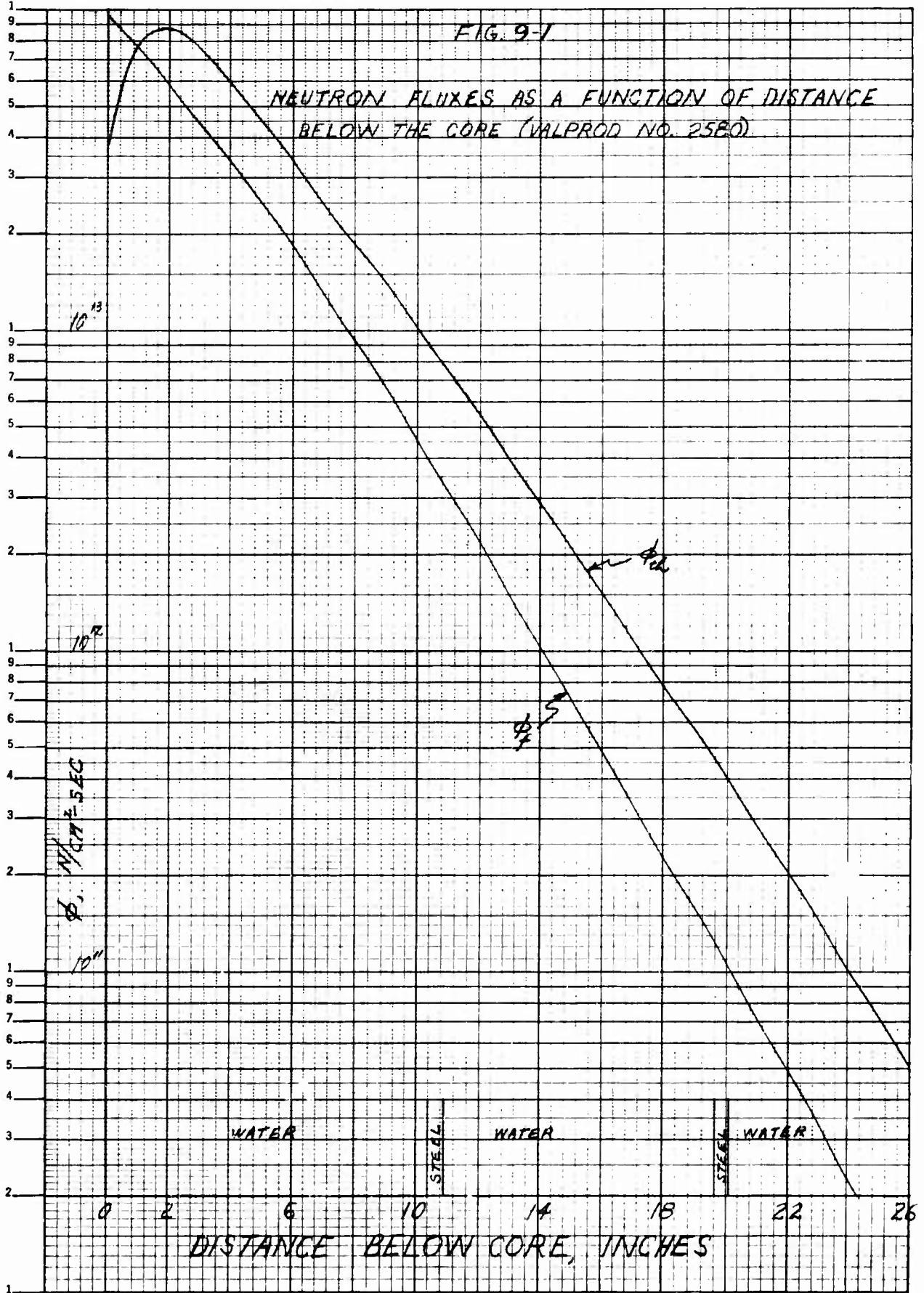
$$\text{Snow density} = 0.6 \text{ gm/cm}^3$$

$$\text{On surface of snow: } H_\gamma(0) = C_e \mu_a \phi_E(0)$$

$$C_e = 2.488 \times 10^{-15} \frac{\text{Btu} - \text{cm}^3}{\text{Mev} - \text{in}^3}$$

FIG. 9-1

NEUTRON FLUXES AS A FUNCTION OF DISTANCE
BELOW THE CORE (VALPROD NO. 2580)



E, Mev $H_{\gamma} (0), \frac{\text{Btu}}{\text{in}^3\text{-sec}}$

| | |
|-------|---|
| 7 | 6.2×10^{-7} |
| 6 | 3.24×10^{-7} |
| 4 | 2.54×10^{-7} |
| 2 | <u>6.45×10^{-7}</u> |
| Total | 1.84×10^{-6} |

Three feet into snow: $H_{\gamma}(3) = Bae^{-\mu t} \phi_{\gamma}(0) \mu_a C_0$

$$t = 91.44 \text{ cm}$$

| E, Mev | μt | $e^{-\mu t}$ | $B_a(\mu t)$ | $H_{\gamma}, \frac{\text{Btu}}{\text{in}^3\text{-sec}}$ |
|--------|---------|----------------------|--------------|---|
| 7 | 1.427 | 0.24 | 1.58 | 2.46×10^{-7} |
| 6 | 1.536 | 0.215 | 1.70 | 1.19×10^{-7} |
| 4 | 1.864 | 0.155 | 2.10 | 8.26×10^{-8} |
| 2 | 2.686 | 6.8×10^{-2} | 3.60 | <u>1.58×10^{-7}</u> |
| | | | | 6.06×10^{-7} |

Six feet into snow:

$$t = 182.88 \text{ cm}$$

| E, Mev | μt | $e^{-\mu t}$ | $B_a(\mu t)$ | $H_{\gamma}, \frac{\text{Btu}}{\text{in}^3\text{-sec}}$ |
|--------|---------|-----------------------|--------------|---|
| 7 | 2.854 | 5.78×10^{-2} | 2.15 | 7.69×10^{-9} |
| 6 | 3.072 | 4.65×10^{-2} | 2.37 | 3.58×10^{-8} |
| 4 | 3.928 | 1.95×10^{-2} | 3.3 | 1.64×10^{-8} |
| 2 | 5.372 | 4.65×10^{-3} | 6.65 | <u>1.99×10^{-8}</u> |
| | | | | 7.98×10^{-8} |

10.0 ACTIVATION OF COMPONENTS

During the course of reactor operation, the various components within the pressure vessel and the components of the primary shield are activated by the neutron flux. The relocation of components of the primary system is dependent upon the activation of the above equipment.

10.1 Pressure Vessel and Primary Shield Component

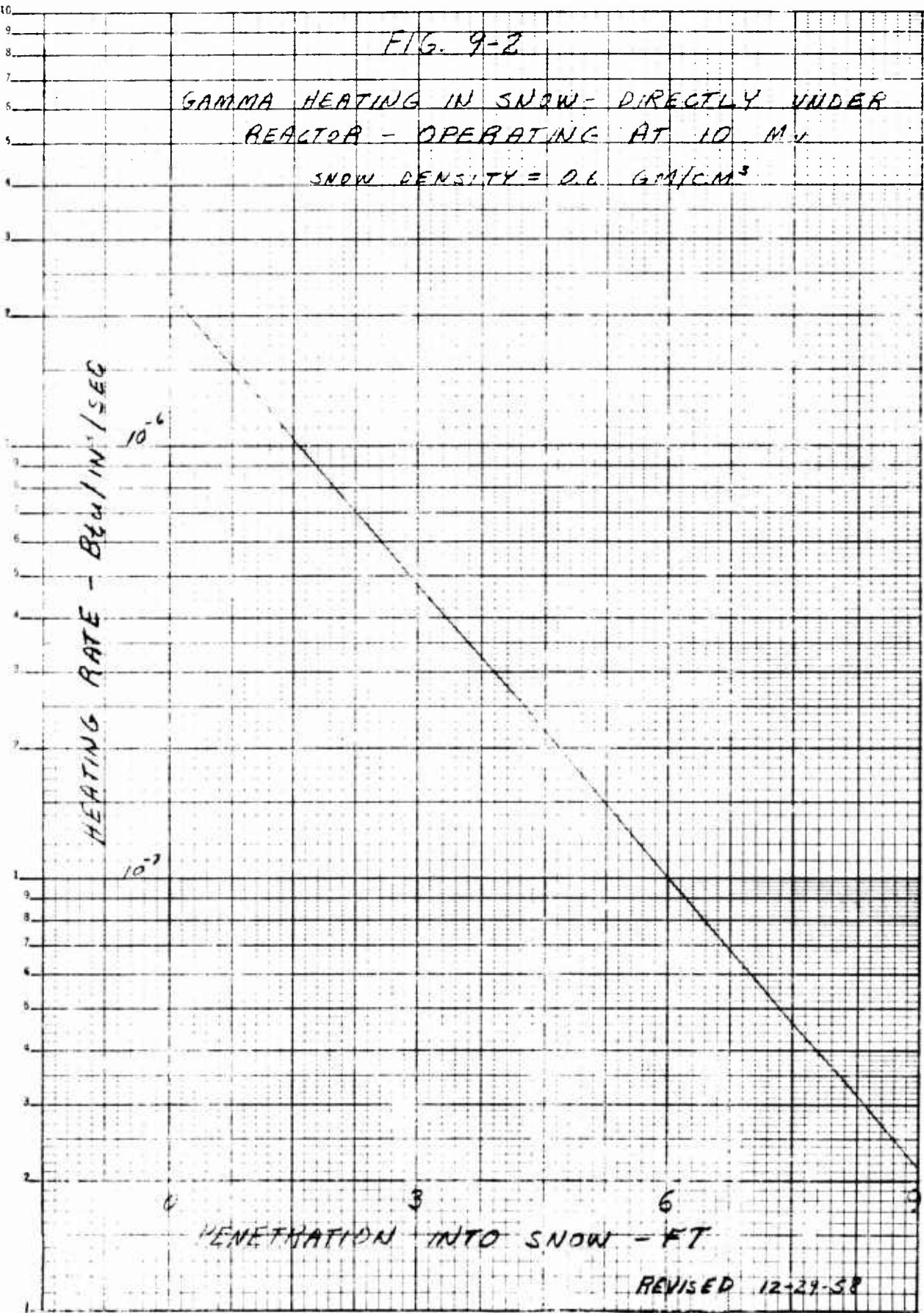
The dose rates five feet from each component after one year full power operation for various shutdown times are given in Table 10-1.

To be able to handle the components, the dose rate due to the activity of each part should not exceed 75mr/hr five feet from the source. The following table is intended to serve as a guide in the determination of the decision as to the feasibility of relocating various components. These rates can be used as a basis for planning but actual dose rates must be measured when actual relocation operations are undertaken. The results given in Table 10-2 are for 1 year of full power operation.

FIG. 9-2

GAMMA HEATING IN SNOW - DIRECTLY UNDER
REACTOR - OPERATING AT 10 MW

SNOW DENSITY = 0.6 GM/CM³



REVISED 12-29-58

TABLE 10-1

DOSE RATES * FROM ACTIVATED COMPONENTS

| Component | Shutdown Times | | | |
|---------------------------------|----------------------|-----------------------|-----------------------|-----------------------|
| | 1 day | 10 days | 30 days | 1 year |
| Thermal Shield | 6.22×10^7 | 5.43×10^7 | 4.44×10^7 | 1.62×10^7 |
| Pressure Vessel | 1.28×10^6 | 1.12×10^6 | 9.15×10^5 | 3.34×10^5 |
| Pressure Vessel Cover | 2×10^3 | 1.75×10^3 | 1.43×10^3 | 5.2×10^2 |
| Pressure Vessel Support Ring | 1.63×10^5 | 1.42×10^5 | 1.16×10^5 | 4.23×10^4 |
| 1st Steel Ring | 3.11×10^4 | 2.72×10^4 | 2.22×10^4 | 8.1×10^3 |
| 2nd Steel Ring | 3.70×10^3 | 3.23×10^3 | 2.64×10^3 | 9.62×10^2 |
| 3rd Steel Ring | 4.19×10^2 | 3.66×10^2 | 2.99×10^2 | 1.09×10^2 |
| 4th Steel Ring | 4.71×10^1 | 4.11×10^1 | 3.36×10^1 | 1.22×10^1 |
| Shield Tank | 6.8×10^{-1} | 5.94×10^{-1} | 4.85×10^{-1} | 1.77×10^{-1} |

* All dose rates are in units of Mr/hr.

TABLE 10-2

FEASIBILITY OF RELOCATION OF COMPONENTS

Shutdown Times

| Component | 1 day | 10 days | 30 days | 1 year |
|------------------------------|-------|---------|---------|--------|
| Control Rod Basket | N | N | N | N |
| Rod Drive Shaft | N | N | N | N |
| Thermal Shield | N | N | N | N |
| Pressure Vessel | N | N | N | N |
| Pressure Vessel Cover | N | N | N | N |
| Pressure Vessel Support Ring | N | N | N | N |
| 1st Shield Ring | N | N | N | N |
| 2nd Shield Ring | N | N | N | N |
| 3rd Shield Ring | N | N | N | N * |
| 4th Shield Ring | R * | R * | R | R |
| Shield Tank | R | R | R | R |

Symbols Used: N - Can not be relocated (dose > 75 mr/hr)

R - Can be relocated (dose < 75 mr/hr)

* Indicates dose rate within a factor of 2 of 75 mr/hr

REFERENCES

II SHIELDING ANALYSIS

1. B. James, et al, "Health Physics Manual for the Army Package Power Reactor", "APAE Memo No. 78 Revision II, May 1, 1958.
2. S. S. Rosen, et al, "APPR-1 Research and Development Program, Shielding Experiments and Analysis, Task No. VI," APAE No 35, October 15, 1958.
3. "Reactor Shielding Design Manual", TID 7004, March 1956.
4. F. H. Clark, "Decay of Fission Product Gammas", NDA 27-39, December 30, 1954.
5. J. Moteff, "Fission Product Decay Gamma Energy Spectrum", APEX 134, 1953.
6. R. L. Marklin and H. S. Pomerance, "Proceedings of the International Conference on Peaceful Uses of Atomic Energy in Geneva, August 1955, Vol. 5, page 96.
7. "Revised Activation Handbook for Aircraft Designers", ANP Document No. NARF-57-50T, FZK-9-124, September 1957, Convair, Fort Worth, Texas.
8. "Allegheny Ludlum Blue Sheet, Allegheny Metal 18-8", Allegheny Ludlum Steel Corporation, Pittsburgh 22, Pennsylvania.
9. "Modern Steels and Their Properties, "Bethlehem Steel Company, Bethlehem, Pa., 1955.
10. C. D. Bopp and D. Sisman, Nucleonics 14, No. 1, page 46, 1956.
11. C. D. Bopp, "Gamma Radiation Induced in Engineering Materials," ORNL 1371, 1953.
12. P. V. Oby, et al, "Primary Shielding Calculations on the IBM 650 (Roc Codes)," APAE Memo 142, October 15, 1958.
13. T. G. Williamson, "APPR-1 Burnout Calculations," APAE Memo 126, April 10, 1958.
14. E. M. Reiback and H. L. Hoover, "Phase III Report, Army Package Power Reactor Field Unit No. 1, APPR-1a, Primary Shield Design Analysis", APAE No. 17, Vol. 1, Supp. 2, July 16, 1958.
15. Herbert Goldstein, "The Attenuation of Gamma Rays and Neutrons in Reactor Shields, "Supt. of Documents, U. S. Government Printing Office, Washington 25, D.C., May 1, 1957.
16. D. J. Hughes and J. A. Harvey, "Neutron Cross Sections," BNL-325, July 1, 1955.

17. F. C. Brooks and H. L. Glick, WAPD-45.
18. Czapek, E., et al, "Gamma Shield Design for Primary Coolant Sources Using the IBM Type 650 Computer", RAS-1, Report No. 74 September 1956.
19. Rosen, S. S., "Supplement to RAS-I", AP NOTE 63, June 26, 1957.
20. Peebles, "Gamma Ray Transmission Through Finite Slabs", R-240, Rand Corporation, December 1, 1952.
21. Moteff, J., "Miscellaneous Data for Shielding Calculations", APEX-176, December 1, 1954.
22. DeYoung, R.C., "Container for Irradiated APPR-1 Fuel Elements", AP MEMO 63, October 31, 1956.
23. Tully, J. P., et al "2000 K.W. Skid Mounted APPR Power Plant", APAE NO. 33, May 1, 1958.
24. Kroeger, H.R., I. M. Neou, and J. L. Meem, "The Effect of Gamma Heating on the APPR-1 Pressure Vessel", 415E2.1, ASTRA, July 1956.
25. "Phase 3 Report APPR Field Unit No. 1, APPR-1A Vol. 1", APAE No. 17 Vol. 1, May 15, 1957.
26. Small, W. J. and J. L. Zegger, "Short Lived Circulating Activity in the APPR", AP MEMO 109, August 28, 1957.
27. Clark, R. J., "Private Communication to M. J. Leibson", October 1958.
28. Chapman, G. T., and C. L. Storrs, "Effective Neutron Removal Cross Sections for Shielding", AECD-3978, September 19, 1955.
29. Mackay, S.D., H. W. Giesler, and J. W. Noaks, "Extended Zero Power Experiment on the Army Package Power Reactor - ZPE-2", APAE No.-21, November 15, 1957

1.0 Primary System Kinetics

1.1 General Kinetic Model

1.1.1 Description

The general kinetic model used is that developed in APAE 38 (1) for the APPR-1. The validity of this model in representing plant transients introduced by control rod and load perturbations was demonstrated by comparison with plant data. The validity of this model in representing the 1500ekw Packaged Nuclear Power Plant is assumed because of its basic similarity to the APPR-1.

1.1.2 Nomenclature

Symbols:

| | |
|---|--|
| A | Heat Transfer Surface Area, ft. ² |
| C | Specific heat, Btu/lb °F |
| F | Coolant Flow Rate, Fraction of Rated Value |
| h | Average core film coefficient, Btu/hr-Ft ² - °F |
| k | Potential power contribution from precursors Btu/sec |
| ℓ | Mean neutron lifetime, birth to absorption, sec ⁻¹ |
| L | Load factor of steam generator power output |
| p | Primary system pressure, psia |
| P | Power output of core, Btu/sec |
| R | Rate of primary system flow, lb/sec |
| S | Slope of pressurizer characteristic, p/ ΔV _{tot} psi/ft ³ |
| t | Time, sec |
| T | Temperature, °F |
| V | Volume, ft ³ |
| W | Weight, lb |
| α | Fraction of power generated in fuel plates and cladding |
| β | Delayed neutron fraction of a group |
| γ | Volume coefficient of primary coolant expansion, °F ⁻¹ |
| δ | Excess reactivity of core |
| ρ | Excess reactivity coefficient, °F ⁻¹ or psia ⁻¹ |
| Θ | Temperature difference at design load, °F |
| λ | Decay constant of a delayed neutron group, sec ⁻¹ |
| τ | Time lag, sec |

Subscripts:

| | |
|---|---|
| C | Mean core coolant condition |
| D | Design power output condition, steady state |
| E | Exchanger tubing |
| F | Mean fuel plate condition |

Subscripts:

| | |
|-----|--|
| G | Mean steam generator condition, primary (tube) side |
| i | ith delayed neutron group |
| L | Liquid in steam generator |
| neg | Negative increase in primary coolant volume |
| p | Primary pressure |
| pos | Positive increase in primary coolant volume |
| r | Control rod insertion |
| S | Mean steam conditions in generator corresp. to saturation |
| tot | Total for primary system |
| 1-8 | Thermo. properties: Condition of location in schematic diagram |
| 1-5 | Nuclear parameters: Particular ith delayed neutron group |

1.1.3 Differential Equations

The following set of differential equations describing primary loop component behavior is derived in APAE 38(1). They are repeated here for ready reference.

Core thermal kinetics:

$$\frac{d}{dt} T_c(t) = \frac{\alpha}{W_F C_F} P(t) - \frac{\alpha P_D}{W_F C_F \theta_{FC}} T_F(t) + \frac{\alpha P_D}{W_F C_F \theta_{FC}} T_c(t)$$

where

$$T_F(0) = \frac{\theta_{FC}}{P_D} P(0)$$

$$\frac{d}{dt} T_c(t) = \frac{1-\alpha}{W_c C_c} P(t) + \frac{\alpha \theta_{1,2}}{\tau_c \theta_{FC}} T_F(t)$$

$$- \left[\frac{\alpha \theta_{1,2}}{\tau_c \theta_{FC}} + \frac{2}{\tau_c} \right] T_c(t) + \frac{2}{\tau_c} T_1(t)$$

where

$$T_c(0) = 0$$

Core nuclear kinetics:

$$\frac{d}{dt} P(t) = \frac{\delta_r / \beta_T T_C(t) / \beta_P P(t)}{\ell} P(t) - \frac{\sum \beta_i}{\ell} P(t) + \sum_{i=1}^5 \lambda_i K_i(t)$$

$$\frac{d}{dt} K_i(t) = \frac{\beta_i}{\ell} P(t) - \lambda_i K_i(t)$$

where

$$K_i(0) = \frac{\beta_i}{\lambda_i \ell} P(0)$$

Kinetics of plenum chambers and piping:

$$\frac{d}{dt} T_1(t / \tau_{5,6}) = \frac{2}{\tau_{6,1}} T_G(t) - \frac{1}{\tau_{6,1}} T_4(t) - \frac{1}{\tau_{6,1}} T_1(t / \tau_{5,6})$$

where

$$T_1(\tau_{5,6}) = T_1(0) = -\frac{P(0)}{2RC_c}$$

$$\frac{d}{dt} T_4(t / \tau_{3,4}) = \frac{2}{\tau_{2,3}} T_C(t) - \frac{1}{\tau_{2,3}} T_1(t) - \frac{1}{\tau_{2,3}} T_4(t / \tau_{3,4})$$

where

$$T_4(\tau_{3,4}) = T_4(0) = \frac{P(0)}{2RC_c}$$

Kinetics of steam generator:

The basic kinetic model developed in APAE 38(1) is used in the study since superheated steam generation is not involved.

$$\frac{d}{dt} T_G(t) = \frac{2}{\tau_G} T_4(t) - \left[\frac{2}{\tau_G} + \frac{2\Theta_{1,2}}{\tau_G \Theta_{Gs}} \right] T_G(t) + \frac{\Theta_{1,2}}{\tau_G \Theta_{Gs}} T_S(t)$$

where

$$T_G(0) = T_C(0) = 0$$

$$\begin{aligned} \frac{d}{dt} T_S(t) = & \frac{P_D}{(W_{LL}^C / W_{EE}^C) \Theta_{Gs}} T_G(t) - \frac{P_D}{(W_{LL}^C / W_{EE}^C) \Theta_{Gs}} T_S(t) \\ & - \frac{P_D}{W_{LL}^C / W_{EE}^C} L(t) \end{aligned}$$

where

$$T_S(0) = -\Theta_{Gs}$$

Pressurizer kinetics:

$$\begin{aligned} \Delta V_{tot}(t) = & \gamma V_c T_c(t) + \gamma V_{2,4} T_4(t) + \gamma V_G T_G(t) + \gamma V_{5,1} T_1(t) \\ & + \text{Constant} \end{aligned}$$

where

$$\Delta V_{tot}(t) = 0$$

$$p(t) = S_{pos} \Delta V_{tot}(t) ; \Delta V_{tot}(t) \geq 0$$

$$p(t) = S_{neg} \Delta V_{tot}(t) ; \Delta V_{tot}(t) \leq 0$$

1.2 Scaled Kinetic Model

1.2.1 Plant Constants

| | | | |
|-----------|----------------------|----------------|------------------------|
| C_C | 1.196 | $W_{6,1}$ | 604.8 |
| C_E | 0.130 | α | 0.94 |
| C_F | 0.121 | β_1 | 0.91×10^{-3} |
| C_L | 1.162 | β_2 | 2.96×10^{-3} |
| l | 2.5×10^{-5} | β_3 | 1.31×10^{-3} |
| P_D | 9486 | β_4 | 1.68×10^{-3} |
| R | 466.8 (4238 GPM) | β_5 | 0.26×10^{-3} |
| S_{pos} | 186 | δ | 1.126×10^{-3} |
| S_{neg} | 111 | γ_p | 3.1×10^{-6} |
| V_C | 3.222 | γ_T | -3.4×10^{-4} |
| V_G | 13.11 | Θ_{FC} | 18.1 |
| $V_{2,3}$ | 6.031 | Θ_{Gs} | 48.9 |
| $V_{3,4}$ | 23.87 | $\Theta_{1,2}$ | 16.99 |
| $V_{5,6}$ | 12.05 | λ_1 | 1.58 |
| $V_{6,1}$ | 12.35 | λ_2 | 0.328 |
| V_L | 85.0 | λ_3 | 0.126 |
| W_C | 157.8 | λ_4 | 0.035 |
| W_E | 2400 | λ_5 | 0.0128 |
| W_F | 429.7 | τ_C | 0.3380 |
| W_G | 641.8 | τ_G | 1.375 |
| W_L | 4370 | $\tau_{2,3}$ | 0.6327 |
| $W_{2,3}$ | 295.3 | $\tau_{3,4}$ | 2.504 |
| $W_{3,4}$ | 1169 | $\tau_{5,6}$ | 1.264 |
| $W_{5,6}$ | 589.8 | $\tau_{6,1}$ | 1.296 |

1.2.2 Time and Amplitude Scaling Factors

A time scaling factor of unity (computer and real time scales equal) was used because of the speed of the transients involved and the ease of scaling.

An amplitude scaling factor of unity (one volt per physical unit) was used for ease of interpreting computer results and for ease of scaling. Proper voltage levels were then obtained by the use of multiples or fraction of the variables.

1.2.3 Potentiometer Settings

A listing of servo-set potentiometer settings is given in Table 1-1. Each setting is stated in terms of both plant symbols and specific numerical value.

1.2.4 Analog Circuit Diagram

The circuit diagram for wiring the electronic analog computer is shown in Fig. 1-1. Feedback connections have been included to demonstrate the many interactions involved.

1.3 Analog Computer Model Response

The transient response of the kinetic model was determined for a series of load perturbations. Fig. 1-2 illustrates response to instantaneous load reductions and Fig. 1-3 to instantaneous load increases. A listing of run numbers and the corresponding conditions applied is given in Table 1-2.

Only plant load perturbations were considered since primary pressure variations due to control rod perturbations would be of less magnitude than those due to the worst load changes considered.

1.4 Selection of Pressurizer Size

A pressurizer vessel containing 12.1 cubic feet of vapor and 5.9 cubic feet of liquid was selected as being more than adequate for any primary system volume changes that would be encountered in the operation of the power plant.

Analog computer analysis of the plant model indicates that the maximum primary pressure variations are ± 230 and -66 psi when the anticipated value of temperature coefficient is used. These pressure swings correspond to instantaneous load drop and rise respectively between 100% and 0% of rating.

An extrapolated value of -3.4×10^{-4} is anticipated for the temperature coefficient of reactivity. Although expectations of this high a coefficient are well justified, it is conceivable that a value as low as -3.0×10^{-4} might exist, though this is a highly conservative extrapolation. Under such circumstances the maximum primary pressure variations are ± 250 and -76 psi corresponding to the extreme load perturbations mentioned.

The computer model is very conservative in determining positive primary pressure surges since adiabatic vapor compression is assumed in the pressurizer. Heat transfer by vapor condensation on vessel walls and liquid free surface is neglected. A comparison of adiabatic model and actual plant response to similar perturbations showed the pressure surges to be in the ratio of about 2 to 1 respectively for the APPR-1. See APAE 38 (1) for further details.

Primary pressure surges of the model are also conservative since secondary system heat losses and auxiliary uses of steam are not included. The minimum load on the steam generator is actually in the order of 1/2 % of rating.

The primary system is designed to structurally withstand under code regulations an internal pressure of 2000 psia, providing for a 250 psi pressure surge from the normal operating pressure of 1750 psia before opening of the safety valve. The pressurizer design is therefore seen to be more than adequate in meeting demands from extreme plant perturbations and uncertainties in specifications of plant constants.

Table 1-1

Servo-set Potentiometer Settings

| Pot No. | Setting | Value | Pot No. | Setting | Value |
|---------|--|--------|--------------------------------------|---|--------|
| 0 | -- | -- | 23 | $2/10 \tau_{2,3}$ | 0.3161 |
| 1 | Recorder Channels | | 24 | $1/10 \tau_{2,3}$ | 0.1580 |
| 2 | | | 25 | $1/10 \tau_{2,3}$ | 0.1580 |
| 3 | | | 26 | $200/RC_c$ | 0.3582 |
| 4 | | | 27 | $12/10 \tau_{3,4}^2$ | 0.1914 |
| 5 | | | 28 | $12/10 \tau_{3,4}^2$ | 0.1914 |
| 6 | | | 29 | $240/C_c W_{3,4}$ | 0.1717 |
| 7 | | | $\alpha P_D / 20 W_{FC} \Theta_{FC}$ | 0.4738 | 30 |
| 8 | $20 \alpha / W_{FC}$ | 0.3616 | 31 | $6/10 \tau_{3,4}$ | 0.2396 |
| 9 | $\alpha P_D / 100 W_{FC} \Theta_{FC}$ | 0.0948 | 32 | $2/10 \tau_G$ | 0.1455 |
| 10 | $200 \Theta_{FC} / P_D$ | 0.3816 | 33 | $2 \Theta_{1,2} / \Theta_{Gs} \tau_G$ | 0.5054 |
| 11 | $400 (1-\alpha) / W_C C_c$ | 0.1272 | 34 | $2/10 \tau_G + \Theta_{1,2} / \Theta_{Gs} \tau_G$ | 0.1707 |
| 12 | $2 \alpha \Theta_{1,2} / 10 \tau_c \Theta_{FC}$ | 0.5221 | 35 | $1000 / (W_{LL} / W_{EE})$ | 0.1856 |
| 13 | $2/10 \tau_c$ | 0.5917 | 36 | $P_D / (W_{LL} / W_{EE}) 2 \Theta_{Gs}$ | 0.0180 |
| 14 | $\alpha \Theta_{1,2} / 10 \tau_c \Theta_{FC} + 2 \tau_c$ | 0.8528 | 37 | $P_D / (W_{LL} / W_{EE}) \Theta_{Gs}$ | 0.0360 |
| 15 | $\gamma_T / 100 \ell$ | 0.1360 | 38 | $84 \Theta_{Gs} / P_D$ | 0.4330 |
| 16 | $35 \gamma V_c$ | 0.1270 | 39 | $2/10 \tau_{6,1}$ | 0.1544 |
| 17 | $3.5 \gamma V_{2,4}$ | 0.1178 | 40 | $1/ \tau_{6,1}$ | 0.7718 |
| 18 | $35 \gamma V_G$ | 0.5165 | 41 | $1/ \tau_{6,1}$ | 0.7718 |
| 19 | $35 \gamma V_{5,1}$ | 0.9614 | 42 | $200/RC_c$ | 0.3582 |
| 20 | $S_{neg} / 210$ | 0.5286 | 43 | $12/10 \tau_{5,6}^2$ | 0.7515 |
| 21 | $S_{pos} / 2100$ | 0.0884 | 44 | $12/10 \tau_{5,6}^2$ | 0.7515 |
| 22 | $3 \gamma_p / 5 \ell$ | 0.0744 | 45 | $240/C_c W_{5,6}$ | 0.3402 |

Table 1-1 (continued)

| Pot No. | Setting | Value | Pot No. | Setting | Value |
|---------|--------------------------------|--------|---------|--------------------------|--------|
| 46 | $6/10 \tau_{5,6}$ | 0.4748 | 58 | λ_5 | 0.0128 |
| 47 | $6/10 \tau_{5,6}$ | 0.4748 | 59 | $2 \beta_1 / 100 \ell$ | 0.7280 |
| 48 | $\Sigma \beta_1 / 500 \ell$ | 0.5696 | 60 | $84 \beta_2 / 10^4 \ell$ | 0.9946 |
| 49 | $\lambda_1 \beta_1 / 100 \ell$ | 0.5751 | 61 | $84 \beta_3 / 10^4 \ell$ | 0.4402 |
| 50 | $\lambda_1 / 10$ | 0.1580 | 62 | $84 \beta_4 / 10^4 \ell$ | 0.5649 |
| 51 | $\lambda_2 \beta_2 / 100 \ell$ | 0.3884 | 63 | $2 \beta_5 / 100 \ell$ | 0.2080 |
| 52 | λ_2 | 0.3280 | 64 | 1/2 | 0.5000 |
| 53 | $\lambda_3 \beta_3 / 10 \ell$ | 0.6602 | 65 | 200/840 | 0.2381 |
| 54 | λ_3 | 0.1260 | 66 | --- | -- |
| 55 | $\lambda_4 \beta_4 / 10 \ell$ | 0.2352 | 67 | --- | -- |
| 56 | λ_4 | 0.0350 | 68 | --- | -- |
| 57 | $\lambda_5 \beta_5 / 10 \ell$ | 0.0133 | 69 | --- | -- |

TABLE 1-2

Analog Computer Model Runs

| <u>Run Number</u> | <u>Conditions Applied</u> |
|-------------------|--|
| 1 | F.L. to 25% inst. |
| 2 | F.L. to 10% inst. |
| 3 | F.L. to 0% inst. |
| 4 | F.L. to 0% inst., no \mathcal{J}_p |
| 5 | F.L. to 0% inst., $\mathcal{J}_t = -3.0 \times 10^{-4}$ |
| 6 | 25% to F.L. inst. |
| 7 | 10% to F.L. inst. |
| 8 | 5% to F.L. inst. |
| 9 | 0% to F.L. inst. |
| 10 | 0% to F.L. inst., no \mathcal{J}_p |
| 11 | 0% to F.L. inst., $\mathcal{J}_t = -3.0 \times 10^{-4}$ |

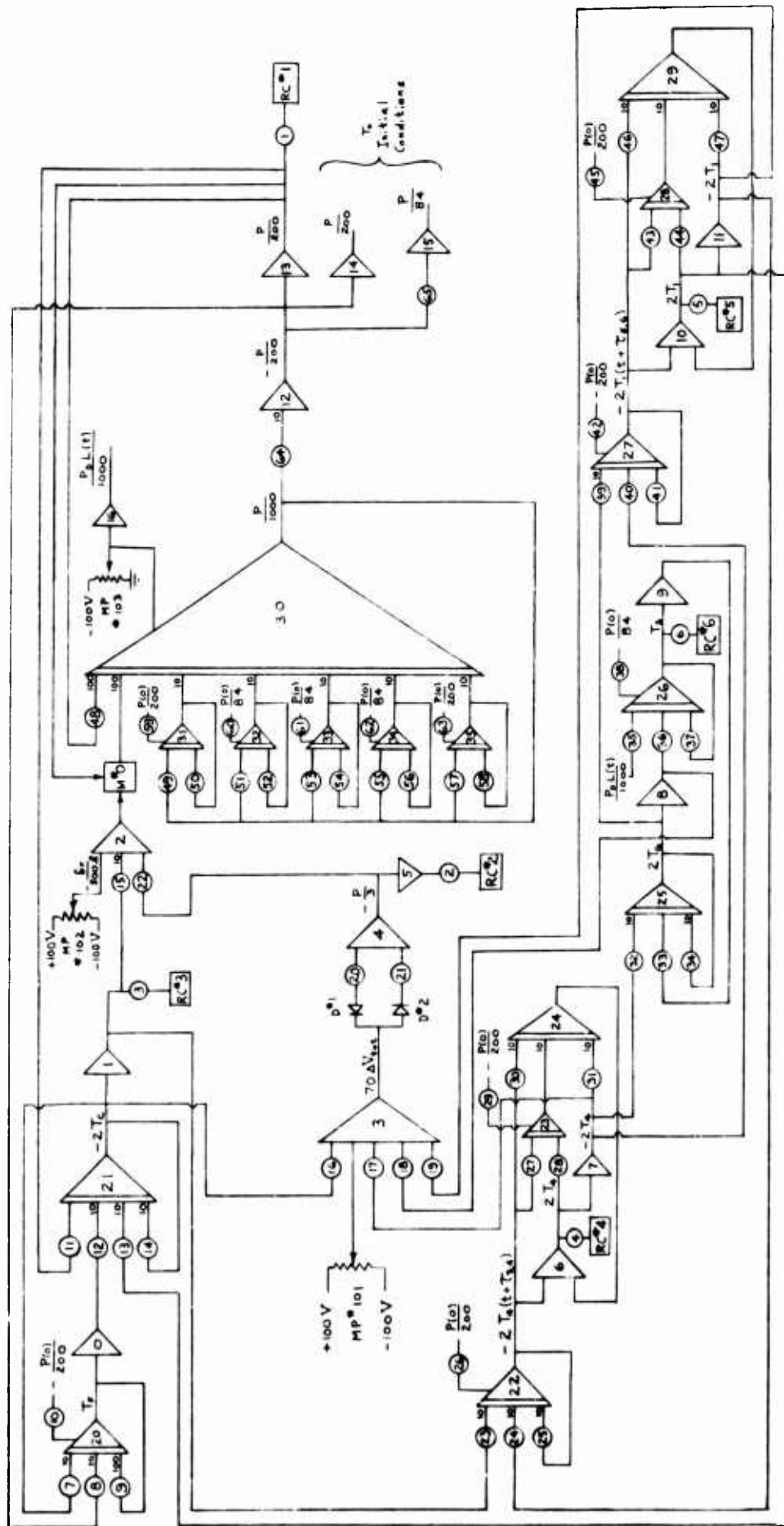
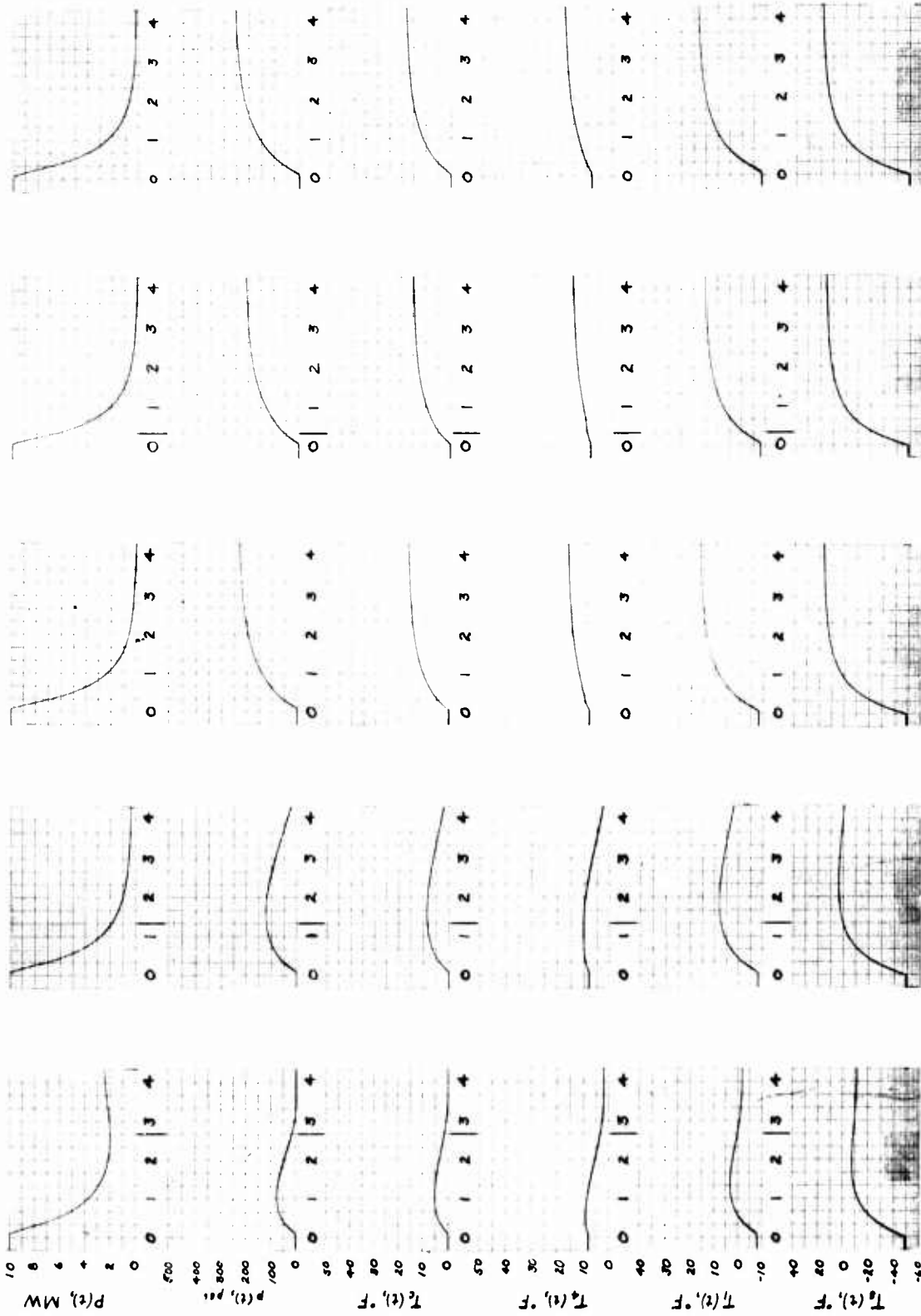


FIG. 1.1.1 -- ELECTRONIC ANALOG COMPUTER CIRCUIT DIAGRAM
FOR PLANT KINETIC MODEL



RUN # 1
FL - 2.5%

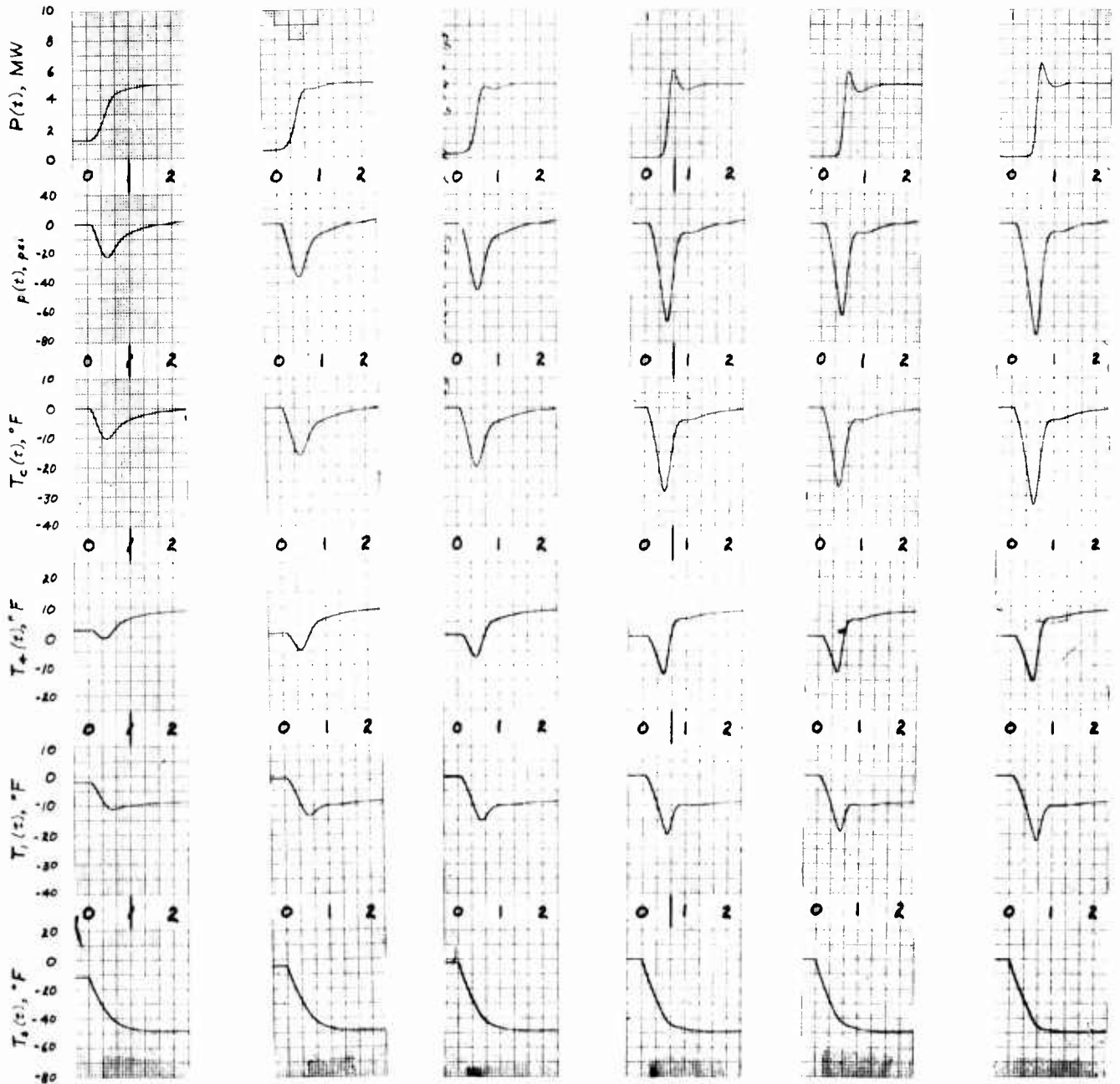
RUN # 2
FL - 10%

ELAPSED TIME, minutes
RUN # 3
FL - 0%

RUN # 4
FL - 0%
NO J_p

RUN # 5
FL - 0%
 $J_p = -3.0 \times 10^{-4}$

FIG. 1-2. PLANT RESPONSE TO INSTANTANEOUS LOAD REDUCTIONS



RUN #6
25% - FL

RUN #7
10% - FL

ELAPSED TIME, minutes
RUN #8
5% - FL

RUN #9
0% - FL

RUN #10
0% - FL
NO J_p

RUN #11
0% - FL
 $J_T = -3.0 \cdot 10^{-4}$

FIG. I-3. PLANT RESPONSE TO INSTANTANEOUS LOAD INCREASES

2.0 REACTOR BEHAVIOR FOLLOWING PUMP FAILURE

2.1 General Kinetic Model

2.1.1 Description

In this study the response of the reactor following a failure of the primary coolant pump was investigated. The nature of this failure was assumed to be one in which the impeller of the pump becomes frozen thus impeding coolant flow. This is a conservative assumption.

Coolant flow due to natural convection is neglected in the computer equations due to the physical location of the steam generator. Murray (2) has shown that when the steam generator is located below the reactor vessel coolant flow due to natural convection will be negligible.

After pump failure the diminishing rate of coolant flow results in increased temperatures both in the fuel and in the coolant within the core. If the reactor continues to operate at rated power this temperature rise will cause boiling within the reactor vessel. It is thus necessary to incorporate a reactor scram system activated when the coolant decreases to a pre-set value of maximum flow rate. This study is intended to indicate whether boiling temperatures will occur before the reactor is scrammed.

2.1.2 Pump Coastdown Characteristics

In calculating the rate of pump coastdown after an accident the kinetic energy possessed by the moving coolant is equated to the friction of the loop. The normalized flow rate "G (t)" is integrated over the range of flow yielding: (3)

$$G(t)^{0.8} = \frac{a}{t^2 g}$$

$$\text{where: } a = \frac{\sum_{i=1}^i \frac{L_i}{A_i} F(t=0)}{0.8 g H(t=0)}$$

L_i = length of pipe section i (ft)

A_i = cross sectional area of pipe (ft²)

$F(t=0)$ = design coolant flow rate (ft/sec)

$H(t=0)$ = head drop around coolant loop (ft)

g = acceleration due to gravity

In the system under consideration, it was assumed that the impeller of the coolant pump had become frozen and thus was further impeding coolant flow. A value of 59.2 ft was used as the negative head. This was obtained from data of a pump similar to that envisioned in this design.

The value of "a" thus becomes:

$$a = \frac{66.751 \times 9.532}{0.8 \times 32.2 \times 98.52} = 0.2507$$

2.1.3 Differential Equations

Utilizing the notation of section 1.1.2 the general kinetic equations are: (1)

$$\frac{dP}{dt}(t) = \left(\frac{0.01 \delta r / \lambda + T_c(t) / \sum_{i=1}^5 \beta_i}{l} \right) P(t) + \sum_{i=1}^5 \lambda_i k_i(t)$$

where: $\frac{dk_i}{dt}(t) = \frac{\beta_i P(t)}{l} - \lambda_i k_i(t)$

The pressure coefficient of reactivity commonly included in the above expression is neglected because there will be insufficient circulation of coolant external to the pressure vessel within the time being considered.

Performing a heat balance on the fuel and coolant within the core yields:

$$\frac{dT_f(t)}{dt} = \frac{\alpha_c P(t)}{W_f C_f} - \frac{Ah}{W_f C_f} (T_f(t) - T_c(t))$$

and

$$\frac{dT_c(t)}{dt} = \frac{(1 - \alpha) P(t)}{W_c C_c} + \frac{hA}{W_c C_c} (T_f(t) - T_c(t)) - \frac{2R}{W_c} (T_c(t) - T_{inlet})$$

where: $T_f(t=0) = \Theta_F, C$
 $T_c(t=0) = 0$

The meaning of symbols used is indicated in section 1.2.2

The flow rate, F(t), is given in section 2.1.2 by:

$$G(t) = \frac{F(t)}{F(t=0)} = \left(\frac{a}{a+t} \right)^{1.25}$$

where: $F(t=0)$ = rated coolant flow

t = time after pump failure accident

The constant a is dependent upon the physical configuration of the primary loop.

The average film coefficient in the core is a function of the flow mass rate to the 0.8 power.

$$\text{then: } \frac{h(t)}{h(0)} = \left(\frac{F(t)}{F(0)} \right)^{0.8} = \left(\frac{a}{a+t} \right)$$

$$h(0) = \frac{P_D}{A \Theta F.C}$$

The previous equations for the fuel and coolant temperatures become:

$$\frac{dT_f(t)}{dt} = \frac{\alpha}{W_F C_F} P(t) - \frac{A}{W_F C_F} h(0) \left(\frac{a}{a+t} \right) (T_f(t) - T_c(t))$$

$$\frac{dT_c(t)}{dt} = \frac{(1-\alpha) P(t)}{W_c C_c} + \frac{A}{W_c C_c} h(0) \left(\frac{a}{a+t} \right) (T_f(t) - T_c(t)) -$$

$$\left[\frac{-2}{W_c} R \left(\frac{a}{a+t} \right)^{1.25} T_c(t) \right]$$

2.2 Constants for Differential Equations

2.2.1 Time and Amplitude Scaling Factors

A scaling factor was chosen in order that ten computer seconds would equal one second in real time. This was dictated by the rapid sequence of events following a pump failure accident and the need to get detailed behavior during this time.

An amplitude scaling factor of one volt equals one physical unit was chosen for this section of the analysis. The magnitude of the quantities generated were scaled proportionally in order that their magnitudes would not exceed ± 100 volts.

2.2.2. Potentiometer Setting

Table 2-1 lists the physical quantities in each potentiometer setting as well as their absolute magnitude in this problem.

TABLE 2 - 1 POTENTIOMETER SETTINGS

| Potentiometer | Quantity | Magnitude | Potentiometer | Quantity | Magnitude |
|---------------|---------------------------|-----------|---------------|-----------------------------|-----------|
| 1 | 1/2 | 0.5000 | 16 | λ_3 /10 | 0.0126 |
| 2 | $84\beta_2$ /10,000 l | 0.9946 | 17 | $\lambda_4\beta_4$ /100 l | 0.0235 |
| 3 | 20/84 | 0.2381 | 18 | λ_4 /10 | 0.0035 |
| 4 | 2 β_1 /100 l | 0.7280 | 19 | $\lambda_5\beta_5$ /100 l | 0.0013 |
| 5 | $84\beta_3$ /10,000 l | 0.4402 | 20 | λ_5 /10 | 0.0013 |
| 6 | $84\beta_4$ /10,000 l | 0.5649 | 21 | 100 $\Theta_{f,c/PD}$ | 0.1908 |
| 7 | $84r_T$ /10,000 l | 0.2285 | 22 | A h_o /10 $W_f C_f$ | 0.9475 |
| 8 | $2\beta_5$ /100 l | 0.0280 | 23 | $10\infty/W_f C_f$ | 0.1808 |
| 9 | T_{in} /200 | 0.0425 | 24 | A h_o /10 $W_c C_c$ | 0.2611 |
| 10 | $\sum r \beta_1$ /50 l | 0.5696 | 25 | 2 R/ W_c | |
| 11 | $\lambda_1\beta_1$ /100 l | 0.5751 | 26 | 50 (1- ∞) $W_c W_c$ | |
| 12 | λ_1 /10 | 0.1580 | 27 | a/10 | 0.0251 |
| 13 | $\lambda_2\beta_2$ /100 l | 0.3884 | 28 | 1 /100 | 0.0100 |
| 14 | λ_2 /10 | 0.0328 | 29 | a/10 | 0.0251 |
| 15 | $\lambda_3\beta_3$ /100 l | 0.0660 | 30 | | |

2.2.3 Analog Circuit Diagram

Fig. 2-1 shows in symbolic form the analog circuitry used in this study. The notation is that utilized and explained in APAE-38(3).

2.3 Results of Analog Pump Failure Simulation

Solution of the coupled differential equations during the pump failure condition yields values of the average fuel surface temperature and the average coolant temperature. These solutions are shown in Fig. 2-2 where the reference value of the temperature coefficient of reactivity has been used. Fig. 2-3 is a plot of the results in which the temperature coefficient has been reduced by 25%.

The statistical hot channel for this system has been designed at 617° F. This is the saturation temperature at design pressure. The hot channel factor has been calculated assuming the simultaneous occurrence of all hot flux factors at the same point. This is definitely a conservative assumption. More

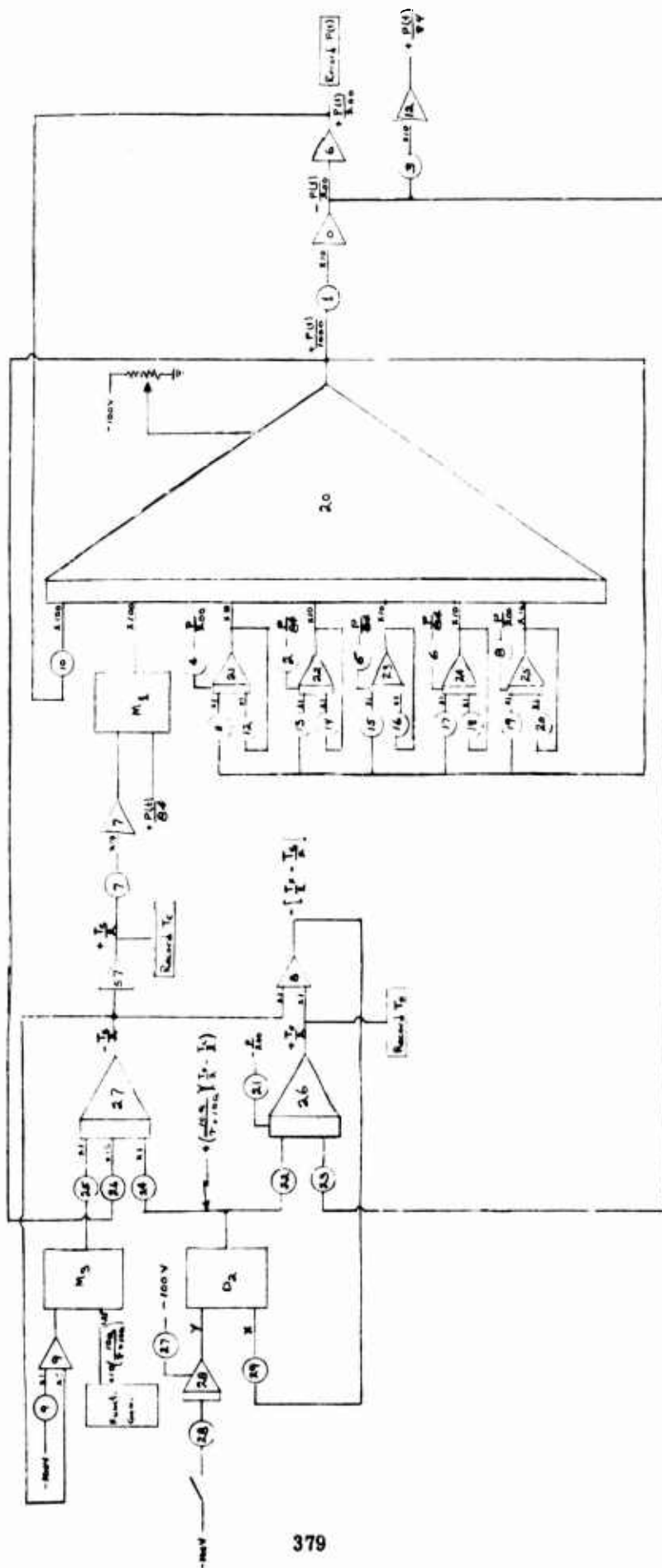
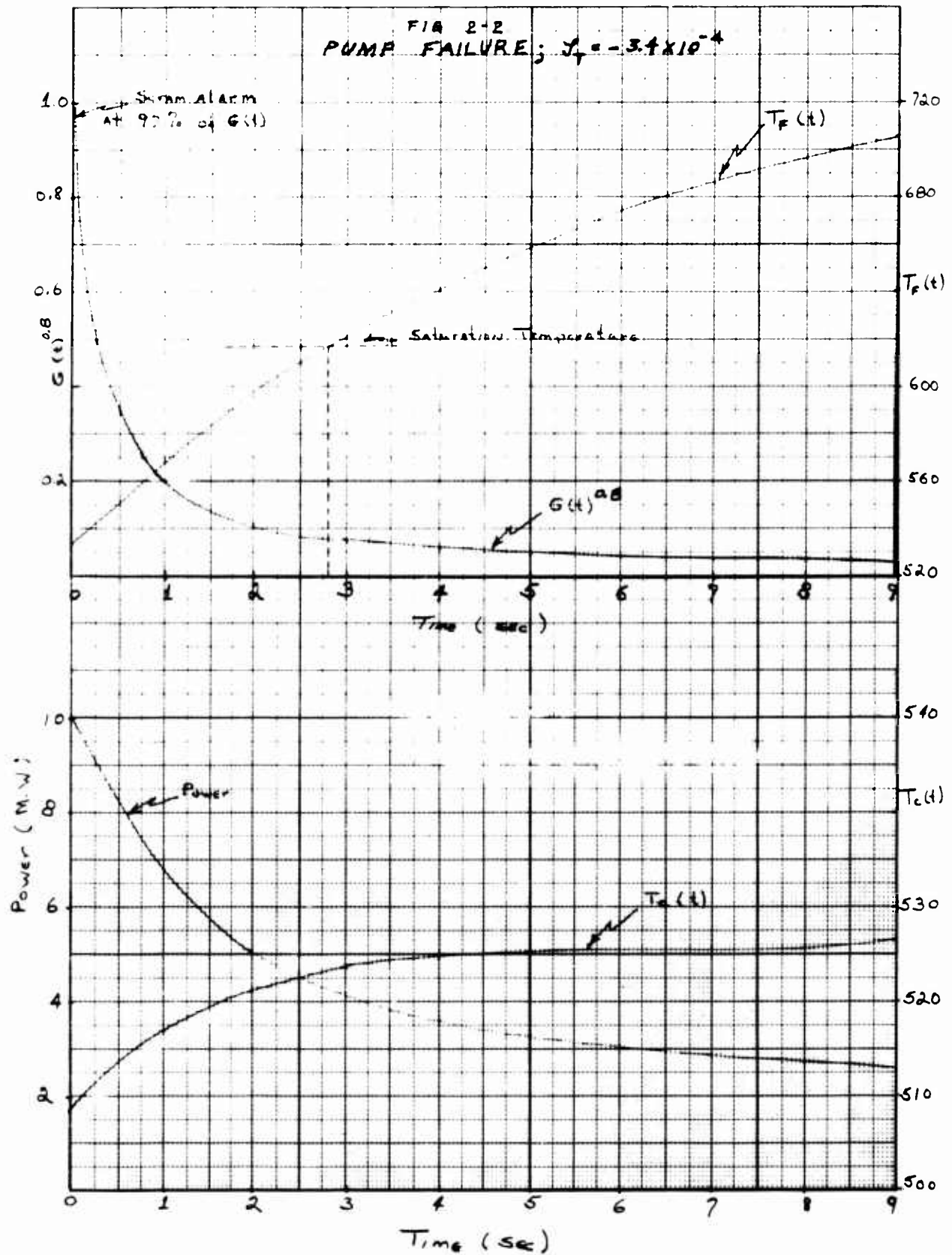
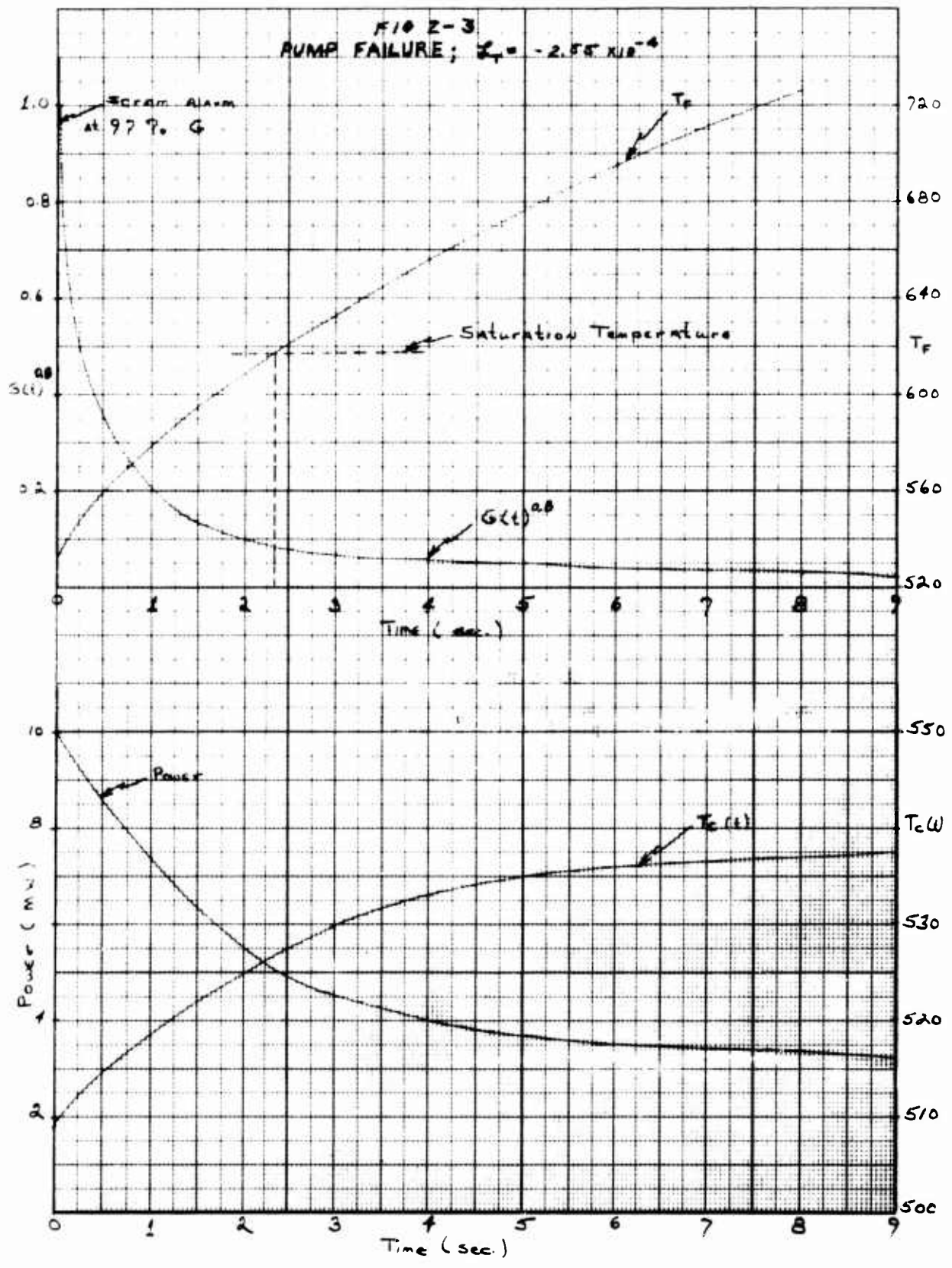


Figure 2-1 Analog Circuit Diagram

FIA 2-2
 PUMP FAILURE; $J_T = -3.4 \times 10^{-4}$





realistically the hottest channel would probably be near 607°F. Experimental data ⁽⁴⁾ indicate that nucleate boiling does not begin until the fuel surface temperature exceeds saturation temperature by as much as 30° F. By conservatively assigning a one second delay between the low flow scram signal and reactor shutdown one can estimate the rise in temperature within the hottest channel. Fig. 2-1 indicates a temperature rise of 43.4° F for the average fuel surface temperature during the second following the reactor scram signal assuming forced convection. The behavior of the hottest channel will follow this trend. Thus only limited nucleate boiling probably will occur within the hottest channel during a pump failure.

The analog results indicate a permissible 2.7 second delay between low flow scram and reactor shutdown. The average fuel surface temperature will not reach saturation before reactor shutdown.

2.4 Conclusions

Results of analog simulation of a pump failure accident in which the pump impeller becomes frozen indicate that only limited nucleate boiling will probably occur before reactor shutdown. The average fuel surface temperature during this accident will not reach saturation before reactor shutdown and therefore no general boiling will occur.

REFERENCES

III TRANSIENT ANALYSIS

1. Brendel, J.O. and J.R. Tomento, "Plant Transient Analysis of the APPR-1 by Analog Methods," APAE-38
2. Murray, R.L., "Notes on Decay Heating after Power Failure," APAE Memo 144.
3. Coneybear, J.F., "Pump Failure and the APPR-1," Astra Repeat 419-E-4.1.
4. Jens, W.H., "Analysis of Heat Transfer, Burnout, Pressure Drop, and Density Data for High-Pressure Water," ANL-4627.

SKID-MOUNTED APPR
DESIGN ANALYSIS

IV. CORE THERMAL & HYDRAULIC DESIGN ANALYSIS

1.0 THERMAL DESIGN CRITERIA

The contract sets forth certain General Objectives and Project Guidelines that affect the thermal design of the Skid Mounted APPR. The most important of these are:

- a. System reliability with minimum downtime for refueling.
- b. Utilization of proven technology
- c. Availability for procurement by January 1, 1959.

On the basis of these project guidelines the Skid Mounted APPR has been designed thermally so that the maximum surface temperature in the hot channel does not exceed the saturation temperature. The thermal design criteria employed on the APPR-1 and APPR-1a has been reviewed prior to start of the thermal analysis of the Skid Mounted APPR.

The following criteria have been established for thermal design of APPR pressurized-water reactors:

1.1 Heat Transfer Coefficient

The heat transfer coefficient is to be calculated by use of the Dittus-Boelter equation with a constant coefficient of 0.021:

$$h = 0.021 \frac{K}{D} \frac{VD}{\mu}^{0.8} (Pr)^{0.4}$$

where:

- h = heat transfer coefficient, Btu/ft²hr^{OF}
k = thermal conductivity, Btu/ft hr^{OF}
D = equivalent diameter of channel, ft
ρ = density of coolant, lb/ft³
V = velocity of coolant, ft/hr
μ = viscosity of coolant, lb/ft-hr
Pr = Prandtl number of coolant

The coefficient 0.021 was established subsequent to a survey of the literature on experimental heat transfer data, and is felt to be conservative, but not extremely so. Papers reviewed are referenced at the end of this section.

1.2 Power Distribution Utilization

A calculated axial power distribution is to be used for the analysis. Values from a calculated radial power distribution are combined with a side plate flux peaking factor and other existing peaking factors to establish in-

dividual nuclear radial factors for the various elements or groups of similar elements. Methods for the establishment of these factors are outlined by B. Byrne in paper entitled, "Thermal Design Basis for APPR Type Elements." In addition a nuclear uncertainty factor of 1.05 is applied to both the bulk coolant temperature rise and the film temperature gradient to account for uncertainties in the calculation of power distributions. In the heat transfer analysis the assumption is made that 95% of the heat released in the core is released in the active fuel elements. The basis for this assumption is explained in 1.6.3 of this section.

1.3 Hot Channel Factors

Manufacturing, orifice sizing, and inlet box effect hot channel factors are derived in 1.6.1 of this section for APPR-1 elements and are listed below. Elements with other dimensions should be treated similarly.

Average factors are those which apply to the bulk coolant temperature rise, and local factors, those which apply to the film temperature gradient.

TABLE 1-1 HOT CHANNEL FACTORS

| <u>Item</u> | <u>Factor</u> | |
|--|----------------|--------------|
| | <u>Average</u> | <u>Local</u> |
| Plate spacing deviation | 1.0706 | 1.1623 |
| Uranium content deviation* | 1.0050 | 1.0250 |
| Length deviation | 1.0357 | 1.0357 |
| Clad thickness deviation | 1.0064 | 1.0128 |
| Orifice sizing | 1.0417 | 1.0332 |
| Inlet box effect: | | |
| Fuel element | 1.0309 | 1.0247 |
| Control rod | 1.0638 | 1.0507 |
| Combined factor (Product of individual factors): | | |
| Fuel element | 1.2044 | 1.3230 |
| Control rod | 1.2428 | 1.3566 |

* This factor includes uranium content of the whole element along with homogeneity within the element.

1.4 Lattice Requirements

Since it is not possible to tailor lattice flow as is done with the internal flow, the entire lattice flow must be based on the maximum fuel element requirement. Calculations (see 1.6.2 of this section) indicate that the larger tolerances on lattice channel dimensions constitute an additional hot channel factor of 1.033. It is therefore felt that the lattice flow should be established on the basis of an average lattice velocity 5% greater than the highest stationary fuel element velocity.

1.5 Instrumentation Tolerances

Instrumentation tolerances for pressurized water reactors have been estimated by R.E. May, and indicated by G. Knighton in memos of 5/14/58 and 6/4/58 to be as follows:

| | |
|-------------------|---------|
| system pressure | ± 2.25% |
| core power | ± 3.5% |
| inlet temperature | ± 4°F |

The above values are conservative and it is feasible to improve same with more accurate, and more costly instrumentation.

1.6 Calculations

1.6.1 Hot Channel Factors

The hot channel factors, as listed in Table 1-1 were calculated on the basis of the following maximum deviations:

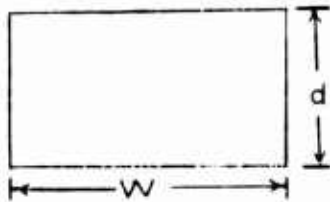
TABLE 1-2

| | <u>Nominal</u> | <u>Max. Deviation</u> |
|--|----------------|--------------------------------|
| Internal Plate spacing | .133" | ± .006 avg ± .0133 local |
| Uranium Content | | ± 0.5% average ± 2.5% local |
| Length | 21.75" | ± 0.75" |
| Clad thickness | .005" | ± .0005 avg ± .001 local |
| Relative Channel Flow as Governed by Orifice Diameter | 1.00 | ± 4% avg. and local |
| Effect of inlet box on flow distribution: | | |
| Fuel element | | 3% |
| Control rod | | 6% |

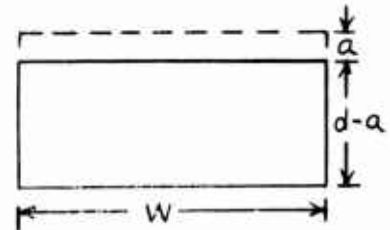
1.6.1.1 Plate Spacing Deviation Factors

(A) Average Hot Channel Factor

A flow passage may be restricted by plate bowing or sagging in the center, or by deviations in the plate edge spacing, the latter case being the most severe thermally.



Nominal Channel



Average Hot Condition

The reduction in flow area = aw

$$A_n = dw$$

$$A_{ha} = dw - aw = (d-a)w$$

$$D_n = \frac{4A_n}{P_n} = \frac{4dw}{2(d+w)} = \frac{2dw}{d+w}$$

$$D_{ha} = \frac{4A_{ha}}{P_{ha}} = \frac{4(d-a)w}{2(w+d-a)}$$

As the pressure drop P across each channel of the same element is essentially equal and as contraction and expansion coefficients for the channels are negligible, velocity variation is only a function of the average hydraulic diameter deviation

$$P = \frac{v^2}{12(2g)} C_c f \frac{L}{D} C_e$$

where C_c and C_e are essentially zero.

$$\frac{v_n^2}{v_{ha}^2} = \frac{D_n}{D_{ha}} \frac{d}{d+w} \times \frac{(w+d-a)}{(d-a)}$$

$$\frac{v_n}{v_{ha}} = \frac{d(w+d-a)}{(d+w)(d-a)}$$

$$F_{TR} = \frac{(TR)_{ha}}{(TR)_n} = \frac{A_n}{A_{ha}} \frac{v_n}{v_{ha}}$$

$$F_{TR} = \frac{d}{d-a} \frac{d+w-a}{d+w} \frac{1}{2}$$

Substituting the numerical values applicable for APPr elements:

$$d = .133''$$

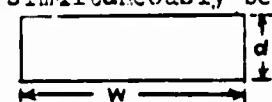
$$a = .006'' \text{ (min. average deviation)}$$

$$w = 2.733''$$

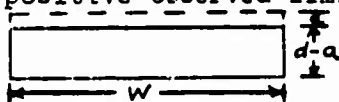
$$F_{TR} = 1.0706$$

(b) Local Hot Channel Factor

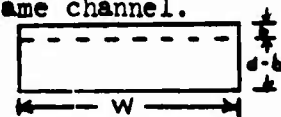
In defining the worst possible channel, thermally, the conservative approach is taken of considering that the average deviation could be the negative observed limit, while a local deviation could simultaneously be at the positive observed limit in the same channel.



Nominal Channel



Average Hot Condition



Local Hot Condition

$$A_n = dw$$

$$A_{hl} = (d-b)w$$

$$\frac{D_{hl}}{D_n} = \frac{A_{hl}}{A_n} = \frac{d-b}{d}$$

The local deviation is assumed to be sufficiently gradual to permit complete diffusion.

$$\frac{V_n}{V_{hl}} = \frac{V_n}{V_{ha}} \times \frac{V_{ha}}{V_{hl}} = \frac{(d/b)}{(d-a)^{3/2}} \sqrt{\frac{d(d/w-a)}{(d/w)}}$$

The film coefficient is reduced not only by the drop in coolant velocity but also by the increase in hydraulic diameter:

$$h = .021 \frac{k}{D} \left(\frac{\rho V D}{\mu} \right)^{0.8} \left(\frac{C_p \mu}{k} \right)^{0.4}$$

$$F_{\Delta T} = \frac{\Delta T_{hl}}{\Delta T_n} = \frac{h_n}{h_{hl}}$$

$$= \left(\frac{V_n}{V_{hl}} \right)^{0.8} \left(\frac{D_{hl}}{D_n} \right)^{0.2}$$

$$= \frac{(d/b)^{0.8}}{(d-a)^{1.2}} \left[\frac{d(d/w-a)}{(d/w)} \right]^{0.4} \left(\frac{d/b}{d} \right)^{0.2}$$

$$F_{\Delta T} = d^{0.2} \frac{(d/b)}{(d-a)^{1.2}} \left(\frac{d/w-a}{d/w} \right)^{0.4}$$

Substituting values for APPR elements:

$$b = .0133''$$

$$F_{\Delta T} = 1.1623$$

1.6.1.2 Uranium Content Deviation

(a) Average Hot Channel Factor

Both fuel elements forming the hot channel are assumed to contain the maximum allowable uranium content per plate.

$$F_{TR} = \frac{TR_{ha}}{TR_n} = \frac{W_{ha}}{W_n}$$

The maximum allowable positive deviation of uranium content per plate is 0.5%.

$$F_{TR} = \frac{W_n (1 + .005)}{W_n} = 1.0050$$

(b) Local Hot Channel Factor

$$F_{\Delta T} = \frac{\Delta T_h}{\Delta T_n} = \frac{W_{hl}}{W_n}$$

In addition to the 0.5% uranium content deviation per plate, there is a maximum allowable non-homogeneity within a plate of 2%. Assuming, conservatively, that the maximum positive deviation per plate and the maximum positive non-homogeneity deviation occur simultaneously, the maximum local uranium content deviation is 2.5%.

$$F_{\Delta T} = \frac{W_n (1 / .025)}{W_n} = 1.0250$$

1.6.1.3 Active Core Length Deviation

For a given volume of meat per plate, a negative deviation in active length increases the amount of meat per unit length and therefore per unit heat transfer area. This affects both the bulk coolant temperature rise and the film gradient. Based on the conservative approach that decreased length increases only meat thickness and not active width:

$$F_{TR} = F_{\Delta T} = \frac{L_n}{L_{min}}$$

for APPR fuel elements:

$$L_n = 21.75''$$

$$L_{min} = 21''$$

$$F_{TR} = F_{\Delta T} = \frac{21.75}{21} = 1.0357$$

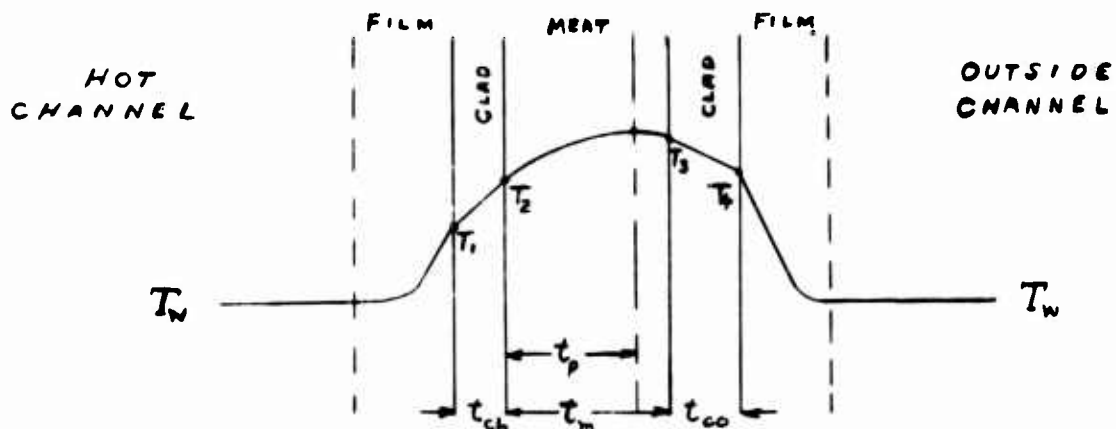
It may be noticed that since the nominal meat width is also the minimum meat width, a corresponding calculation is not necessary for active width deviation.

1.6.1.4 Clad Thickness Deviation Factors

- Derivation of General Equations

If the two clad thicknesses of a fuel plate are unequal, a greater portion of the total heat generated in the meat will pass out through the thinner clad because of lower thermal resistance. A hot channel is, therefore, defined as being composed of two fuel plates whose inner and outer clad thicknesses are at the minimum and maximum observed values respectively. Both the average and local hot channel factors are then equal to the proportional increase in the heat transmitted through the inner sides.

A cross section of the hot channel fuel plate is shown in the diagram below. The water temperatures are conservatively assumed equal.



The determination of hot channel factors is derived in the following steps.

- a) Determine the general differential equation for the temperature distribution through the meat as a volume heat source.
 - b) Determine the general solution for step (a). Substituting boundary conditions, solve for the general constants of integration.
 - c) Determine the location of the temperature peak by setting slope of temperature curve equal to zero. Portion the heat flow through two clads accordingly, in terms of meat boundary conditions.
 - d) Determine the temperature gradient through each clad and water film combination, using the results of step (c). The meat boundary conditions are then defined in terms of physical dimensions and properties.
 - e) Substitute the meat boundary conditions as determined by step (d) into the expressions for proportioning of heat flow as determined in step (c). The hot channel factor is then simply the ratio of the hot channel side flow to the average or nominal flow.
- a) The general differential equation for temperature distribution through a volume heat source is determined as follows:

$$q_{in} = -K_m \left(\frac{dt_m}{dx} \right)_x$$

$$q_{out} = -K_m \left(\frac{dt_m}{dx} \right)_{x/dx}$$

$$q_{out} - q_{in} = Qdx$$

$$\left(\frac{dt_m}{dx} \right)_{x/dx} - \left(\frac{dt_m}{dx} \right)_x \neq \left(\frac{d^2t_m}{dx^2} \right) dx$$

By proper substitution and simplification:

$$q_{out} - q_{in} = -K_m \left(\frac{dt_m}{dx} \right)_{x/dx} \neq K_m \left(\frac{dt_m}{dx} \right)_x$$

$$Qdx = -K_m \left[\left(\frac{dt_m}{dx} \right)_x \neq \left(\frac{d^2t_m}{dx^2} \right) dx \right] \neq K_m \left(\frac{dt_m}{dx} \right)_x$$

$$Qdx = -K_m \left(\frac{d^2t_m}{dx^2} \right) dx$$

$$\frac{d^2t_m}{dx^2} = - \frac{Q}{K_m}$$

b) The differential equation is solved by the reduction of order method:

$$\text{Let } \frac{dt_m}{dx} = y \text{ then } \frac{dy}{dx} = -\frac{Q}{K_m}$$

$$\int dy = -\frac{Q}{K_m} \int dx$$

$$\frac{dt_m}{dx} = y = -\frac{Q}{K_m} x + c_1$$

$$\int dt_m = -\frac{Q}{K_m} \int x dx + c_1 \int dx$$

$$t_m = -\frac{Q}{2K_m} x^2 + c_1 x + c_2$$

Boundary conditions (See Fig. 1):

$$x = c; T_m = T_2$$

$$x = t_m; T_m = T_3$$

By substitution of boundary conditions into the general solution:

$$T_2 = c_2$$

$$T_3 = -\frac{Q}{2K_m} t_m^2 + c_1 t_m = T_2$$

$$c_1 = \frac{T_3 - T_2}{t_m} + \frac{Qt_m}{2K_m}$$

Substituting these results to obtain the specific solution:

$$T_m = -\frac{Q}{2K_m} x^2 + \left[\frac{T_3 - T_2}{t_m} + \frac{Qt_m}{2K_m} \right] x + T_2$$

c) To find the point of temperature peaking, and therefore the point of direction change in heat transfer, determine t_p where $\frac{dT_m}{dx} = 0$:

$$\frac{dT_m}{dx} = -\frac{Q}{K_m} t_p + \left[\frac{T_3 - T_2}{t_m} + \frac{Qt_m}{2K_m} \right] = 0$$

$$t_p = \frac{t_m}{2} + \frac{K_m}{Qt_m} (T_3 - T_2)$$

It is seen from this expression for t_p that the peak temperature normally occurs in the center of the meat, but that a correction is necessary with unequal sink temperatures. This is, of course, as expected.

As heat generation per unit volume is uniform, the fraction of the total heat flow that is leaving the fuel plate on the hot channel side is equal to t_p/t_m . Therefore:

$$q_h = Q t_p \\ = \frac{Qt_m}{2} \cdot \frac{K_m}{t_m} (T_3 - T_2)$$

$$q_c = Q (t_m - t_p) \\ = \frac{Qt_m}{2} - \frac{K_m}{t_m} (T_3 - T_2)$$

d) Since an expression is available for the heat flow rate through the clad and water film on either side, the corresponding temperature gradients can be determined:

$$T_2 - T_w = q_h \left(\frac{1}{h_{ch}} + \frac{1}{h_f} \right) \\ = q_h \left(\frac{t_{ch}}{K_c} + \frac{1}{h_f} \right)$$

Similarly for the other plate side:

$$T_3 - T_w = q_c \left(\frac{t_{co}}{K_c} + \frac{1}{h_f} \right)$$

By subtraction and substitution for q_c :

$$T_3 - T_2 = q_h \left[\frac{t_{co}}{K_c} + \frac{1}{h_f} \right] - q_h \left[\frac{t_{ch}}{K_c} + \frac{1}{h_f} \right] \\ T_3 - T_2 = [Qt_m - q_h] \left[\frac{t_{co}}{K_c} + \frac{1}{h_f} \right] - q_h \left[\frac{t_{ch}}{K_c} + \frac{1}{h_f} \right] \\ T_3 - T_2 = Qt_m \left[\frac{t_{co}}{K_c} + \frac{1}{h_f} \right] - q_h \left[\frac{t_{ch}}{K_c} + \frac{2}{h_f} + \frac{t_{co}}{K_c} \right]$$

For convenience in handling, this latter expression will be written as:

$$T_3 - T_2 = Qt_m \alpha - q_h \beta; \quad \alpha = \frac{t_{co}}{K_c} + \frac{1}{h_f} \\ \beta = \frac{t_{co}}{K_c} + \frac{t_{ch}}{K_c} + \frac{2}{h_f}$$

e) The final expression for q_h can now be determined by substituting this final relationship in paragraph (d) for $T_3 - T_2$ into the equation for q_h in paragraph (c):

$$\begin{aligned}
 q_h &= \frac{Q t_m}{2} \div \frac{K_m}{t_m} (T_3 - T_2) \\
 &= \frac{Q t_m}{2} \div \frac{K_m}{t_m} (Q L_m \alpha - q_h \beta) \\
 &= \frac{Q t_m}{2} \div Q K_m \alpha \\
 &= \frac{K_m}{t_m} \beta \div 1
 \end{aligned}$$

The hot channel factor is now determined by dividing the maximum by the nominal heat flux

$$F = \frac{q_h}{q_n} = \frac{\frac{Q t_m}{2} \div Q K_m \alpha}{\frac{Q t_m}{2}}$$

$$F = \frac{Q t_m \div 2 Q K_m \alpha}{2} \cdot \frac{t_m}{K_m} \cdot \frac{2}{Q t_m}$$

$$F = \frac{t_m \div 2 K_m \alpha}{t_m \div K_m \beta}$$

$$\alpha = \frac{t_{co}}{K_c} \div \frac{1}{h_f}$$

$$\beta = \frac{t_{co}}{K_c} \div \frac{t_{ch}}{K_c} \div \frac{2}{h_f}$$

It is seen that when the two clad thicknesses t_{co} and t_{ch} are equal, then $\beta = 2\alpha$ and $F = 1$ as expected.

(a) Average Hot Channel Factor

The following numerical values are applicable for APPR elements:

$$t_m = .0200 \text{ in. (nominal)}$$

$$t_{ch} = .0045 \text{ in. (minimum average)}$$

$$t_{co} = .0055 \text{ in. (maximum average)}$$

$$k_m = .000205 \text{ Btu/in. } ^\circ\text{F sec (at } 600^\circ\text{F)}$$

$$k_c = .000274 \text{ Btu/in. } ^\circ\text{F sec (at } 600^\circ\text{F)}$$

$$h_f^* = .00459 \text{ Btu/in.}^2 \text{ } ^\circ\text{F sec}$$

By computation:

$$\alpha = 237.94 \text{ in}^2 \text{ } ^\circ\text{F} \text{ } \text{sec/Btu}$$

$$\beta = 472.23 \text{ in}^2 \text{ } ^\circ\text{F} \text{ } \text{sec/Btu}$$

* To be precisely correct, h_f would have to be re-evaluated for each new core and for each element within the core. However, as even a large change in h_f has an insignificant effect on required flow, an average value is used.

Substituting into the expression for hot channel factors developed in section (a):

$$F_{TR} = \frac{TR_h}{TR_n} = \frac{q_h}{q_n} = \frac{t_m / 2 k_m \alpha}{t_m / k_m \beta}$$

$$F_{TR} = 1.0064$$

(b) Local Hot Channel Factor

The following numerical values are applicable for the local factor:

$$t_{ch} = .0040 \text{ in. (minimum local)}$$

$$t_{co} = .0060 \text{ in. (maximum local)}$$

By computation:

$$\alpha = 239.76 \text{ in}^2 \cdot ^\circ\text{F} \cdot \text{sec/Btu}$$

$$\beta = 472.23 \text{ in}^2 \cdot ^\circ\text{F} \cdot \text{sec/Btu}$$

Substituting into the expression for hot channel factors:

$$F_{\Delta T} = \frac{\Delta T_h}{\Delta T_n} = \frac{q_h}{q_n} = \frac{t_m / 2 k_m \alpha}{t_m / k_m \beta}$$

$$F = 1.0128$$

1.6.1.5 Orifice Sizing Factors

The orifice diameter required to yield a given flow rate for a particular fuel element will be determined by a flow test rig. Some flow deviation allowance must be made for instrument error and experimental accuracy. As the calculated value of the proper orifice diameter is expressed to the nearest 1/64" for machining purposes, an additional deviation allowance must be introduced. Experience with the APFR-1 demonstrates that a combined maximum deviation of $\pm 4\%$ is sufficient for both stationary element and control rod flow.

The hot channel factors associated with a 4% reduction in flow from an undersized orifice are determined in a manner similar to that used for the factors associated with plate spacing deviation with the exception that no change in the channel flow area is considered.

(a) Average Hot Channel Factor

$$F_{TR} = \frac{TR_h}{TR_n} = \frac{V_n}{V_h}$$

$$F_{TR} = \frac{V_n}{V_n (1-.04)} = 1.0417$$

(b) Local Hot Channel Factor

$$F_T = \frac{T_h}{T_n} = \frac{h_n}{h_h} = \left(\frac{V_n}{V_h} \right)^{0.8}$$
$$F_T = \frac{V_n}{V_n(1-.04)^{0.8}} = 1.0332$$

1.6.1.6 Inlet Box Effect on Flow Distribution

An allowance is made for uneven flow distribution on leaving the fuel element inlet boxes. For stationary elements, the outer channel flow was assumed to be 3% below average. For control rods the outer channel flow was assumed to be 6% below average. Further investigation of this subject is intended.

(a) Average Hot Channel Factor

$$F_{TR} = \frac{TR_h}{TR_n} = \frac{V_n}{V_h}$$
$$(F_{TR})_{F.E.} = \frac{V_n}{V_n(1-.03)} = 1.0309$$
$$(F_{TR})_{C.R.} = \frac{V_n}{V_n(1-.06)} = 1.0638$$

(b) Local Hot Channel Factor

$$F_T = \frac{T_h}{T_n} = \frac{h_n}{h_h} = \left(\frac{V_n}{V_h} \right)^{0.8}$$
$$(F_T)_{F.E.} = \frac{V_n}{V_n(1-.03)^{0.8}} = 1.0247$$
$$(F_T)_{C.R.} = \frac{V_n}{V_n(1-.06)^{0.8}} = 1.0507$$

1.6.1.7 Symbols and Nomenclature

- a - Max. negative average deviation of plate spacing, in.
- A - Channel flow area, in.²
- b - Max. positive local deviation of plate spacing, in.
- c - Specific heat of water, Btu/lb.-°F
- C - Flow coefficient
- d - Nominal plate spacing, in.
- D - Hydraulic diameter of channel, in.
- f - Channel friction factor
- F - Hot channel factor
- h - Water film heat transfer coefficient, Btu/in.²-°F.-sec.
- k - Thermal conductivity, Btu-in./in.²-°F.-sec.
- L - Channel length, in.
- p - Perimeter of channel, in.

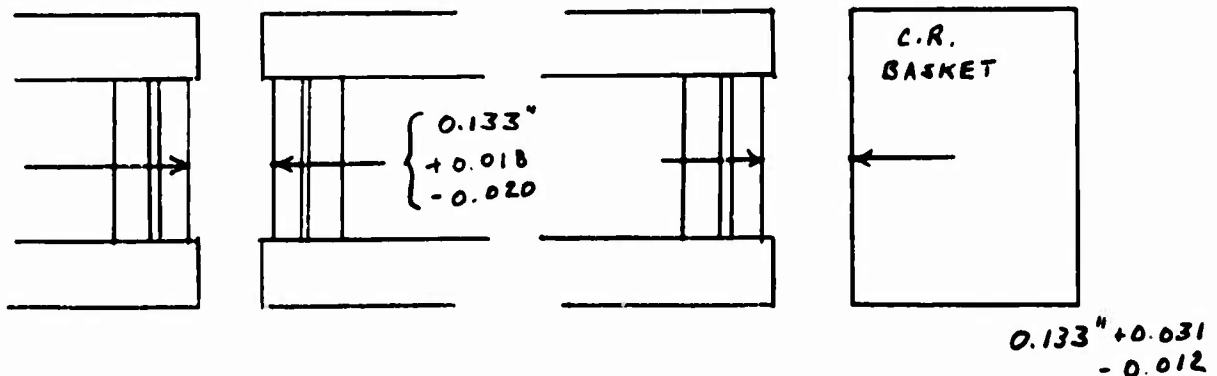
- ΔP - Pressure drop across channel, in. of water
- q - Heat flow rate, Btu/in.²-°F.-sec.
- Q - Volumetric heat generation rate in meat, Btu/in.³-sec.
- t - Thickness of meat or clad in fuel element, in.
- T - Temperature, °F.
- TR - Bulk temperature rise of channel flow, °F.
- Water viscosity, lb./in.-sec.
- V - Water velocity in channel, in./sec.
- w - Width of channel, in.
- W - Relative weight of uranium per plate
- X - Distance to point inside meat, measured from hot channel side perpendicular to plate, in.
- ϕ - Thermal neutron flux
- Water density, lb/in.³

- Subscripts

- a - Average conditions along length of channel
- avg. - Average conditions across width of fuel plate meat
- c - Clad
- C - Contraction flow on entering channel
- E - Expansion flow on leaving channel
- f - Water film
- h - Hot channel conditions
- l - Local conditions along length of channel
- m - Meat of fuel element
- n - Nominal conditions
- o - Outside channel (adjacent to hot channel)
- p - Peak meat temperature
- ΔT - Temperature gradient across water film
- TR - Bulk temperature rise of channel flow
- w - Water

1.6.2 Lattice Requirement Determination

The manufacturing tolerances for the lattice passages are, by necessity broader than those for the internal passages.



Since the larger lattice tolerances are a result of misalignment of entire elements rather than warping of individual plates, it is not possible for the average and local deviations to be in opposite directions. As the pressure drops across the various lattice channels are essentially equal, velocity variation is a function only of average hydraulic diameter deviation.

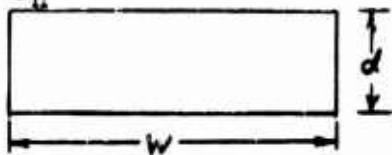
$$\frac{v_n^2}{v_h^2} = \frac{D_n}{D_h}$$

Since the effect on required flow of increased bulk coolant temperature rise hot channel factors is insignificant in comparison with the effect of increased film gradient hot channel factors, only the latter will be derived here.

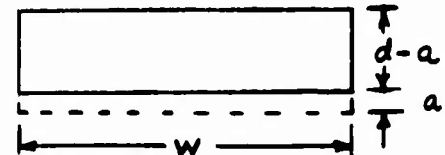
$$h = .021 \frac{k}{D} \left(\frac{\rho v D}{\mu} \right)^{0.8} \left(\frac{C_p \mu}{k} \right)^{0.4}$$

$$F_{\Delta T} = \frac{\Delta T_h}{\Delta T_n} = \frac{h_n}{h_h} = \left(\frac{v_n}{v_h} \right)^{0.8} \times \left(\frac{D_n}{D_h} \right)^{0.2} = \left(\frac{D_n}{D_h} \right)^{0.4} \times \left(\frac{D_h}{D_n} \right)^{0.2}$$

$$F_{\Delta T} = \left(\frac{D_n}{D_h} \right)^{0.2}$$



Nominal Channel



Hot Channel

$$A_n = dw$$

$$A_h = (d-a)w$$

$$F_{\Delta T} = \left(\frac{d}{d-a} \right) \left(\frac{d/w}{d/w-a} \right)$$

$$D_n = 4 A_n / p_n = \frac{2dw}{(d/w)}$$

$$D_h = 4 A_h / p_h = \frac{2(d-a)w}{d/w-a}$$

Between two fuel elements:

$$F_{\Delta T} = 1.033$$

Between fuel element and control rod basket

$$F_{\Delta T} = 1.019$$

It is therefore considered conservative to base the lattice flow on an average velocity 5% greater than the largest internal fuel element velocity.

1.6.3 Heat Release Distribution

The direct fission energy has the following distribution (Proceedings of the Symposium on the Physics of Fission Held at Chalk River, Ontario, May 14-18, 1956. Session C, CRP-642-A (July 1956)).

| <u>Source Energy</u> | CRP-642A 1956 |
|----------------------------|-----------------------|
| KE of Fission Fragments | 167.1 / 2 Mev |
| KE of Fast Neutrons | 5 / 0.5 Mev |
| Prompt Gamma Rays | 7 → 12 Mev |
| Fission Product Gamma Rays | 7.5 Mev |
| Beta Decay Energy | 5.5 Mev } / 2 Mev |
| Totals | 192.1 / 9.5 - 4.5 Mev |

It may be expected that most of the energy of the fast neutrons (5 Mev fissions) is released in the water moderator. Also a large fraction of the prompt gamma rays will be released in the fuel element side plates, end boxes, thermal shield, etc. In addition, there is a net energy gain in the n, α reactions in materials other than the fuel plates. Calculation for the MTR (An Estimate of the Heat Generation and Distribution in the MTR), R.A. Gremesey, (IDO-16443) indicate that only 90% of the heat generated is released in the fuel elements. Until detail heat generation and distribution are available for a particular design, a heat generation rate of 0.95 times the maximum expected shall be used as a basis for thermal design.

2.0 THERMAL ANALYSIS

The thermal analysis of the core is the determination of the core flow requirements, based upon the thermal design criteria previously discussed.

2.1 General Equations and Results

The required core flow is determined by use of the following equations:

$$(1) (T_{s_{\max}})_z = T_{in} + (\Delta T)_z + (\Delta \Theta)_z$$

$$(2) (\Delta T)_z = F_{avg} F_n F_{R\Delta T} \left[\frac{b \varphi}{w c_p} \int_0^{z/L} \frac{\bar{p}}{p} d \left(\frac{z}{L} \right) \right]$$

$$(3) (\Delta \Theta)_z = F_{loc} F_n F_{R\Delta \Theta} \left[\frac{\varphi}{h} \left(\frac{\bar{p}}{p} \right)_z \right]$$

where:

$(T_{s_{\max}})_z$ = maximum surface temperature of fuel plate at Z °F

T_{in} = inlet temperature of coolant fluid °F

$(\Delta T)_z$ = temperature rise of bulk coolant fluid from inlet to Z °F

$(\Delta \Theta)_z$ = temperature gradient across film at Z °F

F_{avg} = bulk coolant temperature rise hot channel factor

F_{loc} = film temperature gradient hot channel factor

F_n = nuclear uncertainty factor

$F_{R\Delta T}$) individual nuclear factors for the various elements,
) which represent the ratio of the heat flux of the
) hottest plate in the element to the average core
) flux and the ratio of the heat flux of the hottest
 $F_{R\Delta \Theta}$) spot on the hottest plate to the average core flux,
) respectively.

b = heat transfer area per flow channel, ft²

φ = average core heat flux, Btu/ft²-hr

w = flow per channel, lb/hr

C_p = specific heat of the bulk coolant fluid evaluated at the mean coolant temperature Btu/# °F.

h = film heat transfer coefficient, Btu/ft²-hr-°F.

L = active length of fuel element, ft.

Z = distance along the active meat length of element, measured from inlet, ft.

$\frac{\bar{p}}{\bar{p}}$ = ordinate of the axial power distribution normalized to an average of unity.

(4) b = 2 (active meat width) x (active meat length) of one fuel plate.

$$(5) \varphi = \frac{P \times 3413,000}{A} \times (.95) \times (F_{inst})$$

where:

P = total core heat output, MW

A = total heat transfer area, ft²

F_{inst} = factor for instrument tolerance

$$(6) h = .021 \frac{k}{D_e} \left[\frac{\rho V D_e}{\mu} \right]^{0.8} \left[\frac{C_p \mu}{k} \right]^{0.4}$$

where:

k = thermal conductivity of coolant, Btu/ft hr °F

D_e = equivalent diameter of one flow channel, i.e., one water gap, ft.

ρ = density of bulk coolant, #/ft³

V = coolant velocity through plates, ft/hr.

μ = viscosity of bulk coolant, #/ft-hr

C_p = specific heat of bulk coolant fluid, Btu/#-°F

$$(7) D_e = \frac{4 \text{ (flow area)}}{\text{wetted perimeter}}$$

Evaluating the above equations for various values of "Z", the maximum surface temperature for each element or group of similar elements for a range of assumed flow rates may be determined. The results are then plotted for each element as " $T_{s_{max}}$ vs. G.P.M." (See Fig. 2.2).

Knowing the saturation temperature corresponding to system pressure and the instrumentation tolerances on pressure and inlet temperature, a maximum allowable surface temperature can be determined. The required flow for each element can then be determined by use of the previously mentioned plots. Lattice flow is calculated on the basis outlined in item 1.4, Thermal Design Criteria.

The required flow thus calculated constitutes minimum core flow only. It is conservative in that the analysis assumes all worst possible factors and tolerances to occur simultaneously.

Since the calculated required flow was determined on the basis of a fully tailored core, i.e. equal maximum surface temperatures in all elements, it would be necessary to install, within the reactor vessel, a suitable orifice plate, designed to achieve the required velocity distribution. The proper size of the orifice holes for said plate would have to be determined experimentally on a flow rig, using simulated components prior to the completion of core and vessel fabrication.

It should be noted that since it is not possible to orifice control rod elements externally, and since the elements must be interchangeable, the flow for each control rod must be equal to the flow required by the hottest one, in this case the center element.

By the previously described method of analysis, the following results were arrived at as the tailored flow requirements for the Skid-mounted core:

| | |
|----------------------------------|----------|
| Inlet temperature | 500°F |
| Outlet temperature | 518.1°F |
| Max. plate surface temperature | 610°F |
| Minimum flow requirement of core | 4117 gpm |

The corresponding required velocity schedule for orificing the core is given in Table 2-1 as V/V_{avg} , where V_{avg} is the average core velocity.

As may be noticed from the velocity schedule, the variation of stationary fuel element flow requirements is very small. In fact the additional flow required in order to establish the flow through each stationary element equal to that through element 34, the hottest stationary element, is only 102 gpm. Since the advantage of tailoring is so minute for this core, it has been decided to use uniform flow.

Table 2-1

Velocity Schedule

| <u>Element No.</u> | <u>V/V avg core</u> |
|--------------------|---------------------|
| 44 | 1.0511 |
| 34 | 1.0138 |
| 33 | 0.9984 |
| 23 | 0.9006 |
| 22 | 1.0087 |
| Lattice | 1.0646 |

that is to allow equal flow for all stationary elements. It may be noticed, however, that some orificing is still necessary to compensate for plenum chamber effects and for the difference between pressure drop through a control rod and that through a stationary element. On the above basis, the following design conditions were established:

| | |
|------------------------------|----------|
| Flow per fixed element | 98.5 gpm |
| Flow per control rod element | 94.5 gpm |
| Lattice flow | 595 gpm |
| Total core flow | 4219 gpm |
| Inlet temperature | 500 °F |
| Outlet temperature | 517.6 °F |
| Maximum surface temperature | 610 °F |

2.2 Calculations

2.2.1 General Constants and Dimensions

| | |
|--------------------|-----------|
| Full thermal power | 10.0 MW |
| System pressure | 1750 psia |
| Inlet temperature | 500 °F |

Stationary fuel element nominal dimensions

| | |
|---|-----------|
| Meat thickness | 0.020 in. |
| Meat width | 2.500 in. |
| Meat height | 22 in. |
| Channel width | 2.733 in. |
| Channel depth | 0.133 in. |
| No. of plates per element | 18 |
| No. of plates per core, 18 x 32 elements | 576 |

Control rod fuel element nominal dimensions

| | |
|---------------------------|-----------|
| Meat thickness | 0.020 in. |
| Meat width | 2.281 in. |
| Meat height | 21 in. |
| Channel width | 2.513 in. |
| Channel depth | 0.133 in. |
| No. of plates per element | 16 |
| No. of plates per core | 80 |
| 16 x 5 elements | |

2.2.2 Heat Transfer Area

Heat transfer area per plate:

$$b = 2 \text{ (meat length) (meat width)}$$

$$b_{F.E.} = 2 \frac{(22)(2.5)}{144} = 0.7639 \text{ ft}^2$$

$$b_{C.R.} = 2 \frac{(21)(2.281)}{144} = 0.6653 \text{ ft}^2$$

for a control rod insertion of 9.25"

$$b_{C.R.} \frac{(9.25)}{21} = 0.2930 \text{ ft}^2$$

Total heat transfer area

$$A = 576 b_{F.E.} / 80 b_{C.R.} \frac{(9.25")}{21"} = 463.45 \text{ ft}^2$$

2.2.3 Average Heat Flux

Assuming that 95% of the total core power is generated in the fuel plates, and applying the instrumentation tolerance on power:

$$\phi = \frac{P \times 0.95 \times F_{inst} \times 3413,000}{A}$$

$$\phi = \frac{10.0 \times 0.95 \times 1.035 \times 3413,000}{463.45}$$

$$\phi = 72,410.2 \text{ Btu/ft}^2 \text{ - hr}$$

2.2.4 Bulk Coolant Temperature Rise

$$(\Delta T)_Z = F_{avg} F_n F_{R\Delta T} \left[\frac{b \phi}{w c_p} \int_0^{Z/L} \frac{p}{p} d \left(\frac{Z}{L} \right) \right]$$

where:

$$(F_{avg})_{F.E.} = 1.2044; (F_{avg})_{C.R.} = 1.2428$$

$$F_n = 1.05$$

$$b_{F.E.} = 0.7639 \text{ ft}^2; b_{C.R.} = 0.6653 \text{ ft}^2$$

$$Q = 72,410.2 \text{ Btu/ft}^2 \text{ hr}$$

$$C_p = 1.179 \frac{\text{Btu}}{\text{lb-}^\circ\text{F}} @ 510 \text{ F}$$

$$(\Delta T)_{Z_{F.E.}} = 5.93310 \times 10^4 \frac{F_{RAT}}{W} \int_0^{Z/L} \frac{\bar{p}}{p} d\left(\frac{Z}{L}\right)$$

$$(\Delta T)_{Z_{C.R.}} = 5.33205 \times 10^4 \frac{F_{RAT}}{W} \int_0^{Z/L} \frac{\bar{p}}{p} d\left(\frac{Z}{L}\right)$$

The integral represents the area under the curve of the axial normalized power distribution plotted versus Z/L.

The radial factors, F_{RAT} and $F_{RA\Theta}$, have been calculated by the nuclear group and are as follows (element numbers refer to Fig. 2-1):

| <u>Element No.</u> | <u>F_{RAT}</u> | <u>$F_{RA\Theta}$</u> |
|--------------------|-----------------------------|----------------------------------|
| 44 | 1.238 | 1.490 |
| 24 | 1.113 | 1.321 |
| 34 | 1.211 | 1.472 |
| 33 | 1.208 | 1.454 |
| 23 | 1.146 | 1.319 |
| 22 | 1.143 | 1.483 |
| 14 | | |
| 13 | | |

2.2.5 Heat Transfer Coefficient

$$h = .021 \frac{K}{D} \left[\frac{eVD}{\mu} \right]^{0.8} \left[\frac{C_p \mu}{K} \right]^{0.4}$$

where:

$$D_{FE} = 0.02144 \text{ ft}$$

$$D_{CR} = 0.02105 \text{ ft}$$

at 510 F

$$k = 0.3496 \text{ Btu/ft-hr-}^{\circ}\text{F}$$

$$\rho = 48.52 \text{ lb/ft}^3$$

$$\mu = 0.253 \text{ lb/hr ft}$$

$$Pr = \frac{c_p \mu}{k} = 0.853$$

$$h_{F.E.} = 0.99614 \text{ } v^{0.8}$$

$$h_{C.R.} = 0.99986 \text{ } v^{0.8}$$

2.2.6 Water Film Temperature Gradient

$$(\Delta\theta)_z = F_{loc} F_n F_R \Delta\theta \left[\frac{\varphi}{h} \left(\frac{\bar{p}}{\bar{p}} \right)_z \right]$$

where

$$(F_{loc})_{F.E.} = 1.3230; (F_{loc})_{C.R.} = 1.3566$$

$$F_n = 1.05$$

$$\varphi = 72,410.2 \text{ Btu/ft}^2 \text{ - hr}$$

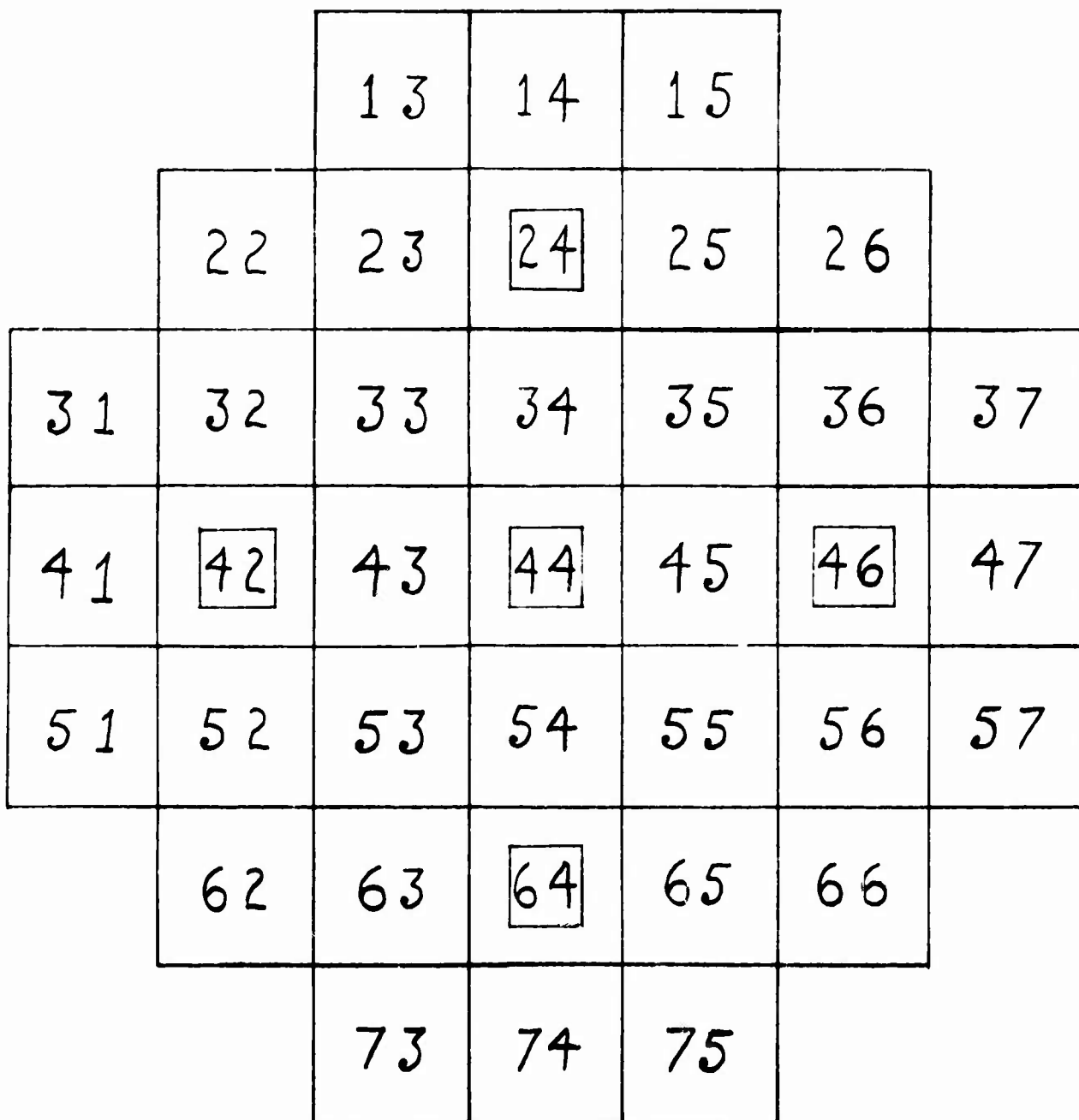
$$(\Delta\theta)_{z_{F.E.}} = 1.00749 \times 10^5 \frac{F_R \Delta\theta}{v^{0.8}} \left[\frac{\bar{p}}{\bar{p}} \right]_z$$

$$(\Delta\theta)_{z_{C.R.}} = 1.03158 \times 10^5 \frac{F_R \Delta\theta}{v^{0.8}} \left[\frac{\bar{p}}{\bar{p}} \right]_z$$

2.2.7 Maximum Surface Temperatures

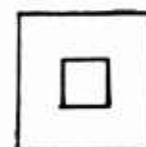
The above equations for $(\Delta T)_z$ and $(\Delta\theta)_z$ were evaluated for 1/2" increments along the length of the core for various elements and flow rates. It was thus established that the hot spot always occurs

FIGURE 2.1
 CORE FUEL ELEMENT ARRANGEMENT AND NUMBERING SYSTEM FOR
 SKID-MOUNTED REACTOR



— STATIONARY ELEMENT

CONTROL ROD —



axially, for the range of flows considered, at a position approximately 7.5" from the inlet to the active core. The values of $(T_s)_{max}$, as evaluated at this position for the various elements and a flow range from 30 - 100 gpm, are plotted in Figure 2-2.

2.2.8 Flow Requirements

By applying to the saturation temperature at 1750 psia tolerances for instrumentation on system pressure and inlet temperature, a maximum allowable surface temperature of 610°F was determined. The required flow for the various elements, corresponding to this temperature are listed in Table 2-2. The corresponding lattice flow is calculated as follows:

$$\text{Lattice flow} = \text{Max. F.E. flow} \times \frac{\text{Lattice area} \times 1.05}{\text{F.E. area}}$$

$$\begin{aligned} \text{Lattice flow} &= 98.5 \text{ gpm} \times \frac{0.2465 \text{ ft}^2}{0.0429 \text{ ft}^2} \times 1.05 \\ &= 594.3 \text{ gpm} \end{aligned}$$

Table 2-2

Total Required Flow

| | <u>Flow per Element GPM</u> | | <u>No. of Similar Elements</u> | | |
|----|-----------------------------|---|--------------------------------|---|---------------------------------|
| 44 | 94.5 | x | 5 | = | 472.5 |
| 34 | 98.5 | x | 4 | = | 394.0 |
| 33 | 97.0 | x | 4 | = | 388.0 |
| 23 | 87.5 | x | 8 | = | 700.0 |
| 22 | 98.0 | x | 16 | = | <u>1568.0</u> |
| | | | | | Total internal flow 3522.5 |
| | | | | | Lattice flow <u>594.3</u> |
| | | | | | Total Required Core Flow 4116.8 |

The summation of the various element flows and the lattice flow composes the minimum required core flow.

For uniform flow the total flow requirement is composed of the following:

Control rods

$$94.5 \text{ gpm/element} \times 5 \text{ control rods} = 473 \text{ gpm}$$

Stationary elements

$$98.5 \text{ gpm/element} \times 32 \text{ elements} = 3152 \text{ gpm}$$

Lattice

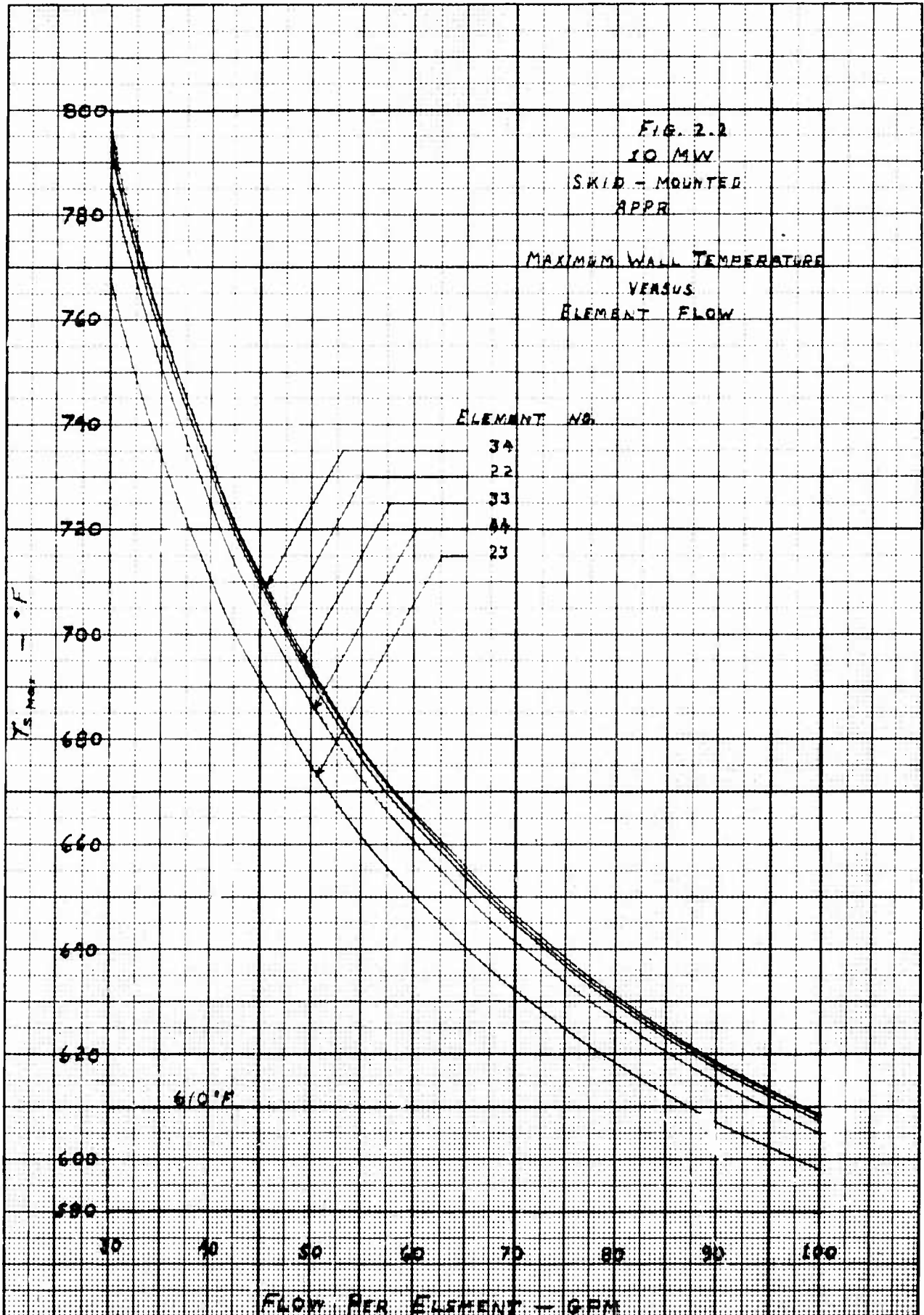
$$594.3 \text{ gpm} \quad \text{or} \quad \underline{594} \text{ gpm}$$

$$\text{Total core flow} = 4219 \text{ gpm}$$

For uniform flow through the stationary elements the minimum core flow requirement is therefore 4219 gpm.

2.3 Conclusions

The thermal analysis has determined the required flow for the core to be 4117 gpm for the case of tailored flow, and 4219 gpm for a uniform flow core. Since tailoring the flow in the core would result in a savings of only 102 gpm, tailoring is of little advantage for this particular core and it therefore has been decided to use uniform flow. This will still necessitate a small amount of orificing to compensate for plenum effects and for the larger pressure drop which occurs through the control rod elements.



3.0 RATIO OF OPERATING TO BURNOUT HEAT FLUX

This section consists of the calculation of the maximum ratio of operating to burnout heat flux. This ratio is of interest in-so-far as it affects the core operation during an accident.

3.1 Operating Heat Flux

The maximum operating heat flux in the hottest control rod is determined by:

$$(\varphi_{op})_{CR_{max}} = \varphi_{avg} \times (F_{R \Delta \Theta})_{CR_{max}} \times \left(\frac{\bar{P}}{P}\right)_{max}$$

where

$$(\varphi_{op})_{CR_{max}} = \text{maximum control rod operating heat flux, Btu/ft}^2\text{-hr}$$

$$\varphi_{avg} = \text{average core heat flux, Btu/ft}^2\text{-hr}$$

$$(F_{R \Delta \Theta})_{CR_{max}} = \text{maximum radial control rod power distribution factor}$$

$$\left(\frac{\bar{P}}{P}\right) = \text{maximum ordinate of the normalized axial power distribution}$$

For the skid-mounted core:

$$\varphi_{avg} = 72,410 \text{ Btu/ft}^2\text{-hr}$$

$$(F_{R \Delta \Theta})_{CR_{max}} = 1.490$$

$$\left(\frac{\bar{P}}{P}\right) = 1.650$$

$$\begin{aligned} (\varphi_{op})_{CR_{max}} &= (72,410) (1.490) (1.650) \\ &= 178,020 \text{ Btu/ft}^2\text{-hr} \end{aligned}$$

Correspondingly, the maximum operating heat flux in the hottest stationary channel is:

$$\begin{aligned} (\varphi_{op})_{FE_{max}} &= \varphi_{avg} \times (F_{R \Delta \Theta})_{FE_{max}} \times \left(\frac{\bar{P}}{P}\right)_{max} \\ &= (72,410) (1.483) (1.650) \\ &= 177,184 \text{ Btu/ft}^2\text{-hr} \end{aligned}$$

3.2 Burnout Heat Flux

The burnout heat flux is calculated, using the Jens and Lottes equation (Ref. ANL-4627), as follows:

$$\left(\frac{\varphi}{10^6}\right)_{\text{B.O.}} = C \left[\frac{G}{10^6}\right]^m (t_{\text{sat}} - t_b)^{0.22}$$

where:

$(\varphi)_{\text{B.O.}}$ = burnout flux, Btu/ft²-hr

G = mass flow, lb/hr - ft²

t_{sat} = saturated temperature corresponding to flow conditions, °F

t_b = water temperature at the position of burnout, °F.

C, m = constants, function of total pressure (p. 52, ANL-4627)

For the hottest control rod:

$$G = 926,304 \text{ lb/hr - ft}^2$$

$$t_{\text{sat}} = 617.09\text{F} @ 1750 \text{ psia}$$

$$t_b = 515.58\text{F}$$

$$C = 0.48 @ 1750 \text{ psia}$$

$$m = 0.442 @ 1750 \text{ psia}$$

$$\left[\frac{\varphi_{\text{BO}}}{10^6}\right]_{\text{CR}} = (0.48)(0.926304)^{0.442} (101.51)^{0.22}$$

$$\left[\varphi_{\text{BO}}\right]_{\text{CR}} = 1,282,215 \text{ Btu/ft}^2 - \text{hr}$$

For the hottest stationary element:

$$G = 893,493 \text{ lb/hr - ft}^2$$

$$t_{\text{sat}} = 617.09 \text{ F}$$

$$t_b = 515.16\text{F}$$

$$C = 0.48$$

$$m = 0.442$$

$$\left[\frac{\varphi_{BO}}{10^6} \right]_{FE} = (0.48) (0.893493)^{0.442} (101.93)^{0.22}$$

$$\left[\varphi_{BO} \right]_{FE} = 1,263,196 \text{ Btu/ft}^2 \text{ - hr}$$

3.3 Flux Ratios

The ratio of operating to burnout heat flux, for the hottest control rod, is:

$$\left[\frac{\varphi_{op}}{\varphi_{BO}} \right]_{CR} = \frac{178,020}{1,282,215} = 0.1388$$

The corresponding ratio for the hottest stationary elements, those in the outer ring, is:

$$\left[\frac{\varphi_{op}}{\varphi_{BO}} \right]_{FE} = \frac{177,184}{1,263,196} = 0.1403$$

3.4 Application of Hot Channel Factors

The hot channel factors which are concerned with uranium content and meat thickness, and therefore affect the maximum possible operating flux, are the uranium content deviation factor and the meat length deviation factor. Locally these factors are 1.0250 and 1.0357, respectively. If these factors are applied to the flux ratios, the results are:

$$\left[\frac{\varphi_{op}}{\varphi_{BO}} \right]_{CR} = 0.1388 \times 1.0250 \times 1.0357 = 0.1474$$

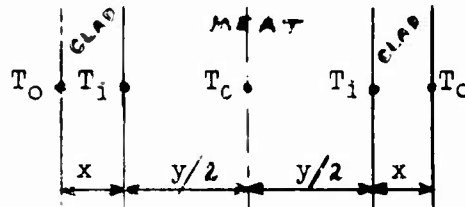
and

$$\left[\frac{\varphi_{op}}{\varphi_{BO}} \right]_{FE} = 0.1403 \times 1.0250 \times 1.0357 = 0.1489$$

4.0 Internal Plate Temperatures

The maximum internal plate temperature is calculated and is of interest for determination of the thermal stresses in the elements.

4.1 Method of Calculation



Considering the heat generation rate within the meat to be uniform:

$$T_{c_{max}} = T_{0_{max}} + (T_1 - T_0)_{max} + (T_c - T_1)_{max}$$

$$(T_1 - T_0)_{max} = \frac{\varphi_{max} (\chi)}{K_c}$$

$$(T_c - T_1)_{max} = \frac{\varphi_{max} (y/2)}{2 K_m} = \frac{\varphi_{max} (y)}{4 K_m}$$

where:

$T_{c_{max}}$ = maximum internal temperature, °F

$T_{0_{max}}$ = maximum surface temperature, °F

$(T_1 - T_0)_{max}$ = maximum temperature difference across the clad, °F

$(T_c - T_1)_{max}$ = maximum temperature difference between the center of the meat and the meat - clad interface, °F

φ_{max} = maximum core heat flux, Btu/ft² hr

χ = thickness of the clad, ft

y = thickness of the meat, ft

K_c = thermal conductivity of the clad, Btu/ft-hr °F

K_m = thermal conductivity of the meat, Btu/ft-hr °F

The maximum core heat flux can be determined as follows:

$$\varphi_{max} = \varphi_{avg} \times (F_{r_{meat}})_{max} \times (\bar{p}/\bar{p})_{max}$$

4.2 Numerical calculation

For the Skid-Mounted APPR Core:

$$\varphi_{avg} = 72,410 \text{ Btu/ft}^2 \text{ hr}$$

$$(FR_{AS})_{\max} = 1.490$$

$$(\bar{p}/\bar{p})_{\max} = 1.650$$

$$Q_{\max} = (72,410) \times (1.490) \times (1.650)$$

$$Q_{\max} = 178,020 \text{ Btu/ft}^2 \text{ hr}$$

$$\lambda = 0.005 \text{ inches}$$

$$y = 0.020 \text{ inches}$$

$$K_c = 11.1 \text{ Btu/ft hr } ^\circ\text{F @ } 612 \text{ F}$$

$$K_m = 9.64 \text{ Btu/ft hr } ^\circ\text{F @ } 612 \text{ F}$$

$$(T_o)_{\max} = 617.09^\circ\text{F}$$

Therefore:

$$(T_1 - T_o)_{\max} = \frac{(178,020)(.005)}{(11.1)(12)} = 6.68^\circ\text{F}$$

$$(T_c - T_1)_{\max} = \frac{(178,020)(.020)}{4(9.64)(12)} = 7.69$$

$$T_{c_{\max}} = 617.09 + 6.68 + 7.69 = 631.46^\circ\text{F}$$

4.3 Application of Hot Channel Factors

If the hot channel factors concerned with uranium content and meat thickness (see Article 3.4) are applied to these values the results are as follows:

$$(T_1 - T_o)'_{\max} = 6.68^\circ\text{F} \times 1.025 \times 1.0357 = 7.09^\circ\text{F}$$

$$(T_c - T_1)'_{\max} = 7.69^\circ\text{F} \times 1.0250 \times 1.0357 = 8.16^\circ\text{F}$$

$$T'_{c_{\max}} = 617.09 + 7.09 + 8.16 = 632.34^\circ\text{F}$$

4.4 Comparison with APPR-1

Since the primary system pressure of the APPR-1 is 1200 psia in comparison with the system pressure of the Skid-Mounted core (1750 psia) the surface temperatures, and therefore the absolute values of the maximum internal temperatures, are not comparable. However, the magnitude of the thermal stresses is mainly dependent upon the temperature differences across the clad and across the meat, rather than the absolute temperatures.

Calculations completed for the APPR-1 (see Ref. 9) showed the temperature difference across the clad, and the temperature difference from the clad-meat interface to the center of the meat each to be 9.9°F. Corresponding values for the Skid-Mounted APPR Core have been shown to be 7.1°F and 8.2°F respectively. It may be noticed that the corresponding values for the Skid-Mounted Core are smaller than those of the APPR-1. The calculation for the APPR-1 had been based upon equal thermal conductivities in the clad and in the meat. For the Skid-Mounted Core calculations the more conservative approach was taken, that of considering the thermal conductivity of the meat to be somewhat smaller than that of the clad.

5.0 THERMAL STRESS IN THE ELEMENTS

Thermal stresses are caused by temperature differences between points in the fuel element. The stresses are proportional to the temperature differences and the temperature differences are approximately proportional to heat flux, decreasing somewhat with increasing coolant velocity.

5.1 Use of Experimental Data

A program was begun in 1954 to test a stainless steel fuel element, of the type used in the APPR-1, in the STR mock-up. The element was to be tested for mechanical stability under combined hydraulic, thermal, and irradiation conditions present in the STR. Additional tests have been performed with a different element in the MTR.

The table below compares the irradiation conditions in the MTR with those in the APPR-1 (Ref 11):

Table 5-1

| | Units | MTR-APPR | | APPR-1 |
|------------------------------|------------------------|----------|---------|--------|
| | | Type I | Type II | |
| Average heat flux | Btu/ft ² hr | 449,000 | 461,000 | 55,900 |
| Specific Power | Kw/Kg | 9,000 | 9,000 | 550 |
| Fuel Concentration in Matrix | gm/cm ³ | 1.240 | 1.817 | 1.31 |
| Fuel loading | gm/cm ² | 0.0315 | 0.0324 | 0.066 |
| Fuel loading per plate | gm | 10.36 | 10.67 | 23.65 |
| Maximum temperature of fuel | °F | - | - | 566 |

A similar comparison is made with the STR in Ref 11. However, as this information is classified, it is not reported here.

5.2 Experimental Test Conditions and Results

A six-plate element was tested in the STR at a cooling water temperature and pressure of 500°F and 2050 psia, respectively. It was removed from the reactor after 157 full power hours of satisfactory operation, examined, and found to be in excellent condition. It was then returned to the reactor an additional 100 hours, the total burnup of U²³⁵ estimated to be 3%. Further information, which is classified, may be found in references 10 and 11.

Two series of tests were undertaken in the MTR. The first was performed with an 13plate element and the second with small capsulated fuel plate specimens.

The small specimens were of two types. Their basic characteristics are listed below:

| | <u>Type I</u> | <u>Type II</u> |
|---------------------------------|--|--|
| Design life (MW-Yr) | 15 | 30 |
| Clad-core-clad thickness (mils) | 5-10-5 | 6.5-7.-6.5 |
| Core composition (weight %) | 17.93 UO ₂ 0.19 B ₄ C | 25.81 UO ₂ 0.35 B ₄ C |
| Clad Material | 81.88 stainless 304L stainless steel | 73.84 stainless |

The full size plates were of three types. Their basic characteristics are as follows:

| | <u>Type I</u> | <u>Type II</u> | <u>Type III</u> |
|--------------------------------|--|----------------|-------------------|
| Design life (MW-Yr) | 15 | 22.5 | 30 |
| Plates of each type | 6 | 6 | 6 |
| Plate Clad-core-clad thickness | 9-12-9 | 10-10-10 | 11-8-11 |
| Core mixture composition | UO ₂ 18.75 B ₄ C 0.21 | 22.18 0.27 | 26.89 0.39 |
| Distance between plates | Stainless 81.04 | 77.55 | 72.75 117 mils |

The plates were inserted in the core for an estimated burn-up of 25-42%. The velocity in the MTR core is approximately 30 fps. The specimens were removed from the core and examined. No gross damage occurred and there was no evidence of defects.

5.3 Comparison with Skid-Mounted Core Conditions

It may be noticed that the average heat flux in the MTR was greater than that of the 10 MW Skid-Mount by a factor of 6.37.

In APMemo 43,⁽⁹⁾ the temperature distributions and thermal stresses were calculated for a total power of 10 MW and a peak to average power of 4, corresponding to a maximum heat flux of 224,000 Btu/ft²-hr. The maximum stress calculated was a tensile stress in the side plate near the outermost fuel plate. This value numerically was 28,300 psi. This calculation was based on extremely conservative assumptions and is an indication of the upper limit of possible stresses, rather than an actual expected value.

The product of the maximum ordinate of the axial power distribution normalized to an average of unity and that of the radial power distribution (determined on an analogous basis) gives the ratio of peak to average power. For the Skid-Mounted Core:

$$\frac{\varphi_{\text{Max}}}{\varphi_{\text{Av}}} = (1.650) (1.490) = 2.46$$

Then:

$$\varphi_{\text{Max}} = \left(\frac{\varphi_{\text{Max}}}{\varphi_{\text{Av}}} \right) \varphi_{\text{Av}} = (2.46) (72,410) = 178,000 \text{ Btu/ft}^2\text{-hr.}$$

Since the maximum heat flux in the 10MW Skid-Mounted Core is 178,000 Btu/ft²-hr, the corresponding upper stress limit is:

$$\frac{178}{224} \times 28,300 \text{ psi} = 22,490 \text{ psi}$$

It is therefore evident that the Skid-Mounted Core has an even larger safety factor than the APPR-1 (which has been operating satisfactorily for 1-1/2 years).

5.4 Conclusions

On the basis of the comparison with experimental test data presented, the comparison with thermal stress calculations presented, and the fact that the APPR-1 has been operating satisfactorily for 1-1/2 years with thermal stresses approximately 26% greater than those expected in the Skid-Mounted Core, it has been concluded that the thermal stresses in this core will be below the allowable value. It is therefore considered not necessary to undertake a detailed analysis of thermal stresses in the fuel plates.

6.0 THERMAL STRESS IN REACTOR VESSEL

In addition to hydraulic stresses in the vessel, thermal stresses occur, caused by a temperature gradient across the vessel wall. This temperature gradient is caused by the heat generation of gammas absorbed or experiencing collisions in the vessel.

6.1 Method of Calculations

If the heat generation rate in the wall is plotted versus distance through the wall on semi-log paper, it may be seen that it closely approximates a straight line. The heat generation rate through the wall may therefore be represented by an exponential of the form:

$$q_x = q_0 e^{-ux}$$

where

q_0 = heat generation rate at the inner surface of the vessel wall

x = distance through the wall, measured from the inner surface

u = slope of the curve on semi-log paper

q_x = heat generation rate at " x " distance from the inner surface

6.1.1 Temperature Difference Equation

If the equation of the heat generation rate is substituted in the general heat transfer equation:

$$-k \frac{d^2t}{dx^2} = q_x$$

integration results in the following equation:

$$-kt = \frac{q_0 e^{-ux}}{u^2} + Cx + D$$

Utilizing the boundary conditions:

$$x = 0, T = T_1$$

and $x = w, \frac{dT}{dx} = 0$ (since the vessel wall is insulated at its outer surface).

the constants may be evaluated:

$$C = \frac{q_0}{k} e^{-uw}$$

$$D = -kT_1 - \frac{q_0}{ku^2}$$

The final equation for the difference between the temperature at some distance x through the wall (T), and the temperature at the inner surface of the wall (T_1) is given by:

$$(T - T_1) = \frac{q_0}{k u^2} (1 - e^{-ux} - uxe^{-uw})$$

where:

k = thermal conductivity of the vessel wall
 w = thickness of the vessel wall.

At $x = w$ the equation reduces to:

$$(T_0 - T_1) = \frac{q_0}{ku^2} [1 - e^{-uw} (1 + uw)]$$

6.1.2 Thermal Stress Equation

If T_1 is considered as a base temperature or an initial uniform temperature, then the increase above T_1 , ($T - T_1$) may be represented by t and:

$$t = \frac{q_0}{ku^2} (1 - e^{-ux} - uxe^{-uw})$$

Assuming the temperature distribution to be symmetrical with respect to the axis of the cylinder and constant along this axis, at a cross section distant from the ends of the cylinder the tangential stress at some radius (r) may be represented by (Ref. 21):

$$\sigma_t = \frac{E}{1-\mu} \left[\frac{1}{r^2} \int_a^r \alpha t r dr + \frac{r^2 - a^2}{r^2 (b^2 - a^2)} \int_a^b \alpha t r dr - \alpha t \right]$$

where:

- σ_t = tangential stress at radius (r)
- E = Young's modulus
- μ = Poisson's ratio
- a = inner radius of the vessel
- b = outer radius of the vessel
- α = coefficient of linear expansion
- t = increase in temperature above the uniform initial temperature.

- (2) Inside wall insulated.
- (3) Outside wall insulated.
- (4) Equal bulk coolant temperatures in inside and outside channels.

Utilization of case (3) for determining stresses in the vessel has been found to be accurate within 3% of the values determined by use of the derived equations. It is in general more conservative than the derived equations.

6.2 Thermal Stress in APPR-1

For purpose of comparison of calculated values with actual values, the calculated and experimental temperature differences and thermal stresses of the APPR-1 will be presented here.

6.2.1 Calculated and Measured Temperature Difference

As indicated on page 195, Ref. 23, the measured temperature difference between the bulk coolant temperature and the outside vessel wall temperature in the APPR-1, operating at 10 MW, was 12.6° F.

In determining the corresponding calculated value, the following equations are used.

The temperature difference across the vessel wall ($T_0 - T_1$) is given by:

$$(T_0 - T_1) = \frac{q_0}{ku^2} \left[1 - e^{-uw} (1 / uw) \right],$$

and the temperature gradient across the film ($T_1 - T_w$) is represented by:

$$(T_1 - T_w) = \frac{1}{ha} \int_{r=a}^{r=b} q_0 e^{-ux} r dr$$

or integrating and simplifying,

$$(T_1 - T_w) = \frac{q_0}{u^2 ah} \left[(ua / 1) - e^{-uw} (ub / 1) \right]$$

where: h = heat transfer coefficient.

For the APPR-1 parameters:

$$T_0 - T_1 = 13.12^\circ \text{ F}$$

$$T_1 - T_w = 6.09^\circ \text{ F}$$

or the total temperature difference as calculated is 19.2° F, as compared with the measured value, 12.6° F.

Since $x = r - a$, the increase in temperature above T_1 may also be represented by:

$$t = \frac{q_0}{k u^2} (1 - e^{-u(r-a)} - (r-a) u e^{-uw})$$

or

$$t = \frac{q_0}{k u^2} \left[(1 - a u e^{-uw}) - e^{ua} e^{-ur} (u e^{-uw}) r \right]$$

Substituting the above expression for (t) in the equation for determining the tangential stress (σ_t), and integrating results in the following expression for σ_t :

$$\sigma_t = \left[\frac{E}{1-\mu} \right] \left[\frac{\alpha q_0}{k u^2} \right] \left[\frac{(1 - a u e^{-uw})}{2} \left(1 - \frac{a^2}{r^2}\right) e^{-u(r-a)} \frac{(ur - 1)}{u^2 r^2} - \frac{(ua - 1)}{u^2 r^2} - u e^{-uw} \left(r - \frac{a^3}{r^2}\right) \left\{ \frac{r^2 - a^2}{r^2 (b^2 - a^2)} \right\} \left\{ \frac{(1 - a u e^{-uw})}{2} (b^2 - a^2) - \frac{e^{-uw}}{u^2} (ub - 1) - \frac{ua - 1}{u^2} - \frac{u e^{-uw}}{3} (b^3 - a^3) \right\} - 1 - e^{-u(r-a)} - (r-a) u e^{-uw} \right]$$

Since the thermal stress in the vessel goes from a compressive stress at the inner surface to a tensile stress at the outer surface, the maximum stress must be at one of these surfaces. Evaluating the above equations at $r = a$ and $r = b$ yields:

$$\sigma_t(r = a) = \left[\frac{E}{1-\mu} \right] \left[\frac{\alpha q_0}{k u^2} \right] \left[\frac{2}{b^2 - a^2} \right] \left[\frac{(1 - a u e^{-uw})}{2} (b^2 - a^2) - \frac{e^{-uw}}{u^2} (ub - 1) - \frac{(ua - 1)}{u^2} - \frac{u e^{-uw}}{3} (b^3 - a^3) \right]$$

and

$$\sigma_t(r = b) = \sigma_t(r = a) - \left[\frac{E}{1-\mu} \right] \left[\frac{\alpha q_0}{k u^2} \right] \left[1 - e^{-uw} (1 - uw) \right]$$

It is obvious that for reasonable values of "u" and "w" the maximum thermal stress will occur at the inner radius ($r = a$) of the vessel.

A similar equation could be derived for calculating the radial stress. However, as the tangential stress will always be larger than the radial stress, further derivations are not necessary.

In "Thermal Stresses in Reactor Vessels" (Ref. 22) sets of curves are presented (based on IBM 704 calculations, for determining thermal stresses in vessels with various parameters and conditions. The curves presented represent 4 cases:

- (1) Equal wall temperatures at inside and outside surfaces.

6.2.2 Thermal Stress in APPR-1

The thermal stress corresponding to the measured temperature difference (12.6° F) is 1975 psi. The stress corresponding to the calculated temperature difference (19.2° F) is 2977 psi.

As may be noticed, the method of calculation yields values of temperature difference and thermal stress considerably higher than those actually existing, as evidenced by experimental measurements. It is felt that this will also be true of values calculated for the Skid-Mounted Core.

6.3 Calculated Temperature Difference and Thermal Stress at Mid-Plane

In designing the reactor vessel several possibilities were considered and investigated with respect to thermal stress. Since the Skid-Mounted APPR is a package reactor, it is desirable to keep the vessel as close to the core as possible, although in doing so the thermal stress is increased. The various designs investigated in arriving at one satisfactory with respect to thermal stress are indicated in Table 6-1. The results of cases 3-7 are represented graphically in Figure 6-1.

As may be noticed from the table, the thermal stress corresponding to the final design (Case 7) is 6800 psi. The temperature difference across the wall is 46.9° F.

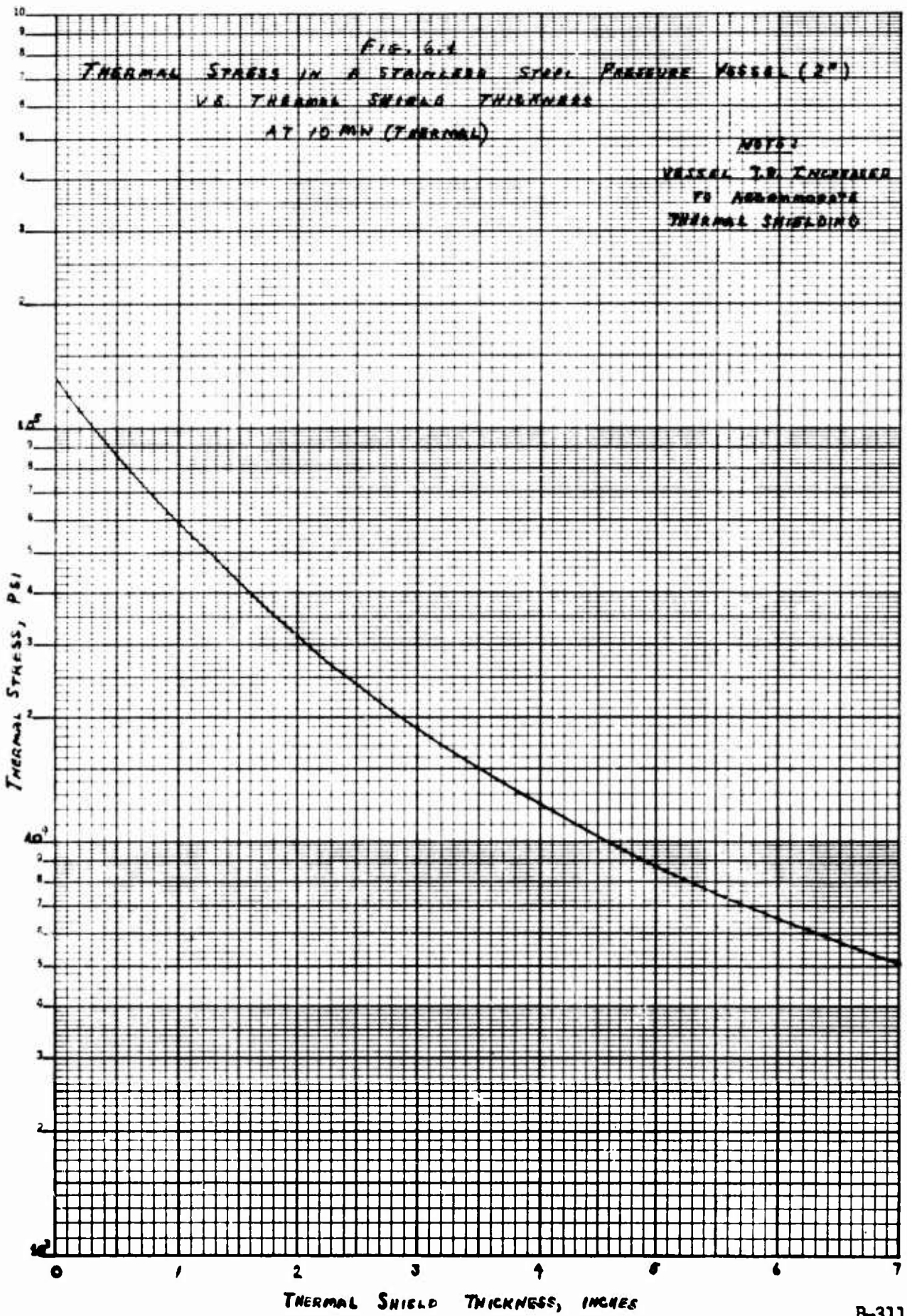
Table 6-1

Reactor Vessel Thermal Stresses

| Case No. | Reactor Vessel | | | Thermal Shield | | | Thermal Stress psi |
|----------|-----------------|---------------------------------|------------------|-----------------|-----------|-------------------|-----------------------|
| | Inside Diameter | Thickness | Material | Inside Diameter | Thickness | Material | |
| 1 | 25" | 2" | 304-SS | | None | | 132,200 |
| 2 | 25" | 1 3/4" | 304-SS | | None | | 111,500 |
| 3 | 28.5" | 2" | 304-SS | 23.5 | 2" | 304-SS | 30,800 |
| 4 | 30.5" | 2" | 304-SS | 23.5" | 3" | 304-SS | 18,800 |
| 5 | 30.5" | 2" | 304-SS | 23.5" | 3" | Borated 304-SS | 16,420 |
| 6 | 37.75" | 1/8" clad 1/2 3/8" vessel | 304-SS SA-212 | 33" | 1" | 304-SS | 12,400 |
| 7 | 37.75" | 1/8" clad 1/2 3/8" vessel | 304-SS SA-212 | 23.5" | 2" | 304-SS | 6,800 |

6.4 Calculated Thermal Stress in the Thermal Shield

Since the data presented in Ref. 22 has been found to be accurate within 3% of values calculated from derived equations, this data was used for calculating the stress in the thermal shield. For this purpose Case 4, equal bulk coolant temperatures inside and outside the channel, was utilized.



The stress was calculated to be 62,000 psi. Since the thermal shield is not a structural member, however, this value is not too large.

6.5 Calculated Thermal Stress In Vessel Flange

An analytical expression for maximum thermal stress is derived on page 11 of WAPD-CE-43 and is here applied to the vessel flange of the Skid-Mounted Reactor.

For the case of a pressure vessel with the inner wall surface at zero temperature (above some datum), the outer wall surface perfectly insulated, and an exponential heat generation rate in the wall the maximum thermal stress occurs at the inner wall surface and is given by:

$$S_o = \frac{E\alpha q_o}{2(1-\mu)k\beta^2} \left[2 - \frac{2}{\beta a} + \left(\frac{2}{\beta a} - \beta a \right) e^{-\beta a} \right]$$

where

| | | |
|----------|--|---|
| S_o | = stress at inside wall surface | psi |
| E | = modulus of elasticity | 26.4×10^6 psi |
| α | = linear coefficient of thermal expansion | 8.0×10^{-6} ($^{\circ}\text{F}$) ⁻¹ |
| q_o | = volumetric heat generation rate at the inside wall | BTU/ft ³ (hr) |
| μ | = Poisson's ratio | 0.3 |
| k | = thermal conductivity | 25 BTU/(hr)(ft)($^{\circ}\text{F}$) |
| β | = linear absorption coefficient | 5.4408 ft ⁻¹ |
| a | = wall thickness | ft |

This equation may be safely used for the vessel flanges of the Skid-Mounted Reactor as the conditions restricting the use of the equation approximate those of the Skid. Values of the heat generation rate at the inside surface of the wall of the flange were determined and presented in Section 5.2 of the Shielding Design Analysis. The flange wall-thickness is also variable and in this case insertion of the maximum value of the thickness in the equation with the corresponding heat generation rate yields the maximum thermal stress; that is when $a=0.63333$ feet and $q_o = 2.76 \times 10^4$ BTU/(ft³)(hr). Then $\beta a = (5.4408)(0.63333) = 3.4458$.

and

$$S_o = \frac{(26.4 \times 10^6)(8.0 \times 10^{-6})(2.76 \times 10^4)}{2(1-0.3)(25)(5.4408)^2} \left\{ 2 - \frac{2}{3.4458} + \left[\frac{2}{3.4458} - 3.4458 \right] e^{-3.4458} \right\}$$

= 7470 psi

The allowable thermal stress in the flange is 8750 psi. This exceeds the calculated value of the maximum thermal stress, 7470 psi, by 17% which is a sufficient margin of safety.

6.6 Calculated Thermal Stress in Integral Nozzle

The same analytical expression for maximum thermal stress in a pressure vessel which was applied to the vessel flange in Section 6.5 is used here to determine the maximum thermal stress in the vessel outlet nozzle.

The nozzle is so designed that it is considered an integral part of the vessel and its allowable thermal stress is that of the vessel. The volumetric heat generation rate in the inside vessel wall surface at the nozzle is 3.965×10^4 BTU (hr) (ft³) as determined in Section 5.2 of the Shielding Design Analysis. The gamma attenuation path-length through the nozzle is 0.75 feet. The linear absorption coefficient is 8.644 (feet)⁻¹. Then $\rho a = (8.644)(0.750) = 6.483$ and the maximum thermal stress is:

$$S_0 = \frac{(26.4 \times 10^6)(8.0 \times 10^{-6})(3.965 \times 10^4)}{2(1-0.3)(25)(8.644)^2} \left\{ 2 - \frac{2}{6.483} + \left[\frac{2}{6.483} - 6.483 \right] e^{-6.483} \right\}$$

= 5390 psi

This stress is less than the allowable by a factor of (8750/5390) or 1.62. Since the outlet nozzle is closer to the core than the inlet nozzle (which is also integral by design) the inlet nozzle will undergo less thermal stress and a calculation is not necessary.

6.7 Conclusions

As was indicated in Section 6.3, the thermal stress in the vessel was calculated to be 6,800 psi. Since the allowable thermal stress in the vessel is 8750 psi, the vessel and thermal shield designs are satisfactory, in this respect. As was pointed out in Section 6.2, the calculated stress value is considered quite conservative.

The thermal stresses in the flange and integral nozzle are safe by factors of 1.17 and 1.62 respectively.

7.0 Core Pressure Drop

The following calculations have been made for the pressure drop across the active core only, and do not include the inlet and outlet plenum chambers. All other pressure drops have been established as a separate calculation.

7.1 Comparison of Calculated and Experimental Data

Pressure drops through the stationary fuel elements were calculated by use of the IBM 650 Digital Computer (Ref. 19). Verification of the accuracy of this program is illustrated in Fig. 7-1, where both computed pressure drops and experimental pressure drops for air flow through a fixed fuel element are plotted vs flow. It may be noticed that the slopes of both curves are identical and that the calculated data is conservative in comparison with the experimental data. Since the method of calculation of pressure drop is the same for all fluids, the values calculated by the computer program for water flow are equally valid.

7.2 Calculation of Pressure Drops

Although good results were achieved in calculating the stationary fuel element pressure drops by use of the computer, it was not feasible to perform similar calculations for the control rod elements, because of the more complex geometry.

As experimental data for air flow through the control rods was available, the following method of analysis was utilized. Several cases for air flow through fixed fuel elements were calculated on the computer and plotted versus Reynolds number. The experimental data for air flow through the control rods was plotted on the same graph (Fig. 7-2). Assuming that the ratio of control rod pressure drop to fixed element pressure drop for a particular Reynolds number is constant for either air or water flow, the control rod pressure drop for water flow was determined by plotting the fixed element pressure drop for water flow versus Reynolds number and applying the ratio for that Reynolds number, as determined from Figure 7-2. This assumption was based upon the fact that friction factor for a particular Reynolds number is independent of the fluid under consideration.

The plots for water flow are shown in Figure 7-3. From the plot of control rod pressure drop versus Reynolds number for water flow it was possible to determine the values needed for plotting Figure 7-4, "Control Rod Pressure Drop vs Flow Per Element".

7.3 Results and Conclusions

The pressure drop through a control rod element is plotted versus coolant flow in gpm in Figure 7-4. For the coolant flow required through

the control rod elements in the Skid-Mounted APPR core, as established in Section 2.0, the pressure drop is 5.07 ft H₂O. This is also the total pressure drop across the core, as the control rod is the governing element with respect to pressure drop.

It may be noticed that these values are for the unmodified control rods. It is expected that the control rods to be used in the Skid-Mounted APPR will have a slightly smaller pressure drop. However, as the modifications were not completed at the time this analysis was undertaken, and as the experimental data was for an unmodified element, Figure 7-4 gives a conservative estimate of the desired values. It has been estimated that the corresponding values for the modified elements will be 10-15% lower.

The pressure drop through the fixed elements is plotted in Figure 7-5 versus coolant flow in gpm. It may be noticed from this plot that the pressure drop through a fixed element is considerably less than that through the rods. It will be necessary to orifice these elements in order to equalize all pressure drops. Since the pressure drop through the fixed elements is 2.37 ft at the flow required for the Skid-Mounted core, the orificing required will be approximately 2.70 ft H₂O.

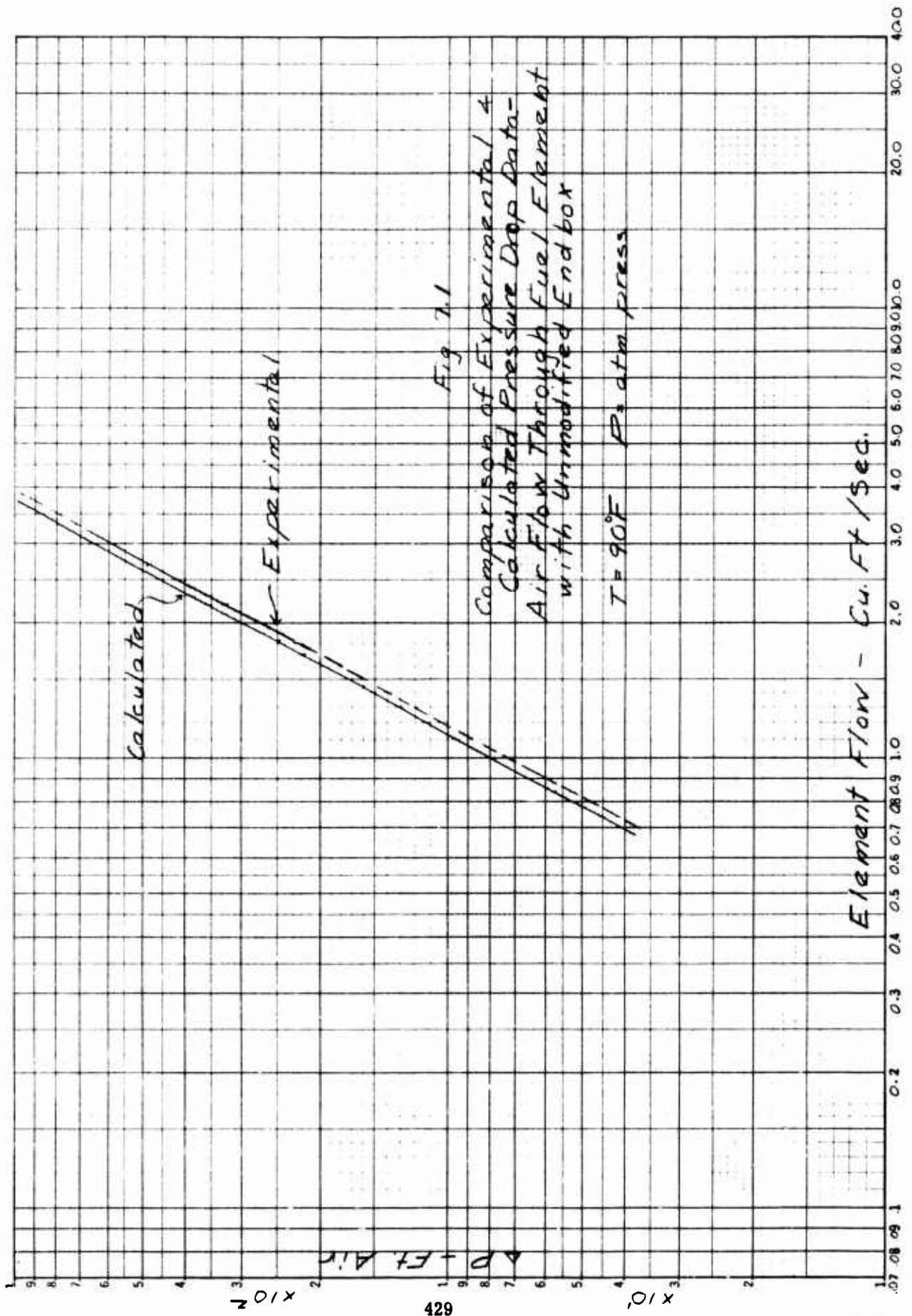


Fig. 7.2

Fuel Element Pressure Drop vs Reynolds Number
Air Flow

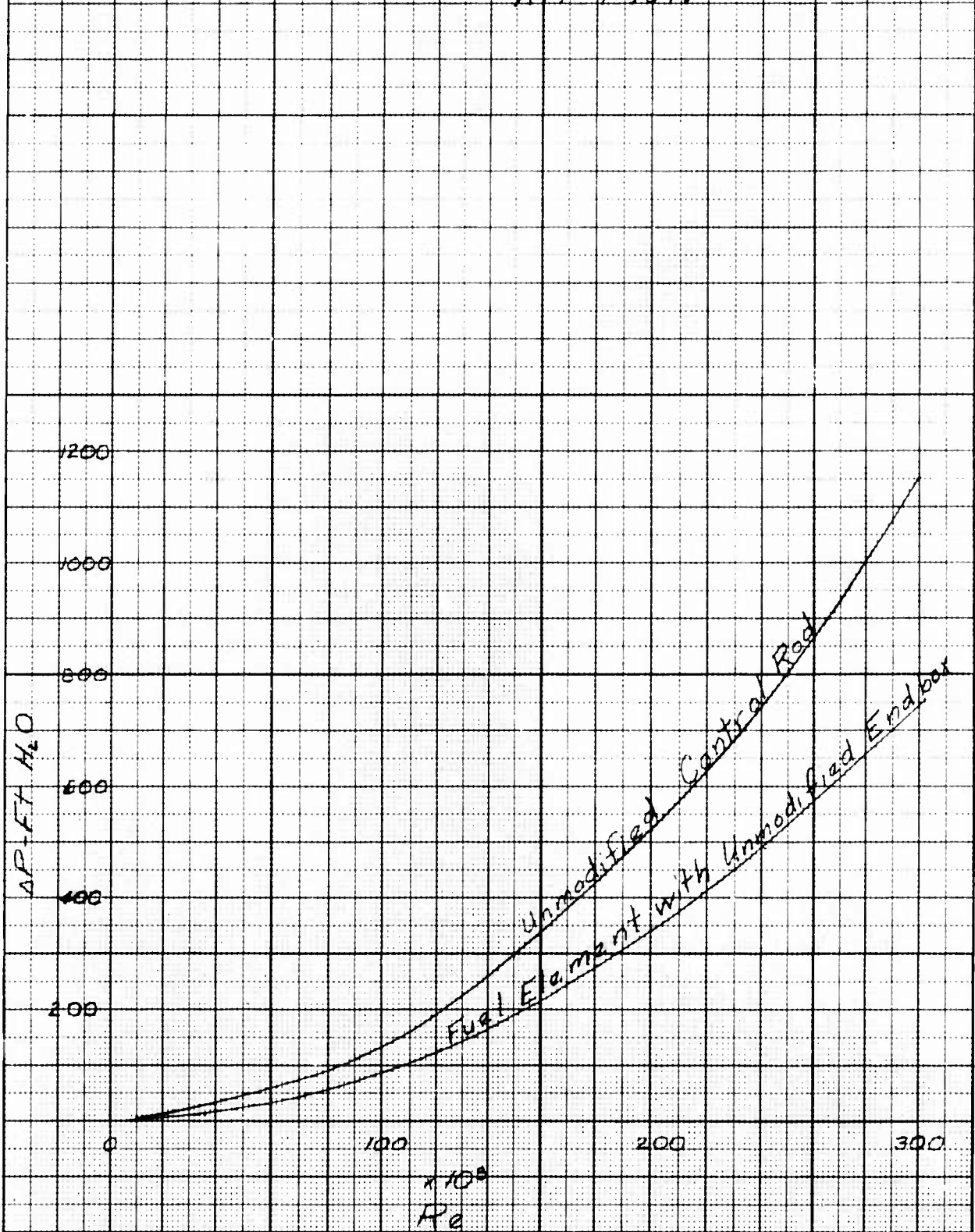


Fig. 7.3

Fuel Element Pressure Drop vs Reynolds Number

Water Flow

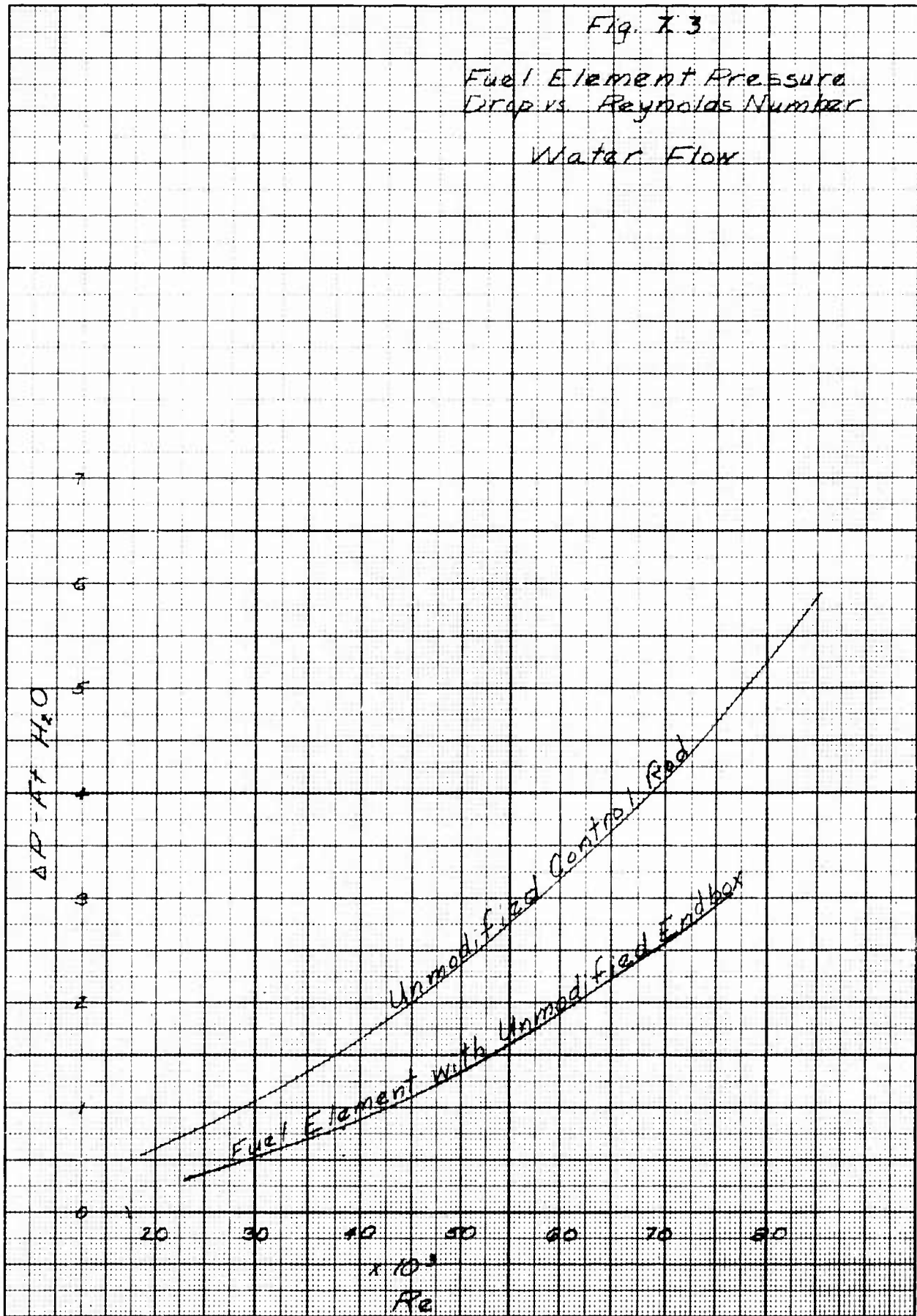


Fig. 7.1

Control Rod Pressure Drop
vs. Flow Per Element

Unmodified Control Rod

Skid-Mounted APPR

$T_{max} = 512 F$ $P = 1750 \text{ psia}$

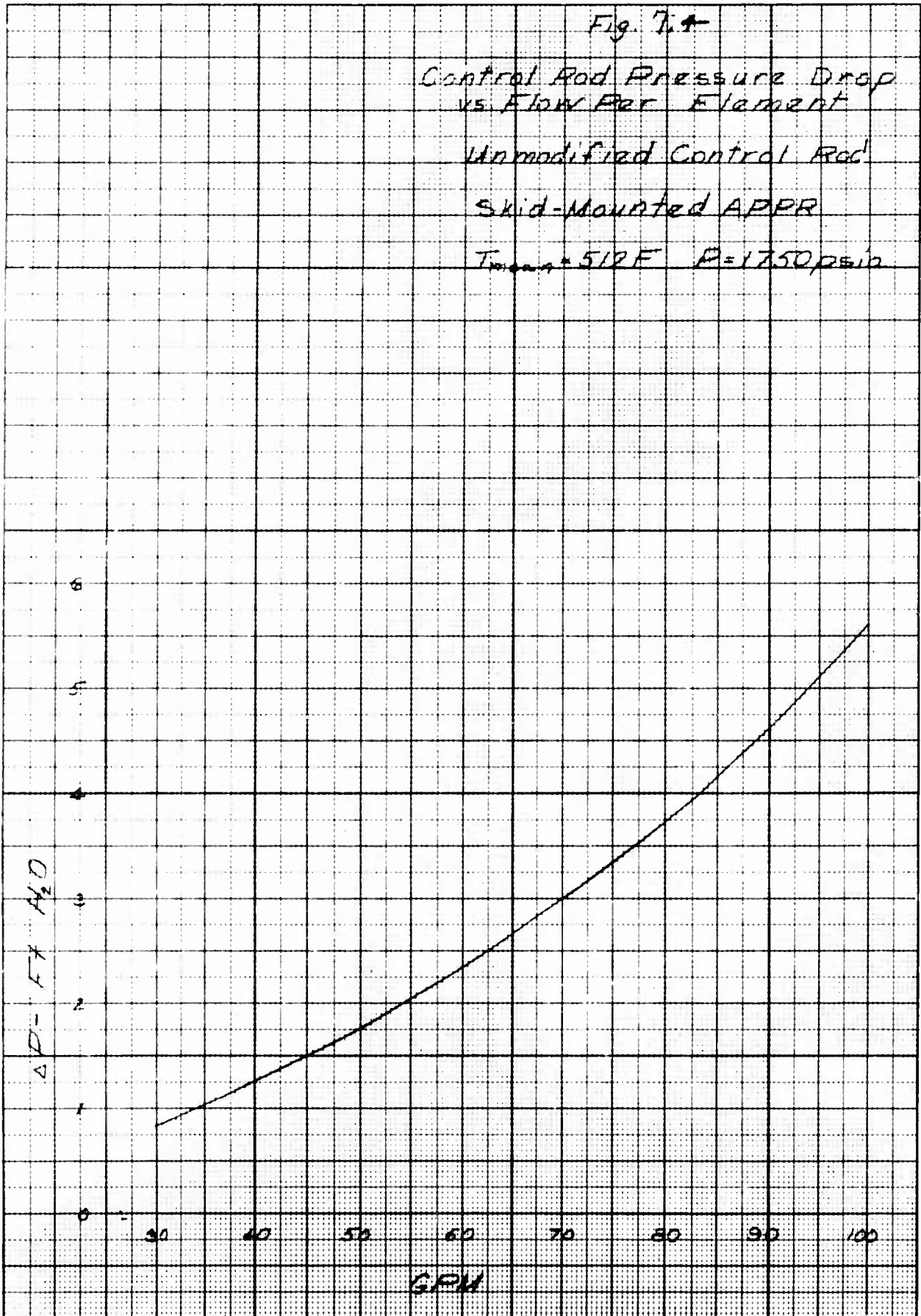
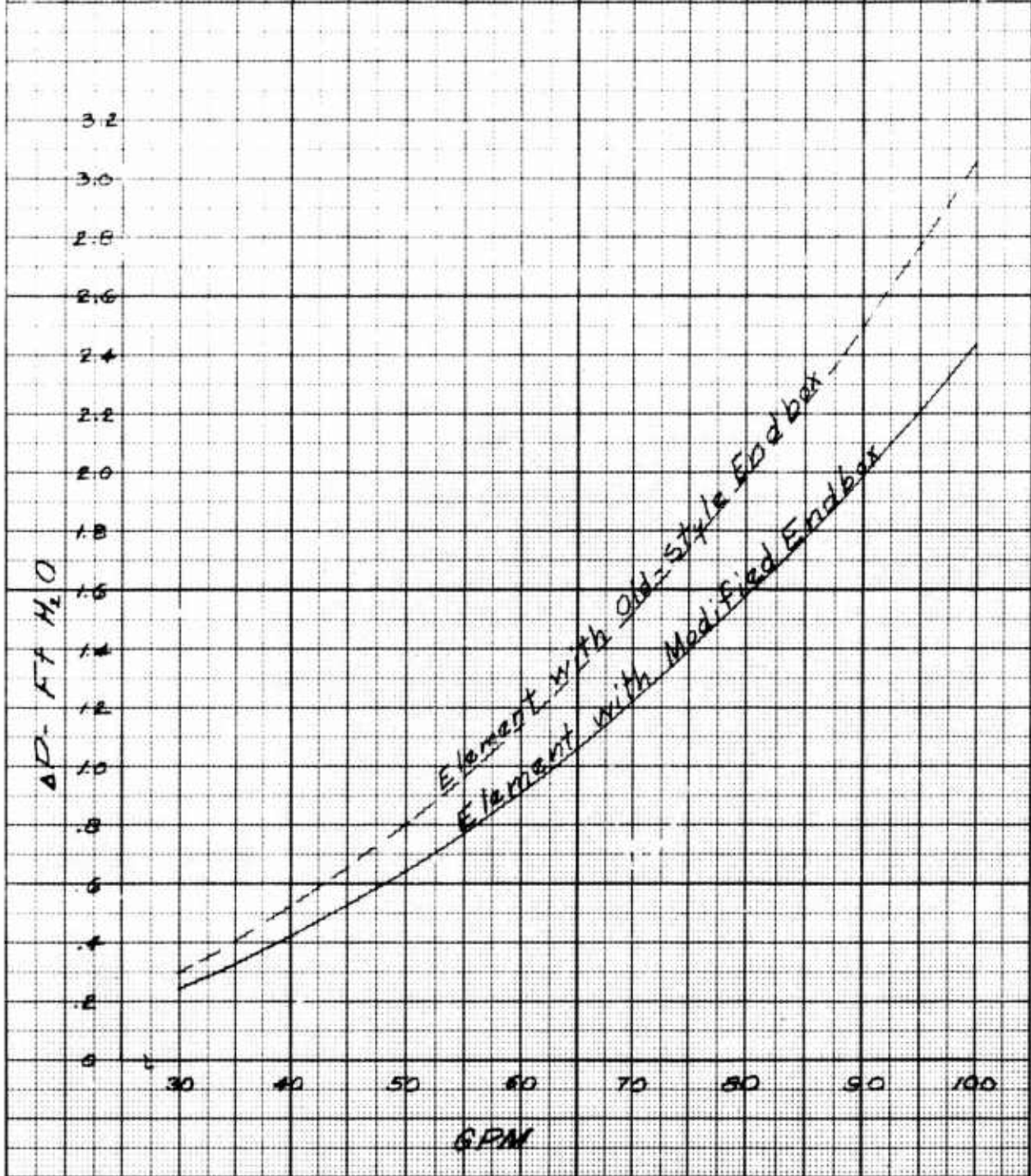


Fig. 7.5

Stationary Fuel Element
Pressure Drop vs Flow
Per Element

Skid-Mounted APPR

$T_{mean} = 512F$ $P = 1750psia$



8.0 FUEL PLATE DEFLECTIONS

Since the internal core flow and the lattice flow through the core are in parallel, the over-all pressure drop through each flow passage must be equal. However, since the geometry of the passages is not the same for both types of flow paths, and since the amount of orificing varies between flow paths, the breakdown of the over-all pressure drop axially is not alike for all passages. This leads to pressure differentials across the outer fuel plates, causing deflection of the plates. If this deflection becomes greater than the allowable tolerance, burnout may result.

8.1 Calculation of Pressure Differential

It has been previously stated (Section 2.0) that the Skid-Mounted APPR will be a uniform flow core. However, as the worst possible conditions have been considered for both uniform and tailored flow, the results of both cases will be included.

The over-all core pressure drop has been shown to be 5.07 ft H₂O. From Figure 5-5 it may be noticed that the pressure drop through a fixed element with a flow of 98.5 gpm is 2.37 ft H₂O, and that the corresponding value for a flow of 87.5 gpm (the minimum required stationary element flow for a tailored core) is 1.88 ft H₂O. The corresponding required pressure drops across the orifice holes are 2.70 ft and 3.19 ft respectively.

The various losses through the elements, which make up the over-all pressure drop across the core, are listed in Table 8-1. The notation refers to Figure 8-1.

TABLE 8-1

Head Loss Through Stationary Elements

| <u>Position</u> | <u>Type of Loss</u> | <u>Ft H₂O</u> | |
|---------------------------------|-----------------------------------|--------------------------|-----------------|
| | | <u>87.5 gpm</u> | <u>98.5 gpm</u> |
| h ₁ | sudden contraction | 0.2226 | 0.2828 |
| h ₂ | gradual enlargement | 0.0263 | 0.0334 |
| h ₃ | sudden contraction | 0.0394 | 0.0501 |
| h ₄ | friction loss | 0.7817 | 0.9752 |
| h ₅ | sudden enlargement | 0.0238 | 0.0302 |
| h ₆ | friction loss | 0.0101 | 0.0126 |
| h ₇ * | sudden enlargement | ----- | ----- |
| h ₈ / h ₇ | orifice loss / sudden enlargement | 3.9661 | 3.6857 |

* Since in the calculation of pressure drop across the elements, the model did not include an orifice plate, the calculations included a loss due to sudden enlargement at the outlet. For actual conditions this loss will be a part of the orifice pressure drop.

The flow rate throughout the lattice passages is essentially equal. The breakdown of the pressure losses axially is illustrated in Table 8-2. The notation again refers to Figure 8-1.

TABLE 8-2

Head Loss Through Lattice

| <u>Position</u> | <u>Type of Loss</u> | <u>Ft H₂O</u> |
|-----------------|------------------------|--------------------------|
| H ₁ | sudden contraction | 0.1322 |
| H ₂ | abrupt change of shape | 0.0491 |
| H ₃ | gradual contraction | 0.0450 |
| H ₄ | friction loss | 1.3000 |
| H ₅ | gradual enlargement | (not needed) |
| H ₆ | abrupt contraction | " |
| H ₇ | orifice loss | " |

The data in Table 8-1 and Table 8-2 is represented graphically in Figure 8-2. As may be noticed from the plot, the maximum pressure differential for a uniform flow core is 0.03 psi. The maximum differential for the core with tailored flow would have been 0.12 psi.

8.2 Experimental Data

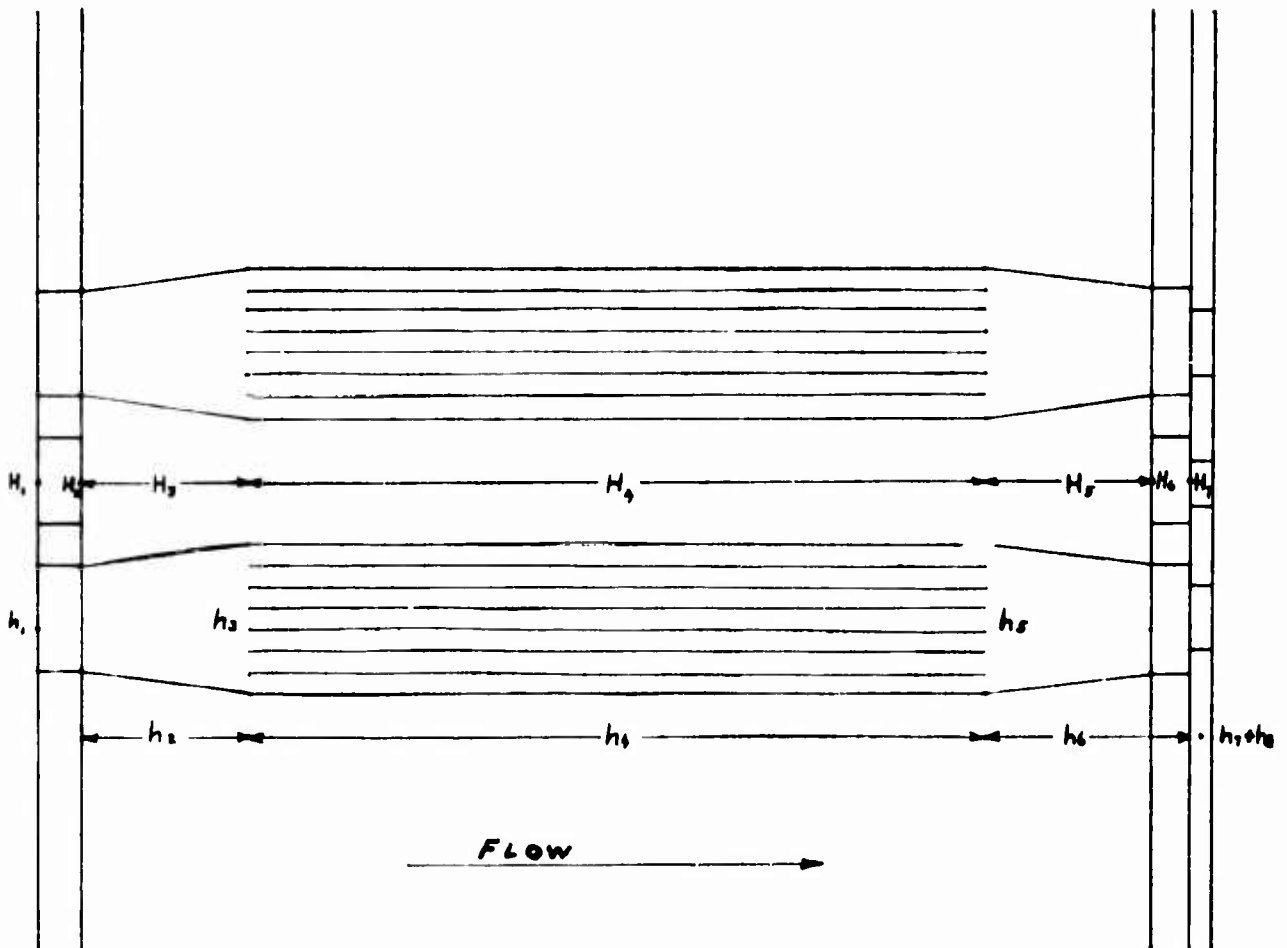
An investigation was conducted at ORNL to determine the effect of pressure differential on the outer plates of an APPR-type fuel element. The fuel elements were pressurized with air, and the deflection of the outer plates measured. (Ref. 20.)

From the experimental data it becomes evident that a differential pressure exceeding 3 psi would result in a deflection of the plate which would cause the adjacent spacings between fuel elements to be beyond tolerance limits (see Ref. 20).

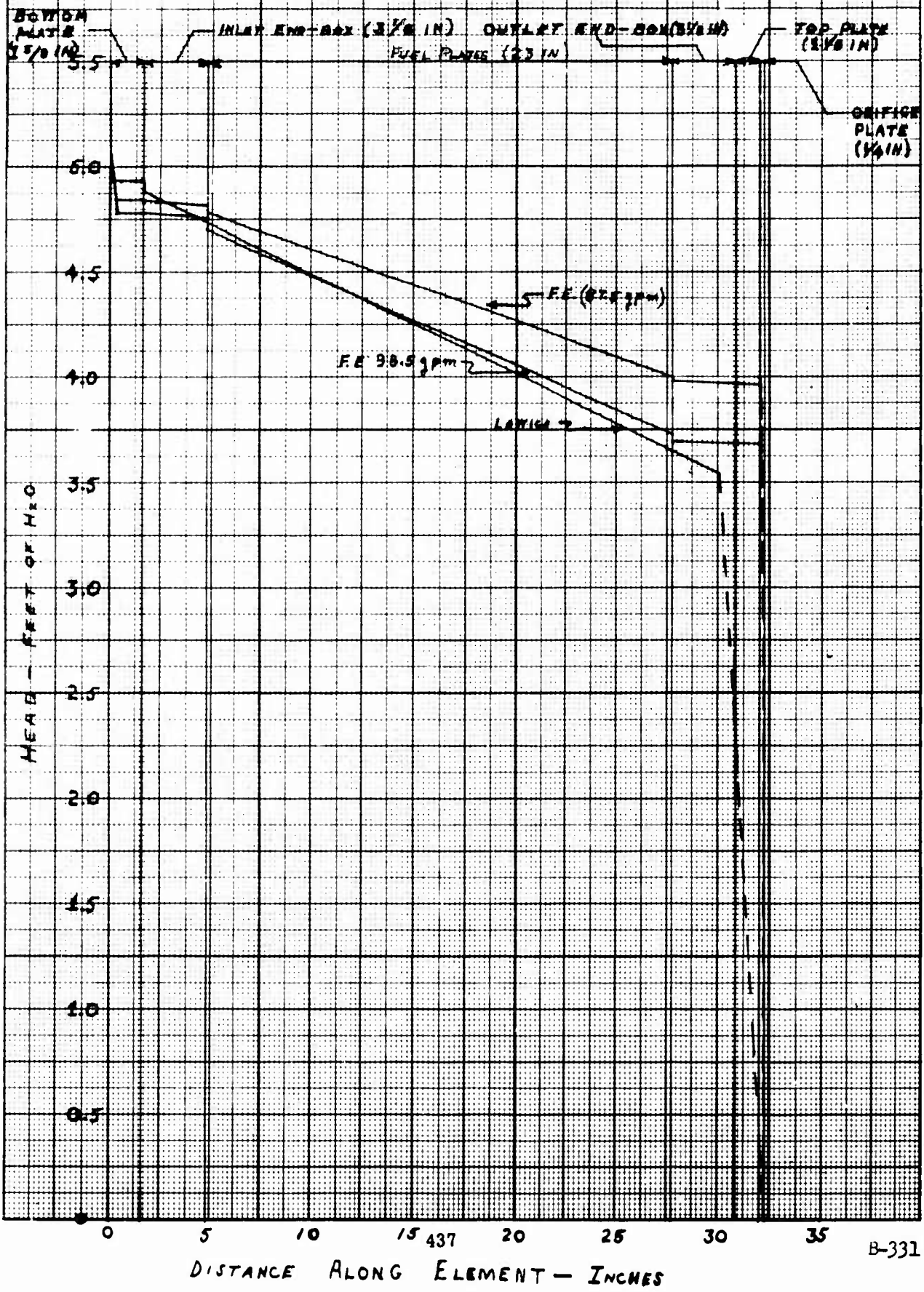
8.3 Conclusions

As was shown in Section 8.1, the maximum expected pressure differential across the outer fuel plates is 0.03 psi. Since the pressure differential required to deflect the plates beyond the allowable tolerance limit is 3 psi, it is apparent that further investigation of this problem is not necessary.

FIG. 8.1
 LOCATION OF HEAD LOSSES
 THROUGH CORE



F. O. B. 2
 HEAD LOSS ACROSS CORE
 STATIONARY ELEMENTS & LATTICE



REFERENCE
IV THERMAL ANALYSIS

1. Clark, Rohsenow, "Heat Transfer and Pressure Drop Data for High Heat Flux Densities to Water at High Subcritical Pressures," Tech Rep #3, Proj. 6627, MIT.
2. Epstein, Chastain, Fawcett, "Heat Transfer and Burnout to Water at High Subcritical Pressures," July 1956, BMI - 1116.
3. Jens, W.H., and Lottes, P.A., "Analysis of Heat Transfer, Burnout Pressure Drop and Density Data for High Pressure Water," May, 1951, ANL-4627.
4. Roarty, J.D., "Application of Forced Convection Heat Transfer and Friction Correlations in Core Design," July, 1954, WAPD-FE-96.
5. Roarty, Sher, "Preliminary Determination of Forced Convection Heat Transfer Coefficients for Rectangular Channels at 2000 psia," 1956, WAPD-TH-217.
6. Zerbe, Chr., "Review of Thermal Design Criteria for Pressurized Water Reactors at 2000 psia," WAPD-SFR-Rs-444.
7. APAE Memo #96, J. Brondel, May 6, 1957.
8. APAE 17 Vol. I, Thermal and Hydraulic Section.
9. AP Memo 43., Temperature Distribution and Thermal Stress in Reactor Core APPR-1.
10. Neill, F.H., and Smith, J.F. Jr., "Stainless Steel Fuel Element Test in STR," CF-54-11-13.
11. Gallagher, J.G., "Status of ORNL - APPR Irradiation Program," CF-55-6-124.
12. Beaver, R.J., "Present Status of Irradiation of APPR Fuel Elements," CF-55-6-167.
13. "Temperature Distribution and Thermal Stress in Reactor Core APPR-1," October 16, 1957, AP Memo 43.
14. Neill, F.H. "Irradiation of Stainless Steel Fuel Element Samples in MTR" CF55-4-153.
15. Beaver, R.J., Feldman, M.J., "MTR Test #3 of APPR Fuel Element" CF-55-4-163.
16. Beaver, R.J., "Post-Irradiation Macroscopic Examination of APPR Stainless Steel Plates Removed from APPR Fuel Element Irradiated in the MTR" CF-56-1-116.

17. "Specifications for Stainless Steel MTR Irradiation Test Element" CF 55-6-31.
18. "Testing of APPR Type UO₂ Stainless Steel Element in the MTR" CF-55-6-47.
19. Bobe, Silks, Stueck, "Program No. 203, Head Loss Calculation on the IBM 650," June 10, 1958, AP Note 105.
20. Erwin, J.H., Beaver, R.J., "Effect of Pressure Differentials on Deflection of the Outer Fuel Plates of Brazed APPR Fuel Elements." February 7, 1957, CF-57-2-34.
21. Timoshenko, S., "Strength of Materials Part II Advanced Theory and Problems," D. Van Nostrand Co., Inc., March 1956.
22. Sonneman, George and Davis, Duane M. "Thermal Stresses in Reactor Vessels," WAPD-BT-1, May, 1957.
23. Meem, J.L. "Initial Operation and Testing of the Army Package Power Reactor APPR-1," APAE-18, August 9, 1957.
24. Langer, B.F., "Design Bases for Reactor Vessels," WAPD-CE-43, 1955.

SKID MOUNTED DESIGN ANALYSIS

INDEX

- SECTION C General Description of Secondary Packages
- 1.0 Turbine Generator Packages
 - 1.1 Operating Characteristics of Machine and Auxiliaries
 - 1.2 Generator Characteristics and Operation at 5500 Feet Elevation
 - 1.3 Total Weight and Weight Distribution
 - 1.4 Provisions for Air Transportability
 - 1.5 Special Doweling and Alignment Requirements
 - 1.6 Heat Release From Turbine Generator to Insulated Enclosures

 - 2.0 Condenser Package
 - 2.1 Condenser
 - 2.1.1 Design and Operating Data
 - 2.1.2 Deaeration
 - 2.2 Air Ejectors
 - 2.2.1 Design and Operating Data
 - 2.2.2 Advantages of Air Ejector Versus Vacuum Pump
 - 2.3 Condensate Pumps
 - 2.3.1 Design and Operating Data
 - 2.4 Heat Release from Package
 - 2.5 Skid Design
 - 2.5.1 Weight and Weight Distribution

 - 3.0 Heat Exchanger Package
 - 3.1 Cooling Water Heat Exchanger
 - 3.1.1 Design and Operating Data
 - 3.2 Evaporator
 - 3.2.1 Design and Operating Data
 - 3.2.2 Description
 - 3.3 Circulating Water Pumps
 - 3.3.1 Design and Operating Data
 - 3.4 Heat Exchanger Circulating Water Pumps
 - 3.4.1 Design and Operating Data
 - 3.5 Blowdown Flash Tank
 - 3.6 Heat Release
 - 3.7 Skid Design
 - 3.7.1 Weight and Weight Distribution

 - 4.0 Air Blast Cooler Packages
 - 4.1 General Description
 - 4.2 Performance and Design Data
 - 4.3 Exhaust Ducts
 - 4.4 Basis of Horsepower Requirements
 - 4.4.1 Air Flow Through Snow
 - 4.5 Weight Distribution
 - 4.6 Skid Design

SKID MOUNTED DESIGN ANALYSIS

INDEX Cont.

- SECTION C General Description of Secondary Packages
- 5.0 Feed Water Package
- 5.1 General Description and Components on the Package
 - 5.2 Low Pressure Feed Water Heater
 - 5.2.1 Description
 - 5.2.2 Design and Operating Data
 - 5.3 High Pressure Heater
 - 5.3.1 Description
 - 5.3.2 Design and Operating Data
 - 5.4 Feed Water Pumps
 - 5.4.1 Performance and Design Data
 - 5.4.2 Selection of Pumps
 - 5.4.3 Pump Mounting
 - 5.5 Chemical Feed System
 - 5.5.1 General Description
 - 5.5.2 Performance and Design Data
 - 5.6 Secondary Water Treatment System
 - 5.6.1 Description and Performance Data
 - 5.6.2 Supplementary Equipment
 - 5.7 Feed Water Storage Tank
 - 5.8 Cooling Water Pumps
 - 5.8.1 Description and Design
 - 5.9 Primary System Auxiliaries
 - 5.10 Shipment
 - 5.11 Heat Release from Package
- 6.0 Switchgear Packages
- 6.1 General Description
 - 6.1.1 Components
 - 6.1.2 Arrangement
 - 6.2 Switchgear Equipment
 - 6.2.1 Equipment Provided
 - 6.3 Motor Control Center
 - 6.4 Station Transformer
 - 6.5 Station Batteries
 - 6.6 Electrical Equipment for Instrumentation
 - 6.6.1 Rectifier
 - 6.6.2 Inverter
 - 6.7 Weight Distribution

SKID MOUNTED DESIGN ANALYSIS

INDEX

SECTION C

DRAWINGS

| <u>Drawing Number</u> | <u>Title</u> | <u>Page Number</u> |
|----------------------------------|--|--------------------|
| <u>Feed Water Package</u> | | |
| M02M3 | General Arrangement | C-21 |
| M02S1 | Structural Skid Arrangement | C-23 |
| M02M4 | Piping - Sheet No. 1 | C-25 |
| M02M5 | Piping - Sheet No. 2 | C-27 |
| M02E6 | Electrical Plan and Elevations | C-29 |
| <u>Condenser Package</u> | | |
| M02M7 | General Arrangement | C-31 |
| M02S2 | Structural Skid Arrangement | C-33 |
| M02M8 | Piping | C-35 |
| M02E7 | Electrical Plan and Elevation | C-37 |
| <u>Heat Exchanger Package</u> | | |
| M02M9 | General Arrangement | C-39 |
| M02S4 | Structural Skid Arrangement | C-41 |
| M02M10 | Piping | C-43 |
| M02E5 | Electrical Plan and Elevation | C-45 |
| <u>Air Blast Cooler Packages</u> | | |
| D-133919 | General Arrangement | C-47 |
| D-133975 | Integral Skid and Supporting Structure | C-49 |
| <u>Turbine Generator Package</u> | | |
| M02M6 | General Arrangement | C-51 |
| M02S5 | Structural Skid Arrangement | C-53 |
| <u>Switchgear Packages</u> | | |
| M02E3 | General Arrangement | C-55 |
| M02S3 | Structural Skid Arrangement | C-57 |
| M02E4 | Conduit Plan | C-59 |

I GENERAL DESCRIPTION OF SECONDARY PACKAGES

The secondary system mechanical and electrical equipment is included in the following ten packages; the turbine generator packages (two sections); the condenser package; the heat exchanger package; the air blast cooler packages (three sections); the feed water heater package; and the switchgear packages (two sections).

1.0 Turbine Generator Packages

The general arrangement of the turbine generator is shown on appended drawing No. MO2M6 and the structural skid on drawing No. MO2S5. The overall dimensions of the erected package are 26 feet 3 inches long by 9 feet 1 inch wide by 6 feet 7 inches high. In order to meet the weight limitations imposed by aircraft transportation, the turbine generator unit is divided into two packages for shipment. The turbine and reduction gear form one package 15 feet 8 inches long by 8 feet 7-1/4 inches wide by 5 feet 11-1/2 inches high. The generator and exciter form the second package 13 feet 4 inches long by 8 feet 10-1/2 inches wide by 6 feet 4 inches high. These lengths include one removable skid end on each package, at the point of joining the skids, between the reduction gear and generator. This unit is a 2000 kilowatt, geared, turbine generator set, consisting of a multi-stage, multiple valve condensing turbine with two uncontrolled extraction points, a single reduction herringbone gear, a 1200 r.p.m. enclosed air cooled generator, a direct connected 10 kilowatt exciter, lubricating oil cooler, generator air cooler, and steam auxiliary lubricating oil pump, all mounted on structural steel bases with an integral lubricating oil storage tank. The turbine is provided with an integral trip and throttle valve, speed control governor, and an overspeed governor.

1.1 Operating Characteristics of Machine and Auxiliaries

The turbine is designed to deliver 2000 kilowatts when supplied with steam at 425 psig., dry and saturated at the throttle and with 8 inches Hg. absolute condenser conditions. The turbine is also designed to receive steam at rising pressure from 425 psig. at full load to 750 psig. at no load.

The turbine can be safely operated at condensing conditions down to approximately 3-1/2 inches Hg absolute, without danger of excessive erosion in the last stage blading.

The turbine operates at 4600 rpm. Two extraction points at 99 psia. and 31.5 psia. are available for feed water heating. Oil pressure for lubrication and operation of the hydraulic governor and control valves is supplied by a direct-connected gear pump, and an automatically controlled steam-driven auxiliary oil pump.

Lubricating oil cooling and generator air cooling are accomplished by built-in heat exchangers which will be cooled with a glycol and water solution circulated through an auxiliary section of the air blast coolers.

1.2 Generator Characteristics and Operation at 5500 Feet Elevation

The generator is totally enclosed, with two outboard bearings, and a direct-connected overhung exciter. It is rated at 2500 kilovolt amperes, 2000 kilowatts at 80 percent power factor and wound for 4160/2400 volts "wye" connected, grounded neutral, 3 phase, 60 cycles, and operates at 1200 rpm. The exciter is rated at 10 kilowatts, 125 volts, direct current, and is self-ventilated. The generator and exciter are designed to N.E.M.A. standards, and proportioned for continuous operation at full load with acceptable temperature rise for operation at an elevation of 5500 feet above sea level.

1.3 Total Weight and Weight Distribution

The total weight of the turbine generator unit is about 67,000 pounds. Since this exceeds the allowable shipping weight of 30,000 pounds, the unit will be divided into two sections, one consisting of the turbine and reduction gear, and the other consisting of the generator and exciter, each weighing approximately 30,000 pounds. Auxiliary equipment, including oil cooler and strainer, trip and throttle valve, and miscellaneous auxiliary devices weighing about 7000 pounds, will be shipped separately.

1.4 Provisions for Air Transportability

To permit shipping this unit by air transportation, the structural frame will be divided into two sections, the line of separation will occur in the vertical plane of the face of the coupling between the reduction gear and the generator, as shown on the turbine generator drawing No. MO2M6. Two temporary skid ends will be provided for bolting onto the divided structural frame to permit each section being handled as a complete skid. These skid ends will also protect the faces of the structural frame from damage during transit. The divided structural frame and temporary skid ends are shown in detail on drawing No. MO2S5. Removable bracing and locking devices will be provided for the turbine and generator by the manufacturer, to prevent axial movement of the rotating parts and to resist the forces developed during air transit.

1.5 Special Doweling and Alignment Requirements

Special dowels will be provided between the two adjoining ends of the structural frame to assure accurate alignment, in the field, of the two parts of the turbine generator unit. Also, adequate and clear markings will be provided on the generator shaft coupling halves to insure recoupling of the unit in the same angular position, thus eliminating the problem of checking the balance of the unit.

1.6 Heat Release From Turbine Generator To Insulated Enclosure

The total heat loss from the unit to the insulated enclosing structure will be approximately 50,000 B.t.u. per hour.

2.0 Condenser Package

The condenser package is shown on the appended drawings No. MO2M7 and No. MO2M8. This package is 24 feet 3 inches long, 8 feet 4-1/2 inches wide, and 9 feet high, and includes the condenser, two condensate pumps, and the steam air ejector. All piping and valving between components and the wiring and locally mounted instrumentation are provided in the package with flanges provided for connection to other packages. All piping on the shell side of the condenser will be welded and flanged to prevent leakage of air into the condenser as completely as possible. As few connections as possible will be located below the water line to minimize this source of oxygen contamination.

Starters for the pump motors are located adjacent to the pumps. All electrical controls are run to one junction box from which connections will be made to the control center.

2.1 Condenser

One 2500 square foot, three-pass, horizontal surface condenser is being supplied. The condenser will be of the deaerating type with a steel hotwell of approximately four-minute storage attached. The unit is 19 feet 0 inch overall length and 51 inch diameter shell. The shell will contain 796, 3/4 inch, 18 B.w.g., Admiralty metal tubes bowed between Muntz metal tube sheets. The condenser is elevated as high on the skid as possible to provide NPSH for the condensate pumps.

2.1.1 Design and Operating Data

The unit is designed to transfer 26.4 million B.t.u. per hour when supplied with 2000 g.p.m. of ethylene glycol solution 60 percent by weight at 110°F., and under these conditions will produce a vacuum at the steam inlet to the condenser of 8 inches of Hg. absolute. The pressure drop on the glycol side of the condenser will not exceed 25 feet of water.

The condenser is equipped with a float-operated level control which will admit water to the condenser from the feed water storage tank. High and low level alarms will indicate difficulty with the control system to the operator.

2.1.2 Deaeration

The condenser is of the deaerating type and is guaranteed to produce condensate with 0 degree depression and with no more than 0.03 c.c. per liter oxygen content. This is the normal guarantee for any condenser, and since this condenser will be of the deaerating type it is expected that it will produce condensate of considerably better quality than guaranteed.

2.2 Air Ejectors

The air ejector selected is a steam jet ejector, with dual, single stage jets discharging into a 75 square foot surface condenser cooled by the condensate.

2.2.1 Design and Operating Data

The air ejector with one element operating is designed to remove at least 3 c.f.m. of free air from the condenser at absolute pressures greater than 3-1/2 inches of mercury when supplied with 305 pounds of 300 psig. steam per hour. The jets require at least 25 gpm. of water for condensing the steam, and hence, it will be necessary to recirculate water back to the condenser at all loads under 700 kilowatts. The recirculation is done automatically by a siphon valve on the discharge side of the air ejector condenser, with the quantity of water recirculated being limited by a fixed orifice.

2.2.2 Advantages of Air Ejector Versus Vacuum Pump

Prior to the selection of the steam jet ejector, a study was made of the steam jet air ejector versus the rotary type vacuum pump. Conclusions indicated that the steam jet ejector was thermodynamically approximately as efficient as the rotary vacuum pump. In addition, its simplicity of operation and small amount of maintenance made it very attractive for the location in a remote area. Costwise, the dual element steam ejector with one spare element was approximately the same as the rotary vacuum pump with no spare capacity, hence, with these factors weighed it was fairly obvious that the steam jet ejector was the proper selection.

2.3 Condensate Pumps

The two condensate pumps are vertical, volute, centrifugal pumps. They are driven by 20 horsepower, 1750 rpm. drip-proof, vertically mounted, solid shaft, normal thrust, squirrel cage, induction motors.

2.3.1 Design and Operating Data

These pumps were selected for their low weight and ability to operate with low NPSH. Due to the head room limitation on the skid, approximately 1-1/2 feet of NPSH is available for the condensate pumps. Each pump will deliver 90 gpm. of condensate at 152°F against a total dynamic head of 325 feet. Although this is slightly more discharge pressure than is required for protection of the boiler feed pumps, it gives an additional margin of safety on the suction of the boiler feed pumps, and those pumps were reduced in head capacity by this margin.

2.4 Heat Release from Package

The expected heat release from this package at full operating temperature is 300,000 B.t.u. per hour with an ambient temperature of 80°F. All piping above 155°F. will be insulated. If all of this radiation cannot be used for heating the enclosure, some of the surfaces will be insulated.

2.5 Skid Design

The structural steel skid is made of a high strength steel capable of withstanding shock at low temperatures. The skid is an all welded frame designed to support the weight of the equipment during transportation, including lifting, skidding, etc. The skid is also designed to resist the inertial forces of the equipment while being transported by air; namely, 8 G's forward, 2 G's aft, 2 G's vertical and 1.5 G's lateral.

2.5.1 Weight and Weight Distribution

The total weight of the condenser package including the structural skid is 28,250 pounds. The skid has been proportioned to distribute the weight of the package in accordance with the allowable floor loading of the C-130 aircraft.

3.0 Heat Exchanger Package

This package is shown on appended drawings No. MO2M9 and MO2M10. This package is 26 feet 9 inches long by 9 feet 0 inch wide by 8 feet 10 inches high. The components included in this package are the cooling water heat exchanger, cooling water heat exchanger pumps, evaporator, the circulating water pumps, and the blowdown flash tank. The evaporator and the cooling water heat exchanger have been held as close to the skid as possible, being elevated only enough to withdraw the bundles over the pumps. All piping has been held as close to the skid as practical for ease of supporting during shipment. All operating controls are accessible from the edge of the skid. The skid is entirely pre-wired with a minimum of connections necessary by the field to place in operation.

3.1 Cooling Water Heat Exchanger

The cooling water heat exchanger is a U-tube heat exchanger, 13 feet 6 inches in overall length with an 18 inch diameter shell.

3.1.1 Design and Operating Data

The heat exchanger is designed to transfer 568,000 B.t.u. per hour from the cooling water entering at 127° F. and leaving at 100°F. to 86 g.p.m. of 60 percent by weight ethylene glycol. The ethylene glycol enters from the air blast cooler at 92° F. and leaves the exchanger at 108.5° F.

3.2 Evaporator

The evaporator is designed to produce 1000 pounds of steam per hour for certain uses outside the plant.

3.2.1 Design and Operating Data

The evaporator is designed to deliver 1000 pounds per hour at 150 psig. of essentially dry steam. Steam for operation of the evaporator is obtained from the main steam line at between 440 and 750 psig., re-

duced in pressure through a pressure control valve to 300 psig., by a control valve with external pilot initiated from the shell of the evaporator.

The evaporator is complete with float-operated inlet valve, which will regulate water returned from outside the station, and level alarms to indicate trouble to the operator at control panel.

While little blowdown is expected with raw water of the purity available at the site the evaporator may be blown down into the flash tank when required.

3.2.2 Description

The evaporator is made up of a shell of 26-3/4 inches outside diameter by 8 feet 1 inch overall length. The heating surface in the shell is comprised of 21 U-tubes of 90-10 copper-nickel material giving a surface of 42 square feet, which is submerged in the lower half of the shell. Steam is taken off in a dry pipe for use by the post.

3.3 Circulating Water Pumps

The circulating water pumps delivering glycol to the condenser in a closed cycle are two, double suction, half capacity, horizontally split case pumps.

3.3.1 Design and Operating Data

Each circulating water pump has a rated capacity of 1000 gpm, against a total head of 65 feet. They operate at 1800 rpm., and require 22.4 brake horsepower when pumping the 60 percent glycol solution at 110° F. The pumps are the standard, cast iron, bronze fitted pumps with ball bearings, and are driven by two General Electric Company's induction motors rated at 25 horsepower, or equal.

3.4 Heat Exchanger Circulating Water Pumps

Two full capacity heat exchanger circulating water pumps deliver water to the cooling water heat exchanger and the air and lube oil coolers on the turbine generator. They are centrifugal pumps, mounted together with a 7-1/2 horsepower induction motor on a common structural steel baseplate.

3.4.1 Design and Operating Data

Each single stage pump operating at 3550 rpm. is designed to deliver 300 gpm. of ethylene glycol solution against a total head of 25 psi. at a temperature of 92° F. The pump has a vertically split steel casing, with cast iron impeller and oil lubricated ball bearings. Only one pump will be operated at a time, and it will deliver approximately 86 gpm. to the heat exchanger, 60 gpm. to the turbine oil cooler, and 100 gpm. to the turbine generator air coolers.

3.5 Blowdown Flash Tank

A small flash tank is located on this skid together with meter and control valves. The tank is sized to handle the maximum flow from the boiler through a 1/2 inch line, flashing the steam and retaining the water until cool.

This tank will also be used to handle the continuous blowdown from the evaporator located adjacent to it.

3.6 Heat Release

The heat release from this package will be 45,000 B.t.u. per hour. All lines on this skid over 140° F will be insulated.

3.7 Skid Design

The structural skid is made of high strength steel capable of withstanding shock at low temperatures. The skid is an all-welded frame designed to support the weight of the equipment during transit, including lifting, skidding, etc. The skid is also designed to resist the inertial forces of the equipment while being transported by aircraft; namely, 8 G's forward, 2 G's aft, 2 G's vertical, and 1.5 G's lateral.

3.7.1 Weight and Weight Distribution

The total weight of the heat exchanger package including the structural skid is about 23,250 pounds. The skid has been proportioned to distribute the weight of the package in accordance with the allowable floor loading of the C-130 aircraft.

4.0 Air Blast Cooler Packages

The general arrangement of the air blast cooler is shown on Drawing No. D-133919.

4.1 General Description

Due to the lack of cooling water at the site, closed circuit air blast coolers are used for condensing steam. An ethylene glycol and water solution is circulated in a closed circuit through the main condenser and air blast cooler sections. Auxiliary cooling is provided by a separate section of the air blast cooler, circulating a glycol solution through the auxiliary heat exchanger in a separate closed circuit. The air blast coolers are extended surface heat exchangers, liquid to air. The coolers are arranged with two banks of cooling sections placed vertically, one on each side of the unit. The liquid flow is horizontal through multiple tubes extending the full length of each bank. The tubes are connected into vertical headers at each end. Air flow is horizontal across the tube banks entering on the outside faces of the banks, flowing to the center. Air flow is produced by induced draft fans located between the tube banks, and placed at the top of the unit. The dis-

charge from the fans is vertically up. The liquid flow in each main bank is two-pass entering and leaving the bank through flanged pipe connections on the headers at the same end. The main banks on each side of a cooler unit are arranged for parallel flow. The auxiliary section of each cooler is arranged for single-pass flow. Weight and dimensional limitations require the air blast cooler to be divided into three separate and identical sections. Each section is 30 feet 0 inch long by 9 feet wide by 9 feet high. The three sections of the air blast cooler are located in three separate snow tunnels, as shown on the plant general arrangement, and the piping is arranged for series flow through the three sections.

4.2 Performance and Design Data

Service - Glycol solution cooler
 Draft type - Induced
 Number of units - One in three sections.

| | | <u>Main Cooler</u> | <u>Auxiliary Cooler</u> |
|---------------------------------------|----------------------|--------------------|-------------------------|
| Duty | B.t.u./Hr. | 26,400,000 | 1,100,000 |
| Extended Surface | Sq. Ft. | 117,400 | 9,600 |
| Air Temperature - In | °F | 35 | 35 |
| Air Temperature - Out | °F | 11C | 73 |
| Liquid Temperature - In | °F | 143.1 | 101 |
| Liquid Temperature - Out | °F | 110 | 92 |
| Total Fluid Entering | Lb./Hr. | 1,057,000 | 160,000 |
| Liquid Side Pressure Drop | p.s.i. | 11 | 5.5 |
| | | | <u>Combined Cooler</u> |
| Total Air Flow at Standard Conditions | c.f.m. | | 354,000 |
| Total Static Pressure | In.-H ₂ O | | 1.25 |
| Fans | | | 68 inch dia. |
| Fans per Section | | | 3 |
| Fans - Total Number | | | 9 |
| Fan Speed | r.p.m. | | 684 |
| Horsepower per fan | h.p. | | 20 |
| Total Horsepower | h.p. | | 180 |
| Materials: | | | |
| Headers | | | Carbon steel |
| Plugs | | | Brass |
| Tubes | | | Admiralty |
| Fins | | | Aluminum |
| Header Type | | | Welded steel |
| Tube Type | | | Pressure wrapped fin |
| Tubes | 1" O.D. by 24' 0" | | 18 B.w.g. |

4.3 Exhaust Ducts

The air discharge from the induced draft fans will be carried to the snow surface by means of insulated ducts. In order to prevent melting of the snow by heat from the exhaust ducts, these ducts will be enclosed with outer casings or ducts separated from the warm inner ducts by a ventilated air space. By this type of construction the snow will be protected from melting.

4.4 Basis of Horsepower Requirements

The power requirements for the coolers is based on a calculated pressure drop across the finned tube coils and the friction of the exhaust stacks of 0.25 inch water, plus a negative pressure of 1 inch water at the face of the coils. Thus the fans are designed to operate at a total static pressure of 1.25 inches water.

4.4.1 Air Flow Through Snow

The air supply to the air blast coolers will be induced to flow from the surface down to the face of the coils. The Army will design and construct the inlet air system such that the pressure drop between the surface of the snow and the inlet to the coils, when maximum required c.f.m. is flowing, does not exceed 1 inch of water.

4.5 Weight Distribution

Each section of the air blast cooler has a total weight of 25,200 pounds. The coolers are designed symmetrically about the longitudinal centerline and the weight of the coils and fans is uniformly distributed along the two side frames.

4.6 Skid Design

The skid is an all-welded structural steel frame designed to support the weight of the equipment during transit, including lifting, skidding, etc. The skid is also designed to resist the inertial forces of the equipment while being transported by aircraft; namely, 8 G's forward, 2 G's aft, 2 G's vertical, and 1.5 G's lateral.

5.0 Feed Water Package

This package is shown on the appended drawings No. MO2M3, No. MO2M4, and MO2M5.

5.1 General Description and Components on the Package

This package is 27 feet 9 inches long by 9 feet 0 inch wide by 9 feet 0 inch high, and contains the low pressure feed water heater, high pressure feed water heater, boiler feed pumps, feed water storage tank, chemical feed system, cooling water pumps, secondary system demineralizer, and the following primary system auxiliaries: primary make-up pump, primary demineralizer, and the primary make-up tank. The two feed water heaters have been

elevated in a horizontal position on the skid to allow the placing of smaller equipment underneath, and to assist in draining the heaters to the condenser. The constant speed, vertical boiler feed pumps and the heaters have all been grouped at one end of the skid to allow complete operation of this equipment within a small area. The feed water storage tank has been located near the center of the skid so that its broad surfaces could be used for mounting the pump starters and controls, and the large amount of small piping from the primary system. The feed water heater level controls are located between the feed water heaters and are easily accessible for maintenance. The primary auxiliaries are all located at one end of the skid and on the outside of the package for ease of maintenance. In general, all of the piping, instrumentation, and electrical control on the panel are completely interconnected on the skid, requiring a minimum of connections being made to other skids.

5.2 Low Pressure Feed Water Heater

5.2.1 Description

The low pressure heater which is mounted along the edge of the skid is 15 feet 3 inches overall with a 16 inch outside diameter shell. The heater which is in the suction to the boiler feed pumps is valved for by-passing in case of difficulty during operation. The heater is a four-pass, U-tube design with the lower pass being shrouded for an integral drain cooler. It will have 37 U-tubes of 3/4 inch outside diameter arsenical copper, comprising a total gross surface of 190 square feet of which 58 square feet is in the sub-cooling zone. The heater will contain the required auxiliary equipment, including high level alarm, gauge glasses, level control, and tube and shell side safety valves.

5.2.2 Design and Operating Data

The low pressure heater is designed to heat 37,000 pounds per hour of condensate after leaving the air ejector to a total temperature of 235°F at full load, operating normally at 27.5 psia. It will receive drains from the evaporator and the high pressure feed water heater, which will be subcooled to approximately 171°F, or 10 degrees above the entering water. The drains from the heater will be returned to the condenser shell and it is expected that the heater will have sufficient pressure differential to return these drains at all loads above 200 kilowatts.

5.3 High Pressure Heater

5.3.1 Description

The high pressure heater is installed in the discharge of the boiler feed pumps and will be subject to the full discharge pressure of these pumps. The heater is 9 feet 11 inches overall length and 14 inches outside diameter of shell. It is a U-tube design heater containing 32 U-tubes of 3/4 inch outside diameter arsenical copper, comprising a total surface of 105 square feet. The heater will be complete with a high water alarm, necessary instruments, relief valves, and drainer. Drains will cascade to the low pressure heater.

5.3.2 Design and Operating Data

The heater water side is designed for 600 psig. at 350°F. and the shell side for 100 psig. at 350°F. It will transfer 2,760,000 B.t.u. per hour heating 37,000 pounds per hour of boiler feed water from 236° F. to 309° F. at full load, operating normally at 89 psia.

5.4 Feed Water Pumps

The two feed water pumps are vertical, 15 stage, double case, centrifugal pumps. Each pump is driven by a 40 horsepower, 3550 r.p.m., drip-proof, vertically mounted, solid shaft, squirrel cage induction motor. Either pump can supply the full load requirement of the boiler.

5.4.1 Performance and Design Data

The pumps are placed between the low pressure and high pressure feed water heaters. Each pump will deliver 90 g.p.m. of feed water at a temperature of 235° F. against a discharge pressure of 465 psi. with a suction pressure of 110 psi., and will deliver 10 gpm. against a discharge pressure of 750 psi. The efficiency at 90 gpm. is 52 percent. The pumps are designed specifically for boiler feed service, the outer shell is of carbon steel, and the casings, impellers, wearing rings, shaft and shaft sleeves are constructed of 11-13 percent chrome steel.

5.4.2 Selection of Pumps

Due to the conditions peculiar to the reactor boiling of rising drum pressure with falling load, a thorough investigation of various types of feed pumps was made before selecting vertical centrifugal pumps. Variable speed, multiple-cylinder, positive displacement pumps were considered because of the high discharge pressure required at low load; however, the high turn down range of 9 to 1 would require complicated speed control of the driver, and a gear speed reducer between the variable speed driver and the pump. Alternating current to direct current drives, hydraulic couplings, eddy-current couplings, and mechanical variable speed drives were considered. In each case the space requirement, weight, and first cost were higher than the centrifugal pumps. The centrifugal pumps operating at constant speed simplify the regulation of feed water to the boiler drum. Whereas by variable speed drive the water level control would have to be translated by control mechanism to pump speed, with the centrifugal pumps the water level controller simply adjusts a throttling control valve in the discharge line between the pump and boiler.

5.4.3 Pump Mounting

The vertical feed water pumps are supported by a mounting flange at the discharge head of the pump. This mounting flange is bolted to the structural supporting frame which forms a part of the complete feed water package skid. The pump casing which contains the multi-stage pump is below the mounting flange, extending down to the bottom of the skid. This results in keeping the center of gravity of the pumps low on the skid, which is advantageous in shipping. The vertical motors which are mounted above the discharge head of the pumps will be removed for shipment for two reasons; one,

to reduce the shipping weight of the package, and two, to protect the pump shaft and impellers from damage during transit.

5.5 Chemical Feed System

5.5.1 General Description

The purpose of the chemical feed system in the secondary side of the plant is to treat the condensate, boiler feed, and steam in such a manner that the corrosion of all equipment will be held to a minimum. Practically all corrosion control systems in power plants accomplish this purpose by controlling the pH of the water in the boiler at a given alkalinity, and providing some means of oxygen scavenging. In this case, morpholine will be added to the condensate ahead of the low pressure heater which will in some degree control the pH of the feed water in the cycle as well as the pH of the water in the boiler. Since morpholine is carried through as a gas with the steam, it will protect the entire system from the boiler outlet back through the condenser.

Sodium sulphite will be added to the condensate stream at the same point prior to entering the low pressure heater. It will be fed continuously into the condensate stream and thereby protect the heaters and piping into the boiler, at which point the residual will be maintained to scavenge oxygen in the boiler. When the condenser is functioning properly, the amount of sulphite required to be pumped into the system will be rather small.

5.5.2 Performance and Design Data

Identical chemical feed pumps and tanks have been selected for both the morpholine and sulphite service since neither chemical is particularly corrosive. Each pump will be a proportioning pump with a single cylinder, having a capacity of 1.7 gph. and being driven by a 1/3 horsepower, 1725 rpm., three phase, 440 volt, alternating current motor. The capacity of the pumps may be varied from zero to full rated maximum capacity by adjustment of the stroke. These pumps take their suction from a 15 gallon stainless steel tank set immediately above the pump. The suctions of the two tanks have been interconnected so that the pumps can be used for pumping either sulphite or morpholine in the event that one pump is out for service.

5.6 Secondary Water Treatment System

The secondary water treatment system consists of one mixed bed deionizer, which will receive melted snow at approximately 50° F and 5 p.p.m. total solids, and deliver water having a specific resistance of over 1,000,000 ohm centimeters. The unit having an overall height of 74 inches will be furnished on a baseplate approximately 40-1/2 inches wide by 29 inches deep, which will contain one deionizing tank 14 inches in diameter and 60 inches high, completely piped with 5/8 inch stainless steel pipe and 1/2 inch stainless steel type valves. The unit will contain 1.1 cubic feet of cation resin and 1.65 cubic feet of anion resin which will be manually regenerated.

5.6.1 Description and Performance Data

With the specified water containing no more than 5 p.p.m. total solids, the deionizer will have a flow rate of 300 gallons per hour and the capacity between regenerations of 75,300 gallons. The unit will be regenerated manually, and should require between 2 and 2-1/2 hours to regenerate. During the regeneration period, the unit will require approximately 200 gallons of water at a rate not exceeding 8 g.p.m. Approximately 5.5 to 8 c.f.m. of air are required at 10 psig. for mixing the beds after regeneration.

5.6.2 Supplementary Equipment

A blower capable of producing 20 c.f.m. at 10 psig. with accessories, and a 3 horsepower, drip-proof motor will be furnished with the unit for operation during periods of regeneration to mix the resin. This demineralizer package will be complete with an inlet integrating flow meter and indicating controller which will close a motor-operated water valve when the purity exceeds a preset standard.

5.7 Feed Water Storage Tank

Forming a part of the skid will be a rectangular storage tank made of 1/4 inch steel plate. The tank will be covered and vented with an access manhole in the top. The tank is 6 feet 0 inch by 7 feet 3 inches long by 7 feet 11 inches high, and contains 2500 gallons of useable capacity. This rectangular shape tank utilizes the available space on the skid to the best degree. The tank will be complete with high and low level alarms and drain connection.

The 2500 gallon tank will have an expected storage capacity equivalent to 10 hours of operation. In case of emergency, the blowdown on the boiler could be cut off and the storage time extended to more than 24 hours. The low level alarm on the tank has been set at approximately 2/3 capacity so that there will be sufficient time to regenerate the demineralizer in case of any difficulty after the alarm. Morpholine will be added to the tank to control pH of the water, and thereby reduce corrosion of this carbon steel tank and associated piping.

5.8 Cooling Water Pumps

The purpose of the cooling water pumps is to supply cooling water to the primary coolant pump, primary heat exchanger, space cooler, spent fuel pit cooling, and the shield tank coolers. This system is a closed circuit, from the cooling water pumps through the various pieces of equipment to be cooled, back through the cooling water heat exchanger, and to the suction of the cooling water pumps. The feed water storage tank is connected into the suction of the cooling water pumps acting as a surge tank for the system.

5.8.1 Description and Design

The cooling water pumps which are provided in duplicate are centrifugal process pumps driven by 3 horsepower, 440 volt, drip-proof motors at 3600 rpm. The pumps are rated at 50 gpm. and deliver 100° F. water

against a total head of 50 psi. The pumps are vertically split, with steel casing, cast iron impellers, and oil lubricated ball bearings. Although this is a heavy-duty, process type pump, a 100 percent spare has been provided which will automatically start in case of loss of discharge pressure.

5.9 Primary System Auxiliaries

While the primary system auxiliaries located on this package have no connection with the other equipment, it provides a convenient place for locating this equipment during shipment, and fits in quite well with the overall arrangement of the plant. Located on this skid are the make-up tank, make-up pumps, and the primary system demineralizer, together with the associated instrumentation and piping which are required to be accessible by the operators. The equipment is located around the edge of the skid for ease of maintenance and operation.

5.10 Shipment

Due to the limitation on height, it will be necessary to remove the safety valves on the heaters and ship separately. Due to the limitation on weight, it will be necessary to remove the primary demineralizer and ship this separately. For practical reasons and limitation on weight, it is desirable to remove the motors from the two vertical boiler feed pumps, and to ship them separately, as will be detailed later. All other equipment will be shipped intact as assembled.

5.11 Heat Release from Package

The expected heat release from this package at full operating temperature is 29,000 B.t.u. per hour. This estimate is based on computations with insulation on all piping and equipment over 140° F.

6.0 Switchgear Packages

6.1 General Description

The electrical packages are shown on drawing No. MO2E3. Due to space and weight limitations, the electrical equipment has been mounted on two skids. The control package is 28 feet 10-7/8 inches long by 9 feet wide by 8 feet 10 inches high. The switchgear package is 13 feet 10 inches long by 9 feet wide by 8 feet 10 inches high.

6.1.1 Components

The switchgear package will contain only the switchgear. The control package will contain the control console, nuclear rack, instrumentation distribution cabinet, motor control center, rectifier, battery rack, and dry-type transformer.

6.1.2 Arrangement

The control package has been arranged with the console, nuclear rack, and instrumentation distribution cabinet at the front of the

package. Due to its length the motor control center will occupy one side of the package and be separated by an aisle from the other remaining components. Access space has been allowed at both sides of the control console.

The switchgear package allows both a walking space and a draw-out aisle for the circuit breakers in the area not occupied by the equipment.

6.2 Switchgear Equipment

6.2.1 Equipment Provided

The switchgear will be an indoor, draw-out unitized, 4160 volt, three phase, four wire, metal enclosed unit consisting of:

- A - 2500 Kilovolt ampere turbine generator air circuit breaker.
- B - Exciter, synchronizing, and auxiliary panel.
- C - Incoming line air circuit breaker.
- D - Auxiliary power air circuit breaker.
- E - Outgoing feeder No. 1 air circuit breaker.
- F - Outgoing feeder No. 2 air circuit breaker.

6.3 Motor Control Center

The motor control center will be an indoor, unitized, 600 volt, 600 ampere, three phase, three wire assembly, including circuit breakers, motor starters, etc., for the 480 volt circuits to the primary, feed water, condenser, heat exchanger, air blast cooler packages, and the station services. The control center will also contain panel boards for the distribution of alternating current and direct current power for instrumentation.

6.4 Station Transformer

The station transformer will be a dry type, self-cooled, 500 kilovolt ampere, 4160 volt, wye primary, 480 volt, delta secondary, three phase, 60 cycle, unit substation type. The transformer will be mounted on "Korfund" vibration isolators to prevent vibration transmission to the control console.

6.5 Station Batteries

The station battery will supply the direct current requirements of the control console and the tripping requirements of the switchgear circuit breakers. The battery will be the nickel cadmium type mounted in trays on a steel battery rack. The rating of the battery of 165 ampere hours at 28 volts is based on supplying the instrumentation load for approximately one hour after station power failure.

6.6 Electrical Equipment for Instrumentation

The rectifier will supply a regulated source of direct current control power and the floating charge on the station battery. By means of an inverter, part of the direct current will be changed to a preferred alternating current supply for the control console, nuclear rack, and monitoring devices. The distribution of the control power is as shown on drawing No. MO2E2.

6.6.1 Rectifier

The rectifier will be a free standing, fully enclosed, ventilated, indoor unit of the solid-state type. It will be rated for the 100 ampere, 28 volt, direct current instrumentation load and the floating charge rate of the battery. It will also be used, if necessary in an emergency, for re-charging the battery from a fully discharged state.

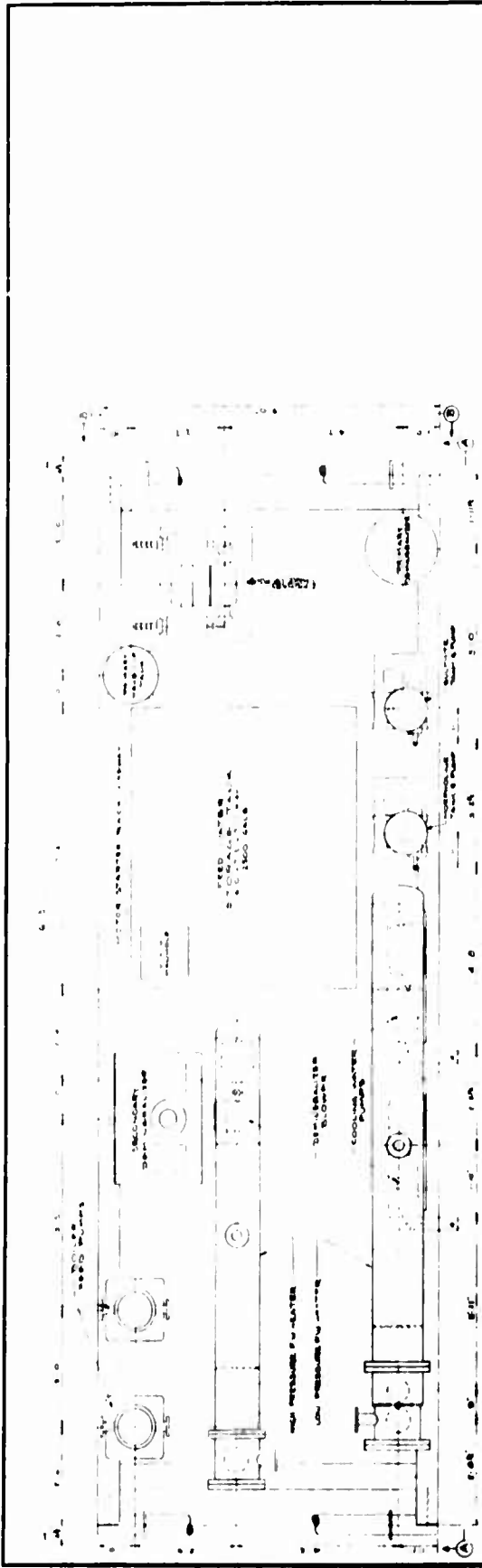
6.6.2 Inverter

The inverter will be a solid-state unit for inverting approximately 3000 watts, 28 volts, direct current to 115 volts, 60 cycle alternating current. The inverter will be designed to mount in the motor control center.

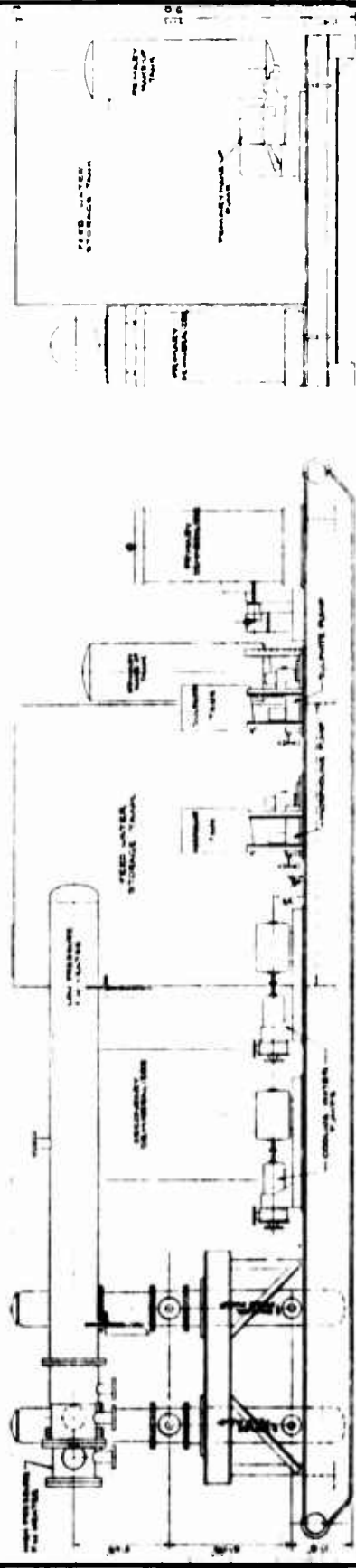
6.7 Weight Distribution

The weight distribution is as follows:

| | <u>Pounds</u> |
|---------------------------------|---------------|
| <u>Control Package</u> | |
| Motor Control Center | 5,000 |
| Primary Instrument Console | 2,700 |
| Instrument Distribution Cabinet | 750 |
| Nuclear Panel | 1,550 |
| Battery | 800 |
| Rectifier | 1,000 |
| Conduit and Wire | 500 |
| Transformer | 6,400 |
| Skid | 6,600 |
| Total | <u>25,300</u> |
| <u>Switchgear Package</u> | |
| Switchgear | 20,000 |
| Skid | 3,000 |
| Total | <u>23,000</u> |



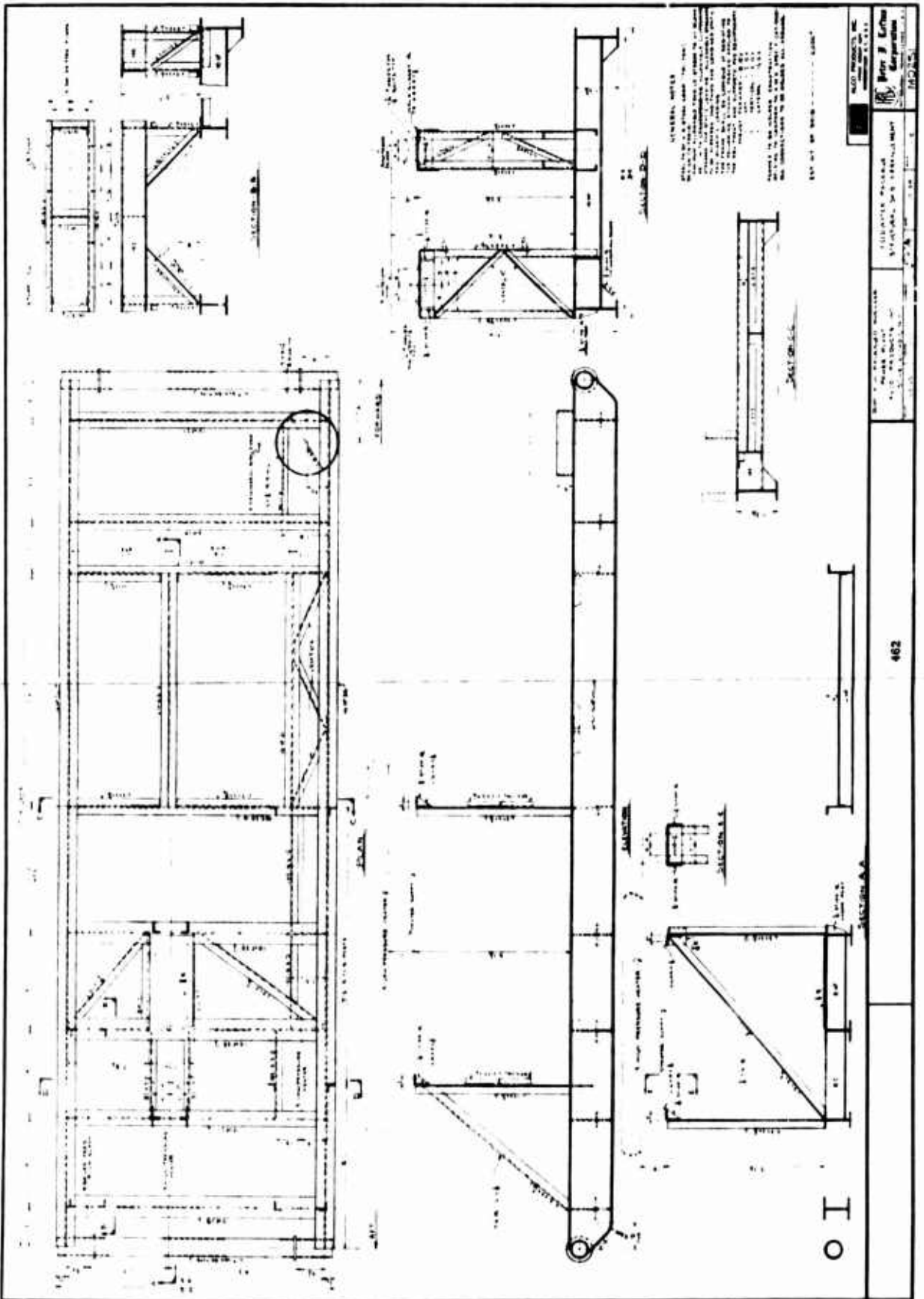
PLAN



ELEVATION A-A

ELEVATION B-B

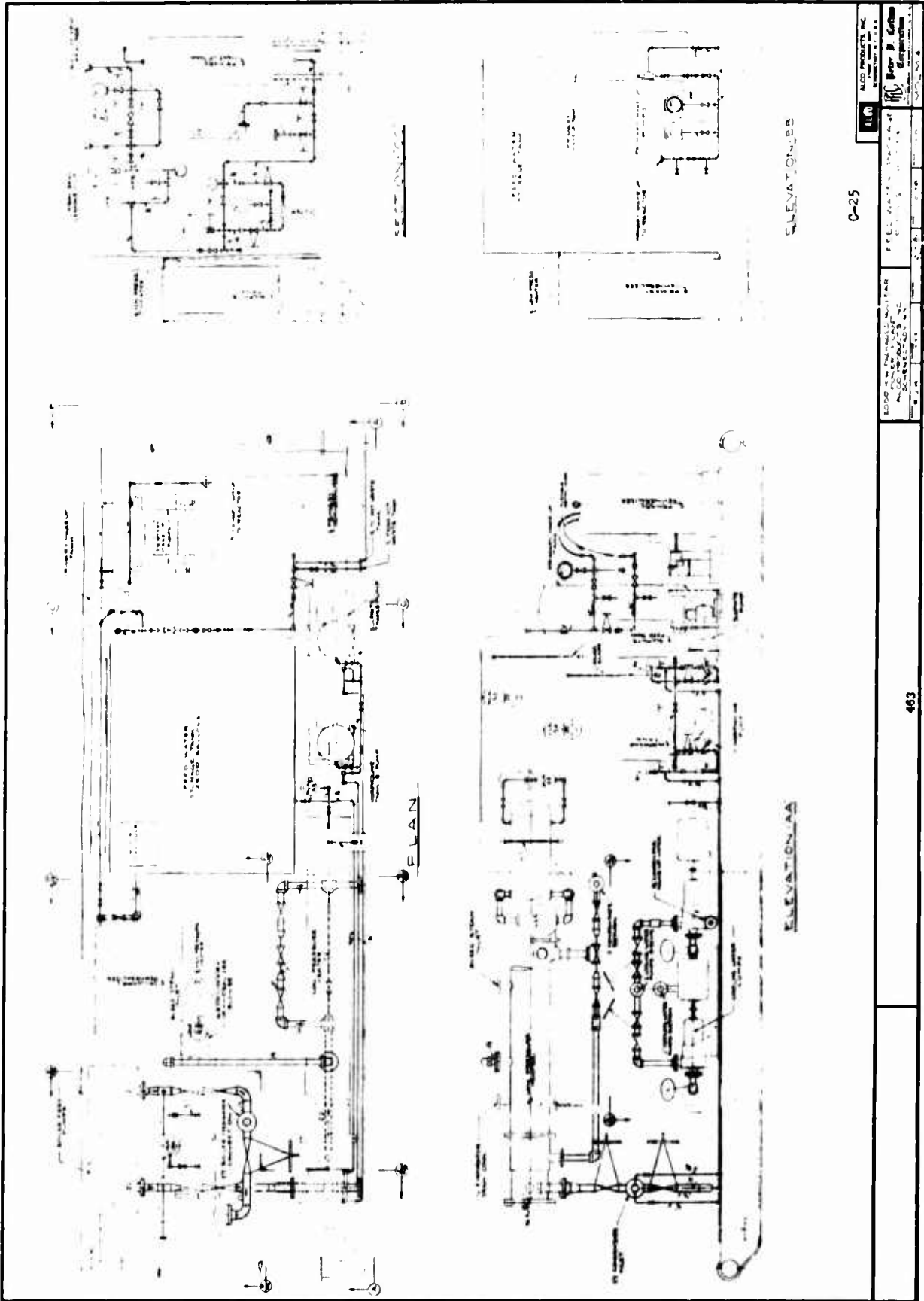
| | | | |
|--|--|---|----------------------------------|
| ALSO PROVIDED BY THE USER: | | FEEDWATER PACKAGE GENERAL ARRANGEMENT Westinghouse Electric Corporation | SHEET NO. 358 OF 410 M.O. 213 |
| 3000 KW PACKAGE POWER PLANT AND REACTOR CONTAINMENT | | | |
| 481 | | C-21 | |



O I

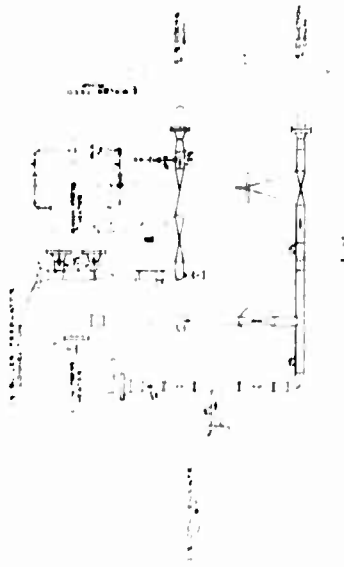
462

| | | | | |
|--|--------------------|--------------|-----------------------|-------------------|
| TITLE STRUCTURAL STEEL SECTION A-A | PROJECT NO. 462 | DATE 1918 | DRAWN BY J. L. ... | CHECKED BY ... |
|--|--------------------|--------------|-----------------------|-------------------|

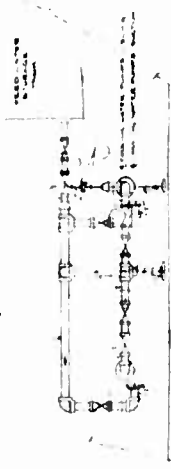


C-25

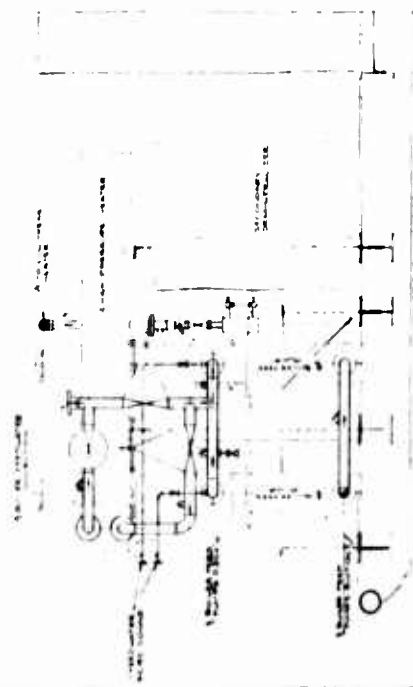
| | |
|-------------|--|
| ALCO | ALCO PRODUCTS, INC. ALCOA BUILDING ALCOA PLANT |
| DESIGNED BY | ALCO ENGINEERING DEPARTMENT |
| DRAWN BY | ALCO ENGINEERING DEPARTMENT |
| CHECKED BY | ALCO ENGINEERING DEPARTMENT |
| DATE | ALCO ENGINEERING DEPARTMENT |



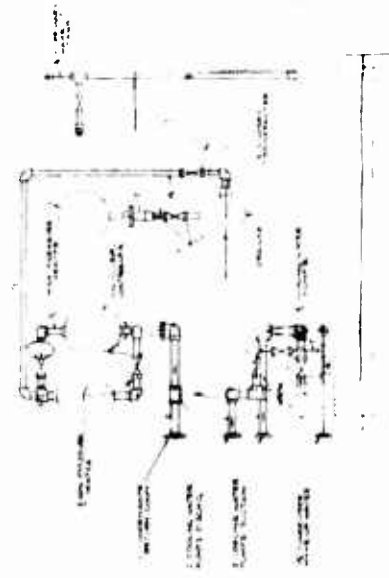
SECTION IEE



SECTION IEE

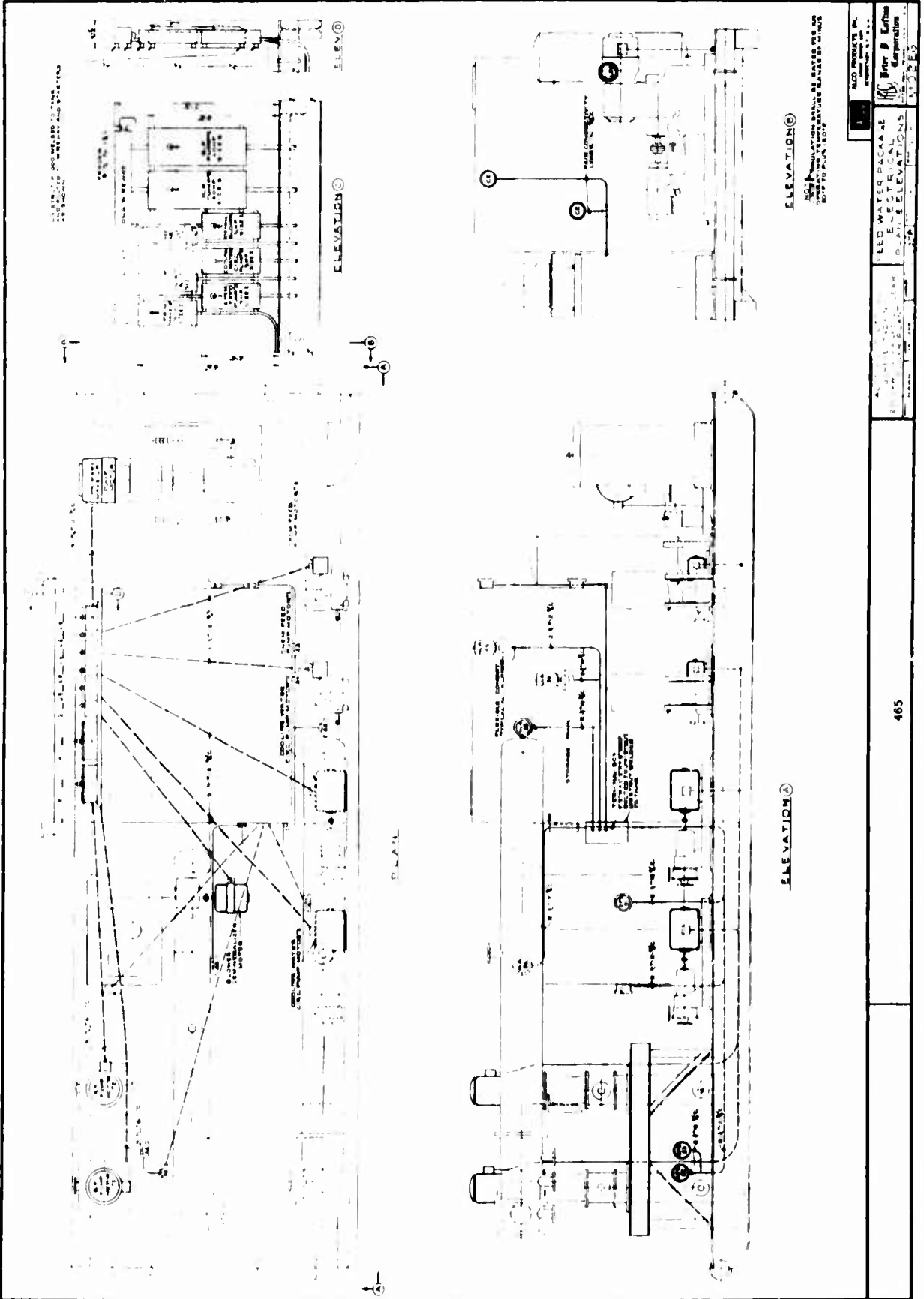


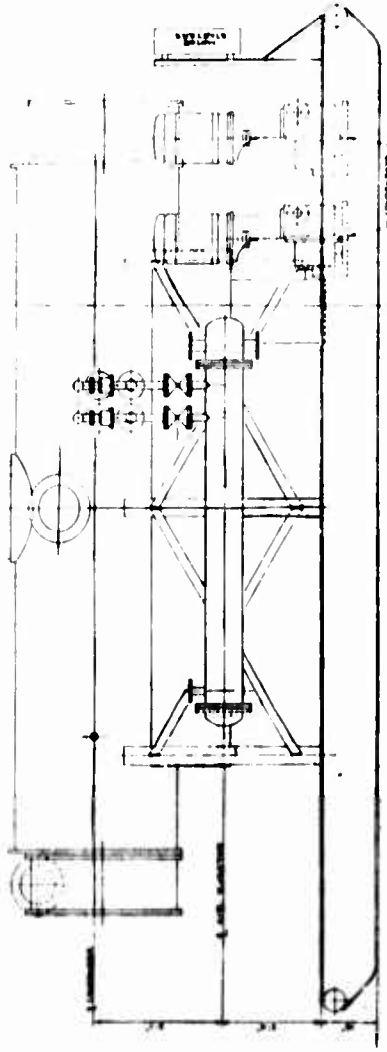
SECTION IEE



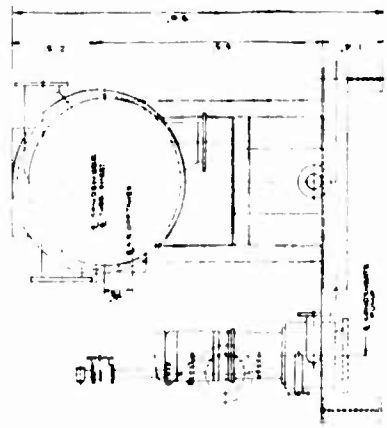
SECTION IEE

| | | | |
|---|--|---|--|
| ALCO PRODUCTS, INC. ALCO PRODUCTS, INC. ALCO PRODUCTS, INC. | | ALCO | |
| FOR SALES AND SERVICE ALCO PRODUCTS, INC. ALCO PRODUCTS, INC. | | FIELD WITH SERVICE ALCO PRODUCTS, INC. | |
| 464 | | 464 | |
| 464 | | 464 | |



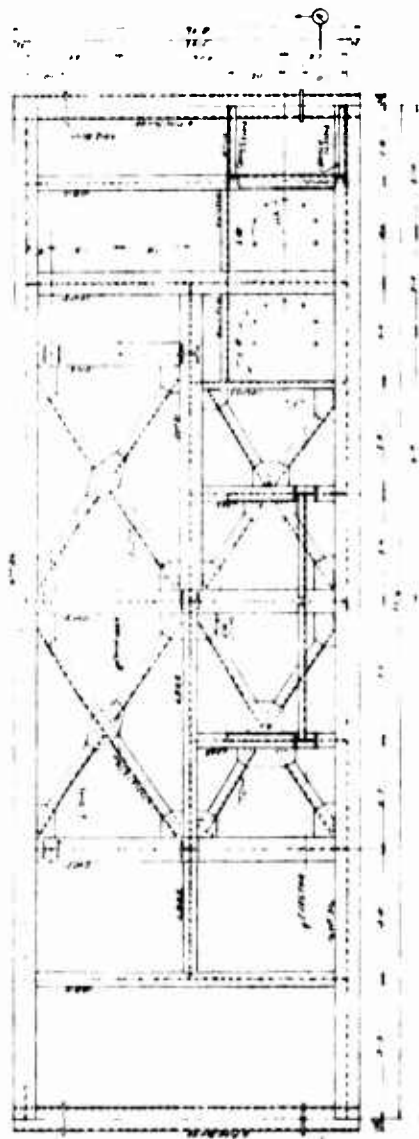


ELEVATION A-A



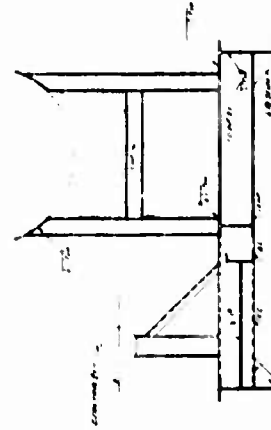
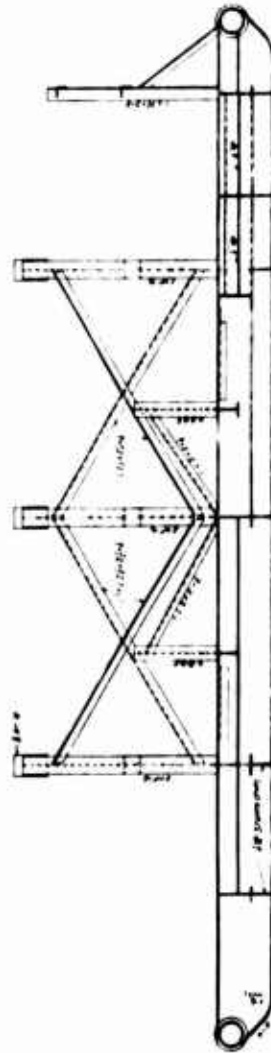
ELEVATION B-B

| | | | |
|---|--|---------------------------------------|--|
| ALCO PRODUCTS, INC. 1000 S. JONES AVE. MONTICELLO, N.C. | | LICENSEE PACKAGE GENERAL AGREEMENT | |
| 406 | | MODEL 7 | |

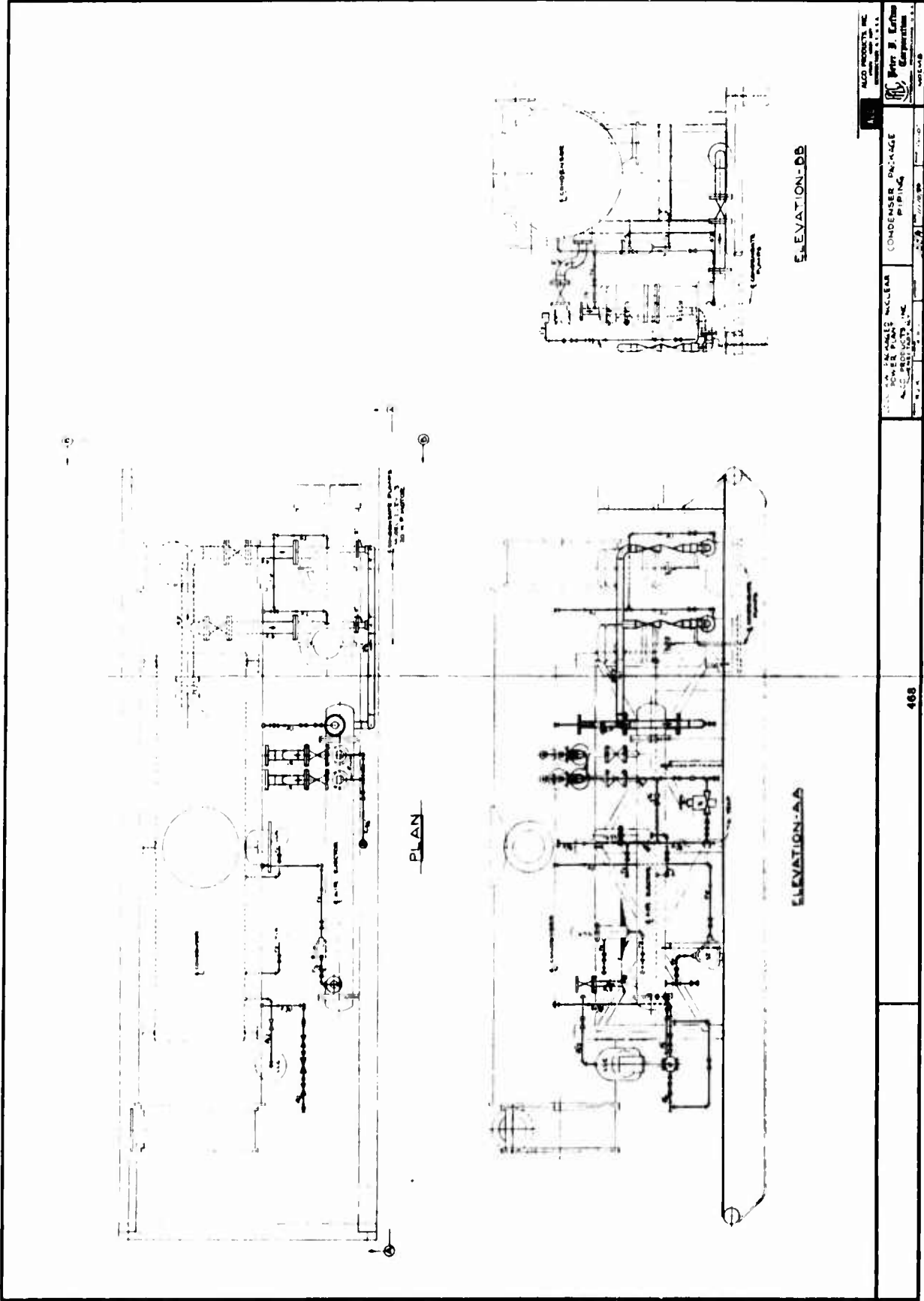


Notes:
 1. All steelwork to be painted with a minimum of two coats of zinc-rich primer and two coats of red oxide paint.
 2. All steelwork to be galvanized.
 3. All steelwork to be fabricated to the American Institute of Steel Construction, Inc. Specification for Structural Steel Buildings, 1950 Edition, Part 5, Allowable Stress Design and Plastic Design.
 4. All steelwork to be fabricated to the American Institute of Steel Construction, Inc. Specification for Structural Steel Buildings, 1950 Edition, Part 5, Allowable Stress Design and Plastic Design.
 5. All steelwork to be fabricated to the American Institute of Steel Construction, Inc. Specification for Structural Steel Buildings, 1950 Edition, Part 5, Allowable Stress Design and Plastic Design.
 6. All steelwork to be fabricated to the American Institute of Steel Construction, Inc. Specification for Structural Steel Buildings, 1950 Edition, Part 5, Allowable Stress Design and Plastic Design.
 7. All steelwork to be fabricated to the American Institute of Steel Construction, Inc. Specification for Structural Steel Buildings, 1950 Edition, Part 5, Allowable Stress Design and Plastic Design.
 8. All steelwork to be fabricated to the American Institute of Steel Construction, Inc. Specification for Structural Steel Buildings, 1950 Edition, Part 5, Allowable Stress Design and Plastic Design.
 9. All steelwork to be fabricated to the American Institute of Steel Construction, Inc. Specification for Structural Steel Buildings, 1950 Edition, Part 5, Allowable Stress Design and Plastic Design.
 10. All steelwork to be fabricated to the American Institute of Steel Construction, Inc. Specification for Structural Steel Buildings, 1950 Edition, Part 5, Allowable Stress Design and Plastic Design.

Structural Member Design - 9/5/50



2000 PLY SHEET PILE
 CONSTRUCTION
 COMPANY
 A DIVISION OF
 THE STEEL INDUSTRIES
 OF AMERICA
 INCORPORATED
 1200 PLY SHEET PILE
 CONSTRUCTION
 COMPANY
 A DIVISION OF
 THE STEEL INDUSTRIES
 OF AMERICA
 INCORPORATED



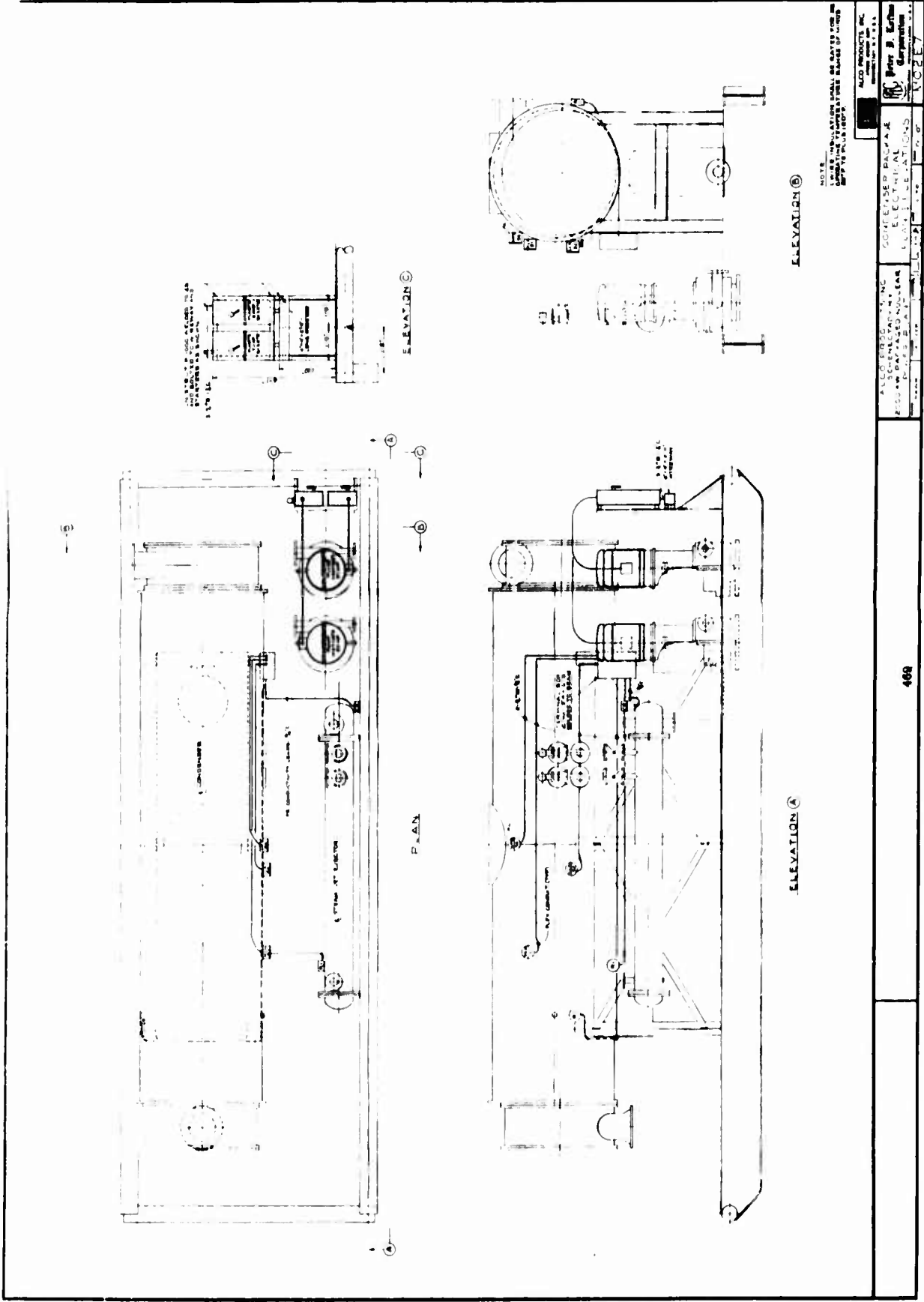
ALCO PRODUCTS, INC.
 1000 WEST 10TH AVENUE
 DENVER, COLORADO 80202 U.S.A.

ALCO PRODUCTS, INC.
 1000 WEST 10TH AVENUE
 DENVER, COLORADO 80202 U.S.A.

ALCO PRODUCTS, INC.
 1000 WEST 10TH AVENUE
 DENVER, COLORADO 80202 U.S.A.

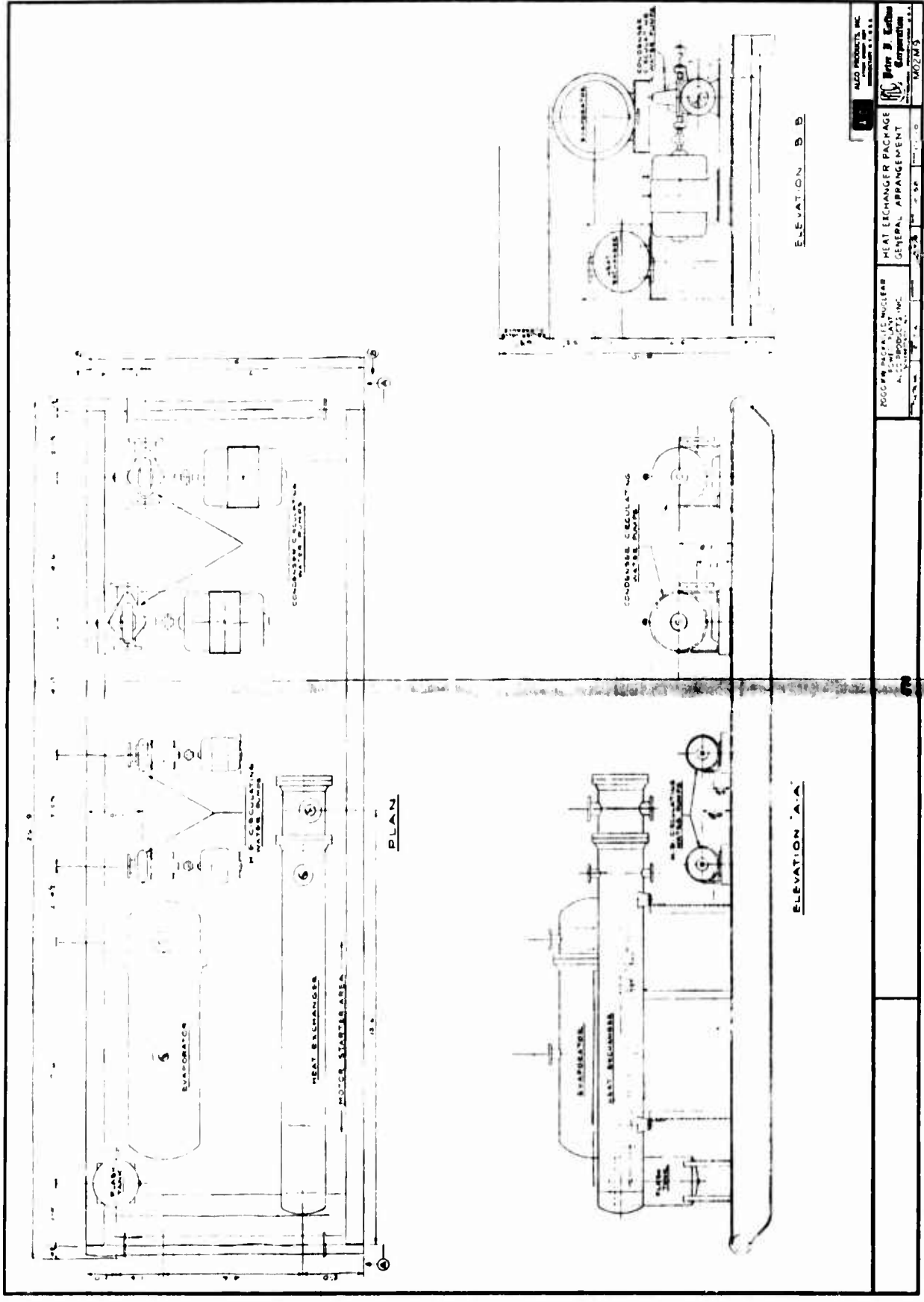
ALCO PRODUCTS, INC.
 1000 WEST 10TH AVENUE
 DENVER, COLORADO 80202 U.S.A.

ALCO PRODUCTS, INC.
 1000 WEST 10TH AVENUE
 DENVER, COLORADO 80202 U.S.A.



NOTE: ALL DIMENSIONS ARE IN INCHES UNLESS OTHERWISE SPECIFIED.

| | |
|---------------------|---------------------|
| ALCO PRODUCTS INC. | |
| 469 | |
| ALCO PRODUCTS INC. | ALCO PRODUCTS INC. |
| CONVERTIBLE PACKAGE | CONVERTIBLE PACKAGE |
| ELECTRICAL | ELECTRICAL |
| INSTALLATIONS | INSTALLATIONS |
| ALCO PRODUCTS INC. | ALCO PRODUCTS INC. |
| 469 | 469 |
| ALCO PRODUCTS INC. | ALCO PRODUCTS INC. |
| CONVERTIBLE PACKAGE | CONVERTIBLE PACKAGE |
| ELECTRICAL | ELECTRICAL |
| INSTALLATIONS | INSTALLATIONS |
| ALCO PRODUCTS INC. | ALCO PRODUCTS INC. |
| 469 | 469 |
| ALCO PRODUCTS INC. | ALCO PRODUCTS INC. |
| CONVERTIBLE PACKAGE | CONVERTIBLE PACKAGE |
| ELECTRICAL | ELECTRICAL |
| INSTALLATIONS | INSTALLATIONS |
| ALCO PRODUCTS INC. | ALCO PRODUCTS INC. |
| 469 | 469 |
| ALCO PRODUCTS INC. | ALCO PRODUCTS INC. |
| CONVERTIBLE PACKAGE | CONVERTIBLE PACKAGE |
| ELECTRICAL | ELECTRICAL |
| INSTALLATIONS | INSTALLATIONS |
| ALCO PRODUCTS INC. | ALCO PRODUCTS INC. |
| 469 | 469 |



ALCO PRODUCTS, INC.
 1000 WEST 12TH AVENUE
 DENVER, COLORADO 80202

MOOSE SIGN AREA
 HEAT EXCHANGER PACKAGE
 GENERAL ARRANGEMENT

ALCO PRODUCTS, INC.
 1000 WEST 12TH AVENUE
 DENVER, COLORADO 80202

CONDENSER
 HEAT EXCHANGER
 STEAM GENERATOR

CONDENSER REGULATING
 VALVE PUMP

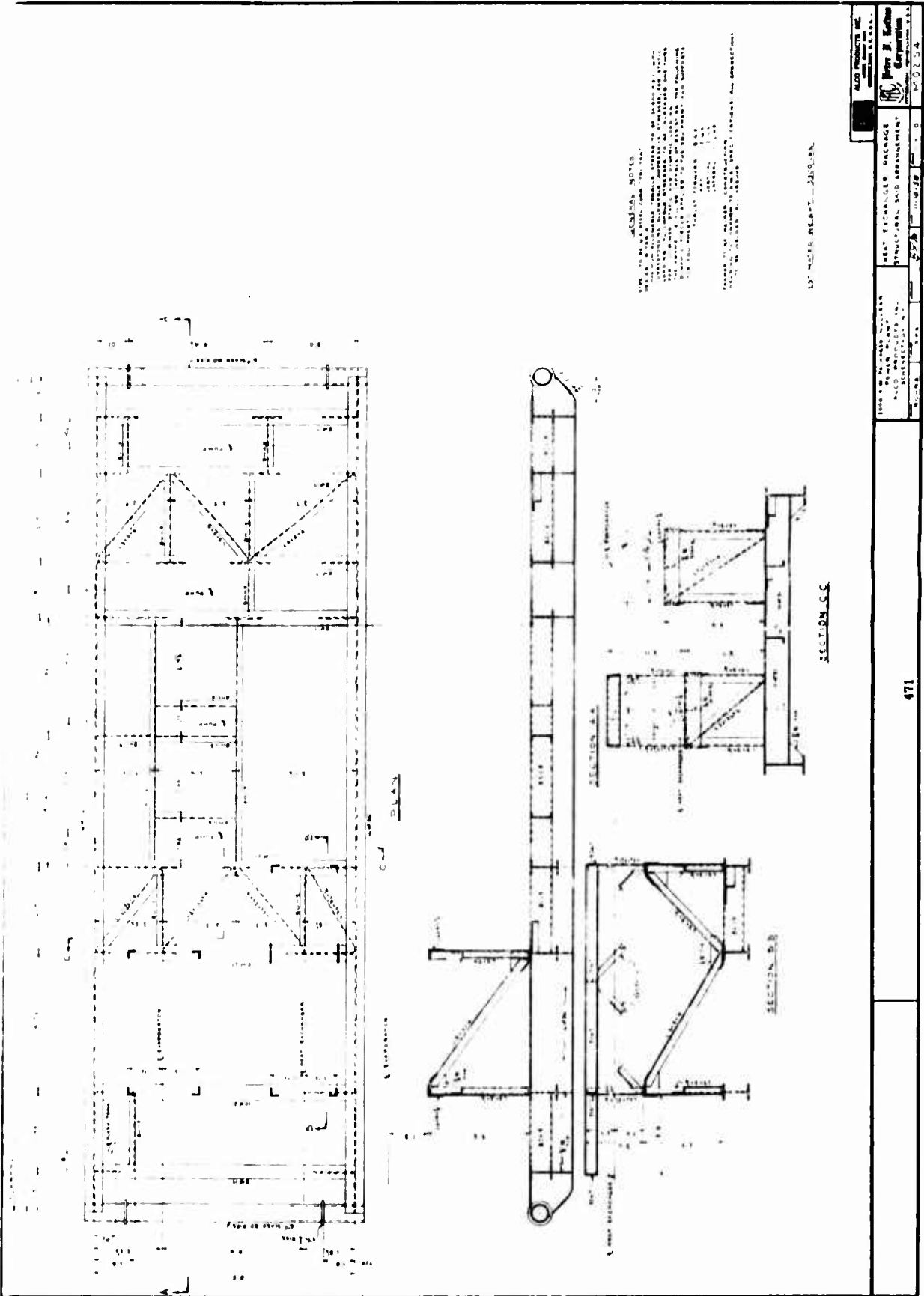
STEAM GENERATOR
 HEAT EXCHANGER

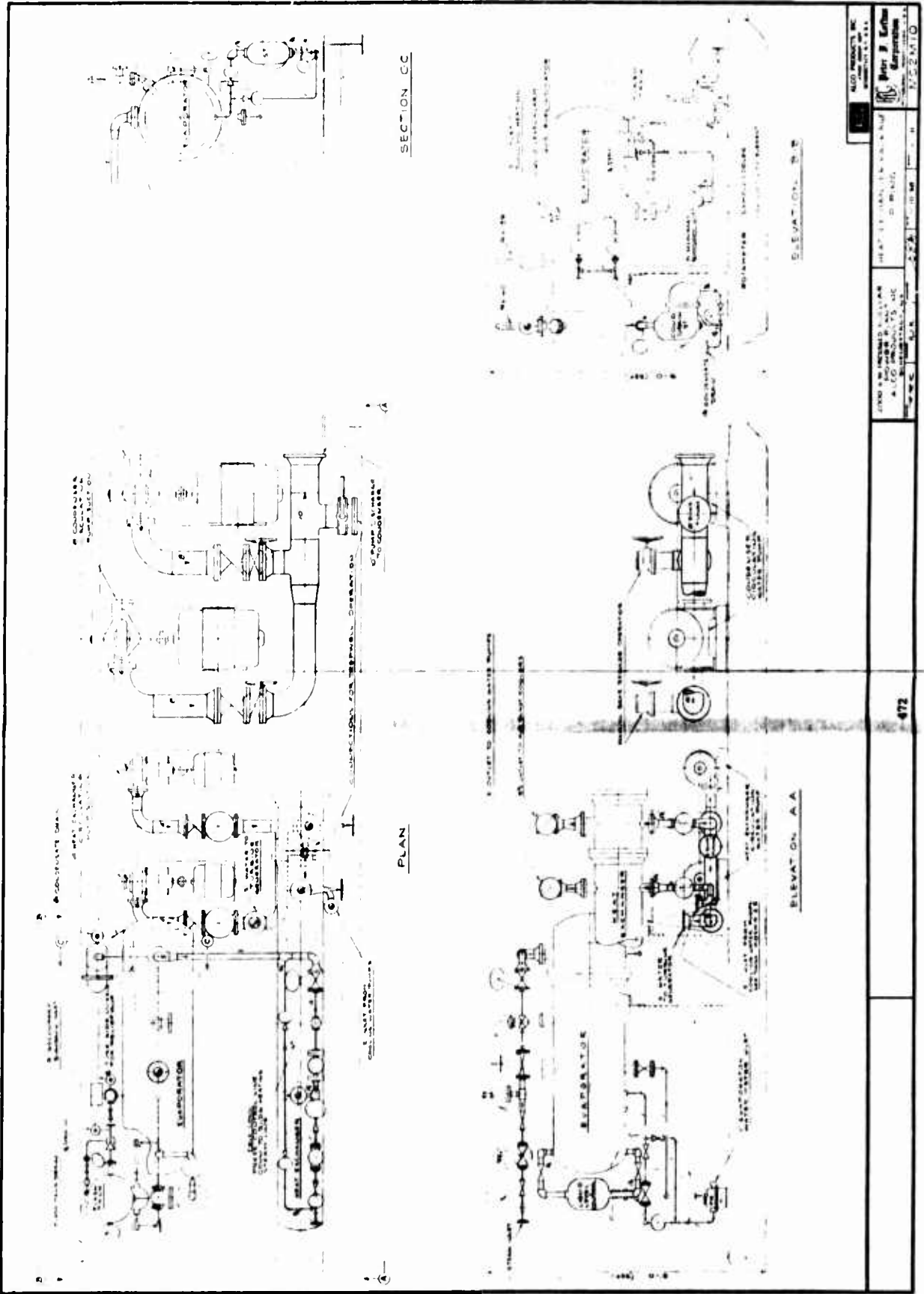
MOOSE SIGN AREA

CONDENSER REGULATING
 VALVE PUMP

CONDENSER
 HEAT EXCHANGER
 STEAM GENERATOR

ALCO PRODUCTS, INC.
 1000 WEST 12TH AVENUE
 DENVER, COLORADO 80202

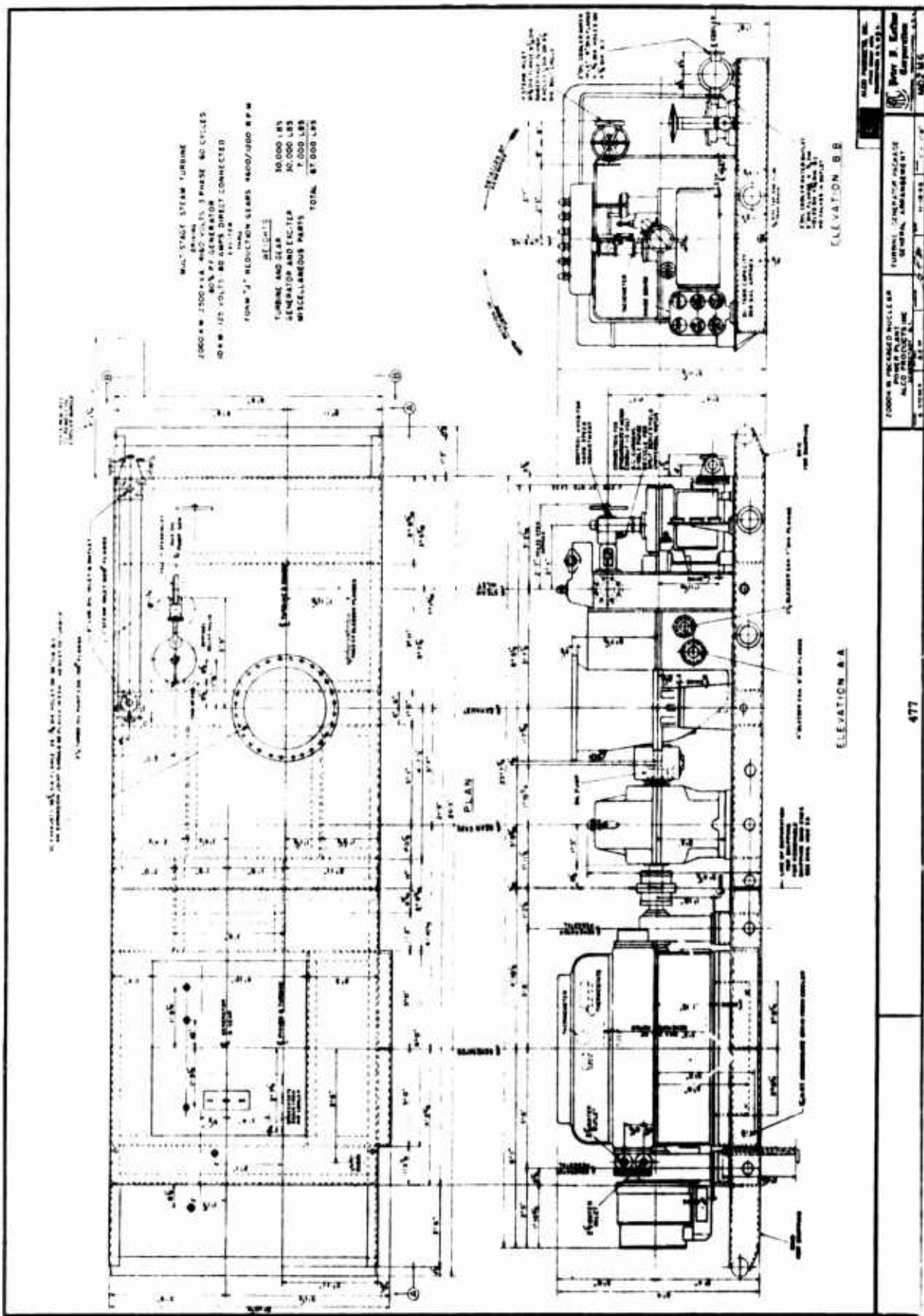


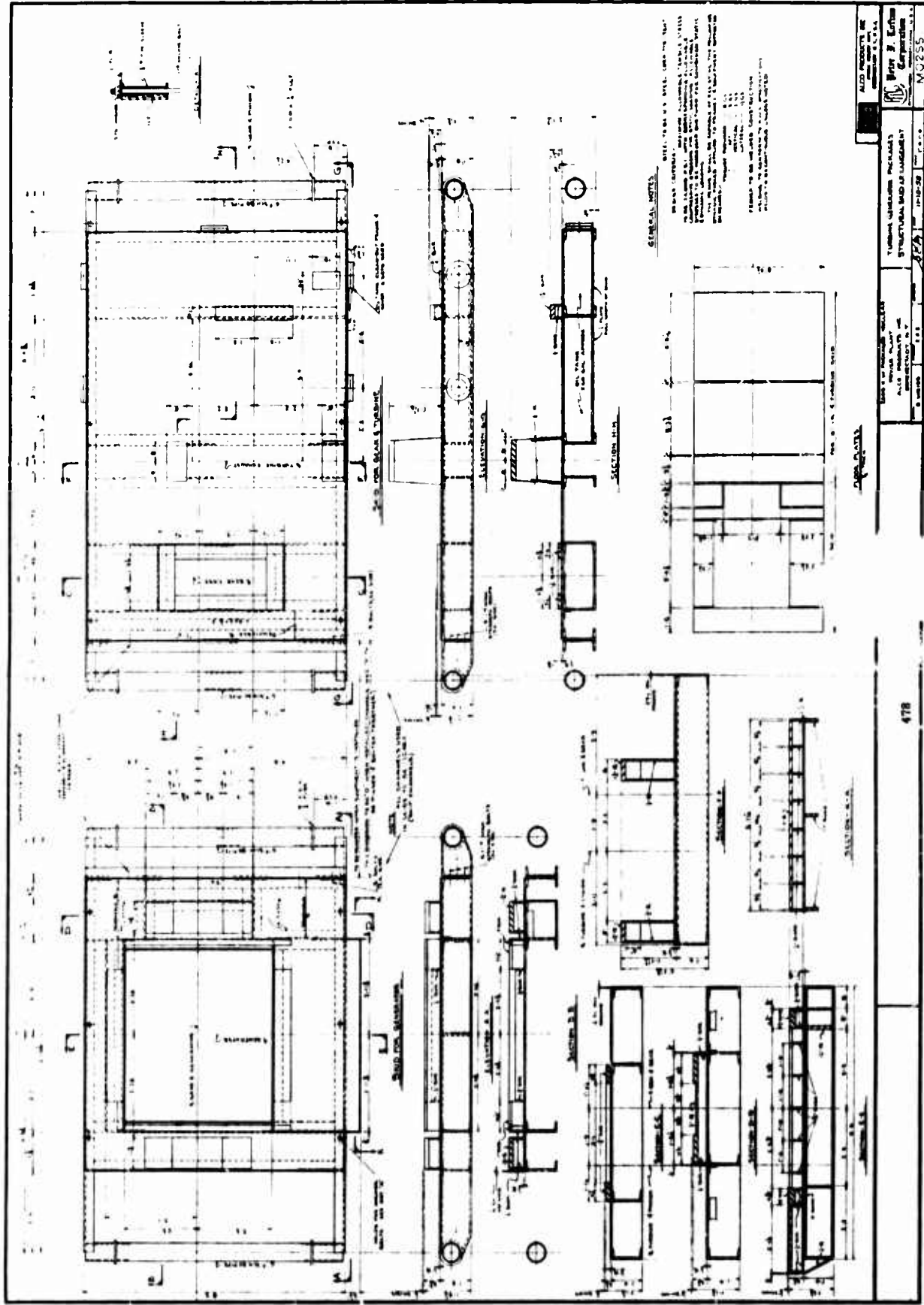


ALCO PRODUCTS, INC.
 1700 WASHINGTON AVENUE
 ALCO PRODUCTS, INC.
 1700 WASHINGTON AVENUE
 ALCO PRODUCTS, INC.

472

ALCO PRODUCTS, INC.
 1700 WASHINGTON AVENUE
 ALCO PRODUCTS, INC.
 1700 WASHINGTON AVENUE
 ALCO PRODUCTS, INC.

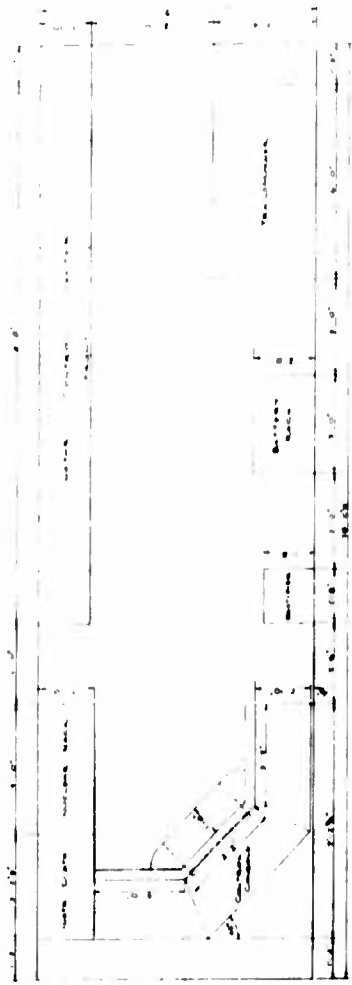




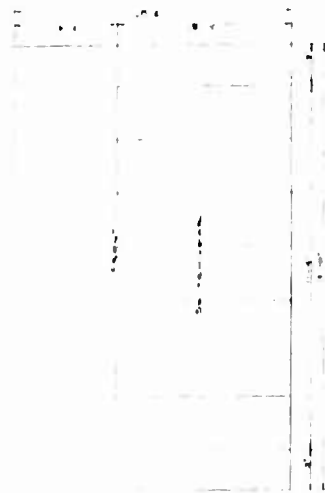
GENERAL NOTES

1. ALL DIMENSIONS ARE TO FACE UNLESS OTHERWISE NOTED.
 2. ALL WALLS ARE CONCRETE UNLESS OTHERWISE NOTED.
 3. ALL FLOORS ARE CONCRETE UNLESS OTHERWISE NOTED.
 4. ALL ROOFS ARE CONCRETE UNLESS OTHERWISE NOTED.
 5. ALL CEILING ARE CONCRETE UNLESS OTHERWISE NOTED.
 6. ALL DOORS ARE TO BE 3' 0" HIGH AND 2' 0" WIDE UNLESS OTHERWISE NOTED.
 7. ALL WINDOWS ARE TO BE 4' 0" HIGH AND 6' 0" WIDE UNLESS OTHERWISE NOTED.
 8. ALL STAIRS ARE TO BE 4' 0" WIDE UNLESS OTHERWISE NOTED.
 9. ALL ELEVATIONS ARE TO BE FINISHED UNLESS OTHERWISE NOTED.
 10. ALL SECTIONS ARE TO BE FINISHED UNLESS OTHERWISE NOTED.

| | | | | | | | |
|---|--|---|--|-------------------------------|--|----------------------------|--|
| <p>ALSO PROVIDED BY ARCHITECTURE & CIVIL</p> | | <p>THIS DRAWING INCLUDES STRUCTURAL AND LAYOUT</p> | | <p>NO. 100-28</p> | | <p>NO. 255</p> | |
| <p>DATE OF PREPARATION: 1954</p> | | <p>SCALE: 1/4" = 1'-0"</p> | | <p>DATE OF REVISION: 1954</p> | | <p>SCALE: 1/4" = 1'-0"</p> | |
| <p>478</p> | | <p>478</p> | | <p>478</p> | | <p>478</p> | |



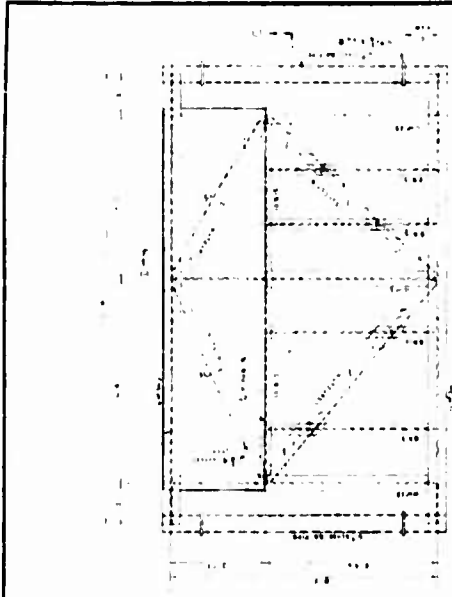
CONTROL PACKAGE PLAN



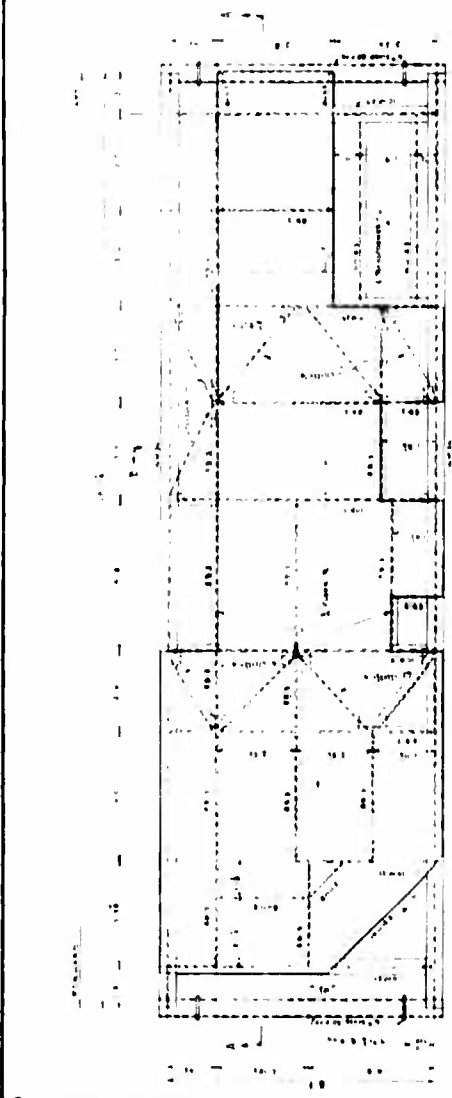
SWITCHGEAR PACKAGE PLAN

- 12" x 12"
- CONTROL PACKAGE
- 1. Control Panel
 - 2. Battery Pack
 - 3. Switchgear
 - 4. Electrical Connections
 - 5. Cable Tray
 - 6. Junction Box
 - 7. Terminal Block
 - 8. Fuse Block
 - 9. Relay
 - 10. Transformer
 - 11. Motor
 - 12. Fan
 - 13. Light
 - 14. Vent
 - 15. Door
 - 16. Lock
 - 17. Handle
 - 18. Knob
 - 19. Switch
 - 20. Plug
 - 21. Socket
 - 22. Receptacle
 - 23. Outlet
 - 24. Inlet
 - 25. Conduit
 - 26. Raceway
 - 27. Cable
 - 28. Wire
 - 29. Busbar
 - 30. Terminal
 - 31. Connector
 - 32. Splice
 - 33. Joint
 - 34. Seal
 - 35. Gasket
 - 36. Pad
 - 37. Shim
 - 38. Washer
 - 39. Nut
 - 40. Bolt
 - 41. Screw
 - 42. Nail
 - 43. Rivet
 - 44. Pin
 - 45. Cotter Pin
 - 46. Spring
 - 47. Padlock
 - 48. Key
 - 49. Lock Key
 - 50. Padlock Key
- SWITCHGEAR PACKAGE
- 1. Switchgear
 - 2. Electrical Connections
 - 3. Cable Tray
 - 4. Junction Box
 - 5. Terminal Block
 - 6. Fuse Block
 - 7. Relay
 - 8. Transformer
 - 9. Motor
 - 10. Fan
 - 11. Light
 - 12. Vent
 - 13. Door
 - 14. Lock
 - 15. Handle
 - 16. Knob
 - 17. Switch
 - 18. Plug
 - 19. Socket
 - 20. Receptacle
 - 21. Outlet
 - 22. Inlet
 - 23. Conduit
 - 24. Raceway
 - 25. Cable
 - 26. Wire
 - 27. Busbar
 - 28. Terminal
 - 29. Connector
 - 30. Splice
 - 31. Joint
 - 32. Seal
 - 33. Gasket
 - 34. Pad
 - 35. Shim
 - 36. Washer
 - 37. Nut
 - 38. Bolt
 - 39. Screw
 - 40. Nail
 - 41. Rivet
 - 42. Pin
 - 43. Cotter Pin
 - 44. Spring
 - 45. Padlock
 - 46. Key
 - 47. Lock Key
 - 48. Padlock Key

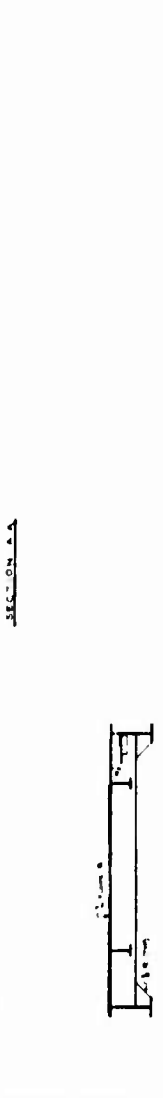
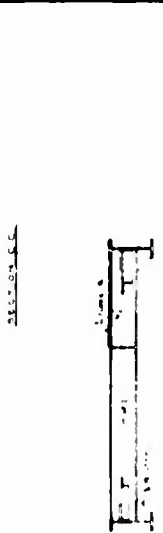
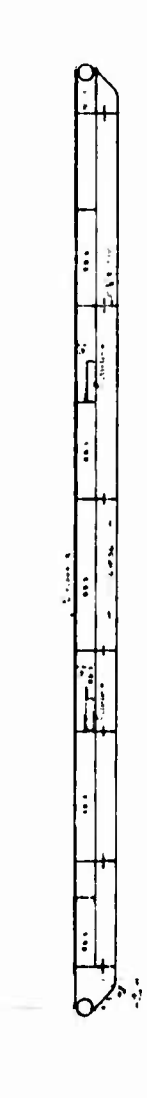
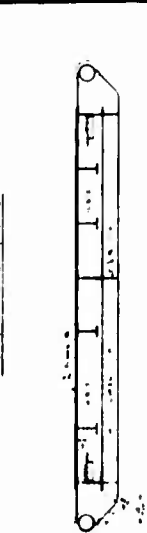
ALCO PRODUCTS, INC.
 479
 ELECTRICAL DEPARTMENT
 1000 W. 10th Street
 Chicago, Ill. 60608
 MADE IN U.S.A.



SECTION A-A



SECTION B-B



GENERAL NOTES

1. ALL DIMENSIONS ARE IN FEET AND INCHES.

2. ALL WALLS ARE 12" THICK UNLESS OTHERWISE NOTED.

3. ALL ROOFS ARE TO BE CONCRETE SLAB ON GIRDS.

4. ALL FLOORS ARE TO BE CONCRETE ON GIRDS.

5. ALL CEILING ARE TO BE CONCRETE ON GIRDS.

6. ALL DOORS AND WINDOWS ARE TO BE AS SHOWN.

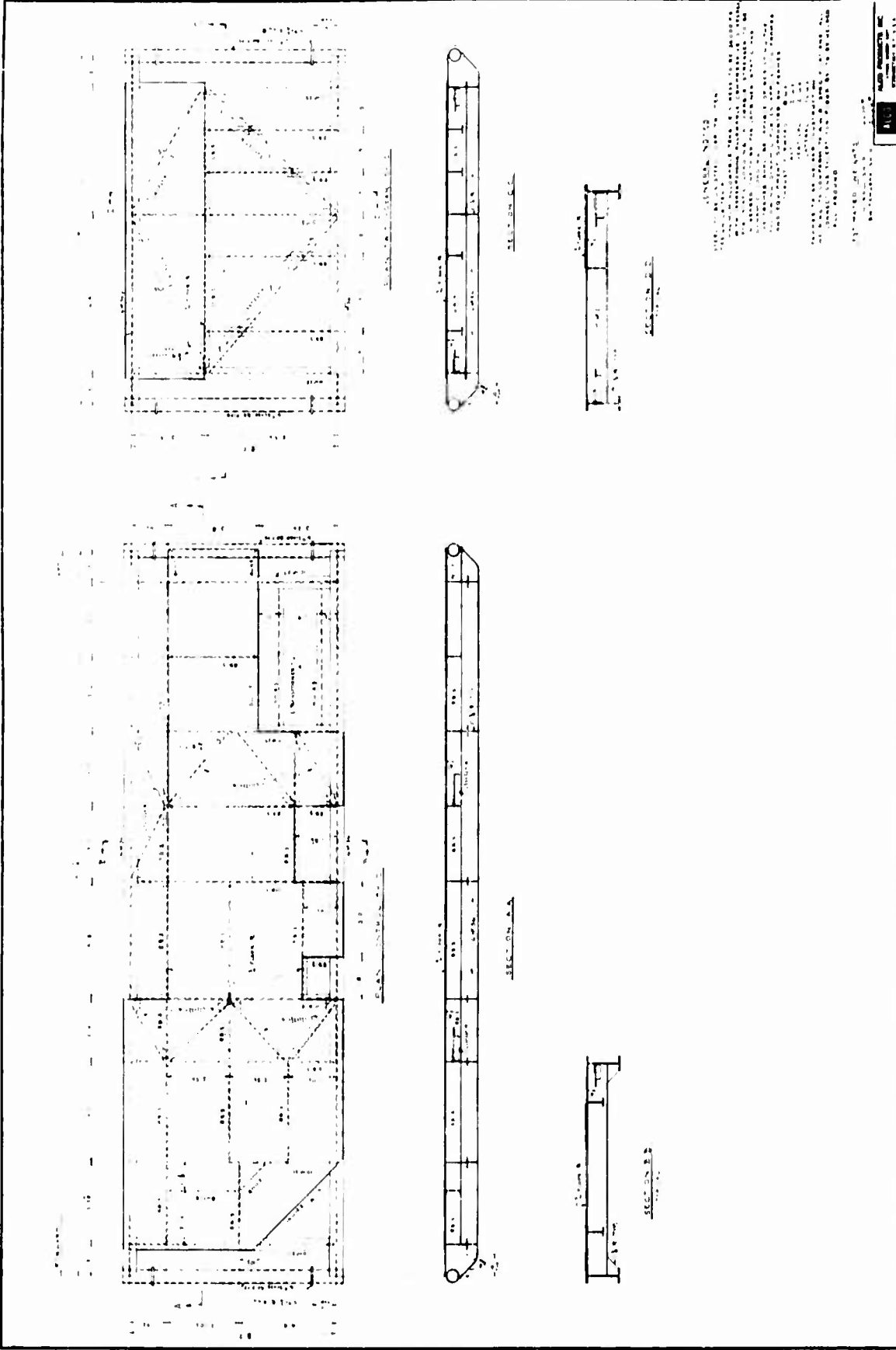
7. ALL MATERIALS ARE TO BE AS SPECIFIED IN THE SPECIFICATIONS.

8. ALL WORK IS TO BE DONE IN ACCORDANCE WITH THE LATEST EDITIONS OF THE BUILDING CODES AND SPECIFICATIONS.

9. ALL WORK IS TO BE DONE IN ACCORDANCE WITH THE LATEST EDITIONS OF THE BUILDING CODES AND SPECIFICATIONS.

10. ALL WORK IS TO BE DONE IN ACCORDANCE WITH THE LATEST EDITIONS OF THE BUILDING CODES AND SPECIFICATIONS.

| | | | |
|-----------------------|--|--|--|
| | | Ernst & Krueger Corporation | |
| PROJECT NO. 12345 | | SHEET NO. 480 | |
| DRAWN BY: J. D. SMITH | | CHECKED BY: A. B. JONES | |
| DATE: 12/15/1925 | | SCALE: AS SHOWN | |



UNLESS NOTED TO THE CONTRARY, ALL DIMENSIONS ARE TO FACE UNLESS OTHERWISE SPECIFIED.

ALL WORK SHALL BE IN ACCORDANCE WITH THE LATEST EDITIONS OF THE BUILDING CODES AND SPECIFICATIONS.

ALL MATERIALS SHALL BE OF THE BEST QUALITY AND SHALL BE SUBJECT TO INSPECTION AND APPROVAL BY THE ARCHITECT.

ALL WORK SHALL BE COMPLETED WITHIN THE SPECIFIED TIME FRAME.

ALL WORK SHALL BE DONE IN ACCORDANCE WITH THE LATEST EDITIONS OF THE BUILDING CODES AND SPECIFICATIONS.

ALL MATERIALS SHALL BE OF THE BEST QUALITY AND SHALL BE SUBJECT TO INSPECTION AND APPROVAL BY THE ARCHITECT.

ALL WORK SHALL BE COMPLETED WITHIN THE SPECIFIED TIME FRAME.